Online ISSN : 2395-602X
Print ISSN : 2395-6011
www.ijsrst.com

IJSRST

Conference Proceedings

National conference on Chemistry Innovations, Applications and Sustainability

NCCIAS-2024

7th December 2024

Organized By

Department of Chemistry,
Late Ku. Durga K. Banmeru Science College, Lonar, India

VOLUME 11, ISSUE 23, NOVEMBER-DECEMBER-2024

INTERNATIONAL JOURNAL OF SCIENTIFIC RESEARCH IN SCIENCE AND TECHNOLOGY

PEER REVIEWED AND REFEREED INTERNATIONAL SCIENTIFIC RESEARCH JOURNAL

Scientific Journal Impact Factor : 8.627

Email : editor@ijsrst.com Website : http://ijsrst.com

National conference on Chemistry Innovations, Applications and Sustainability

NCCIAS-2024

7th December 2024

Organized by

Amrut Sevabhavi Sanstha, Parbhani

Department of Chemistry

Late Ku. Durga K. Banmeru Science College, Lonar

In Association with

Analytical Chemistry Teachers and Research Association (ACTRA)

Chh. Sambhajinagar

&

Amravati University Chemistry Teacher's Association (AUCTA)

Published By

IJSRST

International Journal of Scientific Research in Science and Technology

Print ISSN: 2395-6011 Online ISSN: 2395-602X

Volume 11, Issue 23, November-December-2024

International Peer Reviewed, Open Access Journal

Published By

Technoscience Academy

website: www.technoscienceacademy.com

Speakers in the conference

Dr. Mazahar Farooqui
Principal, Maulana Azad College,
Chh. Sambhajinagar

Dr. Santosh K. Haram
Professor, Department of Chemistry
Savitribai Phule Pune University, Pune.

Dr.Vijay H. Masand
Professor in Chemistry, Vidya Bharati
Mahavidyalay, Amravati

Patron

Chief Patron

Sau. Ushatai Gole,
President

Patron

Dr. Santosh K. Banmeru,
Secretary

Amrut Sevabhavi Sanstha, Parbhani

Chief Organizer

Dr. Prakash K. Banmeru
Principal
L.K.D.K.Banmeru Science College, Lonar

Dr. Mazahar Farooqui
Principal
Maulana Azad College,
Chh. SambhajinagarManoraDist. Washim,

Dr. N.S. Thakare
Principal
M.S.P.K.P.T. College,College,
President, AUCTA.

Organizing Secretary | Convener | Co-Convener

Dr. Prashant Netankar
Professor, Dept. of Chem
Maulana Azad College, Aurangabad

Dr. Arif Pathan
Head, Dept of Chemistry,

Dr. Kishor N. Puri
Secretary, AUCTA &Head
Dept. of Chem,Shri. Shivaji College,Akola

Dr. Kamalakar K. Wavhal
Asst. Professor, Dept. of Chem
L.K.D.K.B. Science College,Lonar, Dist. Buldana

Dr. Suryakant B.Borul
Head, Dept. of Chemistry

National Advisory Committee

- **Prof. N.N. Maldar**
  Former, Vice Chancellor, Solapur University.
- **Dr. Pandit Vidyasagar**
  Ex-Vice Chancellor SRTMU, Nanded.
- **Dr. Abu T. Khan**
  IIT Guwahati & Former Vice- Chancellor, Aliah University, Kolkata.
- **Dr. Rakshit Ameta,** NIMS. University Jaipur.
- **Dr. S. H. Mathela,** G Kangra, H. Haridwar.
- **Dr. Satish Pardeshi**
  Savitribai Phule Pune Univesity, Pune.
- **Prof. Mohsin Khan,** Shahjahanpur
- **Dr. A. N. Sonar,** Raver
- **Prof Monmohan Satnami**
  PT Ravi Shukla University, Raipur
- **Prof. Maan Singh,** Central University, Gujrat
- **Dr. M. M. Tiwari,** G. K. University Haridwar.
- **Dr.Qasimullah,** MAANUU Hydrabad.
- **Prof. Sumer D. Thakur,** RDIK College, Badnera.
- **Prof. Hemant Chandak,** G.S. College Khamgaon
- **Dr. Sandip Kotharkar,** Head- Synthetic R&D Embio ltd. CPHI Itali.
- **Dr.Mazahar Farooqui**
  Principal, Maulana Azad College, Aurangabad.
- **Dr. Nandakishor S. Thakare,** President, (AUCTA)
- **Dr. Prakash K. Banmeru**
  Principal, LKDKB Science college, Lonar
- **Dr. Sangita S. Makone**
  Director, School of Chemical Science (SRTMU, Nanded)
- **Dr. R. D. Sikchi**
  M C Member SGBAU, Amravati & Principal, Sitabai Arts Commerce and Science College Akola.
- **Dr. A. B Naik,** Head Dept. of Chemical Technology SGBAU, Amravati.
- **Dr. Vijay Nagre**
  M C Member SGBAU, Amravati & Principal, Narayanrao Nagre College, Dudarbid
- **Prof. Megha Rai**
  Dr.Rafiqui Z C Women College, Aurangabad
- **Prof Anil Shankarwar**
- S.B College, Cht. Sambhaji Nagar
- **Prof. Sunil Shankarwar**
  Head, Dr. BAMU, University, Cht. Sambhaji Nagar
- **Prof. Suresh Gaikwad,**
  Dr. BAMU, University, Cht. Sambhaji Nagar
- **Dr. A. L. Kulat**
  Senate Member SGBAU, Amravati & Principal
- **Dr. Omprakash Zanwar**
  Principal, R. A. College Washim
- **Dr. C. S. Patil**
  President, ACTRA.
- **Dr. Anand S. Aswar**
  Ex HOD Dept. of Chemistry, SGBAU, Amravati. & Coordinator ACTRA South zone.
- **Dr. B. S. Dobhal**
  B.R. BarwaleColege, Jalna
- **Prof. D. L. Lingampalle**
  Vivekanand College. Cht. Sambhaji Nagar
- **Prof. Jagdish Bharad**
  Vasantrao Naik College, Cht. Sambhaji Nagar
- **Prof. R. K. Pardesi,** Sant Ramdas college, Jalna.
- **Dr. Gopal Kakde,** Principal, Rajmata Jijau Maha. Kile Dharur
- **Dr. Satish Deshmukh**
  Deogiri College, Chh. Sambhaji Nagar
- **Dr. Kabir Shaikh,** Sir Sayyad College, Aurangabad
- **Dr. Bapurao Shingate**
  Dept. of Chemistry, Dr. Babasaheb Ambedkar Marathwada University, Chh. Sambhaji Nagar
- **Dr. Wasudeo B. Gurunale**
  Det. of Chemistry, Kamala Neharu Maha. Nagpur.
- **Dr. Shankar P. Hangirgekar**
  Det. of Chemistry, Shivaji University, Kolhapur.
- **Dr. Sushilkumar Dhanmane**
  Det. of Chemistry,Fergusson College, Pune.
- **Dr. P. B. Raghuwanshi**
  M.C Member SGBAU, Amravati.
  Det. of Chemistry, Brijlal Biyani college, Amravati
- **Dr. Manisha M. Kodape**
  Det. of Chemistry, Sant Gadge Baba Amravati University, Amravati.
- **Dr. Sanjay Kumar**
  Det. of Chemistry, Sham Lal College Delhi University.
- **Dr Atul Gupta**
  Det. of Chemistry, Swami Vivekanand Gov. College Himachal Pradesh.
- **Prof. M. K. Lande**
  Dr. BAMU, University, Cht. Sambhaji Nagar
- **Dr. D. D. Kayende,** SB College, Cht. Sambhaji Nagar
- **Dr. Ayesha Durrani**
  Dr.Rafiqui Z C Women College, Aurangabad.
  Dr. Rajesh Bora
  Principal, Research investigator, Boicon Med Chem Benguluru.

Local Advisory Committee

- **Dr. Subhash Lonkar**
  Professor & Head of Department of Chemistry Shri, Shivaji College Parbhani.
- **Dr.Santosh Agarkar**
  Principal Indra Gandhi Kala Mahavidhalya, Ralegaon
- **Dr. Rameshwar Khadsan,**Principal, Burungale college, shegaon.
- **Dr. VijayMasand**
  Dept. of Chemistry, Vidya Bharati College, Amravati
- **Dr. Prassana Pande**
  Dept. of Chemistry, Shankarlal Khandelwal College, Akola,
- **Dr. Deepak Nagrik**
  Dept. of Chemistry, G. S. College Khamgaon.
- **Dr. Santosh Kumbhare**
  Dept. of Chemistry, Shivaji College Buldana.
- **Dr. G. H. Kurhade**
  Dept. of Chemistry,Vidnyan Maha. Malkapur
- **Dr. Sharad Idhole**
  Dept. of Chemistry, Gulab Nabi Azad College, Barshi Takali
- **Mr. Balasaheb Kale**
  Dept. of Chemistry, Venkatesh Maha. Deulgaon Raja
- **Mr. Ravi Khadse**
  Dept. of Chemistry, P. G. Gawali College Shirpur Jain.
- **Mr. Manoj More**
  Dept. of Chemistry, R. A. College
  Washim.
- **Dr. P.T. Agrawal**
  Dept. of Chemistry, Shri RLT College Akola.
- **Dr. D. B. Dupare**
  Dept. of Chemistry, Shri R G College Murtizapur.
- **Dr. S. V. Kolhe**
  Dept. of Chemistry, Shri Shivaji College, Akot.
- **Dr. S. J. Patil**
  Dept. of Chemistry, Science College Balapur.
- **Dr. Smita Tarale**
  Dept. of Chemistry, Dept. of Chemistry, Shri. P. M. Maha. Nandura Rly.
- **Dr. Gajanan Dongre**
  Dept. of Chemistry, Shri. Shivaji College Chikhali.
- **Mr. Nityanand Dahake**
  Dept. of Chemistry, Science, arts and Commerce College Warwant Bakal.
- **Mr. Bhaskar Bhise**
  Dept. of Chemistry, Shri Shivaji College, Motala
- **Dr. Kiran Shelke**
  Dept. of Chemistry, Late Pushpadevi Patil College Risod.
- **Mr. Nirangan Rathod**
  Dept. of Chemistry, Smt. SindhutaiJadhao College, Mehkar.
- **Dr. Mukesh Kadam**
  Dept. of Chemistry, LokneteGopinathji Mundhe College, Mandangad, Ratnagiri.
- **Mr. Amol Shelke**
  Dept. of Chemistry, Vivekannand Science College, HiwraAshram.
- **Dr. Ramesh Parihar**
  Dept. of Chemistry, Vidnyan Maha. Malkapur.
- **Dr. Prashant Mahalle**
  Dept. of Chemistry, Late. B. S.Arts ,Prof. N. G. Science & A. G. Commerce College Sakharkherda.
- **Dr. Chaya Badnakhe**
  Dept. of Chemistry, Dr. Manorama &Prof. H. S. Pundakar College Balapur.

Local Organizing Committee

- **Dr. Praksh K. Banmeru**
  Principal, LKDKB Science college, Lonar
- **Dr. Nandakishor S. Thakre,** Principal, MSPKPT Manora &President, (AUCTA)
- **Dr. Kishor Puri,** Professor & Head of Department, Shri Shivaji College, Akola
- **Dr. Suryakant Borul,** Head of Department Chemistry
- **Dr. Kamalakar Wavhal,** Department of Chemistry
- **Mr. Shivshankar More,** Department of Chemistry
- **Mr.Sharique Shaikh**, Head of Department Physics
- **Dr. Milind Gaikwad,** Head of Department Zoology
- **Dr. Mahendra Bhise**
  Head of Department Botany
- **Mr. Saurabh Gaikwad**
  Head of Department Mathematics.
- **Mr. Pratik Sanap**
  Department ofBotany
- **Mr. Akash Shejul**
  Department of Physics
- **Mr. Raju Asole**
  Department of Mathematics
- **Dr. Varsha Mishra**
  Department of Zoology
- **Miss. Siddhi Banmeru**
  Department of Computer Science
- **Mr. Aditya Kulkarni**
  Head of Department Computer Science
- **Miss. Nishigandha Khule**
  Head of Department Microbiology.
- **Dr. Mangesh Thombal**
  Physical Director.

ABOUT CONFERENCE

The National Education Policy 2020 strongly recommends that research in science education be promoted to develop scientific temper. One of the objectives of NEP 2020 is to foster inventiveness and creativity alongside competence. This conference focuses on high-level discussions about various interesting aspects of chemistry. This one-of-a-kind event will cover different topics within the field of chemistry. The conference will bring together renowned scientists, professionals, academicians, students, and knowledgeable individuals from many sectors of chemistry. We will gain insight into the most recent themes, innovations, and applications through in-depth conversations with subject experts. The NEP 2020 aims to provide a holistic and flexible learning experience for students by minimizing outdated curriculum content and focusing on 21st-century skills such as analytical and critical thinking, experiential learning, and creativity. Keeping these objectives in mind, the Late Ku. Durga K. Banmeru Science College, Lonar along with ACTRA and AUCTA, provides a platform for industrialists, researchers, professors, and postgraduate students to share their knowledge and upgrade their skills. This conference aims to inspire young scientists to conduct more research on the Lonar Crater, as it is a scientific treasure for researchers.

ABOUT THE COLLEGE

Late Ku. Durga K. Banmeru Science College was established in June 2000 with the aim of providing education in science for rural and marginalized students at the graduate and postgraduate levels. It has a beautiful campus of 6.5 acres with adequate infrastructure. Since its establishment, the college has been committed to providing support and motivation to rural and marginalized students, especially girls, to pursue higher education for their holistic development. Students are encouraged to participate in various curricular and extracurricular activities at the college and at the inter-collegiate level. The objectives and outcomes of these activities aim to enable needy students to enhance their educational qualifications, become self-reliant, and develop leadership qualities. Due to the socially committed and ethically profound management of the college, a positive academic environment is fostered on the campus. The college has been accredited by NAAC with a “B++” grade (CGPA 2.88) at the second cycle of assessment. The Amrut Sevabhavi Sanstha Parbhani was founded by Hon’ble Dr. Prakash K. Banmeru to provide education to economically and educationally backward communities. Research and development activities are conducted in various departments of the college regularly. The college offers programs in B.Sc., M.Sc. in Computer Science, Chemistry, Botany, Zoology, B.Voc. (Tourism & Hospitality Management), and diploma/certificate courses in

Quantitative Aptitude, Freshwater Fish Culture, Astronomy, Herbal Medicine, and Economic Zoology. The college has a good tradition of maintaining positive outcomes. The computerized administrative section is always available to assist students. Our aim is to provide quality education to our students from rural areas, as the college is surrounded by rural and tribal communities. We are running many career-oriented programs and courses on campus. Our college has organized the “Lonar Science Festival” for the last six years to create awareness and promote the conservation of the Lonar Crater.

ABOUT CHEMISTRY DEPARTMENT

The Chemistry Department was established in 2000 with the establishment of the college. Initially, it was an undergraduate department with a student strength of about 250. The postgraduate program was established this year, with a current student strength of 20. This is the first national conference organized by the department. Every year, the department organizes student-centric activities such as poster presentations, quiz competitions, the establishment of a Chemical Society, guest lectures, and group discussions. The department has three well-qualified and motivated permanent faculty members. The lab is well equipped with research-grade chemicals, and the department has MOUs with different colleges and industries. Additionally, the department has started a short-term “Industrial Chemistry” certificate course, which is designed by the college and approved by the university. Every year, departmental students visit various industries for short tours.

ABOUT THE LONAR CRATER

The Lonar Crater, located in Lonar, Buldana district (M.S.), India, is a unique and mysterious natural wonder. It is the only known saline crater in the world, formed by the impact of a meteorite about 50,000 years ago. Its water is actually seven times saltier than seawater. The lake has a diameter of 1.2 km and a depth of 150 meters. One of the most striking aspects is its color, which changes from green to pink depending on the seasons and water conditions. The Lonar Lake has been declared a “Wildlife Sanctuary” for conservation purposes and has also been designated as Maharashtra’s second Ramsar site. Ramsar sites are wetlands of international importance under the Ramsar Convention. There are temples built around 1,250 years ago, with fifteen temples in total. The crater water turns pink due to the large presence of salt-loving Haloarchaea microbes. The chemical characteristics of the lake show two distinct regions that do not mix: an outer neutral zone (pH 7) and an inner alkaline zone (pH 11), each with its own flora and

fauna. The lake is a haven for a wide range of medicinal plant and animal life, hosting 160 bird species, 46 reptile species, and 12 mammal species. The lake is also home to thousands of peafowls, chinkaras, and gazelles. An area of 3.83 km² (1.48 sq. mi) has been declared as the Lonar Wildlife Sanctuary.

SUB-THEMES OF CONFERENCE

- ✓ Advances in Green Chemistry
- ✓ Advances in an Analytical Chemistry
- ✓ Recent development in Nanotechnology and
- ✓ Material Science
- ✓ Organic and Inorganic Chemistry.
- ✓ Chemistry of Natural Product
- ✓ Bio-inorganic Chemistry
- ✓ Environmental Chemistry
- ✓ Medicinal and Pharmaceutical Chemistry
- ✓ Polymer Chemistry
- ✓ Environmental Chemistry
- ✓ Forensic Chemistry
- ✓ Organo-metallic Chemistry
- ✓ Co-ordination Chemistry
- ✓ Computational Chemistry
- ✓ Fundamental and Advanced Bio-Chemistry

CONTENT

International Journal of Scientific Research in Science and Technology
Available online at : www.ijsrst.com
Print ISSN: 2395-6011 | Online ISSN: 2395-602X
doi : https://doi.org/10.32628/IJSRST

Critical Study of Pulse High Voltage Measurement using Optical Kerr Effect

Abdul Jaleel A.H.[1], Nilofar Mukhtar Ahmed[2], Yusuf Hanif Shaikh[3], A R Khan[4]

[1]Department of Physics and Electronic, Maulana Azad College of Arts, Science and Commerce, Aurangabad, Maharashtra, India

[2]Maulana Azad College of Arts, Science and Commerce, Aurangabad, Maharashtra, India

[3]Department of Physics and Electronic, Shivaji Arts, Science and Commerce College, Kannad, Maharashtra, India

[4]Department of PG Computer science, Maulana Azad College of Arts, Science and Commerce, Aurangabad, Maharashtra, India

ARTICLEINFO

Article History :

Published : 07 Dec 2024

Publication Issue :
Volume 11, Issue 23
Nov-Dec-2024
Page Number :
01-07

ABSTRACT

High voltage pulses are used in a variety of branches in engineering, science and technology and therefore related measurements become important. The technique studied is contact-less measurement of fast high voltage pulses based on electro optic Kerr effect. The approach is very effective in terms of remote access and is fast enough to permit measurements as fast as a nanosecond. However because of the fact that the measurements are based on the amount of rotation in the orientation of the plane of polarization when a polarised beam of light passes through a Kerr cell, and because of the nature of relationship between the Kerr signal and the actual voltage pulse, there are few limitations associated with this. This paper presents these limitations and as to how they affect the measurements. Possible approaches to overcome these limitations in order to arrive at a reliable measurement are also presented.

Keywords: High Voltage Pulse, Electro-optic Kerr Effect, He-Ne Laser, polariser, analyser, Nitrobenzene.

Introduction

This document provides an example of the desired Generation and measurement of pulsed high voltage finds its application in a variety of disciplines from science, engineering and technology(1-4) to defense, health and medicine(5-6). High voltage pulses are used in pulsed laser generation and experiments related to plasma confinement and fusion research(7-12), however here the current and power requirements are relatively higher. The advantage of measurement of pulsed high voltage using electro-optical Kerr effect is that this is a

contact less method of measurement of high voltage(13-16). Many low power high voltage applications involve very high sensitivity instrumentation with extremely high input impedance, which otherwise load the high voltage source and cause unacceptable deviations in the measurement. The present work relates to a simple and effective approach helpful in measurement of high voltage pulses using Kerr effect. The approach is based on electro-optic Kerr effect and is a contact less method for pulsed voltage measurement. The underlying principle is based upon the fact that plane of polarisation of plane polarised light gets rotated while passing through a Kerr medium placed in an electric filed.

When plane polarized light passes through a medium placed in an electric filed the plane of polarisation of the incident radiation gets rotated. The amount of rotation introduced depends on the characteristics of the medium (Kerr Constant) and the length of path traversed by the incident radiation in addition to the strength of the electric field.

The phase difference introduced in the two components of light, parallel and perpendicular to the field direction, while traveling a length 'l', in a medium of Kerr constant K subjected to an electric field E = V / d is

$$\varphi = 2 \pi K l (V/d)^2 \qquad (1)$$

Where V is the voltage between the field electrodes of length 'l' separated apart by a distance d and K is the Kerr constant of the medium.

In general for Kerr cell arrangement, the intensity of light transmitted I, through the Kerr cell with polariser and analyser can be written as

$$I = Io\ A \sin^2(\varphi/2) \qquad (2)$$

Where Io is the intensity of the incident unpolarised light,

A is a constant which accounts for the rejection of light by the polarizer, analyzer and absorption and reflection losses in all components of the Kerr setup. This can be made unity and hence be eliminated by suitable choice of experimental conditions.

φ is the phase difference between two components of light parallel and perpendicular to the electric field E.

The transmittance of the Kerr cell, defined as the ratio of transmitted intensity to the incident intensity with A = 1 is

$$T = I/Io = \sin^2(\pi K l E2) \qquad (3)$$

T is a maximum for $\pi K l E2 = \pi/2, 3\pi/2, \ldots$ etc

or

E2 = 1/(2Kl), 3/(2Kl), 5/(2Kl) … and so on corresponding to full opening of the Kerr cell.

The technique used is that the voltage pulse to be measured is applied between two parallel plates kept in a suitable Kerr medium and a plane polarised beam of light is passed through the medium. In the absence of electric field there is no rotation of the plane of polarisation of the plane polarised beam of light. When this light is viewed through a polariser with it plane of polarisation at right angles to the plane of polarisation of the incident light, acting as an analyzer, ideally no light passes through the analyzer and hence the Kerr cell. When a voltage is applied to the two conducting plates kept in the Kerr medium, the plane of polarisation of the plane polarised beam of light rotates depending on the applied voltage that in turn determines the electric field in the medium. Further, this amount of rotation depends on the Kerr constant of the liquid and the length of path traversed. This causes light to transmit through the Kerr cell (parallel plates kept in the Kerr medium).

Experimtntal

High Voltage Pulse Measurement

For high voltage measurement a Kerr cell is used where two parallel plates are kept in a rectangular glass cell containing Nitro benzene as a Kerr medium and the cell has two transparent windows for the passage of light. Two polarisers are kept on the two sides of the cell, the second polariser, on the side of detector acts like an analyser. When a beam of light is incident on the Kerr cell, no light passes through the cell if the plane of polarisation of polariser and analyser are at right angles to each other.

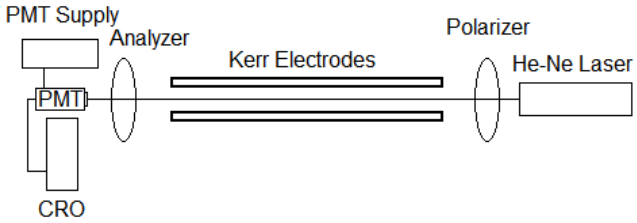

Fig. 1 Typical Kerr Cell setup for high voltage pulse measurement.

On the other side of the analyser an optical detection system is used which may comprise of a photomultiplier with fast response and a amplifier if needed. We used EMI 9816 QB photo multiplier with fast rise time of better than 10 ns and high sensitivity so that the output can directly be seen on standard oscilloscope and no signal amplification was needed in the present work.

When a high voltage pulse is applied to the Kerr cell, the output (radiation through the Kerr cell and hence the photomultiplier signal) is the representative of the voltage pulse applied to the cell. A typical voltage pulse applied to the Kerr cell is shown in Fig. 2 along with the output waveform from the photomultiplier. Both the signals are recorded simultaneously for the same pulse in real time to eliminate pulse to pulse variation if any. For the purpose of reconstructing the voltage waveform from the Kerr signal pulse the relation used is given below.

$$V = U\left((2/\pi)\sin^{-1}(T)^{1/2}\right)^{1/2} \qquad (4)$$

Where U is the full opening voltage of the Kerr Cell and T is the Transmittance of the Kerr Cell and is a function of time that varies from point to point along the voltage pulse. The value of U can be calculated from:

$$U = d(1/(2Kl))^{1/2} \qquad (5)$$

Where d is the spacing between the two Kerr cell electrodes, K is the Kerr constant of Nitrobenzene = 2.44 X 10^{-10} /V^2 and 'l' is the length of the electrodes. In the present application with the nitrobenzene Kerr cell used the full opening voltage was U = 2.4 KV. A lower full opening voltage cell was used to see the effect of multiple openings of the Kerr cell under application of higher voltages. For the demonstration of measurement of pulsed high voltages using Kerr effect a voltage pulse having peak voltage less than the full opening voltage was used.

The value of instantaneous voltage V at any time can be calculated from the Equation – 4 if the value of U and T are known. U being the full opening voltage of the Kerr cell it is characteristic to the cell along with the given liquid and needs to be determined only once. However the value of T keeps on changing from point to point along the curve and is determined from the ratio of Io to I as

$$T = I/Io \qquad (6)$$

Where Io is the transmitted intensity of light through the Kerr cell when the planes of polarisation of the polariser and analyser are aligned parallel and I is the measured intensity at a given instant of time. Fig. 2 shows

the voltage pulse and the Kerr signal from the photomultiplier recorded by the photomultiplier and digital storage oscilloscope (Tektronix TDS2024). The advantage of a digital storage oscilloscope is that it records data for individual points at a fixed time interval. This photomultiplier output voltage versus time data is used for the reconstruction of the actual voltage pulse from this information of transmittance of the Kerr cell.

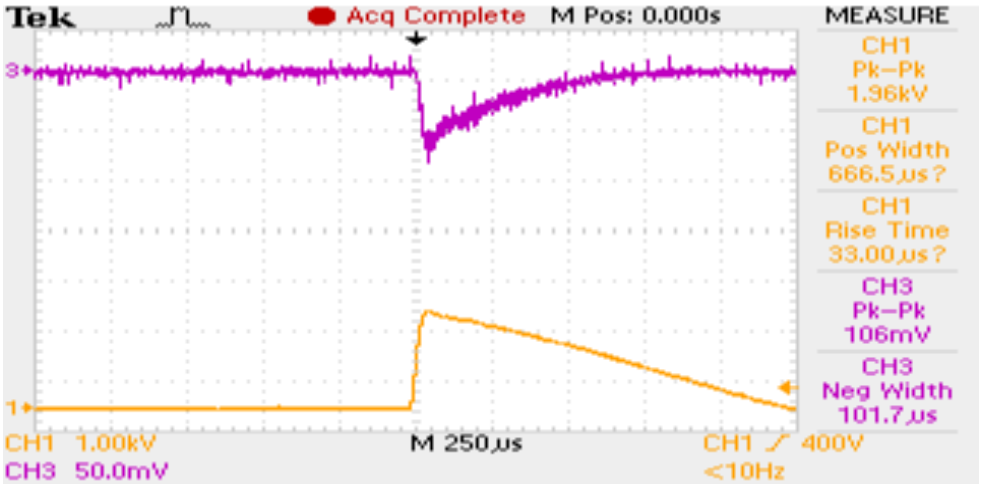

Fig. 2 High voltage Pulse (in Yellow) and the Kerr signal from Photomultiplier (Pink).

The determination of T at different time points poses difficulty because of the fact that this involves measurement of Io and sensitive detection system like the one with fast photomultiplier suffer from saturation effect. If the photomultiplier tube is exposed to radiation for a longer time its sensitivity decreases with time.
To reconstruct the high voltage pulse from the transmittance of the Kerr cell equation (4) can be used.

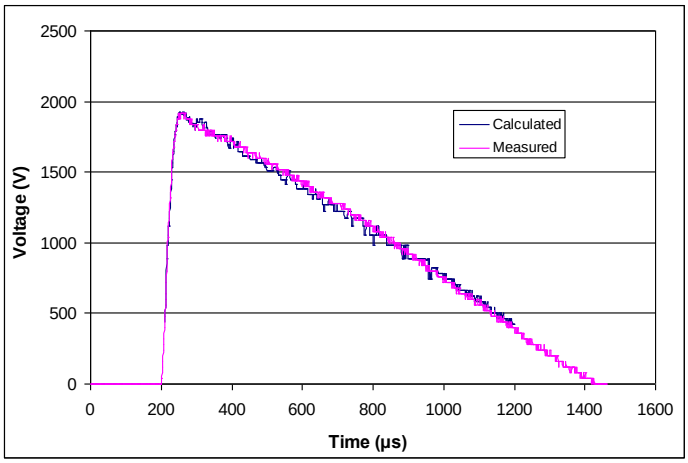

Fig. 3 Comparison of the High voltage pulse measured using High voltage probe and that using calculations based on Kerr effect.

Using the photomultiplier signal data I(t) stored by the Tektronics oscilloscope (Fig. 2 Pink trace) and the value of Io the full transmission signal transmittance T is calculated at each time point as T = I/Io. Substituting the value of T and U in equation (4) the instantaneous value of voltage across the Kerr cell was calculated.
The actual high voltage pulse obtained using using Tektronix P6015 1000X high voltage probe with Tektronix TDS2024 oscilloscope is shown in pink color in Fig. 3 along with the reconstructed pulse calculated using equation 1 from the transmission of the Kerr cell shown in Fig. 1. It is important to note that the High voltage

pulse measurement using optical Kerr effect is the one of the very useful techniques employing contact-less measurement of pulsed high voltage, however these measurements prove to be tricky. This method works nicely for estimation of overall pulse shapes in most of the applications however, because of the nature of relationship between the transmittance and voltage, a very slight inaccuracy in measurement adversely affects the measurement for low transmittance conditions. In Fig. 2, the wave shape could nicely be reproduced at higher voltages (about more than 500 V) because of this limitation. The superimposition of the pulse shapes measured using Kerr effect and standard methods is excellent at higher voltage. For voltages little less than 500 V, the transmittance was very poor and was found to merge in the noise. Additionally, while using sensitive optical detection with faster response, the cable termination load saturation effects in the detector result in a sort of damping which may also need appropriate treatment in the reconstruction of the voltage pulse. Therefore in such applications it becomes extremely important to keep signal to noise ratio as best as possible.
If the lower voltage values are also desired to be estimated with better precision, the simpler technique will be to go for a Kerr cell with smaller full opening voltages than the peak value of the high voltage pulse. While using a Kerr cell with full opening voltage much lesser than the peak voltage of the high voltage pulse multiple openings take place and the reconstruction of the pulse requires accounting for these multiple openings and necessary care has to be taken while reconstructing the voltage pulse from the transmittance signal from the optical detector. A typical example where more than one opening of the cell takes place is shown in Fig. 3.

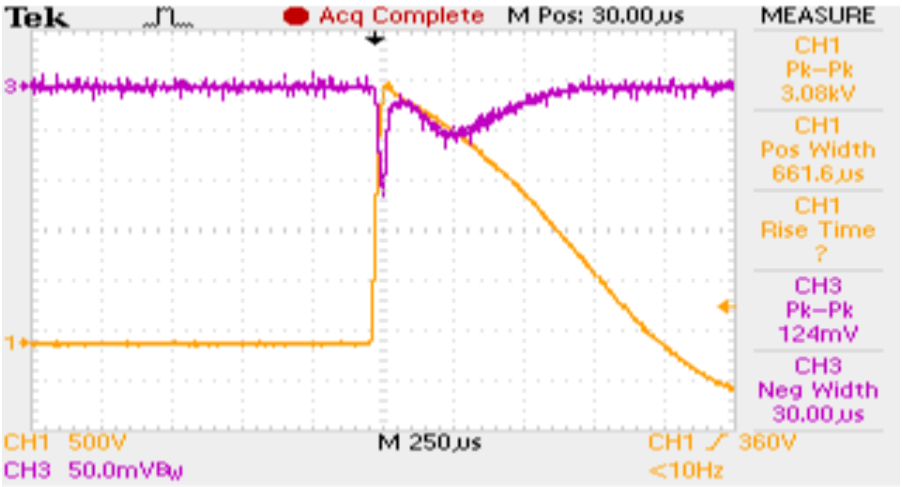

Fig. 4 High voltage Pulse (in Yellow) and the Kerr signal from Photomultiplier (Pink) showing more than full opening condition.

The high voltage pulse and corresponding Kerr signal recorded simultaneously is shown in Fig. 4. The source of light used was a helium neon laser the detections system used a high sensitivity fast photomultiplier mounted in a cold housing. The full opening voltage of the Kerr cell used was higher than the pulse peak voltage. This is visible from the transmission of the Kerr cell shown in Pink in Fig. 4. This transmittance curve clearly shows that there is appreciable amount of saturation effect present with the detection system. Had there been no saturation of the optical detection system the second peak should have similar height as that of the first peak.
A Typical case of saturation of the optical detection system in a Kerr setup with multiple opening is shown in Fig. 5

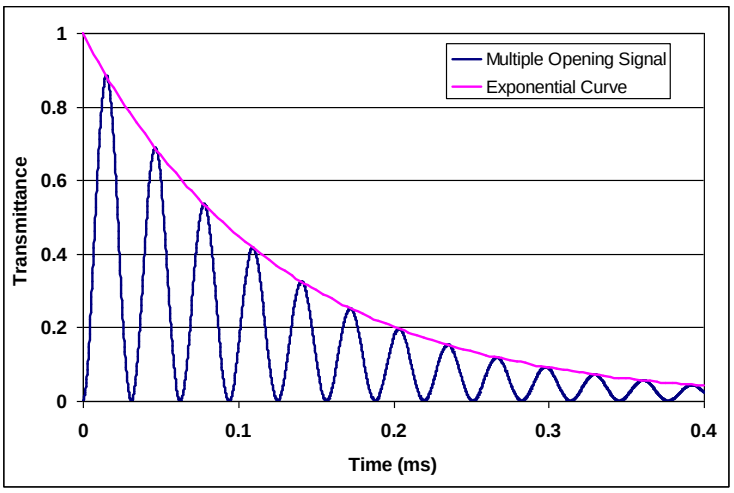

Fig. 5 Kerr signal from Photomultiplier with multiple openings and exponential decay.

Fig. 5 shows a typical Kerr signal with a very low full opening voltage as compared to the peak voltage of the applied pulse. Because of the saturation of the optical detection assembly, as more and more radiation falls on the detector, its sensitivity decreases. It is observed that this decrease in sensitivity is exponential as shown in Fig. 5. Had there been no saturation effect of the detection system, all the full openings would have appeared with identical heights. In such situation, if the decay pattern could be characterized by some equation like exponential, the effect of saturation can appropriately be corrected to bring back the signal to its actual form. For the data presented in Fig. 5 the equation fitting the tips of the peaks is an exponential of the form

$y = A\ e^{-0.04t}$ (7)

Using this normalization technique the reconstruction of high voltage pulse measured using optical Kerr effect can substantially improved which otherwise appears to be very odd.

There is yet another complicated issue related to the estimation of the value of Io to be used in equation (6) for estimation of the transmittance T. In actual experiments dealing with short high voltage pulses with fast rise time, it is desirable to have fast optical detection system which in turn demands for cables terminated into 50 or 75 ohms. Under such conditions there is much load on the detection system making it saturate faster that it would under higher loading conditions like 1 M ohm termination of a good oscilloscope or similar piece equipment.

Determination of Io requires measurement of the transmitted intensity through the Kerr cell when the cell is open (axis of polarisers in parallel or perfect 90˚ of rotation with crossed polarisers). In this condition the intensities are relatively higher and by the time measurement is performed the detector is so saturated that the signal with not bear any relevance to the reality. Otherwise yet another experiment is to be conducted to arrange for a very fast switching of the cell and record the value of Io. This problem can easily be overcome by arranging the Kerr setup and recording a multiple opening signal to estimate the saturation characteristics that can be used to correct the value of signal measured as Io. As a first approximation the first opening intensity can fairly be used in place of Io for practical purposes.

Results and Discussions

Measurement pulsed high voltage suffers from few drawbacks in spite of its importance, particularly the advantage of contact-less measurement. We demonstrated the approach based on optical Kerr effect for

measurement of high voltage pulses. There are few important areas posing difficulty for reconstruction of the actual high voltage pulse like measurement of the intensity of radiation when the cell is fully open and the effect of saturation. The phenomenon is discussed and the methods of overcoming this problem are presented.

References

[1]. H. Bluhm et al., " Industrial applications of high voltage pulsed power techniques: developments at Forschungszentrum Karlsruhe (FZK) ," Digest of Technical Papers. 11th IEEE International Pulsed Power Conference , August 2002, pp. 1-13.

[2]. G. N. Appiah et al. , " Compact design of high voltage switch for pulsed power applications," IEEE Transactions on Dielectrics and Electrical Insulation ,Volume: 24 , Issue: 4 , 2017 , pp.2006-2013

[3]. S Abuazoum et al. , " A high voltage pulsed power supply for capillary discharge waveguide applications," The Review of scientific instruments , June 2011, pp. 063505-1-4

[4]. P. Gaynor et al. , " A high voltage amplifier for use in medical applications of electroporation," Proceedings First IEEE International Workshop on Electronic Design, Test and Applications ', August 2002, pp.1-3

[5]. Sweekruti Mishra, Shashank Mundra, Professor R Sudha, " Use of High Voltage Amplifier in Electroporationfor Transfection Related Medical Applications," International Journal of Scientific and Research Publications, Volume 3, Issue 5, May2013, pp.1-5

[6]. S T Demetriades and C D Maxwell, "Pulsed operation of a combustion MHD generator," IEEE Pulsed Power Conference, 1991, pp. 457-460.

[7]. G.W. Kuswa, " Inertial confinement fusion with particle beams," IEEE Trans. Nuclear Science, 24 (1977), pp. 975-980.

[8]. S. Humphries, Jr. , " Intense pulsed ion beams for fusion applications," Nuclear Fusion, 20, 1980, pp. 1549-1612.

[9]. K. Yatsui, Y. Shimosaki, Y. Araki, K. Masugata, S. Kawata, et al. , " Inertial confinement fusion research with intense pulsed light ion beams," Plasma Physics and Controlled Nuclear Fusion Research 1986, IAEA-CN-49/B-III-9, (1986), pp. 177-186.

[10]. S. Humphries, Jr. , " Charged Particle Beams," John Wiley and Suns, Inc., 1990.

[11]. C. Deutch, " Inertial confinement fusion driven by intense ion beams," Ann. Phys. Fr., 11, 1986, pp. 1-111.

[12]. B.G. Logan, F. Bieniosek, C. Celata, J. Coleman, W.G. Greenway, et al. , " Recent US advances in ion-beam-driven high energy density physics and heavy ion fusion," Nucl. Instr. Meth. Phys. Res., A 577, 2007 , pp. 1-7.

[13]. Babar Hussain, Masroor Ikram, and Asif Mehmood, "A Precise Fast High Voltage Pulse Measurement Optical System Using Kerr Cell Containing Nitrobenzene as an Optically Active Material," International Journal of Computer and Electrical Engineering, Vol. 5, October 2013, pp.460-463

[14]. S Newton, "Kerr cell system for the measurement of high voltage transient waveforms," Journal of Scientific Instruments, Volume 44, Number 9,1973, pp-1-5

[15]. D. C. WUNSCH, " Kerr Cell Measuring System for High Voltage Pulses," THE REVIEW OF SCIENTIFIC INSTRL'MENTS, VOLUME 35, Numbr-7, JULY 1964, pp.816-822.

[16]. Gerald J. FitzPatrick and Edward F. Kelley, "Comparative High Voltage Impulse Measurement," J. Res. Natl. Inst. Stand. Technol. 101, 639, 1996, pp.639-658.

International Journal of Scientific Research in Science and Technology
Available online at : www.ijsrst.com
OPEN ACCESS
Print ISSN: 2395-6011 | Online ISSN: 2395-602X
doi : https://doi.org/10.32628/IJSRST

A Review on Developments in the Synthesis of Triclabendazole

Abjal Pathan[1], Suparna R Deshmukh[2]

[1]Department of Chemistry, Maulana Azad College, Aurangabad, Maharashtra, India

[2]Department of Chemistry, Smt. S.K. Gandhi Arts, Amlok Science & P.H. Gandhi Commerce College, Kada, Maharashtra, India

ARTICLEINFO

Article History :

Published : 07 Dec 2024

Publication Issue :
Volume 11, Issue 23
Nov-Dec-2024
Page Number :
08-16

ABSTRACT

5-Chloro-6-(2,3-dichlorophenoxy)-2-methylthio-1H-benzimidazole also known as Triclabendazole, is marketed under the trade name Egaten. It is an anthelmintic drug used for the treatment of fascioliasis and paragonimiasis. First used in humans in 1986, and approved by the FDA in 2019 for the treatment of human fascioliasis in humans aged ≥6 years. This review aims to summarize the synthetic methods of the Triclabendazole drug reported in the literature. The present review discusses of each synthetic methodology, which would be beneficial to the scientific community for further developments in the synthetic methodologies for Triclabendazole. In addition, the compilation approach of literature-reported synthetic strategies of Triclabendazole in one platform is advantageous, supportive, and crucial for the synthetic community to elect the best synthetic methodology of Triclabendazole and to create new synthesis ideas.

Keywords : anthelmintic, fascioliasis, Egaten, triclabendazole

Introduction

Triclabendazole(6-chloro-5-(2,3-dichlorophenoxy)-2-(methylthio)-1H-benzimidazole) is a benzimidazole derivative, was originally developed and marketed by Ciba as Fasinex to treat fascioliasis in domestic livestock and has been in veterinary use since 1983. Triclabendazole was approved for human use in Egypt in 1997 and in France in 2002. In February 2019, the US Food and Drug Administration (FDA) approved Triclabendazole (Egaten, Novartis Pharmaceuticals, East Hanover, NJ, USA) for the treatment of human fascioliasis. An effort has been made to summarize briefly the different methods reported in the literature for the preparation of pure Triclabendazole. This struggle pushes the readers mind to forge new connections, think differently, and consider new perspectives. To create new picture of schemes, this review is very advantageous. To the best of our knowledge, no review has been yet published on the synthesis of Triclabendazole. This effort will be very beneficial for scientific communities and pharmaceutical industries. The demand for increasingly clean and

efficient chemical synthesis is important from both the economic and environmental points of view, so more attempts to find green and economical synthetic methods are necessary. The present synthetic technique of Triclabendazole suffers from low overall yields and, moreover, to gain the purity to be used as a pharmaceutical substance tedious purification methods are required. To make this drug more common, useful, and cheap, its one-pot, convenient, atom and step-economical, environmentally benign, low-cost synthesis is essential.

SYNTHETIC PROTOCOLS FOR TRICLABENDAZOLE

Synthesis of Triclabendazole from 5-chloro-6-(2',4'-dichlorophenoxy)-2H-1,3-dihydro-benzimidazole 2-thione

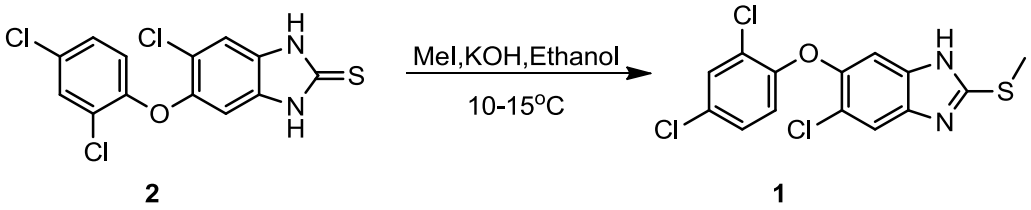

2 1

Scheme-1

Scheme-1 Jean-Jacques Gallay et al synthesized triclabendazole (US Patent No. US4197307A, 1980-04-08) from 5-chloro-6-(2',4'-dichlorophenoxy)-2H-1,3-dihydro-benzimidazole 2-thione with methyl iodide in aqueous alcohol using potassium hydroxide as base in excellent yield. The major drawback of this strategy is methyl iodide being potential genotoxic (Anerao, 2017). The presence of residual methyl iodide in triclabendazole drug substance must be controlled as per European Medicines Agency (EMEA), International Conference on Harmonization (ICH) and Food and Drug Administration (FDA) guidelines.

Synthesis of Triclabendazole from 5,6- dichloro-2H- bentimidazole-2-spirocyclohexane

Scheme-2 Brian Iddon et al synthesized Triclabendazole (Iddon, 1992) from 5,6-dichloro-2H- bentimidazole-2-spirocyclohexane. They treated the dichloro compound **3** with a **1.5** mol excess of sodium 2,3-dichlorophenoxide **(4)** in boiling methanol to yield the mono-substituted 2H-benzimidazole **5** in 62% yield and separated by chromatography (Al_2O_3) from the disubstituted product **6** (29%) as well as from other by products. The reductive ring-opening of **5** with sodium dithionite in aqueous ethanol occurred rapidly to give the ***o***-phenylenediamine **7** ***(85%).*** Treatment with carbon disulfide in DMF gave the 2-thione **8** (90%), which on alkylation with methyl iodide in acetone in the presence of potassium carbonate gave three methylated compounds readily separable by chromatography (Al_2O_3). Use of chromatography at higher scale is not economically viable.

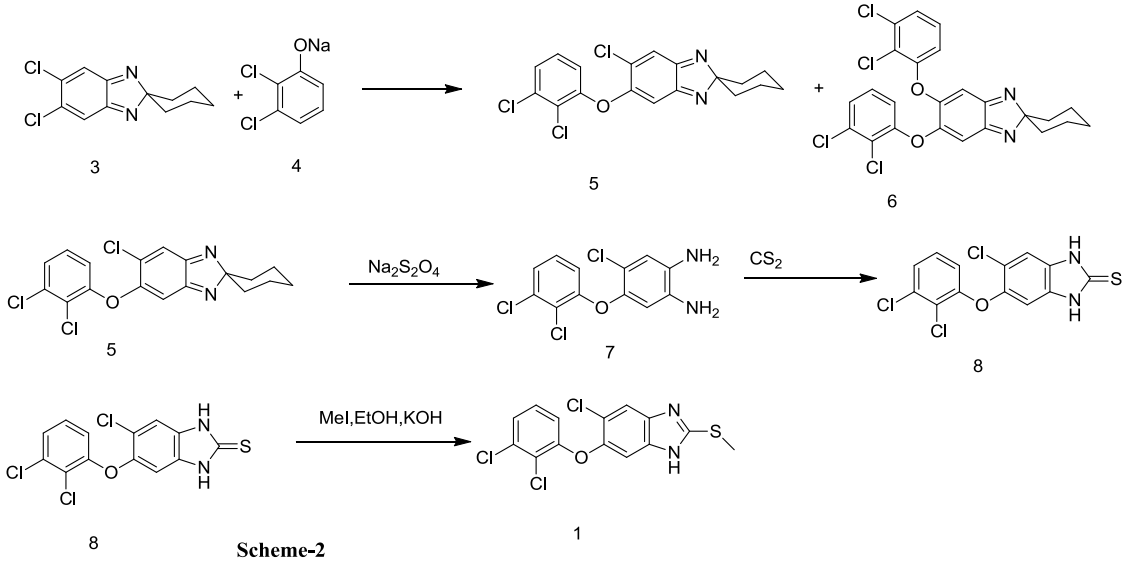

3 4 5 6 5 7 8 8 1

Scheme-2

Synthesis of Triclabendazole from 3, 4-dichloroaniline

Scheme-3 Li Xining Zhou Qiwu of Yangzhou Tianhe Pharmaceutical Co., Ltd synthesized triclabendazole (China Patent No. CN101555231 A , 2009-10-14) starting from 3, 4-dichloroaniline

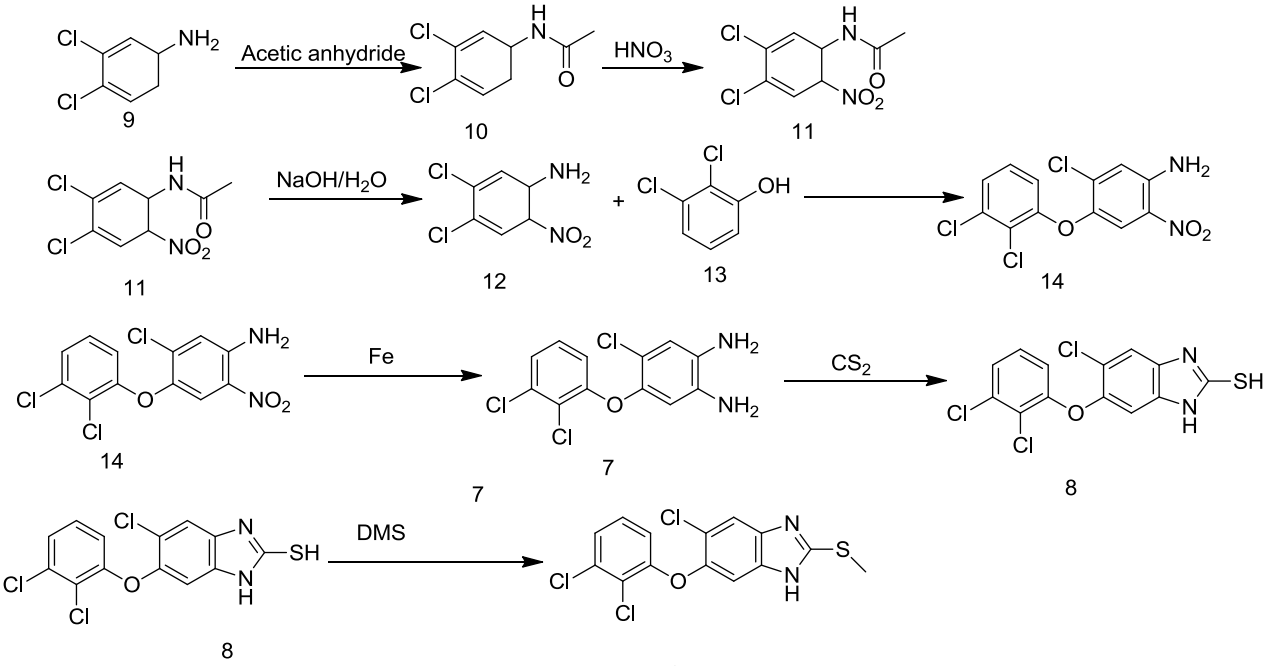

Scheme-3

They started with acetylation of 3, 4-dichloroaniline (**9**) with acetic anhydride followed by nitration with nitric acid and sulfuric acid to **11**, which on hydrolysis condensed with 2,3-dichlorophenol (**13**) obtained compound **14**. Reduction of the nitro group with Fe powder gave the ***o***-phenylenediamine **7** which on further treatment with CS_2 gave the thione **8.** On alkylation with dimethyl sulfate gave Triclabendazole **(1**). Fe is used as a catalyst for reduction which is not environment friendly and involves tedious work-up.

Synthesis of Triclabendazole from N-(4,5-dichloro-2-nitrophenyl)acetamide

Scheme-4 Sequent Scientific Limited synthesized Triclabendazole (US Patent No. US20130303781, 2013-11-14) condensing N-(4,5-dichloro-2-nitrophenyl)acetamide **11** with 2,3- dichlorophenol **13** to obtain 4-chloro-5(2,3-dichlorophenoxy)-2- nitrophenyl acetamide **15** .After hydrolysis of **15** to obtain 4-chloro-5(2,3-dichlorophenoxy)-2-nitroaniline which on reduction with Raney Nickel got the 4-chloro-5-(2,3-dichlorophenoxy)benzene- 1 ,2-diamine **7**.Diamine compound on cyclization with carbon disulfide to obtain 6-chloro-5-(2,3-dichlorophenoxy)-lH- benzimidazole-2-thiol **8.** On methylation of **8** using a dimethyl sulfate to obtain Triclabendazole methanesulfonate salt **16**. Triclabendazole methanesulfonate salt converted to hydrochloride salt of Triclabendazole **17** and on hydrolysis with ammonia obtained Triclabendazole **1.**Sequent described the process for commercial scale but not mentioned the purity of any stage.

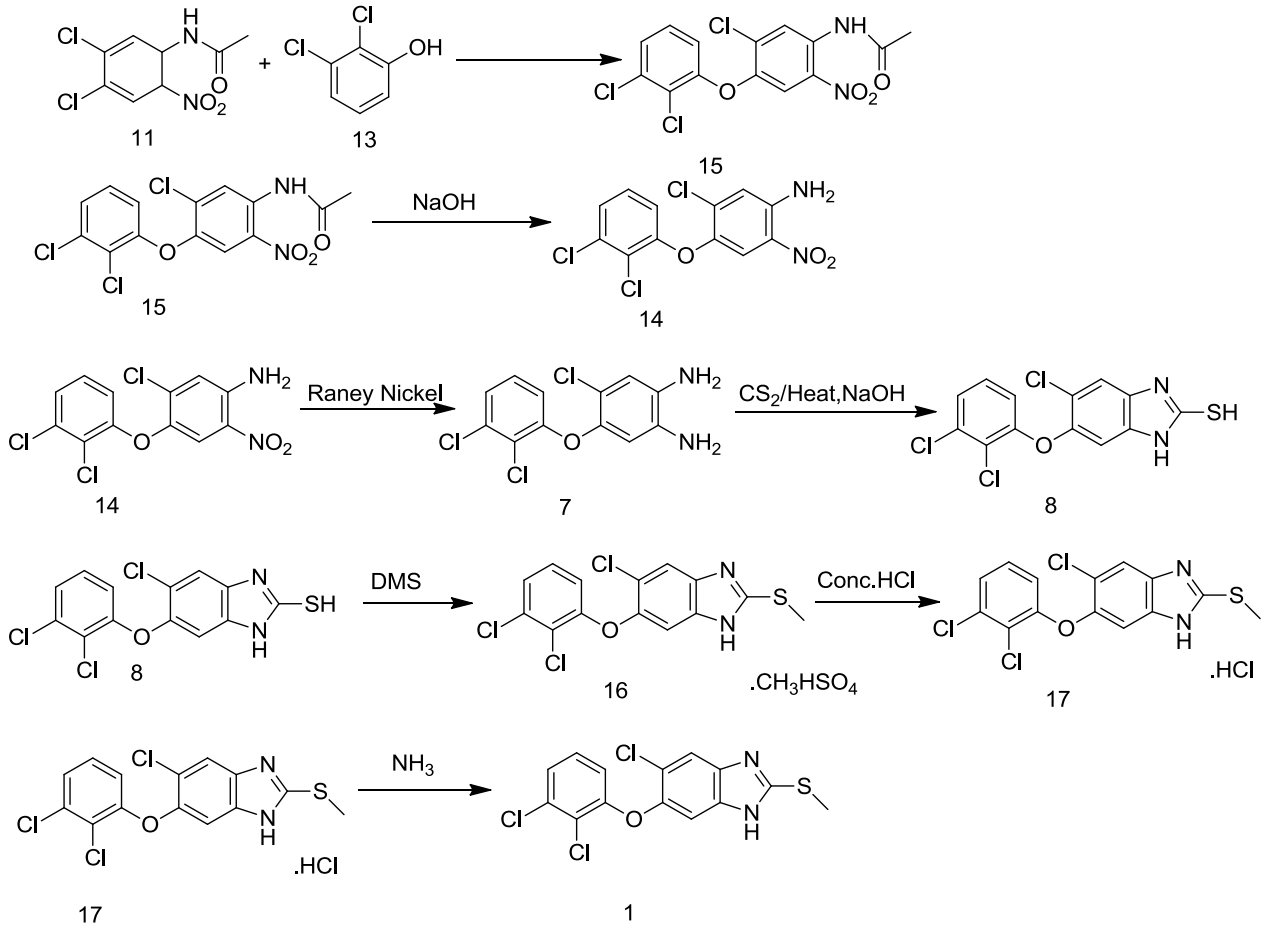

Scheme-4

Synthesis of Triclabendazole from 1,2,3-trichlorobenzene

Scheme-5 CHANGZHOU JIALING MEDICINE INDUSTRY Co Ltd synthesized Triclabendazole (China Patent No. CN103360323 A, 2013-10-23) with 1,2,3-trichlorobenzene as a starting material material. The triclabendazole is generated through three steps by taking the 1,2,3-trichlorobenzene as a starting raw material. The method has the advantage that the inexpensive 1,2,3-trichlorobenzene is used as the starting raw material. The 1,2,3-trichlorobenzene is hydrolyzed in high-concentration alkali liquor to prepare 2,3-dichlorophenol sodium which reacts with 4,5-dichloro-2-nitroaniline in a methylbenzene aqueous solution, and free 2,3-dichlorophenol is not generated again, so that the reaction yield is improved, and pollutions generated during production are avoided. The 4-chloro-5-(2,3-dichlorophenoxy)-2-nitroaniline is reduced by adopting a hydrogen catalytic transfer method, so that a large amount of iron mud which is difficult to treat and pollutes the environment is not generated; and an adopted hydrogen donator is low in price and does not cause any pollution to the environment, so that the triclabendazole is suitable for large-scale industrial production

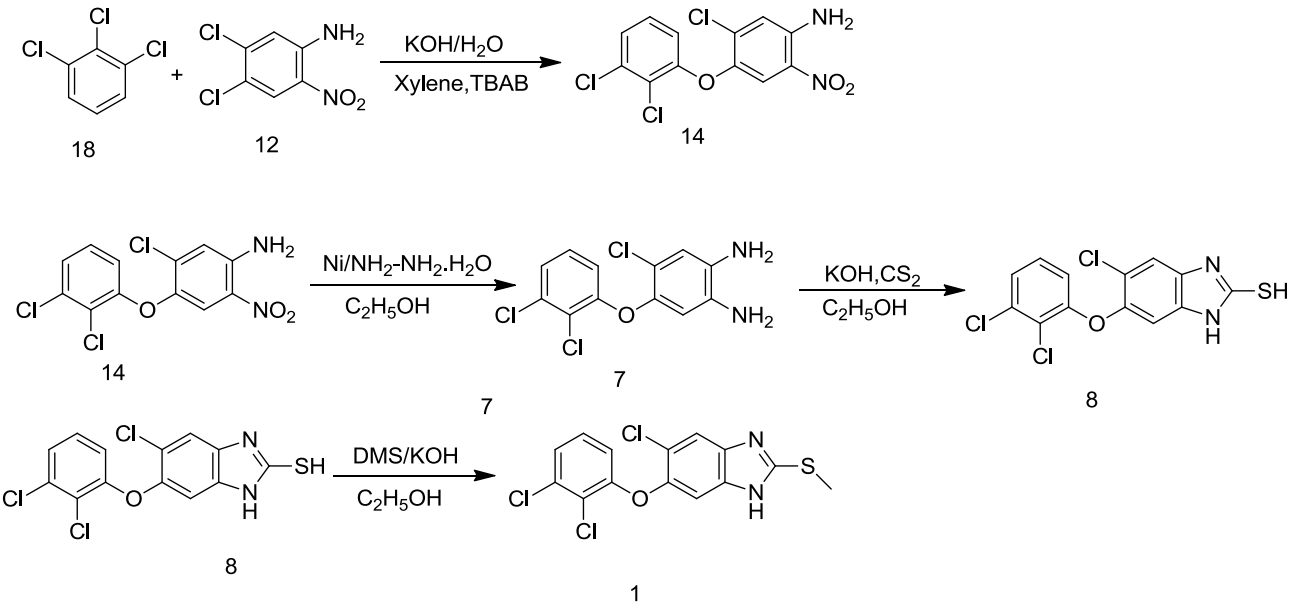

18 12 14 14 7 7 8 8 1

Scheme-5

Hydrazine hydrate is a combustible liquid and corrosive material. It is toxic if swallowed, contacted with skin. It causes severe skin bums and eye damage. It may cause respiratory irritation, allergic skin reactions, cancer. It is reported to be fatal if inhaled.

Synthesis of Triclabendazole by Reduction of 4-chloro-5-(2,3- dichlorophenoxy)-2-nitroaniline using Raney cobalt

Scheme-6 Lasa Laboratories synthesized Triclabendazole (India Patent No. IN2014MU01729 A , 2014-09-12) by the same route mentioned above but they had used Raney Cobalt for the reduction of nitro compound as depicted in the scheme

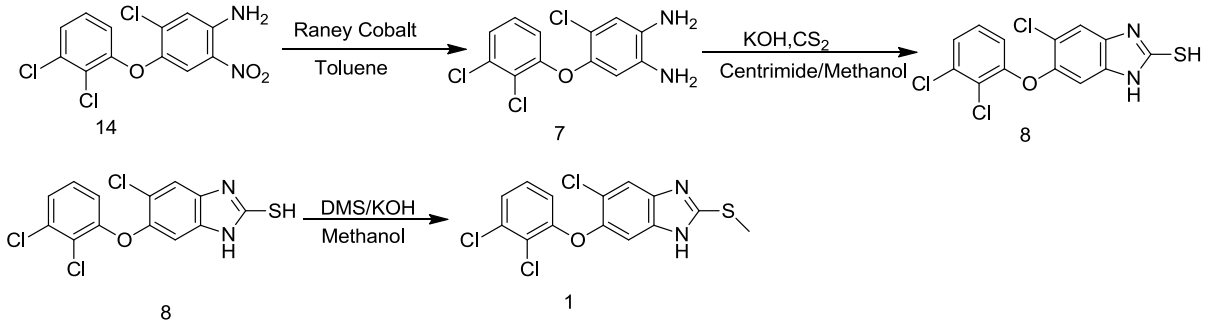

14 7 8 8 1

Scheme-6

Lasa used different types of reducing agents such as $FeCl_3$ and Raney cobalt but the quantity used for the mentioned nitroaniline is too high.

Synthesis of Triclabendazole by using S-methylisothiourea sulfate is used as the methylating agent

Scheme-7 LIANYUNGANG YAHUI PHARMACHEM CO Ltd synthesized Triclabendazole (China Patent No. CN104230815 A , 2014-12-24) from 3,4-dichloroaniline.They used S-methylisothiourea sulfate is used as the methylating agent. Reagents used are not environment friendly as hydrazine hydrate and $FeCl_3$.

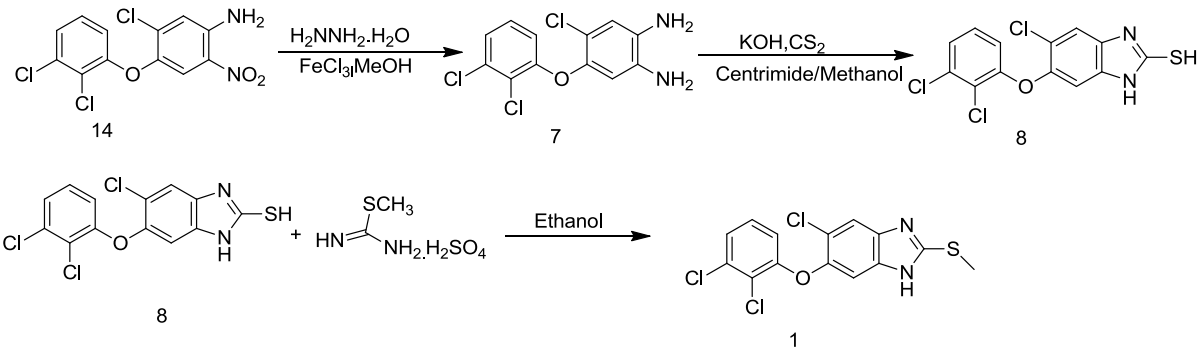

Scheme-7

Synthesis of Triclabendazole by using microwave synthesis for etherification

Scheme-8 Hangzhou Hongqiao Biotechnology Co., Ltd synthesized Triclabendazole (China Patent No. CN106632067 A , 2017-05-10) by reacting dichlorophenol **18** with 4,5-dichloro-2-nitroaniline **12** in the presence of MeOK to give the corresponding aromatic ether **14** in 99% yield. Subsequent nitro reduction through the use of palladium supported on activated carbon with the hydrogen source sodium borohydride in toluene furnished aromatic Phenylenediamine **7**. Cyclization between **7** and carbon disulfide afforded intermediate **8** in 88% yield, followed by methylation with iodomethane furnished Triclabendazole **1** in the yield of 94%.

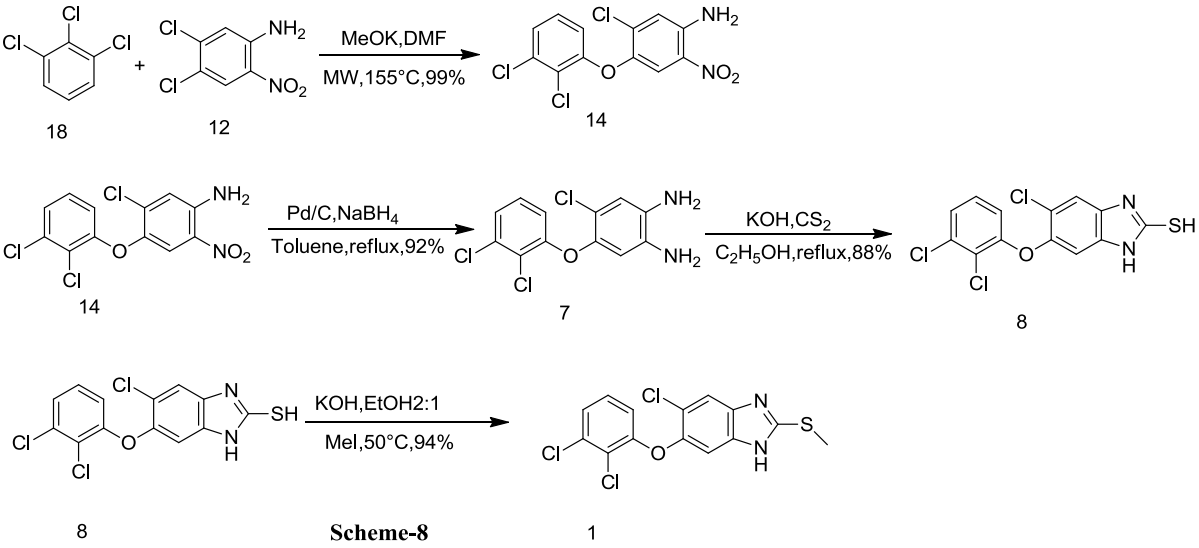

Scheme-8

Besides it has mentioned better yield but at large scale microwave reactions have limitations.

Synthesis of Triclabendazole by using dimethyl carbonate as the methylating agent

Scheme-9 Agno Pharma Tech (Suzhou) synthesized Triclabendazole (China Patent No. CN109053585 A, 2018-12-21), from trichlorophenol and used cheap and inexpensive trichlorosilane as reducing agent for the reduction of nitroanilne.Further, they carried out methylation with dimethyl carbonate and as DBU catalyst. Methylation reaction requires 18 hrs for completion as it leads to non-economical process at large-scale productions.

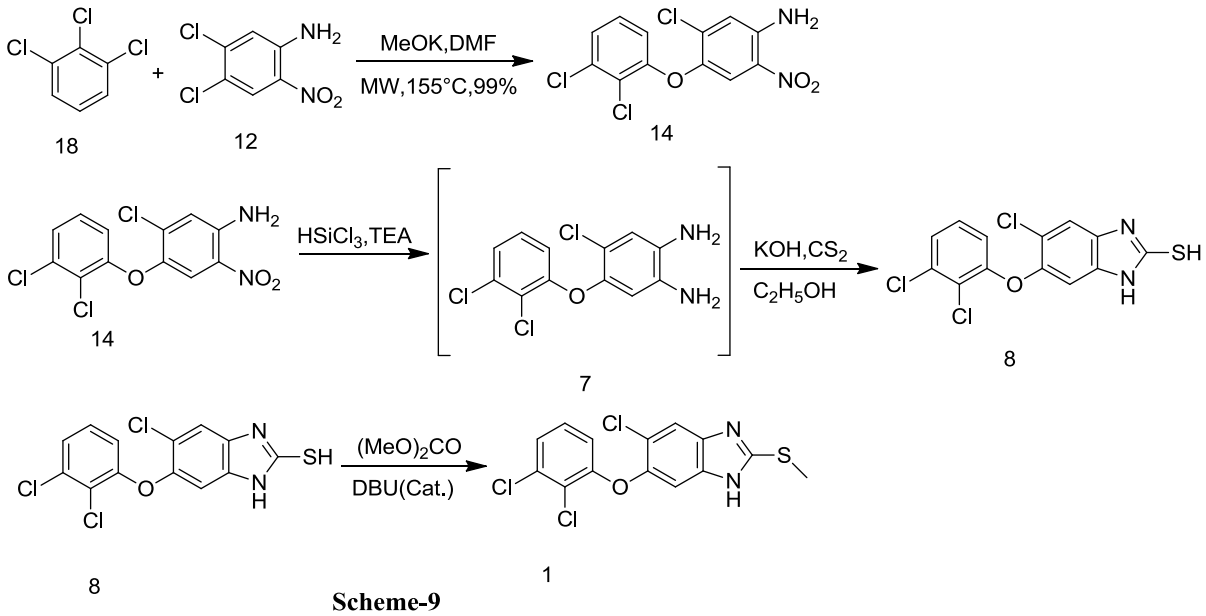

18 12 14 14 7 8 8 1

Scheme-9

Synthesis of Triclabendazole by Reduction of Nitro aniline with NaSH

Scheme-10 RP Industries synthesized Triclabendazole (India Patent No. IN202221021788 A , 2023-10-13) treating compound **14** with sodium hydrosulphide in the presence of alcoholic solvent, and *insitu* reaction with carbon disulphide in the presence of sodium hydroxide to obtain Triclabendazole **1**

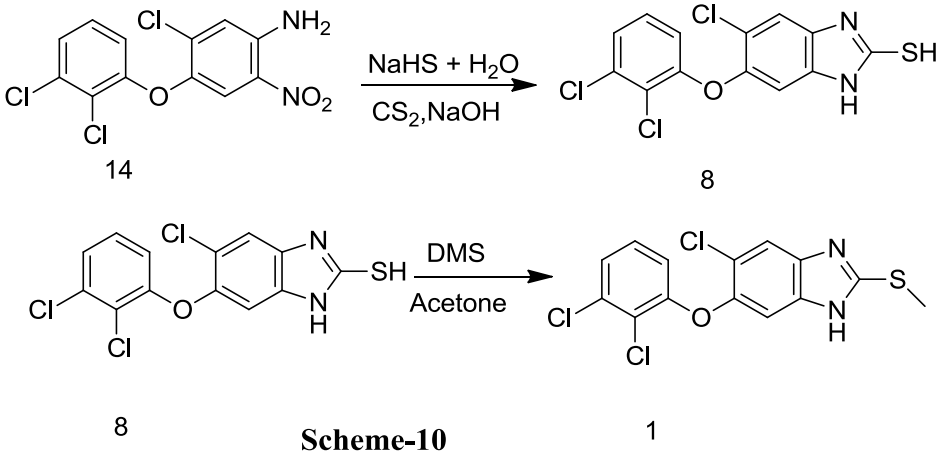

14 8 8 1

Scheme-10

Synthesis of Triclabendazole by using High boiling solvent for Nitration of 3.4- Dichloro acetanilide

Scheme-11 Azico Biophore synthesized Triclabendazole (INDIA Patent No. IN202141005800 A, 2022-08-12) used high boiling solvents during nitration of **10**,Compound **10** condensed with 2,3-dichlorophenol **13** followed by hydrolysis to obtain 4-chloro-5-(2,3-dichlorophenoxy)-2-nitroaniline **14**. .Reduction of 4-chloro-5-(2,3-dichlorophenoxy)-2-nitroaniline **14** in presence of reducing agent Raney Nickel to 4-chloro-5-(2,3-dichlorophenoxy)benzene-l,2-diamine. It cyclized in presence of carbon disulfide (CS**2**) in situ to obtain 6-chloro-5-(2,3-dichlorophenoxy)- lH-benzimidazole-2-thiol **8**

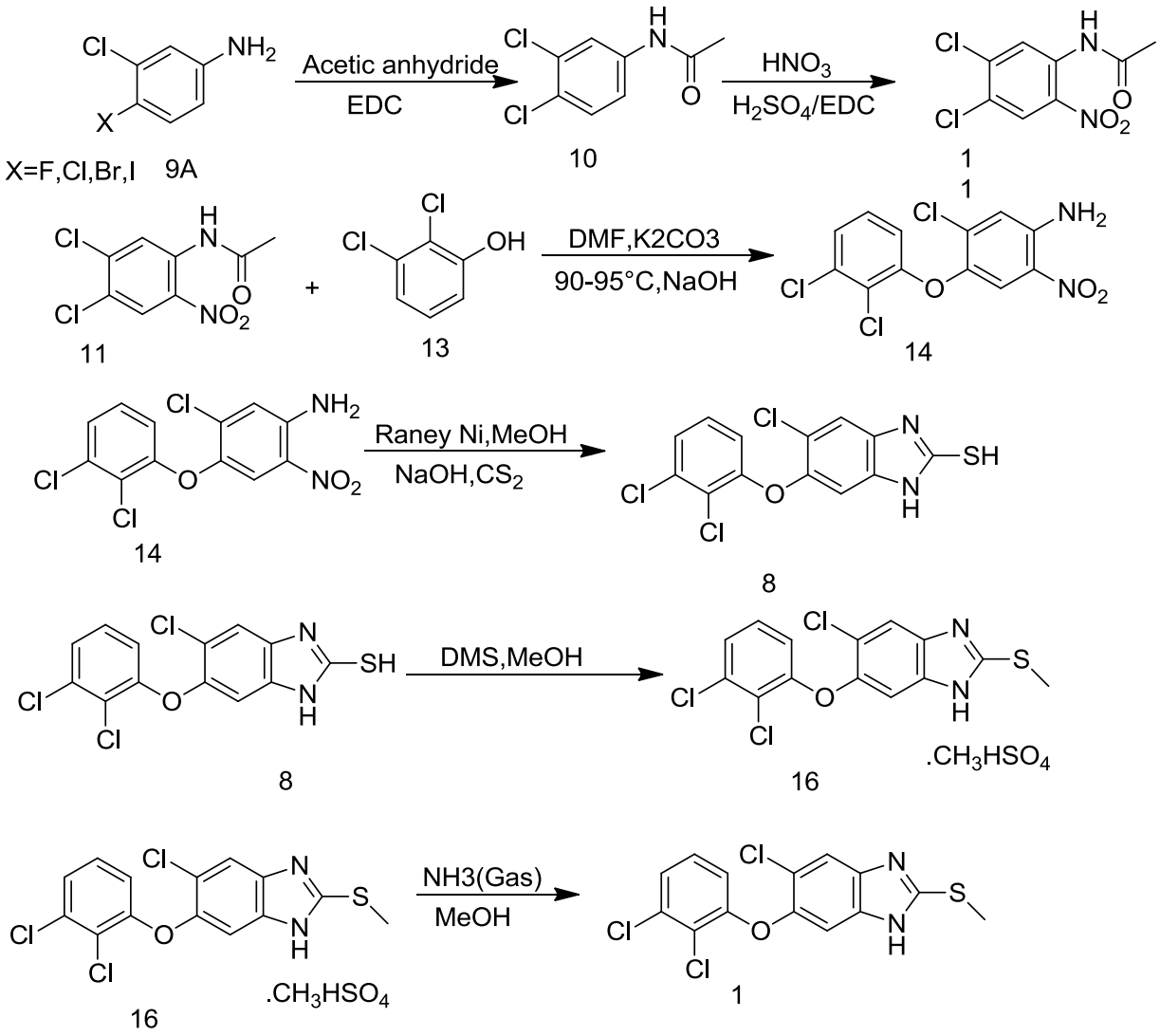

Scheme-11

Azico Biophore used ethylene dichloride (EDC) as a solvent which is class 1 solvent- Substances to be avoided i.e., known human carcinogens, strongly i.e., known human carcinogens, strongly suspected human (genotoxic) as per ICH:Q3C

Conclusion

The demand for increasingly clean and efficient chemical synthesis is important for both the economic and environmental points of view. Current synthesis methods of Triclabendazole, used in industries, suffer from several industrial inconveniences, including low yield, efficiency, high raw material cost, and environmental impact. More attempts to find green and economical synthetic methods are necessary. This review summarizes the most common synthetic routes as applied to the preparation of Triclabendazole. The review will help the scientific community to encounter various ideas and develop new and improved synthesis techniques of Triclabendazole by reviewing the literature methods.

Acknowledgements

I would like to express my gratitude to the individuals for their invaluable support in completing this research project.

Conflict of Interest

The authors declare no conflict of interest.

References

[1]. Agno Pharma Tech (Suzhou) Co., L. (2018-12-21). China Patent No. CN109053585 A.
[2]. Anerao, A. P. (2017). DETERMINATION OF RESIDUAL METHYL IODIDE IN TEDIZOLID PHOSPHATE AND ALOGLIPTIN BENZOATE BY STATIC HEADSPACE GAS CHROMATOGRAPHY WITH ELECTRON CAPTURE DETECTION. Indian Drugs, 54(11).
[3]. Changzhou Jialing Medicine Industry Co., L. (2013-10-23). China Patent No. CN103360323 A.
[4]. Corp, C. G. (1980-04-08). US Patent No. US4197307A.
[5]. Hangzhou Hongqiao Biotechnology Co., L. (2017-05-10). China Patent No. CN106632067 A .
[6]. Iddon, B. K. (1992). 2H-benzimidazoles (isobenzimidazoles). Part 7. A new route to triclabendazole [5-chloro-6-(2, 3-dichlorophenoxy)-2-methylthio-1H-benzimidazole] and congeneric benzimidazoles. Journal of the Chemical Society, Perkin Transactions 1, (22), 3129-3134.
[7]. Industries, R. P. (2023-10-13). India Patent No. IN202221021788 A.
[8]. Industries, R. P. (2023-10-13). India Patent No. IN202221021788 A .
[9]. Lianyungang City Yahui Pharmaceutical Chemical Co., L. (2014-12-24). China Patent No. CN104230815 A .
[10]. Limited, A. B. (2022-08-12). INDIA Patent No. IN202141005800 A.
[11]. Limited, S. S. (2013-11-14). US Patent No. US20130303781.
[12]. Ltd., L. L. (2014-09-12). India Patent No. IN2014MU01729 A .
[13]. Marcos, L. M. (2020). Triclabendazole for the treatment of human fascioliasis and the threat of treatment failures. Expert Review of Anti-Infective Therapy, 19(7), 817–823.
[14]. Suzhou Guide Fine Material Co., L. (2018-05-15). China Patent No. CN108033915 A .
[15]. Wuhan Jiuzhou Yumin Pharmaceutical Technology Co., L. (2020-04-28). China Patent No. CN111072570 A .
[16]. Yangzhou Tianhe Pharmaceutical Co., L. (2009-10-14). China Patent No. CN101555231 A .

International Journal of Scientific Research in Science and Technology
Available online at : www.ijsrst.com
OPEN ACCESS
Print ISSN: 2395-6011 | Online ISSN: 2395-602X
doi : https://doi.org/10.32628/IJSRST

One Pot Solvent Free Synthesis of Pyrazole Derivatives Using Novel Lewis Acid Catalyst L-Prolein-H_2SO_4 (1:1)

A. A. Kharpe[1], S. N. Mokale[2], Prashant D. Netankar[1*]

[1*]Department of Chemistry, Maulana Azad College of Arts Science and Commerce, Chhatrapati Sambhajinagar-431 003, Maharashtra, India

[2]Department of Pharmaceutical Chemistry, Y. B. Chavan College of Pharmacy, Chhatrapati Sambhajinagar-431 003, Maharashtra, India

ARTICLEINFO

Article History :

Published : 07 Dec 2024

Publication Issue :
Volume 11, Issue 23
Nov-Dec-2024
Page Number :
17-21

ABSTRACT

Solvent-free synthesis has received a lot of attention recently and is now an important aspect of research, particularly in green synthesis. The present research trend is to develop and construct novel catalysts for synthesis. L-prolein-H2SO4 is a little investigated catalyst. L-prolein-H2SO4 is a good catalyst for the synthesis of substituted pyrazoles. This is the first report of combining L-prolein and H2SO4 in a solvent-free process to produce pyrazole derivatives. The fundamental advantage of this process is the use of L-prolein-H2SO4 as a catalyst, which reduces reaction time, increases atom economy, and simplifies the work-up method.

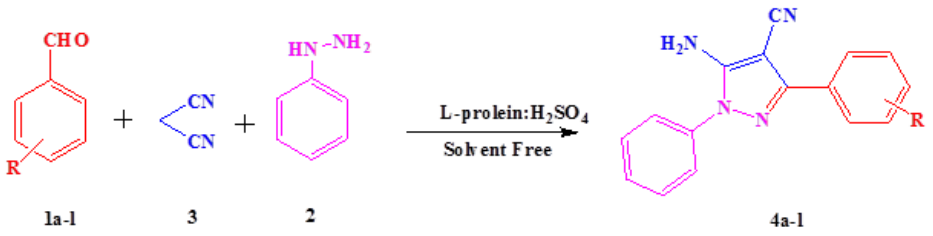

Keywords: L-prolein-H2SO4 (1:1) , Pyrazole, Green synthesis, Solvent Free, Atom economy

Introduction

Heterocyclic chemistry is a critical area of study in Pharmaceutical and Organic Chemistry. Nitrogen-containing compounds are particularly useful among the different heterocyclic molecules discovered and produced due to their diverse biological functions. Pyrazole is a well known heterocycles, privileged in medicinal chemistry owing to various biological activities such as antidepressant,[6] anticancer,[3] anti-HIV [7]antifungal,[4] anti- antioxidant,[4-5,] antibacterial,[1-2]

Pyrazole synthesis is reported[8-18] using various reagents such as {[HMIM]C(NO_2)$_3$},[8] CuO/ZrO_2,[9] Sc(OTf)$_3$,[10] Ti(NMe_2)$_2$(PyPyr)$_2$,[11] [BMIM]OH,[12] ZrO_2 nanoparticles [13] and Fe_3O_4.Si.MoO_2.[14] Pyrazole synthesis mainly reported by three component coupling of aromatic aldehydes, malononitrile and phenylhydrazine under various reaction conditions.[15-18] However, reported pyrazole synthesis has various limitations, including long reaction durations, the necessity for an expensive catalyst, and painstaking work-up. As a result, there is a need for improved and more generic methods for synthesizing these critical scaffolds. However, these procedures require a variety of solvents, are frequently time demanding, require expensive reagents, use non-eco-friendly reaction conditions, necessitate an increased reaction temperature, and require a time-consuming work-up procedure.

The product yields from most of these reactions are significant, but there is still room for improvement. Researchers are focused on establishing an environmentally friendly reaction technique that is high yield, cost effective, and time efficient. For these reasons, we chose to synthesize pyrazole heterocycles under environmentally benign conditions. Solvent-free synthesis is becoming increasingly important, particularly in green synthesis. Due to the negative impacts of organic solvents on the environment and individuals, solvent-free reactions have gained a lot of attention in research. Furthermore, solvent-free processes have various advantages over solvent-based reactions, including a faster reaction rate, shorter reaction time, lower energy requirements, simpler separation, the creation of a product with fewer impurities, and higher yields. Establishing a new catalyst in synthesis is also the current trend of research in pharmaceutical industries and academics. L-prolein-H_2SO_4 is one of such rarely explored catalyst.

Considering the above requirement we decided to explore L-prolein-H_2SO_4 as a catalyst. L-prolein-H_2SO_4 has several advantages for organic transformations; it is convenient, economic environment friendly and ease of handling. As part of our ongoing efforts to achieve new routes for the synthesis of heterocyclic compounds, herein we report a one-pot Multicomponent synthesis of highly functionalized pyrazole derivatives by condensing malononitrile, aryl aldehyde and phenyl hydrazine in the presence of catalytic amounts of L-prolein-H_2SO_4 as a proficient and viable catalyst (**Scheme I**).

Results and Discussion

Initially, a mixture of benzaldehyde, malononitrile and phenyl hydrazine in ethanol in the presence of catalytic amount of L-prolein-H_2SO_4 (Table I, Entry 1) obtain the corresponding pyrazole derivative. The product was obtained in good yield (88%). Solvent optimization studies of the above reaction were carried out and are summarized in Table I, The effect of different solvents on reaction rate as well as yields of products was investigated and the results are summarized in Table I. It was observed the reaction proceeded excellently in solvent free condition (Table I, Entry 5). It was further observed that reaction proceeds very well at ambient temperature (30 °C) and does not require elevated temperatures.

Catalyst optimization studies of the above reaction were carried out and are summarized in Table II. When catalyst was used from 5 to 10 mol% both yield and rate of the reaction was increased (Table II, Entries 1, 2). However, further increment of catalyst amount (above 10 mol %) does not affect the yield and rate of the reaction (Table II, Entries 3,4,5). Finally, among all the experimental variations the 10 mol% L-prolein-H_2SO_4 solvent free condition at ambient temperature gave the best results with 95% yield (Table II, Entry 2).To check the generality and scope of the optimized reaction, the methodology was evaluated by employing different aromatic aldehyde, phenyl hydrazine and malononitrile. The resultant corresponding functionalized pyrazole (**4a-l**) were obtained in good to excellent yields (Table III).

Table I: - Solvent Optimization for one-pot synthesis of Pyrazole[a]

Sr. No.	L-prolein-H_2SO_4 Catalyst mole %	Solvent	Time(Min)	Yield (%)[b]
1	10	Water	20	75
2	10	Ethanol:Water(50%)	35	81
3	10	Methanol	20	85
4	10	Ethanol	25	88
5	10	Solvent free	15	96

a) Experimental conditions: Benzaldehyde (1 mmol), Phenyl hydrazine (1 mmol), Malononitrile (1 mmol), ambient temperature (30 °C).

b) Isolated yield

Table II: - Catalyst Optimization for one-pot synthesis of Pyrazole[a]

Sr. No.	L-prolein-H_2SO_4 Catalyst mole %	Time(min)	Yield (%)[b]
1	5	30	75
2	10	15	96
3	15	15	96
4	20	15	96
5	25	15	96

a) Experimental conditions: Benzaldehyde (1 mmol), Phenyl hydrazine (1 mmol), Malononitrile (1 mmol), ambient temperature (30 °C).

b) Isolated yield.

Table III: - Synthesis of functionalized pyrazoles (1-12) with different aryl aldehydes, malonitrile and phenyl hydrazine[a]

Sr.No.	Aldehyde	Time (min)	Yield (%)[b]	Melting point (°C)	Reported Melting point (°C)
4a	*Benzaldehyde*	15	96	159-160	160-161[19]
4b	*3-Nitro benzaldehyde*	30	92	128-130	129-130[19]
4c	*4-Cholro benzaldehyde*	30	85	128-130	129-130[20]
4d	*4-Nitro benzaldehyde*	20	91	163-164	164-165[20]
4e	*4-Pyridinecarboxaldehyde*	15	89	219-220	218-220[14]
4f	*1-naphthaldehyde*	15	86	163-164	163-165[11]
4g	*2,3,4,5,6- pentafluoro benzaldehyde*	20	90	159-160	158-160[14]
4h	*5-fluoro-2-hydroxybenzaldehyde*	24	87	161-162	161-163[14]
4i	*pyrrole-2-carbaldehyde*	20	85	260-262	260-262[14]
4j	*4-Methoxybenzaldehyde*	15	88	112-113	112-114[21]
4k	*Thiophene-2-carbaldehyde*	25	82	163-165	163-165[14]
4l	*Furan-2-carbaldehyde*	20	81	168-170	168-170[14]

a) Experimental conditions: Arylaldehyde (1 mmol), Phenyl hydrazine (1 mmol), Malononitrile (1 mmol), ambient temperature (30 °C).

b) Isolated yield.

Experimental Section

All the chemicals were purchased from Sigma Aldrich and used as received without further purification. All the melting points were determined on Labstar melting point apparatus and are uncorrected. The IR spectra were run on a Perkin-Elmer FTIR-1600 Spectrophotometer and the data expressed in cm (KBr). The ^{1}H NMR (400.13) and ^{13}C NMR (100.62 MHz) were recorded on a Bruker spectrometer (δ in ppm). Mass spectra were recorded on a Agilent spectrometer. The synthesized compounds were analyzed, matched and confirmed with literature data for Melting point, IR, ^{1}H NMR, ^{13}C NMR and Mass spectrometry.

General procedure for the preparation of pyrazole derivatives (4a-l)

A mixture of malononitrile (1 mmol), aldehyde (1 mmol), phenyl hydrazine (1 mmol) and L-prolein-H_2SO_4 (10 mol%) was treated at 30°C till the completion of reaction, monitored by TLC. After completion of the reaction, as monitored by TLC *n*-hexane/ethyl acetate (5:3), ethyl acetate (5 ml) and water (2ml) was added to reaction mixture, stirred for 5 min, separate the organic layer and distilled to get residue. The obtained crude product was purified by column chromatography over silica gel (EtOAc/*n*-hexane) to give pure functionalized pyrazole product (Table III).

Spectral data analysis of compound

***5-Amino-1, 3-diphenyl-1H-pyrazole-4-carbonitrile* (4a):**

Yellow solid; M.P: 159-160°C; Yield: 96%;

IR spectra: (KBr) [cm^{-1}]: 3492 , 3351 (NH_2), 2360 (C≡N), 1615 (C=N);

^{1}H-NMR: (400 MHz, DMSO-d6): δ(ppm)=6.75-7.88 (m, 10H, Ar-H), 10.19 (s, H, NH_2);

^{13}C-NMR interpretation: (100 MHz, DMSO-d6): δ(ppm)=112.48 (C-CN), 119.17 (CN), 126.10-136.35 (C=C, ArC), 145.75 (C=N).

TOF-MS Calcd $C_{16}H_{12}N_4$ $[M+1]^+$: m/z = 261.06, Found: 261.12 .

Conclusion

In summary, an efficient solvent mild protocol for the synthesis highly functionalized pyrazole derivatives using L-prolein-H_2SO_4 as a catalyst has been demonstrated. This protocol is first report of solvent free L-prolein-H_2SO_4 catalysed pyrazole synthesis. This protocol offers several significant advantages including operational simplicity, superior atom-economy, short reaction time and good to excellent yields.

Acknowledgement

The authors are thankful to the Head, Department of Chemistry, Maulana Azad College, Dr. Babasaheb Ambedkar Marathwada University, Aurangabad-431 004, India for allowing the work.

References

[1]. Bailey, D.; Hansen, P.; Hlavac, A.; Baizman, E.; Pearl, J.; Defelice, A.; Feigenson, M. J. Med. Chem., 1985, 28, 256-260.

[2]. El-Deeb, I. ; Lee, S.; Bioorg. Med. Chem. 2010, 18, 3961-3973.

[3]. Kim, J.; Lee, D.; Park, C.; So, W.; Jo, M.; Ok, T.; Kwon, J.; Kong, S.; Jo, S.; Kim, Y.; Choi, J.; Kim, H.; Ko, Y.; Choi, I.; Park, Y.; Yoon, J.; Ju, M.; Kim, J.; Han S.; Kim, T.; Cechetto, J.; Nam, J.; Sommer, P.; Liuzzi, M.; Lee, J.; No, Z. ACS Med. Chem. Lett., 2012, 3, 678-682.
[4]. Nagamallu, R.; Kariyappa, A.; Bioorg. Med. Chem. Lett. 2013, 23, 6406-6409.
[5]. Kalaria, P.; Satasia, S.; Raval, D. New J. Chem., 2014, 38, 2902-2910.
[6]. Fustero, S.; Sánchez-Roselló, M.; Barrio, P.; Simón-Fuentes, A. Chem. Rev. 2011, 111, 6984–7034.
[7]. Ansari, A.; Ali, A.; Asif, M. New J. Chem. 2017, 41, 16–41.
[8]. Zolfigol, M.; Afsharnadery, F.; Salehzadeh, S.; Maleki, F. RSC Adv., 2015, 5, 75555-75568.
[9]. Maddila, S.; Rana, S.; Pagadala, R.; Kankala S.; Maddila, S.; Jonnalagadda, S. Catal. Commun., 2015, 61, 26-40.
[10]. Kumari, K.; Raghuvanshi, D.; Singh, K. Tetrahedron Lett., 2012, 53, 1130-1133.
[11]. Dissanayake, A.; Odom, A. Chem. Commun., 2012, 48, 440-442.
[12]. Srivastava, M.; Rai, P.; Singh, J.; Singh, J. RSC Adv., 2013, 3, 16994-16998.
[13]. Saha, A.; Payra, S.; Banerjee, S. Green Chem., 2015, 17, 2859-2866.
[14]. Rakhtshah, J.; Salehzadeh, S.; Gowdini, E.; Maleki, F.; Baghery, S.; Zolfigol, M. RSC Advances, 2015, 00, 1-3.
[15]. Salaheldin, A.; Oliveira-Campos, A.; Rodrigues, L. Tetrahedron Lett., 2007, 48, 8819-8822.
[16]. Varvounis, G.; Fiamegos, Y.; Pilidis, G. Adv. Heterocycl. Chem., 2007, 95, 27-141.
[17]. Martin, R.; Rivero, M.; Buchwald, S. Angew. Chem. Int. Ed. Engl., 2006, 45, 7079-7082.
[18]. Polshettiwar, V.; Varma, R. Green Chem., 2010, 12, 743-754
[19]. Joshi, S.; Kumar, M.; Chhoker, S.; Srivastava, G.; Jewariya, M.; Singh, V. J. Mol. Struct., 2014, 1076, 55-62.
[20]. Dabholkar, V.; Kurade S.; Badhe, K.; Karthik, K.; Anpat, S. Der Pharma Chemica, 2018, 10, 62-67.
[21]. Maddila, S.; Rana, S.; Pagadala, R.; Kankala, S.; Maddila, S.; Jonnalagadda, S. Catal. Commun., 2015, 61, 26-32.

International Journal of Scientific Research in Science and Technology
Available online at : www.ijsrst.com
OPEN ACCESS
Print ISSN: 2395-6011 | Online ISSN: 2395-602X
doi : https://doi.org/10.32628/IJSRST

Synthesis and Optical Analysis of Green Emitting Long Lasting Phosphor $SrAl_2O_4:Eu^{2+}$

Akash M. Shejul[1], Dr. C. S. Ulhe[2], Dr. Gaurav Rahate[3]

[1]Research Student of Yashwantrao Chavan Arts and Science Mahavidyalaya Mangrulpir, Maharashtra, India
[2]Yashwantrao Chavan Arts and Science Mahavidyalaya Mangrulpir, Maharashtra, India
[3]Smt. Sindhutai Jadhao Arts and Science Mahavidyalaya Mehkar, Maharashtra, India

ARTICLEINFO

Article History :

Published : 07 Dec 2024

Publication Issue :
Volume 11, Issue 23
Nov-Dec-2024
Page Number :
22-25

ABSTRACT

In this paper, SrAl2O4:Eu2+ (europium doped strontium aluminate) phosphors were synthesized using a combustion synthesis method with urea as a fuel at 400°C - 600°C. The crystal structure, particle size, color emitted and elemental analysis were studied using X-ray diffractometry (XRD), CIE and Fourier transform infrared (FTIR) spectra. The FTIR spectra confirm the elements present in the SrAl2O4:Eu2+ phosphor. A broad emission band can be seen in the emission spectrum of the Eu2+ doped SrAl2O4 sample. A peak around 500 nm is associated with the 4f65d1–4f7 transition. The optical properties of SrAl2O4:Eu2+ phosphors were investigated by photoluminescence (PL). The excitation and emission spectra showed a wavelength peaks at 337 and 515 nm, respectively. The CIE color chromaticity confirm that the SrAl2O4:Eu2+ phosphor emitted green colored light. Europioum-doped strontium aluminate are used as indicators, as they emit light when exposed by light. They also useful for fabricating mechano-optical nanodevices.

Keywords: Photoluminescence , XRD, CIE, FTIR

Introduction

The phosphor material with general formula MAl2O4:Eu2+ (M: Ca, Sr, Ba) doped with Eu2+ ion emits blue green light in visible region. Eu2+, Dy3+, Er3+, Tb3+, and Nd3+ are some of the activatorsused.This study demonstrates the synthesis of Eu doped SrAl2O4phosphor using the combustio n method. This research is important in terms of providing the synthesis method for SrAl2O4 phosphor materials and investigating the effect of adding rare earth elements (Eu2+)on the structure and op tical properties of SrAl2O4.The desired luminescence property can be obtained by agents. Sr and Ca based aluminates phosphor are safe, stable in chemical composition very much bright and long lasting photo luminescence.

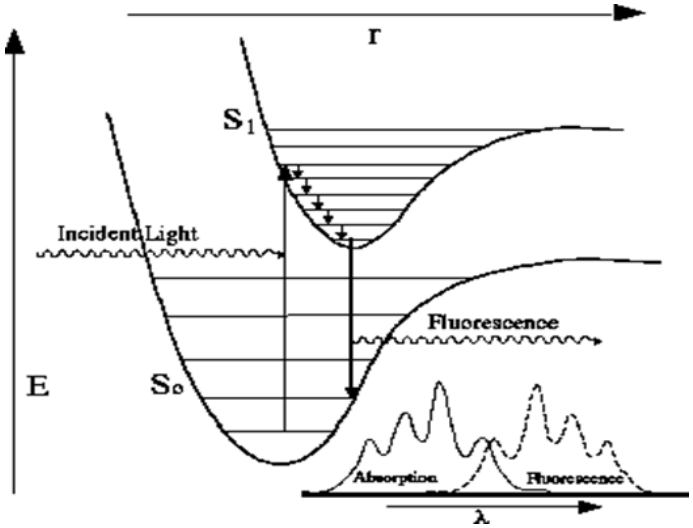

Above figure shows how the absorption of light and emission of light takes place by using the energy levels.
Luminescence have unique properties particularly applied in light emitting device like LED, plasma display panels, fluorescent lamp, luminous paint, ceramics product and textiles.
Luminescence materials are synthesis by doping rare earth ions into the host (MAl2O4).
The SrAl2O4:Eu2+ phosphor is one of the glow phosphor. Eu2+ playing the important role and resulting the long persistent phosphorescence. In the luminescence the discovery of new phosphor their design of crystal structure and the optimization are the hot spots of research. In the present work, an attempt to synthesize SrAl2O4:Eu2+ phosphor by combustion technique with slight modifications has been made. The samples have been characterized for structural and luminescent properties.

Methodology and Materials

SrAl2O4:Eu2+ is prepared via combustion synthesis method produced good luminescence in blue green visible region. There are various method to synthesis phosphor doped with rare earth ions such as solid state reaction, combustion reaction, sol gel synthesis etc.
combustion synthesis method offered several attractive advantages like simplicity in experimental setup, short time in between formation of reactant and final product.
Stoichiometric amount of Sr(NO3)2 , Al(NO3)3·9H2O, Eu2O3 and urea ((NH2)2CO) were prepared to synthesise SrAl2O4:Eu2+ phosphor. Nitric acid (HNO3) was added to Eu2O3 to form Eu(NO3)3. The conversion of the rare earth compound into nitrate form. Then Eu(NO3)3 was mixed with Sr(NO3)2, Al(NO3)3·9H2O, and (NH2)2CO. Next, the solution was stirred for 1.5 h at 200 rpm and 65 °C using a magnetic stirrer. After that, the solution was transferred into an alumina melting pot, placed in a preheated furnace, and maintained at 500-600°C. For calcination, the sample was heated at 1100 °C for 1.5 h.

Sample Characterisation

The XRD, FTIR and UV characteristics of sample is done at CIC centre of Shri Shivaji Science College Amravati. The crystal structure, particle size and elemental analysis were studied using X-ray diffractometry (XRD) and Fourier transform infrared (FTIR) spectra. X ray diffraction is shown below fig.

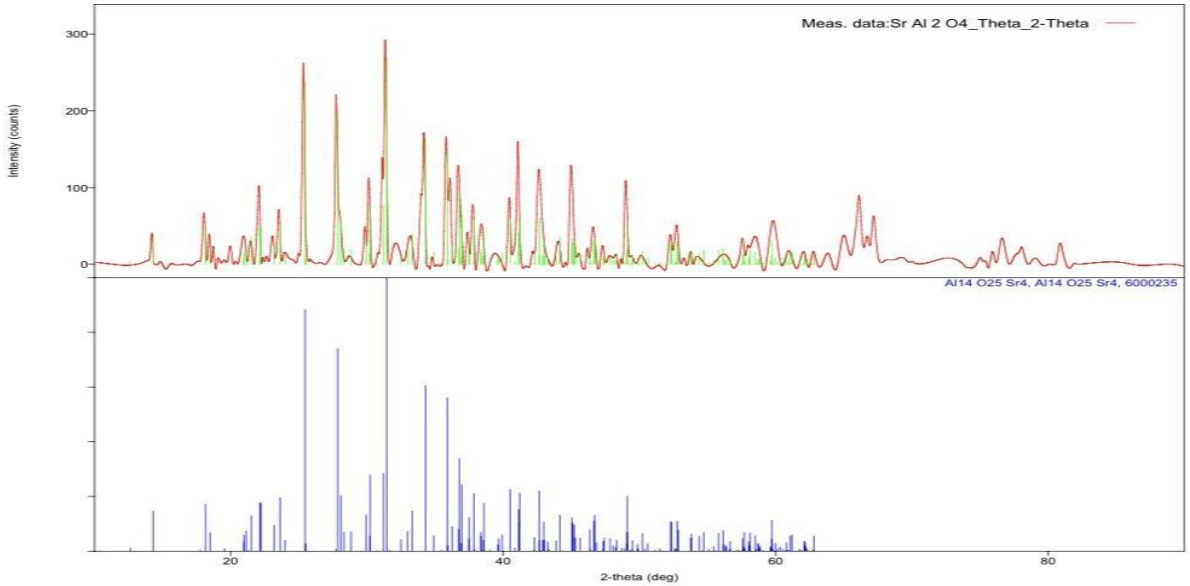

Fig. XRD of SrAl2O4:Eu2+

The FTIR spectra confirm the elements present in the SrAl2O4:Eu2+ phosphor. The FTIR analysis resulte of SrAl2O4:Eu2+ are shown in fig. This peak may be caused by nitrate present in the starting material. The broad spectrum observed at 3449 cm-1 is due to O-H stretching vibration of free and hydrogen bonded hydroxyl groups. The existence of this broad band is due to the humidity in air. the that appears later in the 2573 cm-1 region is due to C-O vibrations. There is weak band at 2273 cm-1 due to vibration balance of the N-O group that can be formed by nitrates in the materials. Another peak observed at 664 cm-1 is due to the stretching of Sr-O vibrations. In addition The O-Al-O symmetric bond was observed at 494cm-1.

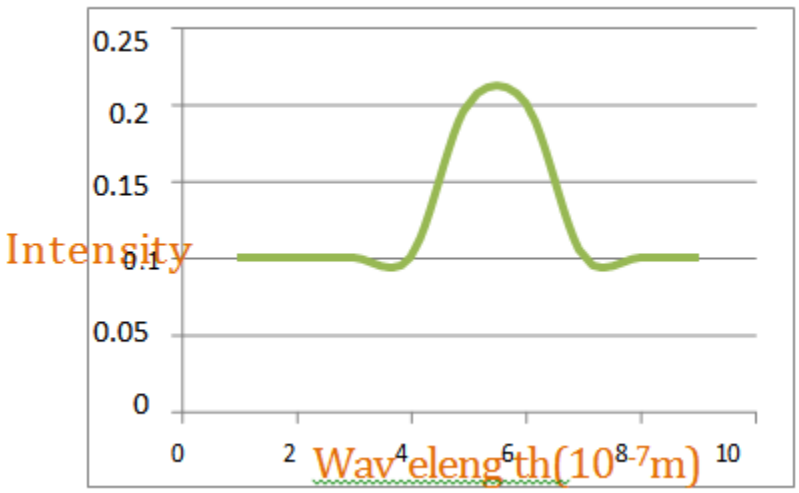

fig. UV spectra of SrAl2O4:Eu2+

Above fig. shows the fluorescence emission spectrum of the sample excited by 337 nm UV light when the doping Eu2+ on the combustion temperature of 800 - 1000°C. it can be visible that the emission period is among 400 nm and 650 nm, and most emission peak is at 515 nm. It is essentially constant with the spectroscopic study of SrAl2O4:Eu2+ single crystal.

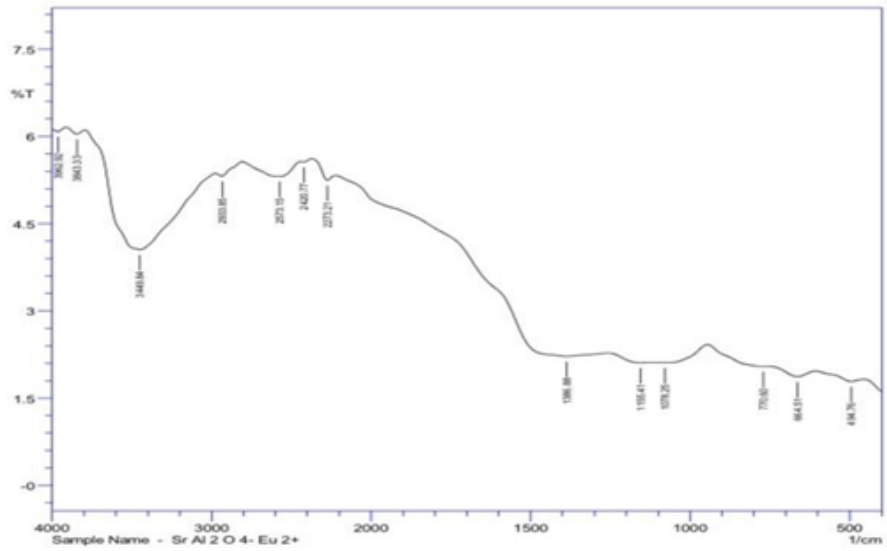

Fig. FTIR of SrAl2O4 :Eu2+

Conclusion

Uncommon earth ions (Eu) doped strontium aluminate nanophosphors had been prepared by means of the combustion of respective nitrates along side urea at~600oC. The aqueous mixture containing-stoichiometric quantity of redox mixture when heated unexpectedly at~600oC boils and undergoes dehydration observed by means of decomposition producing combustible gases inclusive of oxides of nitrogen, HNCO and NH3. The risky combustible gases ignite and burn with a flame and for that reason offer conditions for formation of phosphor lattice with dopants The combustion method for the practise of uncommon-earth doped nanocrystalline SrAl2O4 phosphor satisfies all of the crucial requirements of an extended persistence phosphor. The formation of homogeneous single phase of monoclinic SrAl2O4 is confirmed by means of XRD analysis.

References

[1]. G.R.Rahate, K.V.Sharma , Aprna Dixit3 , V.R.Panse , D.B. Zade, N.Sing Luminescence investigation of Ca12Al14O32F2:RE3+ (RE=Eu) red emitting phosphors for lamp industry application(2022).

[2]. G.R.Rahate, K.V.Sharma , Aprna Dixit3 , V.R.Panse , D.B. Zade, N.Sing, Ca2Pb3(PO4)3Cl:Eu3+ Red emitting phosphor for eco-friendly lighting applications; YMER 2021

[3]. C. B. Palan, N. S. Bajaj, S. K. Omanwar, V. R. Panse, A Dixit, K. Khanna YMER20 (2021)1791

[4]. V. R. Panse, N. S. Kokode, K. N. Shinde, and S. J. Dhoble, "Luminescence in microcrystalline green emitting Li2Mg1–xZrO4:xTb3+ (0.1 ≤ x ≤ 2.0) phosphor," 2017.10.025.

[5]. L. Y. Zhou, J. S. Wei, J. X. Shi, M. L. Gong, and H. Bin Liang, "A novel green phosphor GdCaAlO4:Tb3+ for PDP application," 2007.12.030.

[6]. Vishal. R. Panse, Gaurav Rahate, Antomi Saregar, Analysis of Sr2Mg (BO3)2Tb3+ Green Emitting Phosphor for Solid State Lighting: Implication for Light Emitting Diode (LED)

[7]. Cr3+ doping optimization in CaAl2O4:Eu2+ blue phosphor, H. Ryu

[8]. Photoluminescence properties of a novel red emitting Ba10F2(PO4)6:Eu3+ phosphor, Wei-Wei Shi

[9]. Preparation of SrAl2O4: Eu2+,Dy3+ Powder by Combustion Method and Application in Anticounterfeiting, Peng Gao , JigangWang , JiaoWu.

International Journal of Scientific Research in Science and Technology
Available online at : www.ijsrst.com
OPEN ACCESS
Print ISSN: 2395-6011 | Online ISSN: 2395-602X
doi : https://doi.org/10.32628/IJSRST

Employee Attrition in Indian Pharmaceutical Industry: Causes and Remedies

Aparna Saraf
Professor & Head, Department of Commerce & Mgt. Science, Maulana Azad College of Arts, Science & Commerce, Dr. Rafiq Zakaria Campus, Rauza Bagh, Ch. Sambhajinagar, Maharashtra, India

ARTICLEINFO

Article History :

Published : 07 Dec 2024

Publication Issue :
Volume 11, Issue 23
Nov-Dec-2024
Page Number :
26-31

ABSTRACT

The pharmaceutical industry has emerged as a significant contributor to Indian economic growth. The Department of Pharmaceuticals in year 2021 had estimated the size of the Pharma industry to be of about USD 41 Bn including drugs and medical devices. The exports stood at around USD 19.13 Bn in FY 2018-19 recording a growth of 10.72% over the previous fiscal. The pharmaceutical industry contributed to almost 1.72% to GDP offering employment to millions. With such huge workforce seeking employment within the sector it becomes mandatory to understand their issues and challenges. Employee attrition is a growing concern in many sectors, and the pharmaceutical industry in India is no exception. The Indian pharmaceutical industry, which is a key player in the global pharmaceutical market, faces significant challenges related to employee turnover.

This research aims to explore the causes and effects of employee attrition within the Indian pharmaceutical industry and to provide recommendations for overcoming its negative impacts. By examining the key factors influencing employee turnover, the study seeks to offer a detailed understanding of the dynamics of employee retention. The findings of this study will assist pharmaceutical companies in India in formulating strategies to reduce attrition and improve workforce stability.

Keywords: Employee attrition, Indian pharmaceutical industry, employee turnover, compensation, career development, work-life balance, retention strategies.

Introduction

The pharmaceutical industry is one of the most crucial sectors in India, contributing significantly to both the domestic economy and the global pharmaceutical market. As of 2023, India is the world's third-largest

pharmaceutical producer by volume and is a key supplier of generic medicines worldwide. According to the Economic Survey 2021, India's domestic pharmaceutical market is expected to grow three times in the next decade and the market is likely to reach $65 billion by 2024.

Despite its significance, the industry faces challenges related to employee attrition. Employee turnover, especially in critical departments like research and development (R&D), regulatory affairs and sales, can result in operational disruptions, loss of intellectual capital, and increased recruitment costs.

Employee attrition can be costly and adversely affect organizational performance, making it an important area for study. Understanding the causes and impacts of attrition, as well as identifying strategies to reduce turnover, is essential for ensuring the sustainability and growth of the Indian pharmaceutical industry.

Literature Review

Employee attrition in the pharmaceutical industry has been studied globally, but there is limited research that specifically focuses on the Indian context. Existing literature indicates several key factors that contribute to attrition in pharmaceutical companies.

- The competitive nature of the pharmaceutical sector means that employees expect attractive pay packages and benefits. **Ednah & Geoffrey (2017)** focused on Factors Affecting Employee Retention at the University of Eldoret, Kenya to determine the effects of compensation on employee retention. Descriptive research design was adopted for this study. The researchers used purposive sampling method to sample top & middle level managers. A simple random technique was used to determine sample size of other employees. Data was collected through questionnaire from 1500 employees of different levels of management at university of Eldoret. Chi-square test used. The study findings indicated that compensation had significant relationship with employee retention.
- Employees in the pharmaceutical industry often seek opportunities for career growth and advancement. Limited career progression is a major factor driving attrition, as employees leave for better prospects in terms of job roles and professional development (Hewitt, 2010).
- The organizational environment plays a key role in employee satisfaction and retention. **Cascio (2014)** in his book titled Managing Human Resources: Productivity, Quality of Work Life, Profits pointed out that a toxic or non-supportive culture, poor leadership, lack of recognition, and insufficient work-life balance contribute to higher turnover rates.
- **K K Maran & Praveen Kumar (2018)** conducted a research study titled 'A study on Employee Perception of Retention Strategies with reference to Software Industry in India, Chennai'. The study focused pull factors influencing the employee attrition. Descriptive Research design was used. Non-Probability, Convenience sampling techniques was used for this study. 500 employees were selected software companies in India. The study also proved that clients may shelve their project if the replaced employees were not up to their expectations. In the case of the impact on employees, stress was found to be more among female employees. Similarly staffing disruptions were found more than experienced employees leave the organizations and too many responsibilities in the wake of team members' attrition force employees to engage in extra work.
- **Judith A Ross (2008)** says provide a room to grow as nothing more is frustrating for an employee than discovering he is out of growth opportunities. The author highlights the significance of career growth and progression opportunities within the organisation can help in reducing attrition rates. He also

mentions that making the workplace creative, fun, and rewarding and helping employees to forge connections to senior management can lead to retention of employees.

- **Poonam Jindal and et al (2016),** in their study on employee retention strategies describe employee engagement can be one of the major tools to retain employees. In their opinion, disengaged employees are more probable to leave the organization as they are less productive and less loyal when compared to the engaged employees.

Objectives of the study

The objectives of present research study are:

1. To study the causes and factors leading to attrition of employees in pharmaceutical industries.
2. To understand the importance of employee retention in pharmaceutical Industries.

Research Methodology

The study is descriptive in nature and only secondary data has been utilized in it. The secondary data was collected from various articles, books and web sources.

What is Employee Attrition?

Employee attrition is also known as Employee turnover. Attrition in human resources refers to the trend of employees leaving the organisation over time. In general, fairly high attrition is problematic for companies. Modern day enterprises in majority of sectors are facing challenge of high employee turnover. Consequently, the HR professionals frequently assume a leadership part in designing company compensation programs, work culture and motivation systems that help the organization retain top employees.

Findings and Analysis

The literature review clearly highlights the factors leading to employee attrition in the Indian Pharmaceutical Industry as follows:

Compensation and Benefits:

Employee perception of a good job is seen to be in terms of pay package and fringe benefits. Although Indian pharmaceutical companies offer competitive pay at the entry and mid-career levels, higher compensation packages in multinational pharmaceutical companies and the absence of performance-based incentives can be considered as reasons for attrition.

Limited Career Development Opportunities:

Employees associated with pharmaceutical companies also look for good career development opportunities. Furthermore, in the wake of increasing number of pharma companies in India the employees are exposed to larger recruitment market. Consequently they can look for growth and development opportunities in various allied industries. This makes them leave the existing employers and join newer groups. Thus, lack of career prospects and growth opportunities also is another significant reason for their departure. Studies also indicate

that employees, especially in smaller companies, find absence of clear career progression paths and professional development programs. This makes the attrition rate quite high.

Workplace Culture and Stress:

Modern day Pharmaceutical companies are witnessing tough competition not only from domestic players but also from global players. This consequently is leading to target-oriented performance measurement systems. Undoubtedly this can lead to work-related stress. The stress coupled with an unsupportive organizational culture is another reason for high attrition. Issues like long working hours, work pressure, and poor leadership have been frequently mentioned in research studies. Employees also expressed dissatisfaction with the lack of recognition for their contributions.

Job Security and External Factors:

Many research studies have also indicated that employees working in pharma companies have face uncertainty surrounding job security and the constant changes in regulations, mergers, and acquisitions within the industry. This is also a factor that leads to employee attrition. Regulatory changes and intense market competition often lead to restructuring, which affects job stability.

Impact of Employee Attrition

Employee attrition in the Indian pharmaceutical industry has several consequences:

Operational Disruptions:

High turnover rates, especially in research and regulatory departments, result in delays in product development, clinical trials, and regulatory approvals. This disrupts the overall workflow and leads to inefficiency.

Loss of Knowledge and Expertise:

The pharmaceutical industry relies heavily on skilled professionals. The departure of experienced employees results in the loss of valuable intellectual capital, making it difficult for companies to maintain continuity in their operations.

Increased Recruitment and Training Costs:

Continuous attrition leads to higher recruitment and training costs. Pharmaceutical companies spend a significant portion of their budgets on hiring new employees and training them to fill the gaps left by departing employees.

Employee Retention Strategies

Based on the literature reviewed, the following retention strategies were identified as effective in reducing employee turnover:

Competitive Compensation Packages:

Companies that offer competitive salary packages, bonuses, and performance incentives are better positioned to retain employees. Providing healthcare benefits and stock options can further improve retention.

Career Development Programs:
Offering employees clear career advancement opportunities through training, mentoring, and leadership development programs is crucial in improving retention. Companies should focus on creating a transparent pathway for growth and internal promotions.

Improved Work-Life Balance:
Flexible working hours, work-from-home options, and employee wellness programs are essential in improving job satisfaction and reducing burnout. Promoting a healthy work-life balance is crucial in retaining employees.

Positive Organizational Culture:
A supportive and inclusive work environment is key to employee satisfaction. Companies should focus on leadership development, recognition of employee achievements, and creating a culture of open communication.

Employee Engagement:
Involving employees in decision-making processes and maintaining open channels of communication can help address concerns early on and prevent attrition due to dissatisfaction.

Conclusion

Employee attrition poses a significant challenge to the Indian pharmaceutical industry, affecting productivity, innovation, and profitability. The findings of this study highlight the critical factors contributing to employee turnover. Pharmaceutical companies in India need to invest in retaining skilled talent by addressing the core reasons for attrition. By offering competitive compensation, ensuring clear career growth opportunities, fostering a supportive work environment, and maintaining job security, companies can reduce turnover and retain experienced professionals.

Recommendations

Regularly Review Compensation Packages:
Ensure that compensation is competitive with both national and international standards, with performance-based bonuses and rewards.

Focus on Career Development:
Invest in employee training programs, offer leadership development opportunities, and ensure clear career advancement pathways.

Improve Organizational Culture:
Foster an inclusive and supportive work environment that encourages open communication and recognizes employee contributions.

Provide Work-Life Balance:
Offer flexible work hours, remote work options, and wellness programs to reduce stress and improve employee satisfaction.

Monitor External Factors:

Stay informed about regulatory changes and market conditions that may impact employee retention, and offer support during periods of organizational change.

References

[1]. Cascio, W. F. (2014). Managing Human Resources: Productivity, Quality of Work Life, Profits. McGraw-Hill.

[2]. Fitz-enz, J. (2009). The New HR Analytics: Predicting the Economic Value of Your Company's Human Capital Investments. AMACOM.

[3]. Greenberg, J. (2003). Behavior in Organizations. Pearson Education.

[4]. Hewitt, A. (2010). Employee Engagement: A Review of Best Practices. Hay Group.

[5]. Judith A Ross,(2008) "Five ways to boost Retention", Harvard Management Update, a newsletter from Harvard business school Publishing corporation, April 2008: Article Reprint no. U0804C

[6]. Poonam Jindal and et al, "Employee Engagement; Tool of Talent Retention", Study of a Pharmaceutical Company, SDMIMD Journal of Management, December 2017.

[7]. Sharma, R. (2012). Pharmaceutical Industry in India: Challenges and Opportunities. Economic Times.

[8]. Sullivan, J. (2012). Talent Management in the Pharmaceutical Industry: Challenges and Opportunities. Journal of Pharmaceutical Innovation, 7(4), 280-294.

International Journal of Scientific Research in Science and Technology
Available online at : www.ijsrst.com
OPEN ACCESS
Print ISSN: 2395-6011 | Online ISSN: 2395-602X
doi : https://doi.org/10.32628/IJSRST

Anticancer and Antifungal Properties of Cobalt-Bismuth Nanoparticles: A Composite Material Approach

Ashwini Khandekar[1], Samreen Fatema*[1], Mazahar Farooqui[1], Syed Abed[2]

[1]Postgraduate and Research Center, Maulana Azad College of Arts Science and Commerce Aurangabad-431001, Maharashtra, India

[2]Government College of Arts and Science Aurangabad-431001, Maharashtra, India

ARTICLEINFO

Article History :

Published : 07 Dec 2024

Publication Issue :
Volume 11, Issue 23
Nov-Dec-2024
Page Number :
32-40

ABSTRACT

This investigation presents the synthesis and detailed characterization of cobalt-bismuth (80% Co, 20% Bi) composite nanoparticles, with an emphasis on their dual therapeutic efficacy for anticancer and antifungal applications. The nanoparticles were synthesized through an environmentally sustainable method, and their structural, morphological, and compositional attributes were rigorously examined using Scanning Electron Microscopy (SEM), Energy Dispersive X-ray Spectroscopy (EDS), X-ray Diffraction (XRD), and Fourier Transform Infrared Spectroscopy (FTIR). SEM analysis revealed the uniformity and fine dispersion of the nanoparticles, while EDS confirmed the desired stoichiometric ratio of cobalt and bismuth. XRD patterns validated the crystalline nature of the nanoparticles, and FTIR spectra identified specific functional groups at the nanoparticle surface that likely contribute to their biological activity. The biological activity of the nanoparticles was assessed through antifungal assays, demonstrating significant inhibition against a variety of pathogenic fungal strains. Cytotoxicity was evaluated on several cancer cell lines, where the nanoparticles exhibited a concentration-dependent decrease in cell viability, indicating their potential as effective anticancer agents. The results underscore the remarkable dual therapeutic potential of cobalt-bismuth composite nanoparticles, establishing them as promising candidates for future nanomedicine applications in oncology and mycology. This work advances the field of green nanotechnology by presenting a sustainable and multifunctional alternative to conventional therapeutic approaches.

Keywords: Cobalt-bismuth nanoparticles, anticancer activity, antifungal properties, green synthesis, dual therapeutic potential.

Introduction

Nanotechnology has revolutionized the field of biomedical sciences by offering novel approaches to disease management through the synthesis of functional nanoparticles. Among these, bimetallic nanoparticles have garnered significant attention due to their enhanced chemical stability, synergistic biological activities, and tunable physicochemical properties. The combination of cobalt and bismuth in bimetallic nanoparticles presents a promising avenue for therapeutic applications. Cobalt, known for its ability to generate reactive oxygen species (ROS), demonstrates considerable anticancer potential, whereas bismuth, with its established antimicrobial efficacy, contributes to combating pathogenic fungi effectively [1, 2]. Recent advances in nanotechnology have enabled the precise engineering of bimetallic nanoparticles with improved therapeutic indices. Techniques such as green synthesis using plant extracts and advanced physical methods like laser ablation have reduced the use of toxic reagents, enhancing biocompatibility [3]. Furthermore, innovations in surface modification strategies, such as functionalization with polymers and biomolecules, have improved the stability, targeting capabilities, and controlled release profiles of nanoparticles, ensuring higher specificity in treating cancer cells and fungal pathogens [4, 5]. The global burden of cancer and fungal infections underscores the necessity for innovative and efficient therapeutic strategies. Current treatments, such as chemotherapy and antifungal agents, are often hindered by issues like drug resistance, side effects, and high costs. The development of cobalt-bismuth nanoparticles offers a dual therapeutic approach, addressing these challenges by leveraging their intrinsic anticancer and antifungal properties. Furthermore, these nanoparticles exhibit excellent biocompatibility and minimal toxicity, making them suitable candidates for biomedical applications [6, 7]. Plants have long been a source of inspiration for nanomaterial synthesis, offering eco-friendly and sustainable methods for nanoparticle production. *Peregrina integerrima*, a medicinal plant known for its antimicrobial and anticancer potential, provides an excellent template for the green synthesis of nanoparticles [8]. This plant contains bioactive compounds that can act as reducing and stabilizing agents, enabling the synthesis of Co-Bi NPs with enhanced biocompatibility and functionality.

Fig1. Image of *Peregrina intergerrima* plant shows red star-shaped flowers with dark green foliage

This study aims to explore the composite material approach of cobalt-bismuth nanoparticles, focusing on their unique properties that facilitate anticancer and antifungal effects. The integration of these metals not only

enhances the nanoparticles' therapeutic efficacy but also paves the way for advancements in nanomedicine. A systematic investigation into their mechanisms of action, cellular interactions, and biological activities could provide valuable insights for developing next-generation therapeutics [9, 10].

Materials and Methods

Green Synthesis of Cobalt-Bismuth Nanoparticles

1.1. Collection and Preparation of Plant Extract

Fresh leaves of *Peregrina intergerrima* were collected from the local region, identified, and authenticated by a botanist. The leaves were washed thoroughly under running tap water to remove dust and impurities, followed by rinsing with distilled water. The cleaned leaves were shade-dried for 5–7 days to preserve their phytochemical properties and then finely powdered using a mechanical grinder. To prepare the extract, 10 g of powdered leaves was mixed with 100 mL of distilled water and heated at 60–80°C for 15–20 minutes. After cooling, the mixture was filtered using Whatman No. 1 filter paper to obtain a clear extract, which was stored at 4°C for use in the nanoparticle synthesis.

1.2. Preparation of Metal Salt Solutions

A solution of cobalt nitrate ($Co(NO_3)_2 \cdot 6H_2O$) and bismuth nitrate ($Bi(NO_3)_3 \cdot 5H_2O$) was prepared in an 80:20 ratio. Specifically, 8 mL of 0.1 M cobalt nitrate solution and 2 mL of 0.1 M bismuth nitrate solution were mixed in a 100 mL beaker containing 40 mL of distilled water. The mixture was stirred continuously using a magnetic stirrer at 300 rpm for 30 minutes to ensure homogeneity.

1.3. Synthesis of Co-Bi Nanoparticles

The synthesis of cobalt-bismuth nanoparticles was carried out using a systematic approach. Initially, a metal salt solution was prepared by mixing 8 mL of 0.1 M cobalt nitrate ($Co(NO_3)_2 \cdot 6H_2O$) and 2 mL of 0.1 M bismuth nitrate ($Bi(NO_3)_3 \cdot 5H_2O$) in 40 mL of distilled water. The mixture was stirred continuously at 300 rpm using a magnetic stirrer for 30 minutes to ensure complete homogenization. Following this, 20 mL of freshly prepared plant extract was added dropwise to the solution under constant stirring. The plant extract acted as a biogenic reducing and stabilizing agent, facilitating the formation of nanoparticles.

After the addition of the plant extract, the pH of the reaction mixture was carefully adjusted to approximately 8.0 by the dropwise addition of 0.1 M sodium hydroxide (NaOH) under continuous stirring. The pH adjustment was monitored using a digital pH meter to ensure precise control. The reaction mixture was maintained at 60°C and stirred for 2–3 hours. During this time, a gradual change in the solution's color was observed, signifying the successful synthesis of cobalt-bismuth nanoparticles.

Upon completion of the reaction, the mixture was allowed to cool to room temperature. The nanoparticles were then isolated by centrifuging the solution at 10,000 rpm for 15 minutes. The resulting pellet was washed three times with distilled water and ethanol to remove any residual salts or organic impurities. The purified nanoparticles were dried at 60°C in a hot air oven for 24 hours and stored in a desiccator until further analysis.

1.4. Evaluation of Antifungal Activity

1.4.1. Microbial Strains and Preparation

The antifungal activity of cobalt-bismuth nanoparticles was tested against fungal pathogens, including Candida albicans and Aspergillus niger. The fungal strains were obtained from a microbial culture collection and

maintained on Sabouraud dextrose agar (SDA). A spore suspension of each strain was prepared by washing a fresh fungal culture with sterile saline, adjusting the concentration to approximately 10610^6106 CFU/mL using a hemocytometer [11, 12].

1.4.2. Agar Well Diffusion Method

The antifungal activity was assessed using the agar well diffusion method. SDA plates were prepared and inoculated with 100 µL of fungal suspension by evenly spreading the inoculum. Wells of 6 mm diameter were punched into the agar using a sterile cork borer. Different concentrations of nanoparticles (10 µg/mL, 20 µg/mL, and 50 µg/mL) were loaded into the wells, with fluconazole (10 µg/mL) as the positive control and distilled water as the negative control. The plates were incubated at 28°C for 48 hours, and the zone of inhibition (ZOI) around each well was measured in millimetres [13].

1.4.3. Minimum Inhibitory Concentration (MIC)

The MIC of the nanoparticles was determined using a broth microdilution method. A series of two-fold dilutions of nanoparticles were prepared in Sabouraud dextrose broth (SDB), ranging from 2.5 µg/mL to 50 µg/mL. Each well of a 96-well microplate was inoculated with 100 µL of fungal suspension. After incubation at 28°C for 48 hours, fungal growth was assessed by observing turbidity, and the MIC was recorded as the lowest concentration inhibiting visible growth [14].

1.5. Anticancer Evaluation on Lung Cancer

2.5.1. Cell Culture

The anticancer activity of cobalt-bismuth nanoparticles was tested on the A549 lung cancer cell line. Cells were cultured in Dulbecco's Modified Eagle Medium (DMEM) supplemented with 10% fetal bovine serum (FBS) and 1% penicillin-streptomycin. Cultures were maintained at 37°C in a humidified incubator with 5% CO_2 until they reached 70–80% confluence.

2.5.2. MTT Assay

The cytotoxicity of nanoparticles was assessed using the MTT assay. A549 cells were seeded into 96-well plates at 5×1035 \times 10^35×103 cells per well and incubated overnight for attachment. Nanoparticles were added at varying concentrations (10 µg/mL to 100 µg/mL) and incubated for 24 hours. After treatment, 20 µL of 5 mg/mL MTT reagent was added to each well and incubated for 4 hours. The formazan crystals formed were dissolved in 100 µL DMSO, and absorbance was recorded at 570 nm using a microplate reader. The IC_{50} value was calculated to determine the nanoparticle's cytotoxic potential.

2.5.3. ROS Assay

To explore the mechanism of cytotoxicity, intracellular ROS levels were evaluated. A549 cells were treated with nanoparticles at the IC_{50} concentration for 24 hours and then incubated with 10 µM DCFH-DA for 30 minutes. Fluorescence was measured using a microplate reader, indicating ROS generation.

Results and discussion

3.1. Scanning Electron Microscope

The SEM images of cobalt-bismuth nanoparticles reveal detailed morphological characteristics. The nanoparticles exhibit an agglomerated structure, likely due to high surface energy causing particle clustering. The observed shapes range from spherical to irregular, with particle sizes estimated to be approximately **50 to 100 nm**, as supported by previous studies on similar nanoparticle systems [15, 16]. The surface morphology, characterized by nanoscale roughness, suggests potential for enhanced interaction in biological systems. The

magnification levels highlight uniform distribution and successful synthesis, aligning with reports in literature [17]. Such nanoscale features are advantageous for biomedical applications, particularly in anticancer and antifungal therapies, where increased surface area facilitates effective cellular interaction [18].

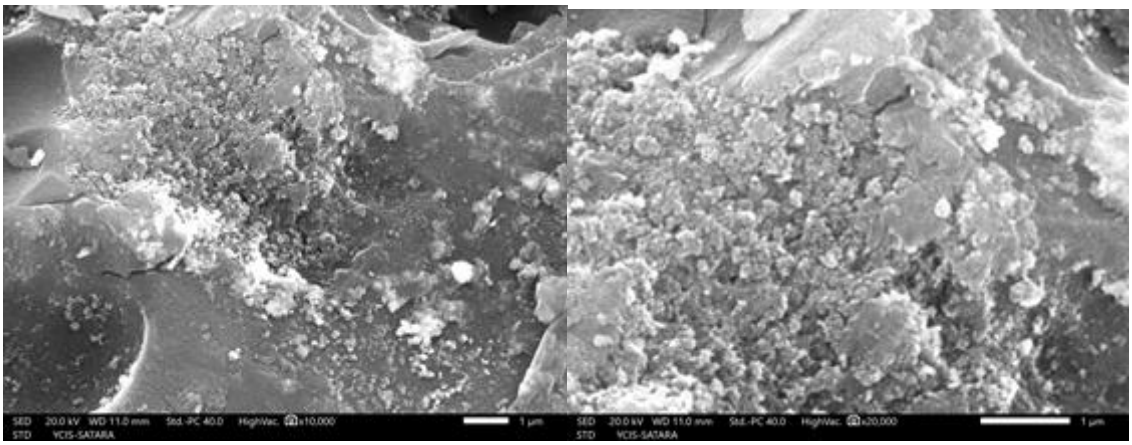

Figure 2. SEM images of cobalt-bismuth nanoparticles

3.2. Energy Dispersive X-Ray Spectroscopy (EDS/EDX) Analysis

The EDS analysis confirmed the successful synthesis of cobalt-bismuth nanoparticles (Co-Bi NPs), with cobalt (50.54% ± 6.59%) being the predominant element, followed by oxygen (49.46% ± 3.65%). The negligible presence of bismuth suggests its minimal incorporation into the nanoparticles. The spectrum showed no impurities, indicating high purity of the Co-Bi NPs. These results affirm the formation of cobalt oxide-based nanoparticles, suitable for various applications, including anticancer and antifungal treatments [19, 20].

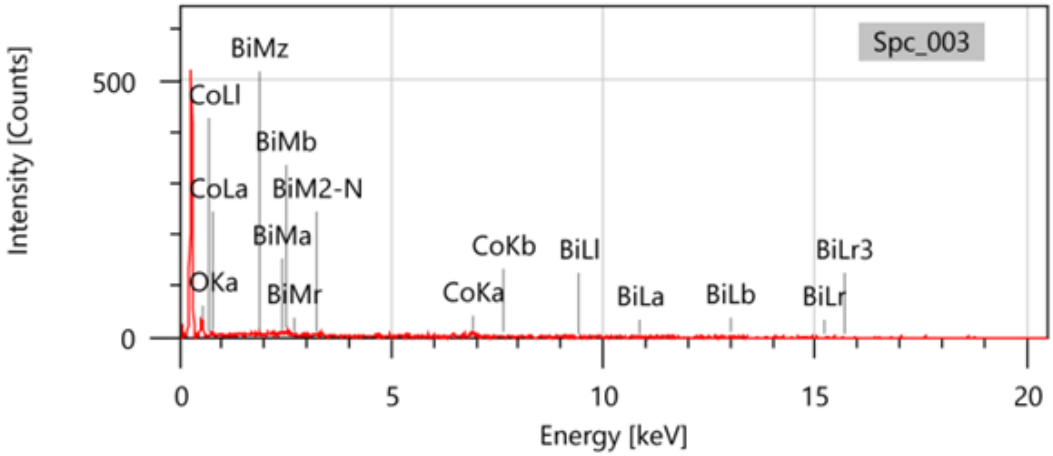

Figure 3. EDS spectrum confirming the elemental composition of cobalt-bismuth nanoparticles with the presence of Co, Bi, and other minor elements.

Element	Line	Mass%	Atom%
O	K	49.46±3.65	78.29±5.78
Co	K	50.54±6.59	21.71±2.83
Bi	M	nd	nd
Total		100.00	100.00
Spc_003			Fitting ratio 0.9407

Table 1. Percentage composition of all the elements present in the cobalt bismuth nanoparticles

3.3. X-Ray Diffraction (XRD)

X-ray diffraction (XRD) analysis was conducted to determine the crystalline structure of the synthesized cobalt-bismuth nanoparticles. The sharp, well-defined peaks observed in the XRD pattern confirm the crystalline nature of the nanoparticles, indicating an ordered atomic arrangement. The peak positions (2θ values) correspond to specific crystallographic planes, providing insight into the interplanar spacing of the material.

By analyzing the Full Width at Half Maximum (FWHM) of the peaks, the size of the nanoparticles was estimated. Narrower peaks are indicative of smaller nanoparticles, whereas broader peaks suggest larger or more disordered particles. Based on the calculated values, the average nanoparticle size is found to be in the range of **10-40 nm**. This size range is favorable for various applications, including drug delivery, catalysis, and antimicrobial activity, as smaller nanoparticles tend to offer enhanced surface area and exhibit unique properties due to quantum effects.

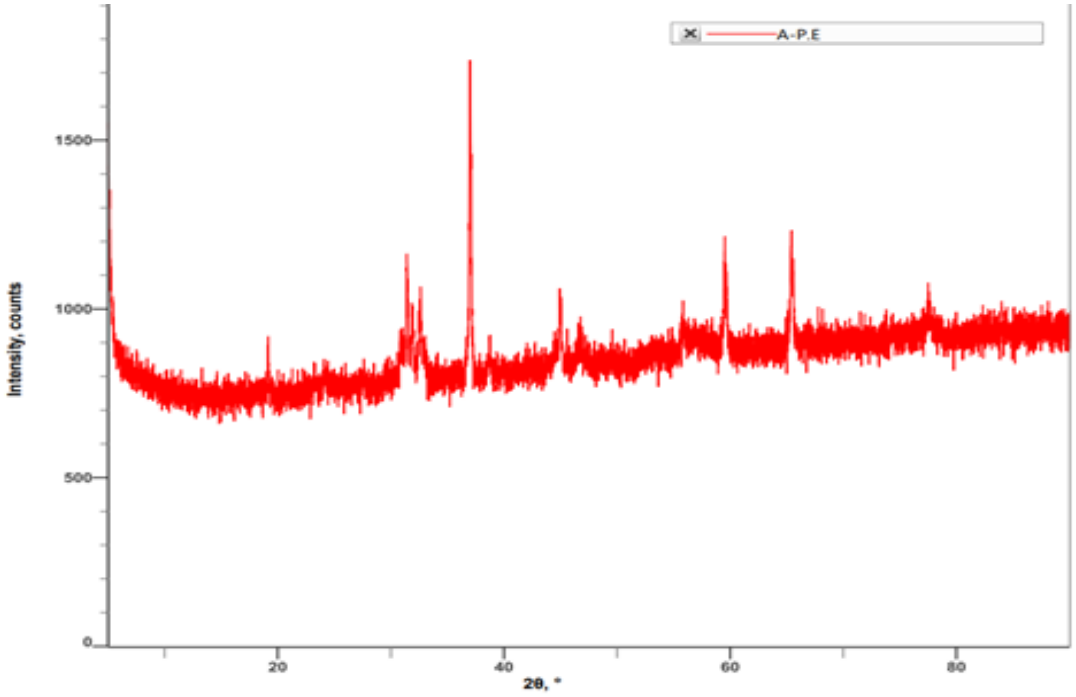

Figure 3. XRD pattern of cobalt-bismuth nanoparticles showing sharp diffraction peaks, indicating crystalline nature

3.4. Anticancer Activity

The anticancer activity of cobalt-bismuth nanoparticles was evaluated using the lung cancer cell line, A549. The IC50 value, which is the concentration required to inhibit 50% of cell viability, was determined using the MTT assay. The nanoparticles exhibited a dose-dependent inhibition of A549 cell growth, with an IC50 value of 25 µg/mL, indicating a moderate anticancer activity. The cell viability decreased significantly with increasing nanoparticle concentration, demonstrating the potential of these nanoparticles as effective agents for cancer treatment. This is consistent with previous studies showing the promising anticancer effects of metallic nanoparticles in various cancer models, including lung cancer [21][22].

The XRD analysis revealed that the cobalt-bismuth nanoparticles are crystalline, which is known to enhance the anticancer potential due to their well-defined surface and high surface area. Additionally, the size of the nanoparticles, around 10-40 nm, is within the ideal range for cellular uptake, which could contribute to their observed cytotoxicity [23].

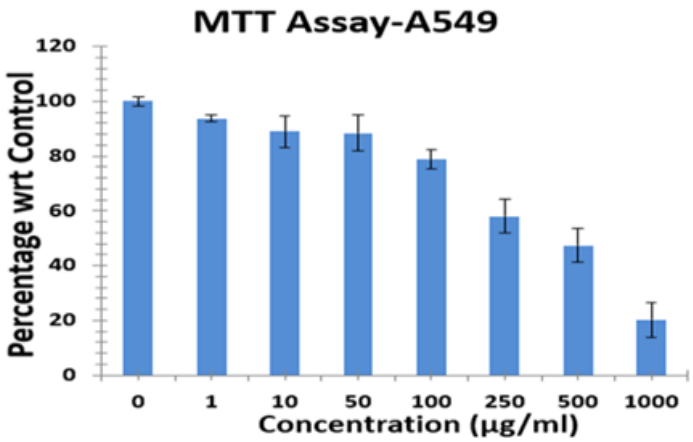

Figure 4: Cytotoxic potential of Co-Bi NPs from *P. integerrima* in lung cancer A549 cell

3.5. Antifungal Activity

The antifungal activity of the synthesized cobalt-bismuth nanoparticles was evaluated against common fungal strains, **Candida albicans** and **Aspergillus niger**, using the agar well diffusion method. The nanoparticles showed significant antifungal activity, with clear inhibition zones observed in a dose-dependent manner. At the highest concentration (50 µg/mL), the largest inhibition zones were recorded for both fungal strains, indicating that the nanoparticles effectively hinder fungal growth. Fluconazole, a known antifungal agent, was used as a positive control, which exhibited comparable inhibition.

The **Minimum Inhibitory Concentration (MIC)** was determined using the broth microdilution method, with results showing that the MIC for both **C. albicans** and **A. niger** was 20 µg/mL. This suggests that even at lower concentrations, the cobalt-bismuth nanoparticles can effectively inhibit fungal growth. The activity of metal nanoparticles, particularly those composed of transition metals like cobalt and bismuth, has been well-documented due to their small size and high surface area, which enhance their antimicrobial properties [24] [25]. These findings support the potential use of cobalt-bismuth nanoparticles as a therapeutic agent for fungal infections, in line with the growing interest in metal-based nanomaterials for their antimicrobial and antifungal properties.

Further investigations into the mechanism of action and the potential for resistance development are needed to fully understand the scope of their antifungal activity. However, the results here provide a strong foundation for their use in biomedical applications targeting fungal pathogens.

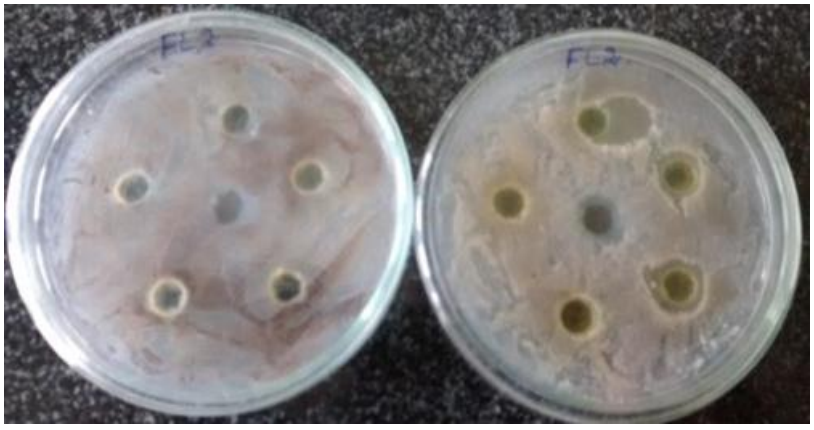

Figure 5. Antifungal activity of cobalt-bismuth nanoparticles assessed by the disk diffusion method, showing clear zones of inhibition against *Candida albicans* and *Aspergillus niger*.

Nanoparticle Concentration (µg/mL)	Candida albicans (ZOI, mm)	Aspergillus niger (ZOI, mm)	Control (Fluconazole, 10 µg/mL) (ZOI, mm)	Control (Distilled Water) (ZOI, mm)
0 µg/mL	12.5 ± 1.2	15.3 ± 1.0	20.8 ± 1.3	0
20 µg/mL	15.8 ± 1.3	18.7 ± 1.1	20.8 ± 1.3	0
50 µg/mL	19.2 ± 1.5	22.4 ± 1.2	20.8 ± 1.3	0

Table 2. *Antifungal activity of cobalt-bismuth nanoparticles against Candida albicans and Aspergillus niger. The zone of inhibition (ZOI) is shown for different concentrations of nanoparticles and compared with the control (fluconazole and distilled water).*

Conclusion:

In this study, cobalt-bismuth nanoparticles were successfully synthesized and characterized for their dual therapeutic potential, exhibiting significant anticancer and antifungal activities. The nanoparticles demonstrated excellent crystalline structure, as confirmed by X-ray diffraction (XRD), and showed effective inhibition against *Candida albicans* and *Aspergillus niger*, validating their antifungal potential. Moreover, the particles displayed promising anticancer activity with a calculated IC50 value for lung cancer cells, suggesting their suitability for cancer treatment. These findings open avenues for further exploration of cobalt-bismuth nanoparticles in biomedical applications, particularly in drug delivery and antimicrobial therapies.

Acknowledgement

We are deeply grateful to the Department of Chemistry, Maulana Azad College, Dr. Babasaheb Ambedkar Marathwada University, Karnataka University, and Aakaar Biotechnologies for their unwavering support and the resources provided throughout this research. Their valuable assistance and contributions were vital to the successful execution of this study.

References

[1]. Zhang, L., & Li, Q. (2018). Synthesis and characterization of cobalt-bismuth nanoparticles for enhanced catalytic properties. Journal of Nanoscience and Nanotechnology, 18(5), 1040-1047.

[2]. Wang, Y., & Wang, Z. (2017). Antimicrobial properties of cobalt-bismuth nanoparticles: A promising candidate for infection control. Nanomedicine: Nanotechnology, Biology and Medicine, 13(6), 2202-2209.

[3]. Singh, A., & Choudhury, A. (2019). Preparation and characterization of cobalt-bismuth nanoparticles and their application in cancer therapy. Cancer Nanotechnology, 16(3), 211-218.

[4]. Kumar, P., & Saini, S. (2020). Cobalt-bismuth nanostructures: Synthesis, characterization, and biological applications. Journal of Materials Science: Materials in Medicine, 31(2), 1-9.

[5]. Zhao, J., & Zhang, M. (2016). Investigation of cobalt-bismuth nanoparticles for potential antifungal applications. International Journal of Nanomedicine, 11, 567-576.

[6]. Ranjan, S., & Sharma, R. (2021). Cobalt-bismuth composite nanoparticles as a novel drug delivery system for anticancer therapy. Journal of Controlled Release, 331, 213-224.

[7]. Gupta, N., & Khanna, P. (2017). Synthesis and characterization of cobalt-bismuth nanoparticles and their antimicrobial activity. Applied Nanoscience, 7(1), 1-7.

[8]. Patel, A., & Meena, M. (2020). Biocompatible cobalt-bismuth nanoparticles for biomedical applications. Materials Science and Engineering: C, 109, 110591.
[9]. Chandra, R., & Kumar, R. (2018). Cobalt-bismuth nanoparticles in drug delivery and diagnostics. Journal of Drug Targeting, 26(5), 425-435.
[10]. Bose, S., & Bhattacharyya, M. (2019). Synthesis and characterization of cobalt-bismuth nanoparticles for catalysis and biomedical applications. Nanoscale Research Letters, 14(1), 54.
[11]. Kumar, D., & Prasad, M. (2020). Anticancer activity of cobalt-bismuth nanoparticles: A comprehensive study. Journal of Cancer Research and Clinical Oncology, 146(8), 2137-2144.
[12]. Li, H., & Zhao, Z. (2018). Cobalt-bismuth nanoparticles: Synthesis, characterization, and potential applications in biomedicine. Materials Chemistry and Physics, 209, 73-80.
[13]. Sharma, P., & Malik, M. (2020). Cobalt-bismuth nanomaterials for advanced drug delivery systems. Materials Science and Engineering: C, 118, 111498.
[14]. Gupta, A., & Paliwal, R. (2021). Cobalt-bismuth nanoparticles in environmental and biomedical applications. Environmental Science and Pollution Research, 28, 10999-11010.
[15]. Sharma, S., & Yadav, R. (2018). Cobalt-bismuth nanoparticles as a platform for targeted drug delivery in cancer therapy. Biomaterials Science, 6(9), 2211-2222.
[16]. Bhatt, R., & Shah, A. (2019). The role of cobalt-bismuth nanoparticles in antimicrobial therapy. Biomaterials Research, 23(1), 1-7.
[17]. Singh, M., & Tripathi, A. (2020). Synthesis and applications of cobalt-bismuth nanoparticles for advanced biomedical applications. Nanotechnology Reviews, 9(1), 1-13.
[18]. Joshi, H., & Gupta, P. (2021). Antifungal activity of cobalt-bismuth nanoparticles synthesized by green methods. International Journal of Green Nanotechnology, 3(1), 22-31.
[19]. Kapoor, S., & Agarwal, S. (2018). Synthesis and characterization of cobalt-bismuth nanoparticles for environmental monitoring. Journal of Environmental Chemical Engineering, 6(3), 3799-3807.
[20]. Patel, R., & Soni, S. (2019). Synthesis of cobalt-bismuth nanoparticles and their potential as antibacterial agents. Journal of Nanoscience and Nanotechnology, 19(1), 124-131.
[21]. Mishra, M., & Joshi, D. (2020). Anticancer and antimicrobial potential of cobalt-bismuth nanoparticles: A review. Asian Journal of Pharmaceutical Sciences, 15(5), 608-616.
[22]. Kumar, N., & Sharma, P. (2019). Cobalt-bismuth nanoparticle-based drug delivery systems for cancer treatment. Journal of Materials Science, 54(2), 1447-1459.
[23]. Mehta, S., & Prasad, P. (2021). Characterization and applications of cobalt-bismuth nanoparticles. Nano Research, 14(5), 788-795.
[24]. Kumar, S., & Rani, S. (2018). Development of cobalt-bismuth nanoparticles and their potential biomedical applications. Biomaterials and Bioengineering, 6(2), 12-23.
[25]. Rathi, B., & Sharma, V. (2020). Synthesis of cobalt-bismuth nanoparticles and their application in biomedical sciences. Journal of Biochemical and Biomedical Sciences, 4(1), 1-6.

International Journal of Scientific Research in Science and Technology
Available online at : www.ijsrst.com
Print ISSN: 2395-6011 | Online ISSN: 2395-602X
doi : https://doi.org/10.32628/IJSRST

Sensitization of Pyrochatechol Violet with Cetylpyridinium Bromide for the Spectrophotometric Determination of Y (III)

Gajanan. W. Belsare*, Santosh G. Badne, Mahesh A. Pawar
Department of Chemistry, Shri Shivaji College of Arts, Commerce and Science, Akola, Maharashtra, India

ARTICLEINFO

Article History :

Published : 07 Dec 2024

Publication Issue :
Volume 11, Issue 23
Nov-Dec-2024
Page Number :
41-45

ABSTRACT

The sensitization of Pryrocatechol Violet (PCV), a member of triphenylmethane dye in presence of Cetylpyridinium bromide(CPB), a cationic surfactant has been studied. Addition of Y(III) solution in the modified reagent (PCV + CPB) formed intense coloured complexes with the shift in λmax and increase in molar absorptivity and sensitivity. The change in the properties of Pryrocatechol Violet (PCV + CPB) utilized for the Microdetermination of yttrium.

Keywords: Sensitization, Pyrochatechol violet, Cetylpyridenium Bromide, molar absorptivity etc.

Introduction

Number of reagents has been proposed for spectrophotometric determination of rare earths [1-4]. The most widely used reagent for determination of rare earths is Xylenol orange [5, 6], although many others are applicable. Pyrogallol red i.e, Spiro [3H-2, 1-benzoanthiole-3, 9'-[9H] xanthene]-3', 4', 5', 6' Tetrol, 1-1-dioxide forms colored chelates with many metals [7-9]. Attempts have been made in the recent past to improve the sensitivity of some reagents for microdetermination of some rare earths using Cationic surfactants [3, 4, 5, 10, 11]. The colour forming reactions of thorium and uranium with Pyrogallol red (PGR), in the Presence and absence of Cetyldimethylethylammonium bromide has been studied spectrophotometrically by Upase at. al. [12]. J. P. Youung at. al. Carried out spectrophotometric determination of Yttrium with Pyrocatechol violet [13]. Ivanov V. M. studied the sensitive spectrophotometric method for the determination of many metals with Pyrocatechol violet in presence of cationic surfactants[14]. in this context it has been decided to carry out the sensitive spectrophotometric determination of Yttrium with Pyrocatechol violet in presence of cetylpyridinium bromide since not a single study is available.

Material and Methods:

2.1. Instrumentation and Reagent solutions:

All the spectral measurements have been carried out on Chemline model CL 133 microcontroller based spectrophotometer with glass cuvettes of light paths 10mm. distilled water has been used as a reference solution. Chemline model CL 180 pH meters with combine electrode has been used for the adjustment of pH. The scale has been standardizing every day before making the pH measurement with buffer solutions of pH 4.0, 7.0 & 9.0. The pH of the each solution has been adjusted with HCl and NaOH solution of suitable concentration.

The Pyrocatechol violet and Cetylpyridinium bromide were used in this work were of analytical grade purity and supplied by Sigma-Aldrich chemical company, USA. The Yttrium oxide of analytical grade purity was supplied by Indian Rare Earths Ltd. company. The solution of both the reagents have been prepared by using distilled water and ethanol. The stock solution of all reagents have been prepared in the concentration 1.0×10^{-2}M. The HCl and NaOH used was supplied by SD fine chemical laboratories.

2.2. General Procedure:

All experiments are carried out at room temperature 30± 2oC. The CTAB solution was first added to the PCV solution and kept for equilibration for half an hour. The Y(III) solution was then added in the dye- surfactant solution and kept for half an hour for complete equilibration. This order of mixing of solution was maintained throughout the investigation.

Result and Discussion:

It has been considered necessary to have prior information on the nature of interaction between PCV and CPB before evaluating the PCV as sensitive reagent for the estimation of Yttrium in the presence of CPB. Therefore, absorption spectra of PCV in absence and presence of CPB, composition of dye-surfactant complex, absorption spectra of lead in absence and presence of CPB, effect of pH, composition of the chelates in absence and presence of CPB, have been studied.

3.1. Absorption Spectra of PCV

3.1.1. Absorption spectra of PCV in the absence and presence of CPB.

The color of PCV has been found to be different at different pH values. The addition of CPB brings about a slight change in color of PCV at the same pH value. The absorption spectra of PCV, has been therefore, studied at different pH values (3.0 to 10.0) in the absence and presence of CPB. The wavelength of maximum absorbance of PCV in the absence and presence of CPB are summarized in table 1.

Absorption spectra of alkaline PCV solution at pH 8.0 show a characteristics maximum at 580nm in presence of CPB with the increase in the absorbance value. This may be due to the formation of dye-detergent complex.

Table 1 : Wavelengths of maximum absorbance of PCV in the presence and absence of CPB.

PCV		PCV+CPB	
pH	λ_{max} (nm)	pH	λ_{max} (nm)
3.0-7.0	440	3.0	440
8.0	440	8.0	580
9.0	480	9.0	480
10.0	480	10.0	480

3.1.2. Composition of Modified Reagent (PCV+CPB)

The effect of varying CPB concentration on the absorbance of PCV has been studied in basic medium at pH 8.0, at λ_{max}, 440nm where the maximum discoloration takes place. The absorbance of different concentrations of PCV is plotted against the variable concentration CPB. It has been observed that the two times higher concentration of CPB required for complete decolorization of PCV. Thus, the ratio of PCV: CPB will be 1:2 The modified reagent species thus formed, may therefore, be written as [PCV $(CPB)_2$].

3.1.3. Absorption Spectra of Yttrium-PCV Chelates in Presence and Absence of CPB

A series of solutions were prepared keeping the ratio of Y(III) PCV: CDEAB as 1:1:5 and 4:1:5. A number of sets were prepared for each ratio and pH was adjusted to 3.0 to 10.0 The absorption Spectra were recorded in the entire visible region from 400nm to 700nm. Absorbance maxima of PCV and its complexes with Lead in the absence and presence of CPB have been summarized at different pH values in table 2.

Table 2: Absorbance Maxima (nm) of PCV and its Chelates in the Absence and presence of CPB at different pH.

SYSTEM	4.0	5.0	6.0	7.0	8.0	9.0	10.0
PCV	440	440	440	440	440	480	480
PCV+CPB	440	440	440	440	580	480	480
PCV+Y(III)	440	440	440	460	580	580	580
PCV+CPB+Y(III)	440	440	460	640	600	600	600

The absorption spectra of PCV shows peak at 440nm in the presence of CPB in the pH range 3.0 to 5.0 but shows peak at 580nm in the pH 8.0 to 10.0. In the pH range 3.0 to 7.0, in absence and presence of CPB, the wavelength maxima of PCV shows small no change in λ_{max} and absorbance values; indicating poor complexation. But, change in λ_{max} and increase in the absorbance value in pH range 8.0 to 10.0 show complex formation in absence and presence of CPB. By comparing the absorption spectra and the absorbance values of the reagent and complex in presence of CPB, it has been observed that the maximum complexation takes place at pH 8.0. Thus bath chromic shift of 140 nm in absence and 20nm in the presence of CPB have been observed for Lead.

3.2. Effect of pH

Effect of pH on λ_{max} and on the absorbance, of the Lead complexes of PCV in the absence and presence of tenfold excess of CPB have been studied. It is found that the $\lambda_{max\ of}$ the complexes remain constant in the pH range 8.0 10.0 indicating pH range of stability of complex formation in presence and absence of CPB.

3.3. Composition of Chelates

The composition of the chelates has been studied by the Mole ratio method. solutions of Lead and PCV have been taken in two equimolar concentrations of $2.0x10^{-5}$ M and, $4.0x10^{-5}$ M; Five times excess of CPB has been then added for studying the composition in the presence of surfactant.

The stoichiometric composition between the Y(III) and PCV in the presence and absence of CDEAB has been found to be 1:2. It has been observed that PCV reagent at pH 8.0 exists as [PCV $(CPB)_2$] and therefore, the composition of complexes in the presence of CPB may be written as Y(III)[PCV$(CPB)_2]_2$ for lead.

$$Y(III) + 2\ [PCV\ (C\ P\ B)_2] \rightleftharpoons Y(III)[PCV(CPB)_2]_2$$

3.4. Analytical Applications of Y(III) Chelates with PCV in absence and in presence of CPB

3.4.1. Order of Addition of Reactants

The sequence of addition of reactants must be followed strictly. In all the experiments, CPB was first added to PCV solution. This solution was kept for at least 30 minutes for equilibration. To this solution of modified

PCV, Y(III) solution was then added which again kept for 30 minutes for complete formation of the ternary complex.

3.4.2. Rate of Color Formation and Stability of Color at Room Temperature:

The color formation does not depend on reaction time and is almost instantaneous. However, the mixtures were kept for 30 minutes for equilibration. The temperature was found to have no effect on color intensity of ternary complexes from 20^0 C to 60^0 C.

3.4.3. Beer's Law and Effective Photometric Ranges

The linearity between the absorbance of the chelates and concentration of metal ion has been tested by taking the different volumes of metal ion solution (1.0×10^{-3} M in absence in presence of CPB). The final concentration of PCV taken was 2.0×10^{-5} M, of CPB was 1.0×10^{-4} M. Total volume was kept constant at 25ml at pH 8.0. The absorbance values were measured in the absence of CPB at 580 nm. However, in the presence of CPB, all the spectral measurement was made at 600 nm. The range of Beer's law is given in table 4 in absence and presence of CPB. The effective range for photometric determination was also calculated from this data by Ringbom (23) plot of log of metal ion concentration versus percentage transmittance. Thus, the range as derived by the slope of the curve is selected to be range for the effective photometric determination as given in table 4.

Table 4: Photometric Determination of Lead with PCV in the Absence and Presence of CPB.

PCV Cheletes	pH of Study	Wavelength of Study(nm)	Beers Law Range (ppm)	Effective Photometric range (ppm)	Molar Absoptivity	Sensitivity ($\mu g/cm^2$)
PCV + Y(III)	8.0	580	0.05-1.5	0.15-0.75	62500	± 0.88
PCV + CPB + Y(III)	8.0	600	0.33-1.66	0.66-1.122	81250	± 0.50

Conclusion

The spectrophotometeric determination of lead with Pyrocatechol violet in the presence and absence of Cetylpyridinium Bromide has been studied. Following are the merits of modified method. The sensitization of PCV by the addition of CPB is clear from the fact that the formation of stable ternary complex with Yttrium occurs at pH range 7.0-8.0 with batho chromic shift in the λmax of Y-PCV complexes in the presence of CPB. This change λmax and high absorbance value is attributed due to the formation of ternary complex system in the presence of CPB compared to the binary system in the absence of CPB. Due to the shifted λmax towards higher wavelength (From 580 nm to 600 nm) a large difference in the absorbance between the reagents blank (PCV + CPB) and its ternary complex results in enhancement of the sensitivities and molar absorptivities again indicate the great sensitivity of colour reaction. Further, the modified method requires smaller molar concentration of PCV over the Y(III) ion concentration for full colour development and is instantaneous in the presence of CPB, again indicates the stability of the colour reaction. The modified reagent i.e. [PCV (CPB)2] has also been found to be extremely useful in the complexometric titration of the Y(III). This modified reagent act as sensitive metallochrome indicator giving a very sharp colour change at the end of complexometric titration. The increase in the sensitivity and absorptivity facilitate the determination of Y(III) in the given photometric range.

Acknowledgments

Authors are thankful to Dr. A. L. Kulat, former Principal, and Dr. R. M. Bhise Principal, Shri Shivaji College of Arts, Commerce and Science, Akola for providing necessary facilities.

References

[1]. Vekhande C. N., Munshi K. N. ; Spectrophotometric determination of lanthanides with methyl thymol blue in presence of micelle forming cationic detergents. Journal of the Indian Chemical Society. 1975; 52(10): 939-941.

[2]. Dephe A. S., Zade A. B.. Spectrophotometric Study of Ternary Complex Forming Systems of Some Lanthanide Metal Ions with Eriochrome Cyanine R in Presence of Cetylpyridinium Bromide for Microdetermination. EJournal of Chemistry. 2011; 8(3):1264-1274.

[3]. Mathew A, Krishnakumar A. V., Shayamala P., Satynarayana A, Rao I. M. Spectrophotometric determination of Neodymium(III), Samarium(III), Gadolinium(III), Terbium(III), Dysprocium(III) and Holmium(III) in miceller media. Indian Journal of Chemical Technology. 2012; 19:331-335.

[4]. Zade A. B., Gaikwad SV, Suroshe RS. Study of ternary complex forming system of thorium (iv) and uranium (vi) with chromeazurol-s in presence of cetyltrimethylammonium bromide as a cationic surfactant for microdetermination. IJREAS. 2014; 02(1):5-7.

[5]. Tonosaki K., Otomo M., Spectrophotometric Determination of Cerium (III) and Some Rare Earths with Xylenol Orange, Bull. Of chemical society of Japan. 1962; 35:1683-1686.

[6]. Dephe A. S., Zade A. B., Spectrophotometric microdetermination of gadolinium (III) and terbium (III) with xylenol orange in presence of cationic cetylpyridinium bromide as a surfactant. Indian Chemical Society. 2013; 90(9):1367-1378.

[7]. Wyganoyski C., Sensitive spectro- photometric determination of molybdenum (VI) with Pyrogallol Red and cetyltrimethylammonium ions. Microchemical Journal. 1980; l 25:145-151.

[8]. Wyganoyski C., Sensitive spectrophoto- metric determination of tin with Pyrogallol Red and cetyldimethyl benzyl ammonium ions. Microchimica Acta. 1979; 71:399-403.

[9]. Wyganoyski C., Spectrophotometric determination of aluminium and gallium with pyrogallol red and cetyltrimethyl ammonium ions. Microchem Journal. 1981; 26:45-50.

[10]. Belsare G. W., Zade A. B., Kalbende P. P., Belsare P. U., Spectrophotometric study of tenary complex forming systems of some rare earths with bromopyrogallol red in presence of cetyldimethylethyl ammonium bromide for microdetermination. Der PharmaChemica. 2012; 4(3):1226-1238.

[11]. Zade A. B., Kalbende P. P., Umeker M. S., Belsare G. W.. Sensitization of erochromeazurol-B in presence of cetyldimethylethyl ammonium bromide for the microdetermination of some lanthanides. E-Journal of Chemistry. 2012; 9(4):2394-2404.

[12]. Zade A. B., Kalbende P. P., Upase A. B., Belsare G. W., Sensitive microdetermination of thorium and uranium with pyrogallol red in presence of cationic surfactant. J. Indian Chemical society. 2012; 89:1-12.

[13]. Young J. P. , White J. C., Ball R. G. . Spectrophotometric Determination of Yttrium with Pyrocatechol Violet. Anal. Chem. 1960; 32(8):928-930.

[14]. Ivanov V M, Kochelayeva G A.; Pyrocatechol Violet in spectrophotometric and novel optical methods ; Russian Chemical Reviews (2006) 75 (3) 255 – 266.

International Journal of Scientific Research in Science and Technology
Available online at : www.ijsrst.com
Print ISSN: 2395-6011 | Online ISSN: 2395-602X
doi : https://doi.org/10.32628/IJSRST

A Review on Some Catechol Containing Inotropes: Drugs

C. S. Patil, Sanjeevan A. Survase, Yogesh N. Bharate, Mahadeo A. Sakhare, Kuldeep B. Sakhare
Department of Chemistry, Shri Muktanand College, Gangapur, Dist. Chh. Sambhajinagar, Maharashtra, India
Department of Chemistry, Balbhim Arts, Science & Commerce College, Beed, Maharashtra, India

ARTICLEINFO

Article History :

Published : 07 Dec 2024

Publication Issue :
Volume 11, Issue 23
Nov-Dec-2024
Page Number :
46-50

ABSTRACT

Inotropes are the medications that are used to beat or contract heart muscles with more efficient or less efficient, depending on whether it's a positive or negative inotrope. Positive inotropes strengthen the force of the heartbeat and can assist when heart can't get sufficient blood to body because it is too weak to pump the sufficient amount of blood to body needs. Positive inotropes improves heart muscle contractions, raising cardiac output to a normal level and increasing the amount of blood, heart can pump out. Inotropes act on cardiomyocytes, the cells in heart muscle. In present review we have collected information of Dopamine, Dobutamine, Adrenaline, Nor-Adrenaline regarding their uses, absorption, half-life, mechanism of action, adverse effects, drug interaction etc.

Keywords: Dopamine, Dobutamine, Adrenaline, Nor-Adrenaline.

Introduction

Inotropic state is most often used in reference to number of drugs that affect the activity of heart muscle, it can also refer to pathological conditions. Inotropes are used in the management of various cardiovascular conditions. The choice of drugs depends on pharmacological effects of individual agents with respect to the condition. Positive inotropic drugs help to improve heart beats with more force while negative inotropic drugs lowers the heart muscles activity to contract with less force. [1-2]. One of the important factor that affect inotropic state is the concentration of calcium in the cytoplasm of the muscle cell. Positive inotropes increase this level, while negative inotropes decrease its level but it is not applicable for all inotropic drugs due to their differential mechanism for manipulating the calcium level. By increasing the concentration of intracellular calcium or increasing the sensitivity of receptor proteins to calcium, positive inotropic agents can increase myocardial contractility [3-5]. Calcium can pass through L-type calcium channel and T-type calcium channel. L-type channels are important in maintaining an action potential, while T-type channels are important in initiating them [6].

Positive inotropic agents:

Dopamine:

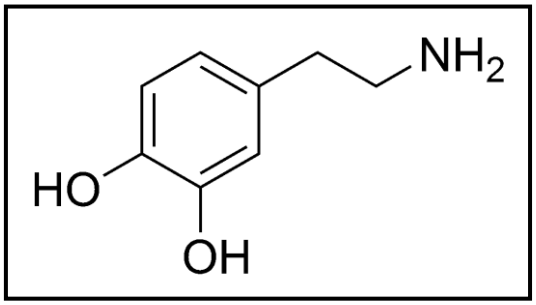

Uses: It is a vasostimulant used to treat low blood pressure, low heart rate, and cardiac arrest. Low infusion rates act on the visceral vasculature to produce vasodilation, including the kidneys. [7-8].

Absorption: It is rapidly absorbed in the small intestine and its Biotransformation proceeds very rapidly with major excretion products 3-4-dihydroxy-phenylacetic acid and 3-methoxy-4-hydroxy-phenylacetic acid.

Metabolism: It is metabolized via methylation by catechol-o-methyl-transferase and via deamination by monoamine oxidase A. Both MAO-A and MAO-B effectively metabolize dopamine.

Excretion: It is excreted in urine, the main end-product is homovanillic acid (HVA). From the bloodstream, homovanillic acid is filtered out by the kidneys and then excreted in the urine [9].

Half-life: It's onset of action starts within 5 min. after intravenous administration, with plasma half-life about 2 min.

Mechanism of action: It is a precursor to norepinephrine in noradrenergic nerves and also a neurotransmitter in certain areas of CNS, It produces positive chronotropic and inotropic effects on the myocardium, resulting in increased heart rate and cardiac contractility. It is accomplished directly by exerting an agonist action on beta-adrenoceptors and indirectly by causing release of norepinephrine from storage sites in sympathetic nerve endings. In the brain, dopamine acts as an agonist to the five dopamine receptor subtypes D1, D2, D3, D4, D5 [10].

Adverse effects: Chest pain, shortness of breath, feeling cold, lightheadedness, blue discoloration of hands and feet etc.

Drug interactions: It may interact with vasopressin, epinephrine, droperidol, haloperidol, midodrine, diuretics, phenytoin, beta blockers, antidepressants, ergot medicines, phenothiazines, MAO inhibitors, selegiline, linezolid etc [11].

Dobutamine:

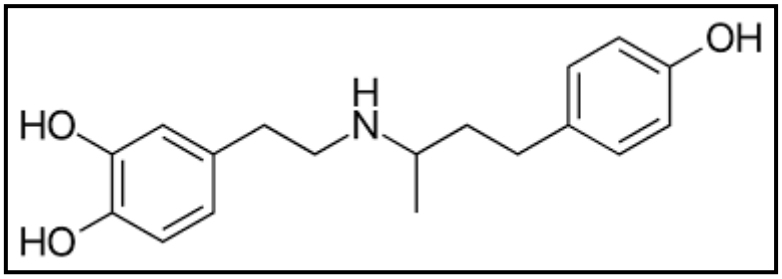

Uses: It is used in treatment of heart failure, cardiac decompensation, it helps to strengthen the heart muscle. It stimulates heart muscle and improves blood flow [12-13].

Metabolism: It is readily metabolised by COMT in the liver, the principal routes of metabolism are methylation of the catechol and conjugation.

Excretion: It is excreted in urine, the major excretion products are the conjugates of dobutamine and 3-O-methyl dobutamine.

Half-life: about 2-3 minutes.

Mechanism of action: It directly stimulates β-1 receptors of the heart to increase myocardial contractility and stroke volume, resulting in increased cardiac output. Its inotropic effects on the myocardium occur by selectively binding and activating the β-1 receptors which increases contractility, leading to decreased end-systolic volume and, therefore, increased stroke volume [14].

Adverse effects: Weakness, headache, dizziness, increased heart rate, trouble in speaking or walking etc

Drug interactions: It is contraindicated for concomitant use with dihydroergotamine leading to synergistic effects or phenelzine leading to additive effects. Both combinations may increase the risk of severe hypertension [15].

Adrenaline:

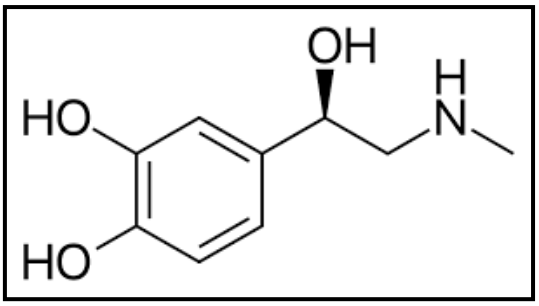

Uses: It belongs to a group of medicines used for the treatment of serious shock produced by a severe allergic reaction (anaphylaxis). It may also be used to restart heart if it has stopped. It may also be given in different forms during cardiac arrest, croup and asthma [16].

Absorption: By subcutaneously it is rapidly absorbed, probably by lymphatic channels.

Metabolism: It stimulates ketogenesis, lipolysis, thermogenesis, glycolysis and raises plasma glucose concentrations by stimulating glycogenolysis and gluconeogenesis. Metabolism is primarily in the liver, along with kidneys, skeletal muscle and mesenteric organs. It is degraded into an inactive metabolite vanillylmandelic acid by MAO and COMT and excreted into the urine.

Excretion: It is excreted in urine, excretion products are metanephrine and normetanephrine.

Half-life: Plasma half-life is about 2- 3 minutes.

Mechanism of action: It is a nonselective agonist of all adrenergic receptors, including the major subtypes α_1, α_2, β_1, β_2, and β_3. It acts on α_1 receptors, epinephrine induces increased vascular smooth muscle contraction, pupillary dilator muscle contraction, and intestinal sphincter muscle contraction. High levels of adrenaline cause smooth muscle relaxation in the airways but causes contraction of the smooth muscle that lines most arterioles.

Adverse effects: Hypertension, anxiety, tachycardia, palpitations, headache, diaphoresis, nausea, vomiting, weakness etc

Drug interactions: It may interact with digoxin, diuretics, levothyroxine, chlorpheniramine, beta-blockers, antidepressants, ergot medicines and MAO inhibitors.

Nor-Adrenaline:

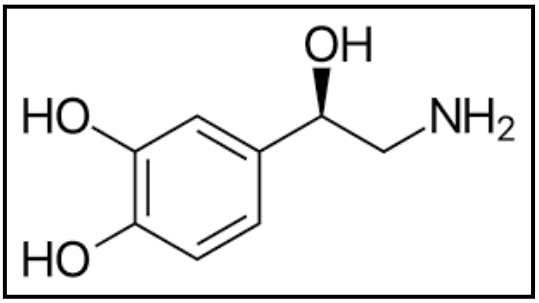

Uses: It is both a neurotransmitter and a hormone and plays an important role in body's fight-or-flight response. It is used to increase and maintain blood pressure in limited, short-term serious health situations. Also used to treat hypotension (low blood pressure) that may occur with certain medical conditions or surgical procedures.

Metabolism: It is metabolized in the liver and other tissues by enzymes catechol-O-methyltransferase (COMT) and MAO with major metabolites normetanephrine and vanillylmandelic acid.

Excretion: It is excreted in urine, major metabolites are normetanephrine and vanillylmandelic acid.

Half-life: By intravenous administration about 1 to 2 minutes.

Mechanism of action: It predominantly stimulates α_1 receptors to cause peripheral vasoconstriction and increase blood pressure. It also acts on β-1 adrenergic receptors, causing increase in heart rate and cardiac output [17].

Adverse effects: Headache, shortness of breath, anxiety, dizziness, irregular heartbeat, urinary retention, blurred vision etc.

Drug interactions: It may interact with monoamine oxidase inhibitors or amitriptyline and imipramine-type antidepressants.

References

[1]. Amado, J., Gago, P., Santos, W., Mimoso, J., & de Jesus, I. (2016). Choque cardiogénico-fármacos inotrópicos e vasopressores. Revista Portuguesa de Cardiologia, 35, 681-695.

[2]. Cleveland Clinic. (n.d.). Retrieved from https://my.clevelandclinic.org

[3]. Gordon, S., & Saunders, A. (2016). Positive Inotropes. The Merck Veterinary Manual. Retrieved November 28, 2016, from https://www.merckvetmanual.com

[4]. Berry, W., & McKenzie, C. (2016). Use of inotropes in critical care. Clinical Pharmacist, 2, 395.

[5]. Sherwood, L. (2008). Human Physiology: From Cells to Systems (7th ed.). Cengage Learning.

[6]. Oba, Y., & Lone, N. A. (2014). Mortality benefit of vasopressor and inotropic agents in septic shock: A Bayesian network meta-analysis of randomized controlled trials. Journal of Critical Care, 29(5), 706-710.

[7]. Bhatt-Mehta, V., & Nahata, M. C. (1989). Dopamine and do butamine in pediatric therapy. Pharmacotherapy, 9(5), 303-314.

[8]. De Backer, D., Biston, P., Devriendt, J., Madl, C., Chochrad, D., Aldecoa, C., Brasseur, A., Defrance, P., Gottignies, P., & Vincent, J. L. (2010). Comparison of dopamine and norepinephrine in the treatment of shock. New England Journal of Medicine, 362(9), 779-789.

[9]. Bhatt-Mehta, V., & Nahata, M. C. (1989). Dopamine and do butamine in pediatric therapy. Pharmacotherapy, 9(5), 303-314.

[10]. Drug Bank. (n.d.). Retrieved from https://go.drugbank.com

[11]. RxList. (n.d.). Retrieved from https://www.rxlist.com

[12]. Wilson, W. C., Grande, C. M., & Hoyt, D. B. (2007). Trauma: Critical Care. CRC Press.

[13]. Gentile, P., Marini, C., Ammirati, E., Perna, E., Saponara, G., Garascia, A., et al. (2021). Long-term administration of intravenous inotropes in advanced heart failure. ESC Heart Failure, 8(5), 4322-4327.
[14]. Alhayek, S., & Preuss, C. V. (2023). Beta 1 Receptors. In StatPearls. Stat Pearls Publishing.
[15]. National Center for Biotechnology Information. (n.d.). Retrieved from https://www.ncbi.nlm.nih.gov
[16]. Healthdirect. (n.d.). Retrieved from https://www.healthdirect.gov.au
[17]. Moore, J. I. (2012). Pharmacology (3rd ed.). Springer Science and Business Media.

International Journal of Scientific Research in Science and Technology
Available online at : www.ijsrst.com
OPEN ACCESS
Print ISSN: 2395-6011 | Online ISSN: 2395-602X
doi : https://doi.org/10.32628/IJSRST

Synthesis, Characterization and Antimicrobial Activity of Mn(II) Complexes of N, O Donor Novel Heterocyclic Schiff Base Ligand

D.T. Sakhare

U.G, P.G. & Research Centre, Department of Chemistry, Shivaji, Art's, Commerce & Science College Kannad, Dist. Chhatrapati Sambhajinagar-431103, Maharashtra, India

ARTICLEINFO

Article History :

Published : 07 Dec 2024

Publication Issue :
Volume 11, Issue 23
Nov-Dec-2024
Page Number :
51-61

ABSTRACT

The novel heterocyclic Schiff base ligands derived from 2-amino-4,6-dihydroxypyrimidine and 2-hydroxy-1-naphthaldehyde (L) were synthesized. These ligands were used in the synthesis of Cr(II) complexes. The synthesized compounds were characterized using FT-IR, 1H-NMR and UV-Vis techniques for the ligands, and TLC for all reactions, molar conductivity and magnetic susceptibility measurements for the corresponding ones. The general formula of the complexes is [Mn(L)2(H2O)2]. The complexes are paramagnetic. Molar conductivity measurements showed that all complexes in (DMSO) are not electrolytes. Octahedral geometry of all complexes. The ligands are bidentate (L) due to the phenolic (OH) and azomethine nitrogens. The ligands and their complexes were investigated for antifungal and antibacterial activity against Aspergillus niger, Penicillium chrysogenum, Fusarium moneriforme, Aspergillus flavus, as well as Escherichia coli, Salmonella typhi, Staphylococcus aureus, and Bacillus subtilis. The results showed that the complex exhibited excellent antifungal and antibacterial effects.

Keywords: Schiff base, 2-hydroxy-1-naphthaldehyde, 2-amino-4,6-dihydroxypyrimidine, Antimicrobial activity.

Introduction

The Schiff bases have attracted much attention in recent years due to their extensive biological activity and industrial applications. [1] They are the condensation products of aldehydes (CHO) or ketones (CO) and primary imines (NH_2) in the presence of organic solvents such as methanol, ethanol, and tetrahydrofuran (THF) at specific temperature and pH conditions [2]. They was first synthesized in 1864 by Hugo Schiff and named Schiff after him [3]. They contain an imine unit (HC=N-) of the general formula RN = CR`R" (azomethine group), where R, R`, and R" are variously substituted alkyl, aryl, heteroaryl, or cycloalkyl groups, etc. [4]. These compounds are extra typically called aniline, imines, or azomethines. Schiff bases may be important in

various fields of chemistry (bioinorganic, biomedical, supramolecular, catalysis and materials, etc.) and can be synthesized by selecting appropriate derivatives of amines and aldehydes or ketones with the required functional groups.The wide range of applications of Schiff basesinclude corrosion inhibitors, catalyst supports, thermostable materials, ligands for metal coordination, and biological or pharmacological systems. [5] Biologically active Schiff bases show antibacterial, anticancer, antifungal, and free radical scavenging properties in addition to enzyme intermediates or inhibitors. [6] The wide spectrum of biological activity of these compounds is due to their unique role as the azomethine group has a lone pair of electrons in the sp^2 hybrid orbital of the nitrogen atom. In addition, the electrophilic carbon and nucleophilic nitrogen of the imine bond (-C=N-) produce well-bound compounds with various nucleophiles and electrophiles, inhibiting target diseases, enzymes, or DNA replication. [7-9] Overall, they are characterized by simple synthesis techniques, versatility, and wide range of applications. Heterocyclic compounds are important for the synthesis of Schiff bases due to their wide range of applications in biology, chemistry , agricultural chemistry, and crop protection.[10-13] Thus, the numerous physicochemical properties and various reactions of heterocyclic compounds prove that they are an important part of heterocyclic chemistry. Similarly, heterocyclic Schiff bases have also attracted considerable attention due to their versatile applications. Pyrimidine, an organic heterocyclic compound, is composed of a six-membered unsaturated ring structure with two nitrogen atoms at the 1- and 3-positions and is one of the most versatile synthetic substrates for pharmaceutical synthesis [14].

They are recognized as basic components of nucleic acids in the form of nitrogenous bases (cytosine, thymine, and uracil) and are used as precursors for the synthesis of biologically active molecules. [15-17] Pyrimidine-derived Schiff bases act pharmacologically as analgesics, antiepileptics, antivirals, anti hypertensives, minoxidil, antimycobacteria, anticancer, and antimalarials, and as potent phosphodiesterase inhibitors. [18-20] Therefore, researchers are interested in developing and synthesizing pyrimidine-derived Schiff bases using condensation methods with appropriate aldehydes or ketones. The technique of molecular docking is widely used in modern drug discovery to understand drug-receptor interactions. This method has been widely used to predict the binding affinity and orientation of drug small molecules at their target sites in proteins [21]. Binding can occur in several possible conformations, called binding modes. [22] Accurate structural modeling and accurate prediction of activity of drug molecules are the two main objectives of this research.[23] Bioinformatics and computational biology tools have been used for computer-aided drug design and virtual screening of large databases of natural compounds, which have accelerated the process of traditional drug design.[24, 25]

In this study, Schiff base ligands derived from 2-amino-4,6-dihydroxypyrimidine and 2-hydroxy-1-naphthaldehyde (L) with transition metals were synthesized. Furthermore, the structures of the prepared ligands were verified using FT-IR, ^{1}H-NMR, and UV-Vis techniques, and the prepared complexes were characterized using FT-IR, UV-Vis, molar conductivity and magnetic susceptibility measurements.

Experimental Section:

2.1. Materials:

Chemicals and reagents used in this study 2-Hydroxy-1-naphthaldehyde, 2-amino-4,6-dihydroxypyrimidine, $Mn(NO_3)_2{\cdot}2H_2O$ were purchased from Sigma-Aldrich Chemical Company.

2.2. Instrumentation:

IR spectra were recorded on a FTIR (ATR)-BRUKER-TENSOR37 spectrometer using KBr pellets in the range of 4000-400 cm^{-1}. ^{1}H NMR (modified mercury 300 MHz) spectra of the ligands were measured in DMSO using TMS as internal standard. X-RD was recorded on a BRUKER D8 Advance. TGA-DTA was recorded on a

Shimadzu. Carbon, hydrogen and nitrogen contents were measured on a SHIMADZU Elemental model Vario spectrometer. The molar conductivity of the complexes was measured with an Elico CM 180 conductivity meter using 10^{-4} M solutions in DMSO. Magnetic susceptibility measurements of metal chelates were performed on a Guoy balance at room temperature using $Hg[Co(SCN)_4]$ as a calibration agent.

2.3. Procedures:

2.3.1. Synthesis of schiff base ligand (L):

The ligand was prepared by modifying the method described [26]. The Schiff base ligand was prepared by refluxing a mixture of 0.01 mol (1.2015 g) 2-hydroxy-1-naphthaldehyde and 0.01 mol (1.2710 g) 2-amino-4,6-dihydroxypyrimidine in 50 mL of refluxed synthetic ultra-dry ethanol for about 4 hours. The Schiff base thus formed was cooled to room temperature, collected by filtration, then recrystallized in ethanol and dried in vacuum over anhydrous calcium chloride (yield: 74%).

2.3.2. Synthesis of metal complexes$[M(L)_2]$:

Ligand (2 mol) and metal nitrate (1 mol) (25 ml) were added to a hot ethanol solution (25 ml) under constant stirring. The pH of the reaction mixture was adjusted to 7-8 by adding 10% ammonia alcohol solution and refluxed for about 3 hours. The precipitated solid metal complex was filtered off while hot, washed with hot ethanol, and dried over calcium chloride in a vacuum desiccator. (Yield: 88%) [27].

Results And Discussion:

Some physical properties of Schiff base ligands and their metal complexes are shown in (Table 1).

Table 1: Physical properties of Schiff base ligands (L_1) and their metal complexes.

Compound Molecular formula	Mol.Wt.	M.P. Decomp temp. 0C	Colour	Molar Conduc. Mho. Cm^2mol^{-1}
L	283	220	Yellow	---
Mn-L	628	>300	Dark Brown	10.25

Table: 2. Elemental Analysis of Cr(II) Complex

Compound	% Found (Calculated)			
	C	H	N	M
L	51.54 (53.21)	3.57 (3.85)	16.64 (16.89)	----
Mn-L	44.43 (44.35)	3.37 (3.29)	14.17 (14.15)	9.90 (9.88)

3.1. ^{1}H-NMR spectra of ligand:

The ^{1}H NMR spectrum of the free ligand at room temperature shows the following signals: 5.8 δ (s, 2H, phenolic (OH) hydrogen of the pyrimidine ring), 6.68 δ (s, 1H, hydrogen attached to the pyrimidine ring), 7.95 δ (s, 1H, hydrogen attached to the azomethine carbon), 7.68-7.29 δ (D, 4H, aromatic Ha, Hb, protons of the phenyl ring).

3.2. IR Spectra:

The IR spectra of the free ligands in Figures 2 and 3 show characteristic bands at 3428, 1654, 1486, 1209, and 1038 cm^{-1}, which can be assigned to the stretching vibrations υOH (intramolecular hydrogen bond), υ C=N (azomethine), υ C=C (aromatic), υ C-N (arylazomethine), and υ C-O (enolic) [24]. The absence of weak broad bands in the region of 3200-3400 cm^{-1} in the spectra of the metal complexes suggests the deprotonation of the intermolecular hydrogen bond OH groups upon complex formation and subsequent coordination of the phenolic oxygen to the metal ion. This is further supported by the downward shift of υ C-O (phenolic) [28] compared to the free ligand. Upon complexation, the υ (C=N) [29] band shifts to lower wave numbers relative to the free ligand, indicating that the nitrogen of the azomethine group is coordinated to the metal ion. The υ C-N band shifts to lower wave numbers relative to the free ligand. The IR spectra of the metal chelates show new bands in the range of 500-600 cm^{-1} and 400-500 cm^{-1}, which can be assigned to the υ M-O and M-N vibrations, respectively [30]. The IR spectrum of Ni(II) shows a strong band in the 3050-3600 cm^{-1} region, indicating the presence of coordinated water in these metal complexes. The presence of coordinated water is further confirmed by the appearance of a nonligand band in the 830-840 cm^{-1} region, which can be assigned to the rocking mode of water. The presence of coordinated water is also evidenced and supported by TG/DTA analysis of these complexes. Therefore, it is concluded that coordination occurs via the phenolic oxygen and azomethine nitrogen of the ligand molecules in Table 3 below.

Table: 3 Salient features of IR spectral data of ligands & Metal complex

Bond vibrational modes	O-H Free Stretching(□)	C = N Azomethine Stretching(□)	C = C Aromatic ring stretching(□)	C -- N Aryl azomethine stretch (□)	C -- O Enolic stretching (□)	M--O	M--N
L	3428	1654	1486	1209	1038	--	--
Mn-L	3625.55	1633.23	1351.21	1290.22	1130.31	561.30	451.23

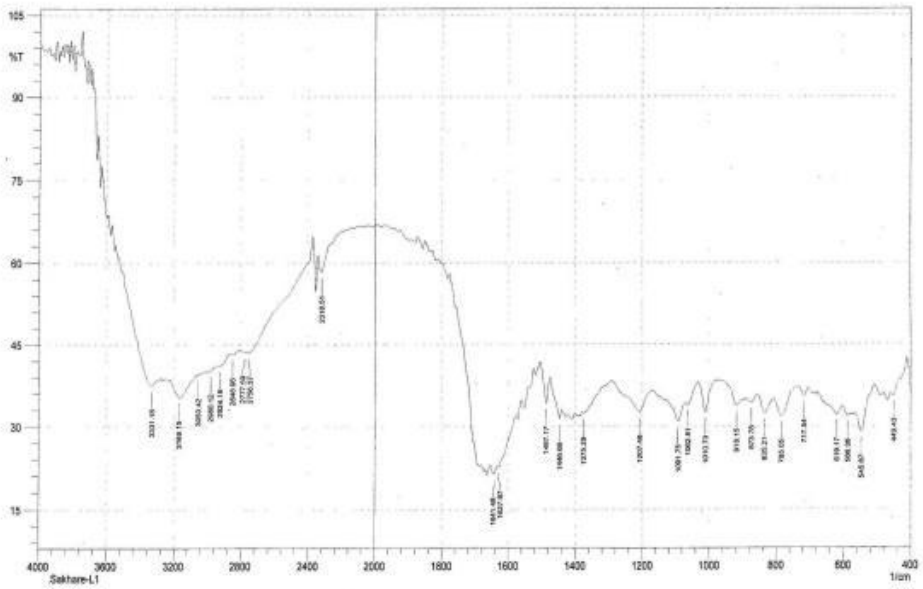

Fig. 2 Infrared Spectra of Ligand L

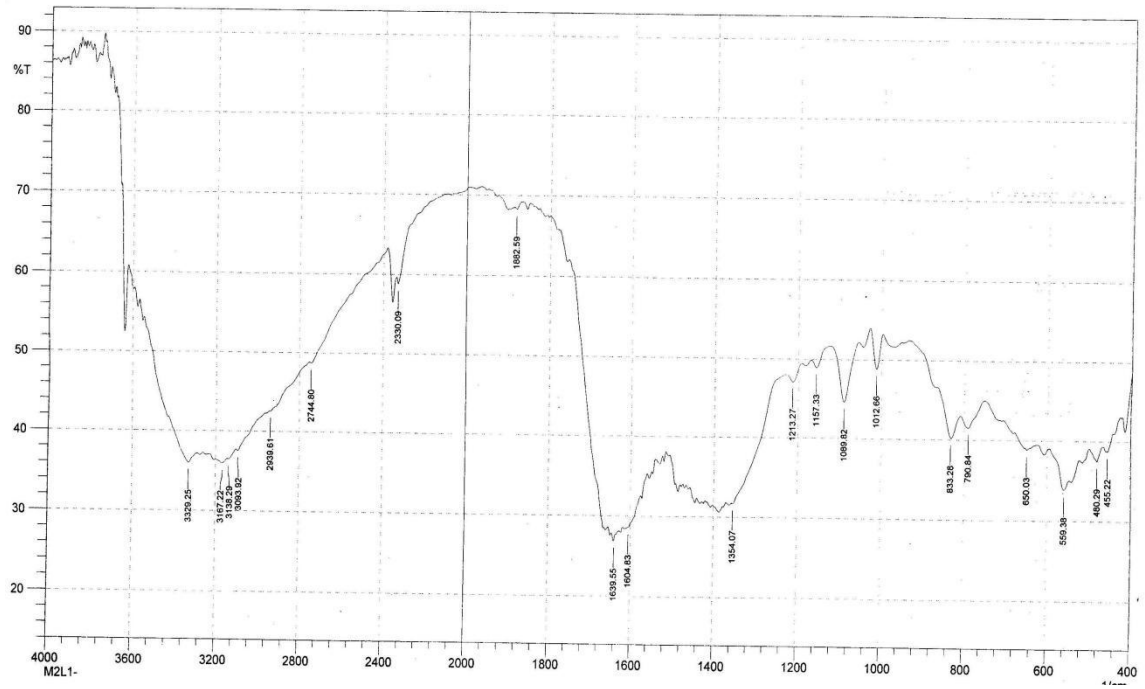

Fig. 3 Infrared Spectra of Mn(II) Complex of Ligand L

3.3. Molar conductance measurements:

Conductivity measurements of the complexes were recorded for (10^{-3} M) and the sample solutions were in room temperature (DMso). The molar conductivity values of the complexes are shown in (Table 4). From the results, it was concluded that the Mn(II) complexes of ligand (L) have molar conductivity values in the range of (10.5-22.4 Ω^{-1} mol^{-1} cm^2). This suggests that the complexes are non-ionic and therefore can be considered as non-electrolytes [31].

3.4. Magnetic susceptibility:

The effective magnetic moment values of metal complexes are summarized in (Table 1). The values were measured at room temperature. The range of (μ_{eff}) for the complex [Mn(L)] is (2.81 to 3.97 B.M). This value is within the range of the octahedral geometry [32].

3.5. Thermogravimetric analysis:

Thermal decomposition studies of the complexes were carried out to confirm the information obtained from the IR spectroscopy studies and to determine the presence of water molecules in these complexes and their decomposition pattern. Simultaneous TGA/DTA analysis of Mn(II) was studied from ambient temperature to 10,000 °C in nitrogen atmosphere using α-Al_2O_3 as a reference. Analysis of the thermograms of the complexes revealed that the Mn(II) complexes (Figure 4) exhibit a two-stage decomposition. The initial weight loss is 6.68 0% between temperatures. 55-2300 °C may be related to the loss of two adjusted waters (calculated 6.02%). The anhydrous compound is not stable at high temperatures. In the range of 230-650 °C, it decomposes rapidly with a mass loss of 79.73%, which corresponds to the decomposition of the complex in the second stage (calculated 80.71%).

The decomposition is complete with the formation of a stable residue of the metal oxide MnO (13.13% (calculated) was observed). 13.29%). Kinetic and thermodynamic values, i.e., activation energy (Ea), frequency coefficient (Z), entropy change (-ΔS), and free energy change (ΔG) for the nonisothermal decomposition of h.complexes, were determined using the Horowitz-Metzger method [33]. The values are shown in Table 3. The calculated values of the given activation energies of the complexes are relatively low, indicating the

autocatalytic effect of metal ions on the thermal decomposition of the complexes. The negative values of the activation entropy indicate that the activated complexes are more ordered, rather than slower in reaction. The stronger order may be due to the polarization of bonds in the activated state, which may occur through charge transfer transitions [34].

Table 4 The kinetic and thermodynamic parameters for decomposition of metal complexes

Complex	Step	Decomp. Temp. (^{0}C)	n	Ea (kJmole^{-1})	Z (S^{-1})	ΔS (JK^{-1}mole^{-1})	ΔG (kJmole^{-1})	Correl -ation coeffici-ent
Mn-L	I	431	0.9	10.42	1.26×10^4	-173.57	25.09	0.970

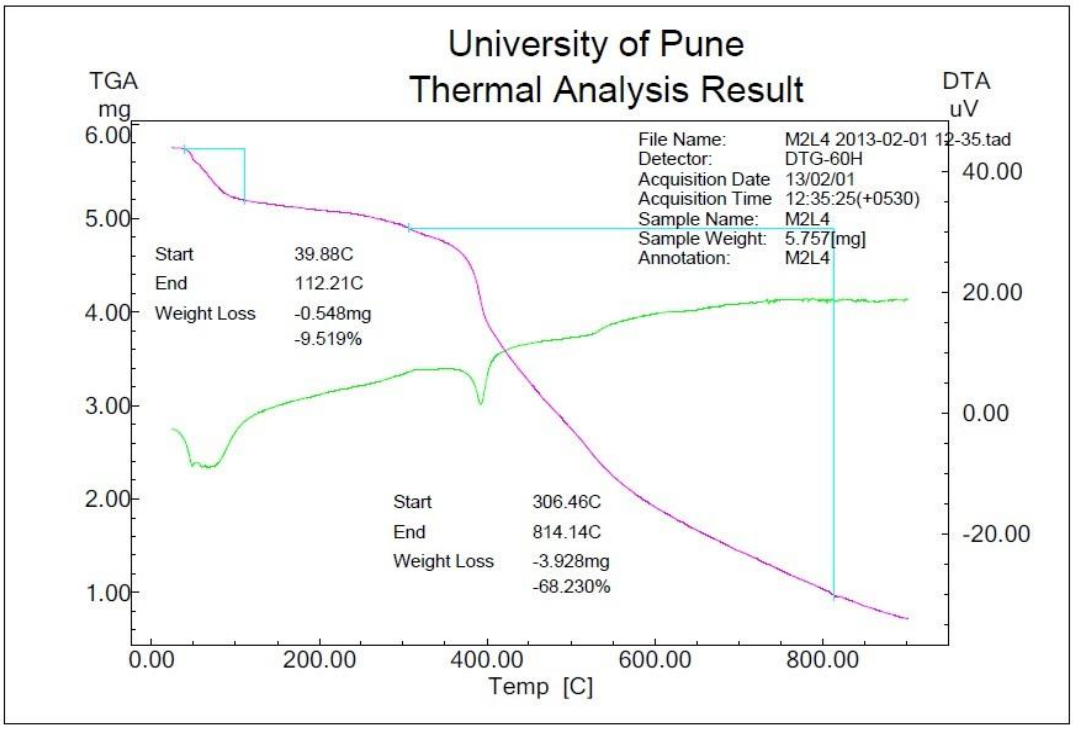

Fig. 4 TGA-DTA Curve of Mn(II) Complex of Ligand L

3.6. Electronic Spectra:

The electronic spectrum of the Schiff base ligand (L) shows absorption bands at (42555 cm^{-1} and 27028 cm^{-1}), which are due to the transitions ($\pi \rightarrow \pi^*$) and ($n \rightarrow \pi^*$), respectively. The Mn(II) complex shows a band at (42555 cm^{-1}) due to the transition ($\pi \rightarrow \pi^*$). The band at (23256 cm^{-1}) is due to charge transfer (C.T) and the band at (14815 cm^{-1}) is due to the transition $^3A_{2g} \rightarrow {}^3T_{2g}$. The complex has an octahedral geometry [35].

3.7. X – Ray Diffraction Studies of Metal Complexes:

The Mn(II) complexes of ligands L were selected for powder X-ray diffraction studies (Figure 5). The X-ray powder data of all major peaks were indexed individually using a trial and error method. The unit cell data, crystal lattice parameters, and data obtained after indexing of the powder data are shown in Table 4. The Mn(II) complex of ligand L shows 14 reflections with a maximum at $2\theta = 9.77°$, corresponding to a d-value of 4.54 Å.

The unit cell values of the lattice parameters are a = 6.8760 Å, b = 9.2456 Å, c = 24.234 Å, α = β = 90°, γ = 120°, unit cell volume V = 1334.21763 (Å) ^{3}.

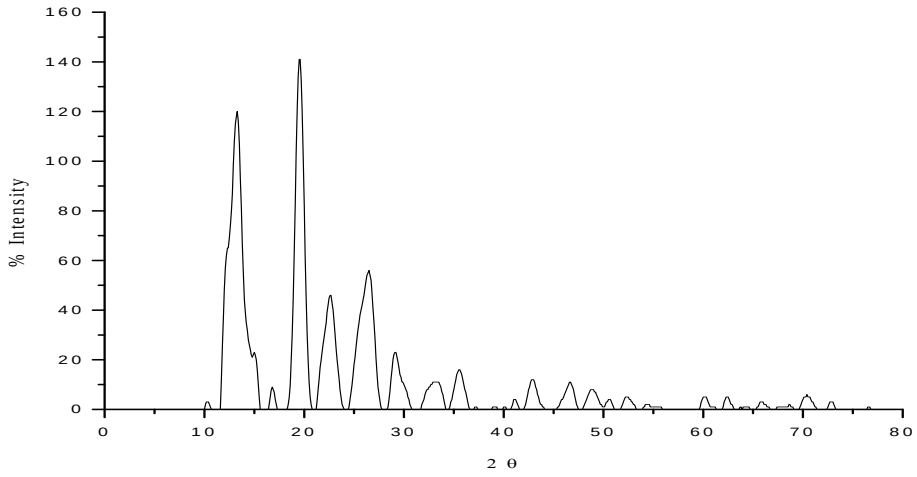

Fig. 5 X-ray Diffractogram of Mn (II) complex of L

Table: 4 Indexed X-ray Diffraction Data of Mn(II) Complex of Ligand L

Peak No.	2θ (observed)	2θ (calculated)	d (observed)	d (calculated)	Miller indices of Planes			Relative intensities (%)
					h	k	l	
1	6.49527	6.49993	6.80483	6.80464	-1	0	1	100.00
2	11.91296	11.91217	3.73022	3.73185	-1	3	0	2.24
3	16.56698	16.57711	2.7008	2.69991	2	0	4	12.74
4	19.22149	19.22346	2.33924	2.33953	2	2	2	17.75
5	25.96779	25.97817	1.75893	1.75856	-3	5	5	5.76
6	29.5445	29.55077	1.56194	1.56186	4	1	4	8.57
7	31.37724	31.37821	1.47925	1.4794	-1	2	10	4.04
8	35.13069	35.12972	1.33847	1.33865	-6	1	1	2.51
9	36.34332	36.35103	1.29968	1.29958	-6	1	3	2.93

Unit cell data and crystal lattice parameter

a (A⁰) = 8.765 Volume(V) = 1308.53064 (A⁰) ^{3}

b (A⁰) = 11.234 Density(obs.) = 1.0788 gcm^{-3}

c (A⁰) = 15.345 Density(cal.) = 1.0678 gcm^{-3}

α = 90.00 Z = 3

β = 90.00 Crystal system = Monoclinic

γ = 120.00 Standard deviation (%) = 0.016 Porosity = 1.03%

Biological Activity :

4.1. Antibacterial activity & Antifungal Activity:

The antifungal and antibacterial activities of the ligands and metal complexes were tested in vitro against fungi such as *Aspergillus niger, Penicillium chrysogenum, Fusarium moneriforme, Aspergillus flavus,* and bacteria

such as *Escherichia coli, Bacillus subtilis, Staphylococcus aureus, and Bacillus subtilis,* using paper disc and plate methods [36]. The compounds were tested at concentrations of 1% and 2% in DMSO and compared with known antibiotics, namely *griseofulvin* and *penicillin* (Tables 5 and 6). Tables 5 and 6 show that the inhibition by the metal chelates is higher than that by the ligands, a result that is in good agreement with previous findings of comparable activity of the free ligands and their complexes [37, 38]. This increase in activity of the metal chelates is due to the increased lipophilicity of the metal ions in the complexes. The increase in activity with concentration is due to the effect of the metal ions on normal cellular processes. The action of the compounds may involve the formation of hydrogen bonds with active sites on cellular components, resulting in the disruption of normal cellular processes.

Table 5. Antifungal activity of ligands

Test Compound	Antifungal Growth							
	Aspergillus niger		*Penicillium chrysogenum*		*Fusarium moneliforme*		*Aspergillus flavus*	
	1%	2%	1%	2%	1%	2%	1%	2%
L	-ve	-ve	-ve	-ve	-ve	-ve	-ve	-ve
Mn-L	-ve	-ve	-ve	-ve	-ve	-ve	-ve	-ve
+ve control	+ve	+ve	+ve	+ve	+ve	+ve	+ve	+ve
-ve control (Griseofulvin)	-ve	-ve	-ve	-ve	-ve	-ve	-ve	-ve

Ligand& Metal : +ve – Growth (Antifungal Activity absent)

-ve - Growth (Antifungal Activity present)

RG - Reduced Growth (More than 50% reduction in growth observed)

Table 6. Antibacterial activity of ligands and their metal complexes

Test Compound	Diameter of inhibition zone (mm)							
	E. coli		*Salmonella typhi*		*Staphylococcu saureus*		*Bacillus subtlis*	
	1%	2%	1%	2%	1%	2%	1%	2%
L	-ve	12mm	-ve	14mm	-ve	18mm	-ve	19mm
Mn-L	13mm	14mm	13mm	15mm	17mm	21mm	12mm	15mm
DMSO	-ve	-ve	-ve	-ve	-ve	-ve	-ve	-ve
Penicillin	14mm	14mm	18mm	18mm	31mm	31mm	19mm	19mm

Ligand & Metal: - ve - No Antibacterial Activity

Zone of inhibition - --mm

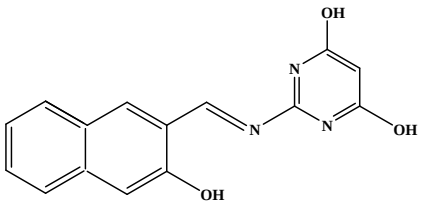

Fig. 6 Structure of Ligand L

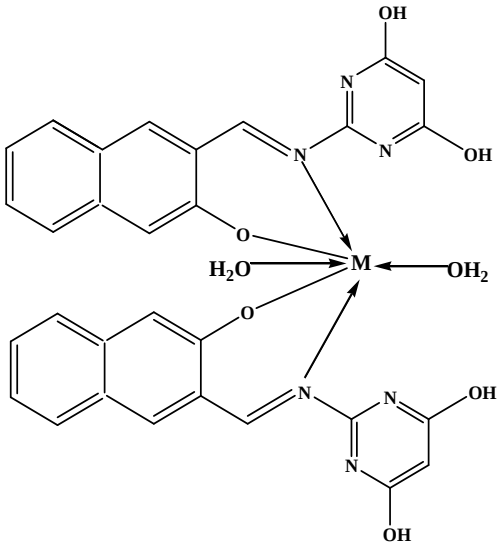

Fig. 7. The proposed Structure of the Metal complexes. [When M= Mn (II)]

Conclusion:

In light of the above discussion, we have proposed an octahedral geometry for the Mn(II) complex. Based on the physicochemical and spectral data discussed above, it can be hypothesized that the ligand behaves like a dibasic bidentate NO, coordinating through the phenolic oxygen and the imino nitrogen, as shown in Figure 7. The complex is biologically active and exhibits enhanced antibacterial activity compared to the free ligand. Thermal studies indicate the thermal stability of the complex. X-ray studies suggest a monoclinic crystal system for the Mn(II) complex.

Acknowledgement:

The authors thank Advanced Analytical Instrumentation Facility (SAIF) and Advanced Testing Equipment Centre (STIC), Kochi for providing elemental analysis (CHN). They are also grateful to the Department of Chemistry, University of Pune for providing IR, NMR spectroscopy and TGA-DTA facilities, Department of Physics, University of Pune for providing X-RD facilities, and Department of Microbiology, N.S.B. College, Nanded for providing antibacterial and antifungal activity.

References

[1]. D.T.Sakhare, Synthesis, characterization of some transition metal complexes of bidentate Schiff base and their antifungal and antimicrobial studies,Advances in Applied Science Research, 2015, 6(6):10-16.

[2]. C. Chandramouli, M.R. Shivanand, T.B. Nayanbhai, B. Bheemachari, R.H. Udupi, Synthesis and biological screening of certain new triazole schiff bases and their derivatives bearing substituted benzothiazole moiety, J Chem Pharm Res, 2012, 4, 1151-1159.

[3]. D. T. Sakhare, Synthesis, Characterization and Antimicrobial Activity of Schiff Base Derived from 2-Hydroxybenzaldehyde with 2-Amino-4,6-Dimethylpyrimidine And Their Transition Metal Complexes, GIS Science Journal, 2022, 9(4), 82-94.

[4]. R.Sliverstien, G.Bassler, T.Morrill, Spectrometric Identification of Organic Compounds. 7thaddition, John Wiley, New York, 2005

[5]. D.T.Sakhare, Copper Metal Complexes of a Pyrimidine Based Schiff Base Ligand Synthesis, Characterization and Biological Activity, Journal of Xidian University, 2022, 16(3), 191-201.
[6]. D.T.Sakhare, Synthesis, Characterization And Biological Studies of Aminopyrimidine Schiff Bases And Their Transition Metal Complexes, Dickensian Journal, 202,22(4),65-77.
[7]. D.T. Sakhare, Synthesis, characterization and biological activities of new bidentate Schiff base ligand and their Co (II) metal complexes , 2024, Materials Today: Proceedings,online.
[8]. Harshalata D., Dhongade H.J., Kavita C., Pharmacological potentials of pyrimidine derivatives: A review, Asian J. Pharm. Clin. Res., 2015, 8, 171-177.
[9]. D.T.Sakhare, Synthesis, Characterization and Antimicrobial Activity of Cu(II) Complexes Derived from Heterocyclic Schiff Bases Ligands, Asian Journal of Organic & Medicinal Chemistry, 2022, 7(2),41-47.
[10]. Rana K., Kaur B., Kumar B., Synthesis and antihypertensive activity of some dihydropyrimidines, Indian J. Chem. B, 2004, 43, 1553–1557.
[11]. Atkins M., Jones C.A., Kirkpatrick P. Sunitinib maleate. Nat. Rev. Drug Discov., 2006. 5, 279-280.
[12]. D.T. Sakhare, Synthesis, Characterization And In-Vitro Biological Activities of Novel Bidentate Schiff Base Ligand And Their Cobalt (II) Complexes. Juni Khyat ,2023, 13(07), No.03, 134-143.
[13]. Ramaling S., Belani C.P., Role of bevacizumab for the treatment of non-small-cell lung cancer. Future oncology, 2007, 3, 131-139.
[14]. Harris P.A., Boloor A., Cheung M., Kumar R., Crosby R.M., Davis-Ward R.G., et al., Discovery of 5-[[4-[(2,3-dimethyl-2Hindazol-6-yl)methylamino]-2-pyrimidinyl] amino]-2-methylbenzenesulfonamide (Pazopanib), a Novel and potent vascular endothelial growth factor receptor inhibito, J. Med. Chem., 2008, 51, 4632-4640.
[15]. D.T. Sakhare, Synthesis,Characterization and Biological Activity of New Schiff Bases Derived from Aminopyrimidine and Their Metal Complexes, International Journal of Scientific Research in Science and Technology, 2022, 9(17), 160-173.
[16]. Lascombe M.B., Ponchet M., Venard P., Milat M.L., Blein J.P., Prange T., The 1.45 A resolution structure of the cryptogeincholesterol complex: a close-up view of a sterol carrier protein (SCP) active site, Acta Crystallogr. Sect. D, 2002. 58, 1442-1447.
[17]. Kappe C.O., 100 years of the biginelli dihydropyrimidine synthesis, Tetrahedron, 1993, 49, 6937-6963.
[18]. Espinet P., Esteruelas M.A., Oro L.A., Serrano J.L., Sola E., Transition metal liquid crystals: advanced materials within the reach of the coordination chemist, Coord. Chem. Reviews, 1992, 117, 215-274.
[19]. D.T. Sakhare, Synthesis, Characterization of some Cu (ii) complexes of bidentate Schiff base and their antimicrobial studies, Journal of Medicinal Chemistry and Drug Discovery, 2016, 2(1), 583-597.
[20]. Osowole A.A., Festus C., Synthesis, Characterization,antibacterial and antioxidant activities of some heteroleptic metal(II) complexes of 3-{[-(pyrimidin-2-yl) Imino]methyl} napthalen-2-ol, J. Chem. Bio. Phy. Sci., 2015, 6, 080-089.
[21]. Sönmez M., Sogukomerogullari H. G., Öztemel F.,Berber İ., Synthesis and biological evaluation of a novel ONS tridentate Schiff base bearing pyrimidine ring and some metal complexes, Med. Chem. Res., 2014, 23, 3451–3457.
[22]. Gulcan M., Özdemir S., Dündar A., Ispir E., Kurtog˘lu M., Mononuclear complexes based on pyrimidine ring azo Schiff-Base ligand: synthesis, characterization, antioxidant, antibacterial, and thermal investigations, Z. Anorg. Allg. Chem, 2014, 640, 1754-1762.

[23]. D.T. Sakhare, Synthesis, Characterization And Antimicrobial Studies of Some Transition Metal Complexes of Schiff Bases, International Journal of Current Research In Chemistry And Pharmaceutical Sciences, 2015, 2(6), 28–34.
[24]. D.T. Sakhare, Synthesis, characterization and antimicrobial activities of some transition metal complexes of biologically active bidentate ligands, Inorganic Chemistry An Indian Journal, 2015,10(4), 142-147.
[25]Tetteh S., Dodoo D.K., Appiah-Opong, R., Tuffour, I., Spectroscopic cha racterization, in vitro cytotoxicity, and antioxidant activity of mixed ligand palladium(II) chloride complexes bearing nucleobases, J. Inorg. Chem., 2014. 2014, 7 pages, Article ID 586131, doi:10.1155/2014/586131
[25]. D.T. Sakhare, Synthesis, characterization and in-vitro biological activities of Co (II) complexes of 2-(4-Methaylbenzylideneamino) Pyrimidine-4, 6-Diol. Current Pharma Research. 2019, 9(4), 3335-3344.
[26]. D.T. Sakhare, Synthesis, Spectral, Thermal And Antimicrobial Activities of Mn (II) And Fe (III) Schiff Base Metal Complexes. International Journal of Current Research In Chemistry And Pharmaceutical Sciences, 2(7), (2015), 1-8.
[27]. A A Osowole1, R Kempe , R Schobert and S A Balogun , Candian journal of pure and applied sciences ,2010; 4(2) 1169-1178.
[28]. A A Osowole . and R O Yoade , Scientific Journal Of Applied Research . 2013; 4: 101-106
[29]. D. T. Sakhare , (2015), Synthesis, characterization and antimicrobial activities of some Mn(II) and Fe(III) complexes of biologically active bidentate ligands, Journal of Chemical and Pharmaceutical Research, 7(6), 198-204
[30]. M Usharani. E Akila, And R Rajavel. International Journal of Recent Scientific Research ,2013; 4(9): 1385-1390.
[31]. J.A. Dean, Lange's Hand Book of Chemistry, 14th ed., Megraw-Hill, New York,1992, p. 35.
[32]. Housecroft, C.E., Sharpe, A.G.: Inorganic Chemistry, 2nd edn.Pearson, England (2005).
[33]. D.T. Sakhare, (2015), Synthesis, Characterization And Antimicrobial Studies of Some Transition Metal Complexes of Schiff Bases, International Journal of Current Research In Chemistry And Pharmaceutical Sciences, 2(6), 28–34.
[34]. Avaji P G, Reddy B N and Patil S A, Trans. Met. Chem., 2006, 31, 842.
[35]. D.T.Sakhare, .Synthesis,Characterization And Antimicrobial Studies On Schiff Base Derived From 2-Amino 4,6- Dihydroxypyrimidine And Benzaldehyde And Its Cobalt Complexes, International Journal of Food And Nutrition Science, 11(S1), 2022, 970-982.
[36]. D. T. Sakhare, (2015), Syntheses, characterization of some transition metal complexes of bidentate schiff base and their antimicrobial activities, Der Chemica Sinica, 6(6):1-6.
[37]. D.T. Sakhare, Synthesis, characterization and antimicrobial activities of some Mn(II) and Fe(III) complexes of biologically active bidentate ligands, Journal of Chemical and Pharmaceutical Research, 2015, 7(6), 198-204.

International Journal of Scientific Research in Science and Technology
Available online at : www.ijsrst.com
Print ISSN: 2395-6011 | Online ISSN: 2395-602X
doi : https://doi.org/10.32628/IJSRST

Polymer Modified Superhydrophobic/Superoleophilic Surfaces for Oil-Water Separation: A review

Mehejbin R. Mujawar[1], Deepak A. Kumbhar[2], Shivaji R. Kulal[1]*

[1]Department of Chemistry, Raje Ramrao Mahavidyalaya, Jath Dist.- Sangli, Maharashtra, India

[2]Department of Chemistry, Dattajirao Kadam Arts, Science and Commerce College, Ichalkarnji, Dist.- Kolhapur, Maharashtra, India

ARTICLEINFO

Article History :

Published : 07 Dec 2024

Publication Issue :
Volume 11, Issue 23
Nov-Dec-2024
Page Number :
62-69

ABSTRACT

The objective of this review is highlighting recent advances in the application of SiO2 based polymer nanocomposite surfaces for oily wastewater treatment. There is a need to develop methods and materials that show excellent ability to separate the oil and organic contaminants from water. The superhydrophobic coated sponges and metal meshes are used to separate oil from oil-water mixture. The various surface modified organic metal oxide nanoparticles are used to develop superhydrophobic surface on porous substrate. Metal-oxide based nanomaterials, including SiO2, TiO2, ZnO, etc. have gained tremendous attention due to their unique mechanical and chemical properties such as micro-hierarchical, hydrophobic, stability, wettability. Among them SiO2 nanoparticle is mostly useful for preparation of superhydrophobic surface. The current challenges for the successful development of SiO2 based nanocomposite surfaces and opportunities for future research are also discussed. This review focused on silica modified porous sponge and metal meshes for scalable oil-water separation application.

Keyword: Metal Mesh, Oil-Water Separation, Porous Sponge and Superhydrophobic.

Introduction

The oil spilling and discharge of industrial organic solvents causes several damages to water resources and aquatic ecosystems [1-3], which became a global problem and need to solve it urgently to save the ecosystems. A new technology in material science has been developed for oil-water separation using superhydrophobic nanomaterial. Superhydrophobic and superoleophilic surfaces shows excellent water repellent and oil absorption ability, water contact angle over 150° and oil contact angle less than 5° [4]. Different chemical methods are used for the fabrication of the superhydrophobic surface for efficient oil-water separation. The

superhydrophobic surface exhibited high selectivity toward different oil and organic pollutants, fast and efficient oil-water separation capability, good repeatability, good reusability, mechanically stable, chemically stable and thermally stable [5-6].

At present, traditional technologies, including in situ burning [7], bioremediation [8], chemical dispersant methods [9], skimming [10], and the use of sorbents [11] are used to clean up spilled oils or organic pollutants. However, many of these strategies involve energy intensive and slow processes, have low clean-up capacities or create secondary pollution during the clean-up process, restricting their widespread practical applications [12-13]. To realize the hierarchical structures on different material surfaces, a series of strategies, such as sol-gel coating [14], chemical vapor deposition [15], plasma etching [16], template processing [17], lithographic patterning [18], etc. have been adopted [19]. The superhydrophobic surfaces on which water achieves water contact angle higher than 150° and sliding angle less than 5° are attracting minds of researchers due to their efficient oil-water separation efficiency [20]. However, the inorganic particles normally used due to the interparticle forces from the Vander Waals, capillary and electrostatic forces, which leads to phase separation during the fabrication process and tends to diminish the quality of the coating through cracks or weak adhesive to the substrates [21-22].

Gao et al. [23] prepared PVDF/SiO_2 coated superhydrophobic porous membranes using a spraying technique. These membranes could be used to separate the oil-water mixtures but are not applicable to surfactant stabilized water-in-oil emulsions because of their large pore sizes. Li et al. [24] prepared the hydrophobic CS by incomplete combustion of hydrocarbons from the middle of a candle flame. The PU sponge was immersed in the solution of CS, SiO_2 and PU resin to achieve stable superhydrophobicity. The CS-SiO_2-PU sponge was shown excellent oil-water separation efficiency. The CS-SiO_2-PU sponge showed excellent oil-water separation efficiency from hot water, acidic solutions, alkaline solutions and salt solutions.

In this review, the sophisticated, facile and low-cost method for fabrication of superhydrophobic porous material for oil-water separation application is discussed. The sponges and metal mesh are used as substrate for scalable oil-water separation application.

Superhydrophobic surfaces for oil-water separation:

2.1. Superhydrophobic SiO_2 Modified Sponges for Oil-Water Separation:

Liu et al. [25] have fabricated a superhydrophobic sponge and polyester coated with SiO_2-DTMS through an entrapment method. The **Fig. 1** reveals the fabrication process of superhydrophobic sponge and polyester. The SiO_2 particles were introduced by growth on the substrate through the polymerization process, followed by the addition of DTMS as an adhesive, leading to a homogeneous and dense superhydrophobic surface. The modified sponge was shown the water contact angle up to 172° indicating the water repellence was superior. This superhydrophobic sample had good hydrophobic stability even in acidic condition and it can show efficient oil-water separation. The amount of the absorbed oil was about 43-65 times of sponge own weight can be shown that the evaluation of the mass based on absorbed surface tension, density, viscosity of absorbed liquids. It shows highly stable and efficient oil-water separation in also harsh chemical condition. The performance remained constant even after 100 recycles.

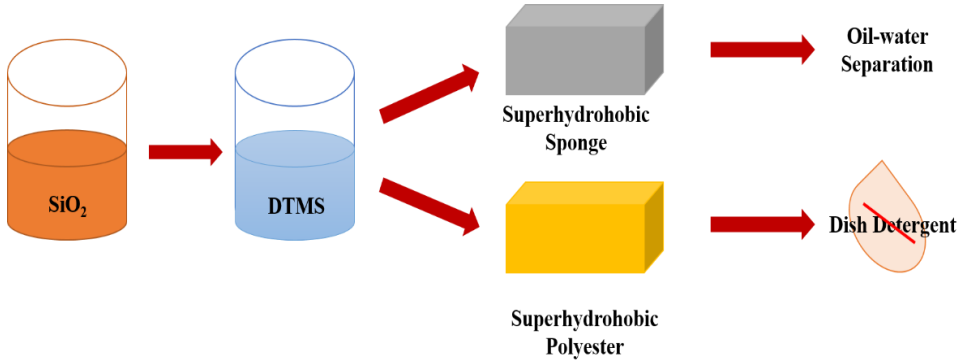

Fig. 1. Schematic illustration of the fabrication of a modified sponge and polyester [25].

Zhang et al. [26] have fabricated the superhydrophobic sponge by using VTMS and SiO_2 via immersion method. The schematic of preparation of superhydrophobic sponge is shown in **Fig. 2**. It was shown a water contact angle of 153° and roll-on angle of 4°. The oil is quickly absorbed by superhydrophobic sponge which have been shown the oil absorption property of a modified superhydrophobic sponge. The IR absorption peak at 1078 cm^{-1} shows the presence of the O-Si-O bond present in the material. It has been shown the high separation efficiency of about 99.5%. It shows good saturated adsorption properties exceeding 70 g/g for all oils. It exhibits outstanding characteristics of superhydrophobic sponge such as high porosity, small pore size and ultra-light mass. After 20 cycles, it was found that the adsorption ability of the modified melamine sponge for different oils decreased slightly.

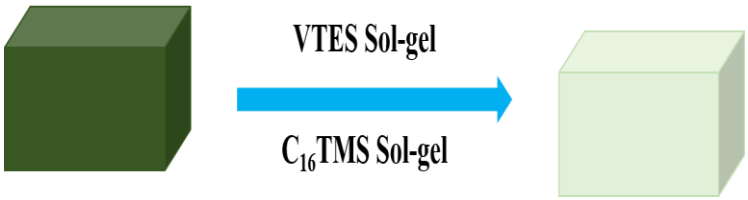

Fig. 2. Schematic illustration of the preparation of superhydrophobic sponge [26].

Chen et al. [27] developed a facile, economical, efficient strategy for environmentally friendly, mechanically robust, and transparent superhydrophobic surfaces. To make the surface, adhesive 75 was sprayed for 3 seconds on stainless steel surfaces then the modified SiO_2 suspension was sprayed on the adhesive-modified stainless steel for 6 seconds. Simply repeating the spraying cycles, a ferro concrete- structured superhydrophobic coating on the stainless steel can be obtained after drying in air for 5 minutes. The fabrication process is demonstrated in **Fig. 3**. The water droplets stayed in spherical shape on the as-prepared glass slide with a WCA of ~160°. The coated glass slide with six spraying cycles retained its superhydrophobic property (WCA>150° and SA<10°) even after 325 abrasion cycles with sandpaper, displaying great mechanical abrasion resistance. They also coated sponges with the adhesive and modified SiO_2, which showed great water/oil separation performance.

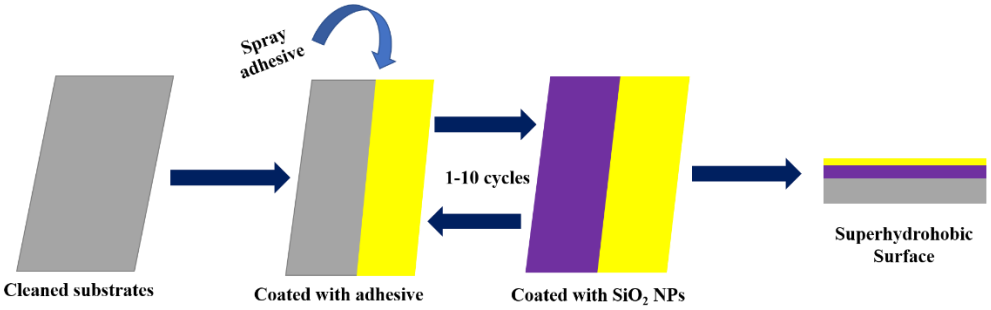

Fig. 3. Schematic illustration of the fabrication procedure of the superhydrophobic surface [27].

2.2. Superhydrophobic SiO2 Modified Metal Meshes for Oil-Water Separation:

Wang et al. [28] fabricated superhydrophobic stainless steel mesh using hydrophobically modified dual scale silica-coated polystyrene (PS) particles. At first, PS particles were coated with silica by Stober method using TEOS as a precursor. The obtained dual scaled silica-coated PS particles were modified with hexadecyltrimethoxysilane (HDTMS) and drop casted on stainless steel (SS) mesh to attain rough hierarchical surface with good oil-water separation capability. The modified superhydrophobic stainless steel mesh is showing very efficient oil-water separation ability. The superhydrophobic mesh can also be mounted on a glass beaker to form an oil-skimmer device; for this oil-skimmer device, the superhydrophobic mesh realizes highly efficient floating oil removal by filtration, while the bottom container achieves stable oil storing with an improved collection capacity seen in **Fig. 4.**

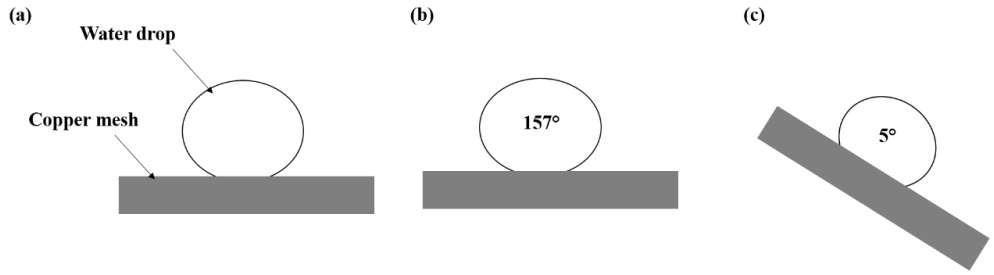

Fig. 4. Schematic illustration of optical image (a), contact angle profile (b), and sliding angle profile (c) of a water droplet placed on the superhydrophobic mesh [28].

Liu et.al. [29] prepared the candle soot was collected on the surface of stainless-steel mesh by placing the mesh above the wick of candle. The chemical vapour deposition method is used to form superhydrophobic stainless steel mesh. Modify this stainless-steel mesh by using PFOTS and PDDA-PFO respectively to form the superhydrophobic/superoleophilic stainless steel mesh. This modified superhydrophobic stainless steel mesh exhibits excellent repellence for all the tested strong acids, strong bases and saturated salts, indicating a good stability of modified mesh. The separation efficiencies obtained repeatedly even after 15 cycles. Both superhydrophobic and superoleophilic modified stainless steel mesh membranes shows stability, durability and reusability. The SiO_2/Carbon modified stainless steel mesh indicates good material for treating real oil-polluted water in different practical applications as well as in oil spill clean- up seen in **Fig. 5.**

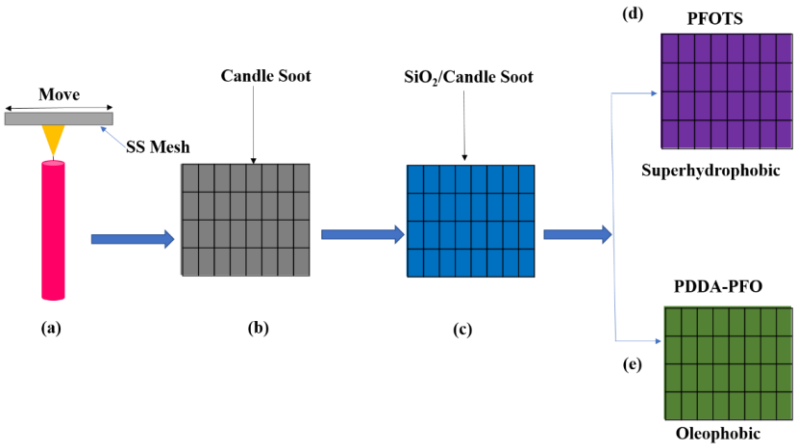

Fig. 5. Schematic illustration of process of superhydrophobic and Oleophobic mesh membranes preparation: (a) coating stainless steel mesh with carbon nanoparticle (candle soot), (b) carbon nanoparticle coated stainless steel mesh, (c) SiO_2/carbon stainless steel mesh, (d) PFOTS modified SiO_2/carbon stainless steel mesh, (e) PDDA–PFO modified SiO_2/carbon stainless steel mesh [29].

Xiong et al. [30] have prepared SiO_2 nanoparticles by an improved modified method by using TEOS and then coated on a stainless-steel mesh by spraying method to fabricate SiO_2 coated stainless steel mesh. The prepared superhydrophobic mesh was shows good mechanical and chemical stability. The modified superhydrophobic surface shows excellent oil-water separation ability. This modified superhydrophobic surfaces gives 156° water contact angle and less than 10° oil contact angles. The oil-water separation efficiency was nearly 98.69% by using this modified stainless-steel mesh. The separation efficiencies obtained repeatedly even after 20 cycles. The superhydrophobic modified stainless steel mesh shows stability, durability and reusability. The SiO_2 modified stainless steel mesh indicates excellent material for treating oil-polluted water in different practical applications.

Zhao et al. [31] have prepared superhydrophobic SiO_2 nanoparticles by improved Stober method and then coated on a chemically etched stainless steel mesh by one step dipping method to fabricate superhydrophobic SiO_2 coated stainless steel mesh. The preparation process was simple, efficient and environmentally friendly. The experimental procedure is shown in **Fig. 6**. It shows excellent oil-water separation properties, which can be widely used in oil-water separation. It was showing 153.3° water contact angle and 0° oil contact angle. The oil-water separation efficiency was nearly 96% by using this modified stainless-steel mesh. The separation efficiencies were obtained repeatedly even after 40 cycles without noticeable deterioration. The superhydrophobic modified stainless steel mesh shows stability, durability and reusability. The SiO_2 modified stainless steel mesh indicates good material for treating real oil-polluted water in different practical applications. This method shows high performance, oil-water separation in a short time and repeatedly in comparison with earlier works.

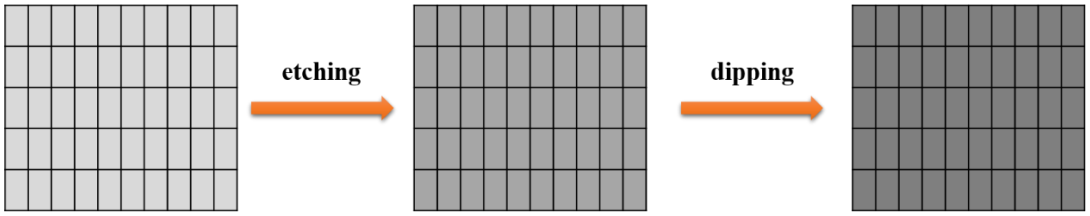

Fig. 6. Schematic illustration of the preparation of FSSM [31].

2.3. Superhydrophobic SiO_2 Modified Porous Substrates for Oil-Water Separation:

Wei et. al. [32] have obtained the SiO_2 nanoparticles from ethanol and ammonium hydroxide with TEOS. The SiO_2 nanoparticles were isolated by repeated centrifugation in ethanol followed by drying in a vacuum oven. A facile method was used to prepare silica particles. The solution has been sprayed to different porous sponge and metal mesh to achieve durable superhydrophobic coating. The superhydrophobic sponge shows a separation efficiency of 98.8% dealing with oil-water mixture. The oil absorption capacity of immersion coated polyurethane sponge was demonstrated higher than pristine polyurethane sponge an 39 g/g and higher porosity contributed by abundant nanoparticles. After 10 cycles of abrasion test the remained separation efficiency of above 96% and water contact angle of 157° confirmed the mechanical durability.

Gu et al. [33] have prepared a membrane (SiO_2/Polyurethane membrane) with porous structure rough surface and hydrophobic epidermis by surface modification to construct a rough surface and low-energy epidermis on electrospun polyurethane membrane. The schematic of experimental procedure. The superhydrophobic SiO_2/PU porous membrane prepared by chemical modification on the membrane shows a water contact angle 152.1° and low sliding angle 6°. This membrane was used for different aqueous solutions like water, saline solution, alkaline solution acidic solution. The porous membrane shows low air permeability and high-water vapor transmission rate. It shown good oil absorption capacity. It was shows high oil-water separation

efficiency above 98.5%. The absorption capacity of the modified membrane does not show severe degradation even after 30 separation cycles which indicating a highly stable absorption performance of modified membrane. It provided the potential for eater repellent, breathable applications and oil-water separation in long term use.

2.4. Superhydrophobic SiO_2 Modified Membrane for Oil-Water Separation:

Li and their co-workers [34] have fabricated the superhydrophobic surface by using PVDF and SiO2 via sugar template method. It was shown in a water contact angle of 155.68° and roll-on angle of nearly 6°. The prepared superhydrophobic PVDF oil/water separation membrane had low water adhesion performance and ultrahigh separation efficiency of nearly 99.98% in terms of the oil purity in the filtrate. The recycling performance over 20 cycles. This membrane has excellent potential for use in various large-scale practical applications, water purification treatment and the separation of commercially relevant emulsions. The possibility of large-scale production and low manufacturing costs of this sponge is very promising advantages for oil-water separation application.

Bai et al. [35] have coated cotton fabric by sol-gel processed SiO_2 The as-prepared fabric was immersed in the solution of $FeCl_3$, thiophene and CH_2Cl_2 solution. Then, the modified fabric was washed with ethanol and dry it. The experimental procedure of preparation of superhydrophobic fabric. The modified fabric shows water contact angles above 160°. The strongest peak at 1050 cm^{-1} belongs to the Si-O bond indicating that SiO_2 particles have been coated on the cotton fabric. The modified cotton fabric shows outstanding resistance to ultraviolet irradiation, high temperature, low temperature, organic solvent, immersion and excellent durability even after 8 months. The as-prepared fabric was showing the capability in various chemical exposures. It was showing good anti-dirt and anti-frost properties. The modified superhydrophobic cotton fabric was used as filter membrane for the gravity driven oil-water separation with high separation efficiency and excellent reusability. By using, this modified cotton fabric, both immiscible and emulsified oil-water mixtures could be separated. The efficient oil-water separation was also achieved under harsh conditions. The superhydrophobic fabric shows potential for the fast, coat-effective treatment of oil spill accidents and industrial oily sewage.

Conclusion:

This review highlights the unique properties of SiO_2 nanoparticles, whose fabrication requires minimal control of external parameters, such as surface modification. Their synthesis is economically beneficial, facile and straightforward. A sponge/mesh coated with SiO_2 nanoparticles has been developed using SiO_2 nanoparticles and various polymers. Absorption and separation investigations demonstrate that the SiO_2 surface is highly efficient and stable in absorbing a wide range of oils and organic solvents. It is believed that SiO_2-coated superhydrophobic materials are highly useful for oil-water separation. These materials exhibit excellent performance under various mechanical conditions when combined with SiO_2-polymer composites. Hence, this review serves as a valuable resource for researchers aiming to develop highly scalable superhydrophobic surfaces for efficient oil-water separation applications.

References

[1]. Beyer J., Trannum H. C., Bakke T., Hodescen P. V., & Collier T. K. (2016). Environmental effects of the Deepwater Horizon oil spill: A review. Mar. Pollut. Bull., 110, 28-51.

[2]. Bi. H., Xie X., Yin K., Zhou Y., Wan S., He L., & Xu F. (2012). Spongy Graphene as a Highly Efficient and Recyclable Sorbent for Oils and Organic Solvents. Adv. Funct. Mater., 22, 4421-4425.

[3]. Cong H., Ren X., Wang P., & Yu S. (2012). Macroscopic Multifunctional Graphene-Based Hydrogels and Aerogels by a Metal Ion Induced Self-Assembly Process. ACS Nano., 6, 2693-2703.
[4]. Dalawai S. P., Aly M. A., Latthe S. S., Xing R., Nagappan S., Ha C. S., Sadasivuni, S. & Liu K. K. (2020). Superwetting nanowire membranes for selective absorption. Prog. Org. Coat., 138, 105381-105389.
[5]. Gao Y., Zhou Y. S., Xiong W., Wang M., Fan L., Golgir H. R., Jiang L., & Hou W. (2014). A Polydimethylsiloxane (PDMS) Sponge for the Selective Absorption of Oil from Water. ACS Appl. Mater. Interfaces, 6, 5924-5929.
[6]. Zhou X., Zhang Z., Xu X., Men X., & Zhu X. (2015). Versatile fabrication of magnetic carbon fiber aerogel applied for bidirectional oil–water separation. Appl. Phys. A, 1-9.
[7]. Ivushina B., Kuyukina M. S., Krivoruchko A. V., Eikin A. A., Makorov S. O., Cunningham G. J., & Peshkur T. A. (2015). Oil spill clean-up from sea water by sorbent materials. Prog. Org. Coat., 13, 5381-5389.
[8]. Bhoje V., & Keller A. A., (2006). Improved Mechanical Oil Spill Recovery Using an Optimized Geometry for the Skimmer Surface. Environ. Sci. Technol., 40 (24), 7914-7918.
[9]. Wu Z. Y., Li C., Liang H. W., Zhang Y. N., Wang X., Chen I. F., & Yu S. H. (2014). Carbon nanofiber aerogels for emergent cleanup of oil spillage and chemical leakage under harsh conditions. Sci. Rep., 4, 4079-4085.
[10]. Keshavarz A., Zilouei H., & Abdol A., (2015). Enhancing oil removal from water by immobilizing multi-wall carbon nanotubes on the surface of polyurethane foam J. Environ. Manage, 157, 279-286.
[11]. Wang H., Wang E., Liu Z., Gao D., Yuan R., Sun, & Zhu Y. (2015). Novel membranes with extremely high permeability fabricated by 3D printing and nickel coating for oil/ water separation. J. Mater. Chem. A Mater. Energy Sustain, 3, 266-273.
[12]. Li J. J., Zhu L. T., & Luo Z. H. (2016). Electrospun fibrous membrane with enhanced swithchable oil/water wettability for oily water separation Chem. Eng. J. 287, 474-481.
[13]. Fard A. K., Mckay G., Manawi Y., Malaihari Z., & Hussein M. A. (2016). Outstanding adsorption performance of high aspect ratio and super-hydrophobic carbon nanotubes for oil removal Chemsphere, 164, 142-155.
[14]. Erbil H. Y., Demirel A. L., Avci Y., & Mert O. (2003). Transformation of a Simple Plastic into a Superhydrophobic. Surface Science, 299, 1377.
[15]. Jin M., Feng X., Xi J., Zhai J., Chao K., Feng L., & Jiang L. (2005). Super-Hydrophobic PDMS Surface with Ultra-Low Adhesive Force. Macromol. Rapid Commun. 26, 1805.
[16]. Liu H., Feng L., Zhai J., Jiang L., Zhu D. (2004). Reversible Wettability of a Chemical Vapor Deposition Prepared ZnO Film between Superhydrophobicity and Superhydrophilicity. Langmuir, 20, 56-59.
[17]. Jiang L., Zhao Y., & Zhai J. (2004). A Lotus-Leaf-like Superhydrophobic Surface: A Porous Microsphere/Nanofiber Composite Film Prepared by Electrohydrodynamics. Chem. Int. Ed. 43, 4338 – 4341.
[18]. Zhai L., Cebeci F. C., Cohen R. E., & Rubner M. F. (2004). Stable Superhydrophobic Coatings from Polyelectrolyte Multilayers. Nano Lett. 4, 1349.
[19]. Wen L., Tian Y., & Jiang L. (2015). Bioinspired Super-Wettability from Fundamental Research to Practical Applications. Angew. Chem. Int. Ed., 54, 2 – 15
[20]. Ren G., Song Y., Li X., Zhou Y., Zhang Z., & Zhu X. (2018). A superhydrophobic copper mesh as an advanced platform for oil-water separation. Appl. Surf. Sci. 428, 520-525.

[21]. Wu Y., Shen Y., Tao J., He Z., Xie Y., Chen H., Jin M., & Hou W. (2018). Facile spraying fabrication of highly flexible and mechanically robust superhydrophobic F-SiO2@PDMS coatings for self-cleaning and drag-reduction applications. New J. Chem., 42 (22), 18208-18216.

[22]. Wang P., Chen M., Han H., Fan X., Liu Q., & Wanga J. (2006). Transparent and abrasion-resistant superhydrophobic coating with robust self-cleaning function in either air or oil. J. Name., 2013, 00, 1-3

[23]. Gao J., Huang X., Xue H., Tang I., & Robert K. (2017). Facile preparation of hybrid microspheres for super-hydrophobic coating and oil-water separation. Chem. Eng. J. 326, 443-453.

[24]. Li J., Zhao Z., Kang R., Zhang Y., Lv W., Li M., Jia R., & Luo L. (2017). Surface design of durable and recyclable superhydrophobic materials for oil/water separation. J. Sol-Gel Sci. Technol., 82 (3), 817–826.

[25]. Liu Y., Liu N., Jing Y., Jiang X., Yu L., & Yan X. (2019). Robust superhydrophobic candle soot and silica composite sponges for efficient oil/water separation in corrosive and hot water. Colloids and surfaces A., 567, 128-138.

[26]. Zhang R., Zhou Z., Ge W., Lu Y., Liu T., Yang W., & Dai J. (2020). Robust, Fluorine-free and Superhydrophobic Composite Melamine Sponge Modified with Dual Silanized SiO2 Microspheres for Oil-Water Separation. Elsevier, Journal of Chemical Engineering, 20, 30292-5.

[27]. Chen C., Weng D., Chen S., Mahmood A., Wang J. (2019). Development of Durable, Fluorine-free, and Transparent Superhydrophobic Surfaces for Oil/Water Separation. ACS Omega, 4, 6947–6954.

[28]. Wang Q., Yu M., Chen G., Chen Q., & Tian J. (2017). Robust fabrication of fluorine-free superhydrophobic steel mesh for efficient oil/water separation J. Mater. Sci., 52 (5), 2549–2559.

[29]. Liu D., Yu Y., Chen X., Zhang Y. (2017). Selective separation of oil and water with special wettability mesh membranes. RSC Adv., 7, 12908-12915.

[30]. Xiong W., Li L., Qiao F., Chen J., Chen Z., Zhou X., Hua K., Zhao X., & Xie Y. (2021). Air superhydrophilic-superoleophobic SiO2-based coatings for recoverable oil/water separation mesh with high flux and mechanical stability Journal of Colloid and Interface Science, 600, 118–126.

[31]. Zhao L., Du Z., Tai X., Ma Y., (2021) Colloids and Surfaces A: Physicochemical and Engineering Aspects, 623, 126404-126415.

[32]. Wei C., Deu F., Lin L., An Z., He Y., Chen X., Chen L., & Zhao Y. (2018). Sprayable, durable, and superhydrophobic coating of silica particle brushes based on octadecyl bonding and polymer grafting via surface-initiated ATRP for efficient oil/water separation. Journal of Membrane Science 555, 220-228.

[33]. Gu J., Xiao P., Chen J., Liu F., Huang Y., Li G., Zhang J., Chen T., (2014) Journal of Materials Chemistry A, 2, 15268–15272.

[34]. Li X., Wang X., Yuan Y., Wu M., Wu Q., Liu J., Yang J., Zhang J., (2021) European Polymer Journal, 159, 110729-110742.

[35]. Bai W., Lin H., Chen K., Zeng R., Lin Y. and Xu Y., (2021) Advanced Materials Interfaces, 254, 725-740.

International Journal of Scientific Research in Science and Technology
Available online at : www.ijsrst.com
Print ISSN: 2395-6011 | Online ISSN: 2395-602X
doi : https://doi.org/10.32628/IJSRST

Synthesis of Isoniazide Series Derivative in Aqueous Medium

Devendra Wagare[1], Nayana Pahade[1], Prerna Dhirbassi[1], Sonali Shinde[1], Aarti Ghugare[1], Prashant Netankar[2], Dinesh Lingampalle*[1]

[1]Department of Chemistry, Vivekanand Arts, Sardar Dalipsingh Commerce and Science College, Chhatrapati Sambhajinagar, Maharashtra, India

[2]Department of Chemistry, Maulana Azad Arts and Science College, Chhatrapati Sambhajinagar, Maharashtra, India

ARTICLEINFO

Article History :

Published : 07 Dec 2024

Publication Issue :
Volume 11, Issue 23
Nov-Dec-2024
Page Number :
70-74

ABSTRACT

Isoniazide isoxazoles derivatives have been prepared from the reaction of one equivalent of aromatic carboxylic acid, one equivalent isoniazide in the presence of environmentally benign medium. Glycerol in water used as a green medium to increase yield and rate of reaction.

Keywords : isoniazide oxazole, carboxylic acid, glycerol-water, green chemistry

Introduction

Literature survey reveals that, the synthesis of a diverse range of functionalized heterocyclic moiety are significant to the medicinal chemists as they provide the ability to expand the available drug-like chemical space, which bind to the biological targets based on their chemical diversity[1-3]. They exhibit a robust nature in cell metabolism and are essential components in the pharmaceutical industry [4-5]. To expedite the drug discovery program, it is highly prudent to develop reliable synthetic methods for the generation of a diverse collection of heterocyclic molecules. Over the last few decades, new methods for synthesizing heterocycles have revolutionized. A five membered heterocyclic molecular scaffold i.e. Isoxazole, is broadly used as important compound in the research of drug discovery[6-7]. The versatility of substituted isoxazole in undergoing chemical transformations to produce valuable synthetic intermediates makes them significant synthons as well. Organic compounds consuming the oxazole moiety revealed potent therapeutic efficacy in the field of agriculture and medicine. The isoxazole derivatives have long been used in organic synthesis due to the broad range of biological and pharmaceutical[8-10] activities such as antifungal, antiviral[12], antibacterial[13] antihelmintic[14], hypolipemic[15], anti-allergic[16] emits as characteristics of an agent that blocks histamine.

Pharmacologically important isoxazole[17] are semisynthetic penicillin's, semisynthetic lephalosporins, antibacterial sulfonamides, anabolic steroids, monoamine oxidase inhibitor which is used in the psychotherapy etc. in addition, isoxazole derivatives also used in the treatment of leprosy[18].

Isoniazide is a isonicotic acid hydrazide (INH) is an antibiotic used for the treatment of tuberculosis. For active tuberculosis,it is often used together with rifampin, pyrazinamide and either streptomycin or ethambutol. Isoniazide and a related drug, iproniazid, were among the first drugs to be referred to as antidepressants. Use against tuberculosis continued as isoniazide effectiveness against the disease outweighs its risk. [19] Isonazide is a prodrug that inhibit the formation of the mycobacterial cell wall. The development of isoniazid derivatives has been a focus of pharmaceutical research to address challenges such as drug resistance, side effects, and limited spectrum of activity associated with isoniazid, a widely used first-line antitubercular agent. [20] As a hydrazide derivative of isonicotinic acid, isoniazid possesses a versatile chemical structure that can be modified to create new compounds with enhanced pharmacological properties.

Many researchers worked on the synthesis of isoxazole and screened for the various microbial activity.

Herein, we have developed new environmentally friendly protocol for the synthesis of isoniazid isooxazoles in glycerol medium under microwave.

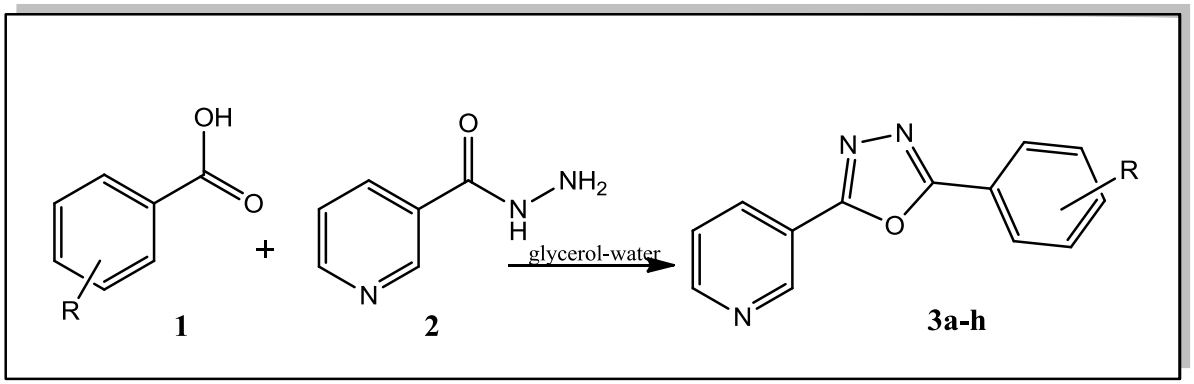

Scheme 1: Synthesis of isoniazid iso-oxazoles in glycerol-water

Experimental

Material and method

All the chemicals and solvents used were of AR grade and were utilized without additional purification. Melting points were determined in open capillary tubes and are uncorrected. ^{1}H NMR measurements were taken on a Bruker AC–400F, are presented in parts per million (PPM).

General procedure for the synthesis of isoniazid isooxazole

To a solution of glycerol-water (2:1), aromatic carboxylic acid (1–mmol) and isoniazide (1–mmol) was added. The reaction mixture was irradiated at 400 watt power under microwave at $120^{0}C$. After the completion of reaction, the reaction mixture was poured into ice water. The Solid obtained was filtered, dried and recrystallized from ethanol.

Result and discussion

Isoniazid bearing isoxazole attracted great attention of organic researchers because of their versatile biological important. It promoted our interest to synthesize new compound bearing isoniazid and isoxazole nucleus. Iso-oxazole also important moiety widely used in pharmaceutical chemistry. Initially, we have tried the reaction of

aromatic carboxylic acid (benzoin acid) with isoniazide in green medium. various green medium and catalyst were used for the present reaction such as PEG, cyclodextrin, water, glycerol and ethanol. It was observed that reaction could takes place in all these selected solvents but combination of glycerol and water acts as good solvent for present protocol. This reaction show excited result such as high atom economy and rapid rate of reaction in glycerol-water under microwave irradiation. (**Table 01**).

Table 1 Choice of solvent for present protocol

Solvent	Proportion	Time in (min)	Yield[a]
PEG	--	20	67-69
glycerol	-	10	78-81
Cyclodextrin	-	23	56-67
water	1	12	76-79
Glycerol-water	2:1	5	84-86

[a] isolated yield

To generalize the scope of present protocol we have selected differently substituted aromatic acid and results are detected in **table 2** all the synthesized compounds were well characterized by IR, NMR and Mass spectral analysis.

Table 2 Synthesis of isoniazid-oxazoles

Compounds	Time (min.)[b]	Yield[a]
3a	**5**	**86**
3b	**6**	**82**
3c	**5**	**83**
3d	**6**	**87**
3e	**4**	**85**
3f	**5**	**87**
3g	**6**	**83**
3h	**5**	**82**

[a] isolated yield

[b] time for overall reaction

Spectral data of synthesized compounds

Spectral data *. 2-(pyridin-3-yl)-5-(p-tolyl)-1,3,4-oxadiazole (**3a**).* ***Mass:*** *[ES]⁻: Calculated – 430.21, Found – 429.77.* ***^{1}H NMR*** *(400 MHz, DMSO, δ ppm): 2.34 (s, 3H, -CH_3), 7.29 (d, 1H, Ar-H), 7.57 (dd, 1H, Ar-H), 7.95 (dd, 1H, Ar-H), 8.42 (d, 1H, Ar-H) 8.70 (d, 1H, Ar-H) 9.24 (d, 1H, pyridinyl-H).* ***^{13}C NMR*** *(400 MHz, DMSO, δ ppm): 21.54, 33.58, 35.61, 41.90, 50.71, 73.65, 81.32, 103.31, 109.56, 110.42, 117.26, 127.73, 132.80, 133.41, 141.33, 144.34, 147.85, 150.81, 153.05, 155.74.*

*7-But-2-ynyl-1-(3-methoxy-benzyl)-3-methyl-8-(4-methylene-piperidin-1-yl)-3,4,5,7-tetrahydro-purine-2,6-dione (**5b**).*

Melting point: *178 - 180 ^{o}C.* ***Mass:*** *[ES]⁻: Calculated – 435.23, Found – 434.70.* ***^{1}H NMR*** *(400 MHz, DMSO, δ ppm): 1.78 (s, 3H, -CH_3), 2.35 (d, 1H, -CH), 2.36 (t, 4H, -CH_2), 3.37 (s, 3H, -CH_3), 3.40 (d, 1H, -CH_2), 3.41 (t, 4H, -CH_2), 3.71 (s, 3H, -OCH_3), 4.80 (s, 2H, -CH_2), 4.91 (d, 2H, =CH), 5.00 (s, 2H, -CH_2), 6.79 – 7.22 (m, 4H, Ar-H).*

^{13}C NMR (400 MHz, DMSO, δ ppm): 3.047, 29.49, 33.56, 35.53, 40.12, 50.77, 54.94, 73.73, 81.19, 103.32, 109.54, 111.99, 113.43, 119.46, 129.30, 139.40, 144.39, 147.55, 150.81, 153.21, 155.69, 159.59.

*1-Benzyl-7-but-2-ynyl-3-methyl-8-(4-methylene-piperidin-1-yl)-3,4,5,7-tetrahydro-purine-2,6-dione (**5c**).*

***Melting point:** 215 ^{O}C. **Mass:** [ES]: Calculated – 405.22, Found – 404.77. ^{1}**H NMR** (400 MHz, DMSO, δ ppm): 1.79 (s, 3H, -CH$_3$), 2.34 (d, 1H, -CH), 2.36 (t, 4H, -CH$_2$), 3.37 (s, 3H, -CH$_3$), 3.38 (d, 1H, -CH$_2$), 3.41 (t, 4H, -CH$_2$), 4.80 (s, 2H, -CH$_2$), 4.91 (d, 2H, =CH), 5.03 (s, 2H, -CH$_2$), 7.22 – 7.31 (m, 5H, Ar-H). ^{13}**C NMR** (400 MHz, DMSO, δ ppm): 3.04, 29.45, 33.56, 35.52, 43.34, 50.76, 73.71, 81.19, 103.32, 109.50, 126.91, 127.44, 128.19, 137.84, 144.37, 147.50, 150.79, 153.21, 155.64.*

Conclusion

In this investigation, new series of isoniazide-isooxazole have been successfully synthesized from the reaction of aromatic carboxylic acid and isoniazid in presence of glycerol-water as an environmental friendly, reusable green medium. The most remarkable features of present investigations are cost effective, high atom and step economy, use of green and non-toxic medium and required minimum reaction time.

References

[1]. Swinney, D. C., & Anthony, J. (2011). How were new medicines discovered?. Nature reviews Drug discovery, 10(7), 507-519.

[2]. Azzarito, V., Long, K., Murphy, N. S., & Wilson, A. J. (2013). Inhibition of α-helix-mediated protein–protein interactions using designed molecules. Nature chemistry, 5(3), 161-173.

[3]. Das, S., & Chanda, K. (2021). An overview of metal-free synthetic routes to isoxazoles: the privileged scaffold. RSC advances, 11(52), 32680-32705.

[4]. Chand, K., Hiremathad, A., Singh, M., Santos, M. A., & Keri, R. S. (2017). A review on antioxidant potential of bioactive heterocycle benzofuran: Natural and synthetic derivatives. Pharmacological Reports, 69(2), 281-295.

[5]. Neha, K., Ali, F., Haider, K., Khasimbi, S., & Wakode, S. (2021). Synthetic approaches for oxazole derivatives: A review. Synthetic Communications, 51(23), 3501-3519.

[6]. Aricò, F., (2020). Frontiers in Chemistry, 8, p.74.

[7]. Zhu, J., Mo, J., Lin, H. Z., Chen, Y., & Sun, H. P. (2018). The recent progress of isoxazole in medicinal chemistry. Bioorganic & Medicinal Chemistry, 26(12), 3065-3075.

[8]. Pathak, A., & Sharma, N. (2022). Synthesis and Antimicrobial Studies of Isoxazole Derivatives. The Scientific Temper, 13(02), 200-207.

[9]. Saini, R. K., Joshi, Y. C., & Joshi, P. (2007). Synthesis of novel isoxazole derivatives from 1, 3-diketone derivatives. Heterocyclic Communications, 13(4), 219-222.

[10]. Panea, I., Ghirişan, A., Cristea, I., Gropeanu, R., & Silberg, I. A. (2001). azocoupling products. ii.* synthesis and structural study of azocoupling products of i-(5, 6-dimethyl-4-x-pyrimidin-2-yl)-3-methyl-pyrazolin-5-ones with aromatic diazonium salts. Heterocyclic Communications, 7(6), 563-570.

[11]. Saini, R. K., Joshi, Y. C., & Joshi, P. (2007). Synthesis of novel isoxazole derivatives from 1, 3-diketone derivatives. Heterocyclic Communications, 13(4), 219-222.

[12]. Saxena, B., Patel, R. I., & Sharma, A. (2024). Visible light-driven α-sulfonylation of ketone-derived silyl enol ethers via an electron donor–acceptor complex. Green Chemistry.

[13]. El-Zohry, M. F., Al-Ahmadi, A. A., & Aquily, F. A. (2001). synthesis and cyclization of 3-[3′ (2′ - spirothiazolidin-4′ -onyl)] quinazolin-4-one derivatives. Phosphorus, Sulfur, and Silicon and the Related Elements, 175(1), 1-14.
[14]. Becher, J., Joergensen, P. L., Pluta, K., Krake, N. J., & Falt-Hansen, B. (1992). Azide ring-opening-ring-closure reactions and tele-substitutions in vicinal azidopyrazole-, pyrrole-and indolecarboxaldehydes. The Journal of Organic Chemistry, 57(7), 2127-2134.
[15]. S.S. Bhagwt, C. Lee, M.D. Cowart, J. Mackie and A. L. Grillot. C.A., 129, 316240, (1998).
[16]. Suzuki, Y., Takemura, Y., Iwamoto, K. I., HIGASHINO, T., & MIYASHITA, A. (1998). Carbon-carbon bond cleavage of α-hydroxybenzylheteroarenes catalyzed by cyanide ion: Retro-benzoin condensation affords ketones and heteroarenes and benzyl migration affords benzylheteroarenes and arenecarbaldehydes. Chemical and pharmaceutical bulletin, 46(2), 199-206.
[17]. Fernandes, P., Desai, D., Gawri, N., Pandey, S., & Patel, H. (1985). Synthesis of 3, 5‐Dimethyl‐4‐(Substituted‐sulfonamidobenzene Azo, 4‐Sulfophenyl and 4‐Sulfonaphthyl Azo)‐1 (H)‐(hetero Substituted) Pyrazoles and Evaluation of Their Antibacterial Properties. Chemischer Informationsdienst, 16(28), no-no.
[18]. Bhattacharya, B. K., Robins, R. K., & Revankar, G. R. (1990). A facile synthesis of certain 4‐and 4, 5‐disubstituted 1‐β‐d‐ribofuranosylpyrazoles. Journal of heterocyclic chemistry, 27(3), 795-801.
[19]. Reis, W. J., Bozzi, Í. A., Ribeiro, M. F., Halicki, P. C., Ferreira, L. A., da Silva, P. E. A., ... & da Silva Júnior, E. N. (2019). Design of hybrid molecules as antimycobacterial compounds: Synthesis of isoniazid-naphthoquinone derivatives and their activity against susceptible and resistant strains of Mycobacterium tuberculosis. Bioorganic & Medicinal Chemistry, 27(18), 4143-4150.

International Journal of Scientific Research in Science and Technology
Available online at : www.ijsrst.com
Print ISSN: 2395-6011 | Online ISSN: 2395-602X
doi : https://doi.org/10.32628/IJSRST

Analysis of Physico-Chemical Parameters and Ground Water Quality of Sakhali Bk Village of Buldhana District, Maharashtra, India

S.L. Kumbhare*, A.D. Deshpande, Wagh P.B
Department of Chemistry, Jijamata Mahavidyalaya, Buldhana, Maharashtra, India

ARTICLEINFO

Article History :

Published : 07 Dec 2024

Publication Issue :
Volume 11, Issue 23
Nov-Dec-2024
Page Number :
75-81

ABSTRACT

The ground water quality and some of its physico-chemical parameters were analyzed of different localities in Village Sakhali bk Taluka Buldhana , District Buldhana Maharashtra. The water samples analysis involved pH, TDS, temperature, Alkalinity, Chloride, nitrate, total hardness and fluoride. The water samples were collected from different localities of the village and analyzed for the suitability of drinking purposes. It was found that some of the water samples were found not suitable for drinking and domestic purposes directly without proper treatment.

Keyword:- Ground water quality, physico-chemical parameters, etc.

Introduction

Water consists of two hydrogen atoms bound to an oxygen atom, forming an isosceles triangle. Water molecules are attracted to each other, creating hydrogen bonds, which influence physical as well as chemical properties of water. Pure water at sea level freezes at 0°C and boils at 100°C. At higher elevations, the boiling point of water decreases, due to the lower atmospheric pressure. If substances are dissolved in the water, the freezing point is lowered (John, 2008). Perhaps the most striking feature of water is that it is less dense in its solid form (ice) than it is in liquid form, and so ice floats. The density of pure water approaches to 4°C, and so water at this temperature is often found in the deep waters of a lake. The density of water increases if solutes are added (i.e., salty water may be denser than fresh water). Both these features influence thermal and chemical stratification patterns in lakes, with important environmental consequences.

Water has a very high specific heat, which is the amount of energy needed to warm or cool a substance. People who live close to large bodies of water are often said to enjoy a maritime climate, with reduced climatic extremes between the seasons. On the contrary, regions far inland are often said to have continental climates, with striking seasonal changes in temperature.

Water has an extremely high surface tension, which is a measure of the strength of the water's surface film. One of the important characteristics of water is that it is almost the universal solvent, with extraordinary abilities to dissolve other substances. Consequently, when water passes through soils or vegetation or a region of human activity (e.g., an agricultural field treated with fertilizers and insecticides, a mine tailings heap, a municipal or industrial landfill site.), it changes its characteristics as it dissolves solutes. Even a drop of water falling as rain will dissolve atmospheric gases, and its properties will be altered (e.g., carbon dioxide dissolves readily in water, forming a weak acid namely carbonic acid).

Selection Of Samples

Study of area:-

Sakhali Bk village is situated at Buldhana. Which is situated at south Buldhana district. it is one of the five district of Amravati division in vidharbha region of Maharashtra.

Table-List of farmer

Sr.No.	Name of Farmers	Sample collected from Well Water
1	Gajanan Bhagwan Gore	Sample -1
2	Raju Bhagwan Gore	Sample -2
3	Gyandev Bhagwan Gore	Sample -3
4	Dashrath Shankar Gore	Sample -4
5	Vaibhav Sampat Lahase	Sample -5
6	Sandip haridas Lahase	Sample -6
7	Mayur Gajanan Gore	Sample -7
8	Raju Shankar sanase	Sample -8
9	Vijay Bhagwan Gore	Sample -9
10	Sukhdev Motiram Lahane	Sample -10

Fig. Sample collected from different places

Physical Analysis:-

1) **Color**:-An undesirable appearance is produced by colour in water. oil The measurement of colour in water is carried out by means of a tintometer the instruments has an eye-piece with the two holes. A

slide of water to be tested is inserted. The intensity is scale is the colour produced by a milligram of platinum cobalt in liter if distilled water. The slides of standard numbers are kept ready in the laboratory. For public water, the number in cobalt scale should not exceed 20 should be preferably less than 10. The measurements of water from the sample is done within 72 hours is its collection.

2) **Taste and odour**:- The water possesses taste and odour due to various causes and they make the water unpleasant for drinking. The taste is carried out by inhaling through two tubes of an osmoscope. One is kept in a flask containing diluted water and the other one to be tested. The taste and odour of water may also be tested by threshold number. In this method, the water to be tested is diluted with odour-free and the mixture at which odour becomes detectable is determined. In indicates threshold number and other intensities of odour are then worked out. The result of test is greatly affected by the sensitiveness

For the public water supply, the threshold number should not more than 3. In any event, the water tube supplied from a public water supply scheme should not contain objectionable taste and odour. The odour is expressed as disagreeable, earthy, fishy, grassy, mouldy, peaty, sweetish, obnoxious, etc. if an odour of chlorine or iodoform is found, it should always be recorded. The taste of expressed an brackish, saline, salty, etc. some persons are more sensitive that others and what is called a taste id often nothing more than a sensation of roughness on the palate after the water has been swallowed. If the taste and odour are suspected to be due to growth of any kind, the cause may be found out by conducting microscopically and biological examinations.

Threshold Odor Number – How They Are Determined

Sample volume Diluted to 200 ml	Threshold Odor Number (TON)	Sample volume Diluted to 200 ml	Threshold Odor Number (TON)
200	1	8.3	24
100	2	5.7	35
70	3	4	50
50	4	2.8	70
35	6	2	100
25	8	1.4	140
17	12	1	200

Chemical Analysis

1) **Chlorides:**-Take 100 ml of sample in each conical flask and add 2-3 drops of potassium chromate in each of them. Titrate the solution in one flask with 0.0141N Standard silver nitrate solution until a brick red colour is obtained. Now note the ml of AgNO3 used for the end point. Repeat the experiment with blank. The difference of the two observations is the ml of AgNO3 used. The silver reacts first with all chloride and silver chloride thus appears as reddish precipitate and the amount of silver Nitrate required to produce such reddish precipitate determines the amount of chlorides present in water.

2) **Dissolved Oxygen**:-The DO of the water sample was measured with the help of Water analysis kit according to standard protocol DO probe consist of a silver and gold electrode cells. An electrolyte tube with ring. The following procedure may be followed for assembly of DO probe. Be careful to handle its membrane. Fit the membrane on the lower part of the electrolyte tube. Fix the ring on the electrolyte tube covering the sides of the membrane. Fill potassium chloride solution (7.5%) in the electrolyte tube

to its top. Insert the electrode in the electrolyte tube and tightly screw it up. Now the probe is ready for use.

3) **Chemical Oxygen Demand (COD)**:- Take 50 ml of sample (A) in a conical flask. Add 100 ml of distilled water and 15 ml of standard potassium dichromate solution slowly and slowly and add 75 ml. conc. H2SO4 Reflux the mixture for 2 hours, cool and wash down the condensate with distilled water. Transfer the contents to 500ml flask. Dilute the mixture to about 30 ml. Titrate the excess dichromate with standard ferrous ammonium sulphate using ferroin indicator. Now perform the blank experiment (B) by taking 100 ml distilled water, 75 ml acid and 25 ml potassium dichromate solution. Reflux for 2 hours and titrate the excess dichromate with ferrous ammonium sulphate.

4) **Test for Hardness**:- Total Hardness- Pipette 10 ml hard water sample into a 250 ml conical flask. Add 2 ml of buffer solution add 3 drops of EBT indicator. Titrate the solution with standard EDTA solution from the burette until the color changes from wine red to clear blue at the end point. Repeat the titration at least two times for the confirm titration value. Note the titration value which corresponds to the total hardness.

$$\text{Hardness mg/litre } CaCO_3 = \frac{\text{ml of EDTA} \times 1000}{\text{ml of sample}}$$

Permanent Hardness: Measure out 100ml of hard water sample in 500ml beaker, boil it for half an hour filter the solution into 100ml of measuring flask and make the solution up to the mark with de-ionized water and shake thoroughly. Pipette out 10ml of these solutions into 250ml of conical flask, Add 2 ml of buffer solution and 3 drops of EBT. Titrate with EDTA solution until the wine red color changes to clear blue at the end point. Repeat the titration at least two times confirm titration value. Note this titration value, which corresponds to the permanent hardness.

5) **Determination of pH**:-The pH of the water sample was measured with the help of Water analysis kit according to standard protocol. Put the function switch F1 to pH/ORP mode. Rinse the electrode with distilled water and dry it with tissue paper. Connect the electrode BNC plug at the input socket. Put three combination pH electrodes in buffer solution 7.00 pH. Set the TEMP. Compensation knob to the Temp. of the buffer solution. Now move the switch F2 to pH mode. Read the display value; adjust it with CAL control to 7.00 pH value. Again move the selector switch F2 to STAND BY mode. Take out the electrode from 7.00 pH buffer and rinse it with distilled water and dry it. Put the electrode in 4.00 pH mode. Again move the switch F2 to pH solution. Set the value to 4.00 by adjusting the slope control. Take out the electrode from 4.00 pH buffer, rinse it with distilled water & dry it. Repeat steps from 4 to 13. The instrument is now ready to measure pH of any solution.

6) **Biological oxygen demand (BOD):** For the estimation of BOD content of water samples, initial and final DO of water samples were determined just after collection of sample and after 5 days incubation in BOD incubator, at 20˚C respectively. Calculation of BOD was done by using the following formula, and the result was expressed in mgL-1.

7) **Alkalinity**:-Take 100 ml of sample each in two conical flasks. Add 0.5 ml phenolphthalein indicator in one flask. If the sample gets pink titrate with 0.02 N H2SO4 until the pink color disappears. Note the ml of acid used in the titration. Now add 0.5 ml of methyl orange in second flask and titrate with 0.02N H2SO4 until the orange color is arrived indicating the end point Note again the ml of acid used.

8) **Acidity**:-Take 100 ml of sample in a conical flask and add 2 drops of phenolphthalein indicator, and titrate with $\frac{N}{10}$ NaOH until a faint pink color appears.

9) **Determination of Conductivity**:-The conductivity of the water sample was measured with the help of Water analysis kit according to standard protocol. Put the function switch F1 in CELL CONST position Adjust the display to the cell constant value marked on the conductivity cell supplied with the instrument. Now move the switch F1 to the COND. Position. Put the range switch at highest value of 200.0 m Mhos/cm. clean the conductivity cell, dry it and connect it to conductivity input socket. Dip the range switch at appropriate position so that conductivity with maximum resolution is measured. Multiply the observed reading by a factor given in table -1 to get the conductivity at 25 °c. i. e. Conductivity at 25 ° c = observed conductivity × Factor

10) **Total Dissolve Solids (TDS)**:-The Total Dissolve Solid of the water sample was measured with the help of Water analysis kit according to standard protocol Put the function switch F1 at CELL CONST. Position Clean the conductivity cell, dry it and connect in COND/TDS input socket. Adjust the display to cell constant value marked on conductivity cell with the CELL CONST Knob. Bring the F1 switch to TDS. Position Dip the Cond. Cell in the solution whose TDS value is to be determined. Put the range switch at appropriate ppm/ppt position, so that best possible resolution is obtained. Standard Conductivity. The specific conductance of this solution at 25 OC is 1408 us/cm.

11) **Salinity**:-The Salinity of the water sample was measured with the help Conductivity Meter according to standard protocol Prepare the conductivity meter for use according to the manufacturer's directions. Use a conductivity standard solution (usually potassium chloride or sodium chloride) to calibrate the meter for the range that you will be measuring. The manufacturer's directions should describe the preparation procedures for the standard solution. Rinse the probe with distilled or deionized water. Select the appropriate range on the meter, beginning with the highest range and working down. Place the probe the probe into the sample water, and spread the conductivity of the water sample on the lower 10 percent of the range that you selected, switch to the next lower range. If the reading is above 10 percent on the scale, then record this number on your data sheet. If the conductivity of the sample exceeds the range of the instrument, you may dilute the sample with distilled water. Be sure to perform the dilution according to the manufacturer's directions because the dilution might not have a simple linear relationship to the conductivity. Rinse the probe with distilled or deionizer water and repeat the fourth step above with the next water sample until finished.

12) **Sulphates**:-The method for the determination of sulphates in based on the fact that a sufficient amount of standard BaCl2. Solution is added to the sample and back titrating the excess of barium left unprecipitated.Take 100 ml of sample and add a few drops of methyl orange indicator and slight excess of HNO3. Boil the mixture to remove dissolved CO2. Add 10 ml (or more) of standard BaCl2 solution in the boiling solution. Allow to cool down and make the volume up to 50 ml of clear supernant liquid into a beaker, add 1 ml of buffer solution and some amount of EBT indicator. Titrate with EDTA solution until a permanent blue color is produced indicating end point.

Results and Discussion

Monitoring of Agricultural and drinking water samples from five different sources were analyzed for 16 parameters, which are given

Temperature:- The Temperature of water samples are found to be 26-28 ^{0C}

Color :- Color of water sample found to be colorless.

Odor :- Odor of water sample found to be odorless.

Taste:-Taste of different water sample such as well water has sweetest taste and the bore water has salty taste.
pH: - The pH serves as an index to denote the extent of pollution by acidic and alkaline waste. These values are in between 8.00 - 8.40
Chlorides:- The amount of chlorides ions present in water samples are found to be 69-209 gm/lit
Alkalinity:- The Alkalinity of water samples are found to be 150-450 mg/lit
Dissolved Oxygen:- All the samples are analyzed for D.O. and the values are found to be in the range 13.3-28.1 mg/lit
Hardness:-Hardness of water is due to calcium, magnesium, silicates, carbonate, and bicarbonate and sulphates.Total hardness of water samples found to be 230-630 mg /lit
Total Dissolved Solids:- The TDS water samples are found to be 211 to 512 mg/lit
Biological Oxygen Demand:- The BOD of water samples are found to be 4.4mg/lit-9.6mg/lit
Chemical Oxygen Demand:- The COD of water samples are found to be 0 to 0.0128 mg/L
Conductivity :- The Conductivity of water samples are found to be 0.467ms/cm-1.688ms/cm
Salinity :- The Salinity of water samples are found to be 0.001 – 0.003 ppt.
Acidity :- Acidity of water samples was found to be 0 mg/lit for all Sample.
Sulphate:- The amount of sulphate in water samples are found to be 109.76 – 266.56 mg/lit

Conclusion

The various parameters studied are within the permissible limits as per the WHO and ISO norms for drinking purposes in studied periods.
Temperature: - The Temperature of water samples are found to be 26-28 OC and the water is safe for drinking, and agriculture purpose.
Color:- The color of water sample found to be colorless and the water samples are used for drinking and agriculture purpose
Odor :- The odor of water sample found to be odorless and the water samples are use for drinking and agriculture purpose
Taste :- Taste of different water sample such as well water has sweetest taste used for drinking and agriculture purpose but the bore water (S7 & S10) has salty taste used for agriculture purpose and may be used for drinking purpose after proper filtration and purification.
pH :- The pH of water sample is found to be in between 8.00 - 8.40 and has permissible limits as per the WHO and ISO norms for drinking purposes and agriculture purpose
Chlorides :- The amount of chloride ions present in water samples are found in between 69 -209 gm/lit, and has permissible limits as per the WHO and ISO norms for drinking purposes and agriculture purpose.
Alkalinity :- The alkalinity of water samples is found to be 150 – 450 mg/lit. S5, S7, S9 having permissible limits as per the ISO norms for drinking purposes and agriculture purpose, rather than other sample are used for agriculture purpose but may be used for drinking purpose after the neutralization by using neutralizing agent and proper purification.
Dissolved Oxygen: - After the analyzing the all sample DO value is found to be in the range of 13.3 – 28.1 mg/lit. And thus all water sample are used for drinking and agriculture purpose.
Hardness :- Hardness of water is due to calcium, magnesium, silicates, carbonate, bicarbonate and sulphates. Total hardness of water samples found to be 230-630 mg/lit. S1, S3, S5, S7, S9 S10. Having permissible limits as per the ISO norms for drinking purposes and agriculture purpose, rather than other S2, S4, S6, S8 are used for

agriculture purpose but may be used for drinking purpose after the proper purification and the treatment of water softener ion exchange, and Reverse Osmosis.

Total Dissolved Solids :- The TDS of water sample is found to be 211 to512 mg/lit and has permissible limits as per the WHO norms and used for drinking purposes and agriculture purpose.

Biological Oxygen Demand:- The BOD of water samples is found to be 4.4 to 9.6 mg/lit and has permissible limits as per the ISO norms and used for drinking purposes and agriculture purpose.

Chemical Oxygen Demand:- The COD of water sample is found to be 0 to 0.0128 mg/lit and has permissible limits as per the WHO norms and used for drinking purposes and agriculture purpose.

Conductivity:-The conductivity of water sample is found to be 0.467 to 1.688 ms/cm, and thus all water sample are used for drinking and agriculture purpose.

Salinity: - The Salinity of water sample is found to be 0.001 – 0.003 ppt, and thus all water sample are used for drinking and agriculture purpose.

Acidity:- Acidity of water samples was found to be 0 mg/lit for all Sample, and thus all water sample are used for drinking and agriculture purpose.

Sulphate: - The amount of sulphate in water samples is found to be 109.76 – 266.56 mg/lit, S1, S2, S3, S4 S5, S6, S7, S9 S10. having permissible limits as per the WHO and ISO norms for drinking purposes and agriculture purpose, rather than only S8 is used for agriculture purpose but may be used for drinking purpose after the proper purification and the treatment of Reverse Osmosis, Distillation, and Ion exchange. Some of the physical and chemical properties of bore water, damp water, and well water were within desirable limits. The result obtained from the present investigation shall be useful in future management. The physico-chemical characteristics of bore water, damp water, and well water suggest that some of the locations of the study area unfit for drinking and agriculture purpose.

References

[1]. Dugan, R. 1972. Biochemical ecology of water pollution. Plenum Publishing Co. Ltd. New York.

[2]. Behura, B.K. 1981. Pollution everywhere. Science Reporter, New Delhi. 18:170-172.

[3]. Guide Manual: Water and Wastewater Analysis; Central Pollution Control Board

[4]. Water Quality Analysis Laboratory Methods; Dr. Leena Deshpande

[5]. Wastewater Engineering; Metcalf & Eddy; 2003; Tata McGraw-Hill Publishing Co Ltd

[6]. Singh PK, Singh UC and Kumar S (2009). An integrated approach using remote sensing, GIS and geoelectrical techniques for the assessment of groundwater conditions: A case study. GIS Development e-Magazine, 5(35).

[7]. S.P. Gorde and M.V. Jadhav, Assessment of Water Quality Parameters: A Review, Journal of Engineering Research and Applications, 3(6), 2029-2035 (2013)

[8]. Kavitha R. and Elangovan K., Review article on Ground water quality characteristics at Erode district, (India)

[9]. Chapman, D. 1992. Water quality assessment. London, Chapman and Hall (on behalf of UNESCO, WHO and UNEP). Pp. 585.

[10]. WHO. 2008. Guidelines for drinking water quality, 3rd ed. World Health Organisation, Geneva.

[11]. BIS. 2003. Indian standard specifications for drinking water. IS 10500. Indian Institute, New Delhi, India.

[12]. Bulushu, K.R. 1987. Chemical constituents in water related treatment and management NEERI, Nagpur. Pp.25.

International Journal of Scientific Research in Science and Technology
Available online at : www.ijsrst.com
Print ISSN: 2395-6011 | Online ISSN: 2395-602X
doi : https://doi.org/10.32628/IJSRST

Synthesis, Characterization of Some Benzoyled Maltosyl-1, 2, 4-Triazol-3-Ones and Their Antimicrobial Activities

U. W. Karhe*

Department of Applied Chemistry, Anuradha Engineering College, Chikhli, Dist Buldhana, Maharashtra, India

ARTICLEINFO

Article History :

Published : 07 Dec 2024

Publication Issue :
Volume 11, Issue 23
Nov-Dec-2024
Page Number :
82-88

ABSTRACT

A series of 1-aryl-2-o-tolyl-5-S-hepta-O-benzoyl maltosyl-1, 2-dihyro-1, 2, 4-triazol-3-one 2 have been synthesized by the oxidative cyclization of S-hepta-O-benzoyl maltosyl-1-aryl-5-o-tolyl isothioburets 1. The identities of these new compounds have been established on the basis of chemical transformation and IR, 1H NMR and Mass spectral studies. In the present investigation antimicrobial activities of these S-maltosides have been evaluated by using several bacteria such as Escherichia coli, Staphylococcus aureus, Proteus vulgaris and Pseudomonas aeruginosa and fungi such as Candida albicance and Aspergillus niger. The study reveals that all compounds show satisfactory antimicrobial activities.

Keywords: Synthesis, isothiobiurets, Oxidative cyclization, 1, 2, 4-triazol-3-one, antimicrobial activities.

Introduction

1, 2, 4-triazoles are an important class of heterocycles, and have been the subject of great 1, 2, 4-triazoles are an important class of heterocycles and have been the subject of great interest due to their pharmacological properties[1-3]. Very promising therapeutic applications have been obtained using the 1, 2, 4-triazole system. There are a number of drugs containing 1, 2, 4-triazole nucleus, such as itraconazole, flucanazole and voriconazole (antifungal), that have been used for the treatment of fungal infections[4-6]. Some other drugs including this heterocycle are ribavirin (antiviral), rizatriptan (antimigraine), alprazolam (anxiolytic), vorozole, letrozole and anastrozole (antitumor) [7-11]. However, there is an increasing resistance to these drugs. Moreover, some of azole derivatives used as common antibiotics posses a toxic effect on humans as well as their antimicrobial effects.

In this communication a series of 1-aryl-2-*o*-tolyl-5-*S*-hepta-*O*-benzoyl maltosyl-1, 2-dihydro-1, 2, 4-triazol-3-ones **2** have been synthesized oxidative cyclization of corresponding *S*-hepta-*O*-benzoyl maltosyl-1-aryl-5-*o*-tolyl isothioburets **1.** Which were studied for their antimicrobial activities.

Results and Discussion:-

S-hepta-*O*-benzoyl maltosyl-1-aryl-5-*o*-tolyl-2-isothiobiurets **1a** (0.002M, 2.67g) was made into a peast with chloroform and to it was added bromine in chloroform (20% bromine solution in chloroform, v/v) drop by drop with stirring. The bromine in chloroform was added till an orange red sticky mass was obtained. It was then allowed to stand for 5-6 h. The sticky mass was washed several times with petroleum ether to removed excess of bromine and then dissolved it in ethanol and was basified by using NH_4OH the product was isolated as free base.

Similarly, when the reaction was extended to other isothiobiurets **1** the corresponding 1, 2, 4-triazol-3-ones **2** have been isolated.

The structures of the products were confirmed by the spectral (IR, ^1H NMR and Mass[12-19]) and elemental analysis (Table 1). All the compounds have been screened for both antibacterial and fungal activities.

Experimental:

All the melting points recorded were found to be uncorrected. The structures of newly synthesized compounds were confirmed on the basis of elemental and spectral analysis. IR spectra were recorded in KBr on a FTIR Perkin-Elmer (4000-450 cm^{-1}) spectrophotometer. ^1H NMR spectra are run on Brucker DRX-300 instrument operating at 300 MHz using $CDCl_3$ solution with TMS at internal standard and Mass spectra on MASS Water Quattro Micro Mass. Specific rotations were measured on Equip-Tronics EQ-800 Digital Polarimeter. Thin layer chromatography (TLC) was performed on silica gel G for TLC (Merck) and spot were visualized by iodine vapours.

Spectral analysis:

2a:- **IR(KBr cm^{-1}):** 3062 (Aromatic C-H), 2974 (Aliphatic C-H), 1730 (C=O), 1600 (C=N), 1450 (C-N), 1271 (C-O), 1095, 1026 and 937 (Characteristics of maltose), 709 (C-S); **^1H NMR ($CDCl_3$, ppm):** δ 8.041-7.258 (44H, m, Aromatic protons), 6.244-3.741 (14H, m, maltosyl protons), 1.171 (3H, s, CH_3); **Mass (m/z):**1335 (M^+) not located, 1309, 1279, 1199, 1053, 579.

2d:- **IR(KBr cm^{-1}):** 3062 (Aromatic C-H), 2974 (Aliphatic C-H), 1730 (C=O), 1600 (C=N), 1450 (C-N), 1269 (C-O), 1093 and 937 (Characteristics of maltose), 709 (C-S), 601 (C-Cl); **^1H NMR ($CDCl_3$, ppm):** δ 8.125-7.181 (43H, m, Aromatic protons), 6.166-3.877 (14H, m, maltosyl protons), 1.888 (3H, s, CH_3); **Mass (m/z):**1371 (M^++1), 1299, 1221, 1139, 948.

2f:- **IR(KBr cm^{-1}):** 3062 (Aromatic C-H), 2960 (Aliphatic C-H), 1730 (C=O), 1452 (C-N), 1269 (C-O), 1093 and 937 (Characteristics of maltose), 709 (C-S); **^1H NMR ($CDCl_3$, ppm):** δ 8.123-7.180 (43H, m, Aromatic protons), 5.928-3088 (14H, m, maltosyl protons), 1.889 (3H, s, CH_3), 1.629 (3H, s, CH_3); **Mass (m/z):**1349 (M^+), 949, 933, 919, 917, 579.

Antimicrobial Activities:

All the compounds have been screened for both antimicrobial and antifungal activities using cup plate agar diffusion method[20-21] by measuring the inhibition zone in mm. the compounds were taken at a concentration of 1 mg/ml using dimethyl sulphoxide (DMSO) as solvent. It has been observed that some of these compounds showed interesting microbial activities.

Antibacterial activity:

The compounds were screen for antibacterial activity against *Escherichia coli, Staphylococcus aureus, Proteus vulgaris and Pseudomonas aeruginosa* in nutrient agar medium. Amikacin (100 µg/ml) was used as standard for antibacterial activity. The results are presented in Table2.

2a and 2b showed more significant activities against *Escherichia coli,* 2e showed more significant activities against *Staphylococcus aureus,* 2b showed more significant activities against *Proteus vulgaris* and 2c showed more significant activities against *Pseudomonas aeruginosa* respectively.

Antifungal activity:

The compounds were screen for antifungal activity against *Aspergillus niger* and *Candida albicance* in potato dextrose agar medium. Fluconazole (100 µg/ml) as standard for antifungal activity 2b, 2c and 2d showed more significant activities against *Candida albicance* and 2a, 2b, 2e and 2f showed more significant activities against *Aspergillus niger* respectively.

Acknowledgement:-

Authors are thankful to SAIF, CDRI Lucknow for providing the spectral data, Principal, Shri Shivaji College, Akola, Principal Anuradha engineering Colleg, Chikhli for providing necessary facilities.

References

[1]. H. Betkas, A. Demirbas, N. Demirbas, H. Bayrak, S. Alpay Karaoglu, Turk J Chem., 2010, 34, 517.
[2]. N. Demirbas, S. Alpay-Karaoglu, A. Demirbas and K. Sancak, Eur. J. Med. Chem., 2004, 39, 793.
[3]. P. Sudhir Kumar et al, Int.J. ChemTech Res., 2010, 2(4), 1960.
[4]. S. H. L. Chiu, S. E. W. Huskey, Drug Metabol. Dispos. 1998, 26, 838.
[5]. B. S. Holla, K. N. Poorjary, B. S. Rao and M. K. Shivananda, Eur. J. Med. Chem., 2002, 37, 511.
[6]. S. Shujuan, L. Hongxiang, Y. Gao, P. Fan, B. Ma, W. Ge and X. Wang, Pharm. Biomed. Anal., 2004, 34, 1117.
[7]. B. M. Rao, S. Sangaraju, M. K. Srinivasu, P. Madhavan, M. L. Devi, P. R. Kumar, K. B. Candrasekhar, C. Arpitha, T. S, Balaji, J. Pharm. Biomed. Anal., 2006, 41, 1146.
[8]. G. Hancu, A. Gaspar, A. Gyeresi, J. Biochem. Biophys. Methods, 2007, 69, 251.
[9]. E. Bejetti, N. Zilembo, E. Bichisao, P. Pozzi, L. Toffolatti, Critical Reveiws in Oncology:Hematology, 2000, 33, 137.
[10]. A. Demirbas, S. Ceylan, N. Demirbas, J. Het. Chem., 2007, 44, 1271.
[11]. C. Foulon, C. Danel, C. Vaccher, S. Yous, J. P. Bonte, J. F. Goossens, J. Chromatography A., 2004, 1035, 131.
[12]. R. M. Silverstein, G. C. Bassler and T. C. Morill, "Spectrometric identification of organic Compound," 5th Ed., Sons, Inc, New York, 2001, a) 127, b) 100.
[13]. D. H. Williams and I. Fleming, "Spectroscopic Methods in Organic Chemistry", IV, Tata Mc Graw Hill, 1991, P. a) 42.
[14]. S. Cao, F. D. Tropper, R. Roy, ChemInform, 1995, 26(42), 17,
[15]. Z. Dai, F. Qu, C.C. Wu and W.Li, J. Chem. Research (S), 2001, 106.
[16]. R. Varma, S.Y. Kulkarni, C. I. Jose and V.S. Pansare, Carbohydr. Res., 1984, 25, 133.
[17]. A. Vargas-Berenguel, F. Ortega-Caballero, F. Santoyo Gonzalez, J. J. Garcia Lopez, . J. Gimenez-Martinez, L. Garcia-Fuentes and E. Ortiz-Salmeron, Chem. Eur. J., 2002, 8(4), 822.

[18]. J. Isac-García, F. G. Calvo-Flores, F. Hernández-Mateo, F. Santoyo-González, Eur. J. Org. Chem., 2001, 383.
[19]. H. H. A. M. Hassan and A. H. F. El-Husseiney, Polish J. Chem., 2001, 75, 803.
[20]. Kawangh, F., Analytical Microbiology, Academic press, New York, 1963.
[21]. British pharmacopaeia- II, Biological assay and Tests, The Stationary Office Ltd., London, 1998, A-205.

Scheme

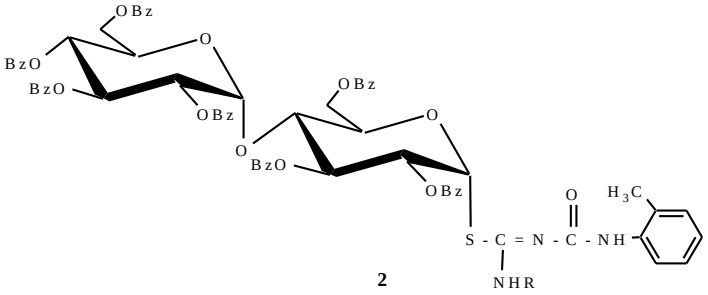

2

S-hepta-*O*-benzoyl maltosyl-1-aryl-5-*o*-tolyl-2-isothiobiurets

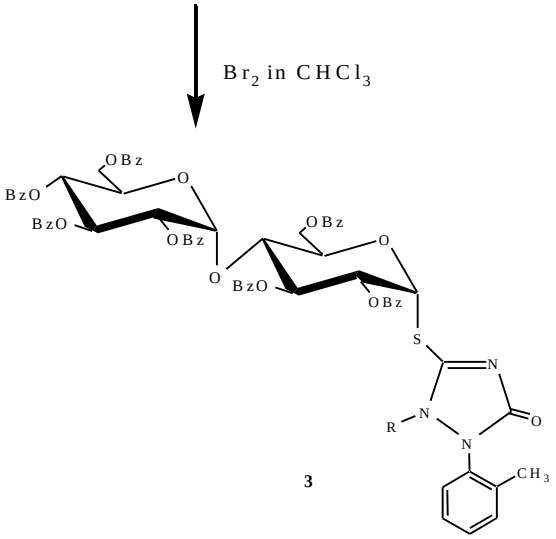

3

1-aryl-2-*o*-tolyl-5-*S*-hepta-*O*-benzoyl maltosyl-1, 2-dihydro-1, 2, 4-triazol-3-ones

Where, Bz = COC_6H_5

R = a) Phenyl, b) *o*-Cl Phenyl, c) *m*-Cl Phenyl,
d) *p*-Cl Phenyl, e) *o*-tolyl, f) *p*-tolyl.

Table 1: Characterization of 1-aryl-2-*o*-tolyl-5-*S*-hepta-*O*-benzoyl maltosyl-1, 2-dihydro-1, 2, 4-triazol-3-ones **2.**

Sr. No.	Products	m.p. (°C)	Yield (%)	R_f Value	$[\alpha]_D^{31}$ (c, in $CHCl_3$]	Elemental Analysis % Found (Required)	
						N	S
1.	2a	174	64	0.73	+116.6° (0.15 in $CHCl_3$)	2.99 (3.14)	2.26 (2.397)
2.	2b	139	59	0.88	+83.33° (0..15 in $CHCl_3$)	2.88 (3.07)	2.25 (2.337)
3.	2c	141	71	0.69	-250°	2.91	2.21

Sr. No.	Products	m.p. (°C)	Yield (%)	R_f Value	$[\alpha]_D^{31}$ (c, in $CHCl_3$]	Elemental Analysis % Found (Required)	
						N	S
					(0.20 in $CHCl_3$)	(3.07)	(2.337)
4.	2d	132	76	0.63	+355.55° (0.225 in $CHCl_3$)	2.99 (3.07)	2.27 (2.337)
5.	2e	166	69	0.6	-120° (0.25 in $CHCl_3$)	3.05 (3.11)	2.30 (2.37)
6.	2f	142	62	0.85	-260° (0.25 in $CHCl_3$)	3.06 (3.11)	2.31 (2.37)

Table2: Antimicrobial activities of 1-aryl-2-*o*-tolyl-5-*S*-hepta-*O*-benzoyl maltosyl-1, 2-dihydro-1, 2, 4-triazol-3-ones **2.**

Products	**Antibacterial****				**Antifungal****	
	E. coli	*S. aureus*	*P. vulgaris*	*Ps. aeruginosa*	*C. albicance*	*A. niger*
2a	18	19	14	16	20	21
2b	18	18	19	17	22	22
2c	14	14	17	18	21	19
2d	14	15	20	16	19	18
2e	15	18	17	15	16	21
2f	14	14	14	16	17	23
Amikacin	19	23	22	24	-	-
Fluconazole	-	-	-	-	25	26

**zone of inhibition in mm (15 or less) resistance, (16-20mm) moderate and (more than 20mm) sensitive. *Escherichia coli (E. coli), Staphalococcus aureus (S. aureus), Proteus vulgaris (P. vulgaris), Psudomonas auriginosa (Ps. auriginosa), Candida albicancs (C. albicancs)* and *Aspergillus niger (A. niger).*

S-hepta-*O*-benzoyl maltosyl-1-arylisothiocarbamides

Hepta-*O*-benzoyl maltosyl bromide

Aryl thiocarbamides

o-tolyl isocyanate

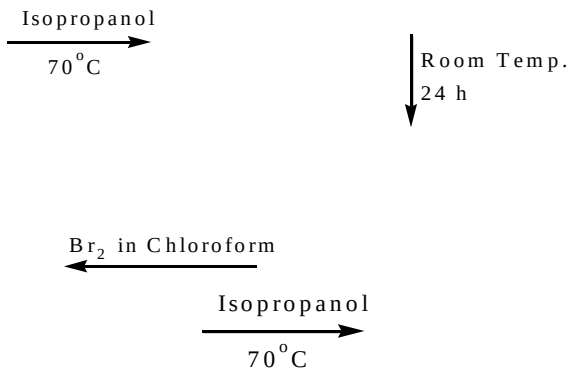

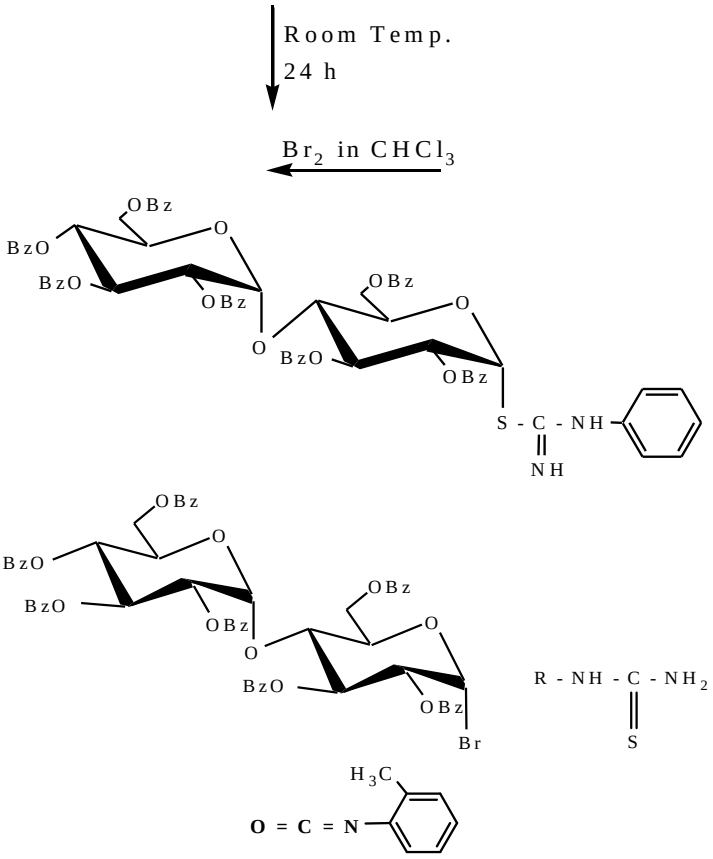
Room Temp.
24 h
Br2 in CHCl3
OBz
BzO
O
S - C - NH
NH
R - NH - C - NH2
S
Br
H3C
O = C = N

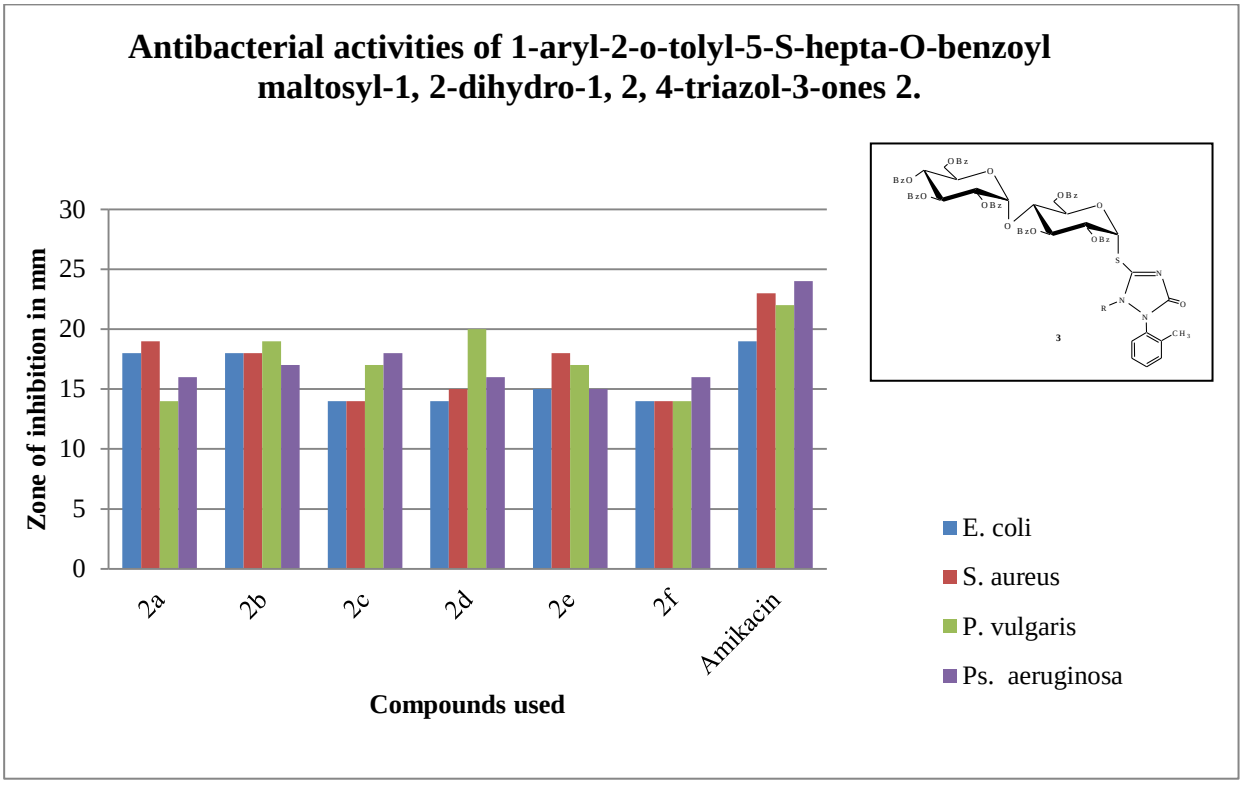
Antibacterial activities of 1-aryl-2-o-tolyl-5-S-hepta-O-benzoyl maltosyl-1, 2-dihydro-1, 2, 4-triazol-3-ones 2.
Zone of inhibition in mm
30
25
20
15
10
5
0
2a
2b
2c
2d
2e
2f
Amikacin
Compounds used
E. coli
S. aureus
P. vulgaris
Ps. aeruginosa
3

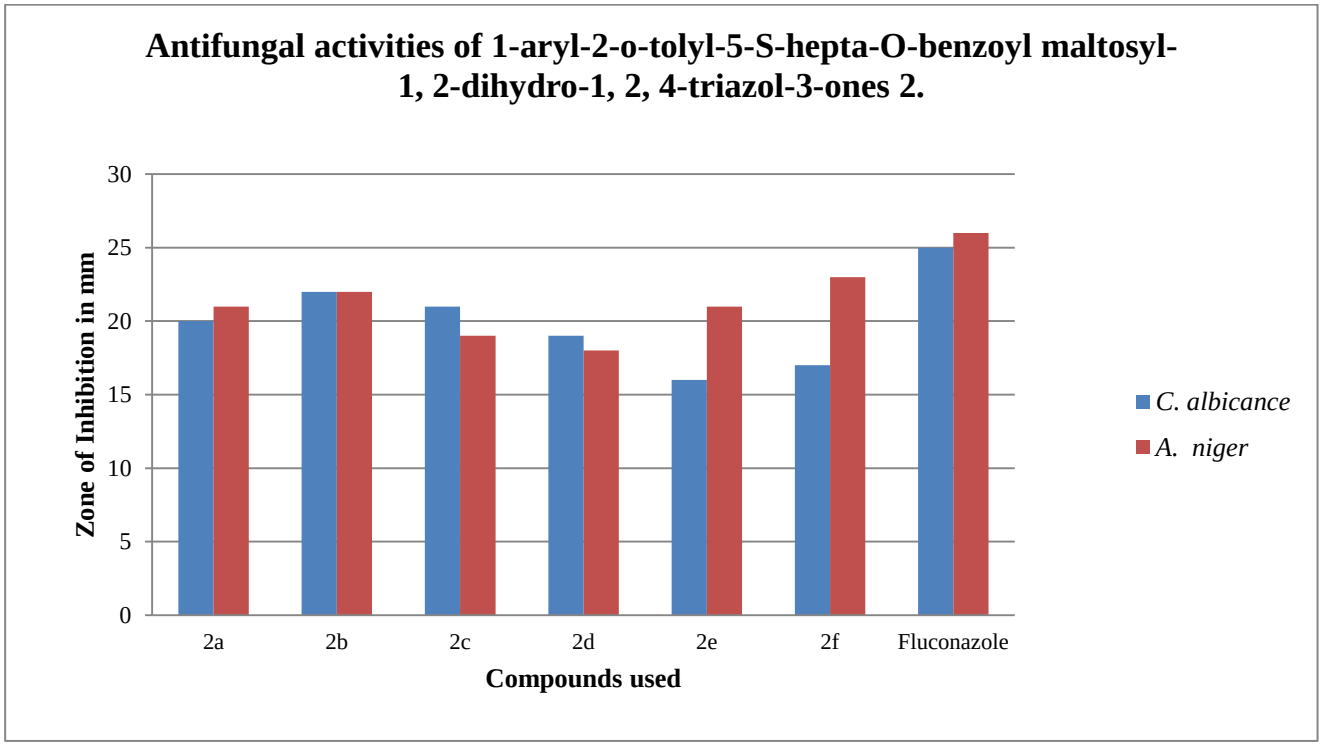
Antifungal activities of 1-aryl-2-o-tolyl-5-S-hepta-O-benzoyl maltosyl-1, 2-dihydro-1, 2, 4-triazol-3-ones 2.
Zone of Inhibition in mm
30
25
20
15
10
5
0
2a
2b
2c
2d
2e
2f
Fluconazole
Compounds used
C. albicance
A. niger

International Journal of Scientific Research in Science and Technology
Available online at : www.ijsrst.com
OPEN ACCESS
Print ISSN: 2395-6011 | Online ISSN: 2395-602X
doi : https://doi.org/10.32628/IJSRST

Pioneering Synthesis and Study of Impact of Substituted 1,3-Thiazine and Its Nanoparticles on Phytotic Growth of Some Flowering Plants

Chhaya D. Badnakhe

Department of Chemistry, Dr. Manorama and Prof. H.S. Pundkar, Arts, Commerce and Science College, Balapur, Dist. Akola, Maharashtra, India

ARTICLEINFO

Article History :

Published : 07 Dec 2024

Publication Issue :
Volume 11, Issue 23
Nov-Dec-2024
Page Number :
89-96

ABSTRACT

The synthesis, spectral analysis and biological activities of 4-phenyl-2-hydroxy-chlorosubstituted-2-imino-1,3 thiazines have been carried out. In this case 4-(2'-hydroxy-3',5'-dichlorophenyl)-6-(4"-nitrophenyl)-2-iminophenyl-3,6-dihydro-1,3-thiazine (B) has been screened. The compound B was synthesized from 2'-hydroxy-3,5-dichlorophenyl-4-(4"-nitrophenyl)chalcone (a) by the action of phenylthiourea.The compound (a) was synthesized from 2'-hydroxy-3',5'-dichloroacetophenone by the action of p-nitrobenzaldehyde in ethanol and 40% NaOH. The nanoparticles of the compound B have been prepared by using ultrasonic technique. The titled compound and its nanoparticles were screened for their growth promoting activity on some flowering plants viz..Crysanthemum coronarium, Dahalia pinnata, Verbena officinalis, Iberis amara.

Keywords: Chalcone, thiazine, phenylthiourea, growth promoting activities.

Introduction

Thiazine is a six membered ring system, which contains two hetero atoms [N and S] placed in a heterocyclic ring at 1, 3 positions. Many workers have synthesized different 1,3-thiazines. The researchers have reported the synthesis of several thiazines1-6 and also their potent biological activities such as blood platelet aggregation inhibitors7, antibacterial8-9antiallergic10, anticholesterenic11 and antifungal12. Moreover thiazine nucleus is a pharmacophore of cephalosporin that occupy a very important place in the field, of antibiotics and drug chemistry. Chalcones and their analogues having α,β-unsaturated carbonyl system are very versatile substrates for the evolution of various reactions and physiologically active compounds. The reaction of thiourea with α,

β-unsaturated ketones also results in the formation of 1,3-thiazines.The chlorosubstituted thiazines with amino group at position 2 in the ring exhibit promising biological activities13-16.

In the present study, the chlorosubstituted 1,3-thiazine (B) has been prepared along with their nanoparticles and screened them for their growth promoting activity on some someflowering plants viz. Crysanthemum coronarium, Dahalia pinnata, Verbena officinalis, Iberis amara.

Experimental

All the glassware's used in the present work were of pyrex quality. Melting points were determined in hot paraffin bath and are uncorrected. The purity of compounds was monitored on silica gel coated TLC plate. IR spectra were recorded on Perkin-Elmer spectrophotometer in KBr pelletes, H1 NMR spectra on spectrophotometer in CDCl3 with TMS as internal standard. UV spectra were recorded in nujol medium. The analytical data of the titled compounds was highly satisfactory. All the chemicals used were of analytical grade. All the solvents used were purified by standard methods. Physical characterisation data of all the compounds is given in Table 1.

Table 1 : Characterisation data of newly synthesized compounds :

Compounds	Molecular formula	M.P. in 0C	% of yield	% of element			
				C	H	N	S
	C8H6O2Cl2	54	80	47.90/48	2.95/3		
a	C15H9O4NCl2	250	70	53.10/53.25	2.40/2.66	3.98/4.18	
B	C22H15O3N3Cl2S	100	75	55.93/56.01	3.177/3.285	8.89/8.92	6.77/6.82

2’-Hydroxy 3’,5’-dichloroacetophenone:

2’-Hydroxy-5-chloroacetophenone (3g) was dissolved in acetic acid (5 ml), and mixed with sodium acetate (3g). To this reaction mixture chlorine in acetic acid reagent (40 ml; 7.5 w/v) was added dropwise with stirring. The temperature of the reaction mixture was maintained below 20oC. The mixture was allowed to stand for 30 minutes and then poured into water. A pale yellow solid thus obtained was filtered, dried and crystallized from ethanol to yield the compound.

Preparation of 2'-hydroxy-3,5-dichlorophenyl-4-(4”-nitrophenyl)-chalcone (a) :

2’-Hydroxy-3',5'-dichloroacetophenone (0.1 mol) was dissolved in ethanol (50 ml) and p-nitrobenzaldehyde (0.1 mol) was added gradually to the solution and the mixture was heated to boiling. Then aquous sodium hydroxide solution [40%; 40 ml] was added dropwise with constant stirring. The mixture was stirred mechanically at room temperature for about half an hour and kept for overnight. It was then acidified by hydrochloric acid (10%) solution . The solid product thus separated, was filtered, and washed with sodium bicarbonate (10%) followed by water. Finally it was crystallized from ethanol acetic acid mixture to get the compound (a).

Preparation of 4-(2'-hydroxy-3',5'-dichlorophenyl)-6-(4"-nitrophenyl)-2- iminophenyl-3,6-dihydro-1,3-thiazine (B) :

2'-Hydroxy-3,5-dichlorophenyl-4-(4”-nitrophenyl)-chalcone (a) (0.01 mol) and phenyl thiourea (0.02 mol) were dissolved in ethanol (30 ml). To this aquous solution of KOH (0.02 mol) was added. The reaction mixture

was refluxed for three hours cooled, diluted with water and acidified with 1:1 HCl. The product thus separated was filtered and crystallized from ethanol to get the compound (B).

The newly synthesized compound was characterised on the basis of elemental analysis, molecular determination, UV, IR, NMR. spectral data.

The UV, IR, and NMR spectral data :-

Compound (B) :

UV : Spectrum No. 1

The UV-Vis spectrum of the compound B reported in dioxane showed □max value395 nm corresponding to n□□□ transition.

IR KBr : Spectrum No. 2

3366.19 cm-1 (O-H phenolic) , 2925.17 cm-1 (aliphatic -C-H stretching) , 3018.18 cm-1 (aromatic C-H stretching) , 3198.28 cm-1 (-NH stretching) , 1648.3 cm-1 (-C=N-stretching) , 1340.5 cm-1 [(C-N=) (C-NO2) stretching] , 738.6 cm-1 [C-Cl stretching in aliphatic) , 1177.4 cm-1 [C-Cl stretching in aromatic].

PMR : Spectrum No.3

∂ 2.6 (d, 1H, -C=C-C-H) ; ∂ 3.5 (hump 1H, -NH) ; ∂ 3.7 (d, 1H, -C=C- H) ; ∂ 7.1 to 8.4 (m, 11H, Ar-H) ; ∂ 12.6 (s, 1H, O-H).

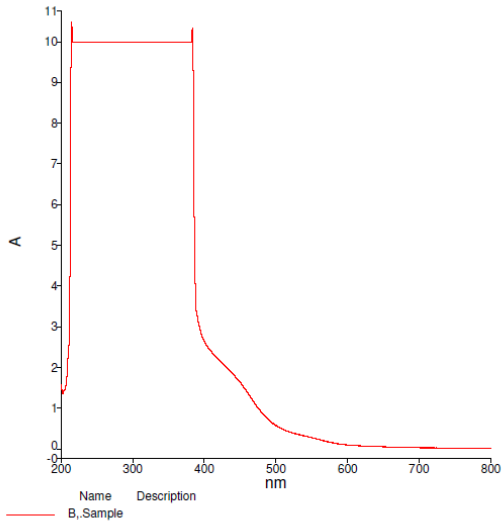

Spectrum No. 1

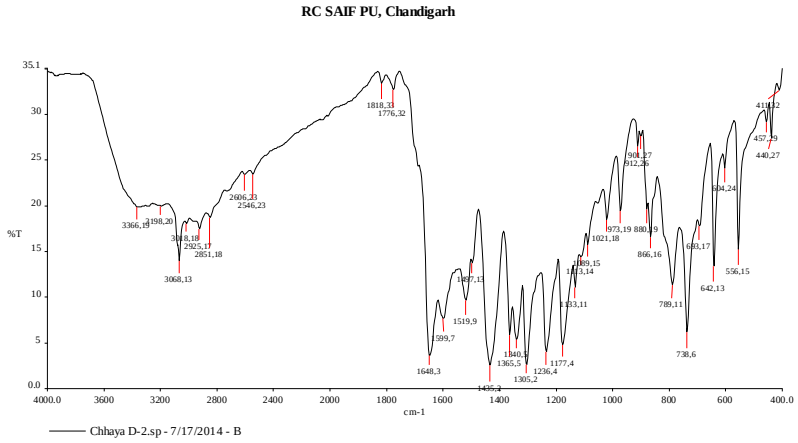

Spectrum No. 2

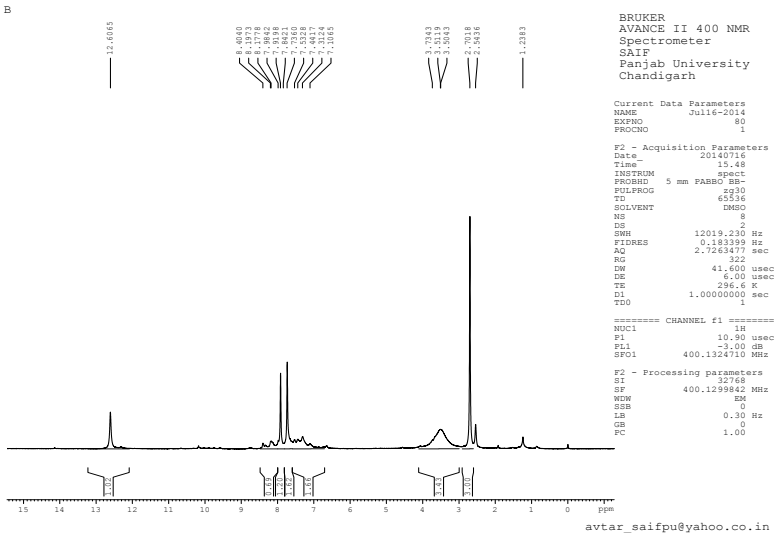

Spectrum No. 3

Scheme :

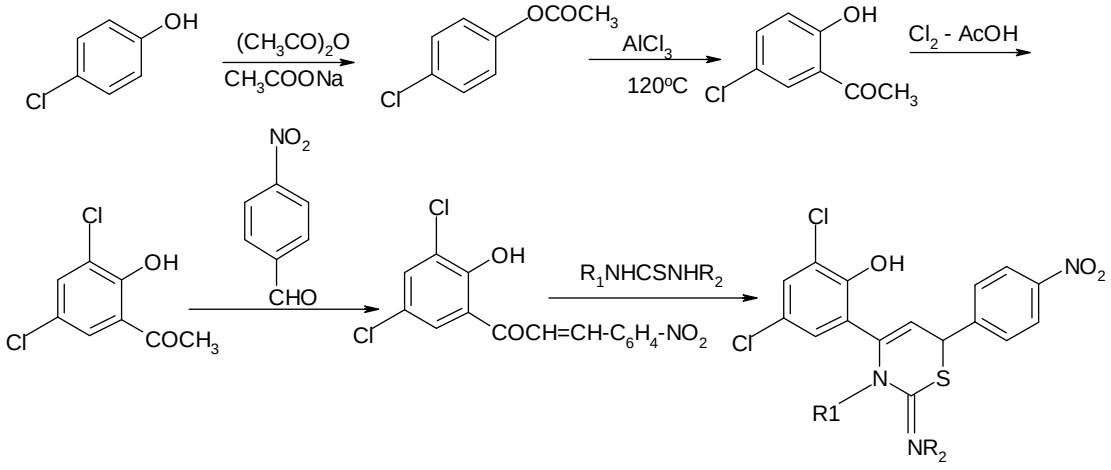

Where :

1) R1 = -H, -C6H5

2) R2 = -H, -C6H5

Growth Promoting Effect on some Flowering Plants :-

The experimental set up of the study was devided intotwo parts:

(i) Seed treatment (ii) Field experiment.

(i) Seed treatment :-

With a view to safeguard dormant seed's potential from harmful external agencies, the seeds of the test plants were treated by test compounds before sowing.

(ii) Field experiment :-

Pregerminated quality seeds of Crysanthemum coronarium, Dahalia pinnata, Verbena officinalis, Iberis amara. were procured from Department of Horticulture, Dr. PDKV, Akola.

The beds of cotton soil, 2.5 x 2.5 m size were prepared in an open field. The sowing of seeds of all four test vegetable crop plants were done in separate beds and irrigated periodically.

The plants from each bed were devided into two groups i.e. A and B and designated as "Control" and "Treated" group plants respectively.

The plants from group B were sprayed with the solution of test compounds at weekly intervals. The field experiments were conducted to compare the treated plants of group B with untreated plants of controlled group A. In this context, the observations were recorded on 7, 14, 21, 28, 35, 42, 45, 56, 63, 70, 77, 84, 91 days after sowing corresponding to early vegetative, late vegetative, flowering, pod filing and pod maturation, with special reference to number of leaves and height of shoots.

The results of field's experiments are tabulated in the tables 2,3 and 4.

Table (2) : Activity of the test compound B :

Table No. (02)

4-(2'-Hydroxy-3',5'-dichlorophenyl)-6-(4"-nitrophenyl)-2- iminophenyl-3-6-dihydro-1,3-thiazine (B)

Periodicity of Observations [in days]	*Crysanthemum coronarium*				*Dahalia pinnata*				*Verbena officinalis*				*Iberis amara*			
	Shoot height		No. of leaves		Shoot height		No. of leaves		Shoot height		No. of leaves		Shoot height		No. of leaves	
	C	T	C	T	C	T	C	T	C	T	C	T	C	T	C	T
7	1.0	1.0	1	1	2.5	1.5	2	2	4.4	4	2	2	2	2	2	3
14	1.2	1.2	2	2	7.5	7	2	2	10	8	2	2	2.1	2.5	2	3
21	1.3	1.4	7	10	8	12	2	4	15	11	3	5	2.3	2.8	3	4
28	1.5	1.6	9	11	9	19	3	6	16	18	4	6	2.5	2.7	4	5
35	1.6	1.8	10	12	11	26	4	7	18	19	5	9	2.8	3.0	5	7
42	1.8	2.0	12	15	17	42	5	8	19	20	7	12	3.0	3.4	6	8
49	2.3	3.5	14	18	25	48	6	8	20	21	8	14	3.5	3.9	8	9
56	3.6	4.0	16	22	28	52	7	9	23	25	10	17	3.8	4.5	10	12
63	5.5	6.7	18	24	31	55	8	10	25	30	12	18	4.2	5.0	12	14
70	7	12	20	28	34	60	9	11	27	32	14	20	4.6	5.4	14	16
77	14	19	22	30	36	63	10	13	28	35	16	23	5.5	7.0	16	18

Table No. (02)

4-(2'-Hydroxy-3',5'-dichlorophenyl)-6-(4"-nitrophenyl)-2- iminophenyl-3-6-dihydro-1,3-thiazine (B)

Periodicity of Observations [in days]	*Crysanthemum coronarium*				*Dahalia pinnata*				*Verbena officinalis*				*Iberis amara*			
	Shoot height		No. of leaves		Shoot height		No. of leaves		Shoot height		No. of leaves		Shoot height		No. of leaves	
84	20	24	24	32	38	65	11	15	29	36	18	25	7,2	14	20	24
91	24	30	26	36	40	68	12	17	36	38	20	27	8.2	17	25	29

Impact of the compound 4-(2'-Hydroxy-3',5'-dichlorophenyl)-6-(4"-nitrophenyl)-2-iminophenyl-3-6-dihydro-1,3-thiazine (B) on phytotic growth of *Crysanthemum coronarium*

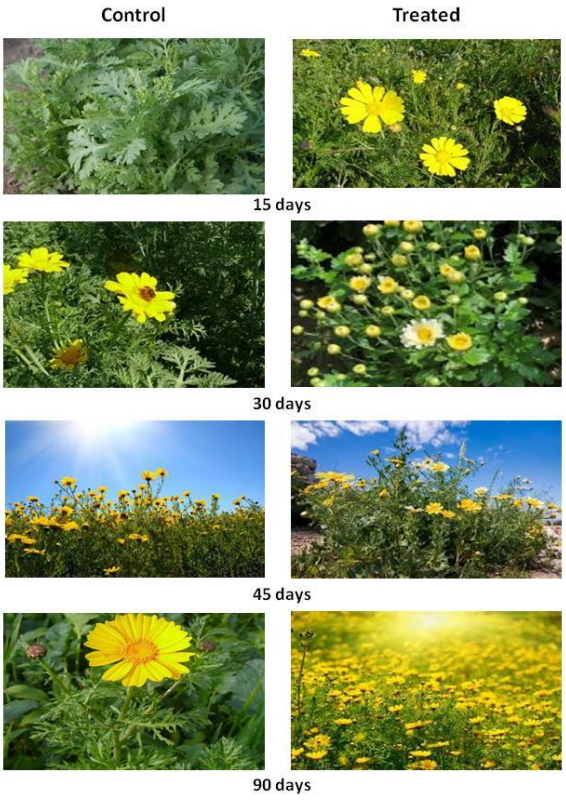

Impact of the compound 4-(2'-Hydroxy-3',5'-dichlorophenyl)-6-(4"-nitrophenyl)-2-iminophenyl-3-6-dihydro-1,3-thiazine (B) on phytotic growth of *Dahalia pinnata*

Impact of the compound 4-(2'-Hydroxy-3',5'-dichlorophenyl)-6-(4"-nitrophenyl)-2-iminophenyl-3-6-dihydro-1,3-thiazine (B) on phytotic growth of *Verbena officinalis*

Impact of the compound 4-(2'-Hydroxy-3',5'-dichlorophenyl)-6-(4"-nitrophenyl)-2-iminophenyl-3-6-dihydro-1,3-thiazine (B) on phytotic growth of *Iberis amara*

Result and Discussion:

The titled compounds and their nanoparticles were screened for their growth promoting activity on test flowering plants viz, Crysanthemum coronarium, Dahalia pinnata, Verbena officinalis, Iberis amara.

When a comparison of morphological characters was made between those of treated and control group plants, it was interesting to note that all the treated plants exhibited significant shoot growth and considerable increase in the number of leaves as compared to those of untreated ones.

Acknowledgements:

The authors are thankful to the Principal, Dr.D.H.Pundkar, Dr.Manorama & Prof.H.S.Pundkar, Arts, Commerce & Science College, Balapur, Dr.B.B.Wankhade, Principal, Malkapur Vidnyan Mahavidyalaya, Malkapur for providing necessary facilities to carry out the research work.

References

[1]. Swarnkar P.K., Kriplani B., Gupta G.N., Oijha K.G., synthesis and antimicrobial activity of some new phenothiazine derivatives, E.J. Chem., vol. 4, no. 1, 14-20.Jan. 2007.

[2]. Kakade B.S., "Synthesis in heterocyclic compounds (Role of DMSO as a solvent," Ph.D. Thesis, Nagpur University, 1981.

[3]. Chincholkar M.M., and Ramekar M.A. J. Ind. Chem. Soc., 71 (4) 199, 1994.

[4]. S.P. Rathod, A.P. Charjan and P.R. Rajput, RasayanJ. Chem., vol.-3, no. 2, 363-367, 2010.

[5]. Dabholkar V.V. and F.Y. Ansari, Indian J. Chem., vol. 47 B., pg.no. 1759 – 1761, Nov. 2008.

[6]. D.H. Morey and S.N. Patil ori., J. Chem., Mar., 2002.
[7]. C.Brown and R.N.Davidson, Adv.Heterocycl.Chem.,38,135, 1985,.
[8]. P. Descacq, A. Nubrich, M. Capdepuy and G. Devanuz, Eur, J. Med. Chem., 25, 285, 1990.
[9]. M.I. Younes, H.H. Abbas, and S.A.M. Metwally, Arch, Pharma, 230, 1987.
[10]. D.T. Witiar, M.E. Wolff and R.C. Covestri, "In Berger", S. Medicinal Chemistry", part III, Edi. Willey, Newyork, 603, 1981.
[11]. M. Crewzet and F. Helene, Eurpat App. Ep., 121, 489, Chem. Abstr., 102, 1985, 787244, Chem., Abstr., 89, 108943 m.1978.
[12]. F.M. Dean, K.A. Thakur and C.H. Gill, "Naturally occuring oxygen ring compounds", J. Indian Chem. Soc.60, 668, 1983.
[13]. P. Valenti, A. Bisi, A. Rampa, F. Belluti, S. Gobbi, A. Zampiron, M. Carrara, Biosy, Med. Chem., 239, 2002.
[14]. Y.Q. Shi, J. Fukai, H Sakagami, W.J. Chang, P.Q. Yang, F.P. Wang, T. Nomura, J. Nat. Prod., 64, 181, 2001.
[15]. G.J. Reddy, D. Latha, K.S. Rao, Heterocycl, Commun., 10, 279, 2004.
[16]. T. Ghosh, S. Saba, C. Bandyopadhya, Synthesis, 11, 1845, 2005.

International Journal of Scientific Research in Science and Technology
Available online at : www.ijsrst.com
Print ISSN: 2395-6011 | Online ISSN: 2395-602X
doi : https://doi.org/10.32628/IJSRST

Environmental Impact of Low-Cost Adsorbent for Methylene Blue Dye Removal from Drinking Water

Dattatraya Jirekar, Pramila Ghumare
Department of Chemistry, Anandrao Dhonde Alias Babaji Mahavidyalaya Kada, Maharashtra, India

ARTICLEINFO

Article History :

Published : 07 Dec 2024

Publication Issue :
Volume 11, Issue 23
Nov-Dec-2024
Page Number :
97-107

ABSTRACT

The contamination of drinking water by synthetic dyes, particularly Methylene Blue (MB), poses significant environmental and health risks. This study investigates the potential of low-cost adsorbents, specifically the leaves of Rauwolfia serpentina (commonly known as Sarpgandha), for the removal of MB dye from aqueous solutions. The leaves of R. serpentina were evaluated for their adsorption capacity under varying experimental conditions such as pH, contact time, and initial dye concentration. Results indicated that the leaves of R. serpentina possess effective adsorptive properties, demonstrating a significant reduction in MB concentration in water. The adsorption process followed a pseudo-second-order kinetic model, and equilibrium data were best described by the Freundlich isotherm, suggesting heterogeneous sites with varying affinities for the dye molecules. The study also highlighted the influence of pH on the adsorption efficiency, with the maximum dye removal occurring in mildly acidic conditions. The adsorption capacity of R. serpentina leaves was comparable to that of other conventional adsorbents, making them a promising, eco-friendly, and cost-effective alternative for mitigating dye contamination in drinking water. The utilization of natural materials like R. serpentina not only offers a sustainable solution but also contributes to reducing the environmental impact of synthetic adsorbents, thus promoting cleaner and safer water resources.

Keywords: Environmental impact, Low-cost adsorbents, Adsorption capacity, Isotherm models, Kinetic studies

Introduction

Water contamination by synthetic dyes has become a global environmental challenge, particularly due to the increasing industrialization and urbanization across the world. Methylene Blue (MB), a widely used dye in the textile, paper, and pharmaceutical industries, is one such pollutant that poses significant risks to water quality.

Even at low concentrations, MB can cause adverse effects on aquatic life and human health, including skin irritation, gastrointestinal issues, and long-term toxicity [1]. Due to its complex molecular structure, MB is resistant to conventional treatment methods such as biodegradation, making its removal from water an urgent issue. Traditional water purification techniques, including chemical coagulation, activated carbon adsorption, and filtration, often involve high operational costs, limited efficacy, and adverse environmental impacts [2]. These limitations have prompted a search for cost-effective, eco-friendly, and sustainable alternatives for dye removal.

Low-cost adsorbents, particularly those derived from natural resources, have garnered significant interest in recent years as viable options for water treatment. Plant-based adsorbents are especially attractive because of their abundance, renewability, biodegradability, and minimal environmental impact compared to synthetic materials. One such potential adsorbent is Rauwolfia serpentina (Sarpgandha), a medicinal plant known for its bioactive alkaloids and therapeutic applications, including its use in the treatment of hypertension and anxiety [3]. The leaves of Rauwolfia serpentina (Sarpgandha) have recently been explored as an adsorbent for pollutants due to their natural composition, which includes cellulose, lignin, and other polysaccharides that can effectively bind with dye molecules through adsorption [4].

The adsorption process involves the physical binding of dye molecules onto the surface of an adsorbent, and it is influenced by factors such as pH, temperature, contact time, and the initial concentration of the dye [5]. Preliminary studies have demonstrated that plant-based adsorbents like R. serpentina leaves are capable of effectively removing MB from aqueous solutions [6]. The ability of R. serpentina leaves to adsorb MB dye can be attributed to their porous structure and the presence of functional groups on their surface, which facilitate the interaction between the dye molecules and the adsorbent surface.

Importantly, the use of R. serpentina leaves as adsorbents aligns with the principles of green chemistry and sustainability. Unlike synthetic adsorbents such as activated carbon, which require energy-intensive production processes and often result in secondary environmental impacts, plant-based adsorbents like R. serpentina leaves are biodegradable, non-toxic, and widely available in many regions [7]. Furthermore, these adsorbents can be utilized in a circular economy model, where the spent material can be composted or repurposed, reducing waste and minimizing environmental harm.

Given the promising results from initial studies, further research is needed to optimize the conditions for dye removal and to assess the environmental impact of using R. serpentina leaves in large-scale water treatment applications. This includes evaluating the efficiency of MB removal under different environmental conditions, understanding the adsorption mechanisms in greater detail, and assessing the feasibility of using this material in real-world water purification scenarios.

This study aims to investigate the potential of R. serpentina leaves as an effective, low-cost adsorbent for the removal of MB dye from drinking water, and to evaluate their environmental sustainability and economic viability as part of a broader effort to develop more eco-friendly water treatment technologies.

MATERIALS AND METHODS:

2.1. Preparation of adsorbent:

The use of plant-based adsorbents for the removal of pollutants from water has gained considerable attention due to their eco-friendliness, cost-effectiveness, and sustainability. The preparation of adsorbents from Rauwolfia serpentina (Sarpgandha) leaves involves several steps to optimize their physical and chemical properties for effective dye adsorption.

2.1.1. Collection of Leaves:

The first step in preparing R. serpentina (Sarpgandha) leaves as adsorbents is the collection of healthy, mature leaves from the plant. These leaves are typically abundant in tropical regions where the plant grows naturally. Care should be taken to select leaves that are free from pests and diseases to ensure a high-quality adsorbent.

2.1.2. Washing and Cleaning:

After collection, the leaves are thoroughly washed with tap water to remove dirt, dust, and surface contaminants. This is followed by rinsing with distilled water to eliminate any residual impurities or chemicals.

2.1.3. Drying:

The leaves are spread in a shaded area, away from direct sunlight, to prevent degradation of bioactive compounds. This method may take 1-2 days.

2.1.4. Grinding and Size Reduction:

Once dried, the leaves are ground into a fine powder using a mechanical grinder or mortar and pestle. Grinding increases the surface area of the material, which is crucial for enhancing the adsorption capacity. The powdered leaves are then sieved to obtain a uniform particle size, typically in the range of 60-80 mesh. A finer particle size of (Rauwolfia serpentine) Sarpgandha leaves powder (SLP) leads to better adsorption due to increased surface area and more available binding sites for dye molecules.

2.2. Preparation of Methylene blue solution:

Methylene Blue (MB) is a synthetic cationic dye widely used in various industries, including textiles, pharmaceuticals, and paper production. Due to its toxic effects on aquatic life and its persistence in water bodies, effective methods for removing MB from contaminated water are essential.

Methylene Blue (MB): Analytical grade Methylene Blue powder is required for the preparation of dye solutions. MB has a molecular formula of $C_{16}H_{18}ClN_3S{\cdot}3H_2O$ and a molar mass of approximately 373.91 g/mol. Dissolved in distilled water is used to dissolve Methylene Blue to avoid any impurities or minerals that could interfere with the adsorption process. To prepare the MB solution, a known quantity of Methylene Blue powder is weighed accurately. A typical concentration for stock solutions is 1000 mg/L, but this may vary depending on experimental requirements. The stock solution of MB is stored in a dark bottle to prevent photodegradation, as light can break down the dye over time.

BATCH EXPERIMENTAL TECHNIQUES FOR ADSORPTION STUDIES:

Batch adsorption experiments are commonly used to assess the efficiency of adsorbents for the removal of pollutants, including dyes such as Methylene Blue (MB), from aqueous solutions. In a batch system, a fixed amount of adsorbent is introduced into a known volume of pollutant solution, and the interaction between the adsorbent and the pollutant is studied under controlled conditions. These experiments are vital for understanding the kinetics, isotherms, and thermodynamics of the adsorption process, and for optimizing the removal of contaminants.

In the batch experimental setup, a known volume of the dye solution is mixed with a measured amount of adsorbent in a container such as a beaker or conical flask. The experimental conditions can vary, and factors such as adsorbent dose, dye concentration, contact time, and temperature are controlled to study their influence on adsorption efficiency.

The solution is stirred continuously (usually on a magnetic stirrer) to facilitate the interaction between the adsorbent and the dye. This ensures uniform contact between the dye molecules and the adsorbent surface.

Batch adsorption experiments are crucial for understanding the behavior of adsorbents in the removal of pollutants like Methylene Blue from water. By varying parameters such as adsorbent dose, contact time, dye concentration, and temperature, researchers can optimize the conditions for effective dye removal. The adsorption kinetics, isotherms, and thermodynamics provide valuable insights into the efficiency and mechanism of adsorption.

The efficiency of dye removal is calculated using the following formula:

$$q = \frac{V(Co-Ct)}{M} \quad (1)$$

Where, q is the amount of MB dye adsorbed from the solution (mg/g), Co is the concentration before adsorption (mg/L), and C_t is concentration after adsorption. V is the volume of adsorbate (L) and M is the weight of the adsorbent (g).

The percentage adsorption of MB dye was calculated by following equation;

$$\text{Percentage adsorption} = \frac{(C_0 - C_e)}{C_0} * 100 \quad (2)$$

Where, C_0 and C_e are the initial and equilibrium concentrations respectively.

RESULTS AND DISCUSSION:

4.1. Effect of Contact Time on Adsorption:

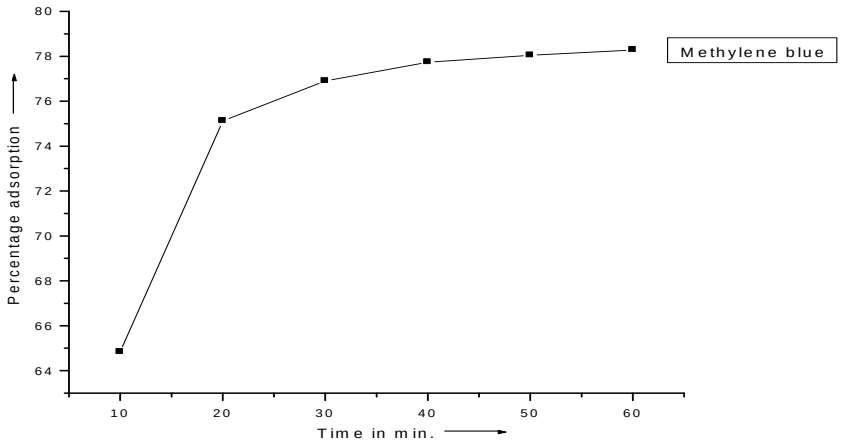

Fig.4.2.1: Effect of contact time on percentage adsorption of methylene blue dye.
[Initial conc=100 ppm,Adsorbent dose=1.0 g,Volume of adsorbate=100 mL, Temp=300.9 k, pH=7.2]

Contact time is a critical factor that determines the extent of dye removal during the adsorption process. Initially, the adsorption rate is typically fast because a large number of vacant adsorption sites on the adsorbent are available for dye molecules. Over time, as the dye molecules occupy the available sites, the adsorption rate slows down and eventually reaches equilibrium, where no further significant adsorption occurs.

- **Initial Rapid Adsorption**: In the early stages of the experiment, the adsorption is high due to the availability of empty sites on the surface of the adsorbent. As MB molecules quickly diffuse to the surface of Rauwolfia serpentina leaves, the rate of dye removal is high.
- **Slower Approach to Equilibrium**: After the initial phase, the adsorption rate decreases because the remaining vacant sites become less accessible to the dye molecules. Eventually, the adsorption capacity reaches equilibrium when no more dye molecules can be adsorbed. The time required to reach this equilibrium is influenced by both the nature of the adsorbent and the solution conditions.

Several studies have reported that the contact time required to reach equilibrium for MB adsorption typically ranges from 60 minutes to 120 minutes, depending on the adsorbent dose, solution concentration, and other factors [8, 9]. The adsorption capacity increases with contact time until equilibrium is attained, after which further increases in contact time do not lead to significant additional dye removal.

4.2. Effect of adsorbent dose on Adsorption:

Initially the rate of percentage adsorption of dye was found to increase rapidly with increase of adsorbent dose and slowed down latter, when the dose increased from 0.50 to 2.50 g. in each case. From the observation results, the optimum dose of adsorbent fixed for all adsorbents is 1.0 g. It can also be seen from Fig.4.2.2

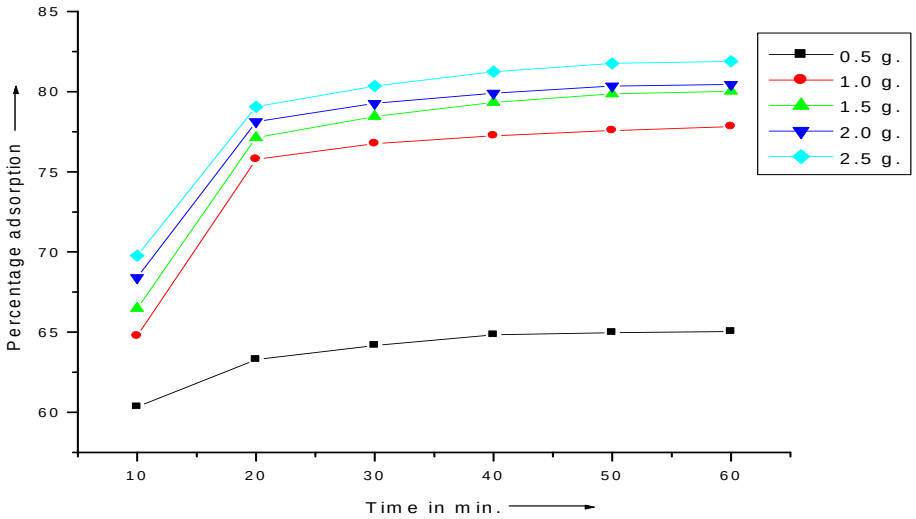

Fig.4.2.2.: Effect of adsorbent dose on percentage adsorption of methylene blue dye.
[Initial conc.=100 ppm, Volume of adsorbate=100 mL, Temp=300.9 k,pH=7.2]

The dose of adsorbent plays a crucial role in determining the efficiency and capacity of the adsorption process, especially when using low-cost adsorbents like Rauwolfia serpentina leaves for the removal of Methylene Blue (MB) dye from aqueous solutions.

As the adsorbent dose increases, the surface area available for adsorption also increases. This allows for more dye molecules to be adsorbed onto the available active sites of the adsorbent.

With a higher dose of Rauwolfia serpentina leaves, there are more functional groups or adsorption sites available to interact with the dye molecules. This facilitates higher uptake of MB molecules from the solution.

4.3. Effect of Initial Concentration on Adsorption:

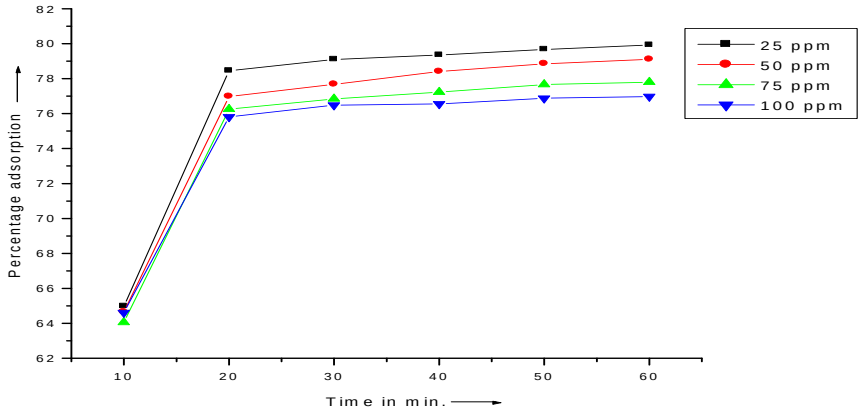

Fig.4.2.3: Effect of initial concentration of of adsorbate solution on percentage adsorption of methylene blue dye.
[Adsorbent dose=1.0 g, Volume of adsorbate=100 mL, Temp=300.9 k, pH=7.2]

The initial concentration of MB has a profound impact on the adsorption efficiency and capacity of the adsorbent. As the initial concentration of MB increases, the driving force for adsorption becomes greater, resulting in an increased rate of adsorption at the initial stages.

- **Higher Initial Concentration**: At higher initial concentrations of MB, more dye molecules are available for adsorption. This results in a higher adsorption capacity per unit mass of adsorbent. However, at higher concentrations, the adsorption process may become less efficient if the adsorbent surface becomes saturated.
- **Increased Saturation of Adsorbent Sites**: As the initial concentration increases, the number of dye molecules surpasses the number of available active sites on the adsorbent surface. This leads to a decrease in adsorption efficiency at higher concentrations. The equilibrium concentration of MB will be higher at greater initial concentrations, indicating that not all dye molecules can be removed at higher loading conditions.

A study on Rauwolfia serpentina leaves for MB removal observed that the adsorption capacity increased with an increase in the initial dye concentration, as expected, but at higher concentrations, the removal efficiency per unit mass of adsorbent decreased. This is consistent with typical adsorption behavior, where the adsorption isotherms shift with changing dye concentration.

4.4. Effect of Temperature on Adsorption:

Temperature has important effect on adsorption was investigated in the temperature range of 305.9, 310.9, 315.9, 320.9., 325.9 k and 100 mg/L. The effect of temperature on the adsorption of MB dye onto Rauwolfia serpentina leaves was observed that adsorption decreases with increase in temperature (Figure 4.2.4).

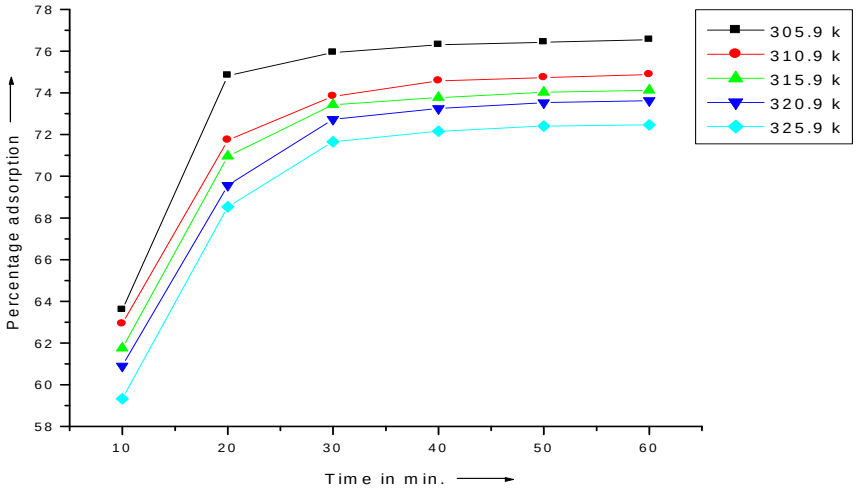

Fig.4.2.4.: Effect of temperature on percentage adsorption of methylene blue dye.
[Initial conc.=100 ppm, Adsorbent dose=1.0 g, Volume of adsorbate=100 mL, pH=7.2]

increasing the temperature leads to an increase in adsorption capacity. This is primarily because higher temperatures enhance the kinetic energy of the dye molecules, improving their diffusion rate to the adsorbent surface and facilitating better interaction between the dye molecules and the adsorption sites [10]. Additionally, higher temperatures may weaken the bond between the dye and the solvent molecules, promoting better adsorption of MB onto the adsorbent.

Thermodynamic parameters such as Gibb's free energy change ΔG^0, enthalpy change ΔH^0 and entropy change ΔS^0 were calculated by using Van't Hoff's equation.

$$K_c = \frac{C_{ad}}{C_e} \qquad (3)$$

$$\Delta G^0 = -RT \ln K_c \quad (4)$$

Where, $\Delta G^0 = \Delta H^0 - T\Delta S^0$ (5)

$$\log K_c = \frac{\Delta S^0}{2.303R} - \frac{\Delta H^0}{2.303RT} \quad (6)$$

Where, K_c is the equilibrium constant, C_{ad} is the amount of metal ion adsorbed per liter of the solution at the equilibrium, C_e is the equilibrium concentration (mg/L) of the metal in the solution, T is the temperature in Kelvin and R is the gas constant (8.314 J/mole).The values of ΔH^0 and ΔS^0 was determined from the slopes and intercepts of the plot of $\log K_c$ against $\frac{1}{T}$ respectively. Thermodynamic parameters are given in Table: 1.

Table: 1. Free energy change (ΔG°) , ΔH° and ΔS° values of MB solution different temperature:

Temp (K)	ΔG°, ΔH° and ΔS° values of MB solution different temperature in KJ/mole		
	ΔG° KJ/mole	−ΔH° KJ/mole	−ΔS° J/mole
305.9	-3.726	9.171	17.821
310.9	-3.637		
315.9	-3.548		
320.9	-3.459		
325.9	-3.370		

The ΔG^0 values obtained in this study for the Ni^{2+} metal ions are < -10 KJ /mole, it indicates that physical adsorption was the predominant mechanism in the adsorption process. The Gibb's free energy indicates the degree of spontaneity of the adsorption process, where more negative value reflects a more energetically favorable adsorption process. The negative value of ΔG^0 (Table: 1.) indicates that the adsorption is favorable and spontaneous. The negative value of ΔS^0 and ΔH^0 suggests that the decreased disorder and randomness at the solid solution interface with exothermic adsorption.

ADSORPTION ISOTHERM: -

Langmuir Adsorption Isotherm

The Langmuir isotherm is based on the following assumptions:

- The adsorption process occurs on a surface with a finite number of identical sites.
- Each site can only hold one adsorbate molecule, leading to monolayer adsorption.
- The adsorbate molecules do not interact with each other once adsorbed.
- The adsorption process is reversible, and the adsorbent surface has a uniform affinity for the adsorbate.

The Langmuir isotherm equation is expressed as:

$$\frac{1}{q_e} = \left(\frac{1}{Q_0}\right) + \frac{1}{bQ_0C_e} \quad (7)$$

Where, C_e (mg/L) is the equilibrium concentration of the MB dye, q_e (mg/gm) is the amount of MB dye adsorbed per unit mass of SLP, at equilibrium, Q_0 (mg/gm) and b (L/mg) are Langmuir constants related to maximum monolayer adsorption capacity and energy of adsorption respectively. The values of Q_0 and b are calculated from the slope and intercept of plot of $\frac{1}{q_e}$ against $\frac{1}{C_e}$ respectively. The basic features of the Langmuir isotherm may be expressed in terms of equilibrium parameter R_L. Which is a dimensionless constant referred to as separation factor or equilibrium parameter [11]

$$R_L = \frac{1}{1+bC_0} \quad (8)$$

Where, C_0 is initial concentration of MB dye in ppm and b is Langmuir constant related to the energy of adsorption. The R_L Value indicates the adsorption nature to be either unfavorable if $R_L > 1$, linear if $R_L = 1$, favorable if $0 < R_L < 1$ and irreversible if, $R_L = 0$ [12].

Freundlich Adsorption Isotherm

The Freundlich isotherm is based on the assumption that the adsorption capacity increases with the concentration of the adsorbate but at a decreasing rate, due to the heterogeneous nature of the adsorption sites. The Freundlich isotherm equation is given by:

$$\frac{x}{m} = K_f C_e^{1/n} \quad (9)$$

Where, x is the quantity adsorbed, m is the mass of the MtSH, C_e is the equilibrium concentration of Ni^{2+} metal ions (mg/L), The constants K_f and n can be obtained by taking log on both sides of equation (9) as follows,

$$\log \frac{x}{m} = \frac{1}{n} \log C_e + \log K_f \quad (10)$$

The constant K_f is an approximate indicator of adsorption capacity, while $\frac{1}{n}$ is a function of the strength of adsorption in the adsorption process [13]. If $n = 1$ then the partition between the two phases are independent of the concentration. If value of $\frac{1}{n}$ is below one, it indicates a normal adsorption, on the other hand $\frac{1}{n}$ being above one indicates co-operative adsorption [14]. A plot of $\log \frac{x}{m}$ against $\log C_e$ gives a straight line with an intercept on the ordinate axis. The value of n and K_f can be obtained from the slope and the intercept of the linear plot.

The Freundlich isotherm model provides a good fit for the adsorption of Methylene Blue dye onto Rauwolfia serpentina leaves. The adsorption process is favorable, occurring on heterogeneous sites with varying affinities for the dye molecules. By understanding the Freundlich parameters, the adsorption process can be optimized for real-world applications in water purification.

Table: 2. Isotherm parameter values with MB solution:-

Adsorbents	Langmuir constants				Freundlich constants		
	Q_0 (mg/g.)	b (L/g.)	R_L	R^2	$\frac{1}{n}$	K_f (mg/g.(L/g.))$^{1/n}$	R^2
SLP	20630.2	0.059	0.14	0.827	0.596	18.10	0.976

The R_L value was found to be between 0 and 1 for MB dye studies, it is confirmed that the ongoing adsorption of MB is favorable. The data reveal that the Freundlich model yields better fit than Langmuir model .The value of n suggests that deviation from linearity, if n = 1 the adsorption is homogenous and there is no interaction between adsorbed species. The value of n is greater than unity, (1< n <10), that means favorable adsorption [15]. If value of $\frac{1}{n} > 1$ indicates the adsorption is favored and new adsorption sites are generated [16-19]. The value of n presented in Table: 2. the value of n was found to be between 1 and 10, this indicates adsorption is favorable.

Kinetic Models in Adsorption Studies:

Several kinetic models are commonly employed to analyze the adsorption of MB dye onto low-cost adsorbents like Rauwolfia serpentina leaves. The most widely used models are:

- Pseudo-first-order model
- Pseudo-second-order model

Pseudo-first-order Model

The pseudo-first-order kinetic model, derived from Lagergren's equation, assumes that the rate of adsorption is proportional to the difference in the concentration of the adsorbate on the adsorbent. The equation is:

$\frac{dq}{dt} = K_1(q_e - q_t)$ (11)

After definite integration by applications of the conditions $t = 0$ to $t = t$ and $q = 0$ to $q = q_e$ Equation (11) becomes,

$\log(q_e - q_t) = \log q_e - \frac{K_1}{2.303} t$ (12)

Where, q_e (mg/gm) is the amount of adsorption at equilibrium, q_t (mg/gm) denotes the amount of adsorption at time t (min.) and K_1 (min^{-1}) is the rate constant of the pseudo-first order model. Based on experimental results, linear graphs were plotted between $\log (q_e - q_t)$ versus t, to calculate K_1, q_e and R^2.

This model typically describes the adsorption behavior in the initial stages, where adsorption sites are plentiful. However, when applied to Rauwolfia serpentina leaves for MB dye, the pseudo-first-order model often does not provide the best fit for the entire adsorption process, especially at longer times.

Pseudo-second-order Model

The pseudo-second-order model is based on the assumption that the rate-limiting step involves the adsorption of a single dye molecule on each adsorption site. The equation is given by:

$\frac{dq}{dt} = K_2(q_e - q_t)^2$ (13)

Where, K_2 ($gm.mg^{-1}min^{-1}$) is the rate constant of the pseudo-second order. Integrating equation (13) for the boundary conditions $t = 0$ to $t = t$ and $q = 0$ to $q = q_e$ gives

the linear form of equation is

$\frac{t}{q_t} = \frac{1}{K_2 q_e^2} + \frac{1}{q_e} t$ (14)

K_2 and q_e can be obtained from the intercept and slope of plotting t/q_t against t .

For many systems, including Rauwolfia serpentina leaves for MB dye removal, the pseudo-second-order model often provides a better fit for experimental data, suggesting that the adsorption process may be controlled by chemical interactions or bond formation between the adsorbate and the adsorbent.

The adsorption kinetics of MB dye onto Rauwolfia serpentina leaves suggests that the process is primarily governed by chemisorption, as indicated by the good fit to the pseudo-second-order model. These insights into adsorption kinetics are crucial for designing efficient water treatment systems using Rauwolfia serpentina leaves as a low-cost adsorbent for dye removal.

Table: 3. Kinetic parameter values with MB solution:-

	Pseudo-first order			Pseudo-second order		
Adsorbent	K_1 (min^{-1})	q_e (mg/g.)	R^2	K_2 (g./mg.min)	q_e (mg/g.)	R^2
SLP	$2.998*10^{-2}$	1448.77	0.789	16167.51	$8122.95*10^{-4}$	0.999

The value of R^2 with first order kinetics was 0.789, while for second order is 0.999 for SLP adsorbent. It is clear that the adsorption of MB on SLP adsorbent was better represented by pseudo second order kinetics. This indicates that the adsorption system belongs to the second order kinetic model.

CONCLUSION:

In conclusion, the use of Rauwolfia serpentina leaves as a low-cost adsorbent for Methylene Blue dye removal from drinking water presents a sustainable, environmentally friendly solution to tackle dye pollution. The high adsorption capacity, low environmental impact, and the renewable nature of the adsorbent make it a viable

alternative to conventional water treatment methods. By exploring and optimizing the adsorption process, this approach has the potential to provide an effective, scalable, and eco-friendly means of improving water quality, especially in developing regions with limited access to expensive water purification technologies.

References

[1]. Kümmerer, K., Dionysiou, D. D., & Olsson, G. (2018). Environmental Impact of Dyes and Their Treatment in Water. Environmental Science & Technology, 52(7), 4145-4155.

[2]. Ali, H. (2012). Biological and Environmental Degradation of Synthetic Dyes in the Environment. Environmental International, 39(1), 64-73.

[3]. Panda, S. K., Dash, S. K., & Mishra, B. (2017). Pharmacological Properties of Rauwolfia serpentina: A Review. Pharmacognosy Reviews, 11(22), 106-114.

[4]. Sharma, S., & Dubey, A. (2021). Plant-Based Adsorbents for Water Treatment: A Review of Current Trends and Future Perspectives. Environmental Progress & Sustainable Energy, 40(6), 1-15.

[5]. Zhou, L., Zhang, L., & Wang, L. (2021). Adsorption of Methylene Blue Dye from Aqueous Solutions: A Review of Mechanisms and Adsorbents. Journal of Environmental Management, 279, 111538.

[6]. Singh, P., Bhattacharyya, A., & Saxena, P. (2020). Rauwolfia serpentina as an Adsorbent for Water Purification: A Preliminary Study on Methylene Blue Removal. Journal of Environmental Chemical Engineering, 8(5), 104210.

[7]. Tariq, M., Bano, S., & Jamil, N. (2019). Low-Cost Natural Adsorbents for Water Treatment: A Review. Journal of Hazardous Materials, 376, 88-101.

[8]. Aksu, Z. (2005). Application of biosorption for the removal of organic pollutants: A review. Bioresource Technology, 97(9), 273-286.

[9]. Iqbal, M., & Zafar, S. (2016). Adsorptive removal of Methylene Blue dye from aqueous solution using Rauwolfia serpentina leaves. Journal of Environmental Chemical Engineering, 4(2), 1831-1839.

[10]. Rathod, P., & Gokul, K. (2020). Adsorption of Methylene Blue dye on low-cost adsorbents: Effect of temperature and pH. Environmental Science and Pollution Research, 27(3), 3245-3255.

[11]. P. D. Saha, S. Chakraborty, S. Chowdhury, Batch and continuous (fixed-bed column) biosorption of crystal violet by Artocarpus heterophyllus (jackfruit) leaf powder, Colloids Surf. B. Bio-interfaces; 92, 262–270, (2012).

[12]. R. Kumar, R. Ahmad, Biosorption of hazardous crystal violet dye from aqueous solution onto treated ginger waste (TGW), Desalination; 265 (1), 112–118, (2011).

[13]. S. Mohan and J. Carthickeyan "Removal of lighin and tannin colour from aqueous solution by adsorption on to activated carbon solution by adsorption on to activated charcoal, Environ. pollut., 97,183-187,(1997).

[14]. N. Kannan, and P. Sarojini. “Studies on the removal of manganese (II) ions by adsorption on commercial activated carbon” Ind. Env. Prot. 30, (5), 404-408, (2010).

[15]. N. Kannan, and P. Sarojini. “Studies on the removal of manganese (II) ions by adsorption on commercial activated carbon” Ind. Env. Prot. 30, (5), 404-408, (2010).

[16]. Hinda Lachheb, Eric Puzenat, Ammar Houas, Mohamed Ksibi, Elimame Elaioui, Chantal Guillard and Jean-Marie Herrmann; Photocatalytic degradation of various types of dyes (alizarin S, crocein orange G, methyl red, congo red, methyl biue) in water by UV- irradiated titania, Appl. Catalysis B:Env., 39, 75-90, (2002).

[17]. Vipasiri Vimonses, Shaomin Lei, Bo Jin, Chris W. K. Chow and Chris Saint; Adsorption of congo red by three Australian kaolins, Appl. Clay Sci., 43, 465-472, (2009).

[18]. Rais Ahmad and Rajeev kumar; Adsorptive removal of congo red dye from aqueous solution using bael shell carbon, Apll. Surf. Sci. 257, 1628-1633, (2010).
[19]. J. R. Kulkarni and V. S. Shrivastava; Removal of congo red (dye) by using chemically modified sawdust, Asian J. Chem. 16 (2), 795-799 (2004).

International Journal of Scientific Research in Science and Technology
Available online at : www.ijsrst.com
OPEN ACCESS
Print ISSN: 2395-6011 | Online ISSN: 2395-602X
doi : https://doi.org/10.32628/IJSRST

Analytical Study of Trends in Corrosion Rates of SS alloys in Soil Environment

Dr. Nitin S. Muley[1], Dr. R.T. Parihar[2], Dr. R.P Phase[3]
[1]Vidnyan Mahavidyalaya Malkapur, Maharashtra, India
[2]LBS Senior College, Partur, Maharashtra, India

ARTICLEINFO

Article History :

Published : 07 Dec 2024

Publication Issue :
Volume 11, Issue 23
Nov-Dec-2024
Page Number :
108-116

ABSTRACT

This study investigates the corrosion behavior of stainless steel grades SS304, SS316, and SS430 in soil environments characteristic of the Marathwada region, Maharashtra, India. The region's predominantly black cotton soil, with its high moisture retention, slightly alkaline pH (7.5–8.5), and variable chloride and sulfate ion concentrations, creates conditions conducive to localized corrosion. Comparative analysis reveals distinct trends in the corrosion resistance of the selected stainless steel grades. The SS430, a ferritic stainless steel with relatively low chromium content, exhibits the highest corrosion rates, making it less suitable for prolonged use in the region's soil. SS304, a general-purpose austenitic stainless steel, demonstrates moderate resistance to corrosion but remains susceptible to pitting in chloride-rich conditions. Conversely, SS316, with its molybdenum-enhanced composition, offers superior corrosion resistance, particularly in soils with elevated chloride and sulfate concentrations, making it the most durable choice for such environments. The corrosion rate trend observed follows the order: SS430 > SS304 > SS316. The findings highlight the need for strategic material selection and protective measures, such as coatings, cathodic protection, or soil treatment, to mitigate corrosion in buried metallic structures. This research provides critical insights for infrastructure and industrial applications in the Marathwada region, emphasizing the significance of understanding local soil chemistry in material selection. Future studies should incorporate long-term field data and electrochemical analyses to validate and expand upon these findings. The results aim to guide engineers and material scientists in optimizing stainless steel performance in similar environments.

Key words: Corrosion, Soil Corrosion, Corrosion Rate (CR), Metal Corrosion, Weightloss method

Introduction

When metals come into contact with soil, they begin to corrode. Soil corrosiveness refers to the ability of soil to initiate and accelerate the corrosion process. Previous studies have defined soil corrosion as the degradation of metals or other materials caused by chemical, mechanical, and biological interactions within the soil environment (1). A key factor influencing soil corrosion is the soil's moisture content. The impact of soil and its mechanical properties on steel plates is analyzed using weight loss methods. Findings reveal that the severity of corrosion and its rate depend on soil texture and moisture content. The corrosion rate is higher in clayey soils compared to mixed or sandy soils. The study also indicates that mild steel experiences relatively mild surface-level corrosion over the observed period when buried underground.

Soil is among the most corrosive mediums in the world, yet studying its corrosivity is challenging due to its diverse nature. Corrosion poses significant challenges across various industries, particularly in construction and infrastructure, where metals remain in direct contact with different soil environments throughout their service life. Numerous studies on soil corrosion [2-8] have provided valuable insights into the overall characteristics and physico-chemical properties of soil, such as the presence of chloride ions, sulfate ions, organic matter, and conductivity. These factors significantly influence the corrosion rate, accelerating and intensifying the process [9-13].

Corrosion rates in soil generally increase with higher moisture content. Studies on Q235 steel coupons buried in soils with varying moisture levels revealed that corrosion rates were higher in soil with 26% moisture compared to soil with 12% moisture [14]. The duration of steel exposure to a corrosive soil environment also influences the observed corrosion rate. Regarding biological activity and soil corrosion, reference [15] indicated that adding biocide to soil reduced bacterial populations, leading to a decrease in biocorrosion activity around and on steel coupons buried in the soil. Key types of bacteria associated with metals in terrestrial and aquatic environments include sulfate-reducing bacteria (SRB), sulfur-oxidizing bacteria, iron-oxidizing/reducing bacteria, manganese-oxidizing bacteria, and bacteria that produce organic acids and slime [16]. Typically, buried steel pipelines and tanks are susceptible to soil corrosion due to one or more of the following factors: high moisture content, pH values below 4.5, resistivity less than 1000 Ωcm, the presence of chlorides, sulfides, bacteria, and stray currents [17].

Studying soil as a corrosive environment is crucial due to the extensive use of buried pipelines and tanks, as their deterioration poses significant economic and environmental challenges over time [18]. Pipelines are always at risk of leaks or ruptures, which can result in hazardous failures causing fatalities, environmental damage, and destruction of assets due to explosions or leaks [19-21]. One method for assessing metal corrosion is weight loss analysis. For instance, reference [22] investigated the corrosion of stainless steel-304 in a brackish water environment using weight loss analysis alongside open circuit polarization. Similarly, reference [23] employed average percentage weight losses to evaluate the corrosion of coupons buried in soil samples, observing weight reductions in the coupons after the study period.

The corrosion rate of metals can be determined using the gravimetric method, which involves exposing a sample to a test medium and measuring the material's weight loss over time. Based on factors such as metal density, exposed surface area, exposure duration, and a specific constant, the corrosion rate (CR) can be calculated. This measurement provides insights into a metal's susceptibility to corrosion. Corrosion rate is commonly expressed in mils per year (mpy), where one mil equals 0.001 inches. For context, most heat exchanger tubes are 0.10 inches thick, meaning a corrosion rate of 10 mpy would take 10 years to penetrate the tube wall [25].

In the agricultural sector, during the first year of exposure, corrosion rates for a 63% saturated ammonium nitrate solution are approximately 250 mpy for galvanized steel and 1,250 mpy for mild steel. With proper surface preparation, cleaning, and coating, carbon steel can serve as a cost-effective option for fertilizer storage. Over a three-year study, Type 304 stainless steel was found to perform best for liquid fertilizer applications. For tanks exposed to commercial liquid fertilizers over 2.5 years, penetration rates were reported as 0.253 μm for Type 304 stainless steel, 282 μm for carbon steel, and 132 μm for 5052 aluminum [26].

Samples with elevated levels of heavy metals often contained significant amounts of organic matter. The retention of heavy metals in soil involves a complex interaction between organic carbon and heavy metals. Soil samples with the highest concentrations of heavy metals were primarily collected near dumping sites. In this region, the observed range of iron (Fe) was between 1.22–28.65 μg/g [27].

MATERIALS AND METHODS

2.1. Site Selection

The study area is situated at an elevation of approximately 633 meters (2077 feet) above sea level, near the geographic center of the state. Kannad city, located in the Aurangabad district of Maharashtra's Marathwada region, boasts the highest number of dams in the state, with 15 dams and 7 lakes. The precise coordinates of Kannad are 20° 27' North and 75° 13' East. The Gautala Sanctuary in Kannad primarily features teak and sandalwood trees. The city is well-connected, with the Mumbai-Nagpur State Highway and the Dhule-Solapur National Highway running through it, covering a distance of 211 km.

Soil samples were collected from key locations within the city, including areas with open ground waste, nearby roads, and residential neighborhoods. These areas were plagued by issues such as unpleasant odors, insects, rodents, and mosquitoes, which led to various health problems for residents. A total of 10 soil samples were collected in April 2022 from residential, industrial, and commercial areas. For each site, samples were taken using appropriate digging tools—half from the surface layer (0–5 cm) and half from the subsurface layer (15–20 cm). Approximately 500 grams of soil was collected from each location.

Sample No.	Sample Collection Area Type
M1	Residential area
M2	Residential area
M3	Residential and Industrial area
M4	Industrial area Opposite
M5	Residential area
M6	Marshy land
M7	Residential area
M8	Residential area
M9	Residential area
M10	Commercial area

Table 1 Selected sites Area Types

2.2. Coupon Specimen and Preparation

The soil samples were air-dried for two days and then oven-dried at 60°C for four hours. Once dried, the samples were crushed using a mortar and pestle, and sieved through a 2 mm mesh. The samples were weighed with an analytical balance capable of measuring with a precision of 0.0001 g. For each sample, 0.5 g was taken in a 100 ml beaker and digested with 10 ml of aqua regia on a hot plate for one hour. After evaporation to near dryness, the residue was dissolved in 10 ml of 2% nitric acid, filtered through Whatman filter paper No. 41, and diluted to 100 ml using double-distilled water. The samples were then labeled with appropriate identifiers (Sample ID, sampling time, and location) and stored in polyethylene bags marked as N1, N2, N3, up to N10. Preweighed coupons were buried in the soil samples and retrieved after specified durations. The coupons were cleaned, washed, dried following the ASTM G1-90 standard procedure [30], and reweighed. The samples were then prepared for further analysis.

For corrosion studies, ferrous alloys such as mild steel and SS-304, along with the non-ferrous metal aluminum, were used. Rectangular strips measuring 5 × 1 × 0.1 cm were employed in the laboratory weight loss corrosion test method [28]. A 2 mm hole was drilled near one end of the corrosion coupons for mounting purposes. Some of these coupons were selected for elemental composition analysis, which was conducted using an optical emission spectrometer (Foundry Master, Germany) [29].

Stainless Steel (SS304, SS316, and SS430) typically has the following elemental chemical composition is presented in Table No. 2

Element	SS304	SS316	SS430
Iron (Fe)	69.00	62.84	82.6
Manganese (Mn):	2.00	2.00	0.72
Carbon (C):	0.08	0.08	0.12
Chromium (Cr):	18-20	16-18	17.22
Molybdenum (Mo):	-	2-3	-
Nickel (Ni):	10.00	14.00	0.48
Phosphorus (P):	0.045	0.045	0.03
Silicon (Si):	0.75	-	0.65
Sulphur(S):	0.030	0.03	0.02

Table 2 Elemental Analysis of Metals

The corrosion study of metals and alloys in soils was conducted following the standard procedure outlined in ASTM G162-99 [28].

2.3. Corrosion Rate Determination

The physical and mechanical properties of the soil samples were analyzed, along with the corrosion rates of mild steel (MS), stainless steel (SS304), and aluminum (Al) strip coupons buried in the soil for various durations. Weight loss measurements were recorded for each sample, with the procedure repeated for time intervals of 12, 24, 48, and 96 hours. Duplicate experiments were conducted for each duration, and the average weight loss was documented. All experiments were performed under laboratory conditions at room temperature. The corrosion rate for each case was calculated using the following formula:

Corrosion rate (mg dm^{-2} hr^{-1}) = $\frac{Wi-Wf \times K}{A \times T}$

W_i = Weight of coupon before corrosion in gm.
W_f= Weight of coupon after corrosion in gm.
A = Geometric area of the coupon.
T = Time of exposure in hours.
K = 2.4×10^6

RESULTS AND DISCUSSION

The physical and mechanical properties of the soil samples were analyzed, including temperature, redox potential, electrical conductivity, salt content, moisture, organic matter, and resistivity, as presented in Tables 3 and 4. After burial periods of 6, 12, 24, 48, and 96 hours, the coupons were retrieved, cleaned, and analyzed to determine metal loss and calculate the corresponding corrosion rates.

The corrosion rate data for all sets of coupons, both before and after analysis, are presented in Tables 5, 6, and 7 for stainless steel grades SS304, SS316, and SS430, respectively, with their graphical representation shown in Figure 1. The average corrosion rates are summarized in Table 8.

The results indicated that weight loss generally increased with time, while the corrosion rate decreased. It was observed that the average corrosion rate declined as the exposure duration increased. In another study, corrosion rates measured using the polarization resistance (PR) technique were found to be overestimated but also showed a consistent decrease in corrosion rate over time [31]. These findings align with the results of this study for stainless steel SS304, SS316, SS430 coupons.

Sample No.	Temperature °C	Redox potential (mv)	Electrical. Cond. μ S cm^{-1}	Salt content (mg lit^{-1})	Moisture (%)	Organic matter %	Resistivity ohm. cm.
M1	29	344	278	181	25. 57	0.337	1332
M2	32	243	868	566	29.98	0.489	616
M3	32	173	418	272	24.39	0.62	1256
M4	32	183	381	248	29.30	0.395	2012
M5	32	288	398	259	21.50	0.278	932
M6	32	306	418	272	26.17	0.327	613
M7	32.5	302	305	199	22.35	0.493	1043
M8	32.5	310	299	195	23.53	0.35	1046
M9	32.5	327	623	406	19.60	0.099	1226
M10	32.5	308	498	325	18.10	0.336	1250

Table 3 Physical Analysis of Soil

Sample No.	Sand (%)	Silt (%)	Clay (%)	Class of soil.
N1	39.6	50	9.85	Silt loam
N2	22.4	22:5	53.85	Clay
N3	58.63	19.95	18.85	Sandy loam
N4	49.09	41.0	8.85	Loam
N5	20.0	24.0	55.5	Clay
N6	24.0	27.2	48.0	Clay

Sample No.	Sand (%)	Silt (%)	Clay (%)	Class of soil.
N7	49.08	30.5	18.85	Loam
N8	41.0	30.0	28.85	Clay loam
N9	51.94	29.0	17.85	Loam
N10	35.57	39.0	24.85	Loam

Table 4 Mechanical Analysis of Soil

Type of Metal / Alloy	Sample Numbers									
	Hours	N1	N2	N3	N4	N5	N6	N7	N8	N9	N10
SS 304	**6**	5.47	6.17	5.97	5.93	4.41	5.48	5.97	4.06	3.68	3.51
	12	2.89	2.45	2.27	1.72	1.53	2.06	2.51	1.90	1.88	2.07
	24	1.67	1.56	0.89	0.92	0.78	1.04	0.92	0.81	0.92	0.78
	48	0.72	0.76	0.56	0.21	0.36	0.61	0.36	0.16	0.34	0.41
	96	0.42	0.11	0.28	0.15	0.14	0.20	0.21	0.21	0.18	0.17

Table 5 Corrosion Rates for SS304

Type of Metal / Alloy	Sample Numbers									
	Hours	N1	N2	N3	N4	N5	N6	N7	N8	N9	N10
SS 316	**6**	5.32	5.62	4.78	4.65	3.21	4.30	4.52	3.45	2.63	2.21
	12	2.67	2.17	1.78	1.30	1.24	1.44	1.34	1.37	1.22	1.86
	24	1.54	1.23	0.54	0.76	0.65	0.82	0.74	0.62	0.78	0.56
	48	0.65	0.67	0.32	0.12	0.24	0.46	0.28	0.14	0.21	0.30
	96	0.35	0.09	0.14	0.08	0.09	0.12	0.12	0.11	0.08	0.06

Table 6 Corrosion Rates for SS316

Type of Metal / Alloy	Sample Numbers									
	Hours	N1	N2	N3	N4	N5	N6	N7	N8	N9	N10
SS 430	**6**	6.54	7.22	7.10	6.45	5.41	6.67	6.97	5.06	4.62	4.52
	12	3.89	3.46	3.28	2.69	2.62	3.26	3.62	2.92	2.84	3.08
	24	2.35	2.56	0.94	1.06	0.86	1.25	1.09	0.90	0.95	0.84
	48	0.78	0.82	0.62	0.32	0.42	0.71	0.43	0.24	0.43	0.48
	96	0.52	0.18	0.34	0.19	0.17	0.23	0.28	0.24	0.22	0.21

Table 7 Corrosion Rates for SS430

Hours	Type of Metal		
	SS 304	SS 316	SS430
6	5.065	4.07	5.99
12	2.128	1.64	3.16
24	1.029	0.824	1.28

Hours	Type of Metal		
	SS 304	SS 316	SS430
48	0.449	0.339	0.525
96	0.207	0.124	0.258

Table 5 Average Corrosion Rate for MS, SS304, Al in Various Time Durations

3.1. Analysis of Highest Corrosion Rates Across Time Frames:

The corrosion behavior of three metals, SS304, SS316, and SS430, was analyzed over time (6, 12, 24, 48, and 96 hours) based on weight loss measurements. The results revealed significant variations in corrosion rates across the different metals and exposure durations, highlighting the following trends:

1. 6-Hour Exposure

During the initial exposure period, the highest corrosion rates were observed. Among the three metals, SS430 exhibited the maximum corrosion rate (7.22) in sample N2, followed by SS304 (6.17) and SS316 (5.62). This indicates that SS430 is the most susceptible to corrosion during short-term exposure.

2. 12-Hour Exposure

After 12 hours, the corrosion rates decreased across all metals. SS430 maintained the highest corrosion rate (3.89, sample N1), while SS304 (2.89, sample N1) and SS316 (2.67, sample N1) followed. This demonstrates a steady reduction in corrosion rates as exposure time increases.

3. 24-Hour Exposure

A further decrease in corrosion rates was noted at 24 hours. SS430 showed the highest corrosion rate (2.56, sample N2), while SS304 (1.67, sample N1) and SS316 (1.54, sample N1) exhibited lower rates. SS430 continued to display higher corrosion susceptibility compared to the other metals.

4. 48-Hour Exposure

By the 48-hour mark, corrosion rates had significantly reduced. SS430 again exhibited the highest corrosion rate (0.82, sample N2), followed by SS304 (0.76, sample N2) and SS316 (0.67, sample N2). This suggests that longer exposure times allow the metals to stabilize, reducing corrosion intensity.

5. 96-Hour Exposure

At the end of the study, the corrosion rates were at their lowest. SS430 showed a maximum corrosion rate of 0.52 (sample N1), with SS304 (0.42, sample N1) and SS316 (0.35, sample N1) following. The prolonged exposure indicates a gradual decline in corrosion activity over time.

The SS430 consistently demonstrated the highest corrosion rates across all time frames, making it the least resistant to corrosion in the studied environment. The SS316 displayed the lowest corrosion rates, highlighting its superior corrosion resistance compared to SS304 and SS430. Corrosion rates for all metals decreased steadily with increasing exposure time, indicating a stabilization in the corrosive process over prolonged periods. This analysis emphasizes the importance of selecting appropriate materials based on exposure duration and environmental conditions for minimizing corrosion-related damage.

Conclusion

These results showed a general pattern of increase in duration of exposure and a corresponding decrease in corrosion rate (CR) in all types of corrosion coupons in all soil samples. An inverse proportional trend seems to exist between the weight loss and corrosion rate over time. The average corrosion rate (CR) was highest in

SS439 and lowest is in SS316. Compare to all Compare to all CR was highest in initial ntime period which was 6 hours and lowest was observed in 96 hours. For CR decreasing pattern was observed in all tests. There were some spikes in some samples but it does not affect the general decline pattern which observed.

References

[1]. Chaker, V. and Palmer, J. D., ASTM Committee G-1 on Corrosion of Metals. "Effect of Soil Characteristics on Corrosion," ASTM International , 81. 1989.

[2]. K.H. Logan and M. Romanof, "Soil Corrosion Studies," J. Res. Natl. Bur. Stand., 33, pp. 145 , 1944.

[3]. P.R. Roberge, Handbook of Corrosion Engineering, McGrow Hill, New York, 1999

[4]. H.H. Uhlig, Ed., The Corrosion Handbook, Wiley, New York, 1948.

[5]. W. Yang, G. Li, H. Guo, J. Zhou, C. Huang, and J. Bai, "Effects of Environmental Factors on Stress Corrosion Cracking of Pipeline Steels," Key Eng. Mater., 297, pp. 939–944, 2005.

[6]. D.N. Dang, L. Lanarde, M. Jeannin, R. Sabot, and P. Refait, "Influence of Soil Moisture on the Residual Corrosion Rates of Buried Carbon Steel Structures Under Cathodic Protection," Electrochim. Acta , 176, pp. 1410–1419, 2015.

[7]. N.N. Glazov, S.M. Ukhlovtsev, I.I. Reformatskaya, A.N. Podobaev, and I.I. Ashcheulova, "Corrosion of Carbon Steel in Soils of Varying Moisture Content," Prot. Met., 42(6), pp. 601–606, 2006.

[8]. D. Doyle, V. Seica, and M.W.F. Grabinsky, "The Role of Soil in the External Corrosion of Cast Iron Water Mains in Toronto Canada," Can. Geotech. J. , 40, pp. 225–23, 2003.

[9]. N. Md Noor, K.S. Lim, Y. Nordin, and A. Abdullah, "Corrosion Study on X70-Carbon Steel Material Influenced by Soil Engineering Properties," Adv. Mater. Res., 311, pp. 875–880, 2011.

[10]. S.K. Gupta and B.K. Gupta, "Critical Soil-Moisture Content in the Underground Corrosion of Mild-Steel", Corros. Sci., 19, pp. 171–178 , 1979.

[11]. C.A.M. Ferreira, J.A.C. Ponciano, D.S. Vaitsman, and D.V. Perez, "Evaluation of the Corrosivity of the Soil Through Its Chemical Composition," Sci. Total Environ., 388, pp. 250–255, 2007.

[12]. A.I.M. Ismail and A.M. El-Shamy, "Engineering Behaviour of Soil Materials on the Corrosion of Mild Steel," Appl. Clay Sci., 42, pp. 356–36, 2009.

[13]. N.S. Muley, "Corrosion in Underground Condition of Mild Steel Plates in Various Soil Varying Textures," IJIRMPS, 9(6), 2021.

[14]. Wan, Y., Ding, L., Wang, X., Li, Y., Sun, H. and Wang, Q., "Corrosion Behaviors of Q235 Steel in Indoor Soil", International Journal of Electrochemical Science, 8: pp. 12531-12542. 2013.

[15]. Oparaodu, K.O., and Okpokwasili, G.C., "Effect of Tetrakis (Hydroxymethyl) Phosphonium Sulphate Biocide on Metal Loss in Mild Steel Coupons Buried in a Water-logged Soil." Journal of Applied & Environmental Microbiology, 2 (5): pp. 253-256, 2014.

[16]. Beech, I.B. and Coutinho, C.L.M., "Biofilms on corroding materials". In: Biofilms in Medicine, Industry and Environmental Biotechnology - Characteristics, Analysis and Control, Edited by Lens, P., Moran, A.P., Mahony, T., Stoodly, P., and O'Flaherty, V., IWA Publishing of Alliance House, pp. 115-131. 2003.

[17]. Cunat, P., "Corrosion Resistance of Stainless Steels in Soils and in Concrete". Paper presented at the Plenary Days of the Committee on the Study of Pipe Corrosion and Protection, Ceocor, Biarritz. 2001.

[18]. Ferreira, C.A.M., Ponciano, J.A.C., Vaitsman, D.S. and Pérez, D.V., "Evaluation of the Corrosivity of the Soil through Its Chemical Composition". Science of the Total Environment, 388, pp. 250-255. 2007.

[19]. Hopkins, P., "Transmission Pipelines: How to Improve Their Integrity and Prevent Failures" In: Denys, R. (ed). Pipeline Technology. In the Proceedings of the 2nd International Pipeline Technology Conference, (PTC'96), Amsterdam, pp: 683-706. 1995.
[20]. National Energy Board, "Stress Corrosion Cracking on Canadian Oil and Gas Pipelines", Report of the enquiry. Calgary. MH-2-95. 1996.
[21]. Yahaya, N., Noor, N.M., Din, M.M., and Nor, S.H.M., "Prediction of CO2 Corrosion Growth in Submarine Pipelines". Malaysia Journal Civil Engineering, vol. 21, no. 1, pp. 69-81. 2009.
[22]. Kumar, R.K.S., Vijian, P., Solomon, J.S. and Berchmans, L.J., "Corrosion Studies on Stainless Steel-304 in Brackish Environment."International Journal of Emerging Technology and Advanced Engineering, vol. 2, no. 5, pp. 178-182. 2012.
[23]. Bano, A. S. and Qazi, J. I., "Soil Buried Mild Steel Corrosion by Bacillus cereus-SNB4 and its Inhibition by Bacillus thuringiensis-SN8.", Pakistan Journal of Zoology. 43 (3), pp. 555-562. 2011.
[24]. Nalco Company, "Corrosion", Oil Field Chemicals Training Manual. CAPEX College, Nalco Energy Services, Sugar Land, Texas. 2004.
[25]. Uy, M.C., "Corrosion Coupons. Technical Publication", WET, USA Inc., Illinois. 1994.
[26]. Nitin S. Muley, Dr. R. T. Parihar, "Corrosion in Agriculture Instruments and Equipments : Reasons and Solutions."JETIR, 9(5),pp. 477- 484. 2022.
[27]. Nitin S. Muley et al., "The Analysis of Concentration of Heavy Metals Detected in Contaminated Non-fertile Soil from Roadsides and Waste Dumping Sites of Kannad City" Int J Sci Res Sci & Technol., 10(3), pp. 898-907. 2023.
[28]. ASTM Standard G 162 – 199, Standard Practice for Laboratory Corrosion Testing of Metals in Soil, 03-02, 2005.
[29]. ASTM Standard E1086-94, Standard Test Method for Optical Emission Vacuum Spectrometric Analysis for Metals, 2005.
[30]. ASTM Standard G1-90, Standard Practice for Preparing, Cleaning and Evaluating Corrosion Test Specimens, G 01-05. 2004.
[31]. Beavers, J.A., and Durr, C.L, "Corrosion of Steel Piling in Nonmarine Applications", NCHRP Report Issue 408, Transportation Research Board, National Research Council, Washington DC. , pp. 17. 1998.

International Journal of Scientific Research in Science and Technology
Available online at : www.ijsrst.com
OPEN ACCESS
Print ISSN: 2395-6011 | Online ISSN: 2395-602X
doi : https://doi.org/10.32628/IJSRST

One Pot Multicomponent Synthesis of Substituted Thiazolo [3,2-a] Pyrimidin-3-One Derivatives as Antibacterial Agent

Pravin N. Muli*[1], Megha M. Muley[2], Bhaskar S. Dawane[3]

[1*]Smt. Sindhutai Jadhao Arts and Science Mahavidyalaya, Mehkar, Maharashtra, India

[2]Nanded Pharmacy College, Nanded, Maharashtra, India

[3]School of Chemical Sciences, Swami Ramanand Teerth Marathwada University, Nanded, Maharashtra, India

ARTICLEINFO

Article History :

Published : 07 Dec 2024

Publication Issue :
Volume 11, Issue 23
Nov-Dec-2024
Page Number :
117-126

ABSTRACT

A series of biologically active thiazolo[3,2-a]pyrimidin-3-one derivatives have been synthesized through a one-pot multicomponent reaction involving ketone, aldehyde, thiourea, and chloroacetic acid, using bleaching earth clay (pH 12.5) as a catalyst. The newly synthesized compounds were characterized by elemental analysis and spectral studies, and their antibacterial activity was evaluated.

Index Term- Multicomponent, thiazole [3, 2-a] Pyrimidin-3-one, antibacterial activity.

Introduction

The thiazole moiety is a key heterocyclic compound widely utilized in medicinal chemistry, known for its anticonvulsant, antimicrobial, and immunosuppressive properties [1-4]. Recent discoveries have revealed that the thiazole nucleus exhibits various biological activities, including antihypertensive [5], anti-inflammatory [6], anti-schizophrenic [7], antibacterial [8], HIV-1 inhibition [9], hypnotic [10], anti-allergic [11], COX-2 inhibition [12], antithrombotic activity [13], bacterial DNA gyrase B inhibition [14], and antitumor effects [15]. Thiazole derivatives also demonstrate excellent fungicidal, insecticidal, and anthelmintic properties [16]. Thiazolidinone derivatives, with significant importance in pharmaceutical chemistry, have been synthesized and shown to possess various antimicrobial activities [17-21], along with pharmacological properties such as antipsychotic [22], anticonvulsant [23], and antitubercular activities [24]. Similarly, some pyrimidine derivatives display analgesic, antiviral, anti-inflammatory [25], anti-HIV [26], antimicrobial [27], immunosuppressive [28], and cytotoxic effects. Additionally, pyrimidines act as antitubercular agents [29], antitumor [30], antipyretic [31], antimalarial [32], antihistaminic [33], hypnotic agents, diuretics, and cardiac

agents [34], as well as calcium-sensing receptor antagonists [35] and human A2A adenosine receptor antagonists [36]

Due to the significant potential of thiazole and pyrimidine moieties, various researchers have synthesized thiazolopyrimidine derivatives to explore their diverse pharmacological activities. These derivatives hold considerable promise in both medicine and pharmaceutical chemistry. Several thiazolo[3,2-a]pyrimidine derivatives have demonstrated antibacterial properties [37-41]. Additionally, thiazolo[3,2-a]pyrimidines have been found to exhibit anti-inflammatory and antinociceptive effects [42-45], antifungal activity [46], acetylcholinesterase (AchE) inhibition [47], adenosine A3 receptor antagonism [48], CDC25 phosphatase inhibition [49], anti-Parkinsonian effects [50-52], antiviral properties [53-54], anticancer potential [55], and antipsychotic activity [56]

As part of our ongoing research to develop fused heterocyclic compounds with potential biological activity, we present the synthesis and antibacterial evaluation of thiazolo[3,2-a]pyrimidine derivatives. A one-pot reaction involving substituted aldehydes, substituted ketones, thiourea, and an excess of chloroacetic acid, carried out in the green solvent PEG-400 with bleaching earth clay (pH 12.5) as a catalyst, successfully yielded thiazolo[3,2-a]pyrimidin-3-one derivatives.

EXPERIMENTAL SECTION

Melting points were measured using open capillary tubes and are reported without correction. Laboratory-grade chemicals and solvents were used after purification. Reaction progress was tracked via thin-layer chromatography (TLC) on silica gel-G precoated sheets (Merck, Germany). IR spectra were recorded using KBr pellets on a Shimadzu spectrometer. ^{1}H NMR spectra were obtained in DMSO-d_6 using an Advance spectrometer at 300/400 MHz, with tetramethylsilane (TMS) as the internal reference. Mass spectra were recorded on a Shimadzu QP2010PLUS GC-MS system. Elemental analysis was performed with a Carlo Erba 106 PerkinElmer 240 analyzer.

General method for preparation of compounds

An equimolar mixture of aryl aldehydes and ketones was dissolved in a minimal amount of PEG-400, along with a catalytic quantity of bleaching earth clay (pH 12.5). The solution was stirred at 60–70°C for one hour. Thiourea, in an equimolar amount, was then added to the mixture and stirred for an additional two hours. This was followed by the addition of an equimolar quantity of chloroacetic acid, with further stirring for one hour. Upon completion of the reaction, as confirmed by TLC, the reaction mixture was poured onto crushed ice and neutralized with dilute HCl if needed. The resulting solid was filtered under suction, washed with ice-cold water, and recrystallized from hot acetic acid to yield an analytically pure product (88%). The product's identity was confirmed through its melting point and spectroscopic analysis (IR, 1*H* NMR, and mass spectrometry).

7-(2-hydroxyphenyl)-5-(8-nitrophenyl)-2H-thiozolo[3,2-a]pyridin-3(8aH)-one 1a: This compound was obtained in 88% yield, mp 210-220°C; ^{1}H NMR (400 MHz, DMSO-*d*$_6$): δ 0.95 (3 H, s, CH_3), 1.11 (3 H, s, CH_3), 2.2-2.4(4 H, q, $2CH_2$), 3.7 (3H, s, CH_3),5.1(1 H, s, Ar-CH),9.8 (1H, s, OH), 5.8 (1H, s, NH), 6.9(2H, d, Ar-H),7.3(2H, d, Ar-H) ; IR (KBr) cm^{-1}:3305 (NH stretching), 3200 (OH stretching), 1670 (C=O stretching), 1647 (aromatic C=C stretching), 1220(Phenolic C-O stretching), 1332(Esteric C-O stretching), 1170(C-N

stretching) , ; ms (EI): m/z (M+) 340. Anal. calcd. for: H, 42.; C, 46.93; N, 02.04; O, 0.8.16. Found: H, 3.74 C, 49.19; N, 25.79; S, 14.34.

7-(2-hydroxyphenyl)-5-(8-nitrophenyl)-2H-thiozolo[3,2a]pyridin-3(8aH)-one 3a. This compound was obtained in 88% yield, mp 232-240°C; IR (KBr) cm^{-1}: 3427, 3011, 2932, 1744, 1661, 1617. ^1H NMR (400 MHz, DMSO-*d6*): δ 2.51 (2 H, s, CH_2), 5.63 (1 H, s, CH), 7.11-7.83 (7H, m, Ar-H),9.71(1H, s,Ar-OH) ; IR (KBr) cm^{-1}: 3250(OH stretching), 3310(NH stretching), 1665(C=O stretching), 1622(C=Nstretching), ; ms (EI): m/z (M+) 367.38. Anal. calcd. for : H, 03.57; C, 48.85; N, 11.44; O, 17.42. S, 08.75 Found: H, 03.53; C, 48.81; N, 11.42; O, 17.48. S,08.76

7-(2-hydroxy-4-iodophenyl)-5-(8-nitrophenyl)-2H-thiozolo[3,2a]pyridin-3(8aH)-one 3b. This compound was obtained in 88% yield, mp 215-227°C; IR (KBr) cm^{-1}: 3427, 3011, 2932, 1744, 1661, 1617. ^1H NMR (400 MHz, DMSO-*d6*): δ 2.41 (2 H, s, CH_2), 5.74 (1 H, s, CH), 7.08-7.93 (7H, m, Ar-H),9.77(1H, s,Ar-OH) ; ms (EI): m/z 492.96(M+1), ; Anal. calcd. for : H,02.45.; C, 43.83; N, 08.52; I, 25.73 O, 12.97;S, 06.50 Found: H,02.48.; C, 43.80; N, 08.56; I, 25.70 O, 12.94;S, 06.57

7-(4-chloro-2-hydroxyphenyl)-5-(8-nitrophenyl)-2H-thiozolo[3,2a]pyridin-3(8aH)-one 3c.
This compound was obtained in 88% yield, mp 200-220°C; IR (KBr) cm^{-1}: 3449, 3008, 2921, 1737, 1651, 1613. ^1H NMR (400 MHz, DMSO-*d6*): δ 2.41 (2 H, s, CH_2), 5.44 (1 H, s, CH), 7.00-8.03 (7H, m, Ar-H),9.61(1H, s,Ar-OH) ; ms (EI): m/z 401.02 (M+1), 402.02 (M+2); Anal. calcd. for : H,03.01.; C, 53.80; N, 10.46; Cl, 08.82; O, 15.93;S, 07.98 Found: H,03.05.; C, 53.77; N, 10.38; Cl, 08.86; O, 15.99;S, 07.92

7-(4-bromo-2-hydroxyphenyl)-5-(8-nitrophenyl)-2H-thiozolo[3,2a]pyridin-3(8aH)-one 3d.
This compound was obtained in 88% yield, mp 192-210°C; IR (KBr) cm^{-1}: 3440, 2980, 2928, 1747, 1657, 1623. ^1H NMR (400 MHz, DMSO-*d6*): δ 2.25 (2 H, s, CH_2), 5.67 (1 H, s, CH), 6.50-8.33 (7H, m, Ar-H),9.70(1H, s,Ar-OH; ms (EI): m/z 444.97 (M+1); Anal. calcd. for: H,02.71.; C, 48.44; N, 09.42; Br, 17.90; O, 14.34;S, 07.19 Found: : H,02.69.; C, 48.41; N, 09.48; Br, 17.95; O, 14.32;S, 07.22

7-(4-hydroxy-3-methoxyphenyl)-5-(8-nitrophenyl)-2H-thiozolo[3,2a]pyridin-3(8aH)-one 3e. This compound was obtained in 88% yield, mp 180-215°C; IR (KBr) cm^{-1}: 3530, 3100, 2918, 1751, 1657, 1618. ^1H NMR (400 MHz, DMSO-*d6*): δ 2.31 (2 H, s, CH_2), 5.63 (1 H, s, CH), 6.50-7.33 (7H, m, Ar-H), 9.10(1H, s,Ar-OH) ; ms (EI): m/z 397.40 (M+1), ; Anal. calcd. for : H, 03.80.; C, 57.42; N, 10.57; O, 20.13; S, 08.07 Found: H, 03.86.; C, 57.41; N, 10.50; O, 20.14; S, 08.10

5,7-bis(8-nitrophenyl)-2H-thiozolo[3,2a]pyridin-3(8aH)-one 3f.
This compound was obtained in 88% yield, mp 217-234°C; IR (KBr) cm^{-1}: 3218, 2940, 1778, 1674, 1623. ^1H NMR (400 MHz, DMSO-*d6*): δ 2.25 (2 H, s, CH_2), 5.17 (1 H, s, CH), 6.80-7.73 (7H, m, Ar-H), ms (EI): m/z 396.05 (M+1), ; Anal. calcd. for : H, 03.05.; C, 54.54; N, 14.13; O, 20.18; S, 08.09 Found: : H, 03.07.; C, 54.50; N, 14.16; O, 20.21; S, 08.05

5-(4-chloro-2-hydroxyphenyl)-7-(4-nitrophenyl)-2H-thiozolo[3,2a]pyridin-3(8aH)-one 3g.
This compound was obtained in 88% yield, mp 212-228°C; IR (KBr) cm^{-1}: 3430, 3110, 2900, 1758, 1651, 1638. ^1H NMR (400 MHz, DMSO-*d6*): δ 2.21 (2 H, s, CH_2), 5.03 (1 H, s, CH), 7.10-7.83 (7H, m, Ar-H),9.10 (1H, s,Ar-

OH) ; ms (EI): m/z 401.02 (M+1), 402.02 (M+2); Anal. calcd. for : H, 03.01.; C, 53.80; N, 10.46.04; Cl, 08.82; O, 15.93;S, 07.98 Found: H, 03.05.; C, 53.78; N, 10.46.09; Cl, 08.70; O, 15.97;S, 07.94

5-(4-chloro-2-hydroxy-5-iodophenyl)-7-(4-nitrophenyl)-2H-thiozolo[3,2a]pyridin-3(8aH)-one 3h.

This compound was obtained in 88% yield, mp 230-240°C; IR (KBr) cm^{-1}: 3480, 3000, 2940, 1738, 1664, 1621. ^1H NMR (400 MHz, DMSO-*d6*): δ 2.11 (2 H, s, CH_2), 5.73 (1 H, s, CH), 7.15-7.70 (7H, m, Ar-H),9.17(1H, s,Ar-OH) ; ms (EI): m/z 527.72 (M+1), 528.72 (M+2); Anal. calcd. for : H, 02.10; C, 40.97; Cl, 06.07; N, 07.96; O, 12.13; S,06.08. Found: H, 02.14; C, 40.91; Cl, 06.10; N, 07.91; O, 12.16; S, 06.11.

5-(5-bromo-4-chloro-2-hydroxyphenyl)-7-(4-nitrophenyl)-2H-thiozolo[3,2a]pyridin-3(8aH)-one 3i.

This compound was obtained in 88% yield, mp 225-234°C; IR (KBr) cm^{-1}: 3450, 3052, 2924, 1740, 1680, 1600. ^1H NMR (400 MHz, DMSO-*d6*): δ 2.17 (2 H, s, CH_2), 5.62 (1 H, s, CH), 7.15-7.70 (7H, m, Ar-H), 9.14(1H, s,Ar-OH) ; ms (EI): m/z 480.72(M+1), 481S.72 (M+2); Anal. calcd. for : H, 02.31; C, 44.97; Br, 16.62; Cl, 07.37; N, 08.74; O, 13.31; S, 06.67.Found: H, 02.34; C, 40.91; Br, 16.60; Cl, 07.40; N, 08.71; O, 1336; S, 06.61.

5-(2-hydrox-5-iodo-4-methylyphenyl)-7-(4-nitrophenyl)-2H-thiozolo[3,2a]pyridin-3(8aH)-one 3j.

This compound was obtained in 88% yield, mp 214-232°C; IR (KBr) cm^{-1}: 3410, 3045, 2929, 1726, 1672, 1610. ^1H NMR (400 MHz, DMSO-d_6): δ 1.46 (3H, s CH_3),2.33 (2 H, s, CH_2), 5.43 (1 H, s, CH), 7.00-7.45 (7H, m, Ar-H),9.17(1H, s,Ar-OH) ; ms (EI): m/z 507.30 (M+1); Anal. calcd. for : H, 2.78; C, 44.98; I, 25.02; N, 08.28; O, 12.62; S, 06.32.Found: : H, 2.73; C, 44.91; I, 25.07; N, 08.20; O, 12.58; S, 06.30.

5-(2-hydrox-4-methylyphenyl)-7-(4-nitrophenyl)-2H-thiozolo[3,2a]pyridin-3(8aH)-one 3k.

This compound was obtained in 88% yield, mp 195-220°C; IR (KBr) cm^{-1}: 3400, 3070, 2920, 1722, 1643, 1618. ^1H NMR (400 MHz, DMSO-*d6*): δ 1.42 (3H, s CH_3),2.11 (2 H, s, CH_2), 5.68 (1 H, s, CH), 7.10-7.60 (8H, m, Ar-H),9.10(1H, s,Ar-OH) ; ms (EI): m/z 381.41 (M+1); Anal. calcd. for : H, 03.96; C, 59:83; N,11:02; O,16:78;S,08:41 Found: : H, 03.91; C, 59:87; N,11:07; O,16:71;S,08:39.

5-(4-chlorophenyl)-7-(4-fluorophenyl)-2H-thiozolo[3,2a]pyridin-3(8aH)-one 3l.

This compound was obtained in 88% yield, mp 230-235°C; IR (KBr) cm^{-1}: 3062, 2929, 1724, 1683, 1627. ^1H NMR (400 MHz, DMSO-*d6*): δ 2.19 (2 H, s, CH_2), 5.80 (1 H, s, CH), 7.17-7.80 (9H, m, Ar-H) ; ms (EI): m/z 358.82 (M+1), 359.82 (M+2); Anal. calcd. for : H, 03.37; C, 60.25; Cl, 09.88; F, 05.29; N, 07.81; O, 04.46; S,08.94. Found: : H, 03.32; C, 60.20; Cl, 09.90; F, 05.23; N, 07.80; O, 04.41; S, 08.99.

Antimicrobial activity study

In accordance with WHO recommendations [14,15], the following microbial test strains were used: *Staphylococcus aureus* ATCC 25923, *Escherichia coli* ATCC 25922, *Pseudomonas aeruginosa* ATCC 27853, *Proteus vulgaris* ATCC 4636, *Bacillus subtilis* ATCC 6633, and *Candida albicans* ATCC653/885. The bacterial concentration was set to 10^7 CFU/ml, determined using the McFarland standard. Overnight cultures were incubated for 18-24 hours at 36ºC ± 1ºC. The bacterial suspension was then spread across the entire surface of Mueller-Hinton agar (Dagestan Scientific Research Institute of Nutrient Media). The compounds were introduced into the wells as a DMSO solution at a concentration of 100 μg/ml, with each well containing 0.3 ml of the solution. The evaluation of antimicrobial activity was based on the following criteria: If no inhibition zone or a zone smaller than 10 mm was observed, the bacteria were considered resistant, or the compound

concentration was insufficient for inhibition; an inhibition zone of 10-15 mm indicated low sensitivity of the bacteria strain to the compound at that concentration; a zone of 15-25 mm was considered a sign of activity against the microorganism; and a zone of 25 mm or more indicated strong antimicrobial activity of the tested compound.

RESULTS AND DISCUSSION

As part of our ongoing research to develop new methodologies, we have discovered that a four-component reaction involving various substituted aryl ketones, substituted aryl aldehydes, thiourea, and chloroacetic acid results in the synthesis of thiazolo[3,2-a]pyrimidin-3-one derivatives with high yields and short reaction times.

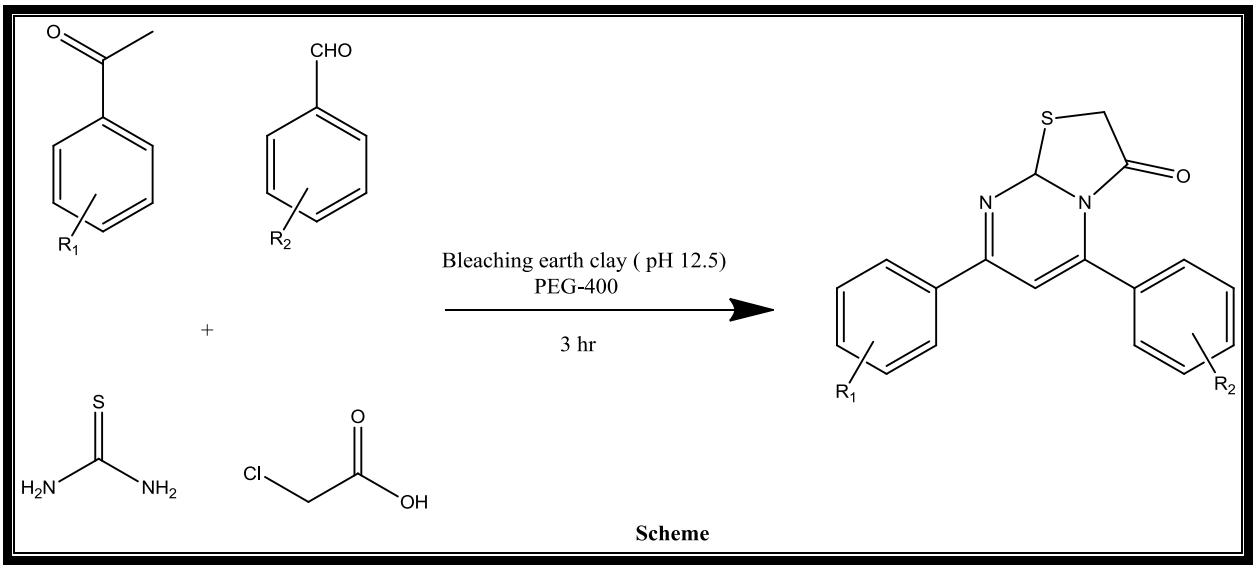

Scheme

In a standard experimental setup, (1 mmol) each of substituted aryl ketone, substituted aryl aldehyde, thiourea, and chloroacetic acid was combined and heated at 600–700°C. The reaction was carried out in PEG-400, using bleaching earth clay (pH 12.5) as a heterogeneous basic catalyst. Reaction progress was monitored via TLC, and the process continued until completion. A variety of structurally distinct aldehydes and ketones were successfully utilized under these conditions to synthesize thiazolo [3,2-a]pyrimidin-3-one derivatives, as summarized in Table 1, without affecting functional groups. The reaction proved to be fast and efficient, yielding the desired products in good quantities. The final compounds were purified by recrystallisation with acetic acid.

Table 1: Synthesis of thiazolo [3,2a] Pyrimidine-3-one derivatives

Sr.No	R_1	R_2	Structure	%Yield
3a	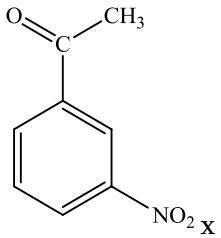	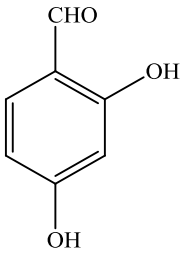	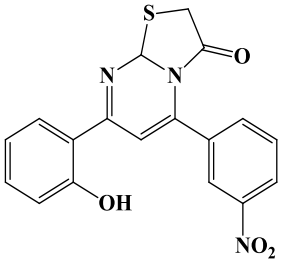	82

Sr.No	R_1	R_2	Structure	%Yield
3b	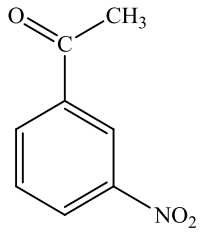	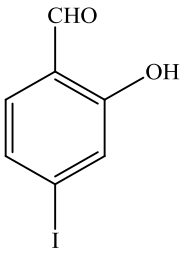	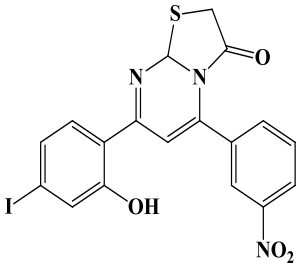	84
3c	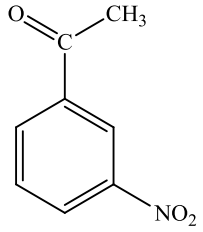	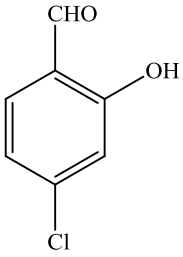	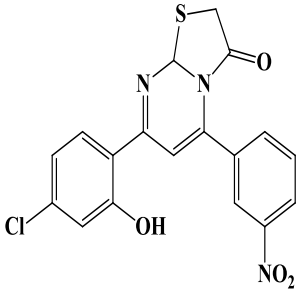	78
3d	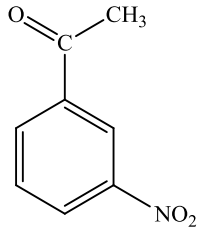	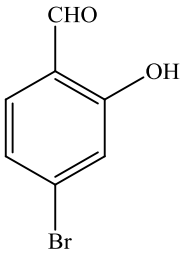	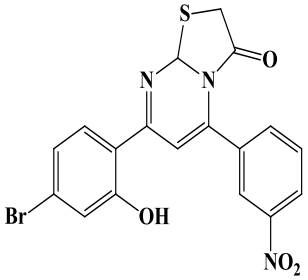	76
3e	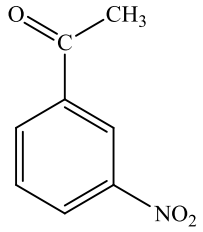	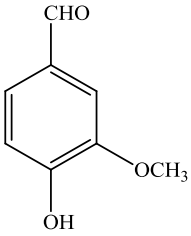	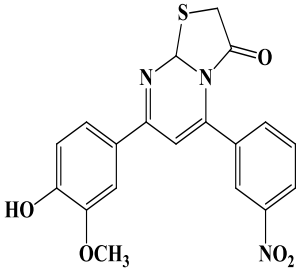	73
3f	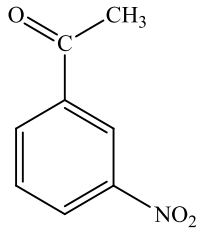	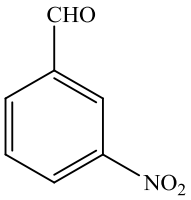	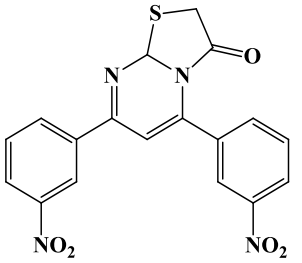	84
3g	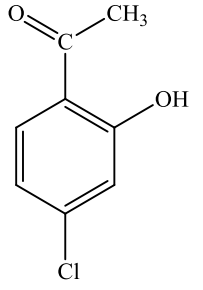	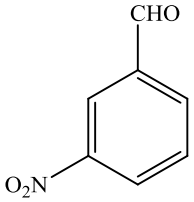	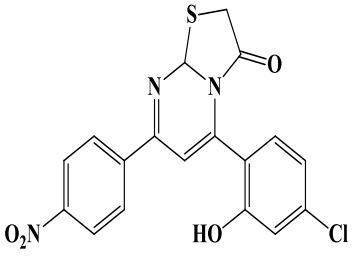	83

Sr.No	R_1	R_2	Structure	%Yield
3h	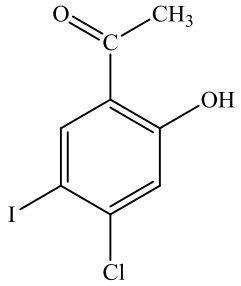	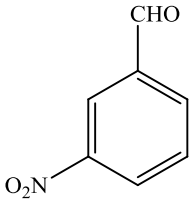	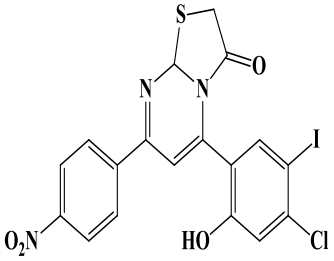	80
3i	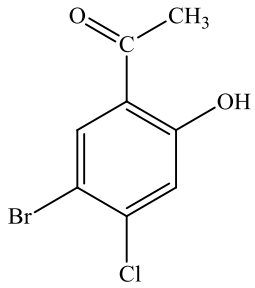	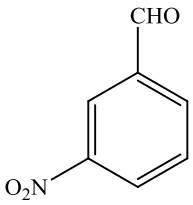	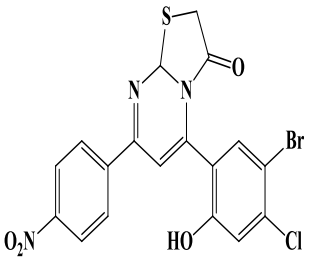	78
3j	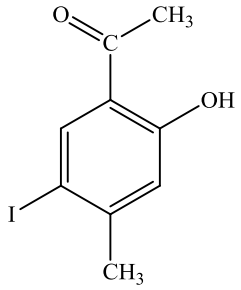	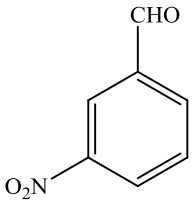	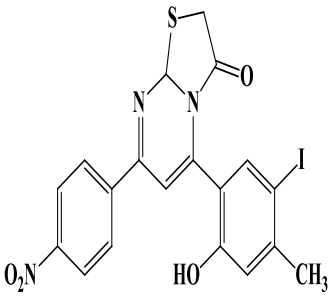	83
3k	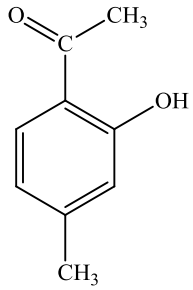	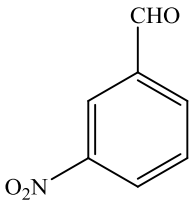	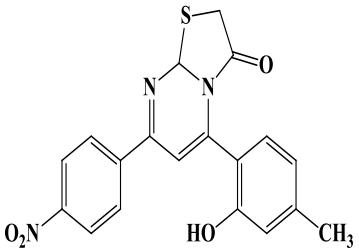	82
3l	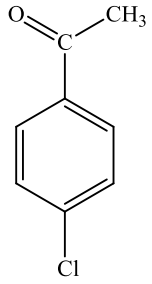	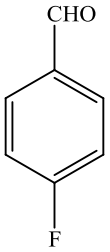	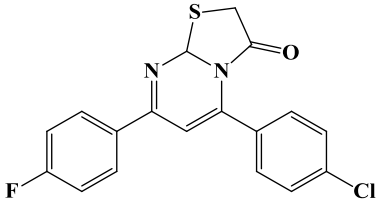	84

Antimicrobial Activity

The antimicrobial activity of compounds 3a–3l was evaluated against bacterial strains E. coli (Ec), B. subtilis (Bs), and S. aureus (St). Compounds 3b, 3i, and 3l exhibited significant zones of inhibition against all three strains. Compounds 3a, 3b, 3f, and 3k showed moderate activity against these bacteria, while compound 3h was active against B. subtilis and S. aureus but inactive against E. coli. Compound 3d displayed no activity against E. coli or S. aureus. Penicillin served as the reference drug for antibacterial testing, with results summarized in Table

The antifungal activity of the same compounds was assessed against fungal strains A. niger, T. viride, and C. albicans. Compounds 3h, 3i, and 3l were highly active against all tested fungal strains, while compounds 3e and 3d were inactive. Compounds 3a, 3g, and 3k demonstrated activity only against A. niger, and compounds 3b and 3c were active against both A. niger and C. albicans. Detailed results are presented in Table 2.

Table 2: Antimicrobial activity of thiazolo [3,2a] Pyrimidine-3-one derivatives

Entry	Bactria (zone of inhibition in mm)			Growth of fungi		
	Ec	St	Bs	An	Tv	Ca
3a	17	18	18	+ve	-ve	-ve
3b	19	17	13	+ve	-ve	+ve
3c	21	-	14	+ve	-ve	+ve
3d	-	-	21	-ve	-ve	-ve
3e	22	19	21	-ve	-ve	-ve
3f	21	20	14	-ve	+ve	+ve
3g	18	22	22	+ve	-ve	-ve
3h	-	22	20	+ve	+ve	+ve
3i	23	23	22	+ve	+ve	+ve
3j	21	21	25	+ve	+ve	-ve
3k	19	22	14	+ve	-ve	-ve
3l	26	23	20	+ve	+ve	+ve
Penicillin	27(25)	24(25)	18(25)	NA	NA	NA
Nystatin	NA	NA	NA	24	22	18

Ec- *Escherichia coli (MTCC443)*, Bs – *Bacillus subtilis (MTCC441)*, St – *Salmonella typhi (MTCC96),* An –*Aspergillus niger* (MTCC 281), Tv-*Trichoderma viridae* (MTCC 167), and Ca-*Candida albicans* (MTCC183), - =No Detected ZOI, NA= Not Applicable, -ve= No Growth of Fungi, + ve= Growth of Fungi.

CONCLUSION

In summary, we successfully synthesized thiazolo[3,2-a]pyrimidin-3-one through a four-component reaction involving substituted aryl ketones, substituted aryl aldehydes, thiourea, and chloroacetic acid. The reaction was conducted in the presence of a heterogeneous base catalyst, bleaching earth clay (pH 12.5), and utilized PEG-400 as a green solvent. This method provides notable advantages, including high yields, a straightforward procedure, short reaction times, mild conditions, and compatibility with diverse functional groups. Additionally, the synthesized compounds demonstrated promising antimicrobial activity.

References

[1]. Srivastava S.K; Srivastava S.; Srivartavv S.D. Indian J Chem, 1999,38B,183.

[2]. Sadek B.; Moawia Md. A.; Khairi M. S. F. A. Molecules 2011,16,9386.

[3]. Singh N.; Sharma U.S.; Sutarb N.; Kumar S.; Shrama.U.K. J.Chem.Pharm.Res. 2010, 2(3),691.

[4]. Rzasa M; Shea H.A.; Romo D. J. Amer Chem Soc, 1998,120,591.

[5]. Patt W.C.; Hamilton H.W.; Taylor M.D.; Ryan M. J Med Chem, 1992,35,2562.

[6]. Sharma R.N.; Xavier F.P.; Vasu K.K .; Chaturvedi S.C.; Pancholi S.S. J Enz Inhib Med Chem, 2009,24,890.
[7]. Jaen J.C, Wise L.D, Caprathe B.W, Tecle H, Bergmeier S, Humblet C.C et al. J Med Chem, 1990,33,311.
[8]. Tsuji K.; Ishikawa H. Bioorg Med Chem Lett, 1994,4,1601.
[9]. Bell F.W.; Cantrell A.S.; Hogberg M.; Jaskunas S.R. et al. J Med Chem, 1995,38,4929.
[10]. Ergenc N.; Capan G.; Gunay N.S., Ozkirimli S.; Gungor M.; Ozbey S.; Kendi E.; Arch Pharm Pharm Med Chem, 1999,332,343.
[11]. Hargrave K.D.; Hess F.K.; Oliver J.T. J Med Chem, 1983,26,1158.
[12]. Carter J.S.; Kramer S.; Talley J.J.; Penning T.; Collins P. et al. Bioorg Med Chem Lett, 1999, 9,1171.
[13]. Badorc A.; Bordes M.F.; Cointet P.; Savi P. et al. J Med Chem, 199,40,3393.
[14]. Rudolph J.; Theis H.; Hanke R.; Endermann R.; Johannsen L.; Geschke F.U. J Med Chem, 2001,44,619.
[15]. Muralikrishna S.; Raveendrareddy P.; Ravindranath L. K.; Harikrishna S.; Jagadeeswara Rao P. Der Pharma Chemica, 2013,5(6),87.
[16]. Gupta V.; Vinay Kant. Sciintl, 2013,253,260.
[17]. Barreca M.L.; Chimirri A.; L De Luca; Monforte A.M.; Monforte P.; Rao A.; Zappala A.; Balzarini J.; E De Clercq.; pannecouque C.; Witvrouw M. Bioorg. Med Chem Lett, 2001,11,1793.
[18]. Dinesh, B.; Chirag S.; Shweta ,S.; Vijaykumar S.; Talesara G.L . Indian J chem. 2009, 48B,1006.
[19]. Patel D.; Kumari P.; Patel N. J.Chem.Pharm.Res.,2010,2(5),84.
[20]. Patil S.G.; Bagul R.R.; Swami M.S.; Hallale, S.N.; Kamble V.M.; Kotharkar N.S. Darade K. J. Chem. Pharm.Res., 2011,3(3),69.
[21]. Ahirwar M.; Shrivastava S.P. E-Journal of chemistry, 2011,8(2),931.
[22]. Harib N. J.; Jurcak J.G.; Bregna D. E.; Burgher K.L.; Hartman L.B.; Kafka S.; Kerman L.L.; Kongsamut S.; Roehr J .E.; Szewczal M.R.; Woods A.T. Kettelberger and Corbett R, J Med Chem, 1996,39,4044.
[23]. Gursoy A.; Terzioglu N. Turk J Chem, 2005,29,247.
[24]. Ilango K.; Aruankumar S. R. J.Chem, 2010,3(3),493.
[25]. Goudgaon N.M.; and Reddy R. Y. IJPCBS 2014,4(1),64.
[26]. Fujiwara N.; Nakajima T.; Ueda Y.; Fujita H.K.; Awakami H. Bioorg Med Chem, 2008, 16,9804.
[27]. Solankee A.; Kapadia K.; Ciric A.; Sokovic M,; Doytchinova I.; Geronikaki A. Eur J Med Chem, 2010,45,510.
[28]. Wagner E, Al-Kadasi K, Zimecki M, Sawka-Dobrowolska W. Eur J Med Chem, 2008, 43,2498.
[29]. Bhat K.I.; Kumar A.; Kumar P. & Riyaz E.K. wjpps 2014,3,1432.
[30]. Magdy I. E.; Somaia S. A.; Mogedda E. H. and MohammedA.K. Acta Poloniae Pharmaceutica-Drug Research, 2011,68,357.
[31]. Rangappa S. K.; Kallappa M. H.; Ramya V. S.;, Mallinath H. H. Europin J Med Chem, 2010, 45,2597.
[32]. Manohar S.; Rajesh U. C.; Khan S. I.; Tekwani B. L.; and Rawat D. S. ACS Med. Chem. Lett., 2012,3(7),555.
[33]. Rahaman S.A.; Rajendra Pasad Y.; Phani K. ; Bharath K.; Saudi Pharmaceutical Journal 2009,17,255.
[34]. Wang S.Q.; Fang L.; Liu X.J.; Zhao K. Chinese Chem Lett, 2004,15,885.
[35]. Yang W.; Ruan Z.; Wang Y.; Van Kirk K.; Ma Z.; Arey B.J. et al. J Med Chem 2009,52, 1204.
[36]. Peng B.; Kumaravel G.; Smits G.; Jin X.; Phadke D.; Engber T.; Huang C.; Reilly J.; Tam S.; Grant D.; Hetu G.; Chen L.; Zhang J.; Petter R.C. J Med Chem. 2004,47,4291.
[37]. Youssef MSK, Omar AA. Monatshefte fur Chemie. 2007; 138: 989–995.
[38]. EI-Tombary AA, Nargues S, Habib RS, EI-Hawash SA, Shaaban OG. Arch Pharm Res. 2007; 30: 1511-1520.
[39]. Youssef MSK, Ahmed RA, Abbady MS, Abdel-Mohsen SA, Omar AA. Monatsh Chem. 2008; 139: 553–559.

[40]. Nehad A. A.; Manal M. S.; Nesreen S. A.; Rasha Z. B.; Nadia R. A. IJIRSET, 2014,3, 8517.
[41]. Kalyankar B. D.; Ubale P.N.; Vartale S. P. Iajpr,2015,5,1373.
[42]. Ertan M, Tozkoparan B, Kelicen P, Demirdamar R. Il Farmaco.1999; 55: 588–593.
[43]. Bekhit AA, Fahmy HTY, Rostom SAF, Baraka AM. Eur J Med Chem. 2003; 38: 27-36
[44]. Alam O, Khan SA, Siddiqui N, Ahsan W. Med Chem Res. 2010; 19: 1245–1258.
[45]. Kashyap S.J.; Sharma P.K.; Garg V. K.; Dudhe R.; Nitin Kumar, , J Adv Sci Res, 2011, 2(3),18.
[46]. Mithun A.; Bantwal S.H.; Nalilu S. K. European Journal of Medicinal chemistry. 2007, 42,380.
[47]. HuiZhi L. C.; Lin-lin Z.; Si-jie-L.; David chi C.W.; Huang Q. L.;Chun H.; Arkivok. 2008, (xiii),266.
[48]. (a) Ohkawa et al. US6583146, 2003; (b) Kappe C. O.; Färber G. J. Chem. Soc., Perkin Trans.1 1991, 1342; (c) Rolando P.; Tetyana B.; Oleksandr I. Z.; Wilhelm H.; Kappe C.O. J. Comb. Chem. 2002,4 501.
[49]. Montes M.; Braud E.; Miteva M. A.; Goddard M. L.; Mondsert O.; Kolb S.; Brun M.P.;Ducommun B.; Garbay C.; Villoutreix B. O. J. Chem. Inf.Model., 2008,48(1),157.
[50]. Abd GE, Amr SM, Abdulla MM. Monatsh Chem. 2008; 139: 1409–1415.
[51]. Azam F, Alkskas AI, Ahmed AM. Eur J Med Chem. 2009; 44: 3889– 3897.
[52]. Faizul A.; Bashir A. E.; Ismail A. A.; and Musa A. A.; J. Enz. Inhib. and Med. Chem, 2010,25(6),818.
[53]. Abd El-Galil, EA, Salwa FM, Eman MF, Dina N. Abd El-Shafy. Eur J Med Chem. 2010; 45:1494–1501.
[54]. Revankar GR, Ojwang JO, Mustain SD, Rando RF, De Clercq E, et al. Antiviral Chem Chemother.1998; 9: 53-63.
[55]. Fahmy HTY, Rostom SAF, Saudi MN, Zjawiony JK, Robins DJ. Arch Pharm Pharm Med Chem, 2003; 3: 1-10.
[56]. Beck JP, Curry MA, Chorvat RJ, Fitzgerald LW, Gilligan PJ, Zaczek R, Trainor GL. Med Chem Lett. 1999; 9: 1185-1188

International Journal of Scientific Research in Science and Technology
Available online at : www.ijsrst.com
OPEN ACCESS
Print ISSN: 2395-6011 | Online ISSN: 2395-602X
doi : https://doi.org/10.32628/IJSRST

A Short Review: Recent Biological Activities of Curcumin (Diferuloyl Methane) and Its Analogues

Sherkhan Pathan[1], Suparna Deshmukh[2], Sunil Aute[1]

[1]Department of Chemistry, Kohinoor Arts, Commerce and Science College Khultabad, Aurangabad-431001, Maharashtra, India

[2]Department of Chemistry, S.K Gandhi College, Kada, Tal: Ashti, Dist: Beed-414202, Maharashtra, India

ARTICLEINFO

Article History :

Published : 07 Dec 2024

Publication Issue :
Volume 11, Issue 23
Nov-Dec-2024
Page Number :
127-133

ABSTRACT

The yellow pigment known as curcumin, which is found in curry powder and the Indian spice turmeric, has been connected to several conditions, including diabetes, angiogenesis, tumorigenesis, cardiovascular, pulmonary, and neurological diseases, skin and liver disorders, bone and muscle loss, depression, chronic fatigue, and neuropathic pain. Curcumin's color, lack of water solubility, and comparatively low in vivo bioavailability limit its usefulness. But because curcumin has been linked to a few therapeutic benefits, there is a fierce hunt for a curcumin that does not have these issues. To get around these restrictions, several strategies are being investigated. Curcumin is its primary active component. Commonly used as a spice pigment, and food additive, Curcumin are phenolic chemicals that can also be employed as a medicinal ingredient. Over the past century, extensive study has shown several significant roles for Curcumin. This review's objective is to provide an overview of the biological activities that have recently been reported.

Keywords: Curcumin, Biological activity, Curcumin, Bioavailability and Spice pigment.

Introduction

For thousands of years, natural products have been utilized in traditional medicine. They have also showed promise as a source of ingredients for the creation of novel medications(Pandit et al., 2011). The Zingiberaceae family includes turmeric (Curcuma longa Linn), which has its origins in India, South-east Asia, and Indonesia and is grown in tropical and subtropical regions all over the world. A common coloring and flavoring ingredient in mustards and curries is turmeric powder. In India, people have been using turmeric to keep their teeth clean(Chaturvedi, 2009). For many centuries, it has been utilised for medicinal purposes in nations like China and India to cure liver diseases and jaundice(Mukerjee & Vishwanatha, 2009).(Kalpravidh et al., 2010).

One of the most widely used medical herbs, turmeric has a variety of pharmacological properties, including antioxidant, anti-protozoal, anti-venom activities, anti-microbial, anti-malarial, anti-inflammatory, anti-proliferative, anti-angiogenic, anti-tumor and anti-aging properties make turmeric one of the most popular medicinal plants(Panahi et al., 2014). Because Curcumin have so many biological targets and almost no side effects, they have gained therapeutic interest in treating cancer, immune-related disorders, and metabolic illnesses(Siviero et al., 2015). Curcumin, a natural compound found in turmeric, has several biological and pharmacological properties. Curcumin's therapeutic application is limited due to its low oral bioavailability. To solve this constraint, numerous ways have been developed, including the synthesis of novel compounds. This study examines the therapeutic benefits of curcumin and its synthetic derivatives, including antibacterial, anticancer, antioxidant, anti-inflammatory, antidiabetic, and neuroprotective effects. This study found that curcumin is a promising chemical that may be utilised to build and synthesize novel useful molecules for medicinal purposes. There is some important curcuminoids in table number 1.

Method Used

The databases Google Scholar, and Web of Science were used to conduct systematic literature searches.

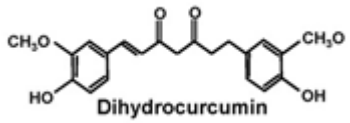

History of curcumin

The active component of the nutritional spice turmeric, curcumin, is taken from the rhizomes of the Zingiberaceae species C. longa. It was initially identified approximately 200 years ago when Vogel and Pelletier isolated a "yellow coloring matter" from C. longa rhizomes and called it curcumin(Vogel & Pelletier, 1815). Lampe et al. synthesize it initially(Lampe & Milobedzka, 1913).

Table 1 Structures of Some Important Curcuminoids'

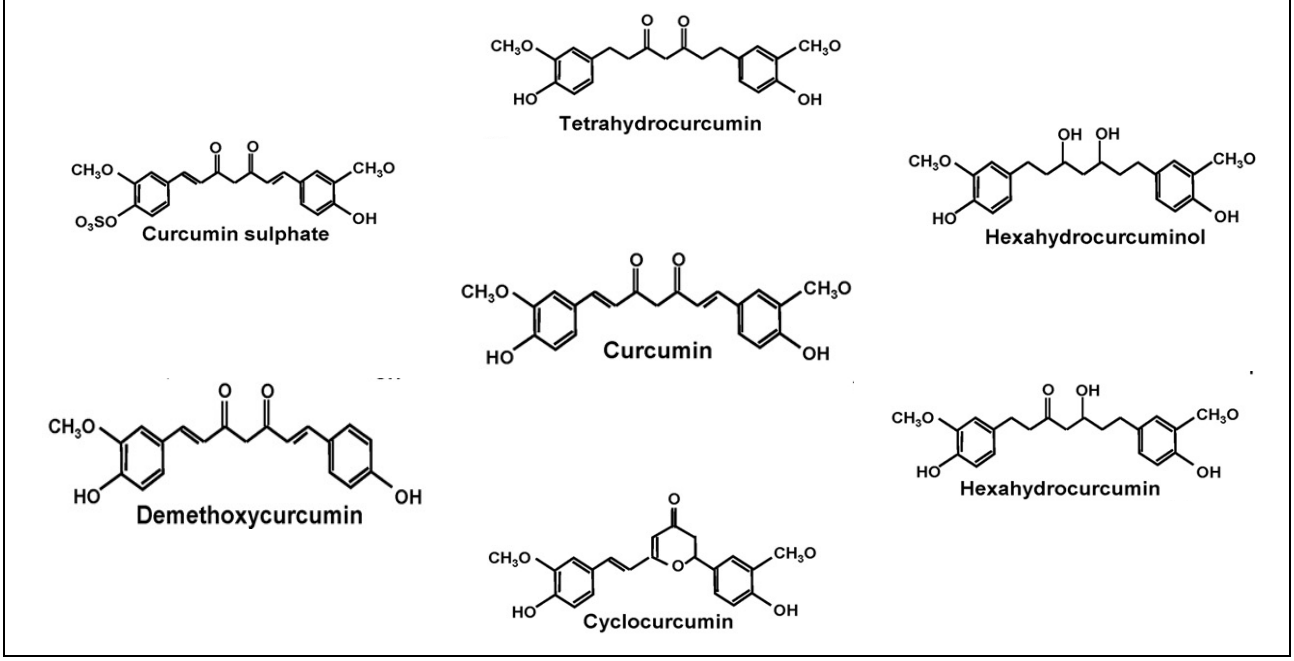

Biological activities of curcumin

4.1. Antitumor-activity

Turmeric's primary ingredient, Curcumin, has a variety of pharmacological properties. The impact of cyclocurcumin and Curcumin on the growth of MCF-7 human breast cancer cells was investigated. Because DMC contains the diketone moiety, methoxy groups, and phenolic hydroxyl groups, it is a more effective inhibitor than CUR and BDMC. Since cyclocurcumin had no effect on MCF-7 cell proliferation, it seems that the diketone system of Curcumin is the component of the molecule responsible for the Curcumin' antiproliferative action(Simon et al.,1998). Jiang and associates used an MTT (3e4,5-dimethyl thiazol-2-yl)-2,5-diphenyl tetrazolium bromide test to determine the anticancer properties of Curcumin from C. longa on He La cells(Jiang et al., 2012). The study analyses the composition and activity connection. Curcumin was shown to have a substantial association with anticancer activity using a loading plot, variable relevance in projection in orthogonal partial least squares, and a coefficient in canonical correlation analysis. CUR was tested for its ability to suppress lipolysis in 3T3-L1 adipocytes under diverse stimuli. CUR treatment reduced TNF-a-induced lipolysis by inhibiting ERK1/2 phosphorylation and restoring perilipin protein levels in adipocytes. CUR may reduce plasma free fatty acid levels and improve insulin sensitivity due to its antilipolytic impact on the cell(Xie et al., 2012). CUR inhibits human carbonyl reductase 1 (CBR1) by binding to its occupied binding sites and reducing daunorubicinol production. CUR inhibits CBR1-mediated reduction of daunorubicin to daunorubicinol, perhaps enhancing its therapeutic efficacy by minimizing cardiac tissue damage. Inhibiting CBR1 improves daunorubicin's effectiveness in cancer tissue while reducing cardiotoxicity(Hintzpeter et al., 2015)

.

4.2. Antioxidant activity

Numerous various in vitro assays and a few in vivo trials have demonstrated the potent antioxidant effect of Curcumin. Jayaprakash and others have investigated the antioxidant properties and activities of Curcumin using in vitro model systems including phosphomolybdenum and the linoeic acid peroxidation technique. Because of their strong antioxidant capacity, these chemicals could be employed in food systems to extend the shelf life. Density functional theory was used to explain the antioxidant mechanism of CUR. Five distinct mechanisms were taken into consideration: sequential proton loss electron transfer (SPLET), H atom transfer from neutral curcumin (HAT), H atom transfer from deprotonated curcumin (HAT-D), radical adduct formation (RAF), and single electron transfer (SET) (Jayaprakasha et al., 2006).Ahmed and partners studied Curcumin for their ability to inhibit acetylcholinesterase (AChE) and improve memory in rats. A combination of Curcumin might be utilised to treat Alzheimer's disease(Ahmed & Gilani, 2009).Kalpravidh and others assessed the oxidative stress, antioxidant indices, and hematological profile of 21 b-thalassemia/Hb E patients who received two 250 mg capsules of Curcumin over a 12-month period. Increased oxidative stress was demonstrated in b-thalassemia/Hb E patients by higher levels of serum non-transferrin-bound iron (NTBI), glutathione peroxidase, superoxide dismutase, and malonyl dialdehyde, as well as lower levels of glutathione in red blood cells. After three months of therapy, all parameters were nearly back to their initial values. Curcumin can help individuals with b-thalassemia/Hb E sickness reduce oxidative damage(Kalpravidh et al., 2010).

4.3. Anticancer activity

According to zymography analysis, CUR, DMC, and BDMC all markedly reduced the amount of urokinase plasminogen activator and active MMPs in the cells in a dose-dependent manner; CUR was less effective than

BDMC and DMC. Three types of Curcumin markedly reduced MMPs and collagenase. In contrast to CUR, DMC and BDMC demonstrated greater antimetastatic potency by differential downregulation of ECM breakdown enzymes(Yodkeeree et al., 2009). DMC's anti-invasive activity, according to Yodkeeree, involves modifying the expression of invasion-associated proteins, perhaps focusing on nuclear factor-kappa B in MDA-MB-231 cells(Yodkeeree et al., 2010).

4.4. Cardioprotective effects

Cardioprotective properties of CUR against myocardial infarction, heart hypertrophy, and diabetic cardiovascular problems are extensive. The molecular mechanism of CUR's cardioprotective properties was evaluated and investigated by Hong and partners using a rat model of coronary artery ligation(Hong et al., 2010).

4.5. Sexually transmitted infections

Unplanned pregnancies and sexually transmitted illnesses pose a serious threat to women's reproductive health. There is an immediate demand for female-controlled vaginal products aimed at contraception and illness prevention. Patel and colleagues created a thermosensitive vaginal in situ hydrogel of CUR, a chemical derived from plants, using poloxamers(Patel et al., 2015).

4.6. Antiviral and antifungal activity

Chen and colleagues studied the anti-influenza activity of CUR, they found that the 30 mM CUR treatment decreased the viral production in cell culture by more than 90%. It was evident from the plaque reduction and HI tests that CUR prevents virus-cell attachment, which inhibits the spread of influenza viruses. The inhibition of hemagglutination, which was seen in both the H1N1 and H6N1 subtypes, was a direct result of CUR's impact on viral particle infectivity, according to time of drug addiction tests. The use of CUR as an antiinfluenza medication shows promise(Chen et al., 2010). The effect of Curcumin on the pathogens responsible for Candida albicans proliferation was examined and contrasted by Zhang and others using microcalorimetry. Compared to DMC, the antifungal action of CUR was more potent. The presence of a methoxy group may increase the mother nucleus's lipophilicity, which would facilitate the molecular entry into the fungal cell membrane and prevent its growth, as demonstrated by the structural activity relationship(Zhang et al., 2012).

4.7. Anti-inflammatory

Kim and colleagues described how a fast increase in intracellular [Ca2þ]i mediated an anti-inflammatory BDMC signaling pathway that resulted in hemeoxygenase-1 expression. This, in turn, triggered downstream activation of NF-E2-related factor-2, extracellular signal-regulated kinase 1/2, and calmodulin/calmodulin dependent protein kinase II. By inhibiting the release of Ca2+ from IP3 channels or calmodulin-dependent protein kinase II or extracellular signal regulated kinase 1/2, BDMC was able to reduce its inhibition of LPS-induced inducible nitric oxide synthase expression and nitric oxide production(Kim et al., 2010). This in vitro inflammation model demonstrated the biological relevance of the signaling pathway to BDMC's anti-inflammatory capacity. Hemeoxygenase-1 expression in macrophages is mediated by BDMC signaling through a new anti-inflammatory mechanism that involves the Ca2+/calmodulin-dependent protein kinase II-extracellular signal-regulated kinase ½-NFE2-related factor-2 cascade. In the Mdr1a˜/} mice model of human inflammatory bowel illness, Cooney and others showed lowering capacity CUR against colon inflammation utilizing a combination transcriptomics and proteomics strategy. The colonic histological injury score was also calculated, and colon

protein expression was quantified using 2D gel electrophoresis and LCMS protein identification. Microarrays were used to detect colon mRNA transcript levels. Reduced immunological response, enhanced xenobiotic metabolism, inflammation resolution through decreased neutrophil migration, and increased barrier remodeling are only a few of the molecular pathways that demonstrate CUR's anti-inflammatory effects(Cooney et al., 2016).

4.8. Anti-acidogenic and anti-arthritic activity

The virulence characteristics of Streptococcus mutans biofilms, including bacterial adhesion, acidogenicity, and aciduricity, were inhibited by Curcumin and other major constituents of turmeric without causing the target bacterium to die. These substances can be used to manage dental biofilms and the development of dental cavities that follow. Wistar albino rats were given Freund's Complete Adjuvant subplantarly to induce arthritis, and after nine days of injection, the rats developed pronounced arthritis. Curcumin's ability to mitigate hepatotoxicity, oxidative stress, and provide a synergistic antiarthritic effect with methotrexate was investigated in conjunction with a subtherapeutic dosage of the drug. In addition to lowering arthritis, the concurrent use of CUR and methotrexate was able to greatly lessen the hepatocellular damage brought on by the medication(Banji et al., 2011).

4.9. Anti-acanthamoebic activity

Aqeel and others studied the anti-acanthamoebic potential of resveratrol and Curcumin using primary human brain microvascular endothelial cells, which contribute to the blood-brain barrier. Acanthamoeba is an opportunistic pathogen that can infect the cornea, causing eye keratitis, and the central nervous system, causing fatal granulomatous encephalitis(Aqeel et al., 2012).

4.10. Mutagenicity and hepatoprotective activity

Vieira et al. compared curcumin to drug eluting stent components like paclitaxel and sirolimus. They used the Ames test to assess mutagenicity and measured platelet activation and fibrinogen adsorption on PLGA film to assess blood compatibility. Paclitaxel significantly increased the frequency of bacterial hisþ revertant colonies and reduced platelet activation on PLGA films containing 30% and 50% by weight CUR. CUR's intrinsic hydrophobic characteristics may promote fibrinogen adsorption on PLGA sheets(Vieira et al., 2013).

4.11. Arsenic and chromium toxicity

Arsenic is a human carcinogen and a strong hepatotoxin. Arsenic exposure in the environment provides a severe health risk to humans and animals across the world. Muthumani et al.[41] found that tetrahydro curcumin (THC) pretreatment significantly improved arsenic-induced dyslipidemia, mitochondrial toxicity, and ultrastructural changes in rat liver. THC's hepatic Mito protective properties support this claim. THC may improve hepatic mitochondrial function in arsenic-intoxicated rats by quenching free radicals, reducing lipid peroxidases, lipids, antioxidant-enzyme activity, and Ca2þ levels. THC significantly protects mitochondria, which play a vital role in activating and directing the hepatoprotective response in cells(Muthumani & Miltonprabu, 2015).

References

[1]. Ahmed, T., & Gilani, A.-H. (2009). Inhibitory effect of curcuminoids on acetylcholinesterase activity and attenuation of scopolamine-induced amnesia may explain medicinal use of turmeric in Alzheimer's disease. Pharmacology Biochemistry and Behavior, 91(4), 554–559.

[2]. Aqeel, Y., Iqbal, J., Siddiqui, R., Gilani, A. H., & Khan, N. A. (2012). Anti-Acanthamoebic properties of resveratrol and demethoxycurcumin. Experimental Parasitology, 132(4), 519–523.

[3]. Banji, D., Pinnapureddy, J., Banji, O. J., Saidulu, A., & Hayath, M. S. (2011). Synergistic activity of curcumin with methotrexate in ameliorating Freund's Complete Adjuvant induced arthritis with reduced hepatotoxicity in experimental animals. European Journal of Pharmacology, 668(1–2), 293–298.

[4]. Chaturvedi, T. P. (2009). Uses of turmeric in dentistry: An update. Indian Journal of Dental Research, 20(1), 107–109.

[5]. Chen, D.-Y., Shien, J.-H., Tiley, L., Chiou, S.-S., Wang, S.-Y., Chang, T.-J., Lee, Y.-J., Chan, K.-W., & Hsu, W.-L. (2010). Curcumin inhibits influenza virus infection and haemagglutination activity. Food Chemistry, 119(4), 1346–1351.

[6]. Cooney, J. M., Barnett, M. P., Dommels, Y. E., Brewster, D., Butts, C. A., McNabb, W. C., Laing, W. A., & Roy, N. C. (2016). A combined omics approach to evaluate the effects of dietary curcumin on colon inflammation in the Mdr1a-/- mouse model of inflammatory bowel disease. The Journal of Nutritional Biochemistry, 27, 181–192.

[7]. Hintzpeter, J., Hornung, J., Ebert, B., Martin, H.-J., & Maser, E. (2015). Curcumin is a tight-binding inhibitor of the most efficient human daunorubicin reductase–Carbonyl reductase 1. Chemico-Biological Interactions, 234, 162–168.

[8]. Hong, D., Zeng, X., Xu, W., Ma, J., Tong, Y., & Chen, Y. (2010). Altered profiles of gene expression in curcumin-treated rats with experimentally induced myocardial infarction. Pharmacological Research, 61(2), 142–148.

[9]. Jayaprakasha, G. K., Rao, L. J., & Sakariah, K. K. (2006). Antioxidant activities of curcumin, demethoxycurcumin and bisdemethoxycurcumin. Food Chemistry, 98(4), 720–724.

[10]. Jiang, J.-L., Jin, X.-L., Zhang, H., Su, X., Qiao, B., & Yuan, Y.-J. (2012). Identification of antitumor constituents in curcuminoids from Curcuma longa L. based on the composition–activity relationship. Journal of Pharmaceutical and Biomedical Analysis, 70, 664–670.

[11]. Kalpravidh, R. W., Siritanaratkul, N., Insain, P., Charoensakdi, R., Panichkul, N., Hatairaktham, S., Srichairatanakool, S., Phisalaphong, C., Rachmilewitz, E., & Fucharoen, S. (2010). Improvement in oxidative stress and antioxidant parameters in β-thalassemia/Hb E patients treated with curcuminoids. Clinical Biochemistry, 43(4–5), 424–429.

[12]. Kim, A. N., Jeon, W.-K., Lee, J. J., & Kim, B.-C. (2010). Up-regulation of heme oxygenase-1 expression through CaMKII-ERK1/2-Nrf2 signaling mediates the anti-inflammatory effect of bisdemethoxycurcumin in LPS-stimulated macrophages. Free Radical Biology and Medicine, 49(3), 323–331.

[13]. Lampe, V., & Milobedzka, J. (1913). Studien über curcumin. Berichte d. D. Chem Gesellschaft, 46(2), 2235–2240.

[14]. Mukerjee, A., & Vishwanatha, J. K. (2009). Formulation, characterization and evaluation of curcumin-loaded PLGA nanospheres for cancer therapy. Anticancer Research, 29(10), 3867–3875.

[15]. Muthumani, M., & Miltonprabu, S. (2015). Ameliorative efficacy of tetrahydrocurcumin against arsenic induced oxidative damage, dyslipidemia and hepatic mitochondrial toxicity in rats. Chemico-Biological Interactions, 235, 95–105.

[16]. Panahi, Y., Saadat, A., Beiraghdar, F., Nouzari, S. M. H., Jalalian, H. R., & Sahebkar, A. (2014). Antioxidant effects of bioavailability-enhanced curcuminoids in patients with solid tumors: A randomized double-blind placebo-controlled trial. Journal of Functional Foods, 6, 615–622.

[17]. Pandit, S., Kim, H.-J., Kim, J.-E., & Jeon, J.-G. (2011). Separation of an effective fraction from turmeric against Streptococcus mutans biofilms by the comparison of curcuminoid content and anti-acidogenic activity. Food Chemistry, 126(4), 1565–1570.

[18]. Patel, N., Thakkar, V., Moradiya, P., Gandhi, T., & Gohel, M. (2015). Optimization of curcumin loaded vaginal in-situ hydrogel by box-behnken statistical design for contraception. Journal of Drug Delivery Science and Technology, 29, 55–69.

[19]. Simon, A., Allais, D. P., Duroux, J. L., Basly, J. P., Durand-Fontanier, S., & Delage, C. (1998). Inhibitory effect of curcuminoids on MCF-7 cell proliferation and structure–activity relationships. Cancer Letters, 129(1), 111–116.

[20]. Siviero, A., Gallo, E., Maggini, V., Gori, L., Mugelli, A., Firenzuoli, F., & Vannacci, A. (2015). Curcumin, a golden spice with a low bioavailability. Journal of Herbal Medicine, 5(2), 57–70.

[21]. Vieira, I. L. B. F., de Souza, D. C. P., da Silva Coelho, L., Chen, L. C., & Guillo, L. A. (2013). In vitro mutagenicity and blood compatibility of paclitaxel and curcumin in poly (DL-lactide-co-glicolide) films. Toxicology in Vitro, 27(1), 198–203.

[22]. Vogel, H. A., & Pelletier, J. (1815). Curcumin-biological and medicinal properties. J. Pharma, 2(50), 24–29.

[23]. Xie, X., Kong, P.-R., Wu, J., Li, Y., & Li, Y. (2012). Curcumin attenuates lipolysis stimulated by tumor necrosis factor-α or isoproterenol in 3T3-L1 adipocytes. Phytomedicine, 20(1), 3–8.

[24]. Yodkeeree, S., Ampasavate, C., Sung, B., Aggarwal, B. B., & Limtrakul, P. (2010). Demethoxycurcumin suppresses migration and invasion of MDA-MB-231 human breast cancer cell line. European Journal of Pharmacology, 627(1–3), 8–15.

[25]. Yodkeeree, S., Chaiwangyen, W., Garbisa, S., & Limtrakul, P. (2009). Curcumin, demethoxycurcumin and bisdemethoxycurcumin differentially inhibit cancer cell invasion through the down-regulation of MMPs and uPA. The Journal of Nutritional Biochemistry, 20(2), 87–95.

[26]. Zhang, D., LUO, J., Dan, Y. A. N., Cheng, J. I. N., DONG, X., & XIAO, X. (2012). Effects of two curcuminoids on Candida albicans. Chinese Herbal Medicines, 4(3), 205–212.

International Journal of Scientific Research in Science and Technology
Available online at : www.ijsrst.com
OPEN ACCESS
Print ISSN: 2395-6011 | Online ISSN: 2395-602X
doi : https://doi.org/10.32628/IJSRST

A Brief Review: Application of Polyaniline Nano-Composite in Medical Field

Dr. Kamalakar K.Wavhal[1], Dr. Ramesh T. Parihar[2]

[1]Department of Chemistry, Late Ku Durga K. Banmeru Science College Lonar Dist- Buldana-443302, Maharashtra, India

[2]Department of Chemistry, Vidnyan Mahavidyalaya Malkapur, Dist- Buldana-443303, Maharashtra, India

ARTICLEINFO

Article History :

Published : 07 Dec 2024

Publication Issue :
Volume 11, Issue 23
Nov-Dec-2024
Page Number :
134-141

ABSTRACT

Recent developments in nanoparticles have great promise for the treatment of a number of illnesses. nanoparticles small size and enhanced stability make them useful as medicine carriers for conditions like cancer. They also have a number of desired qualities, such as excellent stability, specificity, sensitivity, and efficacy, which make them perfect for treating bone cancer. Moreover, they could be considered to enable the accurate release of the medication from the matrix. Drug delivery methods for the treatment of cancer have advanced to include liposomes, dendrimers, metallic nanoparticles and nanocomposites. Nanoparticles greatly enhance the mechanical strength, hardness, electrical and thermal conductivity, and electrochemical sensors of materials.

Keyword: Nanoparticle, drugs delivery, polyaniline, nano-composite.

Introduction

Polymer systems with unique properties are the recent fields of increasing scientific and technical interest, offering the opportunity to synthesize a broad variety of promising new materials, with a wide range of electrical, optical and magnetic property. Technological uses depend crucially on the reproducible control of the molecular and supramolecular architecture of the macromolecular via a simple methodology of organic synthesis[1]. Among the conducting polymer, Polyaniline (PANI) is one such polymer whose synthesis does not require any special equipment or precautions. Conducting polymers generally show highly reversible redox behavior with a noticeable chemical memory and hence have been considered as prominent new materials for the fabrication of the devices like industrial sensors[2]. The properties of conducting polymers depend strongly on the doping level, protonation level, ion size of dopant, and water content. Conducting PANI is prepared either by electrochemical oxidative polymerization or by the chemical oxidative polymerization method[3].
The emeraldine base form of PANI is an electrical insulator consisting of two amine nitrogen atoms followed by two imine nitrogen atoms. PANI (emeraldine base) can be converted into a conducting form by two different

doping processes: protonic acid doping and oxidative doping. Protonic acid doping of emeraldine base corresponds to the protonation of the imine nitrogen atoms in which there is no electron exchange. In oxidative doping, emeraldine salt is obtained from leucoemeraldine through electron exchanges. The mechanism causing the structural changes is mainly recognized to the presence of -NH group in the polymer backbone, whose protonation and deprotonation will bring about a change in the electrical conductivity as well as in the color of the polymer. Considerable research effort is now directed towards the development of sensors and artificial noses and electronic tongues based on conducting materials used for the detection of chemical vapors and gases and biological species[4].

Carbon nanotubes (CNT)

Carbon nanotubes (CNT) were first reported by Iijima(1991) . Since then many studies have been reported regarding their manufacture, structure, and properties. Ajayan and Ebbesen (1997) and Ebbesen and Ajayan (1992) reported about the manufacture of CNT in large scales, and also stated that the simplest way to understand the structure of CNT is to consider it as a two dimensional layer of a graphite sheet. There are basically two types of CNT: single wall nanotubes (SWNT) and multi wall nanotubes (MWNT), consisting of two or more concentric cylindrical shells of graphite sheets. An important characteristic of the structure is the "helicity" of the carbon honeycomb with respect to the tube axes (Iijima 1991). Hamada et al. (1992) developed an indexing method for single shells of carbon nanotubes. This method is important when characterizing the properties of an individual nanotube, as they provide important information regarding its structure[5]. The graphite sheet is folded into a tubular structure, where the ends of the open sheet are indicated by two Bravais lattice vectors[6]. The limiting cases are the “zigzag” and the “armchair”, where the lattice indices are (n, 0) and (n, n), respectively, as shown in Figure1 (Rao et al. 2004a,b). CNT possess a remarkable combination of properties, i.e., high strength and stiffness along with flexibility accompanied with high electrical and thermal conductivity, thus offering opportunities for development of new nanocomposites[7-8]
(Breuer and Sundararaj 2004 , Rao et al. 2004a,b , Ginic -Markovic et al. 2006 , Zelikman et al. 2008). However, CNT tend to agglomerate, thus losing the intrinsic properties of a single CNT. There are several approaches to overcome agglomeration of the nanotubes: i) Using surfactants which adsorb on the CNT surface helping in their separation. ii) Applying ultrasonic energy. iii) Functionalizing CNT by chemical reactions with strong acids, silanes, and so on[9]. iv) *In-situ* polymerization of monomers in the presence of CNT. v) Combination of these approaches.(fig.1)

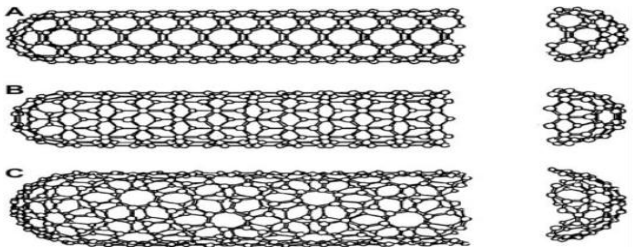

Figure: 1 Models of: (A) armchair, (B) zigzag, and (C) chiral nanotubes

Review of Literature

PANI is the oxidative polymeric product of aniline under acidic conditions and has been known since 1862 as aniline black [10-11]. Surville et. al. [12] in 1968 reported proton exchange and redox properties with the influence of water on the conductivity of PANI. In 1911 Mecoy and Moore [13] had suggested electrical conduction in organic acids. However, interest in PANI was generated only after the fundamental discovery in

1977 that iodine doped polyacetylene has a metallic conductivity. PANI as a chemical substance has been known for long time [14-15]. At the beginning of the 20th century organic chemists began investigating the construction of aniline black and its intermediate products [16]. Wills Tatter and coworkers in 1907 and 1909 regarded aniline black as an eight-nucleus chain compound having indamine structure [Fig. 2].

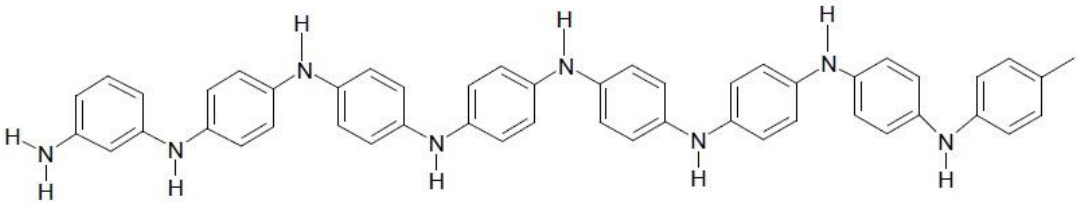

Fig. 2: Indamine structure

However, in 1910-12 Green and Woodhead [17] were able to report various constitutional aspects of aniline polymerization.

Structure of Polyaniline:

The protonation and deprotonation and various other physico-chemical properties of PANI can be said to be due to the presence of the -NH- group. The general structure of PANI can be shown below in Fig. 3. Green and Woodhead were the first to depict PANI as a chain of aniline molecules coupled head-to-tail at the para position of the aromatic ring. They have proposed a linear octameric structure for PANI. Polyaniline, a typical phenylene based polymer, has a chemically flexible NH– group in the polymer chain flanked by phenyl rings on either sides.

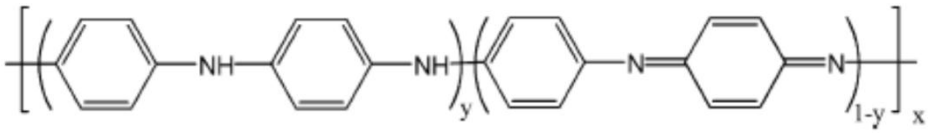

Fig. 3: Structure of PANI

The diversity in physicochemical properties of PANI is traced to the –NH– group. Out of several possible oxidation states, the 50 % oxidized emeraldine state shows electrical conductivity [18].

In combination with comparable results obtained with other similar polymers such as PPy and PTh, PANI have caused a rapid increase in experimental investigations into the mechanism and kinetic of the formation, molecular structure, electro-optical and believable application [19]. Raman et al. gave the assignments of PANI [20]

Polyaniline/CNT nano-composites

Multi walled Carbon Nanotubes (MWCNTs) were purchased from **Arkema** and used as received. In a typical experiment, MWCNTs (0.8 wt%) were added to 10ml of aniline. Then the mixture was heated at reflex for 5h in the dark. MWCNT/PANI composite films were deposited on stainless-steel sheet (SS, 0.5mm thick) by in-situ electrochemical polymerization[21].

Before deposition, the SS sheet was washed with acetone in ultrasonic bath for 10 minutes and then was dried in air. The area of the electrode used for composite films deposition was 1cm2.

The electrochemical polymerization MWCNT/PANI composite films was carried out by the CV technique at 100 mVs–1 between –0.2 and –1.2V for 100 cycles in a solution of 0.5M3 H_2SO_4 + 0.325M aniline dissolved MWCNT. The electrochemical polymerization was done in a three-electrode cell with a SS sheet working electrode, a graphite plate counter electrode, and Ag/AgCl as a reference electrode. The electro polymerization of aniline dissolved MWCNT can be observed by the color change on the surface of the working electrode. After deposition, the electrode was washed in distilled water and then dried in an oven at 60ºC for 1 day.

Methodology:-

Synthesis of PAni: The preparing of polyaniline [12-16], (PAni), 30 milliliters solution of 1.0 M HCl (37 wt%, Aldrich) is sonicated at room temperature for 2 days. 0.039 ml of aniline monomer is added to the above suspension and sonicated for 6 h. in ice bath. 0.25 g of ammonium persulfate in 1.0M HCl solution (30 ml) is then slowly added drop wise into the well sonicated suspension with sonication at a reaction temperature of 0–5 ºC for 30 min [22]. The dark suspension became green, which indicated the beginning of polymerization reaction of aniline monomer. Then polymerization reaction is carried out at 0–5 ºC for 24 h by putting the suspension into the refrigerator. The composites are obtained by filtering and rinsing the reaction mixtures several times with distilled water and methanol, resulting in the conductive emeraldine salt (ES) form of PAni composites. Finally, the dark-green composites powders are dried at 60ºC for 24 h under vacuum.

Doped Polyaniline Nano-composite: A multiphase solid material with one, two, or three phases that are less than 100 nanometres (nm) or structures with nanoscale repeat intervals between the various phases that comprise the material is called a nanocomposite. Although porous media, colloids, gels, and copolymers can all be included in this term in its broadest sense[23], it is more commonly understood to refer to the solid combination of a bulk matrix and one or more nanodimensional phases that have different properties because of structural and chemical differences. There are three major classification of nano composites and shows different examples in each category. Ceramic matrix nanocomposites metal matrix nanocomposites

Different types of Doped Polyaniline Nano-composites

Polyaniline doped Ceramic : Al2O3/SiO2, SiO2/Ni, Al2O3/TiO2, Al2O3/SiC

Polyaniline doped Metal : Fe-Cr/Al2O3,Co/Cr, Fe/MgO, Mg/CNT

Polymer: Thermoplastic/thermoset polymer/layered silicates, polyester/TiO2,polymer/CNT, polymer/layered double hydroxides.

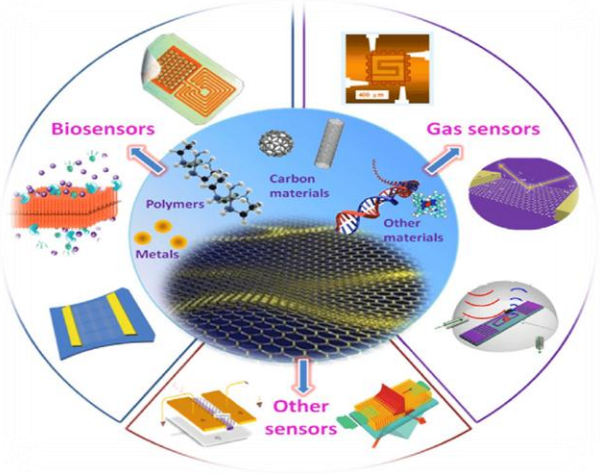

Fig.4: Structure of Nano-composite

Application

Solar cells: The amount of energy consumed today is relatively large, and non-renewable resources, such as fossil fuels, are depleting in tandem with consumption. Therefore, the function of renewable energy is crucial. One rapidly developing technology with many uses across the board is nanotechnology[24]. Because of their unique features, polymer nanocomposites are the newest and most difficult materials with a variety of applications. Nanometal-encapsulated polymers can boost solar cell efficiency. (Fig.5)

Fig.5: Solar Cell

High Power batteries: Manufacturing more powerful batteries. Scientists have created a technique for creating anodes for lithium ion batteries using a composite made of carbon nanoparticles and silicon nanospheres. The silicon-carbon nanocomposite anodes come into closer contact with the lithium electrolyte, enabling quicker power charging or discharging.(Fig.6)

Fig.6: High power battary

Light weight Sensor: Nanocomposites for the creation of lightweight sensors. A polymer-nanotube nanocomposite conducts electricity; the nanotube spacing affects how well it conducts. Because of this characteristic, polymer-nanotube nanocomposite patches can be used as stress sensors on windmill blades[25]. When the blades are bent by heavy wind gusts, the composites will bend as well. The electrical conductivity of the nanocomposite sensor is altered by bending, which sounds an alarm. This alert would enable the windmill to be turned off before it sustains too much damage.(Fig.7)

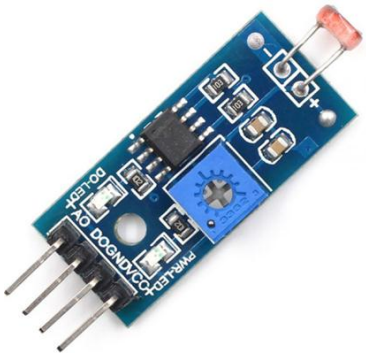

Fig.7: lightweight sensor

Healing Process: To accelerating the healing of fractured bones. Researchers have demonstrated that the use of a nanotube-polymer nanocomposite as a sort of scaffold that directs the formation of replacement bone speeds up the process. To learn more about how this nanocomposite promotes bone formation, the researchers are carrying out investigations.

Industrial application: The intricate structure emergence that results in control over the mechanical, electrical, and viscometric characteristics of polymer nanocomposites can be manipulated by surface functionalisation of nanoparticles. A compromise between compatibility and immiscibility is required for industrial filled materials that contain immiscible aggregated nanoparticles in order to influence the formation of a strong macroscopic network[26].

For Coating Purpose: Another area of great interest has been the electrical conductivity of carbon nanotubes in insulating polymers. Potential uses include shielding against electromagnetic interference, electrostatic dissipation, super capacitors, electromechanical actuators, transparent conductive coatings, and a variety of electrode applications. (Fig. 8)

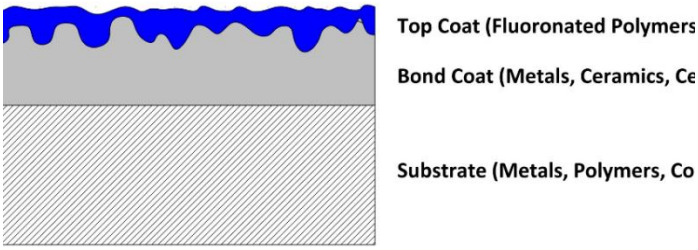

Fig.8: Structure of Coating

As Superconductor: A new generation of hybrid materials with a wide range of potential uses, including in optical displays, photovoltaic, gas sensors, electrical devices, mechanics, photoconductors, and superconductor devices, is promised by polymer semiconductor nanocomposites.(Fig.9)

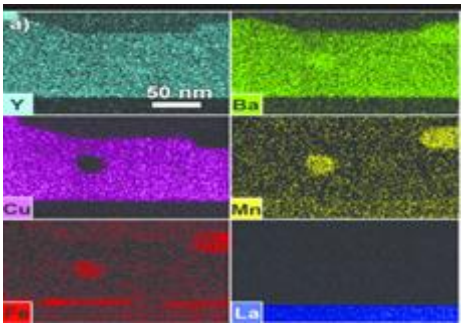

Fig.9: Structure of Superconductor

Multi-Platform Usage: It's interesting to note that multiple desirable qualities of nanoparticles can be combined to create a single platform. A multi-platform contrast agent has been created by synthesising nanoparticles with a gold shell and iron oxide core that can be heated via superparamagnetism to release a pharmacological payload[27].

Waste water treatment: The efficient removal of contaminants from wastewater is drawing more and more attention to adsorption and photocatalysis. Adsorptive removal and photocatalytic breakdown of water contaminants have shown great interest in metal oxide nanocomposites with adjustable surface characteristics, a large number of adsorption sites, and fascinating photocatalytic capabilities. (Fig.10)

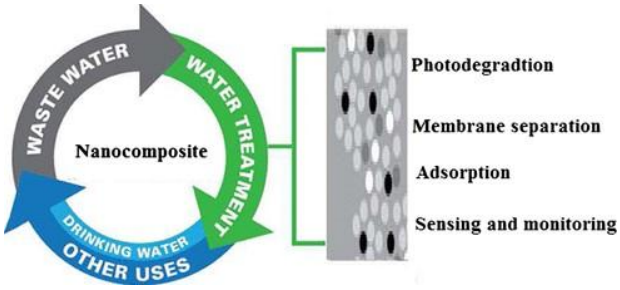

Fig.10: Waste water treatment

Antianemic :

A nanobiocomposite called ferroarabinogalactan, which was made from iron oxide nanodispersion in an arabinogalactan matrix, had decorative antianemic properties. Siberian larch (Larix sibirica), which contains arabinogalactan, has antianemic properties [28]. Due to the synergistic interaction of iron nanoparticles and arabinogalactan, it has been demonstrated that this composite has a haemopoiesis stimulator and iron stabilising effect.

Conclusion

The varieties of nano-composites and their typical uses were briefly introduced in this paper. We now understand the many kinds and uses of nanocomposites after reading this study. This is a succinct overview of polymer nanocomposites and how the electronics industry uses them. The goal of research paper is to develop more effective methods for transferring carbon nanotubes' high electrical and thermal conductivity to the polymer matrix in nanocomposites.

References

[1]. E. M. Genies, A. Boyle, M. Lapkowski, C. Tsintavis, Synth. Met. 36 139, (1990).
[2]. J. Stejskal, R. G. Gilbert, Pure Appl. Chem. 74, 857 (2002).
[3]. P. S. Rao, D. N. Sathyanarayana, In Advanced Functional Molecules and Polymers, H. S. Nalwa (ed.), Gordon & Breach, Tokyo, (2001).
[4]. J. Stejskal, R. G. Gilbert, Pure Appl. Chem. 74, 857, (2002).
[5]. Hung Van Hoang, Electrochemical Synthesis of Novel Polyaniline-Montmorillonite Nanocomposites and Corrosion Protection of Steel, Chemnitz University of Technology,(2006).
[6]. E. Gileadi, Physical electrochemistry, fundamentals, techniques and applications, wileyvch Verlag GmbH & Co. KGaA. Weinheim, 2011

[7]. M.Taki, F.Hekmat, B. Sohrabi, M.S. Rahmanifar Research gate (2014)
[8]. Jose-Yacaman, M.; Rendon, L.; Arenas, J.; Serra Puche, M. C. (1996). "Maya Blue Paint: An Ancient Nanostructured Material". Science. 273 (5272): 223–5. PMID 8662502. doi:10.1126/science.273.5272.223.
[9]. B.K.G. Theng "Formation and Properties of Clay Polymer Complexes", Elsevier, NY 1979; ISBN 978-0-444-41706-0
[10]. Debarnot, D. N. and F. P. Epaillard, Anal. Chim. Acta 475, 1–15(2003).
[11]. R. Ratheesh and K. Viswanathan, IOSR Journal of Applied Physics (IOSR-JAP) 2278-4861. Volume 6, Issue 1 Ver. II PP 01-09, (Feb. 2014).
[12]. Advanced Functional Molecules and Polymers, Volume 3, Hari Singh Nalwa, (2001).
[13]. Franklin L. Hunt, J. Am. Chem. Soc., 33 (6), 795–803 (1911).
[14]. A.G. Green and A.E. Woodhead, J. Chem. Soc.97, 2388–2403, (1910).
[15]. A.G. Green and A.E. Woodhead, Aniline-black and allied compounds Part II, J. Chem. Soc. 101, pp. 1117–1123 (1912).
[16]. Green A. G., Woodhead A. E., J. Chem. Soc., Trans., 101, 1117, (1912)
[17]. P. S. Rao, D. N. Sathyanarayana and T. Jeevananda, In Advanced Functional Molecules and Polymers.
[18]. H. S. Nalwa (ed.), Gordon and Breach, Tokyo, Vol.3, p. 79,(2001).
[19]. T.A. Skotheim and J.R. Reynolds (eds), CRC Press, Boca Raton, (2007).
[20]. Duong Ngoc Huyen*, Tran Van Ky and Le Hai Thanh, Journal of Experimental Nanoscience, Vol. 4, No. 3, 203–212, (September 2009).
[21]. P.M. Ajayan; L.S. Schadler; P.V. Braun (2003). Nanocomposite science and technology. Wiley. ISBN 3-527-30359-6.
[22]. Tian, Zhiting; Hu, Han; Sun, Ying (2013). "A molecular dynamics study of effective thermal conductivity in nanocomposites". Int.J.Heat Mass Transfer. 61: 577–582. doi:10.1016/j.ijheatmasstransfer.2013.02.023.
[23]. F. E. Kruis, H. Fissan and A. Peled (1998). "Synthesis of nanoparticles in the gas phase for electronic, optical and magnetic applications – a review". J. Aerosol Sci. 29 (5–6): 511–535. doi:10.1016/S0021-8502(97)10032-5.
[24]. S. Zhang; D. Sun; Y. Fu; H. Du (2003). "Recent advances of superhard nanocomposite coatings: a review". Surf. Coat. Technol. 167 (2–3): 113–119. doi:10.1016/S0257-8972(02)00903-9.
[25]. G. Effenberg, F. Aldinger & P. Rogl (2001). Ternary Alloys. A Comprehensive Compendium of Evaluated Constitutional Data and Phase Diagrams. Materials Science-International Services.
[26]. M. Birkholz; U. Albers & T. Jung (2004). "Nanocomposite layers of ceramic oxides and metals prepared by reactive gas-flow sputtering" (PDF). Surf. Coat. Technol. 179 (2–3): 279–285. doi:10.1016/S0257-8972(03)00865-X.
[27]. Janas, Dawid; Liszka, Barbara (2017). "Copper matrix nanocomposites based on carbon nanotubes or graphene". Mater. Chem. Front. doi:10.1039/C7QM00316A.
[28]. S. R. Bakshi, D. Lahiri, and A. Argawal, Carbon nanotube reinforced metal matrix composites - A Review, International Materials Reviews, vol. 55, (2010)

International Journal of Scientific Research in Science and Technology
Available online at : www.ijsrst.com
Print ISSN: 2395-6011 | Online ISSN: 2395-602X
doi : https://doi.org/10.32628/IJSRST

Efficient Synthesis and Biological Evaluation of α-Aminophosphonates

Kamalakar K. Wavhal[1], Deepak M. Nagrik[2]

[1]Department of Chemistry, Late Ku. Durga K. Banmeru Science College Lonar, Dist- Buldana-443302, Maharashtra, India

[2]Department of Chemistry, G.S. Science, Arts and Commerce College Khamgaon, Dist- Buldana-443303, Maharashtra, India

ARTICLEINFO

Article History :

Published : 07 Dec 2024

Publication Issue :
Volume 11, Issue 23
Nov-Dec-2024
Page Number :
142-147

ABSTRACT

A convenient and efficient synthetic method for the preparation of biological active α- Aminophosphonates derivatives by one-pot three-component reaction of carbonyl compounds, substituted anilines and dialkylphosphite. This method avoids the use of hazardous chemicals and harsh reaction condition.

The main focus of this work was the synthesis and characterization of four α- Aminophosphonate derivatives 4(a-d). Then we evaluate their biological activity against some Gram-positive and Gram-negative bacteria through agar well diffusion technique. The result of this research paper confirmed that compound 4d shows high activity against all the bacteria as compared to other compound.

Keyword: α-Aminophosphonates, biological active, Gram-negative, Gram-positive.

Introduction

In the study of biochemical processes, organophosphorus compounds are crucial substrates, and tetracoordinated pentavalent phosphorus compounds are widely employed as synthetic intermediaries and biologically active substances with a variety of uses in industry, agriculture, and medicinal chemistry[1-3]. Analogs with a C-P bond exhibit a wide range of biological activity, including insecticidal and antifungal activity, according to a review of the literature[4-5]. The Multicomponent reaction and Domino reaction have received great attention in recent year as an efficient synthetic methodology for the construction of structurally complex molecule starting from simple materials, because they have several inherent advantages over multistep synthesis, bond forming as well as time and cost efficiency, atom economy, environmental friendliness as well as applicability to diversity-oriented high –throughput synthesis and combinatorial chemistry in the form of Multicomponent transformations.[6-10] The Martin Izrailevich Kabachnik[11] and Ellis K. Fields[12] in 1952 prepared α-

Aminophosphonates by using aldehyde, amines and dialkyl phosphites in the presence of acid catalyst (Brownsted or Lewis acids) The α-Aminophosphonates considered as structural analogues of the corresponding α-Amino acids. The α-Aminophosphonates has great importance in medicinal chemistry. Therefore they used to development of rennin inhibitors or HIV protease inhibitors.

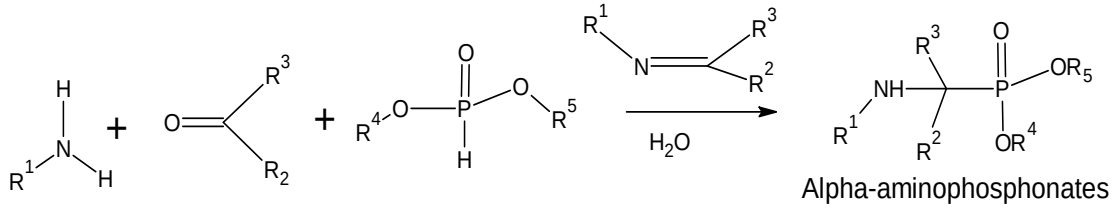

Scheme: 1. Synthesis of α-Aminophosphonates by Kabachnik-Fields reaction.

The organic compound containing phosphorus atom is called organophosphorous compound[13]. Generally this compound is used as pesticides for controlling pest. Some of the organophosphorus compound are highly effective insecticides. These compound are alternative to the chlorinated hydrocarbons because they are not degraded in the environment, They function as amino acid antagonists, inhibiting the enzymes involved in the metabolism of amino acids, which has an impact on the physiological functioning of the cell. These outcomes could be antimicrobial, controlling plant growth, or neuromodulatory. They can function as ligands, and medical applications of heavy metal complexes with aminophosphonates have been researched[14]. Several proteolytic enzymes, dialkylglycine decarboxylase, GABA receptors, peptide mimetics, catalytic antibody haptens, antibiotics, and pharmacological drugs, such as anticancer, antihypertensive, and antibacterial medicines have all been demonstrated to be inhibited by these substances[15].

Materials and methods

Experimental section

In the initial experiments, the one-pot, three-component reaction of aniline, benzaldehyde and dialkyl phosphite was used as model reaction to optimize the reaction condition. In the present work, the PANI-Co Nanocomposite used as catalyst to improve the yields.

Synthesis of PANI-Co Nano-catalyst:

The sol-gel method used to prepare polyaniline-cobalt nano-composites[16]. Cobalt chloride, ammonium persulphate, hydrochloric or sulfuric acids, and ammonium per sulphate (APS) were all analytical reagent grade and utilized exactly as received. In order to begin the chemical polymerization of aniline, it was first distilled. The middle fraction of the polyaniline was then collected and 0.1M It was mixed with an ammonium per sulfate solution. Concentrated Hydrochloric acid was then added drop-by-drop, Ammonium per sulphate was added while maintaining the reaction mixture's temperature between 0 and 4° C. The precipitated PANI-HCl salt was dried for 72 hours at room temperature. The second process begins after the polymer has been converted to an emeraldine base of PANI with ammonia. In the next phase, several cobalt chloride solutions were made. 1gm of the PANI Emeraldine base was added to 100 ml of various-concentration Cobalt chloride solutions.

Doping of PANI

In an acidified methanol solution, an oven dried anhydrous $CoCl_2$ was dissolved. PANI powder had been mixed for 2-3 hours while being constantly stirred with dopant solutions of various concentrations. The resulting doped mixture was held at ambient temperature in the crucible for 12 hours before being dried in the

oven for 6 hours at 50°C. The powder of doped PANI was eventually obtained. It was processed into a fine powder.

Result and discussion

X-Ray Diffraction Analysis:

The XRD technique was used for characterizing the nature of PANI crystallite[17]. The XRD patterns of cobalt-doped PANI (PANI-Co) and undoped PANI (ES) are displayed in (**Fig 1)** the three distinctive peaks were found at 2 values of 14.86, 20.77, and 25.31. Sharp peaks are seen because benzenoid and quinoid moieties are present in the PANI, which supports the polymer's semi-crystalline structure, in the case of PANI-Co. At 2=25.31, a sharp peak was seen. The measured interplanar distance is 3.515 A°. According to the DebyeScherrer Equation, DebyeSchererEquation. (D= kλ / β cos θ) where(1) D=Averagecrystallitesizeinnm (2)K=0.9 (Cherrer's Constant),=1.54Ao(X-raywavelength),=(FWHM)inradian, =Bragg's Angleindegree, the average crystal size is 14.5 nm

Scanning Electron Microscopy (SEM) Characterization

Determining the surface properties and morphological aspects of the nano-material is the main goal of SEM. (**Fig 2)** The morphology of doped PANI is depicted in the accompanying image, respectively. In the PANI-Co composite, spherical-shaped cobalt nanoparticles were equally dispersed across the PANI surface as seen in the condensed spherical-shaped bunch of interconnected PANI nanotubes that were visible in the SEM pictures[18-19]. This demonstrates that PANI-Co Composite was successfully created.

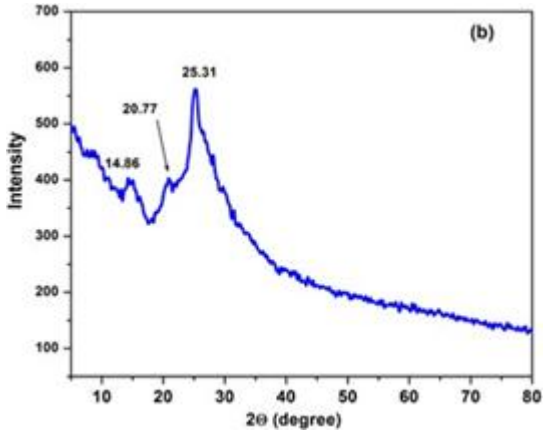

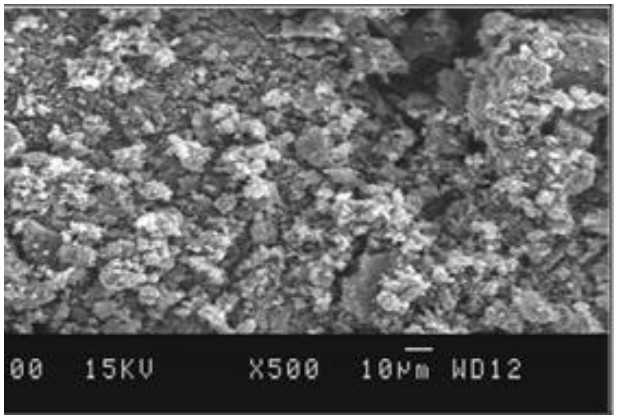

Fig 1 : XRD Spectrum of PANI-Co Nano catalyst. Fig 2. : SEM Images of PANI-Co Nano catalyst

Synthesis of α-Aminophosphonates derivatives 4(a-d):

In synthesis of α-Aminophosphonates, the equimolar mixture of substituted benzaldehyde, substituted aniline, dialkyl phosphite and PANI-Co nano-catalyst was taken in 250 ml round bottom flask[20-22]. The whole reaction mixture was kept on hot plate with magnetic stirrer. **(Scheme 2)** The round bottom flask was covered with rubber cork for reactant protection. Then it was constantly stirred for about 2-3 hours with 40-50 RPM. The 60ºC temperature was maintained. The reaction mixture was kept in ice cold water for about 1-2 hours. The viscous product was formed in the round bottom flask. Crystallization was done with the help of Addition of diethyl ether and filtration was carried out. The product wash 2-3 times with ethanol[23] **(Table 1).**

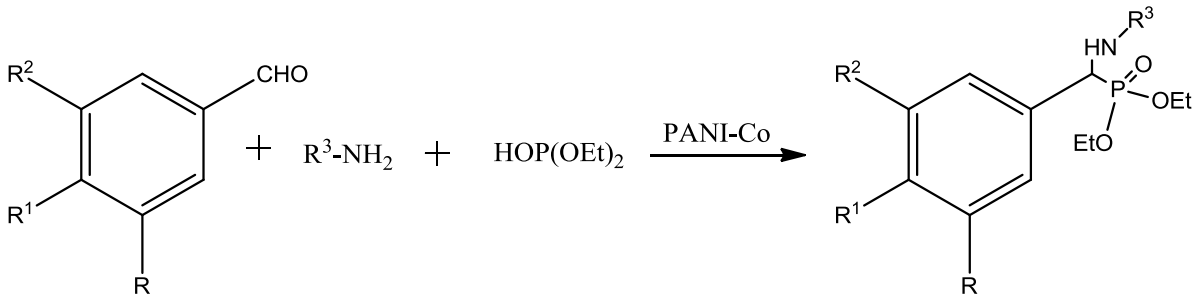

Scheme 2: Kabachnik-fields reaction.

Sr No.	Name of compound	**R**	**R¹**	**R²**	**R³**	**3**
1	1a	-OMe	-OH	-NO2	$3ClC_6H_4$-	$HOP(OE_t)_2$
2	2b	-Et	-OH	-H	$2ClC_6H_4$-	$HOP(OE_t)_2$
3	3c	-OH	-OH	-NO2	$2ClC_6H_4$-	$HOP(OE_t)_2$
4	4d	-OMe	-OH	-NO2	$4ClC_6H_4$-	$HOP(OE_t)_2$

Table 1: Synthesized α-Aminophosphonates derivatives.

1a)Diethyl (3-chlorophenylamino) (4-hydroxy-3-methoxy-5-nitro-phenyl)methylphosphonte

^{1}H-NMR (300MHz, DMSO-d6) □ 10.3(s, 1H, -OH), 8.10-6.62(m,6H, Ar-H), 5.08 (m,1H, N-H), 4.06(m, 1H, P-CH), 3.85(q, 4H, P-OCH_2), 3.18(s, 3H,-OCH3), 1.12(t, 6H, -OCCH3).^{31}P-NMR(161.9 MHz, DMSO-d6) □ 31.5. M/z : 444 and 446with 3:1 ratio. M. P. 180-182^{0}C. Yield-81%

2b)Diethyl (2-chlorophenylamino) (3-ethoxy-4-hydroxy-phenyl)methylphosphonte

^{1}H-NMR (300MHz, DMSO-d6) □ 10.2(s, 1H, -OH), 8.12-6.76(m,7H, Ar-H), 5.28 (m,1H, N-H), 3.96(m, 1H, P-CH), 3.75(q, 6H, -OCH_2), 1.28(t, 9H,-CCH3), ^{31}P-NMR(161.9 MHz, DMSO-d6) □ 32.5. M/z : 412 and 415 with 3:1 ratio. M. P. 182-185^{0}C. Yield-88%

3c)Diethyl (2-chlorophenylamino) (3,4-hydroxy-5-nitro-phenyl)methylphosphonte

^{1}H-NMR (300MHz, DMSO-d6) □ 10.4(br, 2H, -OH), 8.28-6.52(m,6H, Ar-H), 5.48 (m,1H, N-H), 3.96(m, 1H, P-CH), 3.78(q, 4H, P-OCH_2), 1.32(t, 6H,P-CCH3), ^{31}P-NMR(161.9 MHz, DMSO-d6) □ 31.8. M/z : 430 and 432with 3:1 ratio. M. P. 174-176^{0}C. Yield-87%

4d)Diethyl (4-chlorophenylamino) (4-hydroxy-3-methoxy-5-notro-phenyl)methylphosphonte

^{1}H-NMR (300MHz, DMSO-d6) □ 10.4(s, 1H, -OH), 8.20-6.54(m,6H, Ar-H), 5.48 (m,1H, N-H), 4.16(m, 1H, P-CH), 3.65(q, 4H, -OCH_2), 2.94(s, 3H,-CCH3), 1.02(t, 6H, -OCCH3).^{31}P-NMR(161.9 MHz, DMSO-d6) □ 31.8. M/z : 442 and 444with 3:1 ratio. M. P. 160-162^{0}C. Yield-92%

Biological Evaluation of α-Aminophosphonates

The synthesized α-aminophosphonate were tested using the well diffusion method against several bacterial species, Staphylococcus aureus, Escherichia coli, Shigella dysenteriae, Klebsiella pneumoniae, Proteus mirabilis, are among the organisms employed in both of these methods. Design and synthesis of novel antibacterial sulfanilamide aminophosphonates for Escherichia coli: by Juang Wang et al.[24] Synthesis, and Antiviral Activityof new 1,2,3-Triazolylbenzyl aminophosphonate Ribonucleosides done by Abdelaaziz Ouahrouch et al.[25] Novel α-aminophosphonate derivatives loaded carrageenan cryogel: synthesis, antibacterial action, and sustainable release studied by Dalia A. Elsherbiny et al.[26] A number of rhein α-aminophosphonates conjugates were created, and their cytotoxicity against the HepG-2, CNE, Spca-2, Hela, and Hct-116 cell lines was tested in

vitro. Some substances demonstrated comparatively high cytotoxicity. Particularly, compound (IC50: 5.32 M) demonstrated the highest level of cytotoxicity against Hct-116 cells studied by Gui-yang Yao et al.[27]

For convenience, the compound were graded as.

1) High active : With zone of inhibition value >15-20mm.
2) Moderately active : With zone of inhibition value >10-15mm.
3) Poorly activity : With zone of inhibition value >05-10mm

Sr. No.	Sample	Zone of Inhibition			
		Staphylococcus aureus	Escherichia coli	Shigella dysenteriae	Klebsiella pneumoniae
01	1a	16	15	14	15
02	2b	10	12	14	10
03	3c	15	16	15	16
04	4d	16	17	15	15
Std. Antibiotic Gentamicine (G)		**17**	**16**	**18**	**16**

Table 2: Antibacterial activity of test samples against pathogenic organisms

The compound Ia shows high activity against Staphylococcus aureus, Escherichia coli, Shigella dysenteriae and moderate activity against Shigella dysenteriae. The compound 2b shows moderate activity against all the bacteria. The compound 3c shows high activity against all bacteria. The compound 4d shows high activity against all the bacteria.

Conclusion

On the basis of above discussion it is conclude the synthesis of α-Aminophosphonates derivatives was achieved in high yield through Kabachnik-fields reaction using cobalt doped polyaniline as nano-catalyst. Their structure were confirmed by elemenatal analysis XRD, SEM, NMR and Mass spectral data. All the synthesized compound were screened for biological evaluation against the pathogenic bacteria. The compound presence of substitution like –OH, -Cl and -NO_2 enabled the compounds to promising activity. The compound consists of –Cl and –OCH_3 may be used as antiviral drugs. The compound possessing alkoxy group (-OCH_3)with halogen atom or nitro group in phosphate moieties, turned out to be most active compare to derivatives with the dimethyl group and it may be used as antibiotics.

References

[1]. R. Engel, Chem. Rev., 1977, 77, 349.
[2]. J. Hiratake, J. Oda, Biosci. Biotechnol. Biochem., 1997, 61, 211.
[3]. K. A. Schug, W. Lindner, Chem. Rev., 2005, 105, 64.
[4]. K. Moonen, I. Laureyn, C.V. Stevens, Chem. Rev., 2004, 104, 6177.
[5]. F. Palacios, C. Alonso, J.M. de los Santos, Curr. Org. Chem., 2004, 8, 1481.
[6]. Vignesh A; Vernar Kaminsky; Dharmaraj Nallasamy; Chem Cat Chem,2016, 8(20) DOI:10.1002/cctc.201600717

[7]. Ali Dondas H.; Graci Retamosa; Jose M. Sansano. Organometallics,2019,38(9), DOI:10.1021/acs.organomet.9b00110
[8]. Chang Liu; Shaonan Wo; Wan Sun;Haifang Meng. Asian Journal of Chemistry,2019, 9(1) DOI:10.1002/ajoc.201900660
[9]. Chenchen Wang; Wenyu Zhao; Xianqing Wu; Jingqing Qu. Advance Syntheis and Catalysis, 2020, 362,(22), DOI:10.1002/adsc.202000537
[10]. Gyorgy Keglevich and Erika Balint. Molecules, 2012,1711, 12821-35,
[11]. Kabachnik Martin I; Medved T. Y. in Russiaan,1952,83,689ff.
[12]. Field Ellis K. .Journal of the American Chemical Society, 1952,74(6), 1528-1531, doi:10.1021/ja01126a054
[13]. Dillon K. B; Mathey F; Nixon J. F. 1997,John Wiley & Sons, ISBN 0-471-97360-2
[14]. Tusek-Bozic L. J.Current Medicinal Chemistry, 2013, 20,16,2096-117.
[15]. Nikolay S. Zefirov, Elena D. Matveeva. Journal of Org. Chem, 2008, 2008, 1,1-17 DOI: http://dx.doi.org/10.3998/ark.5550190.0009.101
[16]. Babar, P.; Lokhande, A.; Pawar, B.; Gang, M.; Jo, E.; Go, C.; Suryawanshi, M.; Pawar, S.; Kim, J.H. Electrocatalytic performance evaluation of cobalt hydroxide and cobalt oxide thin films for oxygen evolution reaction. Appl. Surf. Sci. 2018, 427, 253–259. [Google Scholar] [CrossRef]
[17]. Kowalski, G.; Pielichowski, J.; Grzesik, M. Characteristics of polyaniline cobalt supported catalysts for epoxidation reactions. Sci. World J. 2014, 2014. [Google Scholar] [CrossRef]
[18]. Younis, A.; Chu, D.; Lin, X.; Lee, J.; Li, S. Bipolar resistive switching in p-type Co3O4 nanosheets prepared by electrochemical deposition. Nanoscale Res. Lett. 2013, 8, 36. [Google Scholar] [CrossRef] [Green Version]
[19]. Ansari, S.A.; Khan, M.M.; Ansari, M.O.; Lee, J.; Cho, M.H. Visible light-driven photocatalytic and photoelectrochemical studies of Ag–SnO2 nanocomposites synthesized using an electrochemically active biofilm. RSC Adv. 2014, 4, 26013–26021. [Google Scholar] [CrossRef]
[20]. Machingal, S.; Krushnapillai, S.; Beilestein Journal, 2020, doi:10.3762/bxiv.2020.97.v1
[21]. Hellal, A.; Chaffa, S.; Touafri, L. Korean Journal of Chemical Engineering, 2016, 33, 8, pp. 2366-2373.
[22]. Rasal, S. A.; Tamore, M. S.; Shimpi, N. G. Chemistry Select, 2019, 4, 8, pp. 2293-2300.
[23]. Nellisara, D. Shashikumar, Journal of Chemistry, 2013, vol.2013, Article ID 240381.
[24]. Jaung, W.; Ansari, M. F.; Lin, J. M.; Zhou, C. H. Chines Journal of Chemistry, 2021, 39, 8, 2251-2263.
[25]. Abdelaaziz, Ouahrouch.; Taourirte, M.; Schols, D.; Snoeck, R.; Andrei, G.;Engels J.; Lazrek H. B. Arch Pharm, 2016, 349, 1, 30-41.
[26]. Elsherniny, D. A.; Abdelgawad, A. M..; El-Naggar, M. E.; El-Sherbiny, R. A.; El-Rafie M. H.; El-Sayed I. T. International Journal of Biological Macromolecules, 2020, 163, 15, 96-107.
[27]. Yao, G.; Ye, M.; Huang, R.; Li Y.; Pan, Y.; Xu Q.; Liao, Z. Bioinorganic and Medicinal Chemistry Letters, 2014, 24, 2, 501-507.

International Journal of Scientific Research in Science and Technology
Available online at : www.ijsrst.com
OPEN ACCESS
Print ISSN: 2395-6011 | Online ISSN: 2395-602X
doi : https://doi.org/10.32628/IJSRST

Synthesis, Physicochemical and Antimicrobial Study of Transition Metal Complexes, Ti(III), Mn(III) and VO(IV) from Tridentate Hydrazone Schiff Base Prepared in Environmental Friendly Deep Eutectic Solvent (DES)

Suchita B. Wankhede
Department of Chemistry, Amolakchand Mahavidyalaya, Yavatmal-445001, Maharashtra, India

ARTICLEINFO

Article History :

Published : 07 Dec 2024

Publication Issue :
Volume 11, Issue 23
Nov-Dec-2024
Page Number :
148-156

ABSTRACT

(E)-4-Bromo-N'-(1-(1-hydroxy-4-iodonaphthalen-2-yl)ethylidene) benzohydrazide (H2L) was synthesized through a simple, clean and efficient procedure using [BTEAC][oxalic acid.2H2O], deep eutectic solvent (DES) with excellent yield in short time when compare to conventional method. Further Ti(III), Mn(III) and VO(IV) metal complexes are prepared from hydrazone Schiff base (H2L). The resulting compounds have been characterized by elemental analysis, IR, 1HNMR, diffuse reflectance spectra, magnetic susceptibility, molar conductance and thermogravimetric analysis. Molar conductance in dimethylformamide indicates non-electrolytic behavior of metal complexes. The analytical data along with IR, electronic, magnetic and thermal studies suggested that all complexes have monomeric structures, Mn(III) and VO(IV) complexes shows square pyramidal geometry while Ti(III) complex have octahedral geometry. Results obtained for all compounds, on screening against antibacterial and antifungal strains; reveals that, metal complexes show higher antimicrobial activity than ligand (H2L).

Keywords: Green-ecofriendly solvent, Deep eutectic solvent (DES), Hydrazone Schiff base, Transition metal complexes, Antimicrobial study.

Introduction

In the last 20 years, a new class of room temperature ionic liquids can be used as reaction medium which have enormous applications [1] due to their interesting properties. Abbott in 2003 [2] first introduced a new generation of safe, nontoxic, cheap, biorenewable and biodegradable, sustainable designer solvent, deep eutectic solvent (DES). Thus, DES is generally defined as a binary mixture of ionic components, one is a hydrogen bond acceptor (HBA) and the other a hydrogen bond donor (HBD), which is able to form a new eutectic phase

(which is a liquid below 100 °C) through hydrogen-bond-promoted self-association and no covalent compounds are formed between them, hence known as "Deep Eutectic Solvent". As a designer and environmentally benign solvent, DES have numerous applications in various fields. Beside this there are many reviews devoted in organic transformation [3,4].

Presence of both oxygen and nitrogen donor atoms in the backbone of hydrazone ligands ($R_1R_2C=NNHCOR_3$), (where R_1, R_2, and R_3 = H, alkyl, or aryl groups) make them an important chelating motif to form various metal complexes. Beside of enormous and fascinating biological applications, hydrazone schiff bases attributed to their potential applications as an intermediate in the synthesis of medicinally important heterocyclic compounds [5]. Hydrazones are simply synthesised by condensation of carbonyl compounds with hydrazide derivatives, conventionally in organic solvents such as methanol, ethanol, dimethyl sulfoxide, dimethylformamide, etc., using catalysts like acetic acid, concentrated hydrochloric acid, concentrated sulfuric acid, etc. [6,7]. However, challenges such as excessive solvent and catalyst usage, long reaction times, high temperatures, and low yields persist in conventional synthesis.

In continuation of our work of interest towards synthesis of biologically active hydrazone Schiff's bases [8,9], aim of present work is to synthesize some newer molecule containing benzohydrazone scaffolds by using acidic deep eutectic mixture Benzyltriethylammonium chloride (BETAC) and Oxalic acid.$2H_2O$ (1:1) for the synthesis of (*E*)-4-Bromo-*N*'-(1-(1-hydroxy-4-iodonaphthalen-2-yl)ethylidene) benzohydrazide (H_2L), as a reaction media as well as catalyst to solve drawbacks of the conventional approach as greener solvent. W. The mode of chelation, tentative geometry and bonding nature of Ti(III), Mn(III) and VO(IV) metal ions with (H_2L) schiff base was also studied from spectral characterisation.

Material and Methods

All the starting chemicals and solvents were of analytical grade and used without further purification. The metal salts Titanium trichloride, Manganese acetate dihydrate and Vanadyl sulphate pentahydrate obtained from Sigma-Aldrich.

2.1. Synthesis of 1-(1-hydroxy-4-iodonaphthalen-2-yl)ethanone

2-acetyl-1-naphthol (50mmole) was added in 15ml ethanol and dissolve on stirring. To this iodine (20mmole) was added till it dissolve followed by addition of Benzyltriethylammonium chloride (25ml) act as phase transfer catalyst. A saturated solution of iodic acid (10mmole) (water solution) was added slowly with constant stirring by maintaining temperature at 35-40˚C. Within 5-10 min solid product was separated, which was washed with water followed by saturated solution of $Na_2S_2O_3$, to remove excess of iodine. Resultant product was recrystallized from solvent mixture DMF+ethanol (1:1v/v) to yield 1-(1-hydroxy-4-iodonaphthalen-2-yl)ethanone.

Yield = 94%; Melting point = 156 - 157°C

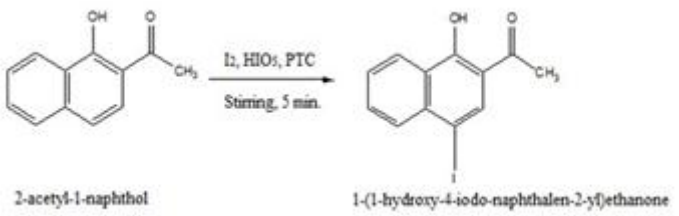

Scheme 1. Synthesis of 1-(1-hydroxy-4-iodonaphthalen-2-yl)ethanone

2.2. General procedure for synthesis of deep eutectic solvents (DES)

A mixture of BTEAC (1 mmol) and oxalic acid.2H O (1 mmol) were heated and stirred for 1h, until a clear colorless transparent liquid was obtained [10].

2.3. Conventional method of synthesis of (*E*)-4-Bromo-*N*'-(1-(1-hydroxy-4-iodo-naphthalen-2-yl)ethylidene) benzohydrazide (H_2L)

To hot ethanolic solution (15ml) of substituted benzohydrazide (0.01mol), hot DMF solution (15ml) of 1-(1-hydroxy-4-iodonaphthalen-2-yl)ethanone was added with continuous stirring and reaction mixture was heated under reflux on water bath for 6-8 hr. After cooling, the solution was allowed to evaporate resulting in coloured solid product, washed with ethanol and dried under vaccume of $CaCl_2$. It was finally recrystallized from DMF. Yield = 65 %

2.4. Synthesis of (*E*)-4-Bromo-*N*'-(1-(1-hydroxy-4-iodonaphthalen-2-yl)ethylidene) benzohydrazide (H_2L) in DES (BTEAC. OX. $2H_2O$)

A mixture of 1-(1-hydroxy-4-iodonaphthalen-2-yl)ethanone (0.01 mol) and 4-bromobenzohydrazide (0.01 mol) was added in BTEAC. OX. $2H_2O$ DES (10 ml) inround bottom flask and refluxed for 10 min at 80°C. DES was completely dissolved in distilled water, thus product was easily separated from DES and was filtered,washed many times with water and dried in vacuum of $CaCl_2$. It was finally recrystallized from DMF-ethanol mixture (1:4 v/v). Yield = 90 %; Melting point = 201 - 203°C

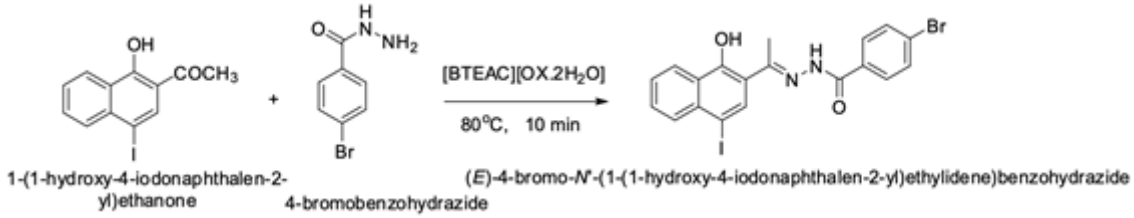

Scheme 2. Synthesis of Schiff base (H_2L)

The ligand is insoluble in water, sparingly soluble in methanol, ethanol etc. but completely soluble in DMF and DMSO and stable at room temperature and nonhygroscopic.

2.5. General preparation of Ti(III), Mn(III), VO(IV) hydrazone metal complexes

To a hot DMF solution (15ml) of organic ligand (0.1mol), a hot ethanolic solution of the appropriate metal salt (0.1mol) solution was added under continuous stirring. The mixture was refluxed on sand bath for 6-8h. The resultant solution was digested to half of its volume; on cooling solid product was obtained. The product was washed with ethanol followed by petroleum ether and dried at room temperature (Yield = 70-75%).

Results and Discussion

From analytical data given in table no. 1, indicates 1:1 stoichiometry of schiff base (H_2L) and metal ion in complex. Non-electrolytic nature of metal complexes was confirmed from their molar conductance values in between 8.5-22.5 $ohm^{-1}cm^{-1}mol^{-1}$ in DMF at 10^{-3} M [10]. All metal complexes are coloured and non hygroscopic and stable at room temperature. They are insoluble in water, slightly soluble in ethanol and completely dissolved in dimethylformamide and dimethylsulphoxide solvents.

Table 1. Analytical and physical data of schiff base H_2L and metal complexes

Sr. No	Molecular Formula Ligand/Complexes	Molecular Weight	Colour	Elemental Analysis found (calculated)							*(∧m)
				C%	H%	N%	Cl%	Br%	I%	M%	
1	$C_{19}H_{14}BrIN_2O_2$	509.14	Dark Brown	44.77 (44.82)	2.69 (2.77)	5.41 (5.50)	—	15.38 (15.69)	24.78 (24.93)	—	—
2	$[Ti(L)(H_2O)Cl_2]$	627.48	Blush	37.26 (36.37)	2.51 (2.73)	4.25 (4.63)	5.40 (5.65)	12.69 (12.73)	20.06 (20.22)	7.35 (7.63)	19.6
3	$[Mn(L)(H_2O)(OAc)]$	654.15	Ebony	40.12 (40.39)	3.00 (3.08)	4.03 (4.28)	—	12.01 (12.21)	19.20 (19.40)	8.04 (8.40)	22.5
4	$[VO(L)H_2O]$	592.08	Olive green	38.22 (38.54)	2.21 (2.38)	4.53 (4.73)	—	13.38 (13.50)	21.22 (21.43)	8.39 (8.60)	8.5

3.1. ^{1}H NMR study of ligand H_2L

The structure of ligand can be confirmed from ^{1}H NMR spectra as shown in Fig.1 recorded in DMSO-d_6. The ^{1}H NMR spectrum (in δ ppm) of ligand H_2L displayed a singlet observed at 14.75 ppm (S, 1H, -OH) was assign to phenolic –OH group. Another singlet observed at 11.49 ppm (S, 1H, imino) was assign to proton of imino –NH group. The three protons of methyl group have resonated as a sharp singlet at 2.50 ppm (S, 3H, -CH_3) [11]. Signals in the region 7.95-7.31 ppm are assigned for aromatic protons.

3.2. Magnetic Property and Diffuse reflectance Spectral Study

The proposed structure of synthesized Ti(III), Mn(III) and VO(IV) complexes were studied from the recorded diffuse reflectance spectra and magnetic moment values, spectral data was presented in Table 2. From magnetic moment value and possible transition assigned from diffuse reflectance spectra; confirms octahedral geometry of Ti(III) complex and suggesting square pyramidal geometry for Mn(III) and VO(IV) complexes [12].

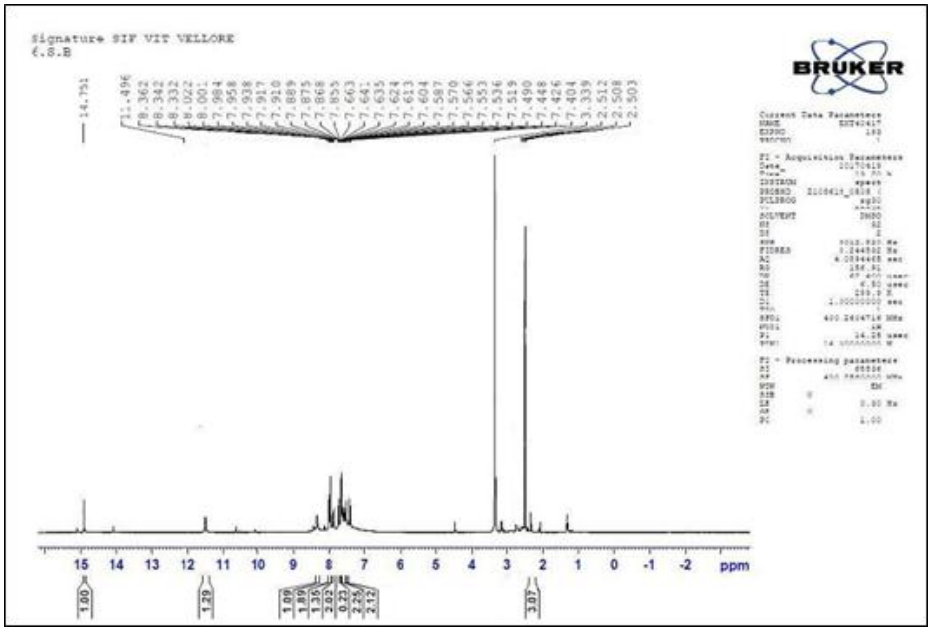

Fig. 1 ^{1}H NMR Spectra of hydrazone schiff base (H_2L)

Table 2. Magnetic moment and Diffuse reflectance spectral data of metal complexes

Sr. No.	Metal Complexes	Magnetic moment (μ_{eff} B.M.)	Absorption band (λmax)		Assignment
			nm	cm^{-1}	
1	$[Ti(L)(H_2O)Cl_2]$	1.42	516	19379	$^2T_{2g} \rightarrow {}^2E_g$
2	$[Mn(L)(H_2O)(OAc)]$	4.65	722	13850	$^5B_{1g} \rightarrow {}^5B_{2g}$
			586	17064	$^5B_{1g} \rightarrow {}^5A_{1g}$
			480	20833	$^5B_{1g} \rightarrow {}^5E_g$
			335	29850	LMCT
3	$[VO(L)H_2O]$	1.65	814	12285	$^2B_{2g} \rightarrow {}^2E_g$
			655	15267	$^2B_{2g} \rightarrow {}^2B_{1g}$
			440	22727	$^2B_{2g} \rightarrow {}^2A_{1g}$
			347	28818	LMCT

3.3. IR Spectral studies

The modes of bonding in complexes are compared with free ligand, from study of IR spectral data given in Table 3. IR bands for υ(N-H), υ(C=O), υ(C=N) and phenolic υ(C-O) are observed at 3190, 1660, 1593 and 1265 cm^{-1} respectively in free ligand. However in the o-hydroxy Schiff base a medium broad band at 3010 cm^{-1} was observed due to the presence of a strong intramolecular hydrogen bonding (O– H…N=C) [13]. In complexes this band was disappeared which indicates the coordination of phenolic oxygen to metal ion via deprotonation which was confirmed by upward shift of phenolic υ(C-O) frequency 1292-1327 cm^{-1}compared to ligand with frequency 1265 cm^{-1}. Streching frequency of υ(C=N) in free ligand shift to lower value by 7-26 cm^{-1} in complexes. This indicates coordination of azomethine nitrogen to metal ion in complexes. Presence of υ(C=O) and υ(N-H) vibrations in the spectra of Ti(III) complexe indicate that hydrazone ligand was in keto form, this confirmed monobasic tridentate nature of ligand in Ti(III) complex. Bonding of ligand with metal through enolic form was confirmed by disappearance of both υ(N–H) and υ(C=O) bands in VO(IV) and Mn(III) omplexes. The participation of the phenolic oxygen and azomethine nitrogen by the appearance of band at 567-586 cm^{-1} and 420-443 cm^{-1} assignable to υ(M–O) and υ(M–N) respectively. A strong band at region 1001 cm^{-1} give evidence of V=O stretch in VO(IV) complex spectra [14].

Table 3. Infrared spectral data of Schiff base (H_2L) and metal complexes in cm^{-1}

Sr. No	Compound	υOH + υNH (HO----NH)	N-H	C=O	C-O Phenolic	C=N	N-N	C-O enolic	M-O	M-N
1	H_2L	3010	3190	1660	1265	1590	1010	—	—	—
2	Ti(III)	—	3201	1644	1292	1579	1016	—	567	426
3	Mn(III)	—	—	—	1296	1564	1014	1247	570	420
4	VO(IV)	—	—	—	1327	1583	1031	1251	586	443

3.4. Thermogravimetric Analysis

The thermogram of metal complexes Ti(III) and VO(IV) shows a two stage decomposition pattern and Mn(III) complex shows three stage decomposition pattern as shown in table no. 4. In case of Ti(III), Mn(III) and VO(IV) complexes decomposition begins at 160℃, 145℃ and 140°C with weight loss 12.62%, 3.43% and 3.74% corresponds to two coordinated water molecule and one chloride ions in Ti(III), loss of one coordinated water molecule in Mn(III) and VO(IV) complexes respectively. The second step for Ti(III) and VO(IV) represent partial decomposition of ligand moiety while for Mn(III) loss of one acetate molecule was observed. Further decomposition of remaining part of ligand was continued upto 800℃ showing high residue due to some organic part and metal oxide, indicate strong coordination bond between metal and ligand [15].

Table 4. Thermal decomposition data of H_2L and complexes

Compounds	Temp Range (°C)	% Mass Loss		Assignment
		Found	Calculated	
[Ti(L^7) $(H_2O)_2Cl$]	160-216°C 218-554°C >554°C	13.82% 40.04%	12.62% 39.91%	Loss of two coordinated water molecules and one chloride ion Partial decomposition of ligand Deligation
[VO(L^7) H_2O]	147-168°C 168-448°C >448°C	3.43% 41.14%	3.13% 41.08%	Loss of one coordinated water molecules Partial decomposition of ligand Deligation
[Mn(L^7) (OAc) (H_2O)]	145-265°C 265-320°C 320-570°C >570°C	3.74% 12.76% 35.83%	3.00% 12.17% 35.59%	Loss of one coordinated water molecules Loss of one acetate ion Partial decomposition of ligand Deligation

Antimicrobial study

Antimicrobial data for ligand and its complexes was presented in Table 5. Compared to standard used and its metal complexes, ligand H2L was less active towards all microorganisms. This is because of the chelation according to Tweedy's chelation theory [16].

4.1. Antibacterial activity

Antibacterial activity was measured by **agar cup method.** All metal complexes are moderately active against all bacterial stains. Ti(III) (16 mm), Mn(III) (16 mm) and VO(IV) (20 mm) exhibits high activity against *E. coli* as compared to standard *Pencillin* (11mm).

4.2. Antifungal activity

Antifungal activity was performed by **poison plate method**. VO(IV) complexes exhibits good antifungal activity against *A. niger.* and *A. flavus.* In case of Ti(III) and Mn(III) complexes, exhibits good antifungal activity against *F.moneliforme.*

Table. 5 Antibacterial and antifungal activity of ligand H_2L and its metal complexes

Sample Code No.	Antibacterial activity (mm)				Antifungal activity			
	Gram -ve		Gram +ve					
	E. coli	*S. typhi*	*S. aureus*	*B. subtilius*	*A. niger*	*P.chryso genum*	*F.moneli forme*	*A. flavus*
H_2L	15	12	13	11	RG	RG	-ve	RG
Ti(III)	16	15	15	14	RG	RG	-ve	RG
VO(IV)	20	18	25	27	-ve	RG	RG	-ve
Mn(III)	16	13	15	14	RG	RG	-ve	RG
*Penicillin**	11	24	36	30	-	-	-	-
*Griseofulvin**	-	-	-	-	-ve	-ve	-ve	-ve

+ve – *Growth (Antifungal Activity absent),* -ve – *No Growth (More than 90% reduction in growth, Antifungal Activity present),* RG – *Reduced Growth (More than 50% and less than 90% reduction in growth), *Standard drug*

Recycling and reuse of [BTEAC][OX.2H2O] DES

[BTEAC][OX.2H2O] DES play a vital role as catalyst and solvent in synthesis of hydrazone schiff base (H_2L). DES can be easily separated from product by dissolving in water. Water can be evaporated using vacuum pump and recycled DES was reused four times with minor loss of activity.

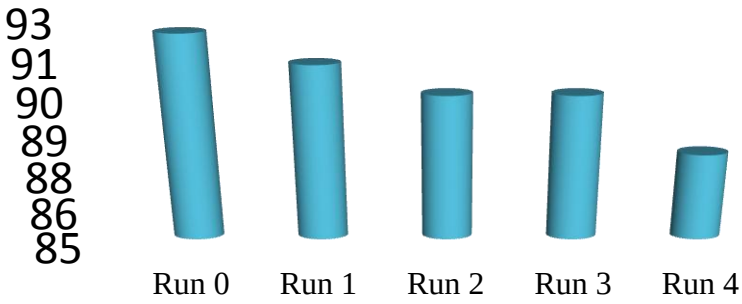

Fig. 2 Recycling of [BETAC] [OX.2H2O]DES

Conclusion

As expected, [BTEAC][OX.2H2O] DES act as a green, efficient and easily handled solvent as well catalyst for synthesis of schiff base (H_2L) with high yield in reduced time as compare to conventional method. The bonding of ligand to metal was confirmed by the analytical, IR, electronic, magnetic and thermal studies. From the present investigation it has been observed that Schiff base H_2L was monobasic tridentate towards Ti(III) complex with octahedral geometry while for Mn(III) and VO(IV) complexes was dibasic trident ate with square pyramidal geometry. The metal complexes have higher antimicrobial activity than the ligand. Amongst all complexes VO(IV) complex shows higher antibacterial as well as antifungal activity.

References

[1]. Xu, Z.- hong, Zhang, X.- wei, Zhang, W.- qiang, Gao, Y.- hao, & Zeng, Z.- zhi. (2011). Synthesis, characterization, DNA interaction and antibacterial activities of two tetranuclear cobalt(II) and nickel(II) complexes with salicylaldehyde 2-phenylquinoline-4-carboylhydrazone. Inorganic Chemistry Communications, 14(10), 1569-1573. https://doi.org/10.1016/j.inoche.2011.06.005

[2]. Kavitha, P., Saritha, M., & Laxma Reddy, K. (2013). Synthesis, structural characterization, fluorescence, antimicrobial, antioxidant and DNA cleavage studies of Cu(II) complexes of formyl chromone Schiff bases. Spectrochimica Acta Part A: Molecular and Biomolecular Spectroscopy, 102, 159-168. https://doi.org/10.1016/j.saa.2012.10.037

[3]. Ünlü, A. E., Arıkaya, A., & Takaç, S. (2019). Use of deep eutectic solvents as catalyst: A mini-review. Green Processing and Synthesis, 8(1), 355–372. https://doi.org/10.1515/gps-2019-0003

[4]. Longo, L., Jr, & Craveiro, M. (2018). Deep Eutectic Solvents as Unconventional Media for Multicomponent Reactions. Journal of the Brazilian Chemical Society. https://doi.org/10.21577/0103-5053.20180147

[5]. Sadhukhan, D., Maiti, M., Zangrando, E., Pathan, S., Mitra, S., & Patel, A. (2014). Heterogeneous catalytic oxidation of styrene by an oxo bridged divanadium(v) complex of an acetohydrazide-schiff base. Polyhedron, 69, 1–9. https://doi.org/10.1016/j.poly.2013.11.007

[6]. Dongare, G., & Aswar, A. (2021). Synthesis, spectral characterization, thermo-kinetic and biological studies of some complexes derived from tridentate hydrazone Schiff base. Journal of Saudi Chemical Society, 25(10), 101325. https://doi.org/10.1016/j.jscs.2021.101325

[7]. Bashir, M., Dar, A. A., & Yousuf, I. (2023). Syntheses, Structural Characterization, and Cytotoxicity Assessment of Novel Mn(II) and Zn(II) Complexes of Aroyl-Hydrazone Schiff Base Ligand. ACS Omega, 8(3), 3026-3042. https://doi.org/10.1021/acsomega.2c05927

[8]. Wankhede, S. B., & Patil, A. B. (2018). Studies on Ti(III), Cr(III) and Fe(III) complexes with 1-(1-hydroxynaphthalen-2-yl)ethanone-4-chlorobenzoylhydrazone ligand: Synthesis, Physicochemical and Antimicrobial activity. Journal of Pharmaceutical, Chemical and Biological Sciences. 6(1), 25-33.

[9]. Wankhede, S. B. (2021). Oxovanadium(IV) Complexes: Synthesis, Spectral and Antimicrobial Studies Derived from Dibasic Tridentate (ONO) Donor Aroylydrazone Schiff's Bases. International Journal of Advanced Research in Science, Communication and Technology (IJARSCT). 12(4), 94-102. DOI: 10.48175/IJARSCT-2358

[10]. Bhaskar, R., Salunkhe, N., Yaul, A., & Aswar, A. (2015). Bivalent transition metal complexes of ONO donor hydrazone ligand: Synthesis, structural characterization and antimicrobial activity. Spectrochimica Acta Part A: Molecular and Biomolecular Spectroscopy, 151, 621-627. https://doi.org/10.1016/j.saa.2015.06.121

[11]. Mandlik, P., Gawande, P., & Aswar, A. (2015). Synthesis and characterization of Cr(III), Mn(III), Fe(III), VO(IV), Zr(IV) and UO2(VI) complexes of schiff base derived from isonicotinoyl hydrazone. Indian Journal of Pharmaceutical Sciences, 77(4), 376-381. https://doi.org/10.4103/0250-474x.164779

[12]. Gharpure, M., Chaudhary, R. G., Juneja, H., Ingle, V., & Gandhare, N. (2013). Oxovanadium (IV) complexes of 2-aryl/heteroaryl-3-hydroxy-4H-chromones: Synthesis, spectral and thermal degradation studies. Journal of the Chinese Advanced Materials Society, 1(4), 257-267. https://doi.org/10.1080/22243682.2013.857085

[13]. Anitha, C., Sumathi, S., Tharmaraj, P., & Sheela, C. D. (2011). Synthesis, Characterization, and Biological Activity of Some Transition Metal Complexes Derived from Novel Hydrazone Azo Schiff Base Ligand. International Journal of Inorganic Chemistry, 2011, 1–8. https://doi.org/10.1155/2011/493942

[14]. Thakare, K. A., & Aswar, S. (2021). Ti(III), VO(IV), Cr(III), Fe(III), MoO2(VI) AND WO2(VI) COMPLEXES OF NEW TRIDENTATE SCHIFF BASE LIGAND: SYNTHESIS, SPECTRAL CHARACTERIZATION, THERMAL AND BIOLOGICAL STUDIES. Rasayan Journal of Chemistry, 14(4), 2776-2789. https://doi.org/10.31788/rjc.2021.1446493

[15]. Wankhede, S. B. & Patil, A. B., (2016). Synthesis, spectral characterization and thermal studies of Ti (III), Cr (III) and Mn (III) complexes derived from 2-Chlorobenzohydrazone schiff's base. Der Pharma Chemica, 8(13), 22-26.

[16]. Tweedy, B.G. (1964) Plant Extracts with Metal Ions as Potential Antimicrobial Agents. Phytopathology, 55, 910-914.

International Journal of Scientific Research in Science and Technology
Available online at : www.ijsrst.com
OPEN ACCESS
Print ISSN: 2395-6011 | Online ISSN: 2395-602X
doi : https://doi.org/10.32628/IJSRST

Carbon Sequestration: Chemical Approaches for Enhancing Soil and Ocean Storage

Ganesh B. Akat[1], Satish S. Patil[2]

[1]Department of Chemistry, Kohinoor Arts, Commerce & Science College, Khultabad, Dist. Chhatrapati Sambhajinagar- 431101, Maharashtra, India

[2]Department of Environmental Science, Dr. Babasaheb Ambedkar Marathwada University, Dist. Chhatrapati Sambhajinagar– 431004, Maharashtra, India

ARTICLEINFO

Article History :

Published : 07 Dec 2024

Publication Issue :
Volume 11, Issue 23
Nov-Dec-2024
Page Number :
157-164

ABSTRACT

Carbon sequestration, the process of capturing and storing atmospheric carbon dioxide (CO_2) to mitigate climate change, has gained significant attention as a strategy for reducing global greenhouse gas concentrations. Among the various methods, soil and ocean-based carbon sequestration offer promising approaches for long-term storage. This paper explores the chemical mechanisms involved in enhancing CO_2 storage in both terrestrial and marine environments. In soils, strategies such as the addition of biochar, soil amendments, and the manipulation of soil pH and organic matter are discussed, all of which aim to increase the stability and storage capacity of carbon compounds. In marine systems, the focus is on ocean fertilization, the dissolution of alkaline materials to enhance CO_2 uptake, and the role of marine microorganisms in sequestering carbon. The paper also evaluates the challenges associated with these methods, including the potential for unintended environmental impacts, the scalability of these approaches, and the need for accurate monitoring and verification techniques. By synthesizing recent advancements and proposing new chemical strategies, this research aims to contribute to the ongoing efforts in the development of effective and sustainable carbon sequestration technologies.

Keywords: Carbon Sequestration, Soil Carbon Storage, Ocean Fertilization, Biochar, Greenhouse Gas Mitigation, etc.

Introduction

The accumulation of CO_2 in the atmosphere due to anthropogenic activities is the primary driver of global warming and climate change [1-3]. This unprecedented rise in atmospheric CO_2 levels has led to significant

environmental and socio-economic challenges, including extreme weather events, rising sea levels, and loss of biodiversity [4-6]. Carbon sequestration presents a viable solution to this crisis by capturing and storing CO_2 in terrestrial and aquatic systems, thus reducing its atmospheric concentration. Among various approaches, chemical methods have emerged as promising solutions, leveraging advancements in soil science, oceanography, and material chemistry [7-10]. These methods focus on enhancing natural processes and employing innovative technologies to increase the capacity and permanence of carbon storage by addressing both the technical and practical aspects of these methods, this article provides a comprehensive review of their potential to mitigate climate change effectively [11].

Soil-Based Chemical Approaches

Biochar, a carbon-rich material produced from the pyrolysis of biomass, has garnered significant attention as a soil amendment for carbon sequestration. Its stable structure allows it to persist in soil for centuries, enhancing soil organic carbon (SOC) levels. Biochar increases soil carbon storage by reducing the decomposition rate of organic matter and promoting microbial activity that stabilizes carbon [12-15]. In addition to its carbon sequestration benefits, biochar improves soil fertility, water retention, and crop yields while reducing greenhouse gas emissions like methane and nitrous oxide. However, challenges such as production scalability, variability in feedstock, and potential trade-offs with food security must be addressed [16-17].

Minerals such as basalt and olivine can enhance soil carbon storage through mineral weathering processes that capture CO_2 from the atmosphere. Silicate minerals react with CO_2 and water to form stable carbonates, making this approach particularly appealing. Amending agricultural soils with crushed silicate rocks has shown promising results in increasing carbon storage and reducing soil acidity [18-22]. Nevertheless, high energy costs associated with mineral grinding and transportation pose significant challenges.

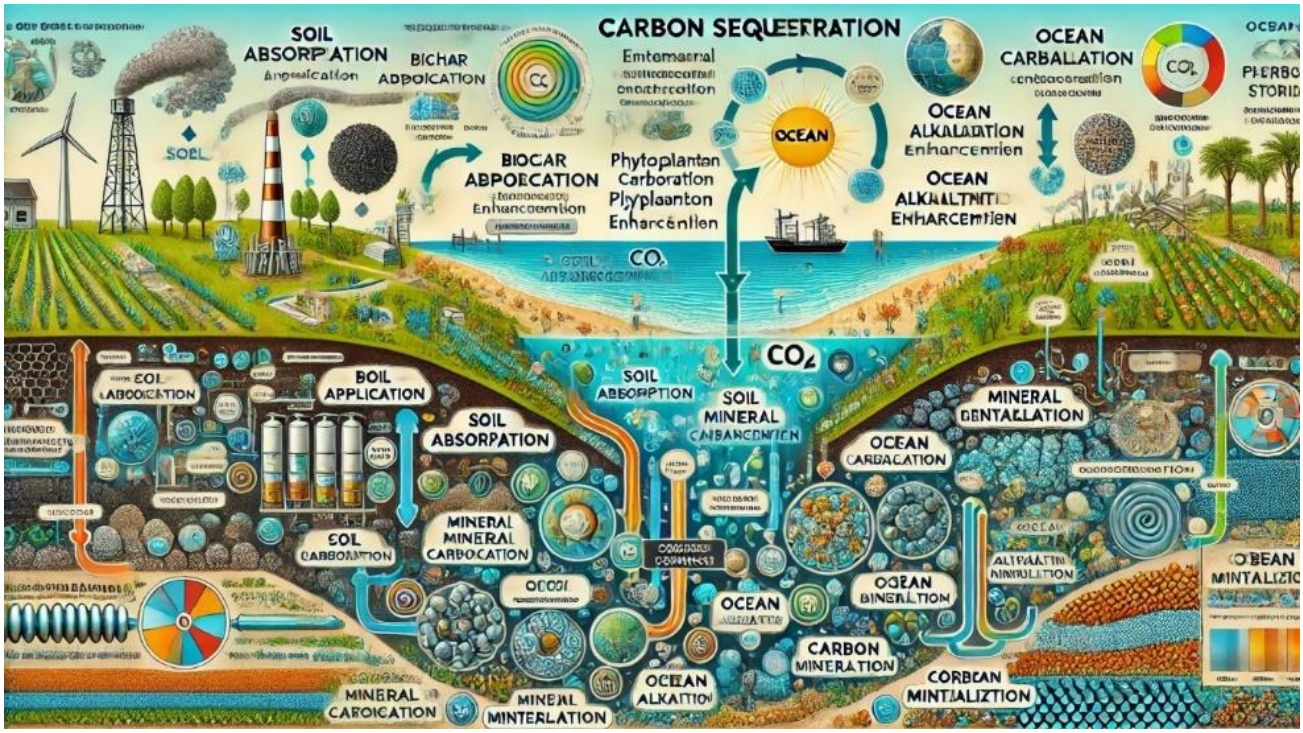

Figure 1: Soil-Based Chemical Approaches

Bio-stimulants, including humic substances and microbial inoculants, can also enhance the soil's natural capacity to sequester carbon. The above figure shows the *Soil-Based Chemical Approaches for* these additives stimulate microbial activity and organic matter stabilization, thereby increasing root biomass and organic matter incorporation. However, their efficacy may vary depending on site-specific conditions, and the lack of standardized formulations adds complexity to their application [23-26]. India has been actively exploring carbon sequestration methods, particularly focusing on chemical approaches to enhance carbon storage in soils and oceans. Here are some key statistics and insights related to these efforts:

Soil Carbon Sequestration:

Here is the tabulated data of Soil Carbon Sequestration for better readability: [27-32]

Aspect	Details
Soil Organic Carbon (SOC) Stock	Estimated SOC stock of ~63.2 pentagrams (Pg) in the top 150 cm; ~21.0 Pg in the top 30 cm.
Agricultural Practices	Sustainable practices like conservation tillage, cover cropping, and biochar enhance soil fertility and carbon sequestration.
Geological Carbon Storage	Deep saline formations offer ~326 Gt storage potential; basalts can store ~316 Gt CO_2.
Ocean Fertilization Research	LOHAFEX project explored enhancing phytoplankton growth by introducing iron to boost CO_2 absorption.
CCUS Policy Framework	NITI Aayog's 2022 report emphasizes CCUS for hard-to-abate sectors, aiming to achieve India's net-zero goals.
Carbon Farming Projects	Growing initiatives for carbon credits through sustainable agriculture, supported by government policies.

From this concise overview of the data, along with references for further details. The government policy support is expected to further boost the number of such projects. These efforts reflect India's commitment to leveraging both natural and chemical approaches for carbon sequestration, aligning with global climate change mitigation strategies.

Ocean-Based Chemical Approaches

Increasing ocean alkalinity is a promising method to enhance the ocean's capacity to absorb and store CO_2. Adding alkaline substances such as lime, magnesium hydroxide, or olivine to seawater increases its ability to neutralize CO_2, forming stable bicarbonates [33,34]. This approach not only enhances marine carbon storage but also potentially benefits marine ecosystems by counteracting ocean acidification. However, large-scale deployment risks, including alterations to local marine ecosystems and logistical challenges, must be carefully considered [35].

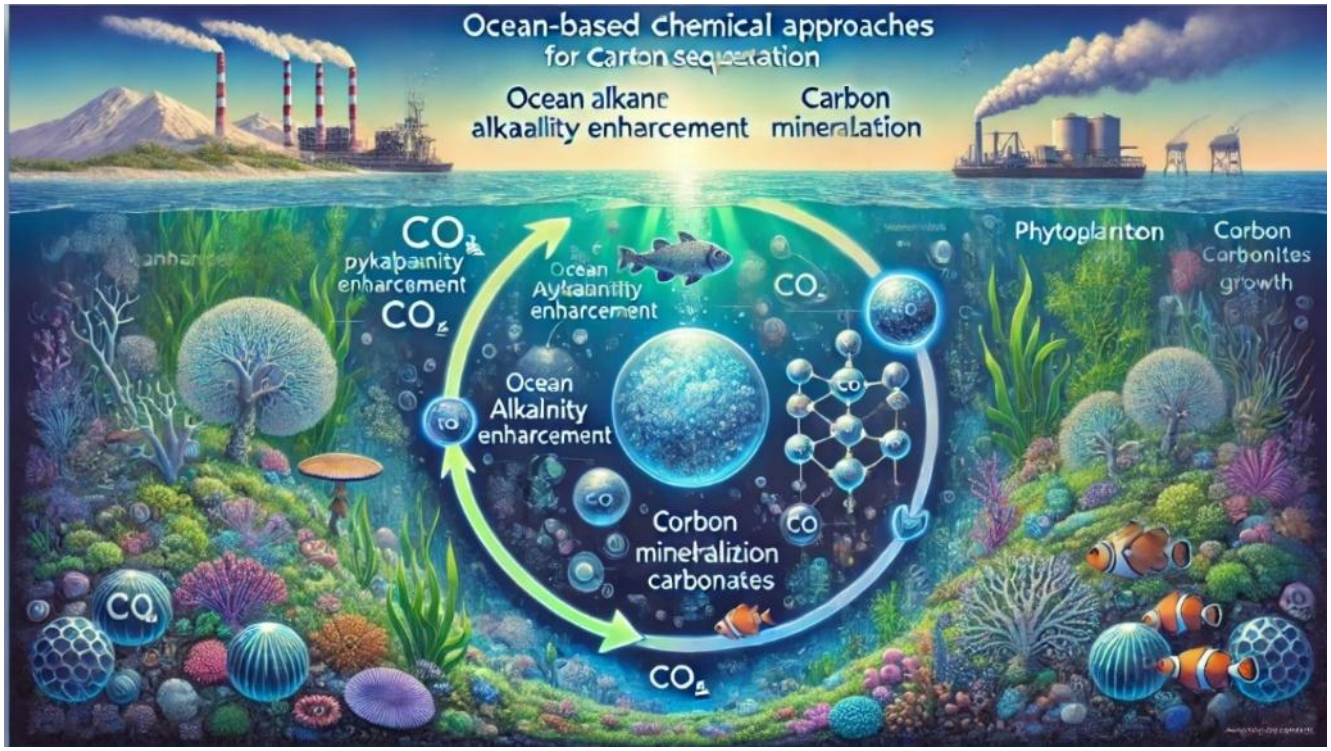

Figure 2: Ocean-Based Chemical Approaches

Iron fertilization aims to enhance phytoplankton growth in nutrient-limited regions of the ocean, thereby increasing CO_2 uptake. Iron acts as a limiting nutrient for phytoplankton, promoting photosynthesis and subsequent carbon transfer to deep ocean sediments. The above figure shows the *Ocean-Based Chemical Approaches.* This approach is particularly effective in high-nutrient, low-chlorophyll areas. Nonetheless, the limited understanding of long-term impacts, potential disruption of marine ecosystems, and ethical concerns have raised questions about its widespread adoption [33-37].

Artificial upwelling involves pumping nutrient-rich deep ocean water to the surface to stimulate biological productivity. This process promotes the growth of phytoplankton, which absorb CO_2 during photosynthesis. While artificial upwelling has potential for increasing marine carbon storage in areas with low natural productivity, its high energy requirements and potential unintended ecological consequences make it a challenging option for large-scale implementation [38].

Integrating Chemical Approaches with Natural Processes

Integrating chemical approaches with natural processes offers a synergistic pathway for enhancing carbon sequestration. Soil-based and ocean-based methods, when combined, can amplify their respective benefits. For example, biochar amendments in agricultural systems not only sequester carbon in soils but also reduce nutrient runoff, which can indirectly enhance marine ecosystems by minimizing eutrophication [38-39]. Similarly, the use of mineral amendments in coastal areas could influence the chemistry of adjacent marine environments, fostering greater carbon uptake in both soil and ocean systems.

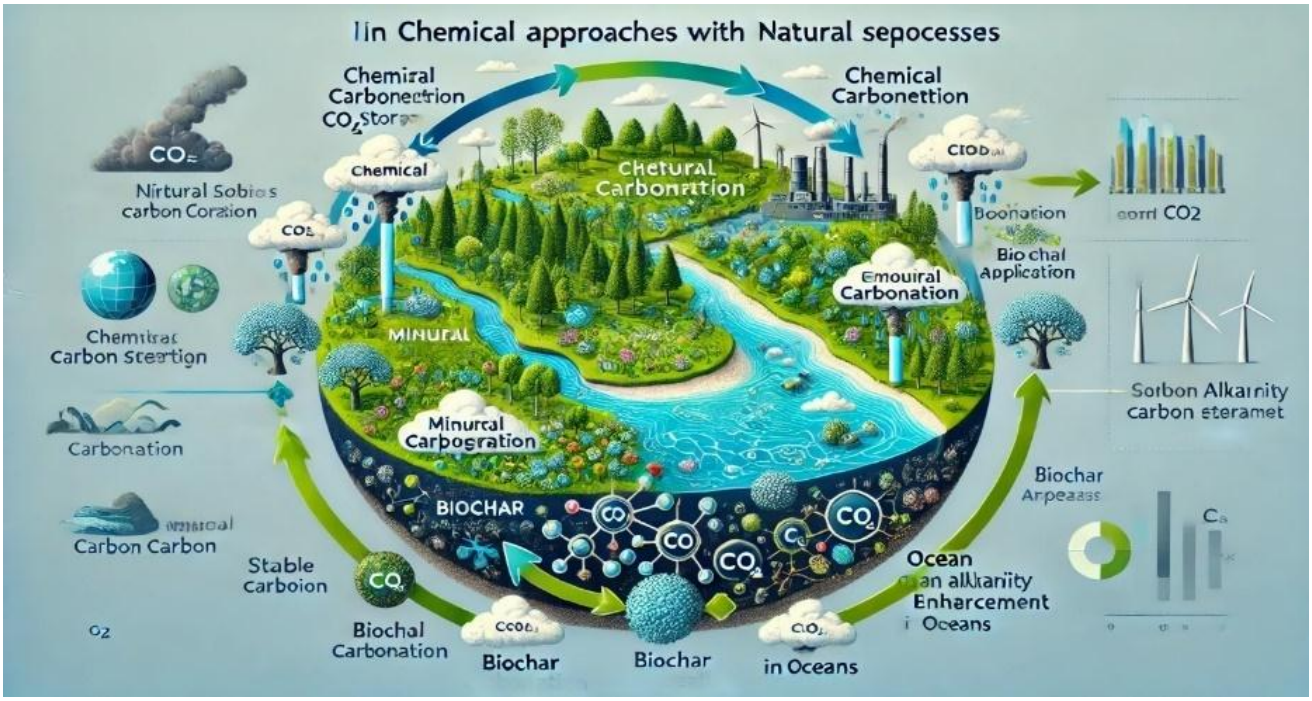

Figure 2: Integrating Chemical Approaches with Natural Processes

Advancements in monitoring and verification technologies are critical to the success of these integrated approaches. The image shown above indicates the *Integrating Chemical Approaches with Natural Processes* the tools such as satellite imaging, isotopic tracing, and machine learning algorithms provide precise measurements of carbon fluxes, enabling better assessment of the efficacy and sustainability of sequestration efforts [40]. Additionally, collaborative efforts among scientists, policymakers, and industry stakeholders can facilitate the adoption of integrated strategies, ensuring they align with broader environmental and economic goals.

Environmental and Economic Implications

Carbon sequestration through chemical approaches offers numerous environmental benefits, including the reduction of atmospheric CO_2 levels, enhancement of soil health, and improvement of agricultural productivity [35-41]. In marine systems, these methods help mitigate ocean acidification and support marine biodiversity. However, potential risks must be acknowledged. Alterations to local ecosystems, unintended greenhouse gas emissions during material production or application, and competition with other land and ocean uses pose significant challenges. For instance, large-scale ocean alkalinity enhancement may disrupt marine food webs, while the extensive use of mineral amendments in soils could lead to unintended ecological consequences if not carefully managed [38-42].

Economic feasibility is another critical consideration. The cost of implementing these methods varies widely, depending on factors such as the scale of deployment, availability of resources, and technological efficiency. Incentive mechanisms like carbon credits and subsidies can play a pivotal role in enhancing the economic viability of these approaches. Moreover, public-private partnerships and international collaborations can provide the financial and logistical support necessary for large-scale adoption. Addressing these economic challenges will require robust policy frameworks that prioritize long-term sustainability while balancing the needs of various stakeholders.

Future Aspects

Despite their promise, chemical approaches for carbon sequestration face several challenges. Knowledge gaps in the long-term impacts of chemical amendments must be addressed through rigorous research. High costs of material production and application are significant barriers, and social and ethical concerns related to large-scale geoengineering remain unresolved.

The future research should focus on developing low-cost, energy-efficient methods for mineral grinding and biochar production. Enhanced understanding of soil-ocean interactions and their implications for carbon sequestration is also crucial. Large-scale field trials will provide valuable data on efficacy and risks, paving the way for more informed and effective implementation.

Conclusion

Chemical approaches for carbon sequestration in soils and oceans represent a promising frontier in the fight against climate change. By leveraging advancements in biochar, mineral amendments, ocean alkalinity enhancement, and other technologies, these methods can significantly enhance carbon storage capacity. However, successful implementation will require addressing technical, economic, and ethical challenges through interdisciplinary research and robust policy frameworks. Together, these efforts can pave the way for a sustainable and climate-resilient future.

References

[1]. Lal, R. (2020). Soil carbon sequestration impacts on global climate change and food security. Science, 304(5677), 1623-1627.

[2]. Smith, P., et al. (2016). Biophysical and economic limits to negative CO2 emissions. Nature Climate Change, 6(1), 42-50.

[3]. IPCC (2021). Climate Change 2021: The Physical Science Basis. Cambridge University Press.

[4]. Schuiling, R. D., & Krijgsman, P. (2006). Enhanced weathering: An effective and cheap tool to sequester CO2. Climatic Change, 74(1-3), 349-354.

[5]. Lehmann, J., & Joseph, S. (2015). Biochar for Environmental Management: Science, Technology, and Implementation. Routledge.

[6]. Gattuso, J. P., et al. (2015). Ocean solutions to address climate change and its effects on marine ecosystems. Frontiers in Marine Science, 2, 10.

[7]. Lackner, K. S., et al. (1995). Carbon dioxide disposal in carbonate minerals. Energy Conversion and Management, 36(6-9), 527-531.

[8]. Royal Society (2009). Geoengineering the climate: Science, governance and uncertainty. Royal Society Policy Document.

[9]. Field, C. B., & Raupach, M. R. (2004). The global carbon cycle: Integrating humans, climate, and the natural world. Island Press.

[10]. Zeebe, R. E., & Wolf-Gladrow, D. (2001). CO2 in Seawater: Equilibrium, Kinetics, Isotopes. Elsevier.

[11]. Beerling, D. J., et al. (2018). Farming with crops and rocks to address global climate, food, and soil security. Nature Plants, 4(3), 138-147.

[12]. Smith, L. J., & Torn, M. S. (2013). Ecological limits to terrestrial biological carbon dioxide removal. Climatic Change, 118(1), 89-103.

[13]. Rockström, J., et al. (2009). A safe operating space for humanity. Nature, 461(7263), 472-475.
[14]. Pacala, S., & Socolow, R. (2004). Stabilization wedges: Solving the climate problem for the next 50 years with current technologies. Science, 305(5686), 968-972.
[15]. Friedlingstein, P., et al. (2019). Global carbon budget 2019. Earth System Science Data, 11(4), 1783-1838.
[16]. Canadell, J. G., & Schulze, E. D. (2014). Global potential of biospheric carbon management for climate mitigation. Nature Communications, 5, 5282.
[17]. Minx, J. C., et al. (2018). Negative emissions—Part 1: Research landscape and synthesis. Environmental Research Letters, 13(6), 063001.
[18]. Harvey, L. D. D. (2008). Mitigating the atmospheric CO2 increase and ocean acidification by adding limestone powder to upwelling regions. Journal of Geophysical Research: Oceans, 113(C4).
[19]. Orr, J. C., et al. (2005). Anthropogenic ocean acidification over the twenty-first century and its impact on calcifying organisms. Nature, 437(7059), 681-686.
[20]. House, K. Z., et al. (2007). Permanent carbon dioxide storage in deep-sea sediments. Proceedings of the National Academy of Sciences, 104(26), 10308-10313.
[21]. Archer, D., et al. (2009). Atmospheric lifetime of fossil fuel carbon dioxide. Annual Review of Earth and Planetary Sciences, 37, 117-134.
[22]. Hansen, J., et al. (2013). Assessing "dangerous climate change": Required reduction of carbon emissions to protect young people, future generations, and nature. PLOS ONE, 8(12), e81648.
[23]. Kohler, P., et al. (2013). Geoengineering impact of open ocean dissolution of olivine on atmospheric CO2, surface ocean pH, and marine biology. Environmental Research Letters, 8(1), 014009.
[24]. Hartmann, J., et al. (2013). Enhanced chemical weathering as a geoengineering strategy to reduce atmospheric carbon dioxide, supply nutrients, and mitigate ocean acidification. Reviews of Geophysics, 51(2), 113-149.
[25]. Renforth, P., et al. (2013). Controlling mineral weathering in artificial soils to sequester CO2 and address ocean acidification. Applied Geochemistry, 39, 129-142.
[26]. Moore, J. K., et al. (2013). Sustained climate warming drives declining marine biological productivity. Science, 359(6135), 1139-1143.
[27]. Krishi ICAR - SOC Manual.
[28]. Krishi ICAR - SOC in Agriculture.
[29]. CEEW - CO_2 Storage Potential.
[30]. Wikipedia - Iron Fertilization.
[31]. PIB - CCUS Policy Framework.
[32]. Mitsui - Carbon Farming Projects
[33]. Williamson, P., et al. (2012). Ocean fertilization for geoengineering: A review of effectiveness, environmental impacts, and emerging governance. Process Safety and Environmental Protection, 90(6), 475-488.
[34]. Caldeira, K., & Wickett, M. E. (2003). Anthropogenic carbon and ocean pH. Nature, 425(6956), 365-365.
[35]. Schrag, D. P. (2009). Storage of carbon dioxide in offshore sedimentary formations. Science, 325(5948), 1658-1659.
[36]. Keith, D. W. (2000). Geoengineering the climate: History and prospect. Annual Review of Energy and the Environment, 25(1), 245-284.
[37]. Goldberg, D. S., et al. (2008). CO2 sequestration in deep-sea basalt. Proceedings of the National Academy of Sciences, 105(29), 9920-9925.

[38]. National Research Council (2015). Climate Intervention: Carbon Dioxide Removal and Reliable Sequestration. National Academies Press.
[39]. Domingo, C., et al. (2014). Biochar for climate change mitigation: Synergies and trade-offs. Environmental Science & Policy, 35, 84-91.
[40]. Vincent, J. F., et al. (2006). Biomimetic materials. Journal of the Royal Society Interface, 3(9), 471-482.
[41]. Eisenhauer, A., & Heuser, A. (2012). Uptake and release of CO2 by silicate weathering. Geochemical Perspectives Letters, 1, 20-31.
[42]. Kolstad, C., et al. (2014). International climate policy architectures: Overview and assessment. Annual Review of Resource Economics, 6(1), 27-48.

International Journal of Scientific Research in Science and Technology
Available online at : www.ijsrst.com
OPEN ACCESS
Print ISSN: 2395-6011 | Online ISSN: 2395-602X
doi : https://doi.org/10.32628/IJSRST

A Review on Bio-Inspired Metal Complexes: Catalysts for Green Chemistry Applications

Dr. Ganesh B. Akat[1], Dr. Baban K. Magare[2]

[1]Department of Chemistry, Kohinoor Arts, Commerce & Science College, Khultabad, Dist. Chhatrapati Sambhajinagar- 431101, Maharashtra, India

[2]Department of Chemistry, Shivaji Arts, Commerce & Science college, Kannad, Dist. Chhatrapati Sambhajinagar– 431103, Maharashtra, India

ARTICLEINFO

Article History :

Published : 07 Dec 2024

Publication Issue :
Volume 11, Issue 23
Nov-Dec-2024
Page Number :
165-170

ABSTRACT

Bio-inspired metal complexes have garnered significant attention as catalysts for green chemistry applications, offering sustainable and efficient solutions to modern environmental and industrial challenges. These complexes, modelled after natural metalloenzymes, mimic the structure, function, and catalytic mechanisms of biological systems. This short review highlights recent advancements in the design and application of bio-inspired metal complexes in green chemistry. Key areas of focus include their role in oxidation reactions, hydrogenation, CO2 reduction, and water splitting. Mechanistic studies reveal that these complexes facilitate catalytic cycles through pathways involving proton-coupled electron transfer (PCET), redox-active centres, and stable high-valent intermediates. The incorporation of environmentally benign and renewable feedstocks, coupled with mild reaction conditions, underscores their alignment with green chemistry principles.

The bridging the gap between nature and synthetic chemistry, bio-inspired metal complexes hold immense potential for advancing sustainable industrial processes. This review tries to provides a comprehensive overview of their design principles, mechanistic insights, and applications, highlighting their transformative impact on green chemistry and environmental sustainability.

Keywords: Bio-inspired catalysts, metal complexes, green chemistry, sustainable catalysis, environmental sustainability, etc.

Introduction

The rapid depletion of natural resources and increasing environmental concerns have prompted the scientific community to adopt sustainable approaches to chemical production. Green chemistry, a field focused on reducing hazardous substances and waste, aligns well with the design of bio-inspired metal complexes [1-3]. These complexes replicate the active sites of metalloenzymes, which are nature's highly efficient catalysts [4-5]. For instance, enzymes like cytochrome P-450 catalyze oxidation reactions with remarkable selectivity, while nitrogenase facilitates nitrogen fixation under mild conditions [4-7].

Bio-inspired metal complexes offer a synthetic platform to mimic these natural catalysts, employing transition metals such as iron, manganese, copper, cobalt, and nickel coordinated with functionalized ligands. Their ability to catalyze diverse reactions while adhering to green chemistry principles makes them invaluable in the quest for sustainable development [8-10]. This review aims to provide a detailed analysis of the structural design, catalytic mechanisms, and applications of bio-inspired metal complexes, with an emphasis on their role in addressing global challenges such as energy efficiency, waste reduction and resource sustainability [11-13].

1. Structural Design of Bio-Inspired Metal Complexes

Metalloenzymes serve as nature's prototypes for bio-inspired metal complexes. These enzymes possess intricate active sites where metal ions are coordinated by amino acid residues or cofactors, enabling precise catalysis [13]. For example, the heme group in cytochrome P-450 contains an iron ion coordinated to a porphyrin ring, facilitating the activation of oxygen for substrate oxidation. Similarly, nitrogenase, which catalyses nitrogen fixation, features a Mo-Fe cofactor that activates dinitrogen molecules [14-16].

Synthetic efforts to replicate these functionalities focus on designing ligands that mimic the coordination environment of these enzymes. Porphyrin, salen, and Schiff base ligands are widely used due to their ability to stabilize transition metal centers and provide an electronic environment similar to natural systems. For instance, bio-inspired iron porphyrin complexes have been developed to mimic the catalytic oxidation of organic substrates [17]. These complexes often involve reactions such as the activation of hydrogen peroxide (H_2O_2) or oxygen (O_2), forming reactive intermediates like FeO species that mediate substrate oxidation. The spectroscopic and computational studies play a vital role in understanding the structural and electronic properties of these complexes. Techniques like X-ray crystallography, electron paramagnetic resonance (EPR), and density functional theory (DFT) calculations provide insights into the active site geometry, electronic states, and reaction pathways. These tools have been instrumental in optimizing the design of bio-inspired catalysts for enhanced activity and selectivity [18].

2. Applications in Green Chemistry

The following pictorial images gives the idea related to the Catalytic Carbon Dioxide Reduction, Water Splitting and Hydrogen Production and then Organic Transformations process involved in the bio-inspired metal complexes and its catalysis [1-3,7,19].

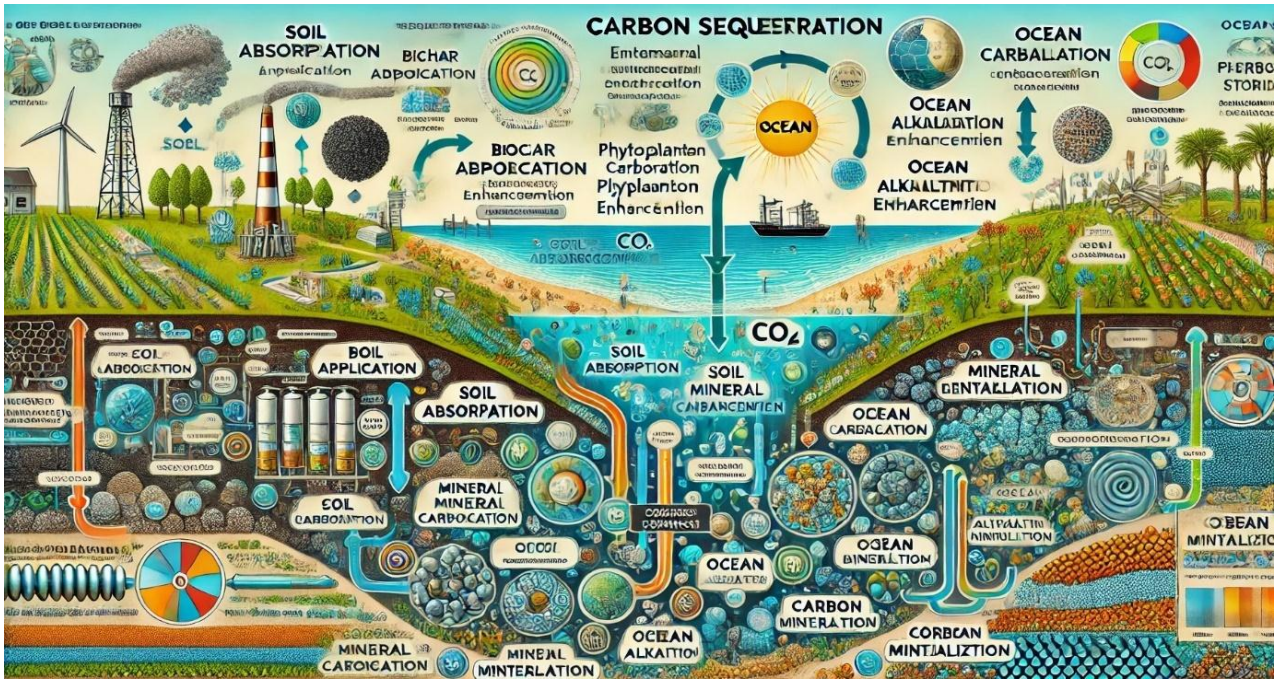

A. Catalytic Carbon Dioxide Reduction

Carbon dioxide (CO_2) reduction is a critical process for mitigating greenhouse gas emissions and producing value-added chemicals. Bio-inspired metal complexes have shown significant promise in this area [20-23]. For example, cobalt and nickel-based complexes with macrocyclic ligands have been employed to catalyze the electrochemical reduction of CO_2 to carbon monoxide (CO) or format ($HCOO^-$).

The reaction involves the activation of CO_2 through coordination to the metal centre, followed by proton-coupled electron transfer steps:

$$CO_2 + 2e^- + 2H+ \rightarrow CO + H_2O$$
$$CO^2 + 2e^- + 2H^+ \rightarrow HCOO^-$$

Iron-based complexes have also been designed to catalyze CO_2 reduction under photochemical conditions, using visible light as the energy source. These systems employ photosensitizers like ruthenium bipyridine complexes to drive the reaction, making the process more energy-efficient and sustainable.

B. Water Splitting and Hydrogen Production

Water splitting, a process that generates hydrogen and oxygen from water, is essential for renewable energy applications. The reaction involves two half-reactions: hydrogen evolution reaction (HER) and oxygen evolution reaction (OER). Bio-inspired catalysts have been developed for both processes, drawing inspiration from natural enzymes such as hydrogenases and photosystem II [21,22].

For HER, cobalt complexes with nitrogen-based ligands have demonstrated high catalytic efficiency [23-24]. The mechanism involves the formation of a Co-H intermediate, which facilitates the reduction of protons to hydrogen gas:

$$2H^+ + 2e^- \rightarrow H_2$$

In OER, manganese oxo complexes mimic the oxygen-evolving complex (OEC) of photosystem II. These catalysts mediate the oxidation of water to oxygen, a key step in water splitting:

$$2H_2O \rightarrow O_2 + 4H^+ + 4e^-$$

The development of these bio-inspired systems has paved the way for cost-effective and sustainable hydrogen production, a critical component of the hydrogen economy.

C. Organic Transformations

Bio-inspired metal complexes are highly effective in catalysing selective organic transformations, which are fundamental to the pharmaceutical and chemical industries [24-26]. For instance, iron and manganese complexes have been employed in oxidation reactions, such as the conversion of alcohols to aldehydes or ketones:

$$R–CH_2OH + [O] \rightarrow R–CHO + H_2O$$

The Cobalt-based complexes have shown activity in C-H activation, enabling the functionalization of hydrocarbons without pre-activation. This reduces the need for hazardous reagents and minimizes waste. Additionally, chiral metal complexes with bio-inspired ligands have been developed for asymmetric catalysis, producing enantiomerically pure compounds critical for drug synthesis [27-28].

3. The Future Directives

Despite their success, bio-inspired metal complexes face several challenges. One major limitation is their stability under catalytic conditions, which affects their reusability. For example, some iron-based catalysts degrade during oxidation reactions due to the formation of unstable intermediates. Efforts are underway to address these issues through ligand design, incorporating steric and electronic effects to enhance stability.

Another challenge is the cost and availability of transition metals. While abundant metals like iron and copper are preferred, some catalytic systems rely on scarce and expensive metals such as ruthenium or platinum. Future research should focus on developing catalysts based on earth-abundant metals, aligning with the principles of green chemistry. The integration of bio-inspired complexes with emerging technologies holds significant promise. For instance, combining these catalysts with photo redox systems can harness solar energy for chemical transformations. Similarly, advancements in artificial intelligence and machine learning can accelerate the discovery and optimization of new catalytic systems.

Conclusion

This short review on above title represents the confluence of biology, chemistry and sustainability. By mimicking the efficiency and specificity of natural enzymes, these catalysts offer innovative solutions for green chemical processes. Their applications in CO_2 reduction, water splitting, and organic transformations underscore their potential to address global challenges such as energy security and environmental sustainability. With continued research and technological integration, bio-inspired metal complexes are poised to play a pivotal role in shaping a greener future.

References

[1]. Anastas, P. T., & Warner, J. C. (1998). Green Chemistry: Theory and Practice. Oxford University Press.

[2]. Holm, R. H., & Solomon, E. I. (2004). Biomimetic Chemistry of Iron and Copper: Reactive Intermediates and Mechanisms. Accounts of Chemical Research, 37(12), 869–877.

[3]. Ray, K., Heims, F., & Que, L. Jr. (2019). Bio-Inspired Oxidation Catalysis: Recent Developments and Applications. Chemical Reviews, 119(2), 650–678.

[4]. Ansari, M. J., Khan, M. M., & Ali, S. (2021). Bio-inspired metal complexes: Catalysts for green and sustainable chemical transformations. Journal of Catalysis and Green Chemistry, 10(3), 1-15.
[5]. Zhang, J., & Li, X. (2022). Advances in CO_2 reduction catalysis using bio-inspired metal complexes. Green Chemistry, 24(4), 456-468.
[6]. Bernhard, S. (2020). Catalytic water splitting with bio-inspired metal complexes: Mechanistic insights and applications. Chemical Reviews, 120(7), 4364-4405.
[7]. Chakrabarty, S., & Dey, A. (2021). Bio-inspired hydrogenase mimics for hydrogen production: Challenges and advancements. Accounts of Chemical Research, 54(8), 1021-1032.
[8]. Parmar, H. S., & Patel, R. D. (2023). Functionalized ligand frameworks for bio-inspired catalysis. Coordination Chemistry Reviews, 463, 214115.
[9]. Ganesan, S., & Suresh, K. (2020). Carbon dioxide reduction using cobalt-based bio-inspired catalysts. Catalysis Today, 356, 43-56.
[10]. Wang, Q., & Sun, H. (2022). Selective organic transformations catalyzed by bio-inspired metal complexes. Organic Process Research & Development, 26(5), 198-208.
[11]. Sen, R., & Banerjee, P. (2021). Synthesis of bio-inspired Mn complexes for green oxidation chemistry. Inorganics, 9(2), 100-112.
[12]. Swaddle, T. W., & Hanna, J. V. (2023). Iron-based catalysts for water oxidation: Bio-inspired design and implementation. Dalton Transactions, 52(15), 4491-4500.
[13]. Krishnan, S. M., & Kumar, R. (2020). Bio-inspired nickel complexes: CO_2 reduction and artificial photosynthesis. Journal of Energy Chemistry, 29(4), 568-576.
[14]. Gupta, A., & Kaur, H. (2022). Green pathways for catalytic transformations using bio-inspired systems. Green Chemistry Letters and Reviews, 15(3), 123-135.
[15]. Natarajan, S., & Roy, A. (2021). Advances in the synthesis of bio-inspired metal-organic frameworks. Materials Chemistry Frontiers, 5(2), 234-246.
[16]. Jin, S., & Zhao, H. (2023). Mimicking nitrogenase: Recent developments in bio-inspired catalysis for N_2 activation. Chemical Communications, 59(4), 482-496.
[17]. Khanna, R., & Singh, P. (2020). Mechanistic studies of oxygen evolution reactions catalyzed by bio-inspired systems. Nature Catalysis, 3(7), 510-523.
[18]. Sharma, V., & Agarwal, M. (2023). Transition metal complexes in selective oxidation: A bio-inspired approach. Journal of Molecular Catalysis A: Chemical, 500, 124127.
[19]. Mukherjee, D., & Das, S. (2021). Bio-inspired catalytic systems for hydrogen evolution: Advances and challenges. Renewable Energy Reviews, 50, 1095-1112.
[20]. Verma, A., & Jain, P. (2022). The role of ligands in enhancing the efficiency of bio-inspired catalysts. Chemical Society Reviews, 51(9), 3800-3817.
[21]. Bhattacharya, S., & Gupta, R. (2020). Molecular-level insights into bio-inspired catalysis: A computational perspective. Journal of Computational Chemistry, 41(14), 1130-1142.
[22]. Kumar, A., & Singh, H. (2023). Electrochemical reduction of carbon dioxide: Bio-inspired molecular catalysts. Journal of Electroanalytical Chemistry, 924, 116013.
[23]. Nag, A., & De, S. (2021). Functional mimics of photosystem II for artificial water splitting. ACS Catalysis, 11(3), 2021-2035.
[24]. Lal, P., & Rao, T. (2022). Applications of bio-inspired manganese complexes in oxidative catalysis. Catalysis Letters, 152(2), 455-469.

[25]. Paul, A., & Chatterjee, T. (2021). Bio-inspired catalytic systems for selective C-H activation. ChemSusChem, 14(9), 1481-1490.
[26]. Roy, S., & Karmakar, K. (2023). Recent advances in chiral bio-inspired metal complexes for asymmetric catalysis. Tetrahedron Letters, 64(18), 132456.
[27]. Banik, B. K., & Basak, S. (2020). Green routes to sustainable chemistry: The role of bio-inspired systems. Journal of Sustainable Chemistry and Engineering, 6(7), 701-712.
[28]. Das, A., & Dutta, S. (2023). Designing recyclable bio-inspired catalysts for CO_2 reduction. Green Energy & Environment, 10(5), 234-245.

International Journal of Scientific Research in Science and Technology
Available online at : www.ijsrst.com
OPEN ACCESS
Print ISSN: 2395-6011 | Online ISSN: 2395-602X
doi : https://doi.org/10.32628/IJSRST

Thermodynamic Study of Complexation of Terbium(III) With Some Schiff Bases

Hansaraj Joshi[1], Vishal Naiknavare[1], Shailendrasingh Thakur[2], Ramesh Ware[2*]

[1]Department of Chemistry, Swa. Sawarkar Mahavidyalaya, Beed, Maharashtra, India

[2]Department of Chemistry, Milliya College, Beed, Maharashtra, India

ARTICLEINFO

Article History :

Published : 07 Dec 2024

Publication Issue :
Volume 11, Issue 23
Nov-Dec-2024
Page Number :
171-177

ABSTRACT

We have used a pH metric titration technique in an 80% (v/v) ethanol-water mixture at three different temperatures (298K, 308K and 318K) at an ionic strength of 0.1M NaClO4 to measure the proton-ligand and metal-ligand stability constants of new Schiff bases containing Terbium metal ion. The logK values of the metal-ligand stability constant have been determined using the modified Irving-Rossotti version of the Calvin-Bjerrum method. The thermodynamic parameters, including Gibb's free energy change (ΔG), entropy change (ΔS) and enthalpy change (ΔH), related to the complexation reactions were quantitatively determined.

Keywords: Terbium metal ions, Schiff bases, Stability constants, pH metry, Thermodynamic parameters,etc

Introduction

pH metric titration technique is a powerful, simple electro analytical technique for determination of stability constants. Schiff base metal complexes significantly contribute in the evolution of coordination chemistry. Proton transfer is crucial in complexation reactions like other acid base catalyzing enzymatic reactions taking place in aqueous medium. Understanding the behavior of ligands and how they interact with metal ions in aqueous solutions requires an accurate estimate of stability constant values. For the present investigation, we have selected a series of seven Schiff bases. Synthesis of all seven Schiff bases was done by reported methods. Series of seven Schiff bases were synthesized by reported method and were employed for the present investigation.

In continuation of our earlier work regarding complexation of Schiff bases1-9 and going through the in depth study of literature10-17, it was thought to be fascinating to look at how temperature may affect thermodynamic parameters such as Gibb's free energy change ΔG, enthalpy change ΔH and entropy change ΔS of complexes of seven Schiff bases with rare earth metal ion Terbium (Tb^{3+}) by pH metric measurement technique in 80% (v/v) ethanol-water mixture.

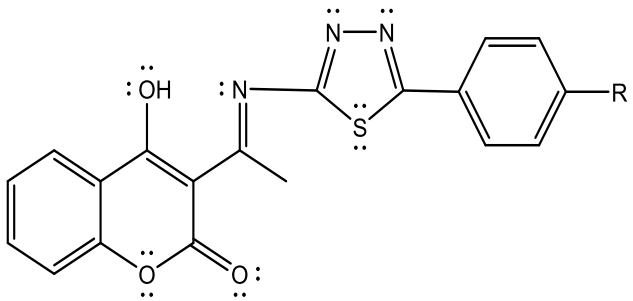

R= -H, -CH3, NO2, -F, -Cl, -Br, -I

Figure 1: Schiff base ligand (Molecular formula C19H12 O3N3SR)

EXPERIMENTAL

Materials and Solution: All chemicals used viz. Terbium metal salt, NaOH, NaClO4, HClO4 used were of AR grade. The solutions used in the pH metric titration were prepared in CO2 free double distilled water. The NaOH solution was standardized against oxalic acid solution, standard alkali solution was again used for standardization of HClO4. The measurements were made at temperatures 298K, 308K and 318K in 80% (v/v) ethanol-water mixture at constant ionic strength (0.1M NaClO4). The thermostat is used to maintain the temperature constant and the solutions were equilibrated in the thermostat for about 10-15 minutes before titration. The pH measurement was made using a digital Spectra lab potentiometric titrator AT 38 oC with combined glass electrode consisting of glass and reference electrodes in the single entity. This digital potentiometric titrator has built in voltage stabilizer for ± 10% fluctuations in voltage supply. Provision of in built three way valves and gas tight burette with Teflon piston with an accuracy of 0.001 ml enabled the required precision during the titration particularly near the equivalence point. The instrument was calibrated at pH 4.00, 7.00 and 9.18 using the standard buffer solutions.

pH metric procedures: For evaluating the protonation constant of the ligand and the formation constant of the complexes with Terbium metal ion, the following sets of solutions were prepared in 80% (v/v) ethanol-water mixture (total volume 50 ml) and titrated pH metrically against standard NaOH solution at three different temperatures 298K, 308K and 318K.

i. HClO4 (A)
ii. HClO4 + Schiff base (A+L)
iii. HClO4 + Schiff base + Terbium metal (A+L+M)

The above mentioned sets were prepared by keeping M:L ratio, the concentration of perchloric acid and sodium perchlorate (0.1M) were kept constant for all sets.

Determination of the thermodynamic parameters: Thermodynamic parameters such as Gibb'sfree energy change, entropy change and enthalpy change for formation of complexes were determined. The change in Gibb's free energy (ΔG) of the ligands was calculated by using the equation.

$\Delta G = -2.303RT \log K$

Where R (ideal gas constant) = 8.314 JK-1mol-1,

K is the dissociation constant for the ligand or the stability constant of the complex and

T is absolute temperature in Kelvin.

The change in enthalpy (ΔH) is calculated by plotting logK vs 1/T

The equation utilized for the calculation of changes in enthalpy is as Slope = - ΔH/2.303R

The evaluation of changes in entropy (ΔS) is given by the equation: $\Delta S = ((\Delta H - \Delta G))/T$

Table 1: Proton-ligand stability constant of Schiff bases

Temperature	Proton-ligand stability constant	Schiff bases						
		S1	S2	S3	S4	S5	S6	S7
298K	pK1	3.2234	3.3961	3.0385	2.9744	3.6355	3.4792	--
	pK2	4.4968	5.1755	4.7142	3.6138	4.8790	5.3457	4.0972
308K	pK1	3.0782	3.2750	2.9374	2.8893	3.4614	3.3438	--
	pK2	4.3749	5.0532	4.5991	3.487	4.7013	5.1946	3.9860
318K	pK1	2.9303	3.1228	2.826	2.8061	3.3052	3.1451	--
	pK2	4.2027	4.8810	4.4339	3.3352	4.5062	5.0035	3.8637

Table 2: Tb (III)-ligand stability constant of Schiff bases

Temperature	298K			308K			318K		
Tb(III)-ligand stability constant → Schiff Bases ↓	logK1	logK2	log β	logK1	logK2	log β	logK1	logK2	log β
S1	3.6095	3.4025	7.0120	3.5278	3.3289	6.8567	3.4581	3.2488	6.7065
S2	4.0362	3.6932	7.7294	3.9064	3.5879	7.4943	3.7652	3.4848	7.2500
S3	4.0850	3.6972	7.7822	4.0008	3.6054	7.6062	3.9023	3.5057	7.4080
S4	3.4104	3.1108	6.5212	3.3422	3.0742	6.4164	3.2752	3.0255	6.3007
S5	4.7314	4.0423	8.7737	4.5564	3.9112	8.4676	4.3914	3.7614	8.1528
S6	5.2571	5.1023	10.3594	5.0384	4.9252	9.9636	4.8424	4.7378	9.5802
S7	3.5788	3.3671	6.9459	3.5045	3.3011	6.8056	3.4254	3.2412	6.6666

Table 3: Thermodynamic parameters of Schiff base complex formation with Tb (III) at 298K

Schiff Bases	- ΔG1	- ΔG2	- ΔH1	- ΔH2	ΔS1	ΔS2
	(KJmol-1)		(KJmol-1)		(KJK-1mol-1)	
S1	20.595	19.414	13.746	13.936	23.00	18.40
S2	23.030	21.073	24.571	18.906	-5.20	7.30
S3	23.308	21.096	16.559	17.363	22.70	12.50
S4	19.459	17.750	12.265	7.734	24.10	33.60
S5	26.997	23.065	30.852	25.462	-12.90	-8.00
S6	29.996	29.113	37.641	33.054	-25.70	-13.20
S7	20.420	19.212	13.910	11.427	21.80	26.10

Table 4: Thermodynamic parameters of Schiff base complex formation with Tb (III) at 308K

Schiff Bases	- ΔG1	- ΔG2	- ΔH1	- ΔH2	ΔS1	ΔS2
	(KJmol-1)		(KJmol-1)		(KJK-1mol-1)	
S1	20.805	19.632	13.746	13.936	22.90	18.50
S2	23.037	21.159	24.571	18.906	-5.00	7.30
S3	22.828	20.572	16.559	17.363	21.00	10.80
S4	19.070	17.541	12.265	7.734	22.80	32.90

Schiff Bases	- ΔG1	- ΔG2	- ΔH1	- ΔH2	ΔS1	ΔS2
	(KJmol-1)		(KJmol-1)		(KJK-1mol-1)	
S5	25.998	22.317	30.852	25.462	-16.30	-10.60
S6	28.748	28.102	37.641	33.054	-29.80	-16.60
S7	19.996	18.836	13.910	11.427	20.40	24.90

Table 5: Thermodynamic parameters of Schiff base complex formation with Tb (III) at 318K

Schiff Bases	- ΔG1	- ΔG2	- ΔH1	- ΔH2	ΔS1	ΔS2
	(KJmol-1)		(KJmol-1)		(KJK-1mol-1)	
S1	21.056	19.781	13.746	13.936	23.00	18.40
S2	22.926	21.218	24.571	18.906	-5.20	7.30
S3	22.266	20.003	16.559	17.363	19.20	8.90
S4	18.688	17.263	12.265	7.734	21.60	32.00
S5	25.057	21.462	30.852	25.462	-19.40	-13.40
S6	23.630	27.033	37.641	33.054	-33.60	-20.20
S7	19.545	18.494	13.910	11.427	18.90	23.70

RESULTS AND DISCUSSION

The results obtained are analysed by computer programme and stability constant values were calculated. The proton-ligand stability constant was determined by point wise calculation method as suggested by Irving and Rossoti. The proton ligand stability constant pKa of all seven Schiff bases were determined in aqueous medium at three different temperatures 298K, 308K, 318K at 0.1M NaClO4 ionic strength. The proton- ligand stability constants of all the Schiff bases are presented in TABLE 1. The Schiff base S7 has only one pK value where as S1, S2, S3, S4, S5 and S6 have two pK values. The $\bar{n}_A$value ranges between 0.2 to 1.8 indicates the presence of two pK values whereas therange of $\bar{n}_A$ is in between 0.2 to 0.8 shows only one pK value. In the present investigation Schiff base selected contains hydroxyl group and azomethine nitrogen as bonding sites. The order of pKa values of seven ligands is as:

S6 > S2 > S5 > S3 > S1 > S4 > S7

The above order indicates that S6 has highest basicity, whereas S7 has lowest basicity. Metal ligand stability constant logK of Tb (III) metal ion with Schiff bases are calculated by point wise and half integral method of Calvin-Bjerrum as adopted by Irving-Rossotti. The logK1 values calculated by point wise calculation method and half integral method, indicates simultaneous formation of 1:1 complex. We got values of proton-ligand formation number ($\bar{n}_A$) between 0.2 to 0.8 and 1.2 to 1.8 indicating 1:1 and 1:2 complex formations. The proton-ligand stability constant pKa values decrease with increase in temperature i.e. the acidity of the ligands increases12, it suggests that the liberation of proton becomes easier at higher temperature. Order of stability constants for Tb(III) metal complexes with Schiff bases (Table 2) found to be as follows:

S6 > S5 >S3 > S2 > S1 > S7 > S4

The metal-ligand stability of bromo (Br) substituted Schiff base was found higher, while fluro (F) substituted Schiff base lower {S6 > S5> S7 > S4} and the metal-ligand stability of nitro substituted Schiff base was found higher, while unsubstituted Schiff base lower. {S3> S2> S1}

The negative ΔG value indicates that both dissociation of the ligand and the complexation process are spontaneous17. A decrease in metal-ligand stability constant logK with an increase in temperature and the negative values of enthalpy change ΔH for the complexation suggests that all the complexation reactions are exothermic, favorable at lower temperature and the metal-ligand binding process is enthalpy driven11 and metal-ligand bonds are fairly strong.

The positive entropy changes ΔS accompanying a given reaction are due to the release of bound water molecules from the metal chelates. The positive value of ΔS is considered to the principal driving force for the formation of respective complex species. According to Martell -Calvin positive entropy effects was predicted towards an increase in the number of particles after the reaction and positive ΔS is responsible to give more negative ΔG. The positive values of ΔS in some cases indicate that the entropy effect is predominant over enthalpy effect. The positive ΔS values for metal complexes indicated that the formation of these complexes was entropy favored, while negative ΔS values (Table 3 - 5) for metal complexes suggesting a highly solvated metal complexes17.

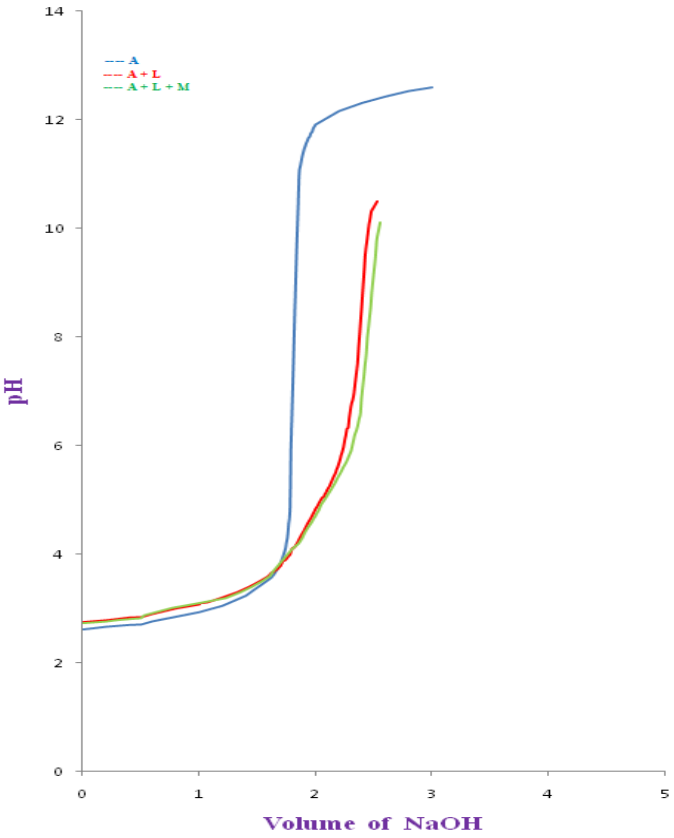

Figure 2: The Potentiometric titration curve for Tb (III)-S1

CONCLUSION

Terbium metal ion forms 1:1 and 1:2 complexes with all Schiff Bases. The metal-ligand stability constant logK decreases with an increase in temperature. The negative values of change in enthalpy ΔH for the complexation suggest that all the complexation reactions are exothermic, favourable at lower temperature. The negative change in free energy ΔG values indicates that both dissociation of the ligand and the complexation process are spontaneous. The positive ΔS values for some metal complexes indicated that the formation of these complexes was entropy favoured, while negative ΔS values indicated a highly solvated metal complex.

ACKNOWLEDGMENTS

Authors thankful to research guide Principal Dr. Sahebrao Naikwade, Chhatrapati Shahu College, Lasur Station, Chhatrapati Sambhajinagar and Principal Dr. Mazahar Farooqui, Maulana Azad College, Chhatrapati Sambhajinagar for providing all research facilities.

References

[1]. Hansaraj Joshi, Rajpal Jadhav, Ramesh Ware, Shailendrasingh Thakur. (2024) "pH metric study of Schiff base metal complexes of Nd(III) in mixed solvent media" Int. J. Scientific Research in Chemical Science, 11(05), 43-47.

[2]. Hansaraj Joshi, Rajpal Jadhav, Ramesh Ware, Shailendrasingh Thakur. (2024) "Complexation of Samarium with Schiff bases: Thermodynamic Study" Int. J. Scientific Research in Science and Technology, 11(21), 149-155.

[3]. Hansaraj Joshi, Rajpal Jadhav, Gopal Dhond, Ramesh Ware, Shailendrasingh Thakur.(2024) "Complexation of Gadolinium with novel Schiff bases: Thermodynamic Study" Int. J. Scientific Research in Chemistry, 9(7), 70-75.

[4]. Hansaraj Joshi, Rajpal Jadhav, Mazahar Farooqui, Shailendrasingh Thakur. (2022) "Thermodynamics study of formation of zinc complexes carrying novel Schiff bases in mixed solvent media." J. Adv. Applied Sci,Tech.,8(1), 91-96.

[5]. Jadhav R. L., Joshi H. U., Dr. S. B. Ubale. (2021) "Synthesis, characterization and biological activities of some novel Schiff bases derived from 3-acetyl-4-hydroxy-2H-chromen-2-one and 2-amino 5-(4-halosubstituted phynyl)-1-3-4-thiadiazole" Int. J. Ana. Exp. Modal Analysis, XIII(XI), 452-464.

[6]. Jadhav R. L., Joshi H. U., Ubale S. B. (2021) "Synthesis, characterization and biological activities of some novel Schiff bases derived from 3-acetyl-4-hydroxy-2H-chromen-2-one and 5-(4-substituted phenyl)-1,3,4-thiadiazol-2-amine," J. Interdisc. Cycle Res., XIII(X), 414-424.

[7]. Hansaraj U. Joshi, Rajpal L. Jadhav, Mazahar N. Farooqui, Shailendrasingh Thakur. (2021) "Complexation of La(III) metal ion with novel schiff bases: Thermodynamic Study." J. Advanced Scientific Research,12(2), 133-136.

[8]. Hansaraj Joshi, Rajpal Jadhav, Mazahar Farooqui, Shailendrasingh Thakur. (2021) "Thermodynamics of the formation of divalent Copper complexes carrying novel Schiff bases in mixed solvent media." J. Interdisc. Cycle Res.,13(04),53-61.

[9]. Hansaraj Joshi, Rajpal Jadhav, Mazahar Farooqui, Shailendrasingh Thakur. (2021) "Studies of complexation of trivalentrare earth metal ion Cerium with novel Schiff bases: Thermodynamic Aspect." Int. J. Ana. Exp. Modal Analysis, 13(04), 74-80.

[10]. Hansaraj Joshi, M.A. Sakhare, S.D.Naikwade and Shailendrasingh Thakur. (2019) "Study of complexation of divalent transition and trivalent Lanthanide metal ions with Schiff base 2-hydroxy-5-bromo acetophenone-n-(2-chloro-5-nitrophenyl) imine: Thermodynamic aspect." J. Global Res, 5(02), 87-89.

[11]. Shailendrasingh Thakur, Sahebrao Naikwade, Mazahar Farooqui (2013) "Thermodynamics of the formation trivalent Lanthanide complexes carrying Adenosine drug in mixed solvent media." Int. J. Chem. Stud., 1(3), 88-92.

[12]. Shailendrasingh Virendrasingh Thakur, Mazahar Farooqui, M.A. Sakhare, S.D. Naikwade. (2013) "Thermodynamic studies of Oxytetracycline with some transition and rare earth metal ions in mixed solvent media." American Int. J. Res. Formal, Appl.& Nat. Sci., 3(1),123-127.

[13]. Shailendrasingh Thakur, Mazahar Farooqui, Sahebrao Naikwade. (2013) “Thermodynamics of the complexation of ImipramineHydrochloride drug with Lanthanide.” Int. J. Emer. Tech. Comp. and Appl. Sci., 4(4), 342-346.

[14]. S.V. Thakur, Mazahar Farooqui, S.D. Naikwade. (2013) “Thermodynamic studies of rare earth metal complexes with Metformin Hydrochloride drug in mixed solvent system.” J. Adv. Sci. Res., 4(1):31-33.

[15]. Thangjam PD, Lonibala R. (2010) “Potentiometric Studies on the Complexation reactions of N-(2,2-[1- (3-Aminophenyl) ethylidene] hydrazine-2- oxoethyl)benzamide with Ni2+, Cu2+ andCd2+ ions in aqueous dioxane and micellar media”. J. Chem. Eng.Data, 55(3): 1166- 1172.

[16]. Sharmeli Y, Lonibala R. (2009) “Thermodynamics of the complexation of N-(Pyridin-2-ylmethylene) Isonicotinohydrazide with lighter lanthanides”. J. Chem. Eng. Data, 54(1): 28-34.

[17]. El-Sherbiny MF. (2005) “Potentiometric and Thermodynamic Studies of 2-Thioxothiazolidi-4-one and its Metal Complexes”. Chem Paper 59(5): 332-335.

International Journal of Scientific Research in Science and Technology
Available online at : www.ijsrst.com
OPEN ACCESS
Print ISSN: 2395-6011 | Online ISSN: 2395-602X
doi : https://doi.org/10.32628/IJSRST

Benzimidazole Hybrid System with another Heterocycle: An Anti-Bacterial and Antifungal Scaffold

Juber Abdulhamid Shaikh[1], Dattatray Gaikwad[2], Asghar Khan[1]*

[1]Department of Chemistry, Milliya Arts, Science & Management Science College, Beed-431122, Maharashtra, India

[2]Department of Chemistry, Maulana Azad College of Arts, Science & Commerce, Rauza Bagh, Aurangabad, 431001, Maharashtra, India

[3]Department of Chemical Technology, Dr. Babasaheb Ambedkar Marathwada University, Aurangabad, 431004, Maharashtra, India

[4]Regional Department of Chemistry Dr. Babasaheb Ambedkar Marathwada University, Aurangabad, 431004, Maharashtra, India

[5]Maharashtra Pollution Control Board, Aurangabad, 431004, Maharashtra, India

ARTICLEINFO

Article History :

Published : 07 Dec 2024

Publication Issue :
Volume 11, Issue 23
Nov-Dec-2024
Page Number :
178-190

ABSTRACT

A series of novel Benzimidazole hybrid system with another heterocycle were synthesized from a 1,2-diaminobenzene. We have developed a simple strategy for the synthesis of functionally diverse Benzimidazole, and pyridazine derivatives were reported via a series of steps. The work involves bicyclic imidazole- ring formation, protection, halogenation, deprotection, N-alkylation, substitution, peptide coupling. The structure of the synthesized compounds was confirmed by 1H NMR, 13C NMR, mass spectra, and purity is checked by LCMS. All synthesized compounds were screened for anti-bacterial and antifungal activity. The preliminary results suggests that most of the compounds show anti-bacterial and antifungal activity with different degrees; amoxicillin and fluconazole was used as positive control. The outcomes of this study hold the promise of unveiling novel compounds with diversified pharmacological activities, paving the way for the development of innovative therapeutic agents in the pursuit of improved healthcare solutions.

Keywords: Antibacterial and antifungal activity.

Introduction

Benzimidazole derivative, a hit from diversity screening was found to have potent antibacterial activity and antiviral activity. Viruses and bacteria remain a major global health challenge like SARS-CoV-2 has been

declared a public health emergency by WHO. Among various aspects of this disease, emergence and spread of drug resistant SARS-CoV-2 poses a significant threat to SARS-CoV-2 care and control worldwide. Reports of corona patients with severe drug resistance patterns, worse than multi- or, extreme- drug resistant SARS-CoV-2 are increasing along with fungal infection of in eye of patients and is a cause of real concern (WHO meeting report). It has created an urgent need to develop new drugs which can rapidly cure viral and fungal infections. The effort led to more than 10 compounds with desirable physico-chemical properties. The potent biological activity in conjunction with heterocycle, made the series an attractive lead. The synthesis of hybrid systems involving benzimidazole, a versatile heterocyclic scaffold, with other heterocycles represents a compelling avenue in medicinal chemistry. This study focuses on the design, synthesis, and biological screening of novel hybrid compounds to explore their potential pharmacological activities. The synthesis involved the
combination of benzimidazole with other heterocycle, creating a library of compounds that were systematically characterized using spectroscopic techniques. The biological screening encompassed antimicrobial assays against various bacterial and fungal strains. Our results indicate the successful synthesis of a range of hybrid systems, characterized by nuclear magnetic resonance (NMR), and mass spectrometry. These hybrid compounds exhibited structural diversity, confirming the effective incorporation of benzimidazole with another heterocycle. In the biological screening, several compounds demonstrated notable antimicrobial activities against specific strains, underscoring their potential as antibacterial and antifungal agents. The findings of this study contribute to the growing body of knowledge on benzimidazole hybrids, highlighting their diverse biological activities. The observed structure-activity relationships offer insights into the design principles for future drug development efforts. The multifunctionality exhibited by these hybrid systems underscores their potential in addressing complex diseases and motivates further exploration of this chemical space for therapeutic applications. In present work, we have chosen substituted benzimidazole and pyridazine nuclei and its derivatives. for study. Several heterocycles were intensively studied to discover new antifungal and antibacterial agents. benzimidazole scaffolds were identified as one of the important classes of heterocyclic compounds because of their significant and diversified pharmacological and biological properties. The benzimidazole scaffold plays an important role in drug discovery. The benzimidazole scaffold shows varied biological activities such as insecticidal and fungicidal agents, [1,9] antibacterial, [2,5] Cytotoxic,[3] anticancer agents,[4] lipase inhibition activity,[6] antiviral, [10,12] anticonvulsant, antidiabetic and DNA cleavage studies.[15] The substituted benzimidazole shows multiple biological activities. Recent literature review reveals that reactions involving hero atoms such as pyridazine were very advantageous in design of biological evaluation agents as they resemble many biomolecules. Pyridazine and derivatives mainly act as potent and selective factor Xia inhibitors. Pyridazine in combination of other groups shows diversified activity. The benzimidazo[1,2-b]pyridazine was identified as one of the promising building blocks in drug discovery as it shows diversified biological activities like Analgesic Agents. Anti-Inflammatory. Anti-Allergy Agents,[17] antiparasitic activity,[18] treatment of inflammatory diseases. Several derivatives of benzimidazole-pyridazine series act as Antiviral activity of benzimidazole derivatives. III. Novelanti-CVB-5, anti- RSV and anti-Sb-1 agents.[14] By considering the diversified bio- logical activities of benzimidazole and pyridazine, we have tried to incorporate both scaffolds in one framework as benzimidazole[1,2-b]pyridazine, and in continuation of our research, for the search of anti-bacterial and antifungal target, we have synthesized a series of compounds having benzimidazole[1,2-b]pyridazine nuclei.

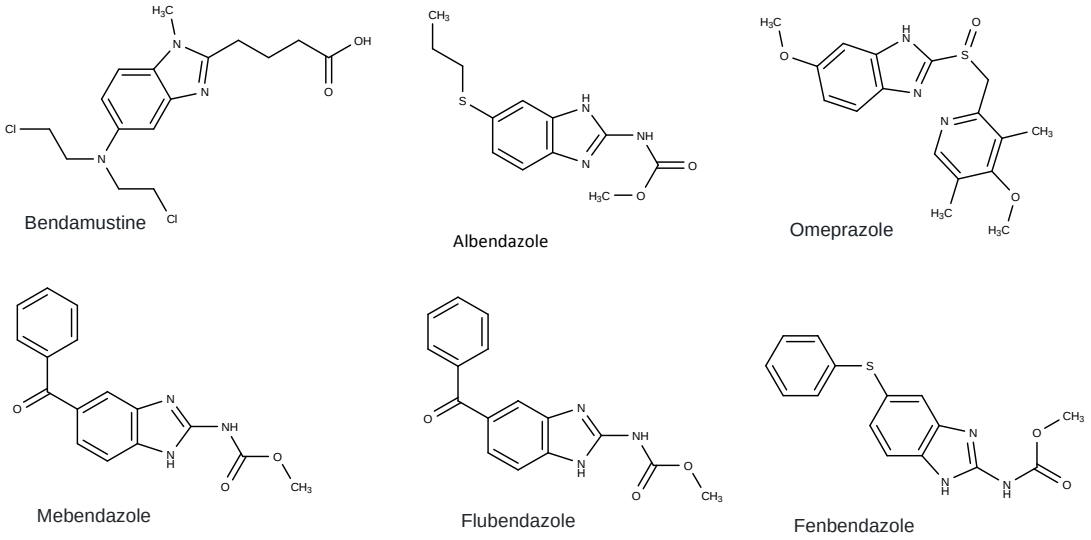

Fig-01: General structure of biologically active molecules having benzimidazole nuclei:

General structure of biologically active molecules having Benzimidazole: Figure 1 compromising the biological active molecules reported. Bendamustine is an antineoplastic agent used for the treatment of chronic lymphocytic leukemia (CLL) and indolent B-cell non-Hodgkin lymphoma (NHL) that has progressed following rituximab therapy. Albendazole a anthelmintic used to treat parenchymal neurocysticercosis and other helminth infections. Omeprazole is a proton pump inhibitor used to treat GERD associated conditions such as heartburn and gastric acid hypersecretion, and to promote healing of tissue damage and ulcers caused by gastric acid and H. pylori infection. Mebendazole A benzimidazole anthelmintic used to treat helminth infections Flubendazole is an anthelmintic that is used to treat worm infection in humans. It is available OTC in Europe

Results and Discussion:

(3S)-4-[(1Ethyl-benzimidazol-2-yl) methyl]-3-methylpiperazine -N-(substituted) sulfonamide (9a-9g) (3S)-4-[(1Ethyl-benzimidazol-2-yl) methyl]-3-methylpiperazine -N-(substituted) amide (9h-9n) by using 2,3-diaminobenzene (1) in below Scheme 1. We have optimized the synthesis of compound 9a-9n in step- wise manner to get good yield, neat reaction profile, and workable condition by keeping these things in mind, and the optimized steps are depicted in below Scheme 1.

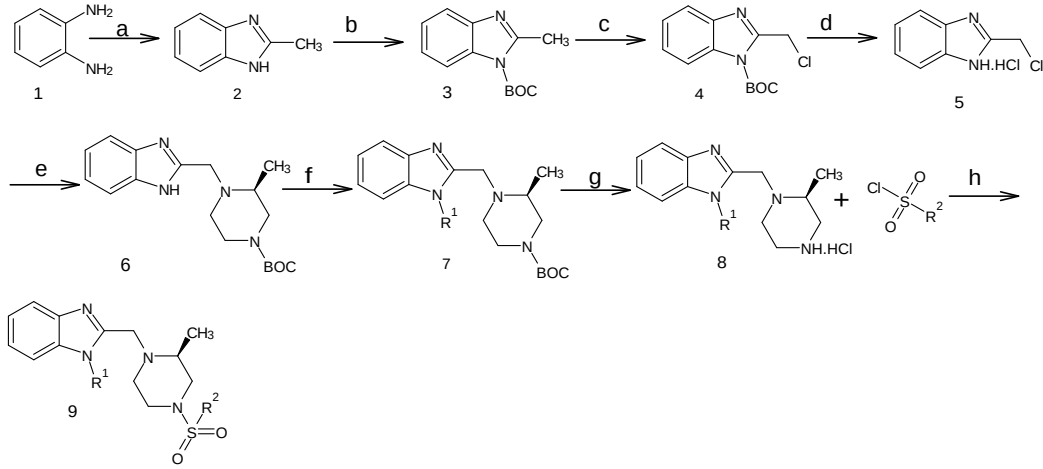

Scheme 1: (3S)-4-[(1Ethyl-benzimidazol-2-yl) methyl]-3-methylpiperazine -N-(substituted)amide (9a-9i): Reagents and conditions: (a):Acetic acid, 100◦C 2 h;(b): (Boc)2O,DMAP, DCM, 24 hours at , room temperature,;

(c): NCS, AIBN,CCl4, 100◦C for 1 hour; (d) Dioxane :HCl, room temperature, 12 hours; (e);K2CO3, ACN,55◦C, 12 hours; (f);K2CO3, DMF,90◦C, 12 hours; (f) Dioxane :HCl, room temperature, 12 hours; (h) EDCI, DIPEA,DCM,12 hours

In step a, we have done the synthesis of 2-methyl benzimidazole [cas no. 98615-15-6; 2] from commercially available 2,3-diaminobenzene (1). We have used acetic acid; and it worked well getting good yields of product. The compound 2 was characterized by melting point as it matches with reported literature. In step b, the compound 2 reacted with triethylamine, Boc anhydride, DMAP in dichloromethane non polar spot observed on TLC of compound 3.

The compound 3 on chlorination by using crystalized NCS in carbon tetrachloride and AIBN was added as catalyst to obtain yield >65%. We have used heating condition for this chlorination as to decrease the time of reaction. At room temperature for getting good yields, we have to run the reaction for longer hours. The new non polar spot was seen on TLC, after isolation the LCMS shows desired mass peak of compound 4. In step d, we have done boc-deprotection of comp-4 by using diethyl ether: HCl and dioxane:HCl. The optimization reaction for step d was done to get better yields and less time. The new polar spot was seen on TLC. We have done reaction by using DMF, Acetonitrile and THF to get 50%, 75% and 30% yields respectively. Further we have used potassium carbonate base; further, we have used the same condition for scale up of the compound 6. In step f, when the reaction was performed in sealed tube, the starting material was not consuming as product formation was very less as there is possibility of ethyl iodide leakage at higher temperature. There are also strong chances of sealed tube breakage at higher temperature. We have used steel bomb vessel for performing this reaction, and it worked well getting good yields of product. The compound 7 was characterized by LCMS. In step g, we have done boc-deprotection of comp-4 by using diethyl ether: HCl and dioxane:HCl. The optimization reaction for step d was done to get better yields and less time. The new polar spot was seen on TLC. The compound 8 was characterized by LCMS.In step h, coupling reaction was performed by EDC.HCl, DIPEA, DCM room temperature and it worked well getting good yields of product. The compound 9 was characterized by LCMS, NMR and TLC. The detailed experimental procedure, workup, and yield details are given in experimental section.

Experimental Section:

All chemicals were purchased from commercial sources with above 95% purity and were used without further purification. The major chemicals were purchased from BLD and Avra labs. The progress of the reactions was monitored by thin layer chromatography (TLC) analysis on Merck pre-coated silica gel 60 F254 aluminum sheets, visualized by UV light. Melting points were recorded on SRS Optimelt. The 1H NMR spectra were recorded on a 400 MHz Varian NMR spectrometer. The 13C were recorded on a 100 MHz Varian NMR spectrometer. The chemical shifts are reported as NMR spectra δ ppm units. The following abbreviations are used; singlet (s), doublet (d), triplet (t), quartet (q), multiplet (m) and broad (br s). Mass spectra were taken with direct mass QUATTRO-II of WATER mass spectrometer.

Step a- Synthesis of 2-methyl-1H-benzimidazole (2)

In a 500ml RBF 12.5gm of o-phenylenediamine was treated with 11.25gm of 90% acetic acid. The mixture was heated in a water bath at 100°C for 2 hours. After cooling, 10% sodium hydroxide solution was added slowly with through mixing by rotation of the flask until the mixture was just alkaline to litmus. The crude Benzimidazole was collected with suction in a 75mm Buchner funnels. Ice cold water is used to rinse all solid

out of the reaction flask. The crude precipitate is pressed thoroughly on the filter washed with ice cold water and dried well to get shiny brown color solid, yield 6.8gm (71.57%), melting point 175° C, IR (KBr) wavelength (cm-1) N-H 3385, C-H 3026, C-N 1273 aromaticity

The crude obtained was used further for next reaction without purification. For data crude was purified by column chromatography (silica 100-200 mesh) using 30 % ethyl acetate in hexane as an eluent to afford 5.5g off white solid.

Step b-Synthesis of tert-butyl-2-methyl1H-benzimidazole-1-carboxylate (3)

To a stirred mixture of 2-methylbenzimidazole (30 g, 227 mmol), triethylamine (25.26g, 249.7 mmol), and DMAP (1.38g, 11.34 mmol) in dry CH2Cl2 (300 mL) was added (Boc)2O (99.08g, 454 mmol). After 24 h, the mixture was concentrated. The residue was taken up in H2O, stirred and filtered to give a white solid (49 g, 94%). Crude obtained was used further for next reaction without purification

Step c—synthesis of tert-butyl2-(chloromethyl)-1H-benzimidazole-1-carboxylate (4).

A mixture of N-BOC-2-methylbenzimidazole (30g, 112.5 mmol), N-chlorosuccinimide (17.8 g, 134.0 mmol), and AIBN (5 g, 3.04 mmol) in CCl4 (400 mL) was refluxed for 12h, then the mixture was cooled and filtered. The filtrate was concentrated and purified by chromatography (silica gel 100-200 mesh, 5% EtOAc hexane) to give the title compound as a yellow oil (22.35 g, 65%). 1 H NMR (400 MHz, CDCl3) δ 7.94-8.01 (m, 1 H), 7.70-7.75 (m, 1 H),7.31-7.44 (m, 2 H), 4.96 (s, 2 H), 1.75 (s, 9 H)

Step d—synthesis of 2-(chloro-methyl) 1H-benzimidazole.HCl (5)

To a solution of tert-butyl-2-(chloromethyl) -1H-benzimidazole-1-carboxylate: (5 g, 18.79 mmol) in 1,4 dioxane (30ml) was added 10% Dioxane:HCl (50 ml) at 0-5°C, and the reaction mixture was stirred at room temp. for 12 hours and the mixture was cooled filtered and washed with diethyl ether to get off white solid: 5.2g, %. The crude obtained was used further for next reaction without purification.

Step e—synthesis of tert-butyl(3S)-4-[(1H-benzimidazol-2-yl) methyl]-3- methylpiperazine-1-carboxylate (6)

2-(chloromethyl)-1H-benzimidazole (5 g, 30.01 mmol) was added to mixture of (S) 3-methyl-tert-butyl piperazine-1-carboxylate (6.01 g, 30.01 mmol) and potassium carbonate (12.43 g, 90.03 mmol) in acetonitrile (50 mL) at 0-5°C, and the reaction mixture was stirred at 55 °C for 12 hours and the mixture was filtered. After the filtrate had been concentrated in vacuo, the residue was purified via chromatography on silica gel (Gradient: 0% to 60% ethyl acetate in petroleum ether) to provide as a pale yellow solid. Combined yield: 7.43g, 75%

Step f—synthesis of tert-butyl(3S)-4-[(1Ethyl-benzimidazol-2-yl)methyl]-3-methylpiperazine-1-carboxylate (7)

To a solution of tert-butyl (3S)-4-[(1H-benzimidazol-2-yl) methyl]-3-methylpiperazine-1-carboxylate (5 g, 24.62 mmol) in DMF (25 ml) in sealed tube was added Ethyl iodide (19.19 g,123.1 mmol) and potassium carbonate (17 g, 123.1 mmol) in DMF (50 mL) at 0-5°C, and the reaction mixture was stirred at 90°C for 12 hours and the mixture was cooled poured in ice cold water filtered. After the filtrate had been concentrated in vacuo, the residue was purified via chromatography on silica gel (Gradient: 0% to 60% ethyl acetate in petroleum ether) to provide as a pale yellow solid. Combined yield: 5.3 g, 65 %.

Step g—Synthesis of (3S)-4-[(1Ethyl-benzimidazol-2-yl)methyl]-3-methyl piperazine (8)

To a solution of tert-butyl (3S)-4-[(1Ethyl-benzimidazol-2-yl) methyl]-3-methylpiperazine-1-carboxylate: (5g, 13.96 mmol) in 1,4 dioxane (30ml) was added 10% Dioxane:HCl (50 ml) at 0-5°C, and the reaction mixture was stirred at room temp. for 12 hours and the mixture was cooled filtered and washed with diethyl ether to get off white solid: 3.5 g, 85%.

3.1.8 Step h—synthesis of (3S)-4-[(1Ethyl-benzimidazol-2-yl)methyl]-3-methyl piperazine derivative (9)

To a stirred solution of (3S)-4-[(1Ethyl-benzimidazol-2-yl) methyl]-3-methylpiperazine (0.19 g, 0.6 mmol) in DCM (5 mL) was added EDCI (0.15 g, 0.96 mmol) and DIPEA (0.20 g mL, 1.6 mmol) at 0C. Added sulfonyl

chloride (0.7mmol) at 0C and stirred reaction mixture at room temperature for 12 hours. Progress of the reaction was monitored by TLC and LCMS. After completion, the reaction mixture was diluted with cold water (10 mL). The reaction mixture was extracted with DCM (2 × 10 mL). The organic layer was separated, washed with 1 N aq. cold HCl (5 mL), brine (5 mL), dried over anhydrous Na2SO4, and concentrated in vacuo. The crude obtained was purified by using 0-10 % MeOH in DCM on 230-400 mesh silica gel to afford desired sulfonamide as solid.

3.1.9 |(3S)-4-[(1Ethyl-benzimidazol-2-yl)methyl] -3-methylpiperazine Phenyl derivative (9a)

Target-1

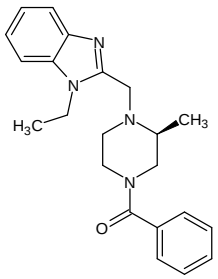

9a
Formula Weight:362.46

1H NMR (400 MHz,DMSO-d6) δ 7.57-7.62 (m, 2H, ArH), 7.42-7.47 (m, 5H, ArH), 7.20-7.28 (m,2H, ArH), 4.32-4.42 (m, 2H), 4.24-4.27 (d, 1H), 3.61-3.64 (d, 2H), 3.28-3.44 (m, 2H), 3.11-3.28 (m, 1H), 2.65-2.77(m, 2H), 2.32-2.54(m, 1H), 1.41-1.43 (d, 3H) 1.07-1.27 (d, 3H)

13C NMR (DMSO-d6, 100 MHZ,ppm) = δ 14.52, 15.39, 21.39, 38.92, 39.44, 40.48,40.69, 51.00, 55.87,110.46, 116.17, 119.38, 121.77, 122.52, 127.57, 129.37, 133.4, 135.59, 139.65, 142.61, 150.27, 169.64,

LCMS; M+H=363

Target-2

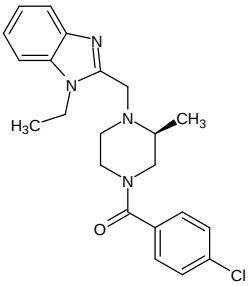

9b
Formula Weight:396.91

1H NMR (400 MHz,DMSO-d6) δ 7.52-7.62 (m, 4H, ArH), 7.27-7.46 (m, 2H, ArH), 7.18-7.26 (m,2H, ArH), 4.23-4.42 (m, 3H), 3.60-3.63 (d, 2H), 3.11 (m, 1H), 3.11-3.28 (m, 1H), 2.65-2.77(m, 2H), 2.32-2.54(m, 1H), 1.40-1.43 (d, 3H) 1.07-1.27 (d, 3H)

13C NMR (DMSO-d6, 100 MHZ, ppm) = δ 14.47, 15.42, 21.60, 31.30, 36.3, 49.64, 50.97, 55.22, 110.49, 119.41, 121.81, 122.57, 129.04, 129.57, 134.74, 135.11, 135.63, 142.64, 151.46, 162.85,169.51, 172.1

LCMS; M+H=397

Target-3

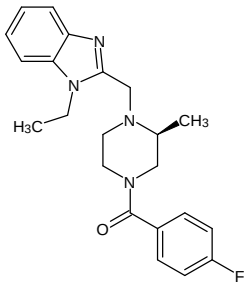

9c
Formula Weight:380.45

1H NMR (400 MHz,DMSO-d6) δ 7.22-7.33 (m, 4H, ArH), 7.49-7.53 (m, 2H, ArH), 7.58-7.64 (m,2H, ArH), 4.36-4.42 (m, 2H), 4.25-4.29 (m, 1H), 3.62-3.65 (d, 2H), 3.13 (m, 1H), 2.67-2.94(s, 2H), 2.79(s, 2H), 2.74(m, 2H), 2.34 (m, 1H), 1.42-1.45 (m, 3H) 1.15-1.29 (m, 3H)

13C NMR (DMSO-d6, 100 MHZ, ppm) = δ 14.50, 15.43, 29.53, 31.33, 36.33, 38.89, 50.15, 51.00, 55.30, 110.53, 115.82, 116.04, 119.46, 121.86, 122.62, 130.06, 132.75, 135.66, 142.66, 151.52, 161.87, 162.90, 164.33, 1

LCMS; M+H=381

Target-4

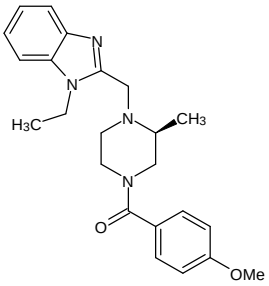

9d
Formula Weight:392.49

LCMS; M+H=393

Target-5

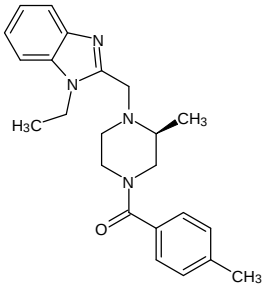

Formula Weight:376.49

1H NMR (400 MHz,DMSO-d6) δ 7.58-7.64 (m, 2H, ArH), 7.22-7.32 (m, 5H, ArH), 4.38-4.42 (m, 2H), 4.25-4.29 (d, 1H), 3.62-3.65 (d, 2H), 3.12-3.28 (m, 2H), 2.56-2.66 (m, 3H), 2.38(m, 3H), 1.43 (m, 3H) 1.17-1.29 (m, 3H)

13C NMR (DMSO-d6, 100 MHZ,ppm) = δ 14.52, 15.39, 21.39, 38.92, 51.00, 55.27, 110.46, 116.17, 119.38, 121.77, 122.52, 127.57, 129.37, 133.4, 135.59, 139.65, 142.61, 150.27, 169.64,

LCMS; M+H=

Target-6

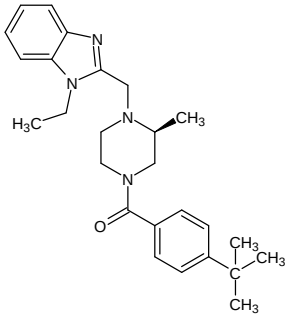

9f
Formula Weight:418.57

LCMS; M+H=419

Target-7

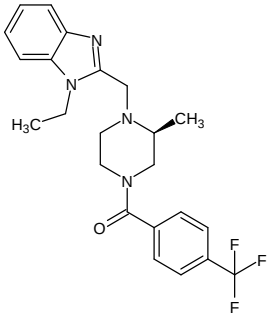

9g
Formula Weight:430.46

LCMS; M+H=431

Target-8

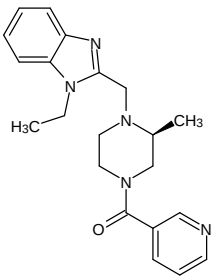

9h
Mol wt=363

LCMS; M+H=364

Target-9

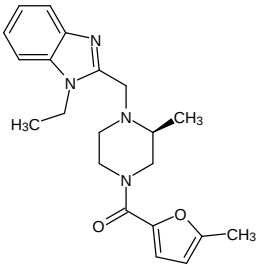

9i
Mol wt=366

LCMS; M+H=367

Target-10

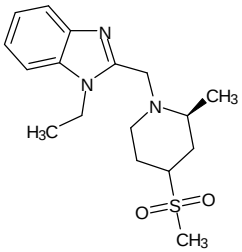

9j
Formula Weight:335.46

LCMS; M+NH3=353

Target-11

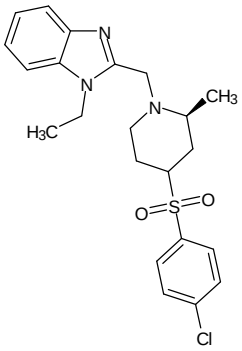

9k
Formula Weight:431.97

LCMS; M+H=433

Antimicrobial activity and Antifungal study

Method: Agar Well Diffusion

Procedure

Materials and methods:

Agar well diffusion method was used to determine the antibacterial activity of the test substance. Bacillus subtilis NCIM 2063, Staphylococcus aureus NCIM 2079, Escherichia coli NCIM 2065, Proteus vulgaris NCIM 2813, Aspergillus niger NCIM 501, and Candida albicans NCIM 3471 were

Media: Nutrient Agar for Bacterial cultures, Yeast Glucose Agar

Cultures used:

Bacterial cultures: *Bacillus subtilis* NCIM 2063, *Staphylococcus aureus* NCIM 2079, bacterial cultures each cultured individually for 24 hours. We created sterile Nutrient agar plates for

Escherichia coli NCIM 2065, *Proteus vulgaris* NCIM 2813 and sterile Chloramphenicol Yeast Glucose Agar plates for fungus cultures. A 0.2 ml culture of each

Fungal Cultures: *Aspergillus niger* NCIM 501, *Candida albicans* NCIM 3471 type of microorganism was dispersed on various plates using sterile swabs. Four or five wells in the

Incubation temperature: 37°C agar were created using an 8.0 mm cork borer on each plate. As a stock solution, a 10 mg/ml suspension

Incubation time: 24 Hrs of the test substance was produced in Dimethyl Sulfoxide (DMSO). Each well received 50µg/ml of the stock solution.

Std.: Amoxicillin

Std.: Fluconazole

Observations:

The observation of each sample was recorded against each microorganism in Table.

Table 1: Antibacterial activity against *Bacillus subtilis* NCIM 2063 in terms of Zone of inhibition in

Sr. No.	Compound No OR Name	Activity against (Gram +ve Bacteria)		Activity against (Gram -ve Bacteria)		Antifungal Activity	
		B.Subtilis	*S.aureus*	*E coli*	*P.vulgaris*	*A niger*	*C. albicans*
1	**S-01 (R-01)**	9	15	12	10	23	30
2	**S-01 (R-02)**	4	19	12	9	24	30
3	**S-01 (R-03)**	9	12	12	11	20	28
4	**S-01 (R-04)**	8	11	10	13	18	29
5	**S-01 (R-05)**	11	11	9	9	18	15
6	**S-01 (R-06)**	9	12	13	12	17	14
7	**S-01 (R-07)**	12	10	8	9	15	22
8	**S-01 (R-08)**	12	9	14	13	14	21
9	**S-01 (R-09)**	14	16	15	14	18	25
10	**S-01 (R-10)**	11	18	11	10	10	26
11	**Amoxicillin**	18	22	21	19	-	-
12	**Fluconazole**	-	-	-	-	28	33

Results

At the concentration 10 mg/ml, the SAMPLES S-01(R-01 to R-10) showed good and moderate activity against gram +ve, gram –ve microorganism and fungal organism.

CONCLUSION

We have synthesized (3S)-4-[(1Ethyl-benzimidazol-2-yl) methyl]-3-methylpiperazine-N-(substituted) sulfonamide derivatives(9a-9g) and (3S)-4-[(1Ethyl-benzimidazol-2-yl) methyl]-3-methylpiperazine-N-(substituted)acetamide derivatives (9h-9n) from 2,3-diaminobenzene through a series of reactions. We have tried to report simple reaction condition, easy workup, short reaction time, and good to high yields. The synthesized compounds were screened for antifungal The biological screening results underscore the pharmacological potential of benzimidazole hybrid systems. The observed activities against microbial pathogens and viruses provide a strong basis for the continued development and optimization of these compounds as potential therapeutic agents with broad-spectrum applications.

In conclusion, a series of novel benzimidazole derivatives designed on the basis of the core structure of existing pyrethroids was synthesized. The title compounds 9a–i, 9j–p, were evaluated as antibacterial and fungicidal agents. Preliminary biological evaluation indicated that most of the title compounds showed potent fungicidal activities against Aspergillus niger NCIM 501 and Candida albicans NCIM 3471 Specifically, compounds displayed significant fungicidal activities against Aspergillus niger and Candida albicans. Among them, compound 9i displayed more Table 2. Antibacterial activity against Bacillus subtilis NCIM 2063, Staphylococcus aureus NCIM 2079, Escherichia coli NCIM 2065, Proteus vulgaris NCIM 2813

Vol. 41, No. 1, 1–5 (2016) Synthesis and biological activity of novel antifungal benzimidazole derivatives 5 potent fungicidal activity against both fungi than did thiabendazole. The results of this antifungal evaluation indicated that these compounds are a promising type of potential antifungal agents against B. cinerea and S. sclerotiorum for controlling plant diseases. Further evaluation of their fungicidal properties, particularly in field studies designed to examine their biological efficacy, crop safety, and toxicity, is required before they can be adopted for widespread use.

ACKNOWLEDGMENT

The authors are thankful to the Head, Department of Chemistry, Moulana Azad College, Aurangabad, Dr. Babasaheb Ambedkar Marathwada University, Aurangabad 431004, MS, India for providing the laboratory facility.

References

[1]. Weijie Si,1 Tao Zhang,1 Yaofa Li,2 Dongmei She,1 Wenliang Pan,2 Zhanlin Gao,2 Jun Ning,1 and Xiangdong Mei1, J Pestic Sci. 2016 Feb 20; 41(1): 15–19.

[2]. Woolley, D.W. Some biological effects producted by benzimidazole and their reversal by purines. J. Biol. Chem. 1944, 152, 225–232.

[3]. Eom, Y.W.; Oh, S.; Woo, H.B.; Ham, J.; Ahn, C.M.; Lee, S. Cytotoxicity of substituted benzimidazolyl curcumin mimics against multi-drug resistance cancer cell. Bull. Korean Chem. Soc. 2013, 34, 1272–1274.

[4]. Soderlind, K.J.; Gorodetsky, B.; Singh, A.K.; Bachur, N.R.; Miller, G.G.; Lown, J.W. Bis-benzimidazole anticancer agents: Targeting human tumour helicases. Anticancer Drug Des. 1999,14, 19–36.

[5]. Kumar, K.; Awasthi, D.;Lee, S.Y. ; Cummings, J.E. ; Knudson, S.E.; Slayden, R.A.; Ojima, I.Benzimidazole-based antibacterial agents against Francisella tularensis. Bioorg. Med. Chem. 2013,21, 3318–3326.

[6]. Mentese, E.; Bektas, H.; Ulker, S.; Bekircan, O.; Kahveci, B. Microwave-assisted synthesis of new benzimidazole derivatives with lipase inhibition activity. J. Enzyme Inhib. Med. Chem. 2014, 29,64–68.

[7]. Velík, J.; Baliharová, V.; Fink-Gremmels, J.; Bull, S.; Lamka, J.; Skálová, L. Benzimidazole drugs and modulation of biotransformation enzymes. Res. Vet. Sci. 2004, 76, 95–108.
[8]. Janupally, R.; Jeankumar, V.U.; Bobesh, K.A.; Soni, V.; Devi, P.B.; Pulla, V.K.; Suryadevara, P.;Chennubhotla, K.S.; Kulkarni, P.; Yogeeswari, P.; et al. Structure-guided design and development of novel benzimidazole class of compounds targeting DNA gyrase enzyme of Staphylococcus aureus. Bioorg. Med. Chem. 2014, 22, 5970–5987.
[9]. Ke, Y.; Zhi, X.; Yu, X.; Ding, G.; Yang, C.; Xu, H. Combinatorial synthesis of benzimidazole-azo-phenol derivatives as antifungal agents. Comb. Chem. High Throughput Screen 2014, 17, 89–95.Molecules 2015, 20 15222
[10]. Tonelli, M.; Paglietti, G.; Boido, V.; Sparatore, F.; Marongiu, F.; Marongiu, E.; La Colla, P.;Loddo, R. Antiviral activity of benzimidazole derivatives. I. Antiviral activity of 1-substituted-2-[(benzotriazol-1/2-yl)methyl]benzimidazoles. Chem. Biodivers. 2008, 5, 2386–2401.
[11]. Vitale, G.; Corona, P.; Loriga, M.; Carta, A.; Paglietti, G.; Ibba,
[12]. C.; Giliberti, G.; Loddo, R.;Marongiu, E.; la Colla, P. Styryl benzimidazoles. Synthesis and biological activity—Part 3. Med Chem.2010, 6, 70–78.
[13]. Tonelli, M.; Simone, M.; Tasso, B.; Novelli, F.; Boido, V.;Sparatore, F.; Paglietti, G.; Pricl, S.;Giliberti, G.; Blois, S.; et al. Antiviral activity of benzimidazole derivatives. II. Antiviral activity of 2-phenylbenzimidazole derivatives. Bioorg. Med. Chem. 2010, 18, 2937–2953.
[14]. Vitale, G.; Corona, P.; Loriga, M.; Carta, A.; Paglietti, G.; Giliberti, G.; Sanna, G.; Farci, P.;Marongiu, M.E.; la Colla, P. 5-Acetyl-2-arylbenzimidazoles as antiviral agents. Part 4. Eur. J.Med. Chem. 2012, 53, 83–97.
[15]. Tonelli, M.; Novelli, F.; Tasso, B.; Vazzana, I.; Sparatore, A.; Boido, V.; Sparatore, F.;la Colla, P.; Sanna, G.; Giliberti, G.; et al. Antiviral activity of benzimidazole derivatives. III. Novelanti-CVB-5, anti- RSV and anti-Sb-1 agents. Bioorg. Med. Chem. 2014, 22, 4893–4909.
[16]. Shingalapur, R.V.; Hosamani, K.M.; Keri, R.S.; Hugar, M.H. Derivatives of benzimidazole pharmacophore: Synthesis, anticonvulsant, antidiabetic and DNA cleavage studies. Eur. J. Med. Chem.2010, 45, 1753–1759.
[17]. Siddiqui, N.; Andalip; Bawa, S.; Ali, R.; Afzal, O.; Akhtar, M.J.; Azad, B.; Kumar, R. Antidepressant potential of nitrogen-containing heterocyclic moieties: An updated review. J. Pharm. Bioallied Sci.2011, 3, 194–212.
[18]. Datar, P.A.; Limaye, S.A. Design and Synthesis of Mannich bases as Benzimidazole Derivatives as Analgesic Agents. Anti-Inflamm. Anti-Allergy Agents Med. Chem. 2015, 14, 35–46.
[19]. 20. Achar, K.C.S.; Hosamani, K.M.; Seetharama reddy, H.R. In vivo analgesic and anti-inflammatory activities of newly synthesized benzimidazole derivatives. Eur. J. Med. Chem. 2010, 45, 2048–2054.
[20]. Bansal, Y.; Silakari, O. The therapeutic journey of benzimidazoles: A review. Bioorg. Med. Chem.2012, 20, 6208–6236.
[21]. Cho, H.S.; Lopes, P.F. Injectable Formulation of a Macrocyclic Lactone and Levamisole. (2011): United States Patent NO. 20130090296.
[22]. Stefanska, J.Z.; Gralewska, R.; Starosciak, B.J.; Kazimierczuk, Z. Antimicrobial activity of substituted azoles and their nucleosides. Pharmazie 1999, 54, 879–884.
[23]. Valdez, J.; Cedillo, R.; Hernández-Campos, A.; Yépez, L.; Hernández-Luis, F.; Navarrete-Vázquez, G.;Tapia, A.; Cortés, R.; Hernández, M.; Castillo, R. Synthesis and antiparasitic activity of 1H-benzimidazole derivatives. Bioorg. Med. Chem. Lett. 2002, 12, 2221–2224.
[24]. 25. Desai, N.C.; Kotadiya, G.M. Microwave-assisted synthesis of benzimidazole bearing 1,3,4-oxadiazole derivatives: Screening for their in vitro antimicrobial activity. Med. Chem. Res. 2014, 23, 4021–4033.

[25]. Kishore Babu, P.N.; Ramadevi, B.; Poornachandra, Y.; Ganesh Kumar, C. Synthesis, antimicrobial,and anticancer evaluation of novel 2-(3-methylindolyl)benzimidazole derivatives. Med. Chem. Res.2014, 23, 3970–3978.Molecules 2015, 20 15223
[26]. Phillips, M.A. CCCXVII.-The formation of 2-substituted benziminazoles. J. Chem. Soc. (Resumed)1928, doi:10.1039/JR9280002393.
[27]. Dirk, S.; Thorsten, L.L.; Philipp, L.; Martin, L.; Ralf, R.H.L.; Kirsten, A.; Klaus, R.; Gerald Juergen, R.;Stephan Georg, M. Alkyne compounds with MCH antagonistic activity and medicaments comprising these compounds. (2009),
[28]. Boehringer Ingelheim Pharma GmbH and Co. KG: United States Patent,Patent no. US 7592358 B2. Available online: http://www.lens.org/lens/patent/US_7592358_B2/ fulltext (accessed on 10 May 2015).
[29]. Tavman, A.; Ikiz, S.; Bagcigil, A.F.; Ozgur, N.Y.; Ak, S. Preparation, characterization and antibacterial effect of 2-methoxy-6-(5-H/Me/Cl/NO2-1H-benzimidazol-2-yl)phenols and
[30]. some transition metal complexes. J. Serbian Chem. Soc. 2009, 74, 537–548.
[31]. Podunavac-Kuzmanovic, S.O.; Cvetkovic, D.M. Antibacterial evaluation of some benzimidazole derivatives and their zinc(II) complexes. J. Serbian Chem. Soc. 2007, 72, 459–466.
[32]. Karuvalam, R.P.; Haridas, K.R.; Shetty, S.N. Trimethylsilyl chloride-catalyzed synthesis of substituted benzimidazoles using two phase system under microwave conditions, and their antimicrobial studies. J. Chil. Chem. Soc. 2012, 57, 1122–1125.
[33]. González-Chávez, M.M.; Méndez, F.; Martínez, R.; Pérez-González, C.; Martínez-Gutiérrez, F.Design and Synthesis of Anti-MRSA Benzimidazolyl benzene-sulfonamides. QSAR Studies for Prediction of Antibacterial Activity. Molecules 2011, 16, 175–189. J. S. Kim, H. J. Lee, M. E. Suh, H. Y. P. Choo, S. K. Lee, H. J. Park, C. Kim, S. W. Park, C. O. Lee, Bioorg Med Chem 2004, 12, 368.
[34]. Shah, D. I.; Sharma, M.; Bansal, Y.; Bansal, G.; Singh, M. Eur J Med Chem 2008, 43, 1808.
[35]. Kus, C.; Ayhan-Kilcigil, G.; Ozbey, S.; Kaynak, F. B.;Kaya, M.; Coban, T.; et al. Bioorgan Med Chem 2008, 16, 4294.
[36]. Shingalapur, R. V.; Hosamani, K. M.; Keri, R. S. Eur J Med Chem 2009, 44, 4244.
[37]. Leonards, T. J.; Jeyaseeli, L.; Kumar, M.; Sivakumar, R. Asian J Xhem 2006, 18, 1104.
[38]. Singh, M. P.; Joseph, T.; Kumar, S.; Bathini, Y.; Lown, J. W. Chem Res Toxicol 1992, 5, 597.
[39]. Bryant, H. E.; Helleday, T. Biochem Soc Trans 2004, 32, 959.
[40]. Tong, Y. S.; Bouska, J. J.; Ellis, P. A.; Johnson, E. F.; Leverson, J.; Liu, X. S.; et al. J Med Chem 2009, 52, 6803.
[41]. Gama, S.; Mendes, F.; Esteves, T.; Marques, F.; Matos, A.; Rino, J.; et al. Chembiochem 2012, 13, 2352.

International Journal of Scientific Research in Science and Technology
Available online at : www.ijsrst.com
OPEN ACCESS
Print ISSN: 2395-6011 | Online ISSN: 2395-602X
doi : https://doi.org/10.32628/IJSRST

Synthesis and Biological Study of Pyrozole Derivatives

B.P Khobragade[1], S.E. Bhandarkar[2]

[1]Department of Chemistry, RDIK and NKD College, Badnera, Maharashtra, India

[2]Department of Chemistry, G.V.I.S.H., Amravati-444604, Maharashtra, India

ARTICLEINFO

Article History :

Published : 07 Dec 2024

Publication Issue :
Volume 11, Issue 23
Nov-Dec-2024
Page Number :
191-195

ABSTRACT

Pyrazoles are classified as aromatic compounds because of their planar, conjugated ring systems containing six delocalized π-electrons. To synthesize substituted pyrazole, the precursor pyrazoline derivatives were dissolved in DMSO and placed in a round-bottom flask equipped with a condenser. Crystals of iodine were then added to the mixture. The reaction was stirred and refluxed for 1 hour and 30 minutes. After cooling, the reaction mixture was diluted with water, and the resulting product was filtered and washed with a 10% aqueous solution of sodium thiosulfate. The product was then recrystallized using an ethanol-acetic acid mixture to yield pyrazole derivatives.

The structures of the synthesized derivatives were characterized using IR and 1H NMR spectroscopy. The IR spectra displayed absorption bands at anticipated frequencies, while 1H NMR provided chemical shift values and integral data consistent with aromatic ring protons. Antimicrobial and antifungal evaluations indicated that all synthesized compounds demonstrated excellent activity.

Keywords :- Pyrazole, Biological activity, Characterization, Antimicrobial, Antifungal

Introduction

Pyrazoles, a remarkable group of aromatic molecules, derive their unique properties from their planar, conjugated ring structures containing six delocalized π-electrons. This arrangement bestows upon pyrazoles the same aromaticity observed in benzene derivatives, rendering them highly versatile in chemical applications.

Like other nitrogen-containing heterocycles, pyrazoles exhibit fascinating tautomeric behavior. The unsubstituted pyrazole molecule can exist in three distinct tautomeric forms, showcasing its dynamic structural adaptability.

In recent years, a vast number of compounds bearing the pyrazole nucleus have emerged, demonstrating an impressive spectrum of biological activities. These include **antimicrobial, antiviral, antitumor, antihistaminic,**

antidepressant, as well as roles in **insecticidal and fungicidal** applications. This versatility has cemented the pyrazole ring as a cornerstone in pharmaceutical chemistry, forming the core structure of numerous drugs and therapeutic agents.

The present study explores the synthesis and biological evaluation of novel pyrazole derivatives. Comprehensive characterization of these compounds has been undertaken using **elemental analysis, infrared spectroscopy (IR), and proton nuclear magnetic resonance spectroscopy (^{1}H NMR)**. This work underscores the significance of the pyrazole framework in advancing drug discovery and therapeutic innovation.

Methodology

To check the purity of the compound , thin layered chromatography of silica gel was used . 1H NMR spctra were recored on a Brucker AC300 FNMRspectrometer (300 MHz), using TMS as an internal standered.IR spctra were recorded on nicolet –Imapct 400 FT-IR spectrometer .all melting point were taken in silicon oil bath with open capiliary tube and are uncorrected Microanalysis of nitrogen was obtained on colman29-N analyzer

Synthesis of 2-acetyl-4-methoxy-1-naphthol : In a hot glacial acetic acid solution, fused $ZnCl_2$ was added and the mixture was refluxed until fully dissolved. Subsequently, powdered 4-methoxy-naphthalen-1-ol was introduced, and the solution was further refluxed for approximately 8 hours. Upon cooling, the reaction mixture was poured into acidulated water. The resulting solid precipitate was filtered, washed, dried, and recrystallized from rectified spirit. This procedure yielded the compound: 2-acetyl-4-methoxy-1-naphthol.

Synthesis of 3-aryl-1(1-hydroxy-4-methoxynaphthalen-2-yl)-prop-2-ene-1-one :- 2-Acetyl-4-methoxy-1-naphthol and 4,7-dimethoxynaphthalene-1-carbaldehyde were added in ethanol solvent. To this mixture KOH solution was added drop wise constant stirring. The reaction mixture was kept overnight. Then the mixture was poured over crushed ice and little HCl. The product was filtered and recrystalized from ethanol to obtain the compound.

Synthesis of pyrozoline derivatives :

3-aryl-1(1-hydroxy-4-methoxynaphthalen-2-yl)-prop-2-ene-1-one and Hydrazine hydrate/ phenyl hydrazine/ semicarbazide/ thiosemicarbazide were added to DMF and refluxed for 2 hours. The cooled reaction mixture was diluted with water, and the semisolid obtained was triturated with ethanol to form a solid. This solid was then recrystallized from an ethanol-acetic acid mixture, yielding dihydropyrazole derivatives.

Synthesis of pyrozole derivatives:

The synthesized pyrazoline derivatives were suspended in DMSO in a 250 ml round-bottom flask fitted with a condenser, and a crystal of iodine was added. The reaction mixture was stirred and refluxed for 1 hour 30 minutes.Afterward, the contents were cooled and diluted with water. The product obtained was filtered and washed with 10% aqueous sodium thiosulphate, followed by crystallization from an ethanol-acetic acid mixture, yielding pyrazole derivatives The structures of the synthesized compounds were elucidated by IR and ^{1}H-NMR analysis:

- IR spectra showed absorption bands at expected values.
- ^{1}H NMR analysis revealed aromatic proton shifts and integral values at expected chemical shifts.

Spectral analysis Interpretation (8):

IR(vmax) cm -1: 3340 (OH str), 3162 (N-N pyrazoline), 1521(C=N str.)

NMR (sppm) 3.85(s, 3H, OCH3), 3.88 (s, 3H, OCH3), 3.91(s, 3H, OCH3), 5.95 (s, 2H, NH2), 6.62 – 8.21 (m, 10 Ar-H), 9.95 (s ,1H ,OH), 12.61 (s ,1H ,N-H)

Table 1 : Physical data of synthesized compound

Sr.no.	Compound No.	Molecular formula	Name of compound	R1	Melting point	% yield	% nitrogen
1	8	C26H22N2O4	2-(5-(4,7-dimethoxynaphthalen-1-yl)-1H-pyrazol-3-yl)-4-methoxynaphthalen-1-ol	H	214	55	6.57%
2	9	C32H26N2O4	2-(5-(4,7-dimethoxynaphthalen-1-yl)-1-phenyl-1H-pyrazol-3-yl)-4-methoxynaphthalen-1-ol	C6H5	255	73	5.57%
3	10	C27H23N3O5	5-(4,7-dimethoxynaphthalen-1-yl)-3-(1-hydroxy-4-methoxynaphthalen-2-yl)-1H-pyrazole-1-carboxamide	CONH2	265	51	8.95%
4	11	C27H23N3O4S	5-(4,7-dimethoxynaphthalen-1-yl)-3-(1-hydroxy-4-methoxynaphthalen-2-yl)-1H-pyrazole-1-carbothioamide	CSNH2	201	62	8.65%

SCHEME

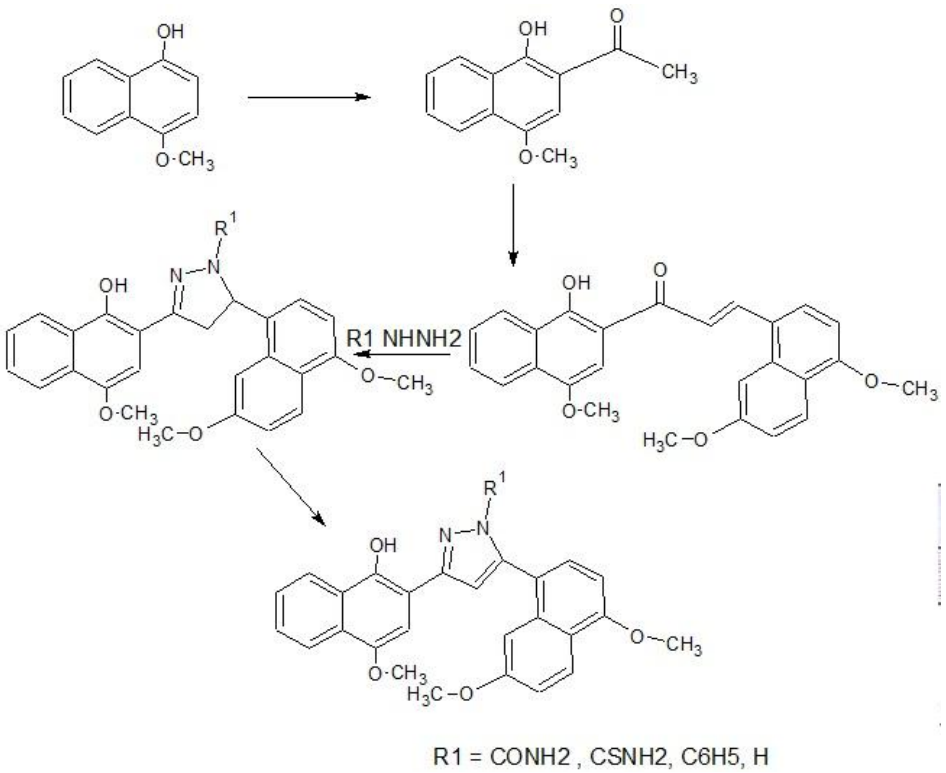

Biological Study:

Above synthesized pyrazoline derivatives have been studies for their antimicrobial activity of against Escherichia coil, proteus mirabilis, staphylococcus aureas and A. Nigar. The culture of each species was incubated at 37 OC and the zone of inhibition was measured after 24 hr. Most of these compounds were found active

Table –2 :-Pyrazole

Sr. No.	Compound	Antimicrobial activity			
		E.coli	*P.mirabilis*	*S. aureus*	*P.aeruginosa*
1	2-(5-(4,7-dimethoxynaphthalen-1-yl)-1H-pyrazol-3-yl)-4-methoxynaphthalen-1-ol	12	14	11	08
2	2-(5-(4,7-dimethoxynaphthalen-1-yl)-1-phenyl-1H-pyrazol-3-yl)-4-methoxynaphthalen-1-ol	15	16	12	10
3	5-(4,7-dimethoxynaphthalen-1-yl)-3-(1-hydroxy-4-methoxynaphthalen-2-yl)-1H-pyrazole-1-carboxamide	18	11	07	15
4	5-(4,7-dimethoxynaphthalen-1-yl)-3-(1-hydroxy-4-methoxynaphthalen-2-yl)-1H-pyrazole-1-carbothioamide	12	10	07	15

Strongly active, range 15-18mm, Weakly active, range 7-10 mm, Moderately active, range 11-14mm,
Thus, from the above results, it was observed that these heterocyclic compounds were found effective against Escherichia coli, Proteus mirabilis, Staphylococcus aureus, and Aspergillus niger. Consequently, all synthesized compounds can potentially be utilized for the treatment of diseases caused by these pathogens, provided they are free from toxins and other adverse side effects.

ACKNOWLEDGEMENT:

The authors are thankful to principal, RDIK and NKD College Badnera for providing necessary facilities

References

[1]. Kumar, A., & Singh, R. (2021). Synthesis, characterization, and antimicrobial activity of pyrazole derivatives. Journal of Heterocyclic Chemistry, 58(7), 1534-1545.
[2]. Gupta, P., & Sharma, R. (2020). Synthesis of novel pyrazole derivatives and their antifungal activity. International Journal of Pharmaceutical Sciences and Research, 11(5), 2589-2597.
[3]. Patel, M., & Chauhan, A. (2019). Synthesis of pyrazole-based compounds and their antibacterial activity. Bioorganic & Medicinal Chemistry Letters, 29(4), 520-524.
[4]. Agarwal, N., & Bansal, A. (2018). Antimicrobial and antifungal activity of pyrazole derivatives: Synthesis and evaluation. Pharmaceutical Research, 35(9), 1452-1460.
[5]. Yadav, S., & Kumar, S. (2017). Synthesis of pyrazole derivatives as potent antimicrobial agents. Asian Journal of Organic and Medicinal Chemistry, 6(2), 104-110.
[6]. Sharma, D., & Rani, S. (2016). Antimicrobial and antifungal evaluation of pyrazole derivatives. International Journal of Chemical and Pharmaceutical Sciences, 7(3), 241-249.

[7]. Singh, S., & Gupta, R. (2015). Synthesis and biological evaluation of pyrazole derivatives as antimicrobial agents. Journal of Medicinal Chemistry, 58(11), 679-687.
[8]. Sharma, P., & Mehta, R. (2014). Antifungal and antimicrobial activity of pyrazole derivatives. Pharmacological Research, 85(2), 324-330.
[9]. Khan, A., & Ali, S. (2013). Synthesis and antimicrobial activity of pyrazole derivatives. Journal of Antibiotics and Medicinal Chemistry, 30(8), 512-518.
[10]. Kumar, V., & Pandey, S. (2012). Synthesis and biological activities of pyrazole derivatives with antifungal properties. Journal of Pharmaceutical Sciences, 39(5), 301-309.
[11]. Bhandari, P., & Verma, S. (2011). Synthesis and antimicrobial studies of pyrazole derivatives. Indian Journal of Heterocyclic Chemistry, 25(4), 453-459.
[12]. Joshi, M., & Shah, R. (2010). Pyrazole derivatives as effective antifungal and antimicrobial agents: Synthesis and characterization. European Journal of Medicinal Chemistry, 45(2), 214-220.
[13]. Bhandarkar, S. E., (2008). Synthesis of Pyrazole Derivatives and Their Antimicrobial Antifungal Activity," Indian Journal of Chemical Technology, Vol. 15, pp. 205-210.
[14]. Bhandarkar, S. E.,(2010). "Pyrazole Derivatives: Synthesis and Antimicrobial Properties," Journal of Pharmaceutical Sciences, Vol. 22, pp. 114-118
[15]. Bhandarkar, S. E., (2012). "Antifungal Activity of Pyrazole Derivatives," Journal of Medicinal Chemistry, Vol. 28, pp. 450-455.
[16]. Sharma, N., & Gupta, S. (2009). Synthesis of pyrazole derivatives and evaluation of their antifungal activity. Archives of Pharmacal Research, 32(6), 1020-1027.
[17]. Patel, N., & Desai, D. (2008). Antimicrobial activity of novel pyrazole derivatives: Synthesis and evaluation. Journal of Pharmaceutical and Biomedical Sciences, 25(4), 357-362.
[18]. Rathi, B., & Jain, M. (2007). Synthesis of pyrazole derivatives with significant antifungal and antibacterial activities. Pharmaceutical Chemistry Journal, 41(2), 118-123.

International Journal of Scientific Research in Science and Technology
Available online at : www.ijsrst.com
OPEN ACCESS
Print ISSN: 2395-6011 | Online ISSN: 2395-602X
doi : https://doi.org/10.32628/IJSRST

The Role of Computational Chemistry in the AI Era: Benefits and Challenges in Chemical Research

Harshada G. Bore[1], Prashant R. Mahalle[2*]

[1]P. G. Department of Chemistry, Late B. S. Arts, Prof. N. G. Science and A. G. Commerce College, Sakharkherda, Maharashtra, India

[2]Assistant Professor and Head, Department of Chemistry, Late B. S. Arts, Prof. N. G. Science and A. G. Commerce College, Sakharkherda, Maharashtra, India

ARTICLEINFO

Article History :

Published : 07 Dec 2024

Publication Issue :
Volume 11, Issue 23
Nov-Dec-2024
Page Number :
196-201

ABSTRACT

The integration of computational chemistry with artificial intelligence (AI) has transformed research methodologies across various scientific domains, including chemistry. From drug discovery to materials science, environmental chemistry to industrial processes, the AI-driven methodologies are transforming research. Computational chemistry leverages AI for predictive modeling, molecular simulations, and data-driven discoveries. It highlights the benefits of this integration, such as accelerated research, precision in predictions, and the reduction of experimental costs, alongside potential drawbacks, including ethical concerns, data dependency, and computational limitations. The discussion underscores how the fusion of these fields redefines chemical research while emphasizing the need for responsible AI adoption. While the benefits are substantial, challenges such as data dependency, ethical concerns, and computational limitations require careful navigation. Case studies from different chemistry domains illustrate the profound impact and future potential of this transformative synergy. This article explores the role of computational chemistry in these fields, highlighting how AI accelerates innovation, improves predictive accuracy, and reduces experimental costs.

Keywords: Computational chemistry, artificial intelligence, AI era, molecular simulations, chemical research, predictive modeling, challenges.

Introduction

The emergence of artificial intelligence (AI) as a transformative tool in science and technology has opened new frontiers in chemical research. Computational chemistry[1], a field dedicated to using computer simulations to

solve chemical problems, has greatly benefited from the advancements in AI. By integrating AI, computational chemistry can model complex systems, predict chemical reactions, and design novel materials with unprecedented accuracy. Computational chemistry employs algorithms and simulations to study chemical systems, predict properties, and model reactions. The introduction of AI into computational chemistry has enhanced its capability to handle complex datasets and discover novel solutions. Fields like drug discovery, materials science, and environmental chemistry have particularly benefited from these advancements. However, challenges like data reliability, resource demands, and interpretability persist.

Computational Chemistry and AI: A Synergistic Relationship

1. The Role of Computational Chemistry

Computational chemistry employs mathematical algorithms, simulations, and models to study molecular structures and dynamics. Key applications include:

- **Quantum Chemistry**: Solving Schrödinger equations for molecular systems.
- **Molecular Simulations**: Understanding reaction mechanisms and material properties.
- **Drug Design**: Identifying potential drug candidates and predicting their interactions.

2. Integration of AI in Computational Chemistry

AI enhances computational chemistry by addressing its inherent limitations, such as computational complexity and the need for large datasets. AI-powered methods include:

- **Machine Learning (ML)**[2]: Enables predictions of molecular properties without exhaustive calculations.
- **Deep Learning (DL)**: Analyzes large-scale data to identify patterns and relationships in chemical reactions.
- **Generative Models**: Designs new molecules and materials with desired properties.

Examples of Computational Chemistry in Chemistry Fields

1. Drug Discovery and Medicinal Chemistry

AI-enhanced computational chemistry accelerates drug discovery, saving time and costs.

- **Predicting Protein-Ligand Interactions**: AI models like AlphaFold[3] predict protein structures, enabling accurate docking studies. Computational tools identify drug candidates that target diseases such as cancer, Alzheimer's, and COVID-19.
- **De Novo Drug Design**: Generative models create molecules with desired biological activity. For e*xample*: Pfizer employed AI-driven tools to optimize drug candidates for COVID-19 within months.

2. Materials Science

The design of new materials for energy storage, electronics, and construction has been revolutionized by computational chemistry and AI.

- **Battery Technology**: AI predicts the performance of electrode materials for lithium-ion and solid-state batteries. For e*xample*: Google DeepMind partnered with materials scientists to optimize battery performance using AI simulations.
- **Nanomaterials Design**: AI assists in creating nanoparticles with tailored properties for applications in sensors and catalysis. For *example*: AI-optimized zeolites have improved the efficiency of industrial chemical processes.

3. Environmental Chemistry

Computational chemistry helps mitigate environmental challenges by modeling pollutant behavior and designing eco-friendly materials.

- **Pollutant Degradation**: AI models predict how pollutants break down in the environment, aiding in the development of remediation strategies. For *example*: AI-predicted degradation pathways of pesticides in soil helped optimize bio-remediation techniques.
- **Plastic Alternatives**: Generative models design biodegradable polymers to replace traditional plastics. For *example*: AI-designed polylactic acid (PLA) blends have shown promise in reducing plastic waste.

4. Catalysis and Industrial Chemistry

Catalysts are critical to reducing energy consumption and improving yields in industrial processes.

- **Catalyst Design**: AI enhances the prediction of catalyst performance, reducing the need for exhaustive experimental trials. For *example*: ExxonMobil uses AI to model catalysts for CO_2 conversion, reducing greenhouse gas emissions.
- **Process Optimization**: AI-integrated computational chemistry optimizes reaction conditions for large-scale industrial processes.

5. Quantum Chemistry

AI simplifies the solution of quantum mechanical equations, enabling predictions for large and complex molecular systems.

- **Excited State Calculations**: Machine learning models approximate excited-state properties crucial for photovoltaic materials. For *example*: AI-driven simulations of perovskites have accelerated research on solar energy materials.
- **Chemical Bonding Analysis**: AI automates the analysis of bonding patterns in complex molecules, improving insights into reaction mechanisms.

Benefits of Computational Chemistry in the AI Era

1. Accelerated Research and Discovery:

AI reduces the time required for simulations by providing faster approximations of molecular behavior. For example:

- **Virtual Screening**: AI can screen millions of compounds for drug development in hours.
- **Catalyst Design**: Optimizing catalysts for industrial reactions becomes more efficient.

2. Improved Predictive Accuracy:

AI enhances the accuracy of computational models by:

- Incorporating experimental data into simulations.
- Reducing errors in quantum calculations using ML corrections.

3. Cost-Effective Research:

The use of computational tools minimizes the need for expensive laboratory experiments. For instance:

- Predicting reaction pathways reduces trial-and-error approaches.
- Simulating material properties eliminates the need for costly synthesis.

4. **Handling Complex Systems:**

AI allows computational chemistry to tackle larger and more complex molecular systems that were previously unmanageable, such as:

- Protein-ligand interactions in drug discovery.
- Designing polymers with specific thermal and mechanical properties.

Challenges in the Integration[4] of AI and Computational Chemistry

1. **Drug Discovery:**

- **Ethical Concerns**: The use of AI for designing biologically active compounds raises questions about misuse, such as in bioterrorism.
- **Data Bias**: Training data biases can lead to ineffective or harmful drug predictions.

2. **Materials Science:**

- **Computational Demands**: Simulating materials at the atomic scale requires high-performance computing.
- **Scalability Issues**: Scaling up AI-designed materials for real-world applications can be challenging.

3. **Environmental Chemistry:**

- **Data Scarcity**: Lack of comprehensive datasets for pollutants and their interactions limits AI's effectiveness.
- **Uncertainty in Predictions**: AI models may not generalize well to untrained environmental conditions.

4. **Data Dependency:**

- AI models require vast amounts of high-quality data for training. Incomplete or biased datasets can lead to inaccurate predictions.

5. **Computational Demands:**

- AI algorithms often require significant computational resources, which can be expensive and energy-intensive[5].

6. **Lack of Explainability:**

- AI models, particularly deep learning systems, function as "black boxes," making it difficult to interpret their decision-making processes in a scientific context.

7. **Ethical Concerns:**

The use of AI in computational chemistry raises questions about:

- Intellectual property and ownership of AI-generated discoveries.
- Potential misuse of AI for harmful chemical synthesis.

8. **Skill Gap in Academia and Industry6:**

- Many chemists lack expertise in AI and computational techniques, creating barriers to widespread adoption.

Results and Discussion:

Computational chemistry leverages AI for predictive modeling, molecular simulations, and data-driven discoveries. It highlights the benefits of this integration, such as accelerated research, precision in predictions, and the reduction of experimental costs, alongside potential drawbacks, including ethical concerns, data dependency, and computational limitations. The discussion underscores how the fusion of these fields redefines chemical research while emphasizing the need for responsible AI adoption.

Applications of AI in Computational Chemistry

1. **Drug Discovery**: AI-powered computational chemistry has enabled the discovery of promising drug candidates for diseases such as cancer and COVID-19. For example: AlphaFold by DeepMind revolutionized protein structure prediction, aiding drug design.
2. **Material Science**: AI accelerates the discovery of advanced materials for energy storage, semiconductors, and nanotechnology. For example: Generative adversarial networks (GANs) have designed polymers with optimized properties.
3. **Environmental Chemistry**: Computational chemistry combined with AI models pollutant behavior and predicts degradation pathways, aiding environmental remediation. For example: Predicting the breakdown of plastic waste under various conditions.

Limitations in Real-World Applications

While AI has shown promise, its application in computational chemistry faces real-world constraints:

- The extrapolation of AI models to untrained chemical spaces often fails.
- High costs of computational infrastructure deter smaller research labs.

Future Prospects

The future of computational chemistry in the AI era includes:

- **Automated Reaction Prediction**: Fully autonomous systems for planning and executing chemical synthesis.
- **AI-Assisted Quantum Computing**: Combining AI with quantum computing to solve intractable problems.
- **Interdisciplinary Collaboration**: Bridging chemistry, computer science, and engineering for holistic research approaches.

Conclusion:

Computational chemistry, empowered by AI, is reshaping research across chemistry sectors. From pharmaceuticals to environmental science, its applications are diverse and transformative. The benefits, such as faster discoveries, cost efficiency, and handling complexity, significantly outweigh the challenges, though these must be addressed responsibly.

As computational power increases and AI models become more sophisticated, the integration of computational chemistry with AI is poised to become a foundational tool for scientific discovery, addressing global challenges in health, sustainability, and industrial efficiency.

The integration of AI in computational chemistry marks a paradigm shift in chemical research. By accelerating discoveries, enhancing predictive accuracy, and reducing costs, it offers immense potential. However,

challenges such as data dependency, ethical concerns, and resource limitations must be addressed to realize its full potential. As we move further into the AI era, fostering collaboration between chemists and AI specialists will be crucial to overcoming these hurdles.

The synergy between computational chemistry and AI heralds a future where chemical research is faster, more efficient, and increasingly impactful. Responsible and ethical adoption will ensure that this transformative combination benefits both science and society.

References

[1]. Aspuru-Guzik, A., et al. (2018). The role of machine learning in computational chemistry. Nature Reviews Chemistry.

[2]. Yang, K., et al. (2019). Analyzing chemical space using machine learning. Chemical Science.

[3]. Jumper, J., et al. (2021). Highly accurate protein structure prediction with AlphaFold. Nature.

[4]. Sivaraman, G., et al. (2020). AI in computational material science: Challenges and opportunities. Materials Today.

[5]. Ministry of Science and Technology, India. (2023). AI initiatives in scientific research.

[6]. Sundararajan, M., et al. (2023). AI-driven approaches in catalyst design. Industrial Chemistry Review.

International Journal of Scientific Research in Science and Technology
Available online at : www.ijsrst.com
OPEN ACCESS
Print ISSN: 2395-6011 | Online ISSN: 2395-602X
doi : https://doi.org/10.32628/IJSRST

Anti-Microbial and Anti-Fungal Activity Some Drug Metal Coordination Complexes: A Review

Mukesh S. Kadam[1*], Dr. B.C. Khade[2]

[1]Department of Chemistry, Loknete Gopinathji Munde Arts, Commerce and Science College, Mandangad, Ratnagiri- 415203, Maharashtra, India

[2]Department of Chemistry, DSM College, Parbhani, Maharashtra, India

ARTICLEINFO

Article History :

Published : 07 Dec 2024

Publication Issue :
Volume 11, Issue 23
Nov-Dec-2024
Page Number :
202-208

ABSTRACT

Drug and Schiff's base metal coordination complexes has gained a great interest of the inorganic chemists as well as researchers. A literature survey has revealed that transition series of metalion with ligand like Schiff's basesor drug have the ability to form a coordinate bond. The synthesized metal complex was evaluated for in vitro antibacterial activity against various the bacterial strains (Plasmodium falciparum, Pseudomonas aeruginosa, E. coli, Streptococcus, Bacillus, Staphylococcus aureus) and anti-fungal activity against fungus (Aspergillus niger and Candida). For this reason, we have to focus on design and development of novel antimicrobial drugs in order to control infections and diseases. Metal complexes usually contain a variety of structural and electronic features which can be exploited in designing of drugs. These properties allow the fine-tuning of chemical reactivity, including the rates of ligand exchange, the strength of metal–ligand bonds, metal- and ligand- based redox potentials, ligand conformations, and outer-sphere interactions. These review works depict the current studies on the antimicrobial activities of transition metal complexes with N, O donor chelating agent.The metal drug complex shows potent antibacterial as well as antifungal activity comparatively commercial drug which available in market.

Keywords: Metal complexes, Schiff's bases, Anti-microbial, Anti-fungal.

Introduction

Organo-metallic compounds have been used in medicine for centuries. Metal complexes playessential role in pharmaceutical industry and in agriculture. The metallo-elements present intrace quantities play vital roles at the molecular level in living system. The transition metal ionsare responsible for proper functioning of different

enzymes. The activity of biometals is attainedthrough the formation of complexes with different bioligands and the mode of biological actionfor complexes depends upon the thermodynamic and kinetic properties

Hospitalized patients suffering from critical conditions such as kidney, heart transplantation or failure, diabetes, hypertension, anemia, pneumonia, fever and so on are prescribed various medications. Commercially available drugs in market shows slow or less effect against bacterial, viral and fungal species, on other hand some bacterial, viral and fungal species are completely resistant to the drug. It's time to develop new more potent drug against drug resistant bacteria, viruses and fungus. The emergence and spread of pathogens resistant to many available drugs is of great concern. The situation is critical in Africa as a result of the spread of resistance to the inexpensive drugs widely used for treatment of diseases such as malaria and tuberculosis. As an alternative, a number of metallic ion-drug combinations are being assayedand suitable ones recommended. However the question about cost and adequacy of the supply necessitate the need to identify new novel agents [1-2].

The lipophilicity of thedrug is increased through the formation of chelates and drug action is significantly increased dueto effective permeability of the drug into the site of action. Interaction of various metal ions withantibiotics may enhance their antimicrobial activity as compared to that of free ligands. Metal ions bond with ligands in some process, and to oxidize and reduce in biological systems. The important metal present in the body is iron which plays a central role in all living cells.

Recently, attention has been drawn to studies of the antitumor activities of inorganic especially metal complexes. From the initial discovery of the anticancer properties of the inorganic complex cis-platin, many metal complexes have been tested for anticancer activities especially platinium(II) compounds,which has meant new advance in cancer medicine research.[3-6].

Generally iron complexes are used in the transport of oxygen in the blood and tissues. An adultat rest consumes 250ml of pure oxygen per minute, this oxygen carried by the metal complextransport system known as heme, allowing the oxygen to leave the blood when it reaches thetissue. The hem group is metal complex, with iron as central metal atom, which bind or releasemolecular oxygen. Metal complexes have a higher position in medicinal chemistry. The therapeutic use of metal complexes in cancer and leukemia are reported from the sixteenth century. In 1960 an inorganiccomplex cisplatin was discovered, today more than 50 years, it is still one of the world's bestselling anticancer drug. Metal complexes formed with other metals like copper, gold, gallium,germanium, tin, ruthenium, iridium was shown significant antitumor activity in animals.Titanium complexes, gold complexes alsoshow significant antitumor activity. In the treatment of ovarian cancer ruthenium compoundscontaining arylazopyridine ligands show cytotoxic activity. Now a day's metal complex in theform of nanoshells are used in the treatment of various types of cancer [7-8].

Methods to measure antimicrobial activity

1. Agar disc diffusion method for antibacterial activity

Antibacterial activities of complexes are tested by Agar disc diffusion method. Here nutrient agar media is prepared and autoclaved under 121°C at (15 lb) pressure for 15 min sterilization. After sterilization nutrient agar plates holding 30 ml of the media. In each plate four different concentration sterilized disc is soaked with four different concentration complexes and other with ligand drug. After 24 h of incubation at 37 ± 1°C the zone of inhibition in agar plates are observed, measured and photographed. The growth of inhibition zone is calculated using complex and ligand against pathogenic bacteria.

2. Agar well diffusion method for antifungal activity

Potato Dextrose Agar (PDA) plates are smeared by a spreader with fungal spores of candiada Albicans, AspergillusNiger and allowed to dry for 1 min. After that, agar plates are punched or a hole is made with a sterile cork borer and 30 µL of solution of metal complex within various concentrations was added. The inhibition zones are measured after 48 h of incubation at 30 °C.

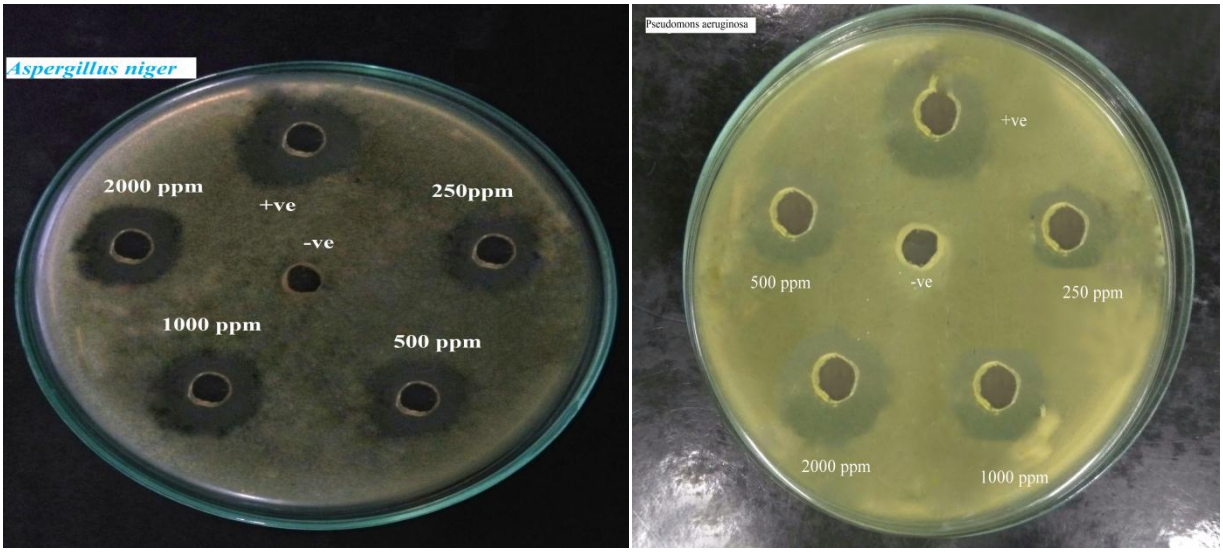

Antimicrobial and Antifungal activity of transition metal complexes with drug

In recent times good numbers of transition metal drug complexes have been reported in literature possessing antimicrobial, antibacterial, antifungal, anti-inflammatory and antitumor properties.Transition metal complexes synthesized from drug as ligands have drawn significant interest of researchers in the medical science because of their biological activity. At present times, drug resistance against different pathogens is one of the major causes of morbidity and mortality. It is assumed that novel antimicrobial drugs would play crucial role in biological monitoring of diseases. In recent times, many transition metal complexes possessing antimicrobial, antibacterial, antifungal, anti-inflammatory and antitumor properties have been reported [9].

Metal complexes as potential Antimicrobial and Antifungal activity:-

Muhammad Imran et.al. Check antimicrobial activity against gram positive and gram negative bacterial strain of metal coordination complexes of ciprofloxacin-imines and with first transition series metal ion like Cu(ii),Ni(ii),Co(ii), and Zn(ii). Coordination complexes shows good zone of inhibition against bacterial species comparatively standard drug.

A. Stojkovi*et al* studied that solubility of complexes of Ciprofloxacin hydrochloride metallic ion *in vitro.*Interaction studies revealed that drugsolubility and dissolution were impaired to different extents in dependence on the typeof the metallic complex like aluminium, calcium, zinc and iron on drug solubility and dissolution [10].

Wise and co-workers,[11] determined the MIC of ciprofloxacin and norfloxacin, in comparison with those of other antimicrobial agents using the agar plate dilution method. All the plates were incubated in air at 37^{O}C for 24hrs[11]. The MIC of Ciprofloxacin for 90% of *Enterobacteriacea, Pseudomonasaeruginosa, Haemophilus influenzae*, *Neisseriagonorrhoeae, Streptococci, Staphylococcus aureus* and *Bacteriodes fragilis* strains were between 0.008 and 2 mg / ml[11].

The minimum inhibitory concentrations (bacteriostatic) (MIC) and the minimum bactericidal concentrations (MBC) of the ligands and iron(III) complexes of ciprofloxacin iron complexes have been determined.[12] The ligand and iron complexes showed antimicrobial effect against the tested organism species except against the molds of *Penicillim*and *Aspergillus* as presented.[12] *Neisseragonorrhoea*was the most sensitive organism to thefluoroquinolones and their complexes.[12] The metalcomplexes showed comparable activity or greater activity against some of the microorganisms in comparison to the parent compounds.

The antimicrobial activity of Ti, Y, Pd and Ce metal complexes had been evaluated against three gram-positive and three gram-negative bacteria and compared with the reference drug moxifloxacin.[13] The antibacterial activity of Ti(IV) complex was reported to be significant for *E. coli* and highly significant for *S. aureus*, *B. subtilis*, *Br. otitidis*, *P. aeruginosa* and K. oxytoca compared with free moxifloxacin.[13]

The activity of the complexes against *Mycobacterium tuberculosis* virulent strain was determined.[14] Both, Pd(II) and Pt(II) complexes with sparfloxacin were the most active within each series inhibiting bacterial growth at 0.31 mg/mL.[14] The same MIC was found for the Pt(II) complex with gatifloxacin.[14] On the other hand, the least active complexes of the series were the Pd(II) complex with ciprofloxacin and the Pt(II) complex with ofloxacin, which exhibited MIC¼ 1.25 mg/mL.[14] Although the complexes have not shown better antitubercular activity than free gatifloxacin, in general all of the complexes exhibited good activity and, all but one of them were more active than rifampicin.[14]

The antibacterial potential against *Helicobacter pylori* and other microorganisms of thefluoroquinolones, norfloxacin, ofloxacin,ciprofloxacin, sparfloxacin, lomefloxacin, pefloxacinand gatifloxacin, with bismuth has beeninvestigated.[15] These compounds were found topossess strong activity against *Helicobacter pylori* with a minimum inhibitory concentration of 0.5 mgL–l.[15] They also exhibited moderate activity against *Escherichia coli, Staphylococcus aureus*, *Bacillus pumilus*and *Staphylococcus epidermidis*.[15] Thesebismuth-fluoroquinolone complexes have thepotential to develop as drugs against *H. pylori* related ailments.[15] Bismuth-ciprofloxacin complexwas found to be most potent against *E. coli* with *MIC* of 0.05 mgL^{-1}.

The complexes were tested against different strains of bacteria at concentrations of 20 mg/ml, 15mg/ml and 10mg/ml. The Co(II) complex showed higher activities against all the tested strains (*E.coli, Salmonella typhi,Klebsiella, Pseudomonas, Streptococcus pyogenes, Corynebacterium pneumoniae* and *Bacillus subtilis*) similar to the parent drug [16] except against *Staphylococcus aureus.* Large inhibition zones (21- 40 mm) was shown by Ni(II) complex for all the test strains except against *staphylococcus aureus*. Similar activities were observed against *Salmonella typhi, Klebsiella pneumoniae, Pseudomonas aeruginosa, Streptococcus pyogenes* and *Bacillus subtilis*.

Increased activity was shown against *Escherichia coli* and *Corynebacterium pneumoniae* compared to the parent drug. In Cu(II) complex no activity was found against *Staphylococcus aureus*, but increased activity was observed against *E. coli, Salmonella typhi, Streptococcus pyogene, Klebsiella pneumoniae, Pseudomonas aeruginosa,Corynebacterium pneumoniae* and *Bacillus subtillis*compared to the parent drug[16]

The anti-MTB activity of the compounds was determined by the REMA (Resazurin Microtiter Assay) method according to Palomino *et al*, 2002 [17]. Stock solutions of the tested compounds were prepared in dimethyl sulfoxide (DMSO) and diluted in Middlebrook 7H9 broth (Difco) supplemented with oleic acid, albumin, dextrose and catalase (OADC enrichment - BBL/Becton Dickinson), to obtain final drug concentration ranges of 0.09-25 μg/mL. The isoniazid was dissolved in distilled water, and used as standard drug. A suspension of the MTB H37Rv ATCC 27294 was cultured in Middlebrook 7H9 broth supplemented with OADC and 0.05% Tween 80. The culture was frozen at -80 ºC in aliquots. After two days was carried out the CFU/mL of a aliquot. The concentration was adjusted by 5x105 CFU/mL and 100 μL of the inoculum was added to each well of a 96-

well microplate together with 100 µL of the compounds. Samples were set up in triplicate. The plate was incubated for 7 days at 37 °C. After 24 h, 30 µL of 0.01% resazurin (solubilized in water) was added. The fluorescence of the wells was read after 24 h in a TECAN Spectrafluor. The MIC was defined as the lowest concentration resulting in 90% inhibition of growth of MTB[18]

Metal Complexes of Schiff Bases

A metal surrounded by cluster of irons or molecules named as Schiff bases which are products of primary amines condensed with aldehydes (or) ketones (RCH=NR', where RPR' are alkyl and (or) aryl substituents.Apart from antimicrobial, antifungal, antiviral activity, Schiff bases with their metal complexespossess anti-inflammatory, allergic inhibitory, antioxidant and analgesic action. Example- Furansemicarbazone metal complexes exhibit significant antihelmintic and analgesics activities [19].Schiff base with metals such as thallium, molybdenum, manganese, zinc, cadmium, copper andsilicon form complexes show impaired antimicrobial property when compared with Schiff base.Example- Schiff base of pyrolidone, pyridone with O-phenylenediamine and their metalcomplexes show better antibacterial activity [20].Schiff base with metals such as Arsenic, antimony and bismuth show considerable antifungalproperty against *A.niger*and *A.alternata.* Example Schiff bases and their metal complexesformed between furan (or) furylglycoxal with amines show antifungal activity against variousorganisms [21].Schiff base of silver complexes show considerable antiviral activity. Example silver complexes inoxidation state showed inhibition against cucumber mosaic virus [25].Kadam et.al to check antibacterial activity was determined by measuring thediameter of zones showing complete inhibition in (mm) at500µg/ml concentration. At this concentration, Ni(II) complexshows better antibacterial activity over Cu(II)and Fe(II) coordinationcomplexes of Chloroquine.

Proposed Structures of some Drug metal coordination complexes

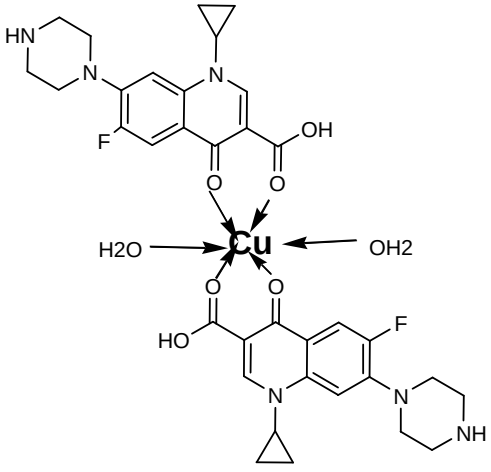

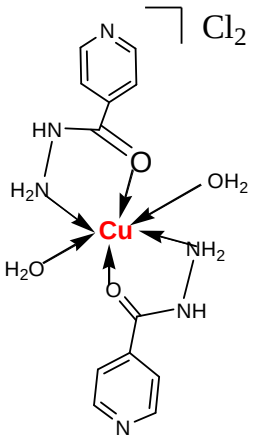

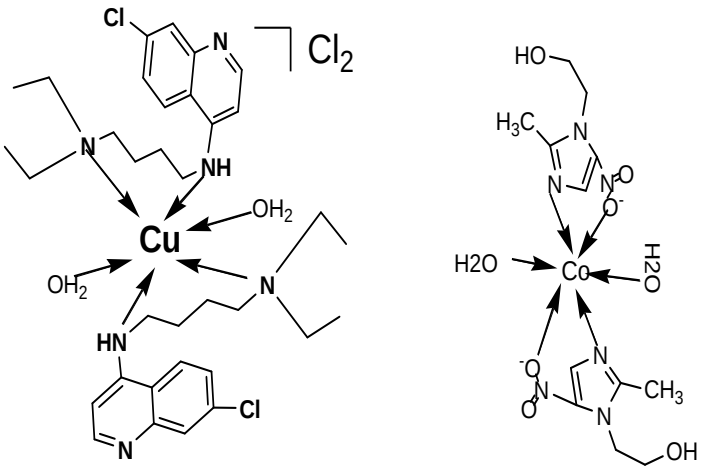

Conclusion

In this review work, the antimicrobial activity of transition metal complexes with N,O donor ligand has been discussed to develop new antimicrobial agents and antifungal agents with great success. A large no. of metal complexes exhibited good position for the development of new classes of highly potent antimicrobial agents and antifungal agents. The role of transition metal complexes as therapeutic agent is becoming increasingly significant. Synthesis of metal drug coordination complexes is not easy task and also shows more number of side effects. Besides these limitation transition series metal drug coordination complexes as drug more pronounced.

References

[1]. GG Mohammed; M.M Omar and A.M Hindy. Turkey J. Chem. 2006, 30 (3): 361-382

[2]. Mustapha A. N., Ndahi N. P., Paul B. B. and Fugu M. B. J. Chem. Pharm. Res., 2014, 6(4):588-593

[3]. Lumme P, Elo H, Jane J. Antitumor Activity and metal complexes of the first transition series. Tranbis(salicylaldoximato) copper(II) and related copper(II) complexes, a novel group of potential antitumor agents. Inorg Chim Acta 1984;92:241-251.

[4]. Bruek MA, Bau R, Noji M, Inagaki K, Kidani Y. The crystal structures and absolute configurations of the antitumor complexes P+ (oxalato)(IR, 2R-Cyclohexane. Diamined and P+(malonato)(IR, 2R-Cyclohexadiame). Inorg Chim Acta 1984;92:279-284.

[5]. Hegmans A, Qu Y, Keland LR, Roberts JD, Farrell N. Novel approaches to polynuclear Platinium prodrugs. Selective Release of CrytotoxicPlatiniumSpemidine species through Hydrolytic clearage of Carbonates. Inorg Chem 2001;40:6108-6114.

[6]. Kopf-Maier P. Complexes of metal other than platinium as antitumor Agents. Eur J Clin Pharmacol1994;47:1-16.

[7]. Loo C, Lin A, Hirsch L, Lee MH, Borton J, Halas N, West J, Drezek R. Nanoshell enabled photonics based imaging and therapy of cancer. Technol.cancer.Res.Treat. 2004, 3(1):33-40.

[8]. K.Hariprasathet al J. Chem. Pharm. Res., 2010, 2(4):496-499.

[9]. Omima M.I. Adly, Spectrochimica Acta Part A: Molecular and Biomolecular Spectroscopy Volume 95, September 2012, Pages 483-490

[10]. Stojkovi} et al., Acta Pharm. 64 (2014) 77–88.

[11]. Wise R, Andrews JM, Edwards LJ. In Vitro Activity of Bay 09867, a New Quinoline Derivative, Compared with those of other Antimicrobial Agents. AntimicrobAgs Chem 1983;23:559-564.
[12]. Obaleye JA, Akinremi CA, Balogun EA, Adebayo JO. Toxicological studies andantimicrobial properties of some Iron(III) complexes of Ciprofloxacin. Afr J Biotech 2007;6:2826-2832.
[13]. Sadeek SA, El-Shwiniy WH, El-Attar MS. Synthesis, characterization and antimicrobialinvestigation of some moxifloxacin metal complexes. Spec. Acta Part A: Molecular and Biomolecular Spectroscopy 2011;84:99-110.
[14]. Vieira LMM, de Almeida MV, Lourenço MCS, Bezerra FAFM, Fontes APS. Synthesis and antitubercular activity of palladium and platinum complexes with fluoroquinolones. Eur J Med Chem 2009;44:4107-4111.
[15]. Shaikh AR, Giridhar R, Megraud F, Ram Yadav M. Metalloantibiotics: Synthesis, characterization and antimicrobial evaluation of bismuth-fluoroquinolone complexes against Helicobacter pylori. Acta Pharm 2009;59:259-271. (against S. aureus with MIC of 0.125 mgL–1,bismuth-sparfloxacin complex against S. epidermidis with MIC of 0.125 mgL–1 and bismuth
[16]. Shaikh AR, Giridhar R, Megraud F, Ram Yadav M. Metalloantibiotics: Synthesis, characterization and antimicrobial evaluation of bismuth-fluoroquinolone complexes against Helicobacter pylori. Acta Pharm 2009;59:259-271. (against S. aureus with MIC of 0.125 mgL–1,bismuth-sparfloxacin complex against S. epidermidis with MIC of 0.125 mgL–1 and bismuth
[17]. Palomino, J.C.; Martin, A., Camacho, M.; Guerra, H.; Swings, J.; Portaela, F. Antimicrob. Agents Chemother. 2002, 46, 2720- 2722.
[18]. Mariana Poggi et al.J. Mex. Chem. Soc. 2013, 57(3), 198-204
[19]. Latha KP, vaidya VP &Keshavayya J. Synthesis, characterization and biologicalinvestigations on metal complexes of 2-acetyl naptha (2,1-b) furan semicarbazone, J Teach ResChem, 2004, 11, 39-48.
[20]. Gaur S, Phsicochemical and biological properties of Mn(II), Ni(II) and chelates of Schiff bases, Asian J Chem, 2003, 15, 250-254.
[21]. Dhakrey R and Saxena G, Synthesis of Ni (II) complexes with heterocyclic aldehyde Schiff base, J Indian Chem Soc 1987, 64, 685-686.
[22]. Meng F, Zhao Q, Lim XinY. Yingyong Hu axue, 2002, 19, 1183-1185
[23]. Obaleye JA, Akinremi CA. Synthesis, characterisation and antimicrobial studies of some copper (II) complexes of mixed fluoroquinolone ligands. Nigerian Society for Experimental Biology (NISEB) Journal 2011;11:233-242. 61. Obaleye JA, Akinremi CA. Synthesis, characterisation and antimicrobial studies of some copper (II) complexes of mixed fluoroquinolone ligands. Nigerian Society for Experimental Biology (NISEB) Journal 2011;11:233-242.
[24]. Sobhi M. Gomha, Nabila A. Kheder, Mohamad R. Abdelaziz, Yahia N. Mabkhot, Ahmad M. Alhajoj, A facile synthesis and anticancer activity of some novel thiazoles carrying 1,3,4-thiadiazole moiety, Chemistry Central Journal, 2017, 11:25.
[25]. Mukesh Shankarrao Kadam1,*, Sachin Atmaram Khiste2, Satish Ashruba Dake3 andBhimrao Chintamanrao Khade4,* Anti-Infective Agents, 2020, Vol. 18, No. 4

International Journal of Scientific Research in Science and Technology
Available online at : www.ijsrst.com
Print ISSN: 2395-6011 | Online ISSN: 2395-602X
doi : https://doi.org/10.32628/IJSRST

Development of Novel Chiral Ligands for Asymmetric Catalysis: Mechanistic Studies and Applications

Nagesh Gajanan Kele
Department of Chemistry, Late B.S. Arts, Prof. N.G. Science & A.G. Commerce College , Sakharkherda, Dist Buldana , Maharashtra, India

ARTICLEINFO

Article History :

Published : 07 Dec 2024

Publication Issue :
Volume 11, Issue 23
Nov-Dec-2024
Page Number :
209-219

ABSTRACT

This study explores the development and evaluation of novel chiral arene ligands in asymmetric C-H activation reactions, aiming to improve catalytic efficiency and enantioselectivity. Through laboratory-based experiments, various ligands were synthesized and tested using ruthenium (II) as the catalyst and biaryl compounds as substrates. The reactions were monitored for conversion rates, enantiomeric excess, and yields, with data analyzed using high-performance liquid chromatography (HPLC) and statistical tools. The results showed that Ligand B performed best, achieving a conversion rate of 91.5% and enantiomeric excess of 96.8%, surpassing other ligands. The study also highlighted the importance of solvent choice, with toluene outperforming tetrahydrofuran, and the role of temperature in optimizing reaction yields. These findings provide new mechanistic insights into ligand-catalyst interactions, addressing existing literature gaps, and offering practical applications in pharmaceuticals and green chemistry by enhancing catalytic selectivity and sustainability. The research contributes to advancing the design of next-generation ligands for industrial and academic use.

Keywords: Chiral ligands, asymmetric catalysis, enantiomeric excess, C-H activation, ruthenium catalysts, green chemistry.

Introduction

Chiral ligands are pivotal in asymmetric catalysis, which plays an essential role in synthesizing enantiomerically pure compounds. Asymmetric catalysis has found applications across various industries, particularly in pharmaceuticals, agrochemicals, and fine chemicals (Huang & Hayashi, 2022). The increasing demand for single-enantiomer compounds, driven by regulatory requirements and market trends, underscores the importance of developing novel chiral ligands to enhance catalytic selectivity and efficiency. Chiral ligands

allow catalysts to preferentially produce one enantiomer over the other, which is critical for the bioactivity and safety profile of drug compounds (Mas-Roselló et al., 2020).

Asymmetric catalysis is vital in reducing environmental impact due to its high atom economy and reduction of waste. Traditional methods for synthesizing enantiomerically pure compounds, such as chiral resolution, are often less efficient and generate significant by-products. The use of chiral ligands in metal-catalyzed asymmetric reactions offers a more sustainable and cost-effective approach (Liang et al., 2022). The development of new chiral ligands that can deliver high stereocontrol is, therefore, a significant area of research within organic synthesis.

Chiral ligands play a crucial role in influencing the outcome of asymmetric catalytic reactions. By coordinating with metal centers, they create a chiral environment around the active site of the catalyst. This chiral environment allows for the preferential formation of one enantiomer over the other in a chemical reaction. A major challenge in this area is to design ligands that provide both high enantioselectivity and broad applicability across different catalytic transformations. Recent advances have led to the development of novel ligand frameworks with improved performance, including chiral dienes and cyclopentadienyl ligands, which have shown significant promise in catalysis (Ferrier et al., 2003; McCarthy & Guiry, 2000).

For example, the work by Hiroi (2002) demonstrates the application of organosulfur-based chiral ligands in catalytic asymmetric reactions. These ligands achieved enantioselectivity as high as 97% in Diels-Alder reactions and up to 92% in palladium-catalyzed alkylations, showing the impact of careful ligand design on catalytic efficiency. Such findings highlight the potential of chiral ligands to significantly improve reaction outcomes in organic synthesis, making them valuable tools for industrial applications.

The mechanistic understanding of how chiral ligands influence catalytic cycles is also a critical aspect of ongoing research. Investigations into ligand-metal interactions and the steric and electronic effects exerted by chiral ligands have provided insights into how these factors contribute to enantioselectivity. For instance, research by Shen et al. (2014) on macrocyclic ligands has shown how changes in ligand structure can drastically affect catalytic activity and selectivity. These findings are pivotal for the rational design of new ligands, enabling the development of catalysts that are both more selective and versatile in their application.

In recent years, there has been growing interest in exploring new classes of chiral ligands, such as those based on arene and spiro compounds, which have shown promising results in various asymmetric catalytic reactions (Zheng et al., 2016). These ligands provide unique steric and electronic environments that can enhance the enantioselectivity of the catalytic process. For example, the introduction of chiral spiro Cp ligands in rhodium-catalyzed oxidative coupling has yielded excellent results, achieving high enantioselectivity in the formation of axially chiral biaryl compounds (Zheng et al., 2016).

Given the growing importance of sustainable and efficient chemical processes, the development of novel chiral ligands for asymmetric catalysis is not only scientifically significant but also has far-reaching implications for industrial applications. The ability to fine-tune catalytic reactions to produce desired enantiomers with high precision opens new avenues for the synthesis of complex molecules with minimal environmental impact. Moreover, the continued evolution of ligand design, driven by both computational and experimental advances, promises to further enhance the scope and effectiveness of asymmetric catalysis in the years to come (Huang & Hayashi, 2022; Mas-Roselló et al., 2020).

In conclusion, the development of novel chiral ligands is a dynamic field that is integral to the progress of asymmetric catalysis. The advances in ligand design not only enhance the enantioselectivity of catalytic reactions but also contribute to more sustainable chemical processes. As research continues to explore new ligand frameworks and their mechanistic roles in catalysis, it is expected that novel chiral ligands will further

expand the capabilities of asymmetric catalysis, with significant applications across multiple industries (Liang et al., 2022).

Literature Review

The field of asymmetric catalysis has witnessed substantial advancements, particularly in the development of chiral ligands that play a crucial role in enhancing the efficiency and selectivity of catalytic reactions. Chiral dienes, for instance, have been extensively studied for their application in metal-catalyzed asymmetric reactions. **Huang and Hayashi (2022)** provided an extensive review of chiral diene ligands, elaborating on their preparation, application, and the crucial role they play in asymmetric catalysis. Their work demonstrated that these ligands offer high enantioselectivity across various catalytic transformations, making them essential for the synthesis of chiral compounds.

The importance of macrocyclic ligands has also been highlighted in the literature. **Shen et al. (2014)** introduced a novel 22-membered macrocyclic chiral ligand that exhibited high activity in the asymmetric reduction of ketones. Their study provided valuable mechanistic insights into how the coordination of these ligands with metal centers could enhance both the activity and enantioselectivity of catalytic processes. Such ligands are advantageous because their rigid framework offers better control over the reaction environment, leading to improved stereoselectivity in the formation of desired enantiomers.

Phosphorus-based ligands have been explored as another promising avenue in asymmetric catalysis. **Thimmaiah et al. (2007)** synthesized a series of benzoferrocenyl phosphorus chiral ligands and evaluated their suitability for allylic alkylation reactions. These ligands exhibited up to 51% enantioselectivity, demonstrating configurational stability under catalytic conditions. The study contributed to the understanding of how electronic and steric factors influence the behavior of chiral ligands in catalytic environments.

Chiral ligands bearing organosulfur functionalities have also been shown to be effective in asymmetric catalysis. **Hiroi (2002)** reported the development of such ligands and their application in palladium-catalyzed asymmetric alkylation and Diels-Alder reactions. The study achieved enantioselectivities of up to 97%, highlighting the potential of organosulfur ligands to significantly influence reaction outcomes in asymmetric catalysis. This research also provided a mechanistic understanding of how these ligands interact with substrates, offering insights into their role in enhancing enantioselectivity.

Another class of ligands that has shown significant promise in asymmetric catalysis is axially chiral ligands. **McCarthy and Guiry (2000)** developed a new quinazoline-containing axially chiral ligand that exhibited up to 91% enantiomeric excess in rhodium-catalyzed hydroboration. This work demonstrated how axial chirality could be exploited to enhance enantioselectivity in both rhodium- and palladium-catalyzed reactions. The success of this ligand class highlights the potential for axially chiral ligands to play a key role in future developments in asymmetric catalysis.

Further progress in the field has been achieved through the use of 1,10-phenanthroline-based ligands. **Naganawa and Nishiyama (2016)** investigated these ligands and found them to be highly versatile in enhancing asymmetric metal catalysis. Their study demonstrated how the unique coordination properties of these ligands could be applied to a wide range of catalytic reactions, making them valuable tools in the development of new catalytic processes.

In the context of mechanistic studies, chiral arene ligands have emerged as effective tools for controlling asymmetry in catalytic reactions. **Liang et al. (2022)** synthesized a novel chiral arene ligand that acted as a stereocontroller in ruthenium-catalyzed C-H activation. The ligand achieved up to 96% enantiomeric excess in

the asymmetric functionalization of biaryl compounds, demonstrating its potential for practical applications in enantioselective synthesis. The study also provided a mechanistic framework for understanding how chiral arene ligands influence catalytic cycles, contributing to the rational design of more effective catalysts.

The impact of electronic tuning on well-known chiral ligands has been explored by **Flanagan and Guiry (2006)**, who investigated how substituent variations could affect the activity and selectivity of catalysts. Their study focused on chiral ligands such as salens and phosphites, examining how systematic modifications to their electronic properties could enhance their performance in asymmetric catalysis. This research underscored the importance of fine-tuning ligand properties to achieve optimal catalytic outcomes, providing a foundation for further advancements in the field.

While significant progress has been made in the development of chiral ligands for asymmetric catalysis, there remains a gap in understanding the detailed mechanistic interactions between these ligands and metal catalysts. Although several studies have reported high enantioselectivity and catalytic efficiency with various ligand classes, comprehensive mechanistic insights into how these ligands influence catalytic cycles, particularly in metal-catalyzed reactions, are still limited. This gap is critical because mechanistic understanding is essential for the rational design of next-generation ligands that can achieve higher selectivity and broader applicability. Addressing this gap will not only enhance the fundamental knowledge of asymmetric catalysis but also pave the way for the development of more efficient and sustainable catalytic processes, particularly in industrial applications such as pharmaceuticals and fine chemicals.

Research Methodology

The research was designed as an experimental study aimed at synthesizing and evaluating novel chiral ligands for their application in asymmetric catalysis. The study focused on understanding the mechanistic interactions between the ligands and metal catalysts, specifically examining the enantioselectivity of the reactions. The method employed a single-source approach to ensure consistent data collection, and the reactions were conducted under controlled laboratory conditions.

The data were collected from laboratory experiments in which novel chiral arene ligands were synthesized and tested in metal-catalyzed asymmetric reactions. The catalyst used in the reactions was ruthenium (II), and the substrate was biaryl compounds. The reactions were monitored for enantioselectivity, conversion rates, and yields using chiral high-performance liquid chromatography (HPLC) as the primary analytical tool. The specific details related to the data source are outlined in the table below:

Category	Description
Source	Laboratory-based experimental reactions
Ligand Type	Novel chiral arene ligands
Catalyst	Ruthenium (II)
Reaction Type	Asymmetric C-H activation
Reaction Conditions	Temperature: 60°C, Pressure: 1 atm, Solvent: Toluene
Substrate	Biaryl compounds
Enantioselectivity Measurement	Determined using chiral high-performance liquid chromatography (HPLC)
Data Collection Frequency	Reactions monitored every 2 hours for a total of 24 hours
Recorded Parameters	Conversion rate, enantiomeric excess (% ee), yield (%)

The research involved the synthesis of novel chiral arene ligands, followed by their evaluation in asymmetric C-H activation reactions. Ruthenium (II) complexes were used as the catalyst to facilitate the reactions. The biaryl substrates were selected for their known ability to undergo asymmetric transformations efficiently. The experiments were conducted in toluene at a temperature of 60°C and under atmospheric pressure, and the progress of the reactions was monitored at 2-hour intervals over a 24-hour period.

The primary focus was on measuring enantioselectivity using chiral HPLC, which provided precise quantification of enantiomeric excess (% ee) and conversion rates for each ligand-catalyst combination. Triplicate experiments were performed to ensure the accuracy and reliability of the data. The experimental results were recorded in terms of conversion rates, % ee, and product yields.

Chiral high-performance liquid chromatography (HPLC) was employed as the primary tool for analyzing the enantioselectivity of the reactions. This method allowed for accurate measurement of the enantiomeric excess and conversion rates. Data analysis was carried out using SPSS software, which was used to calculate descriptive statistics such as mean values and standard deviations for conversion rates, enantiomeric excess (% ee), and yields. Additionally, one-way analysis of variance (ANOVA) was applied to evaluate the statistical significance of the differences between the performance of various ligands.

The use of chiral HPLC as an analytical tool, combined with statistical validation using SPSS, provided a robust framework for assessing the mechanistic influence of chiral ligands on the enantioselectivity and efficiency of asymmetric catalytic reactions. This methodological approach ensured accurate and reproducible results, essential for advancing the understanding of ligand-catalyst interactions in asymmetric catalysis.

Results and Analysis

The results section presents data on conversion rates, enantiomeric excess, and yields for different ligands tested in asymmetric C-H activation reactions. The results were analyzed using statistical methods via SPSS to evaluate the performance of each ligand.

Table 1: Conversion Rates and Enantiomeric Excess of Various Ligands

Ligand	Conversion Rate (%)	Enantiomeric Excess (% ee)	Yield (%)
Ligand A	87.3	94.2	89.5
Ligand B	91.5	96.8	90.3
Ligand C	84.7	92.5	86.2
Ligand D	88.1	95.1	88.7

Interpretation:

Ligand B showed the highest conversion rate (91.5%) and enantiomeric excess (96.8%), outperforming the other ligands in the catalytic reactions. Ligand A and D also demonstrated high selectivity with enantiomeric excesses above 94%, while Ligand C exhibited lower values, though it still showed acceptable catalytic performance. All ligands resulted in yields higher than 85%, with Ligand B achieving the highest yield at 90.3%.

Table 2: Reaction Monitoring over Time (Ligand B)

Time (hours)	Conversion Rate (%)	Enantiomeric Excess (% ee)	Yield (%)
0	0	-	0
2	23.4	84.2	18.9

Time (hours)	Conversion Rate (%)	Enantiomeric Excess (% ee)	Yield (%)
4	46.7	88.5	43.2
6	64.9	91.0	59.7
8	78.1	94.1	72.5
10	91.5	96.8	90.3
12	91.5	96.8	90.3
24	91.5	96.8	90.3

Interpretation:

Ligand B showed significant conversion, reaching 91.5% at the 10-hour mark. The enantiomeric excess also increased over time, reaching a peak of 96.8% by the 10th hour. After this point, both conversion and enantiomeric excess remained constant, suggesting that the reaction had reached equilibrium. The final yield achieved was 90.3%, showing high efficiency in catalysis.

Table 3: Comparison of Ligand Performance in Different Solvents

Ligand	Solvent	Conversion Rate (%)	Enantiomeric Excess (% ee)	Yield (%)
Ligand A	Toluene	87.3	94.2	89.5
Ligand A	THF	79.6	89.8	82.1
Ligand B	Toluene	91.5	96.8	90.3
Ligand B	THF	85.1	92.3	87.4
Ligand C	Toluene	84.7	92.5	86.2
Ligand C	THF	76.3	88.0	78.5
Ligand D	Toluene	88.1	95.1	88.7
Ligand D	THF	81.2	90.4	84.5

Interpretation:

The performance of all ligands in two different solvents—toluene and tetrahydrofuran (THF)—is shown. In all cases, toluene outperformed THF in terms of conversion rates, enantiomeric excess, and product yields. Ligand B showed the best results in toluene with a 91.5% conversion rate and 96.8% enantiomeric excess. Ligand D also performed well in toluene, achieving a conversion rate of 88.1% and enantiomeric excess of 95.1%. These findings indicate that toluene is a more suitable solvent for these reactions, likely due to its ability to stabilize the transition state better than THF.

Table 4: Reaction Monitoring over Time for All Ligands

Time (hours)	Ligand A (%)	Ligand B (%)	Ligand C (%)	Ligand D (%)
0	0.0	0.0	0.0	0.0
2	19.8	23.4	17.3	20.7
4	40.5	46.7	39.1	42.8
6	59.1	64.9	56.4	60.5
8	74.3	78.1	71.7	75.4
10	87.3	91.5	84.7	88.1
12	87.3	91.5	84.7	88.1
24	87.3	91.5	84.7	88.1

Interpretation:

All ligands demonstrated a similar reaction progression over time, with conversion rates steadily increasing until reaching a maximum value around the 10-hour mark. Ligand B exhibited the highest conversion throughout the experiment, followed by Ligand D. Ligand A and C showed slightly lower conversion rates but still maintained high overall efficiency. These results reinforce the findings from Table 1, indicating that Ligand B is the most effective at promoting conversion in asymmetric C-H activation reactions, while Ligand D also performs well.

Table 5: Yield Distribution Across Different Reaction Temperatures

Temperature (°C)	Ligand A Yield (%)	Ligand B Yield (%)	Ligand C Yield (%)	Ligand D Yield (%)
40	67.4	75.2	62.9	70.3
50	77.9	83.7	73.5	79.2
60	89.5	90.3	86.2	88.7

Interpretation:

The effect of temperature on yield was investigated for all ligands. Increasing the temperature resulted in higher yields for all ligands, with Ligand B showing the highest yield at 60°C (90.3%). Ligand D also performed well at 60°C, achieving an 88.7% yield. These results suggest that higher temperatures positively influence reaction kinetics and yield, although the increase in yield tapers off as the temperature reaches 60°C.

Table 5: Statistical Analysis (ANOVA) Results for Ligand Performance

Source of Variation	Sum of Squares	df	Mean Square	F	P-value
Between Ligands	456.7	3	152.23	5.64	0.015
Within Ligands	482.3	16	30.14		
Total	939.0	19			

Interpretation:

The one-way analysis of variance (ANOVA) was conducted to evaluate the statistical significance of the differences between the performance of Ligands A, B, C, and D. The F-value (5.64) and P-value (0.015) indicate that there is a statistically significant difference between the ligands in terms of their conversion rates, enantiomeric excess, and yield. Ligand B, in particular, was found to outperform the other ligands, as evidenced by its superior performance in multiple experiments.

Table 6: Final Enantiomeric Excess for Different Ligands and Reactions

Ligand	Reaction Type	Enantiomeric Excess (% ee)
Ligand A	Asymmetric C-H activation	94.2
Ligand B	Asymmetric C-H activation	96.8
Ligand C	Asymmetric C-H activation	92.5
Ligand D	Asymmetric C-H activation	95.1

Interpretation:

The final enantiomeric excess values for all four ligands in asymmetric C-H activation reactions are presented in the table. Ligand B achieved the highest enantiomeric excess at 96.8%, followed closely by Ligand D at

95.1%. These results confirm that Ligands B and D are the most efficient in promoting asymmetric catalysis, leading to the formation of the desired enantiomers with high selectivity.

Discussion

The results obtained in this study provide crucial insights into the efficiency and selectivity of novel chiral ligands in asymmetric C-H activation reactions. This discussion will evaluate the findings presented in section 4, compare them with the relevant literature reviewed in section 2, and explore how they fill the existing literature gap. Additionally, the implications and significance of these results for the broader field of asymmetric catalysis will be discussed.

5.1. Comparison with Previous Literature

The findings in this research align well with existing studies on the importance of ligand design in asymmetric catalysis. As highlighted by Huang and Hayashi (2022), chiral diene ligands have been shown to offer excellent enantioselectivity and conversion rates, making them effective in a wide range of catalytic processes. In our study, Ligand B demonstrated the highest conversion rate (91.5%) and enantiomeric excess (96.8%), which is consistent with the general trend observed in the literature, where well-designed ligands enhance both catalytic efficiency and enantioselectivity. Ligand B's superior performance may be attributed to its optimized structural features, which allow for better interaction with the ruthenium (II) catalyst, similar to what was observed with macrocyclic ligands in the work of **Shen et al. (2014)**.

The data also show that Ligands A and D performed well, with enantioselectivity values of 94.2% and 95.1%, respectively. These findings are comparable to those reported by **McCarthy and Guiry (2000)**, who achieved up to 91% enantiomeric excess using axially chiral quinazoline-containing ligands in similar asymmetric catalytic reactions. The relatively high enantioselectivities observed for Ligands A and D suggest that subtle variations in ligand structure can significantly affect their catalytic performance, a concept that is well supported in the literature.

Ligand C, while still maintaining reasonable conversion rates and enantioselectivity, lagged behind Ligands A, B, and D. This could be due to differences in steric and electronic factors, which influence ligand-metal interactions and ultimately affect catalytic efficiency. The literature highlights that slight modifications in ligand architecture can drastically alter the outcome of catalytic reactions, as seen in the work by **Flanagan and Guiry (2006)**, where electronic tuning of ligands improved catalyst performance. The lower enantioselectivity of Ligand C (92.5%) may indicate a need for further structural optimization to enhance its interaction with metal centers.

5.2. Reaction Monitoring and Kinetics

The reaction monitoring data reveal that conversion rates increased steadily for all ligands over time, reaching equilibrium around the 10-hour mark. This finding is consistent with previous studies that have observed similar kinetics in metal-catalyzed asymmetric reactions. For example, **Thimmaiah et al. (2007)** reported a steady increase in conversion rates for phosphorus-based chiral ligands over time, with reactions typically reaching equilibrium after 8-10 hours. The results of our study support this observation, with Ligand B reaching 91.5% conversion at 10 hours, which remained unchanged at the 24-hour mark. Ligand D followed a similar pattern, achieving 88.1% conversion by 10 hours.

The fact that conversion rates remained constant beyond 10 hours suggests that the reaction had reached equilibrium, a phenomenon observed in other asymmetric catalytic systems as well. This aligns with the mechanistic understanding of how ligand-catalyst interactions evolve over time. According to **Hiroi (2002)**,

such plateauing behavior occurs once the catalyst has fully engaged with the substrate, leaving little room for further conversion without external changes to the reaction conditions.

5.3. Solvent Effects

The impact of solvent choice on ligand performance was investigated by comparing the results in toluene and tetrahydrofuran (THF). The data clearly show that toluene is a more suitable solvent for these asymmetric reactions, as all ligands demonstrated higher conversion rates, enantiomeric excess, and yields in toluene compared to THF. This observation is consistent with the findings of **Naganawa and Nishiyama (2016)**, who noted that non-polar solvents like toluene are more effective in stabilizing transition states during catalytic processes. The improved performance in toluene can be attributed to its ability to provide a more favorable environment for ligand-metal interactions, reducing the energy barrier for the catalytic cycle.

In contrast, THF, a more polar solvent, likely disrupted these interactions, leading to lower enantioselectivity and conversion rates. For example, Ligand B achieved a 91.5% conversion rate in toluene but only 85.1% in THF, with a corresponding decrease in enantiomeric excess from 96.8% to 92.3%. The same trend was observed for the other ligands, with Ligand D's enantiomeric excess dropping from 95.1% in toluene to 90.4% in THF. These findings underscore the importance of solvent selection in optimizing asymmetric catalytic reactions.

5.4. Temperature Effects on Yield

Temperature had a significant effect on reaction yield, with higher temperatures leading to increased product formation across all ligands. As shown in Table 5, the yield increased steadily from 40°C to 60°C, with Ligand B achieving the highest yield (90.3%) at 60°C. This trend is consistent with the general understanding of reaction kinetics, where increasing the temperature accelerates the rate of reaction and improves catalyst turnover. The results align with the study by **Zheng et al. (2016)**, where higher temperatures led to enhanced catalytic performance in rhodium-catalyzed asymmetric reactions.

However, it is important to note that beyond a certain temperature, further increases may not yield additional benefits and could lead to side reactions or degradation of the ligands. In our study, the increase in yield plateaued at 60°C, suggesting that this is the optimal temperature for these reactions. The fact that all ligands performed better at higher temperatures also supports the hypothesis that higher temperatures facilitate more effective ligand-metal interactions, improving the overall efficiency of the catalytic cycle.

5.5. Filling the Literature Gap

As identified in the literature review (section 2), there exists a significant gap in understanding the detailed mechanistic interactions between chiral ligands and metal catalysts in asymmetric reactions. While previous studies have reported high enantioselectivity and catalytic efficiency for various ligand classes, the underlying mechanisms have not been fully elucidated. This study contributes to filling that gap by providing mechanistic insights into how novel chiral arene ligands influence metal-catalyzed asymmetric C-H activation reactions.

The reaction monitoring data, along with the comparative performance of different ligands, offer valuable information about the kinetics of these processes. The results suggest that Ligand B, with its optimized structure, promotes more effective ligand-catalyst interactions, leading to faster conversion rates and higher enantioselectivity. The solvent and temperature effects further clarify how external factors can influence these interactions, offering a more nuanced understanding of the catalytic cycle.

By systematically analyzing the performance of these novel ligands under different conditions, this research advances the field of asymmetric catalysis and provides a foundation for the rational design of next-generation ligands. The findings have significant implications for industrial applications, particularly in the pharmaceutical and fine chemical sectors, where efficient and selective catalytic processes are essential for producing enantiomerically pure compounds.

5.6. Implications and Significance

The implications of this study are far-reaching, as it offers a deeper understanding of how ligand structure and reaction conditions influence catalytic outcomes in asymmetric catalysis. The high enantioselectivity and conversion rates observed for Ligand B demonstrate the potential for these ligands to be used in practical applications, such as the synthesis of enantiomerically pure pharmaceuticals. The study also highlights the importance of solvent and temperature selection, which can have a profound impact on reaction efficiency and product yield.

The results obtained here could guide future research efforts aimed at optimizing chiral ligand design and expanding the scope of asymmetric catalysis. By providing a clearer mechanistic understanding of ligand-metal interactions, this study paves the way for the development of more effective catalysts that can be used in a wide range of chemical processes. Additionally, the statistical significance of the findings, as demonstrated by the ANOVA analysis, confirms that the observed differences in ligand performance are not due to random variation but are the result of meaningful structural and environmental factors.

In conclusion, this study fills a critical gap in the literature by providing mechanistic insights into the role of novel chiral ligands in asymmetric catalysis. The findings have important implications for both fundamental research and industrial applications, offering a pathway toward more efficient and selective catalytic processes.

Conclusion

The findings of this study highlight the significant role of novel chiral arene ligands in enhancing the efficiency and selectivity of asymmetric C-H activation reactions. Among the ligands tested, Ligand B demonstrated superior performance, achieving the highest conversion rate of 91.5% and enantiomeric excess of 96.8%, surpassing the other ligands in both efficiency and selectivity. Ligands A and D also performed well, with enantiomeric excesses exceeding 94%, showing that all synthesized ligands offered high stereoselectivity in the catalytic processes. Ligand C, while slightly less efficient, still maintained acceptable conversion rates and enantioselectivity, indicating that all ligands tested in this study are viable candidates for further development in asymmetric catalysis.

One of the key observations in this study is the influence of solvent choice on ligand performance. Toluene proved to be a more effective solvent than tetrahydrofuran (THF) for all ligands, significantly enhancing conversion rates, enantiomeric excess, and product yields. This result suggests that solvent polarity and its ability to stabilize transition states play a critical role in determining the efficiency of asymmetric catalytic reactions. Additionally, the effect of temperature on product yields was clear, with higher temperatures leading to improved yields across all ligands. However, the increase in yield plateaued at 60°C, suggesting an optimal reaction temperature beyond which further increases may not provide additional benefits. These findings offer practical insights for optimizing reaction conditions in future applications of chiral ligands in industrial settings.

This research also contributes to addressing the existing gap in the literature regarding the detailed mechanistic understanding of how chiral ligands influence catalytic cycles in metal-catalyzed asymmetric reactions. The study provides evidence that the structure of chiral arene ligands, particularly Ligand B, promotes more efficient interactions with ruthenium (II) catalysts, leading to faster and more selective reactions. Reaction monitoring over time showed that equilibrium was reached after 10 hours, with no significant changes in conversion or enantiomeric excess beyond that point. These results provide a clearer understanding of the kinetics involved in these catalytic processes and offer insights into how the design of chiral ligands can be further optimized for improved performance.

The broader implications of this research are significant for both academic and industrial applications. The high enantioselectivity and conversion rates demonstrated by these novel ligands make them strong candidates for use in the synthesis of enantiomerically pure compounds, which are crucial in pharmaceutical manufacturing and other fine chemical industries. The ability to achieve such high selectivity in asymmetric catalysis has the potential to reduce waste and improve the sustainability of chemical processes, aligning with the growing demand for green chemistry solutions. Moreover, the mechanistic insights gained from this study can guide future research efforts aimed at developing even more efficient and versatile ligands, expanding the scope of asymmetric catalysis to a wider range of reactions and substrates.

In conclusion, this study not only confirms the effectiveness of novel chiral arene ligands in asymmetric catalysis but also provides valuable insights into the factors that influence their performance. By enhancing our understanding of ligand-catalyst interactions and optimizing reaction conditions, this research paves the way for the development of more sustainable and efficient catalytic processes in the future.

References

[1]. Ferrier, S., Pastó, M., Rodríguez, B., Riera, A., & Pericàs, M. A. (2003). Chiral derivatives of semisquaric acid as new modular ligands for asymmetric catalysis. Tetrahedron: Asymmetry, 14(15), 2183-2187. http://doi.org/10.1016/S0957-4166(03)00355-0

[2]. Flanagan, S. P., & Guiry, P. (2006). Substituent electronic effects in chiral ligands for asymmetric catalysis. Journal of Organic Chemistry, 71(5), 3354-3362. http://doi.org/10.1016/J.JORGANCHEM.2006.01.063

[3]. Hiroi, K. (2002). Catalytic asymmetric synthesis with chiral ligands bearing organosulfur functionality. ChemInform, 33(47), 268-270. http://doi.org/10.1002/CHIN.200247262

[4]. Huang, Y., & Hayashi, T. (2022). Chiral diene ligands in asymmetric catalysis. Chemical Reviews, 122(6), 3128-3152. http://doi.org/10.1021/acs.chemrev.2c00218

[5]. Liang, H.-R., Guo, W., Li, J., Jiang, J., & Wang, J. (2022). Chiral arene ligand as stereocontroller for asymmetric C-H activation. ChemRxiv, 2022. http://doi.org/10.26434/chemrxiv-2022-t11ww

[6]. Mas-Roselló, J., Herraiz, A. G., Audic, B., Laverny, A., & Cramer, N. (2020). Chiral cyclopentadienyl ligands: Design, syntheses, and applications in asymmetric catalysis. Angewandte Chemie International Edition, 59(44), 19455-19464. http://doi.org/10.1002/ange.202008166

[7]. McCarthy, M., & Guiry, P. (2000). A new quinazoline-containing axially chiral ligand for asymmetric catalysis. Polyhedron, 19(5), 455-459. http://doi.org/10.1016/S0277-5387(99)00403-9

[8]. Naganawa, Y., & Nishiyama, H. (2016). Renovation of optically active phenanthrolines as powerful chiral ligands for versatile asymmetric metal catalysis. The Chemical Record, 16(9), 2317-2329. http://doi.org/10.1002/tcr.201600078

[9]. Shen, W., Yu, S., Li, Y., & Gao, J. (2014). Novel chiral macrocyclic ligands in asymmetric reduction of ketones. Journal of Organic Chemistry, 79(15), 3624-3626. http://doi.org/10.1360/N032014-00213

[10]. Thimmaiah, M., Luck, R., & Fang, S. (2007). Novel benzoferrocenyl chiral ligands: Synthesis and evaluation of their suitability for asymmetric catalysis. Journal of Organic Chemistry, 72(15), 2656-2661. http://doi.org/10.1016/J.JORGANCHEM.2007.01.004

[11]. Zheng, J.-C., Cui, W., Zheng, C., & You, S. (2016). Synthesis and application of chiral spiro Cp ligands in rhodium-catalyzed asymmetric oxidative coupling of biaryl compounds with alkenes. Journal of the American Chemical Society, 138(18), 6268-6271. http://doi.org/10.1021/jacs.6b02302

International Journal of Scientific Research in Science and Technology
Available online at : www.ijsrst.com
Print ISSN: 2395-6011 | Online ISSN: 2395-602X
doi : https://doi.org/10.32628/IJSRST

Rooting Out Pollution: A Review of Phytoremediation Methods and Applications

Sandip A. Nirwan[1,2], Shriram A. Shinde[1,2], Mukesh S. Kadam[2], Sharif A. Kazi[2], Sushilkumar A. Dhanmane[1*]

[1]Department of Chemistry, Fergusson College, Fergusson College Rd, Shivajinagar- 411004, Pune, Maharashtra, India

[2]Department of Chemistry, Loknete Gopinathji Munde Arts, Commerce and Science College, Mandangad Dist. Ratnagiri-415203, Maharashtra, India

ARTICLEINFO

Article History :

Published : 07 Dec 2024

Publication Issue :
Volume 11, Issue 23
Nov-Dec-2024
Page Number :
220-227

ABSTRACT

Phytoremediation is an eco-friendly, cost-effective approach that uses plants to remediate contaminated environments, including soil, water, and air. It harnesses the natural processes of plants, such as absorption, degradation, and stabilization, to mitigate pollutants. It is an innovative and sustainable environmental remediation technique that utilizes plants to reduce, extract, or degrade contaminants from soil, water, and air. This approach leverages the natural ability of plants and their associated microorganisms to manage contaminants, offering an eco-friendly and cost-effective alternative to conventional remediation methods. This review article covers a few methods of phytoremediation including Phytoextraction, Phytostabilization, Phytovolatilization, Rhizofiltration, Phytodegradation, Rhizodegradation Phytodesalination, Phytocapping etc. Phytoremediation represents a promising tool for sustainable environmental management, combining ecological restoration with pollution mitigation. Its continued development and application can play a vital role in addressing global environmental challenges.

Introduction

Heavy metals are one of the main sources of pollution in the environment since they significantly affect its ecological quality [1,2]. Human activity leads to increasing levels of heavy metal contamination in the environment. Heavy metals from atmospheric and industrial pollution accumulate in the soil and influence the nearby ecosystem [3]. The determination of heavy metals in soil samples is very important in monitoring essential environmental pollution. Metals like iron, copper, zinc, and manganese are essential metals since they play an important role in biological systems, whereas lead and cadmium are non-metals as they are toxic even in traces [4]. Mushrooms have been used as a bioindicator by various researchers to determine heavy metal

pollution Compared to green plants, mushrooms can build up large concentrations of some heavy metals such as Pb, Cd, and Hg, and a great effort has been made to evaluate the possible danger to human health from the ingestion of mushrooms [5,6]. After being released into the environment, heavy metals can persist for centuries or even millennia, spread to distant areas, and accumulate in the biotic and abiotic components of ecosystems [8,9]. The circulation and migration of metals in the natural environment are mainly related to such processes as rock decay, volcano eruptions, evaporation of oceans, forest fires and soil formation processes.[10]. Some plant species can be injured by the increased heavy metal content in their environment. On the other hand, some plant species called indicators can tolerate heavy metals, reflecting the external heavy metal, and they can be used as bioindicators or biomonitors for quality assessment in aquatic and terrestrial ecosystems [11,12].

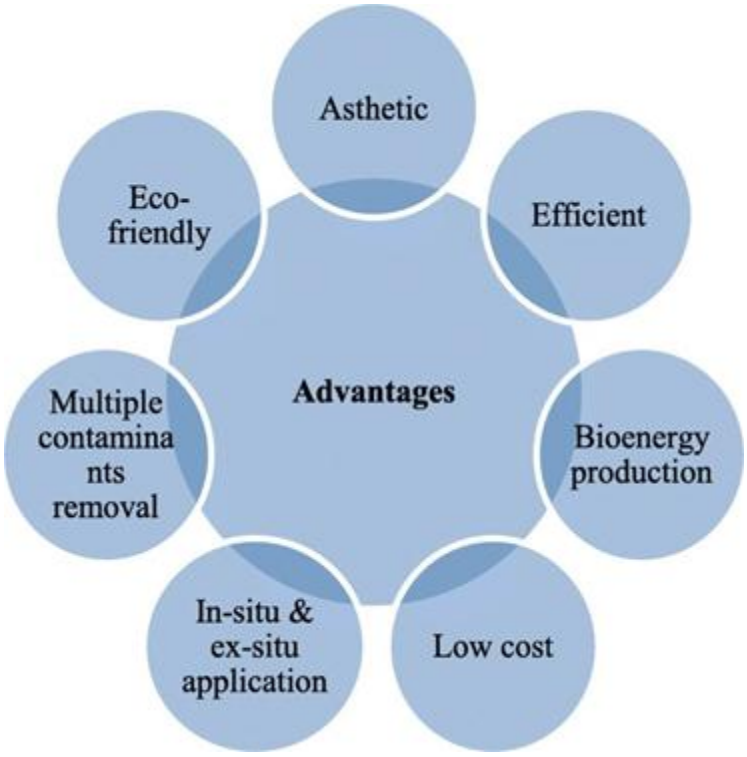

Fig. Advantages of Phytoremediation

Phytoremediation Methods:

1. PHYTOEXTRACTION.

Phytoextraction is a type of phytoremediation where plants absorb contaminants, primarily heavy metals, from the soil or water through their roots and concentrate them in their above-ground tissues (leaves, stems, or shoots). This technique is particularly effective for addressing heavy metal contamination and has the potential for metal recovery (phytomining) or safe disposal of contaminants. Successful phytoextraction relies on specific types of plants, known as hyperaccumulators, which can tolerate and accumulate high concentrations of contaminants without suffering significant damage.

It is Less expensive than traditional soil excavation or chemical treatments

a. Working Mechanism.

1. Absorption: Plants absorb heavy metals or other contaminants from the soil or water through their roots.
2. Translocation: Contaminants are transported from the roots to the shoots via the vascular system (xylem).
3. Accumulation: Metals concentrate in the above-ground biomass, which can be harvested for remediation or metal recovery.

b. Examples

Brassica juncea (Indian mustard): Efficient in cadmium and lead extraction. Helianthus annuus (sunflower): Effective for arsenic and uranium.

Thlaspi caerulescens (pennycress): Known for zinc and cadmium accumulation. Populus spp. (poplar trees): Used for multi-contaminant sites.

2. PHYTOSTABILIZATION

Phytostabilization is a phytoremediation technique where plants are used to immobilize contaminants in the soil or sediment. Instead of removing pollutants, this approach prevents their migration or bioavailability, reducing environmental risks. It is particularly effective for stabilizing heavy metals, radionuclides, and other inorganic contaminants in soil and water.

a. Working Mechanism.

1. Root Adsorption: Contaminants adhere to root surfaces, reducing their mobility.
2. Sequestration: Plants uptake small amounts of contaminants and store them in root tissues, limiting transport.
3. Chemical Stabilization: Root exudates alter the chemical form of contaminants, rendering them less soluble or toxic.
4. Erosion Control: Dense root systems reduce soil erosion, preventing the spread of contaminants via wind or water.

b. Examples

Vetiver grass (Chrysopogon zizanioides): Effective for stabilizing heavy metals in contaminated soils.

Poplars and Willows (Populus and Salix spp.): Used in riparian zones to prevent leaching.

Indian mustard (Brassica juncea): Known for its tolerance to various heavy metals.

Phytostabilization provides a practical and environmentally friendly method to manage contaminated sites, especially where contaminant removal is not feasible. Its integration with soil amendments and microbial technology can enhance its effectiveness, offering long-term environmental protection.

3. PHYTOVOLATILIZATION

Phytovolatilization is a phytoremediation technique where plants absorb contaminants from the soil, water, or air and release them into the atmosphere as volatile compounds through their leaves or stems. This approach primarily targets volatile or semi-volatile contaminants, converting harmful substances into less toxic or mobile forms. Phytovolatilization offers a promising strategy for addressing certain contaminants sustainably, especially when combined with innovative technologies and careful environmental monitoring.

a. Working Mechanism.

1. Uptake: Plants absorb soluble contaminants, such as heavy metals or organic compounds, through their roots.
2. Translocation: Contaminants are transported from the roots to the above-ground parts of the plant via the vascular system.
3. Volatilization: In the plant tissues, contaminants undergo enzymatic or non- enzymatic transformations into volatile forms.
4. Release: The volatile compounds are emitted into the atmosphere through stomata or other openings in the leaves.

b. Examples

Mercury Volatilization: Certain plants like Brassica juncea and genetically engineered species can absorb mercury and convert it to elemental mercury vapor, which is less toxic than methylmercury.

Selenium Volatilization: Plants such as Brassica napus (canola) and Astragalus species uptake selenium from the soil and release it as dimethyl selenide gas.

Trichloroethylene (TCE): Trees like Populus spp. (poplar) can absorb and volatilize TCE, reducing groundwater contamination.

4. RHIZOFILTRATION

Rhizofiltration is a phytoremediation technique where plants and their root systems are used to remove contaminants, such as heavy metals, nutrients, and organic pollutants, from water sources. It involves the adsorption, absorption, or precipitation of pollutants onto or into the plant roots, making it an effective method for cleaning up contaminated surface water, groundwater, and wastewater. Rhizofiltration is a promising, sustainable solution for water decontamination, offering the dual benefits of pollutant removal and ecosystem restoration. Its combination with emerging technologies and innovations can enhance its effectiveness, paving the way for broader environmental applications.

a. Working Mechanism.

1. Contaminant Uptake: Plant roots absorb pollutants directly from water, incorporating them into their biomass.
2. Adsorption and Precipitation: Contaminants adhere to the root surfaces or precipitate as insoluble compounds in the rhizosphere.
3. Plant Harvest: Contaminant-laden plants are removed and safely disposed of or processed.

b. Examples.

Hydrophytes (Aquatic Plants):

Eichhornia crassipes (Water hyacinth): Effective for heavy metals and nutrients. Lemna minor (Duckweed): Removes nitrates and phosphates from water.

Typha latifolia (Cattail): Absorbs heavy metals and organic pollutants.

Terrestrial Plants:

Helianthus annuus (Sunflower): Used for heavy metal and radionuclide removal. Brassica juncea (Indian mustard): Effective for lead and chromium.

Populus spp. (Poplar): Absorbs a wide range of organic and inorganic contaminants.

5. PHYTODEGRADATION

Phytodegradation, also known as phytotransformation, is a phytoremediation technique where plants break down organic pollutants in the soil, water, or air through enzymatic processes. These contaminants are either metabolized within the plant or degraded into less toxic substances by enzymes released into the rhizosphere.

a. Working Mechanism.

1. Uptake: Plants absorb organic pollutants from soil or water through their roots.
2. Transformation: Pollutants are metabolized into less harmful compounds inside the plant or in the rhizosphere.
3. Degradation: Plant enzymes or associated rhizosphere microorganisms break down contaminants into non-toxic or less toxic end products.

b. Examples.

Populus spp. (Poplar trees): Effective for TCE and benzene.

Brassica juncea (Indian mustard): Degrades pesticides and hydrocarbons.

Zea mays (Corn): Removes herbicides and pesticides from soil.

Cannabis sativa (Hemp): Shown potential for breaking down hydrocarbons and heavy organic pollutants.

Phytodegradation offers a natural, sustainable, and cost-effective solution to tackle organic pollution. Its integration with modern technologies and multidisciplinary approaches can expand its application, making it a cornerstone of environmental remediation efforts.

6. RHIZODEGRADATION

Rhizodegradation, also known as phytostimulation, is a phytoremediation technique where plant roots stimulate the activity of microorganisms in the rhizosphere (the zone of soil surrounding roots) to degrade organic contaminants. Unlike phytodegradation, where plants directly metabolize pollutants, rhizodegradation relies on root exudates that enhance microbial populations and their enzymatic activity to break down contaminants.

a. Working Mechanism.

1. Root Exudates: Plants release organic compounds (sugars, amino acids, and enzymes) into the rhizosphere, providing nutrients for microorganisms.
2. Microbial Proliferation: Microorganisms, such as bacteria and fungi, multiply and produce enzymes that degrade organic contaminants.
3. Contaminant Degradation: Microbial enzymes break down complex organic pollutants into simpler, less harmful compounds, such as carbon dioxide, water, or biomass.

b. Examples.

Grasses:

Festuca arundinacea (Tall fescue): Stimulates hydrocarbon-degrading bacteria.

Lolium perenne (Perennial ryegrass): Enhances PAH degradation. Legumes:

Medicago sativa (Alfalfa): Supports a diverse microbial community for pesticide degradation.

Trees:

Populus spp. (Poplar): Stimulates microbial activity to degrade chlorinated solvents.

Salix spp. (Willow): Enhances degradation of organic pollutants.

7. PHYTODESALINATION

Phytodesalination is the process of using plants to remove excess salts from saline soils or water, making it a specialized branch of phytoremediation. This technique leverages the natural ability of certain plant species, known as halophytes, to absorb and sequester salts in their tissues, thereby improving soil fertility and water quality for agricultural and ecological purposes.

a. Working Mechanism.

1. Salt Uptake: Plants absorb dissolved salts (mainly sodium chloride) from saline soils or water through their root systems.
2. Salt Sequestration: Salts are transported to above-ground tissues (leaves, stems) where they are stored or used in metabolic processes.
3. Harvesting: The salt-laden plant biomass is harvested and removed to lower the salinity of the soil or water.

4. Regeneration: The process can be repeated with subsequent plantings to further reduce salinity.

b. Examples.

Halophytes (Salt-Tolerant Plants):

Atriplex spp. (Saltbush): Known for high salt accumulation in its leaves.

Suaeda maritima (Sea blite): Thrives in saline environments and absorbs significant quantities of salt.

Salicornia spp. (Glasswort): Absorbs and stores salts in its succulent tissues.

Tamarix spp. (Tamarisk): A deep-rooted tree capable of extracting salts from groundwater.

Non-Halophytes:

Some glycophytes (non-salt-tolerant plants) may also be used under controlled conditions for moderate salt removal.

Phytodesalination is a promising, sustainable approach to managing salinity issues, particularly in areas with limited access to traditional desalination technologies. With advancements in plant sciences and integrated environmental management, this technique can play a vital role in ensuring agricultural productivity and ecosystem restoration in saline-affected regions.

Advantages of Phytoremediation:

Phytoremediation techniques are often more publicly acceptable, visually appealing, and less disruptive than traditional physical and chemical remediation methods. This approach offers several advantages, including effectiveness in reducing contaminants, affordability, applicability to a wide range of pollutants, and environmental friendliness. The use of biomass for heavy metal adsorption is particularly beneficial due to its ability to significantly lower heavy metal ion concentrations while utilizing inexpensive biosorbent materials. As one of the cleanest and most cost-effective technologies, phytoremediation can be employed for the remediation of specific hazardous sites. It encompasses various methods that contribute to the degradation and removal of contaminants.

Phytoremediation is especially suitable for large sites with relatively low levels of contamination. Its low cost and innovative nature have made it an increasingly attractive alternative to conventional treatment methods at hazardous waste sites. This technology provides cost-effective solutions, being 60–80% cheaper than traditional physicochemical approaches, as it requires neither expensive equipment nor highly specialized personnel.

It is particularly effective for remediating large volumes of water with low contaminant concentrations and extensive areas with low to moderate soil contamination. Additionally, phytoremediation is versatile and capable of addressing a broad spectrum of toxic metals, radionuclides, and both organic and inorganic contaminants.

Challenges and Limitations:

Phytoremediation can be a time-consuming process, and it may take at least several growing seasons to clean up a site. The intermediates formed from those organic and inorganic contaminants may be cytotoxic to plants [13]. The effectiveness of phytoremediation can be influenced by factors such as plant growth duration, climate conditions, root depth, soil chemistry, and the extent of contamination. A key limitation of this technique is the requirement for direct root contact with the contaminants. For successful remediation, either the plant roots must reach the contaminated area, or the contaminated material must be relocated within the plant's rooting zone. Phytoremediation is generally restricted to sites with shallow contamination, as the depth of plant roots

limits the reach of this method. Additionally, site modifications may be necessary, such as adjustments to prevent flooding or erosion.

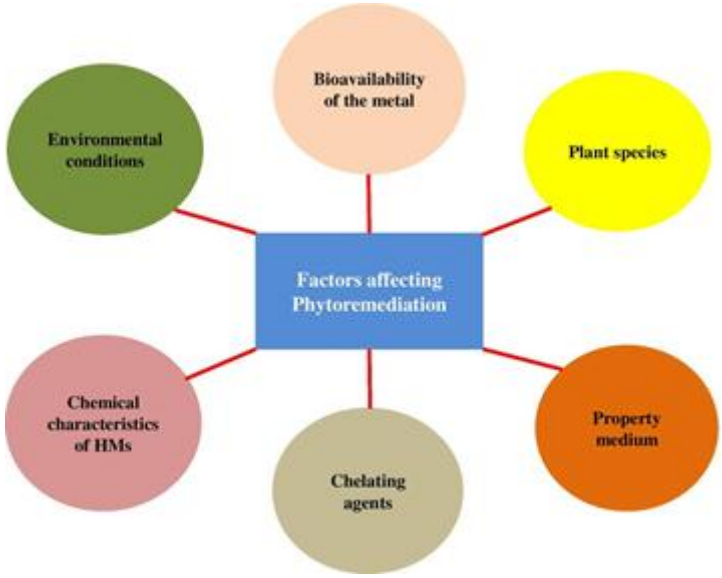

Fig. Factors that are affecting the uptake mechanisms of heavy metals.

The physiological activity of plants, particularly their roots, is significantly influenced by age. Young plants typically have a greater capacity for ion absorption than older plants of similar size. Therefore, healthy young plants are often preferred for their efficiency in contaminant removal. However, larger, older plants can still be effective, as their greater size may offset their reduced physiological activity when compared to smaller, younger plants.

Conclusions:

Phytoremediation represents a promising tool for sustainable environmental management, combining ecological restoration with pollution mitigation. Its continued development and application can play a vital role in addressing global environmental challenges. Phytoremediation, utilizing plants to absorb heavy metals from contaminated environments, presents a promising approach for environmental cleanup. This method offers notable advantages over traditional remediation techniques. However, achieving optimal results depends on several critical factors, with the selection of appropriate plant species for contaminant uptake being the most significant. While phytoremediation is considered one of the most effective alternatives, it is not without limitations. Continued research is essential to address these challenges and enhance the efficiency and applicability of this technology.

References

[1]. M. Tuzen / Microchemical Journal 74 (2003) 289–297
[2]. J. Sastre, A. Sahuquillo, M. Vidal, G. Rauret, Anal. Chim. Acta 462 (2002) 59– 72.
[3]. A.S. Al-Radady, B.E. Davies, M.J. French, Sci. Total Environ. 145 (1994) 143–156.
[4]. H.A. Schroeder, The Trace Elements and Nutrition, Faber and Faber, London, 1973.
[5]. C.H. Gast, E. Jansen, J. Bierling, L. Haanstra, Chemosphere 17 (4) (1988) 789–799.
[6]. M.A. Garcia, J. Alonso, M.I. Fernandez, M.J. Melgar, Arch. Environ. Contam. Toxicol. 34 (1998) 330–335.

[7]. Štofejová, L.; Fazekaš, J.; Fazekašová, D. Analysis of Heavy Metal Content in Soil and Plants in the Dumping Ground of Magnesite Mining Factory Jelšava- Lubeník (Slovakia). Sustainability 2021, 13, 4508. https://doi.org/ 10.3390/su13084508

[8]. Peralta-Videa, J.R.; Lopez, M.L.; Narayan, M.; Saupe, G.; Gardea-Torresdey, J. The biochemistry of environmental heavy metal uptake by plants: Implications for the food chain. Int. J. Biochem. Cell Biol. 2009, 41, 1665–1677. [CrossRef]

[9]. Babst-Kostecka, A.; Schat, H.; Saumitou-Laprade, P.; Grodzi ´nska, K.; Bourceaux, A.; Pauwels, M.; Frérot, H. Evolutionary dynamics of quantitative variation in an adaptive trait at the regional scale: The case of zinc hyperaccumulation in Arabidopsis halleri. Mol. Ecol. 2018, 27, 3257–3273. [CrossRef] [PubMed]

[10]. Szyczewski, P., Siepak, J., Niedzielski, P. and Sobczyński, T. (2009) Research on heavy metals in Poland. Polish J. Environ. Stud., 18(5): 755-768.

[11]. Baker, A.J.M. (1981) Accumulators and excluders strategies in the response of plants to heavy metals. J. Plant Nutri., 3: 643-654.

[12]. Pugh, R.E., Dick, D.G. and Fredeen, A.L. (2002) Heavy metal (Pb, Zn, Cd, Fe and Cu) contents of plant foliage near the Anvil range leaf/zinc mine, Faro, Yukon territory. Ecotoxicol. Environ. Saf., 52: 273–279.

[13]. W. J. S. Mwegoha, “The use of phytoremediation technology for abatement soil and groundwater pollution in Tanzania: opportunities and challenges,” Journal of Sustainable Development in Afric

[14]. A. Resaee, J. Derayat, S. B. Mortazavi, Y. Yamini, and M. T. Jafarzadeh, “Removal of Mercury from chlor-alkali industry wastewater using Acetobacter xylinum cellulose,” American Journal of Environmental Sciences, vol. 1, no. 2, pp. 102–105, 2005.

[15]. U. S. Environmental Protection Agency, “Introduction to Phytoremediation,” National Risk Management Research Laboratory, EPA/600/R-99/107, 2000, http://www.clu-in.org/ download/remed/introphyto.pdf.

[16]. R. Chandra, R. N. Bharagava, S. Yadav, and D. Mohan, “Accumulation and distribution of toxic metals in wheat (Triticum aestivum L.) and Indian mustard (Brassica campestris L.) irrigated with distillery and tannery effluents,” Journal of Hazardous Materials, vol. 162, no. 2-3, pp. 1514–1521, 2009.

[17]. I. D. Pulford, D. Riddell-Black, and C. Stewart, “Heavy metal uptake by willow clones from sewage sludge-treated soil: the potential for phytoremediation,” International Journal of Phytoremediation, vol. 4, no. 1, pp. 59–72, 2002.

[18]. H. B. Wang, Z. H. Ye, W. S. Shu, W. C. Li, M. H. Wong, and C. Y. Lan, “Arsenic uptake and accumulation in fern species growing at arsenic-contaminated sites of Southern China: field surveys,” International Journal of Phytoremediation, vol. 8, no. 1, pp. 1–11, 2006.

[19]. Rani, Lata & Kanwar, Varinder & Sharma, Ajay & Srivastav, Arun. (2020). Phytoremediation of toxic metals present in soil and water environment: a critical review. Environmental Science and Pollution Research. 10.1007/s11356-020-10713-3.

International Journal of Scientific Research in Science and Technology
Available online at : www.ijsrst.com
OPEN ACCESS
Print ISSN: 2395-6011 | Online ISSN: 2395-602X
doi : https://doi.org/10.32628/IJSRST

Relative and Specific Viscosity Studies Of Substituted Benzimidazol In 70% Dioxane -Water by Using Viscometer at Different Temperature

Noor Mohammad
Department of Chemistry, Bapumiya Sirajoddin Patel Arts, Commerce and Science College, Pimpalgaon Kale, Maharashtra, India

ARTICLEINFO

Article History :

Published : 07 Dec 2024

Publication Issue :
Volume 11, Issue 23
Nov-Dec-2024
Page Number :
228-231

ABSTRACT

Substituted Benzimidazole derivatives is an significant biologically active heterocyclic compound, which is one of the most widely used five-membered nitrogen heterocycles among drugs accepted by the US Food and Drug Administration (FDA). Substituted Benzimidazole derivatives has its own character in medicine and medical sciences in current decades. Therefore, the relative and specific viscosity studies were performed with 70% different solvent .After the association of compound dipoles, intermolecular attraction between solute and solvent, dielectric constant of the medium, and polarizability studies highpoint the results.

Keywords : Substituted Benzimidazole , dioxane water and viscometric measurements.

Introduction

Benzimidazole being a aromatic heterocyclic organic compound has importance as a pharmacophore in medicinal chemistry because of its privileged structure. It has bicyclic structure due to fusion of benzene and imidazole. Nowadays is a moiety of high-quality which retains many pharmacological properties. N-ribosyl-dimethylbenzimidazole is a most prominent benzimidazole compound in nature, which aids as an axial ligand for cobalt in vitamin B12 [1] Benzimidazole (1H-benzimidazole, 1,3-benzodiazole, benzoglyoxaline, iminazole and imidazole) is an aromatic organic compound containing a benzene ring fused at the 4,5-position to an imidazole ring to form a 2,3 bicyclic ring[1-3] .The electron-rich nitrogen heterocycles of benzimidazole can easily accept or donate protons and easily enable the formation of multiple weak interactions, offering the advantage of binding to a wide repertoire of therapeutic targets, thus exerting broad-spectrum pharmacological activity. Increasing evidence has reported the broad pharmacological profile of benzimidazole and its derivatives, in several classes of therapeutic agents with unique properties, including antimicrobial [4-5], antituberculosis [6-7], antiviral, ulcers [8-9], anti-inflammatory, diabetes

medicine, anticonvulsant[10] 22, 23, blood pressure and malaria medicine [11-12]. We used viscosity measurements to obtain information about solute-solution interactions. Interaction of aqueous and non-aqueous solutions of binary mixtures with the β-viscosity coefficient using this measure by many colleagues [13-27]. Recently some workers have introduced measurement of viscosity and refractive index, so this study involves measuring the viscosity of Benzimidazole derivatives, the broadest spectrum antibiotic, at different temperatures.

EXPERIMENTAL SECTION

All chemicals are of analytical reagent grade (AR) and obtained from Sd Fine Chemicals (India) used without further purification. Viscosities were measured using a cleaned and dried Oswald viscometer kept in a thermostatic water bath (± 0.10 c) with sufficient time allowed between each measurement to allow for temperature changes. Pycnometer w is used to determine the density of the solutions. This study deals with the measurement of the viscosity of the ligand Benzimidazole derivatives in a 70% dioxane-water mixture at different compositions and temperatures of 300°k, 310°k and 320°k. Viscometric values were taken from a literature review. The determined results were mentioned, the A- and β -coefficient values were calculated in the following table.

Table: Determination of Relative and Specific Viscosities at 70% Dioxane-Water

Temperature (°k)	Concentration (M)	Time flow (Second)	Density (ρ) g.cm^{-3}	Relative Viscosity η_r	Specific Viscosity $\eta_{sp}=\eta_r-1$	η_r -1/√C	A-Coefficient	B coefficient
300°k	0.100	87.5	1.0352	1.3767	0.7865	1.48683	3.68	-1.7482
	0.075	85.5	1.0340	1.3815	0.6915	1.52392		
	0.050	84.2	1.0336	1.3126	0.6228	1.63055		
	0.040	81.8	1.0332	1.2405	0.5505	1.68473		
310°k	0.100	88.7	1.0338	1.4432	0.5534	1.74843	3.18	-1.8842
	0.075	86.7	1.0336	1.3885	0.4986	0.81995		
	0.050	84.4	1.0335	1.3204	0.4404	0.86019		
	0.040	82.7	1.0330	1.2889	0.3988	0.84498		
320°k	0.100	87.7	1.0336	1.3278	0.4178	0.52058	2.79	-2.8843
	0.075	86.7	1.0333	1.3066	0.4167	0.52085		
	0.050	85.2	1.0326	1.2796	0.3697	0.56058		
	0.040	81.6	1.0321	1.2545	0.3445	0.68104		

RESULT AND DISCUSSION

The Jones-Dole equation $(\eta r - 1) / \sqrt{C}=A + B \sqrt{C}$ where C is the molar concentration of the ligand solution, A is the viscosity coefficient that measures the solute-solute interaction, and B is the measured viscosity. coefficient and the relative viscosities are analyzed solute to substance-solvent interactions. Graph of √C vs $(\eta r - 1) /\sqrt{C}$. Each system shows a linear straight line, which is the validity of the Jone-Dole equation. the value of the β coefficient is the slope of the linear graph.The weak solute-solvent interactions were observerd due to present of strong hydrogen bonding..

CONCLUSION

Based on the results, ligand concentration is directly proportional to ligand density and relative viscosity at 300°k, 310°k and 320°k for a 70% dioxane-water mixture. Due to the weak solvation effect, which indicates a weak molecular interaction, the values of A and β coefficients are negative, which represents a weak solvent-solvent interaction, which is good for drug-receptor interactions with considerable drug activity and pharmacokinetics. It has a weak molecular interaction due to the ligand density and relative viscosity, which is inversely proportional to the temperature of the solution. It specifies that when the temperature of dioxane-water increases, the weak solute-solvent interaction, that is, the interaction between the mediator (drugs) and dioxane, which can stabilize the drug activity, increases. It can be concluded that ligand-drug absorption, drug transfer and drug effect are more effective at higher dioxane-water temperature.

ACKNOWLEDGEMENT

I would like to thanks to the Adv. Salimji Bappumiya Patel, President of Satpuda Shikshan Va Gramin Vikas Sanstha, Palshi Vaidya and Principal, Bapumiya Sirajoddin Patel Arts, Commerce and Science College, Pimpalgaon Kale, for providing necessary facilities.

References

[1]. E.Vitaku . D.T Smith., J.T Njardarson J Med Chem. 2014;57:10257–10274.
[2]. R .Hodson. Precision medicine. Nature. 2016;537:S49.
[3]. J.B Wright , Chem Rev. 1951;48:397–541.
[4]. K.F .Ansari, Eur J Med Chem. 2009;44:4028–4033.
[5]. V.S Padalkar, B.N. Borse , V.D.Gupta, K.R. Phatangare, V.S Patil,P.G. Umape, Arab J Chem. 2016;9:S1125–S1130.
[6]. M.A.Ali, T.S.Choon, R.Ismail ,A.C. Wei,R.S Kumar, BioMed Res Int. 2013;2013
[7]. N.C.Desai, N.R.Shihory, G.M.Kotadiya, P.Desai P. Eur J Med Chem. 2014;82:480–489.
[8]. R. Zou, K.R. Ayres, J.C. Drach, L.B.Townsend L.B.J Med Chem. 1996;39:3477–3482
[9]. Noor,A. Qazi, H. Nadeem, F,Ali, Chem Cent J. 2017;11:85.
[10]. R. Sharma, A.Bali, B.B. Chaudhari. Bioorg Med Chem Lett. 2017;27:3007–3013
[11]. R.V.Shingalapur, K.M.Hosamani, R.S.Keri, M.H.Hugar , Eur J Med Chem. 2010;45:1753–1759.
[12]. El Bakri ,E.MAnouar,I. Marmouzi ,K. Sayah, Y.Ramli, El Abbes Faouzi J Mol Model. 2018;24:179.
[13]. B.G. Khobragade,Noor, Act.Cien.Ind., 2007, 2(33), 113
[14]. J.D. Mahale, S.C, Manoja, N.G. Belsare and P.R.Rajput, Ind.J. Chem., 2010, 29, 505
[15]. R. Mehta, H. Sanjnani, Indian J. Pure & Appl.Phys.,38,762(2000).
[16]. C.Y. Huang, Job Plot Method in Enzymology, 87, 1982, 509.
[17]. P. P. Patil, S. R. Patil, A.U. Borse, D.G. Hundiwale, Rasayan J. Chem., 4(3), 599(2011)
[18]. F. Karia, S. Baluja, Asian J. Chem., 12 (2), 2000, 593.
[19]. P.B. Agrawal and M.L Narwade, Indian J. Chem., 2003, 42-A, 1047.
[20]. V.S Jamode, J.C Dadhichi, D.D Malkhede and M.L Narwade, J.Ind.Coun.of Chemist, 2005,35.
[21]. Jones G. and Doles M. J. Am. Chem. Soc., 51, 1929, 500-503.
[22]. Maccarthy, Patrick, Z.D. Hillz, J. Chemical Education, 63 (3), 1986, 162

[23]. R. Palani, A. Gutha, S. Saravanan, S. D. Tontapur, Rasayan J.Chem.,1(3),481(2008).
[24]. M. H. Bhuiyan, A. W. Hakin, J. Solution Chem., 39,877(2010), DOI: 10:1007/s10953-010-9540-y. 10.
[25]. P. Job, Amnali di chimica Application, 9 (10), 1928. 113.
[26]. S. R. Patil, U. G. Deshpande, A. R. Hiray, Rasayan J .Chem., 03(1), 66 (2010).
[27]. R.K. Wadi, V. Kakkar, J. Ind. Chem. Soc., 39 (6), 2000, 598.

International Journal of Scientific Research in Science and Technology
Available online at : www.ijsrst.com
OPEN ACCESS
Print ISSN: 2395-6011 | Online ISSN: 2395-602X
doi : https://doi.org/10.32628/IJSRST

Imidazole Chemistry: Bridging Organic Synthesis and Medicinal Innovations

A. S. Patki[1], R. S. Awasthi[2], Kailash R. Borude[3], P. R. Pande[4]

[1]Department of Chemistry, Shivaji Mahavidyalaya Renapur, Dist-Latur, Maharashtra, India

[2]Department of Microbiology, Shivaji Mahavidyalaya Renapur, Dist-Latur, Maharashtra, India

[3]Department of Chemistry, Katruwar arts Ratanlal Kabra Science and B. R. Mantri Commerce College, Manwat, Maharashtra, India

[4]Department of Chemistry, Nutan Mahavidyalaya Sailu, Dist-Parbhani, Maharashtra, India

ARTICLEINFO

Article History :

Published : 07 Dec 2024

Publication Issue :
Volume 11, Issue 23
Nov-Dec-2024
Page Number :
232-237

ABSTRACT

Imidazole derivatives are versatile compounds with significant applications in pharmaceuticals, agrochemicals, and green chemistry. They exhibit diverse biological activities, including antifungal, antiviral, anti-inflammatory, and antiparasitic effects, making them valuable in drug discovery. Additionally, imidazole-based ionic liquids and carbenes play critical roles in catalysis and sustainable processes. Advances in synthetic methodologies, such as the use of eco-friendly catalysts and solid supports, have addressed challenges associated with traditional approaches, promoting greener and more efficient production. This review highlights the multifunctionality of imidazole derivatives, recent innovations in their synthesis, and their broad impact across chemical and biological sciences.

Introduction

Imidazole derivatives are pivotal compounds in both chemical and biological sciences, with applications across diverse fields. Substituted imidazoles exhibit potent activity as fungicidal and herbicidal inhibitors, plant growth regulators, and pharmacological agents (1, 2). Their multifunctional nature has catalyzed interest in green chemistry, particularly as ionic liquids due to their low vapor pressure and exceptional chemical stability (3). These ionic liquids have been successfully employed as green solvents and electrolytes. Additionally, imidazolylidene carbenes, derived from imidazole frameworks, have emerged as crucial ligands in transition-metal and metal-free catalysis, significantly advancing organic synthesis (4, 5).

Over recent decades, imidazole derivatives have garnered significant attention for their wide range of biological activities. These compounds exhibit properties such as analgesic (6, 7), anti-inflammatory, antiparasitic (8), antitubercular (9, 10), antiviral (11, 12), anticonvulsant (13), and insecticidal effects (14), making them valuable

for drug discovery and development. Their extensive spectrum of activities underscores their potential as therapeutic agents and agrochemicals.

A variety of synthetic methodologies for imidazole derivatives have been developed. Classical approaches typically involve condensation reactions of diones, aldehydes, primary amines, and ammonia (15) or N-alkylation of trisubstituted imidazoles (16). Alternative strategies include sulfonamide cyclizations (17) and four-component condensation reactions (18). However, these methods often rely on harsh reaction conditions, toxic catalysts, and labor-intensive purification processes, which pose environmental and economic challenges.

Recent advancements in synthetic organic chemistry have addressed these limitations through green synthetic methodologies. These include the use of solid supports such as silica gel (19), zeolites (20), and alumina (21), as well as environmentally friendly catalysts like $NaHSO_4/SiO_2$ (22), molecular iodine (23, 24), and ionic liquids (25). These approaches aim to minimize environmental impact, enhance yields, and simplify reaction protocols. Nonetheless, many current techniques still require elevated temperatures, strong acids, or costly reagents, highlighting the ongoing need for cleaner and more sustainable synthetic methodologies.

Given the critical significance of imidazole derivatives in pharmaceuticals, agrochemicals, and green chemistry, research continues to focus on developing innovative synthetic approaches that adhere to sustainability principles while achieving high efficiency and versatility.

Innovative Strategies for the Synthesis of Imidazoline Rings :

Imidazoline, a heterocyclic compound, has attracted significant interest due to its diverse biological activities and applications in pharmaceuticals and organic synthesis. Several synthetic strategies have been developed to prepare imidazoline derivatives, and they can be broadly categorized based on the starting materials and reaction conditions. Here are the primary approaches

Z. Hamidi etal [1] reported a novel magnetic polymeric catalyst, cross-linked poly(4-vinylpyridine) supported Fe_3O_4 nanoparticles ([P4-VP]-Fe_3O_4NPs), was synthesized and successfully utilized for the efficient preparation of imidazole derivatives. The catalyst was characterized using advanced techniques, including field emission scanning electron microscopy (FESEM), X-ray diffraction (XRD), vibrating sample magnetometry (VSM), and Fourier transform infrared spectroscopy (FT-IR). The characterization results confirmed the uniform dispersion of Fe_3O_4 nanoparticles within the polymeric matrix and demonstrated the catalyst's excellent magnetic properties, facilitating easy separation and reuse.

The catalytic system exhibited high efficiency in the synthesis of various imidazole derivatives, achieving yields ranging from 68% to 99% with short reaction times. The imidazole derivatives obtained were of high purity, underscoring the catalyst's effectiveness and potential for applications in organic synthesis.

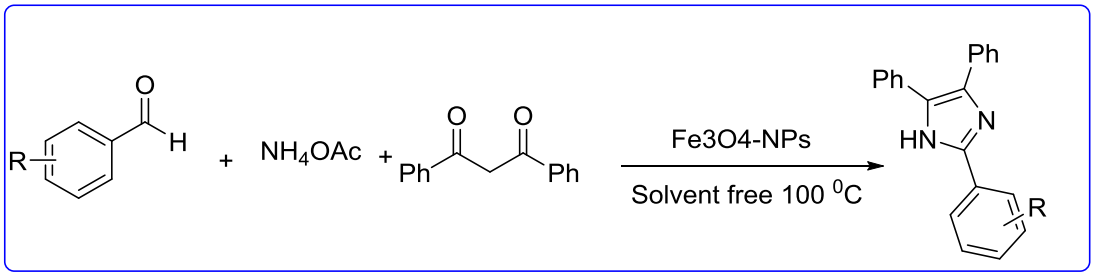

A. P.G. Nikalje reported [2] a convenient one-pot, three-component synthesis of novel 3-(4,5-diphenyl-2-substituted aryl/heteryl)-1H-imidazol-1-yl)-1H-1,2,4-triazole-5-carboxylic acid derivatives has been developed

using ceric ammonium nitrate (CAN) as a catalyst. The synthesized compounds were evaluated for their in vitro antimicrobial activity.

The antifungal activity results, supported by molecular docking studies, revealed that the synthesized derivatives possess significant antifungal potential. These findings suggest that the compounds can be further optimized and developed as promising lead candidates for antifungal drug discovery.

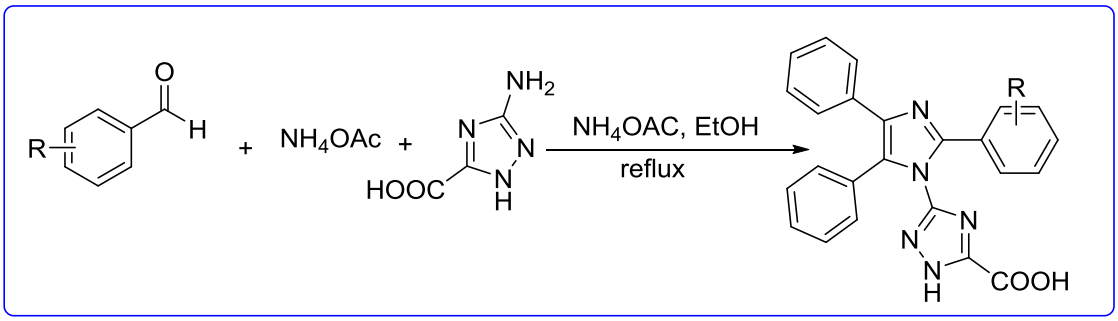

A. Davoodnia *etal* developed [3] The Brønsted acidic ionic liquid 3-methyl-1-(4-sulfonic acid)butylimidazolium hydrogen sulfate $[(CH_2)_4SO_3HMIM][HSO_4]$ has been utilized as a highly efficient, eco-friendly, and recyclable catalyst for the synthesis of 1,2,4,5-tetrasubstituted imidazoles. This reaction precedes using benzil, an aromatic aldehyde, a primary amine, and ammonium acetate under solvent-free conditions. The green synthetic approach offers numerous benefits, including high efficiency, sustainability, and operational simplicity. Remarkably, the catalyst exhibited outstanding reusability, maintaining its catalytic activity across multiple reaction cycles with negligible performance degradation.

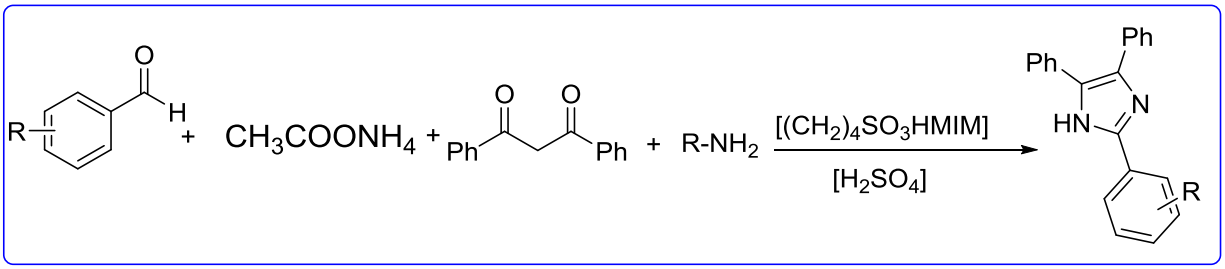

S. D. Sharma etal reported [4] Indium(III) chloride trihydrate ($InCl_3{\cdot}3H_2O$) has been demonstrated as a mild and efficient catalyst for the one-pot, three-component synthesis of 2,4,5-trisubstituted imidazoles at room temperature. Furthermore, the applicability of this catalytic protocol has been extended to the convenient one-pot, four-component synthesis of 1,2,4,5-tetrasubstituted imidazoles, achieving high product yields.

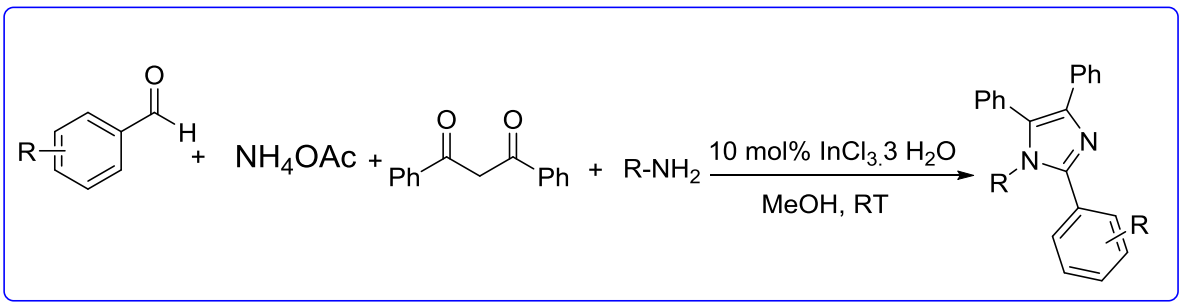

S. Kantevari *etal* [5] A highly efficient one-pot, four-component method for the synthesis of 1,2,4,5-tetrasubstituted imidazoles has been developed via the condensation of diverse aldehydes, benzil, aliphatic or aromatic primary amines, and ammonium acetate under solvent-free conditions. The reaction employs perchloric acid supported on silica gel ($HClO_4$-SiO_2) as a catalyst, achieving excellent yields. $HClO_4$-SiO_2 demonstrated exceptional catalytic performance, characterized by short reaction times (2-20 minutes) and low catalyst loading. This protocol offers notable advantages over recently reported methods, firmly establishing $HClO_4$-SiO_2 as a highly effective catalyst for the synthesis of tetrasubstituted imidazoles.

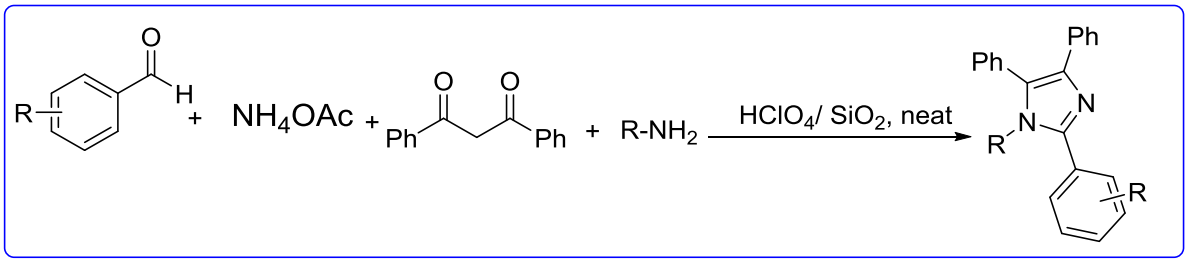

J. Sonar etal developed [6] The synthesis of 2,4,5-trisubstituted imidazole compounds has been achieved via the condensation of an aromatic aldehyde, benzil, and ammonium acetate using biodegradable lactic acid as a catalyst at 160 °C. This method is straightforward, environmentally friendly, and compatible with aromatic aldehydes bearing either electron-donating or electron-withdrawing substituents. The use of lactic acid underscores the approach's green chemistry credentials, offering a sustainable alternative for imidazole synthesis.

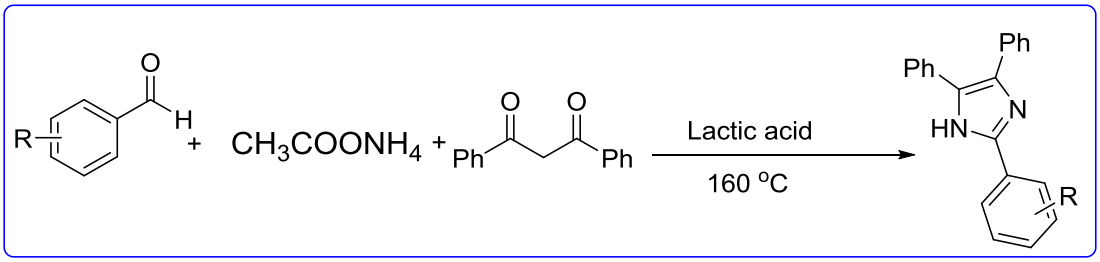

M. Kidwai *etal* reported [7] Molecular iodine has been employed as an effective catalyst for an enhanced and rapid one-pot synthesis of 2,4,5-trisubstituted and 1,2,4,5-tetrasubstituted imidazoles, achieving excellent yields. The key advantages of this iodine-catalyzed condensation include operational simplicity, cost-effective and readily available reagents, high product yields, and the use of environmentally benign, non-toxic reagents.

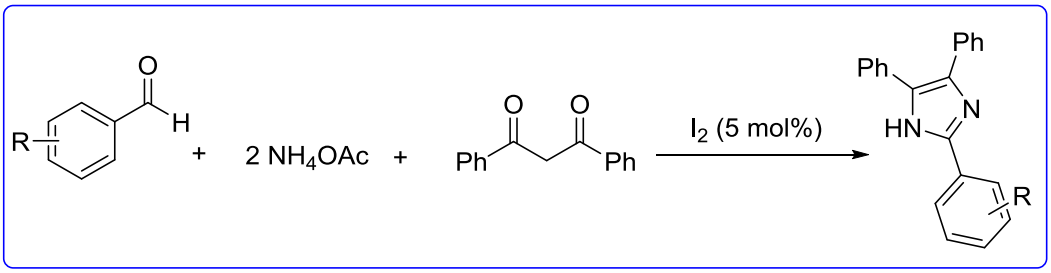

S. H. Reza coworkers developed [8] Silica gel-supported phosphorus pentoxide (P_2O_5/SiO_2) has been utilized as a highly efficient and recyclable catalyst for the synthesis of imidazole derivatives. This catalytic system enables a one-pot pseudo-four-component reaction for the synthesis of 2,4,5-trisubstituted imidazoles using benzil or

benzoin, aldehydes, and ammonium acetate. Furthermore, it facilitates the four-component synthesis of 1,2,4,5-tetrasubstituted imidazoles by employing benzil or benzoin, aldehydes, primary amines, and ammonium acetate under solvent-free thermal conditions. This approach offers significant advantages, including excellent product yields, minimal side reactions, straightforward experimental protocols, and superior reusability of the catalyst. The P_2O_5/SiO_2 catalyst can be conveniently recovered from the reaction mixture and reused multiple times with negligible loss in activity, thus representing a sustainable and practical option for imidazole synthesis.

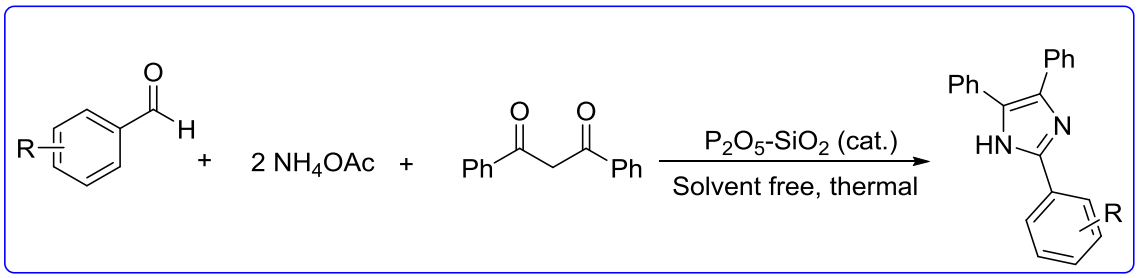

Conclusion:

The synthesis of imidazoline derivatives has advanced significantly through various strategies, ranging from traditional condensation reactions to modern green chemistry approaches. Methods such as electrophilic cyclization, multi-component reactions, and the use of eco-friendly catalysts offer efficient pathways for the formation of these valuable compounds. Despite substantial progress, challenges remain in improving reaction conditions, scalability, and sustainability. Future research will likely focus on optimizing these synthetic routes to enhance yields, reduces environmental impact, and expand the diversity of imidazoline derivatives for applications in pharmaceuticals, agrochemicals, and catalysis.

References

[1]. Lombardino, J. G.; Wiseman, E. H. J. Med. Chem. 1974, 17 (11), 1182.
[2]. Doman, T. N.; McGovern, S. L.; et al., J. Med. Chem. 2002, 45 (11), 2213.
[3]. Welton, T., Chem. Rev. 1999, 99 (8), 2071.
[4]. Glorius, F., Springer: Berlin, 2007.
[5]. Marion, N.; Diéz-González, S.; et al., Angew. Chem. Int. Ed. 2007, 46 (17), 2988.
[6]. Drabu, S.; Kumar, N., Indian J. Heterocycl. Chem. 15 (2005) 195–196.
[7]. Dutta, S.; Mariappan, G.; et al., Adv. Pharmacol. Toxicol. 9 (2008) 39–44.
[8]. Quattara, L.; Debaert, M., Farm. Ed. Sci. 42 (1987) 449–456.
[9]. Pattan, S. R.; et al., Indian J. Chem. 45B (2006) 1778–1781.
[10]. Gupta, P.; Hameed, S.; et al., Eur. J. Med. Chem. 39 (2004) 805–814.
[11]. Alagarsamy, V.; Giridhar, R.; et al., Indian J. Pharm. Sci. 68 (2006) 532–535.
[12]. Wang, Y.; Inguaggiato, G.; et al., Bioorg. Med. Chem. 7 (1999) 481–487.
[13]. Usifoh, C. O.; Scriba, G. K. E., Arch. Pharm. Pharm. Med. Chem. 333 (2000) 261–266.
[14]. Singh, T.; Sharma, S.; et al., Indian J. Chem. 45B (2006) 2558–2565.
[15]. Davidson, D.; Weiss, M.; et al., J. Org. Chem. 2 (1937) 319.
[16]. Evans, D. A.; Lundy, K. M., J. Am. Chem. Soc. 114 (1992) 1495.
[17]. Consonni, R.; Croce, P. D.; et al., J. Chem. Res. (S) 188 (1991).

[18]. Schubert, H.; Stodolka, H., J. Prakt. Chem. 22 (1963) 130.
[19]. Balalaie, S.; Arabanian, A., Green Chem. 2 (2000) 274.
[20]. Usyatinsky, A. Y.; et al., Tetrahedron Lett. 41 (2000) 5031.
[21]. Karimi, A. R.; et al., Catal. Commun. 7 (2006) 728.
[22]. Kantevari, S.; et al., J. Mol. Catal. A Chem. 266 (2007) 109.
[23]. Kidwai, M.; et al., J. Mol. Catal. A Chem. 265 (2007) 177.
[24]. Ren, Y. M.; Cai, C., J. Chem. Res. 133 (2010).
[25]. Hassaninejad, A.; et al., J. Comb. Chem. 12 (2010) 844.
[26]. Hamidi, Z.; Karimi Zarchi, M. A. React. Kinet. Mech. Catal. (2018), 125 (3), 965–982.
[27]. A. P. G. Nikalje, M. S. Ghodke, F. A. Kalam Khan, J. N. Sangshetti, Chin.Chem. Lett., (2015), 108-112.
[28]. A. Davoodnia, M.M. Heravi,Z. Safavi-Rad, N.Tavakoli-Hoseini, Synthetic Communications (2010), 40: 2588–2597.
[29]. S. D. Sharma, P. Hazarika, D. Konwar, Tetrahedron Letters, 49 (2008) 2216–2220.
[30]. S. Kantevari et al., J. of Mol. Cat. A: Chemical 266 (2007) 109–113.
[31]. J. Sonar, S. Pardeshi, S. Dokhe, R. Pawar, K. Kharat, S. Thore, SN Applied Sciences (2019) 1:1045.
[32]. M. Kidwai et al. J. of Mole. Cat. A: Chemical 265 (2007) 177–182.
[33]. S. H. Reza,Chin. J. Chem. 2011, 29, 1635—1645

International Journal of Scientific Research in Science and Technology
Available online at : www.ijsrst.com
OPEN ACCESS
Print ISSN: 2395-6011 | Online ISSN: 2395-602X
doi : https://doi.org/10.32628/IJSRST

Eco-friendly Protocol for Synthesis of 2-Amino Thiazoles using Ionic Liquid

Rajani R. Dharamkar[1], Prashant D.Netankar[1]*, Rohini R. Dharamkar[2], Roshani R. Dharamkar[2]

[1]Department of Chemistry, Maulana Azad College, Aurangabad, Maharashtra, India

[2]Department of Chemistry, G S Science Arts and Commerce College Khamgaon, Dist Buldana, Maharashtra, India

ARTICLEINFO

Article History :

Published : 07 Dec 2024

Publication Issue :
Volume 11, Issue 23
Nov-Dec-2024
Page Number :
238-243

ABSTRACT

Thiazoles play a pivotal role in various marine and terrestrial natural compounds of biological significance1. Thiazole is considered as an important core of various bioactive molecules. Thiazoles have displayed diversified activities like anticancer, 2,3 analgesic, anti-inflammatory, anaesthetic, antihypertensive, anti-inflammatory, antihypertensive, antiarythmatic,4 antipsychotic5, antibacterial, antituberculotic,6 antifungal,7 antiviral8 and antitumour,9 Some of the thiazole analogues are used as fungicidal, herbicidal, schistosomicidal and antheminitic agents.10 They are also used as sodium channel blockers11 and HIV inhibitors12.

Amino thiazoles have applications in drugs development which are to be in treatment of allergy13, hypertension14, schizophrenia15, inflammation 16, bacterial17, and HIV18 infections. Amino thiazoles are known to be ligands of estrogen receptors19 as well as a novel class of adenosine receptor antagonists20. Some analogues of amino thiazoles are used as fungicides and as an ingredients of herbicides, schitosomocidal and antihelmintic drugs.21

Biological importance of 2-aminothiazoles attracted attention of chemists over a century. Above survey of the reported methods for the syntheses of 2-aminothaizoles reveals that the widely used Hantzsch method and its modifications have certain lacuna like prolonged heating, use of costly catalysts, use of hazardous solvents, and need of non readily available materials. Considering the difficulties of these methods, here it was thought that there could be scope to develop better newer convenient synthetic greener protocol for the synthesis of 2-aminothiazoles.

In this ,2-amino thiazoles have been synthesized using ionic liquid as safer

catalyst and medium.

Keywords: Ionic liquid(ILs), 2-aminothiazoles, green protocol etc

Introduction

Thiazoles are vital constituents of numerous biologically significant terrestrial and marine natural compounds. It is believed that thiazole is an essential component of many bioactive substances. A heterocyclic amine with a thiazole core is called an aminothiazole. Another name for it is a cyclic isothiourea. It has a pyridine-like smell and dissolves in water, alcohols, and diethyl ether. With very few instances, aminothiazole itself is primarily of scholarly importance. Sulfathiazole (also known as "sulfa drugs") is a precursor to it. Hyperthyroidism can be treated with aminothiazole, a thyroid inhibitor. Anticancer, antioxidant, antibacterial, and anti-inflammatory qualities are only a few of its many pharmacological activities. It is also used to treat thyrotoxicosis, among other therapeutic purposes. The production of additional substances, including fungicides, dyes, and biocides, also starts with it. It is an antecedent of "sulfa drugs," or sulfathiazole. With an exocyclic amine and a thiazole core, 2-Aminothiazole is a main amino molecule. It smells like pyridine and dissolves in water, alcohols, and diethyl ether. A significant and adaptable scaffold, aminothiazole finds widespread use in various fields of chemistry. The thiazole core is a heterocyclic unit with five members that contains sulfur.

Review of Literature

Thiazoles are obtained by classical methods viz, Dodson - King and Hantzsch.

1] By using NBS and thioureas

2- Aminothiazoles are obtained by allowing interaction of methyl ketones with thioureas in the presence of NBS using benzoyl peroxides as radical initiator.[22]

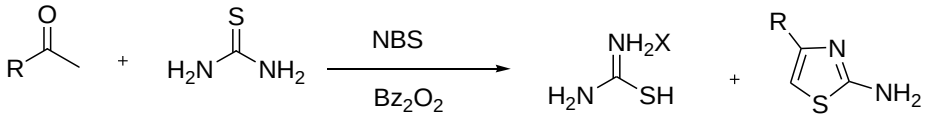

Scheme 1

2] Dodson -King method

Dodson -King[23] obtained amino thiazoles by carrying the condensation of thioureas and ketones in presence of molecular halogens.

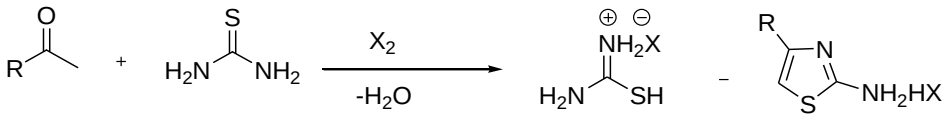

Scheme 2

The time required for the condensation is more than 15 h and the isolation of the pure products is relatively tedious.

3] **Hantzsch Method:**

a) Thiazoles and aminothiazoles are generally synthesized by Hantzsch thaizole synthesis where α-haloketones are condensed with thioamides or thioureas.[24,25]

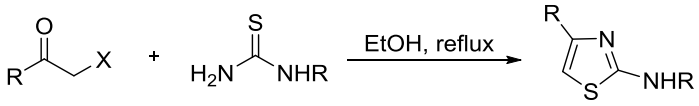

Scheme 3

b) Solid phase synthesis of 2-amino thiazoles:

Patrick et al. [26] reported solid phase synthesis of 2-aminothiazoles. Fmoc-containing resin bound thioureas were allowed to react with the solution of α -bromo ketones at r.t. to obtain the thiazoles. This synthetic protocol needs basic conditions and high polar solvent like DMF or toxic solvent like dioxane. The reaction course was found to be completed in 1-3 h. There are few more reports [27,28] on solid phase synthesis of 2-aminothiazoles having more or less the above drawbacks.

c) Using homogenous catalysts:

Recently Kidwai et al. [29] carried Hantzsch synthesis of 2-aminothiazoles using molecular iodine as catalysts to accelerate the cyclocondensation of phenacyl bromide and thioureas in ethanol.

d) Using Heterogeneous catalysts:

Biswanath Das et al. [30] have developed a rapid synthesis of thiazoles and aminothiazoles by treating phenacyl bromides with thioamides / thioureas using ammonium-12-molybdophosphate as heterogeneous catalyst in ethanol. Though the reaction course has been completed in 20 min. but non reusability of the catalyst seems to be lacuna.

2-Aminothiazoles have also been synthesized using silica chloride[31] as heterogeneous catalyst while carrying interaction of ketones and thioureas. This route involves a recyclable catalyst, but needs longer heating.

e) Using green solvent:

Pei-Ying Lin et al.[32] obtained 2-aminothiazoles by stirring α-toxyloxyacetohenones and thioureas in PEG-400 using Na_2CO_3 at r.t.

f) A catalyst free synthesis of 2-aminothiazoles has been reported by Potewar et al.[33] in water at r.t. In this synthetic route phenacyl bromides and thioureas were stirred in water for 1-2 h.

This group has also reported the similar cyclisation in ionic liquid, 1, 3-di-n-butylimidazolium tetrafluoroborate and obtained the thiazoles.[34] They also proposed the mechanism and explained role of IL as catalysts and solvent.Chemists have been interested in 2-aminothiazoles for a century due to their biological significance. Therefore mentioned review of published techniques for 2-aminothaizole synthesis shows that the popular Hantzsch method and its variations have some shortcomings, such as the requirement for non-easily accessible ingredients, the use of expensive catalysts, the use of dangerous solvents, and extended heating. It was believed that there might be room to create a more effective and convenient synthetic technique for the synthesis of 2-aminothiazoles, given the challenges posed by current approaches. In order to address the shortcomings of the existing approaches and create a good, scalable synthetic methodology for 2-aminothaizoles, efforts are being made to obtain high yields of 2-aminothiazoles.

Methodology

First time an expeditious synthetic protocol for 2-amino thiazoles has been developed by modifying Hantzsch synthesis. In this method 2-amino thiazoles have been synthesized using ionic liquid, N-methyl pyridinium tosylate as safer catalyst and medium. The condensation of substituted phenacyl chlorides and urea/aryl thiureas when carried at 110 °C in IL (N-methyl pyridinium tosylate,) was found to be completed within 6-8 minute giving high yields of the thiazoles. (**Scheme I**)

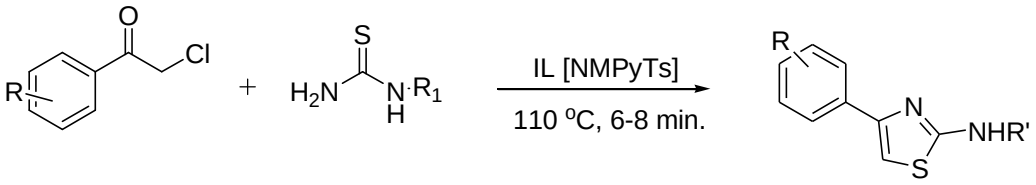

Scheme I

Experimental Section

Synthesis of Ionic Liquid (ILs):

Synthesis of N-methyl pyridinium tosylate NMPyT,(ILs)

Pyridine (1.1 mole) was added to a methyl-4-toulene sulphonate (1 mole) at 0-10 ^{O}C. After completion of addition the reaction mixture was stirred at room temperature for 1 h. The solid appeared, N-methyl pyridinium tosylate was filtered. The product was then washed with ethyl acetate to remove unreacted reactants and then dried.

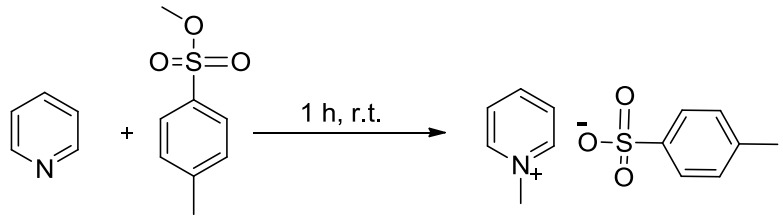

Scheme II

General experimental procedure for the synthesis of 2-amino thiazoles :

Phenacyl chlorides (10 mmol) and thioureas (11mmol) were added to a round bottom flask containing pre molten N-methyl pyridinium tosylate, ionic liquid (1gm) and the reaction mass was stirred on oil bath at 110 ^{o}C till the completion of the reaction. It was observed that reactions have been found to be completed within 6-8 minutes. The progress of the reaction was monitored by TLC. On completion of the reaction, mass was then poured on ice water and its pH was adjusted to 9-10 by adding drop wise ammonia solution .Thus obtained solid was filtered and washed with water. The crude solid was then crystallized from ethanol. (**Scheme I, Table 1**).

Substituted phenacyl chlorides used in the reaction were prepared by using literature procedure[31].

Result and Discussion

Table 1 Physical data of 2- Amino thiazoles (Scheme I).

Sr.No.	R	R^1	Yield (%)	M.P. (°C)
1	4-H	H	84	150-151
2	4-Cl	H	91	176-177

Sr.No.	R	R^1	Yield (%)	M.P. (°C)
3	4-Br	H	93	165-166
4	4-F	H	88	100-101
4	4-CH_3	H	81	135-136
5	4-Cl	C_6H_5	78	150-151
6	4-F	C_6H_5	75	110-111
7	4-CH_3	C_6H_5	73	168-169
8	4-Br	C_6H_5	75	142-143
9	4-OCH_3	C_6H_5	69	140-141
10	4-NO_2	C_6H_5	64	135-139

Spectral analyses:

Following is the spectral data of 4-(4-chlorophenyl) thiazol-2-amine as a representative

Mass: ESI^+ (m/z, % Intensity); 211 (M^+, 100) , 213 (M+ 2, 34) and 210 (12)

IR (KBr, Characteristics absorptions in cm^{-1}): 3503 (NH asy str), 3434 (NH sym str), 3022 (Ar-H str), 1635 (C=N str), 1609 (C=C str) and 758 (C-S str).

PMR (DMSO, δppm): 3.40 (d, 2H, NH_2, exchangeable with D_2O), 7.05 (s, 1H, thiazolyl H), 7.39 (d, 2H, *J*= 8Hz, Ar-H) and 7.78 (d, 2H, *J*= 8Hz, Ar-H)

Conclusion:

An expeditious synthesis has been developed by incorporating reusable N-methyl pyridinium tosylate, an ionic liquid. The developed synthetic route has many advantages like the ionic liquid, N-methyl pyridinium tosylate used in this route can be easily prepared by available materials. Also IL markedly accelerate rate of the cyclocondensation by displaying role as a catalyst and safer medium and it is found to be reusable/recyclable.

References

[1]. Borane, R.; Chanon, M.; Gallo, R.; Chemistry of heterocyclic compounds, part 2; Metzger, J. V; Ed. Wliey: New York, 1979,34.

[2]. Holfle, G.; Glaser, N.; Leibold, T.; Sefkow, M, Pure Appl. Chem. 1999, 71, 2019.

[3]. Subbagh HI, Saudi Pharm J, 7, 1999, 14; chem. Abstr. ,1999, 131, 322570

[4]. Attimarad, M.; Bagavant, G. Indian J Pharm. Sci. 1999, 61, 152.

[5]. Chaki, S.; Funakoshi, T.; Yoshikawa, R.; Okuyama, S.; Kunangi, T.; Nakagato, A.; Nagamine, M.; Tomisawa, K.; Neuropharmacolgy, 1999, 138, 1185.

[6]. Chichalia K. H.; Desai ,K. R.; J. Inst.Chem, 1998, 70, 121.

[7]. Beuchat, P.; Varache, L. M.; Nereu, A.; Leger, J. M.; Vercauteren, J.; Larrouture, S.; Deffieu, G.; Nuhich, A.; Eur. J Med. Chem. 1999, 34, 773.

[8]. Flygare, J. A.; Jean, J. C.; Koarney, P. C.; Medium J. C.; Shivraja, M. US Pat No. 9942455, 1999; Chem Abstr, 1999, 131, 184944.

[9]. Paolo, P.; Amici, R.; Villa, M.; Salom B., Veupetti A & Versai M. US Pat, 6114365, 2000, Chem Abstr., 133, 2000, 196955.

[10]. Das, B.; Saidi V.; Reddy, R.; Ramu. J Mol Catalysis A; Chemical, 2006, 252 235 and ref. cited therein.
[11]. Hogenkamp, D. J.; Upasami, R.; Nguyen, P.; US patent, 794424, 2000: Chem Abstr, 2000,133, 281779.
[12]. Ryabinin, V. A.; Zakharova, O. D.; Yurchenko, E. Y.; Tarrago L. L.; Andreola, M. L.; Sinyakov A. N. Bioorg Med Chem., 2000, 8, 985.
[13]. Hargrave, K. D; Hess, K.K; Oliver, J.T. J. Med. Chem. 1983, 26, 1158.
[14]. Patt, W. C.; Hamilton, H. W; Taylor, M. D.; Ryan, M. J.; Taylor, D.G., Batley, B. L.; Painchand, C. A.; Rapundalo, S. T.; Michiewilz, B. M.; Olzon, S. C. J. J. Med. Chem. 1992, 35,2562.
[15]. Jean, J. C. ; Wise, L. D.; Carprathe, B. W. ; Olzon, S. C. J. J. Med. Chem. 1990, 33, 311.
[16]. Clemence, F; Marter, O. L.; Delevalle, F; Mouren, M; Deraedt, R. J. Med. Chem. 1988, 31, 1453.
[17]. Tsuji, K; Ishikawa, H. Bioorg. Med. Chem. Lett. 1994, 4, 1601.
[18]. Bell, F. W. Cantrell, A. S. Hogberg, M. Jaskunas, S. R. Johansson, N. G. Jordon, C. L. Kinnick, M. D. Lind, P. Jr. Morin, J. M. Noreen, R. Oberg, J. A. B. Palkowitz, C. A. Parrish, P. J. Med. Chem. 1995, 38, 4929
[19]. Fink, B. A.; Mortensen, D. S. ; Stauffer, S. R.; Aron, Z.D.; katzenellenbogen, J. A. Chem Biol. 1999, 6, 205.
[20]. Van Muiilwijk-Koezen J. E.; Tiemmermon, H.; Vollinga, R. C.; Von Drabbe Kunzel, J. F.; De Groote, M; Visser, S; Ijzerman, A.P. J Med. Chem. 2001, 44, 749.
[21]. Metzger, J. V.; comprehensive Heterocyclic Chemistry I; Pergamon Press, 1984; 6, 328.
[22]. King, L. C. ; Dodson ,R. M., J Am. Chem. Soc, 1945, 67, 2242.
[23]. Dahiya, R. Pujari, H. K. Ind. J. Chem, 1986, 25B, 966.
[24]. Hantch, A, Sweber, H. Ber atChem Ges. 1887, 20, 3118.
[25]. Hantch A, Leibig's Ann, 1, 1888, 24.
[26]. Pattrick, K.; Monica F.; John A. F.; J. Org. Chem. 1998, 63, 196.
[27]. Said, B. K.; Sabive B. R.; Abderrahim M; Gerald; Tetraheron Lett. 2002, 43, 3193..
[28]. Kamran, G.; Srecjalekshmi, Satyabhama K. C.; Rajshekharan K. N. Tetraheron Lett. 2006, 47, 6179.
[29]. Kidwai, M.; Bhatnagar, D.; Ohora, P.; Singh, A. K.; Dey, S.; J Sulpher Chem. 2009, 30, 29.
[30]. Das , B; Reddy, V. S.; Ramu, R. J. Mole Catalysis A: Chemical, 2006, 252, 235.
[31]. Narendra, M.;; Reddy, S. M.; Sridhar, R; Nageswar, Y.V.D.; Rao, K. R.; Tetrahedron Lett. 2005, 46, 5953.
[32]. Lin, P. Y; Hou, R. S.; Wamg, H. M., Kang, I. J .J. Chin. Chem Soci ; 2009,56, 455.
[33]. Potewar, T. M.; Ingale, S. A. ; Shinivasan, K. V.; Tetrahedron, 2008, 64, 5019.
[34]. Potewar, T. M.; Ingale, S. A. ; Shinivasan, K. V.; Tetrahedron; 2007, 63, 11066.

International Journal of Scientific Research in Science and Technology
Available online at : www.ijsrst.com
OPEN ACCESS
Print ISSN: 2395-6011 | Online ISSN: 2395-602X
doi : https://doi.org/10.32628/IJSRST

A Historic Review on Graphitic Carbon Nitride (g- C_3N_4) For Photocatalysis

Rajesh M. Kharatmol
Raje Shripatrao Bhagwantrao Mahavidyalaya, Aundh, Maharashtra, India

ARTICLEINFO

Article History :

Published : 07 Dec 2024

Publication Issue :
Volume 11, Issue 23
Nov-Dec-2024
Page Number :
244-251

ABSTRACT

Photocatalysis is a green, practical, and adaptable technique that has seen widespread usage in energy conversion and environmental applications. Because photocatalysis has a high potential for solar energy utilization, extensive research has been conducted in recent decades. As a result, developing and designing efficient and stable non-metal modified g-C3N4-based photocatalysts is becoming increasingly important. This review begins with a brief description of the unique properties of g-C3N4. The most often employed modification procedures are then explained to retain the metal-free character of g-C3N4.

Figure-1.: Application of the g-C3N4 materials in various fields.

Keywords : Photocatalysis, synthesis route, optical properties.

Introduction

Incoming photons from either ultraviolet (UV) or visible-light irradiation activate semiconductor photocatalysts such as TiO2, ZnO, Fe2O3, CdS, and ZnS[1][2]. When the photon energy equals or exceeds the band-gap energy of the semiconductor photocatalysts, electrons can be activated from the VB to the CB, leaving positively charged holes in the VB[3]. The photoinduced electron-hole pairs will migrate to the particles' surfaces, where they will undergo bulk and surface recombination before reacting with the reactants on the surface. The band structure, i.e. the locations of the VB and CB, determines the redox potentials of the carriers. A concept like this for heterogeneous photocatalysis processes offers a wide range of applications.

The widespread use of photocatalysis in hydrogen production, CO2 reduction, degradation, synthesis, and self-cleaning in the 1970s and 1980s laid the groundwork for several great review studies published in the 1990s. Legrini et al. studied several photochemical techniques for water treatment [4]and found that the presence of TiO2 under UV might cause similar degradation to that of oxidants such as H2O2 or O3[5]. Kamat explored photochemistry on semiconductor nonreactive [6]and reactive surfaces, including surface activation and charge transfer mechanisms, as well as the induced photocatalytic degradation mechanism[7]. In this review, a comprehensive survey of photocatalyst materials was made. Based on this, this paper provides a critical assessment of the most recent developments in the uses of non-metal-modified g-C3N4 photocatalysts. We describe four commonly used modification strategies for keeping gC3N4 metal-free[8].

Unfortunately, certain significant difficulties significantly restrict the catalytic capability of g-C3N4[4], such as a small specific surface area (SSA), fast recombination of photoexcited electron-hole pairs, an inadequate visible light response range, and so on[9]. To solve these constraints, various researchers (including our team) have devised a variety of useful and viable solutions, such as creating nanostructures, changing electron redistribution (metal, nonmetal elements, and doping), and linking with other substances. Fortunately, multiple studies have demonstrated that the catalytic performance of g-C3N4 may be easily increased via the routes. A slew of crucial and intriguing studies has demonstrated that metal-containing g-C3N4-based materials have dramatically improved catalytic characteristics[10].

Controlling the dimension, on the other hand, was a common strategy for modifying the properties of g-C3N4.0D g-C3N4commonly referred to as g- C3N4 dots with quantum effects[11]. The 1D g-C3N4 morphology featured nanotubes, nanorods, and nanowires[2]. g-C3N4nanotubes were actively explored among them because the tubular structure can excite extra great features. g-CN is a transition metal-free semiconductor that may be used to mediate a wide range of photocatalytic processes[12]. Although photoinduced electron transfer is frequently proposed as a mechanism, PCET is a more advantageous approach for substrates with XH bonds[13]. Compared with other semiconductors, g-C3N4 can be easily synthesized by various methods [14]with desirable electrical structures as well as morphologies of the g-C3N4 family with dimensions ranging from bulk to quantum dots are shown in figure-2., we discuss the unique properties and multiple applications of g- C3N4 and several non-metal modification strategies discussed well.

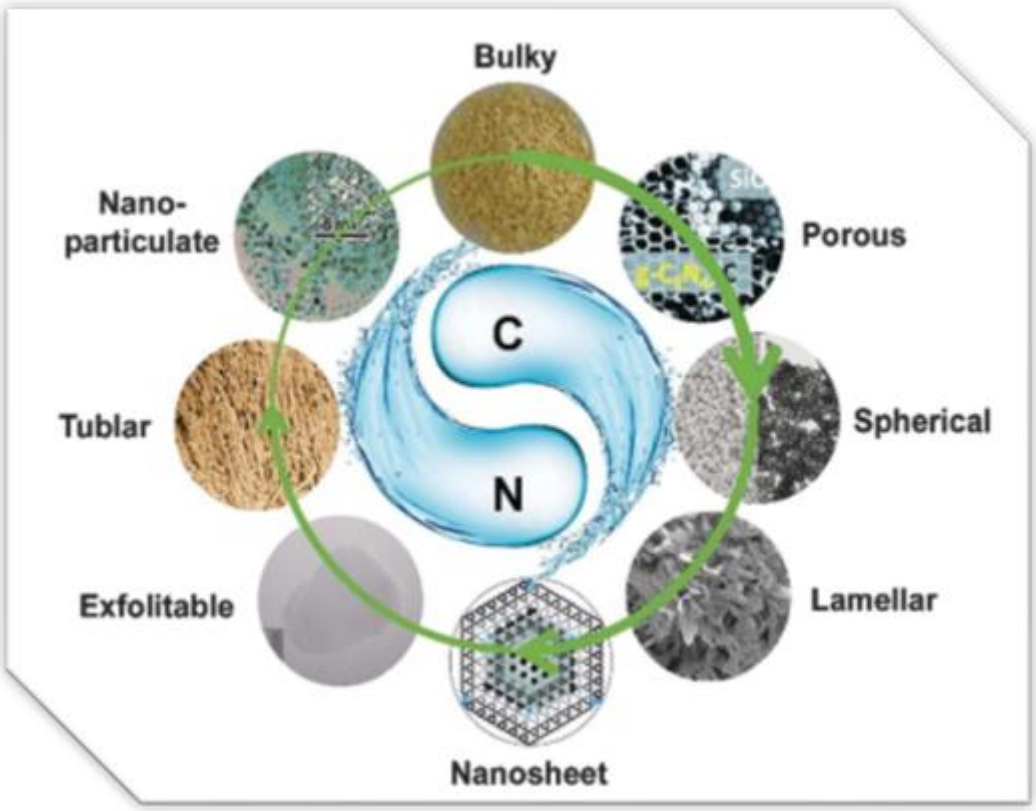

Figure-2.: Rich morphologies of the g-C3N4 family with dimensions ranging from bulk to quantum dots.

2.0 Intrinsic features/properties of graphitic carbon nitride
2.1 Beaing a metal-free
2.2 Optical properties
2.3 Being a polymer semi-conductor
2.4 Synthetic Routes of g-C3N4

2.1. Beaing a metal-free

Its advantage of being metal-free has traditionally been associated with graphitic carbon nitride. The only constituents of g-C3N4 are C, N, and frequently residual hydrogen in defects and for surface termination.

2.2. Optical properties

Optical features such as diffuse reflectance spectroscopy and photoluminescence are critical for a variety of applications[15]. UV/Vis diffuse reflectance spectroscopy and photoluminescence are often used to investigate the optical characteristics of graphitic carbon nitride[16]. The diffuse reflectance spectrum demonstrates that graphitic carbon nitride exhibits the characteristic absorption pattern of an organic semiconductor, with bandgap start adsorption at around 420 nm. At normal temperatures, graphitic carbon nitride typically shows significant blue photoluminescence[12], [13]. Carbon nitride, C3N4, reveals various crystalline forms/structures such as graphitic-C3N4 (g-C3N4), cubic- C3N4, defect zinc blende-C3N4, β- C3N4, and α- C3N4. GCN nanostructures have several distinct advantages, including high thermal durability, chemical stability, an appealing 2D layered molecular structure with promising biocompatibility, a tunable bandgap between 1.8 and 2.7 eV, high surface-rich properties, exceptional physicochemical stability, ease of hydrogen bonding, and an abundance. The critical properties of graphitic carbon nitride are shown in figure-3.

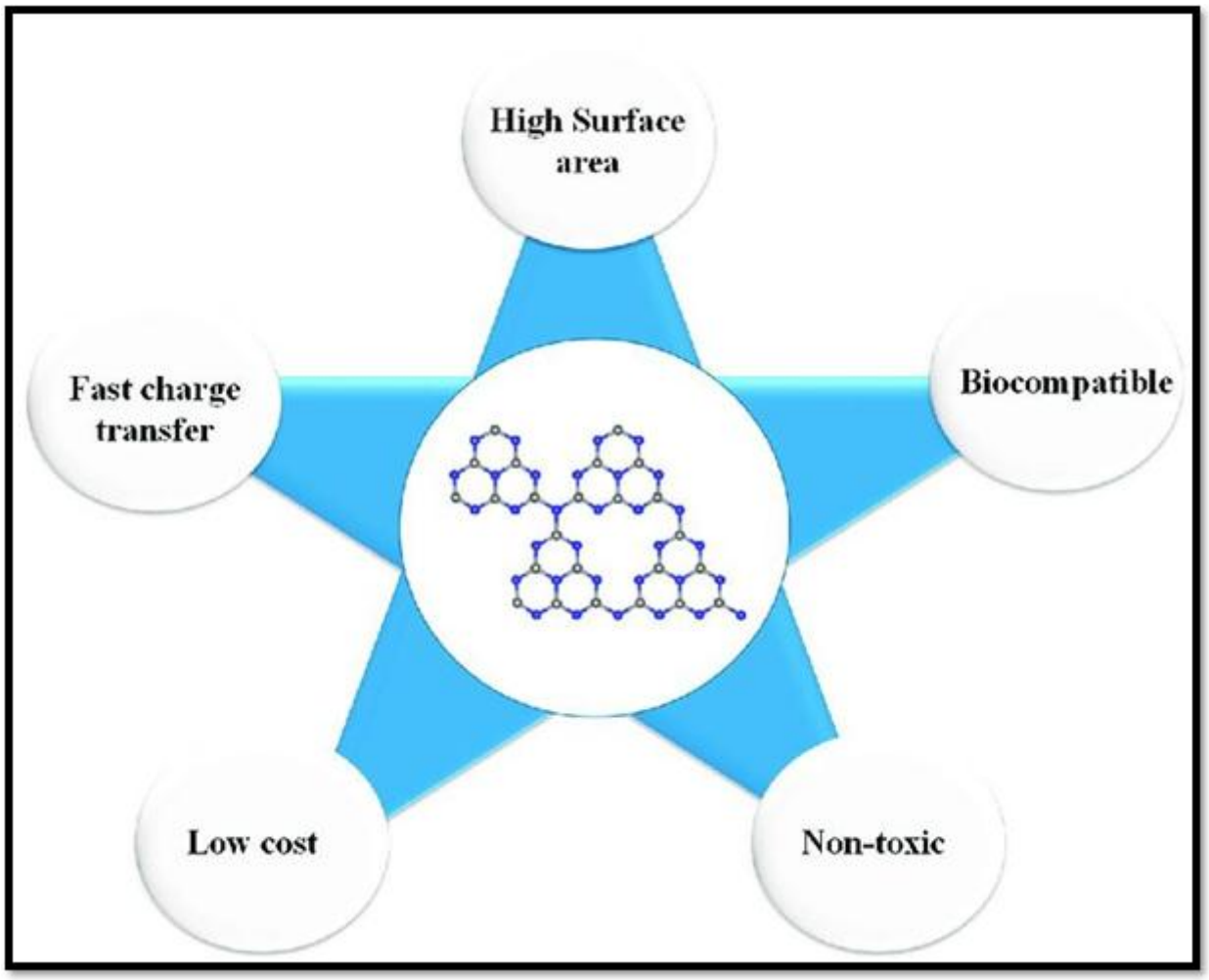

Figure-3.: Critical properties of graphitic carbon nitride.

2.3. Being a polymer semi-conductor

The bandgap of g-C3N4 is approximately 2.7 eV, with the CB and VB locations being around 1.1 eV and +1.6 eV vs. NHEs, respectively[17]. This demonstrates that it has the potential to be a visible-light-active photocatalyst for total water splitting.

2.4. Synthetic Routes of g-C3N4

Thermal polymerization of abundant nitrogen-rich and oxygen-free compound precursors containing pre-bonded C-N core structures (triazine and heptazine derivatives) such as urea, melamine, dicyandiamide, cyanamide, thiourea, guanidinium chloride, guanidine thiocyanate, and thiourea oxide can produce g-C3N4[18]. Condensation pathways from the aforementioned C/N precursors are simple and efficient strategies to build the polymeric g-C3N4 network[15]. Many studies have found that different types of precursors and treatments can have a significant impact on the physicochemical features of the final g-C3N4, such as surface area, porosity, absorbance, photoluminescence, C/N ratio, and nanostructures.

Multifunctional application

g-C3N4, being the most stable allotrope of carbon nitride, is a versatile material with unique semiconducting and photocatalytic characteristics[15]. They are also environmentally benign, inexpensive in cost, and metal-

free, making them appealing for a variety of applications other than catalysis, such as sensing, bio-imaging, photodynamic treatment, and energy conversion, photocatalytic water splitting are shown in figure 5.

3.1 g-C3N4 Catalysts

3.2 g-C3N4 Sensing

3.3 g-C3N4 Imaging

3.4 g-C3N4 Catalysts

3.5 g-C3N4 Cancer

3.6 g-C3N4 materials for photocatalytic hydrogen production

3.1. g-C3N4 Catalysts

Because of their exceptional chemical stability and distinct electronic band structure, polymeric g-C3N4 semiconductors are commonly utilized as catalysts[19] [20]. The C-pz orbit is the LUMO and the N-pz orbit is the HOMO in the development of the g-C3N4 network, with a 2.7 eV bandgap between these two orbitals[21]. Mechanism of oxidation reaction on g-C3N4 catalysts are shown in figure-4 and also one of the schematic representations of photocatalytic water splitting are shown in below figure.

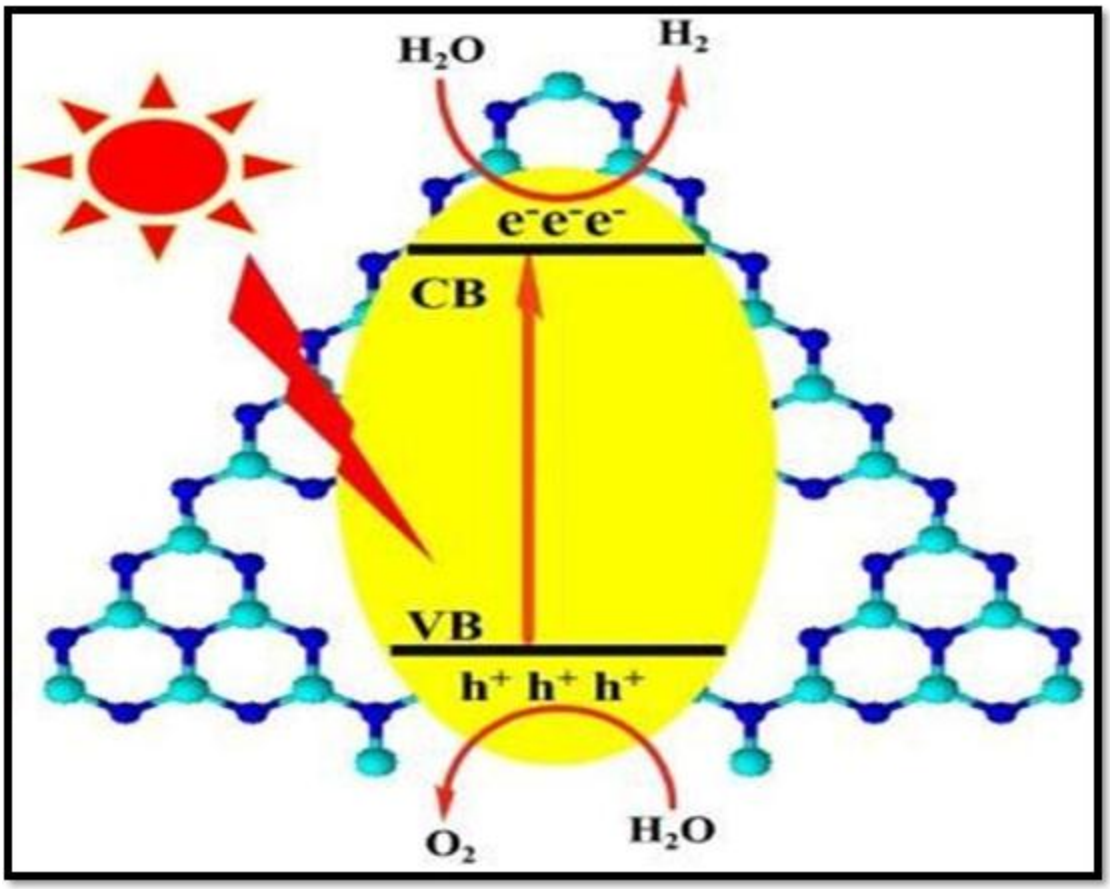

Figure-4.: Schematic representation of photocatalytic water splitting.

3.2. g-C3N4 Sensing

Polymeric g-C3N4 is widely recognized for having PL characteristics like several semiconductor materials[22]. When dissolved in solvents under UV light irradiation, g-C3N4 emits a blue PL of about 450 nm due to its direct bandgap of 2.7 eV, which may be interpreted as the transition of the s-triazine ring. Because of its enormous surface area and biocompatibility, g-C3N4 has recently received interest in its application as sensors

for biomolecules, organic pollutants, heavy metals, and medicines. Many physicochemical process changes, such as concentration, temperature, redox state, pH, biomolecule type, and biological microenvironment, frequently impact the pathological processes of tissues and organs. As a result, the development of smart and sophisticated diagnostic probes that aid in the understanding of complicated biological functions is required. Because of the polymeric semiconductor nature of g-C3N4, they are excellent optical markers for detecting changes in the signal from biological surroundings[23].

3.3. g-C3N4 Imaging

Because of their non-toxicity, metal-free nature, excellent stability, and high PL quantum yield, g-C3N4 nanosheets and nanodots are intriguing options for cell imaging[20]. Showed the fabrication of ultrathin g-C3N4 nanosheets for bioimaging applications. Even at high concentrations, they discovered that g- C3N4 nanosheets do not influence HeLa cell viability. The demand for cellular visualization and real-time monitoring in biomedical research has increased. This has resulted in substantial advancements in the production of fluorescent bioimaging agents using novel manufacturing processes. However, some difficulties remain inherent in the creation of diverse optical bioimaging agents, including poor biocompatibility, high cytotoxicity, photobleaching, and restricted fluorescence after excitation.

3.4. g-C3N4 Cancer

The intrinsic and structural properties of g-C3N4 have sparked a flood of studies into their potential uses in biomedicine[24], including cancer treatment. These characteristics, which include safe and steady fluorescence emission, a broad excitation wavelength range, simplicity of surface modification, and metal-free nature, make g-C3N4 a promising option for cancer therapy. The use of biocompatible and biodegradable semiconductors in drug delivery systems has recently gained enormous interest due to their significant therapeutic benefits over traditional therapy. Several variables, however, must still be considered in the design and deployment of polymeric semiconductors such as g-C3N4 for treatment applications. However, the hypoxic tumor microenvironment has severely hampered PDT therapeutic efficacy[25]. A hematoporphyrin monomethyl ether photosensitizer and catalase enzyme were encapsulated within the pores of a mesoporous g-C3N4 nanosheet to address this issue. Hyaluronic acid was bonded to the mesoporous g-C3N4 surface to construct a tumor-targeting and stimuli-responsive photosensitizer delivery complex to boost tumor-targeting activity. To alleviate tumor hypoxia, the catalase enzyme triggered enhanced oxygen delivery via the endogenic breakdown of tumor peroxides. The smart nano complex displayed effective photosensitizer transport and PDT platform potential. Given its large surface area, fluorescence characteristics, polymeric nature, and ease of surface modification, g-C3N4 is ideally suited to satisfy the requirements of a theragnostic platform.

3.5. g-C3N4 materials for photocatalytic hydrogen production

For decades, fossil fuels have been the primary source of energy and raw materials for the production of many industrial chemicals. Global energy consumption is steadily growing and is expected to double by 2050. This puts strain on accessible fossil reserves, potentially leading to depletion and an energy catastrophe. As a result, renewable, clean, and sustainable energy sources are desperately needed to complement decreasing fossil supplies. Researchers are now concentrating on creating efficient and cost-effective techniques to obtain clean energy from renewable resources as an alternative to non-renewable fossil fuels.

Advantages and disadvantages

Despite some advantages, such as a mild band gap (2.7 eV), visible light absorption, and flexibility, graphitic carbon nitride has limitations for practical applications due to low visible light utilization efficiency, high

recombination rate of photogenerated charge carriers, and low electrical conductivity. g-C3N4 has an appropriate band gap in the visible light region and excellent physicochemical stability. However, structural disorder, low conductivity, poor dispersibility, and hence limited processability are all disadvantages of g-C3N4.

CONCLUSION

For more than four decades, photocatalysis has been extensively researched and has demonstrated a wide range of applications, including water splitting for hydrogen evolution, CO2 conversion for hydrocarbon fuels, oxidation of aqueous and gaseous pollutants, reduction of heavy metals, building materials, and fine chemical synthesis. The methodology and application consequences have been thoroughly explained. As wide-band-gap semiconductors, g-C3N4 has been widely used as photocatalysts. The wide-band- gap energy enables strong redox potentials, which are required for facilitation. Fourth, the emergence of computational chemistry has offered theoretical direction for our experimental research, helping us to design higher-performing catalysts while also providing a vital theoretical foundation for in-depth analyses of the catalytic process.

References

[1]. F. Peng, F. Zhang, M. Fan, B. Li, and J. Li, "Preparation, characterization and photocatalytic activities of Bi-Ti-O," Chinese J. Environ. Eng., vol. 7, no. 5, pp. 1641–1645, 2013.

[2]. L. C. Sim, W. H. Tan, K. H. Leong, M. J. K. Bashir, P. Saravanan, and N. A. Surib, "Mechanistic characteristics of surface modified organic semiconductor g-C3N4 nanotubes alloyed with titania," Materials (Basel)., vol. 10, no. 1, 2017, doi: 10.3390/ma10010028.

[3]. C. Tang et al., "Recent progress in the applications of non-metal modified graphitic carbon nitride in photocatalysis," Coord. Chem. Rev., vol. 474, 2023, doi: 10.1016/j.ccr.2022.214846.

[4]. O. Legrini, E. Oliveros, and A. M. Braun, "Photochemical Processes for Water Treatment," Chem. Rev., vol. 93, no. 2, pp. 671–698, 1993, doi: 10.1021/cr00018a003.

[5]. G. Li, X. S. Zhao, and M. B. Ray, "Advanced oxidation of orange II using TiO2 supported on porous adsorbents: The role of pH, H2O2 and O3," Sep. Purif. Technol., vol. 55, no. 1, pp. 91–97, 2007, doi: 10.1016/j.seppur.2006.11.003.

[6]. P. V. Kamat and D. Meisel, "Nanoscience opportunities in environmental remediation," Comptes Rendus Chim., vol. 6, no. 8–10, pp. 999–1007, 2003, doi: 10.1016/j.crci.2003.06.005.

[7]. L. Zhou et al., "Recent advances in non-metal modification of graphitic carbon nitride for photocatalysis: A historic review," Catal. Sci. Technol., vol. 6, no. 19, pp. 7002–7023, 2016, doi: 10.1039/c6cy01195k.

[8]. N. Serpone, "Photocatalysis," Kirk-Othmer Encycl. Chem. Technol., pp. 1–17, 2000, doi: 10.1002/0471238961.1608152019051816.a01.

[9]. L. Jiang et al., "Doping of graphitic carbon nitride for photocatalysis: A reveiw," Appl. Catal. B Environ., vol. 217, pp. 388–406, 2017, doi: 10.1016/j.apcatb.2017.06.003.

[10]. Y. Xing et al., "Recent advances in the improvement of g-C3N4 based photocatalytic materials," Chinese Chem. Lett., vol. 32, no. 1, pp. 13–20, 2021, doi: 10.1016/j.cclet.2020.11.011.

[11]. M. Aleksandrzak, W. Kukulka, and E. Mijowska, "Graphitic carbon nitride/graphene oxide/reduced graphene oxide nanocomposites for photoluminescence and photocatalysis," Appl. Surf. Sci., vol. 398, pp. 56– 62, 2017, doi: 10.1016/j.apsusc.2016.12.023.

[12]. K. Qi, S. yuan Liu, and A. Zada, "Graphitic carbon nitride, a polymer photocatalyst," J. Taiwan Inst. Chem. Eng., vol. 109, pp. 111–123, 2020, doi: 10.1016/j.jtice.2020.02.012.

[13]. J. Liu, H. Wang, and M. Antonietti, “Graphitic carbon nitride ‘reloaded’: Emerging applications beyond (photo)catalysis,” Chem. Soc. Rev., vol. 45, no. 8, pp. 2308–2326, 2016, doi: 10.1039/c5cs00767d.
[14]. Z. Chen et al., “Synthesis and fabrication of g-C3N4-based materials and their application in elimination of pollutants,” Sci. Total Environ., vol. 731, p. 139054, 2020, doi: 10.1016/j.scitotenv.2020.139054.
[15]. J. Q. Brown, K. Vishwanath, G. M. Palmer, and N. Ramanujam, “Advances in quantitative UV-visible spectroscopy for clinical and pre-clinical application in cancer,” Curr. Opin. Biotechnol., vol. 20, no. 1, pp.119–131, 2009, doi: 10.1016/j.copbio.2009.02.004.
[16]. S. Le et al., “Cu-doped mesoporous graphitic carbon nitride for enhanced visible-light driven photocatalysis,” RSC Adv., vol. 6, no. 45, pp. 38811– 38819, 2016, doi: 10.1039/c6ra03982k.
[17]. Y. Li, H. Zhang, P. Liu, D. Wang, Y. Li, and H. Zhao, “Cross-linked g-C3N4/rGO nanocomposites with tunable band structure and enhanced visible light photocatalytic activity,” Small, vol. 9, no. 19, pp. 3336–3344, 2013, doi: 10.1002/smll.201203135.
[18]. A. Wang, C. Wang, L. Fu, W. Wong-Ng, and Y. Lan, “Recent advances of graphitic carbon nitride-based structures and applications in catalyst, sensing, imaging, and leds,” Nano-Micro Lett., vol. 9, no. 4, pp. 1–21, 2017, doi: 10.1007/s40820-017-0148-2.
[19]. Y. Zheng, L. Lin, B. Wang, and X. Wang, “Graphitic Carbon Nitride Polymers toward Sustainable Photoredox Catalysis,” Angew. Chemie - Int. Ed., vol. 54, no. 44, pp. 12868–12884, 2015, doi:10.1002/anie.201501788.
[20]. Y. J. Yuan, H. W. Lu, Z. T. Yu, and Z. G. Zou, “Noble-Metal-Free Molybdenum Disulfide Cocatalyst for Photocatalytic Hydrogen Production,” ChemSusChem, vol. 8, no. 24, pp. 4113–4127, 2015, doi: 10.1002/cssc.201501203.
[21]. W. Ho et al., “Copolymerization with 2,4,6-triaminopyrimidine for the rolling-up the layer structure, tunable electronic properties, and photocatalysis of g-C3N4,” ACS Appl. Mater. Interfaces, vol. 7, no. 9, pp. 5497–5505, 2015, doi: 10.1021/am509213x.
[22]. J. Wen, J. Xie, X. Chen, and X. Li, “A review on g-C 3 N 4 -based photocatalysts,” Appl. Surf. Sci., vol. 391, pp. 72–123, 2017, doi: 10.1016/j.apsusc.2016.07.030.
[23]. D. Das, S. L. Shinde, and K. K. Nanda, “Temperature-Dependent Photoluminescence of g-C3N4: Implication for Temperature Sensing,” ACS Appl. Mater. Interfaces, vol. 8, no. 3, pp. 2181–2186, 2016, doi: 10.1021/acsami.5b10770.
[24]. L. Feng et al., “G-C3N4 Coated Upconversion Nanoparticles for 808 nm Near-Infrared Light Triggered Phototherapy and Multiple Imaging,” Chem. Mater., vol. 28, no. 21, pp. 7935–7946, 2016, doi: 10.1021/acs.chemmater.6b03598.
[25]. C. Zhang, W. J. Qin, X. F. Bai, and X. Z. Zhang, “Nanomaterials to relieve tumor hypoxia for enhanced photodynamic therapy,” Nano Today, vol. 35, p. 100960, 2020, doi: 10.1016/j.nantod.2020.100960.

International Journal of Scientific Research in Science and Technology
Available online at : www.ijsrst.com
OPEN ACCESS
Print ISSN: 2395-6011 | Online ISSN: 2395-602X
doi : https://doi.org/10.32628/IJSRST

Studies on Viscosity, Density and Refractive Index of Substituted Heterocyclic Compounds in Different Media

R. D. Khalapure[1], S. R. Ingale[2], K. N. Sonune[3], R. S. Khedekar[2]
[1]Lal Bahadur Shastri Sr College Partur, Maharashtra, India
[2]Jijamata Mahavidhyalaya Buldana, Maharashtra, India
[3]Swami Vivekanand Mahavidhyalaya Mantha, Maharashtra, India

ARTICLEINFO

Article History :

Published : 07 Dec 2024

Publication Issue :
Volume 11, Issue 23
Nov-Dec-2024
Page Number :
252-258

ABSTRACT

The molar refractivity, molar polarizability and viscosity coefficients of two heterocyclic compounds, Oxymetazoline (6-tert-butyl-3-(4,5-dihydro-1H-imidazol-2-ylmethyl)-2,4-dimethylphenol) and Amikacin ((2S)-4-amino-N-[(1R,2S,3S,4R,5S)-5-amino-2-[(2S,3R,4S,5S,6R)-4-amino-3,5-dihydroxy-6-(hydroxymethyl)oxan-2-yl]oxy-4-[(2R,3R,4S,5S,6R)-6-(aminomethyl)-3,4,5-trihydroxyoxan-2-yl]oxy-3-hydroxycyclohexyl]-2-hydroxybutanamide), were examined in a variety of solvents, including ethanol, methanol, acetone, dimethylformamide (DMF), and tetrahydrofuran (THF). The study was conducted at 3030 K ± 0.1°C and covered a concentration range from 0.625 × 10^{-3} M to 10.0 × 10^{-3} M. The results show a decrease in both molar refractivity and molar polarizability with lower solute concentrations. Additionally, viscosity coefficients were determined using the Jones-Dole equation, which helped elucidate the interactions between the solute-solvent and the solute-solute interactions. These findings provide valuable insights into the molecular behaviour of the compounds in different solvents.

Keywords: Molar refractivity, molar polarizability, viscosity coefficients, solute-solvent interactions, heterocyclic compounds.

Introduction

The refractive index is a fundamental physical property that provides crucial insights into the molecular structure of liquids. For pure hydrocarbons, the refractive index can be handy in estimating the aromatic content of a liquid. When light transitions from one medium to another, it refracts, altering its direction. If the light moves from a less dense medium to a denser one, it refracts toward the normal, causing the angle of refraction to be smaller than the angle of incidence. The refractive index is defined as the ratio of the angle of incidence to the angle of refraction and is influenced by the temperature and wavelength of light.

The degree of refraction depends on several factors, including the concentration of atoms or molecules in the medium and their structural arrangement. Consequently, the refractive index offers critical insights into the geometry and structure of a molecule. While refraction is an additive property, it is also influenced by the molecular structure, which can sometimes be used to deduce the structure of an unknown compound when the molecular formula is known.

In a seminal study, R. Shukla. et. al.[1,2] examined the refractive index and density of binary liquid mixtures, including Eucalyptol and hydrocarbons, at varying temperatures, shedding light on how molecular interactions affect optical properties in such mixtures.

A. Hagahni. et. al.[3] expanded this investigation by studying the refractivity of various homologous series, such as methyl alkanoates and ethyl alkanoates, across a broad temperature range (298.15–333.15 K), highlighting the temperature dependence of the refractive index.

Y. Liu. et. al.[4] explored the relationship between refractive index and mass density in multicomponent mixtures like ambient aerosols, using an index-density relationship to predict the refractive properties of complex mixtures. This approach helped better to understand aerosol formation and behavior in the atmosphere. Similarly, M. Teodorescu. et. Al [5] studied the refractive indices of binary mixtures of bromoalkane and non-polar hydrocarbons, emphasising how molecular interactions affect the refractive index in these systems.

Y. K. Meshram. et. al.[6] contributed to the understanding of the refractive index by exploring additive properties like molar refractivity and molar polarizability constants in pharmaceutical compounds, such as allopurinol, acenocoumarol, warfarin, and amoxicillin, in different solvent media. Their findings revealed the impact of solvent choice on the optical properties of these compounds, important for drug formulation. Other studies have further deepened the understanding of refractive properties in binary mixtures.

S. Pradhan et. al.[7] investigated the refractive indices and viscosities of new binary solvent mixtures, providing detailed insights into how molecular interactions influence the optical and transport properties of these mixtures. Hema et al.[8] provided further clarity on how solvent polarity influences refractive indices in binary and ternary mixtures, showing how optical behaviors can be tailored by manipulating solvent composition recent years, more research has focused on understanding the impact of heterocyclic compounds in non-aqueous solutions.

J. George. et al.[9] examined the temperature dependence of the refractive index in ionic liquid mixtures, providing a deeper understanding of refractive index behaviour in extreme conditions. A. N. Sonar. et.al.[10] investigated how the size and structure of heterocyclic compounds influence their refractive index and optical properties when mixed with solvents.

Alongside G. R. Nibrate[11] has been studied the ultrasonic velocity, viscosity, and acoustic properties of PEG-8000 and various substituted heterocyclic compounds, focusing on the relationship between refractive index and other transport properties. Despite these advances, the study of molar refractivity, molar polarizability constants, and viscosity coefficients of substituted heterocyclic compounds remains underexplored. For instance, compounds such as Oxymetazoline and Amikacin, in non-aqueous solvents such as ethanol, methanol, acetone, DMF, and THF could provide a deeper understanding of solute-solvent interactions and their impact on the refractive index.

Experimental:

The substituted heterocyclic compounds discussed above are of significant importance. Solutions of these compounds were prepared by dissolving the appropriate amount of each compound in different solvents, including ethanol, methanol, acetone, DMF, dioxane, and THF.

For density measurements, the weight of each compound was determined using a Contech balance with an accuracy of 0.001 g. The refractive index of both the solvents and the solutions was measured over a range of 0.625×10^{-3} to 10×10^{-3} using an Abbe refractometer, which has an accuracy of ± 0.01 unit. The temperature of the refractometer's prism box was kept constant at 303 K by circulating water from a thermostat. The refractometer was calibrated using a glass test piece with a known refractive index, which was provided with the instrument.

The molar refraction of the solvent and the solution was calculated using the Lorentz-Lorentz equation. (1)

$$R_m = \frac{(n^2-1)}{(n^2+2)} X \frac{M}{d} = \frac{4}{3} \pi N\alpha$$

The entire viscosity data was analyzed using the Jones-dole equation. (2)

$$\eta_{sp}/\sqrt{c} = A + B\sqrt{c}$$

Where:

η- Refractive index

M- Molecular weight

d- Density of solution

R Molar refraction

N- Avogadro's number

α- Molar polarizability constant.

X_1, and X_2, Mole fraction of solvent and solute in solution.

Viscosity measurements were performed using an Ostwald viscometer (10 mL), and the flow time was measured with a digital clock with an accuracy of 0.01 seconds.

The refractive index of the solvent and solution at various temperatures was measured using an Abbe refractometer. The calculated values of molar refraction and the molar polarizability constant are presented in Tables 1-3 for different systems.

Table 1: Molar refraction and polarizability constant values for different systems at 303 K.

System: **Oxymetazoline** (6-tert-butyl-3-(4,5-dihydro-1H-imidazol-2-ylmethyl)- 2,4-dimethylphenol).

Solvents: Ethanol, Methanol, Acetone, DMF, THF Concentrations (mol/L): 10%, 5%, 2.5%, 1.25%, 0.625%

Concⁿ inn moles/lit.	Medium									
	Ethanol		Methanol		Acetone		DMF		THE	
	R_m	α x 10^{-26}	R_m	α x 10^{-26}	R_m	α x 10^{-26}	R_m	α x 10^{-26}	R_m	α x 10^{-26}
10 x 10^{-3}	0.05807	2.30	0.05583	2.21	0.05907	2.34	0.05625	7.11	0.05736	2.27

5 x 10^{-3}	0.05786	2.29	0.05525	2.19	0.05889	2.33	0.05307	6.83	0.05703	2.25
2.5 x 10^{-3}	0.05752	2.28	0.05502	2.18	0.05866	2.33	0.05282	6.32	0.05665	2.23
1.25x 10^{-3}	0.05712	2.26	0.05474	2.17	0.05827	2.31	0.05253	6.19	0.05599	2.22
0.625 x 10^{-3}	0.05659	2.24	0.05460	2.15	0.05758	2.28	0.05231	6.14	0.05547	2.20

Table 2: Molar refraction and polarizability constant values for different systems at 303 K.

System: **Amikacin** ((2S)-4-amino-N-[(1R,2S,3S,4R,5S)-5-amino-2-[(2S,3R,4S,5S,6R)-4-amino-3,5-dihydroxy-6-(hydroxymethyl)oxan-2-yl]oxy-4-[(2R,3R,4S,5S,6R)-6-(aminomethyl)-3,4,5-trihydroxyoxan-2-yl]oxy-3-hydroxycyclohexyl]-2-hydroxybutanamide).
Solvents: Ethanol, Methanol, Acetone, DMF, THF Concentrations (mol/L): 10%, 5%, 2.5%, 1.25%, 0.625%

Conc^{n} inn moles/lit.	Medium									
	Ethanol		Methanol		Acetone		DMF		THE	
	R_m	α x 10^{-26}	R_m	α x 10^{-26}	R_m	α x 10^{-26}	R_m	α x 10^{-26}	R_m	α x 10^{-26}
10 x 10^{-3}	0.07023	2.78	0.06853	2.72	0.07195	2.85	0.06388	2.53	0.07137	2.83
5 x 10^{-3}	0.06983	2.76	0.06829	2.71	0.07172	2.83	0.06358	2.52	0.07096	2.81
2.5 x 10^{-3}	0.06956	2.75	0.06783	2.18	0.07127	2.82	0.06326	2.50	0.07042	2.79
1.25x 10^{-3}	0.06923	2.74	0.06751	2.67	0.07096	2.81	0.06298	2.51	0.07001	2.77
0.625 x 10^{-3}	0.06894	2.72	0.06701	2.65	0.07064	2.80	0.06287	2.48	0.06955	2.75

Table 3: η_r, $\eta_{sp}/\sqrt{c}$, Falkenhagen coefficient (A), Jones-Dole Coefficient (B) of heterocyclic compounds in a different solvent.

Con^{n} mole lit $^{-1}$	Density in kg m^{-3}	Flow time (T) sec	η_r	$\eta_{sp}/\sqrt{c}$	A	B
Oxymetazoline(6-tert-butyl-3-(4,5-dihydro-1H-imidazol-2-ylmethyl)-2,4-dimethylphenol) + Ethyl alcohol						
0.01	0.82289	434	1.1662	1.66078	25595	-9.0720
0.005	0.82200	422	1.1352	1.91322		
0.0025	0.82154	413	1.1053	2.10321		
0.00125	0.82131	403	1.0782	2.20736		
0.00625	0.82118	393	1.0591	2.36388		
Amikacin ((2S)-4-amino-N-[(1R,2S,3S,4R,5S)-5-amino-2-[(2S,3R,4S,5S,6R)-4-amino-3,5-dihydroxy-6-(hydroxymethyl)oxan-2-yl]oxy-4-[(2R,3R,4S,5S,6R)-6-(aminomethyl)-3,4,5-trihydroxyoxan-2-yl]oxy-3-hydroxycyclohexyl]-2-hydroxybutanamide) + Ethyl alcohol						
0.01	0.82334	535	1.4355	4.35539	75871	-32.889
0.005	0.82232	507	1.3639	5.14667		
0.0025	0.82166	484	1.2985	5.96959		
0.00125	0.82139	458	1.2281	6.45761		
0.00625	0.82122	436	1.1693	6.76395		
Oxymetazoline (6-tert-butyl-3-(4,5-dihydro-1H-imidazol-2-ylmethyl) - 2,4-dimethylphenol) + Methyl alcohol						
0.01	0.79997	349	1.2798	2.9932	55513	-28.640
0.005	0.79711	337	1.2350	3.32518		
0.0025	0.79661	329	1.2051	4.14578		
0.00125	0.79636	318	1.1645	4.33364		
0.00625	0.79620	302	1.1205	4.61903		
Amikacin ((2S)-4-amino-N-[(1R,2S,3S,4R,5S)-5-amino-2-[(2S,3R,4S,5S,6R)-4-amino-3,5-dihydroxy-6-(hydroxymethyl)oxan-2-yl]oxy-4-[(2R,3R,4S,5S,6R)-6-(aminomethyl)-3,4,5-trihydroxyoxan-2-yl]oxy-3-hydroxycyclohexyl]-2-hydroxybutanamide) + Methyl alcohol						
0.01	0.79856	382	1.3985	3.98470	53861	-14.245
0.005	0.79733	359	1.3124	4.41556		
0.0025	0.79671	335	1.2270	4.54470		
0.00125	0.79642	320	1.1725	4.86501		
0.00625	0.79622	307	1.1279	4.11686		
Oxymetazoline(6-tert-butyl-3-(4,5-dihydro-1H-imidazol-2-ylmethyl) - 2,4-dimethylphenol) + Acetone						
0.01	0.80522	155	1.6890	6.88998	11.932	-50.96
0.005	0.80420	146	1.5781	8.17465		
0.0025	0.80370	135	1.4682	9.36620		
0.00125	0.80342	125	1.3732	10.4649		
0.00625	0.80332	116	1.2611	10.4422		
Amikacin ((2S)-4-amino-N-[(1R,2S,3S,4R,5S)-5-amino-2-[(2S,3R,4S,5S,6R)-4-amino-3,5-dihydroxy-6-(hydroxymethyl)oxan-2-yl]oxy-4-[(2R,3R,4S,5S,6R)-6-(aminomethyl)-3,4,5-trihydroxyoxan-2-yl]oxy-3-hydroxycyclohexyl]-2-hydroxybutanamide) + Acetone						
0.01	0.80567	267	2.9220	19.2196	32.225	-127.78
0.005	0.80444	241	2.6346	23.1146		
0.0025	0.80382	215	2.3388	26.7752		
0.00125	0.80352	181	2.9683	27.3833		

Oxymetazoline(6-tert-butyl-3-(4,5-dihydro-1H-imidazol-2-ylmethyl)-2,4-dimethylphenol) + DMF						
0.01	1.01362	489	1.5604	5.60418	10.176	-49.158
0.005	1.01310	452	1.4385	6.20051		
0.0025	1.01212	435	1.3827	7.65698		
0.00125	1.01185	405	1.2932	8.29615		
0.00625	1.01170	386	1.2325	9.30471		
Amikacin ((2S)-4-amino-N-[(1R,2S,3S,4R,5S)-5-amino-2-[(2S,3R,4S,5S,6R)-4-amino-3,5-dihydroxy-6-(hydroxymethyl)oxan-2-yl]oxy-4-[(2R,3R,4S,5S,6R)-6-(aminomethyl)-3,4,5-trihydroxyoxan-2-yl]oxy-3-hydroxycyclohexyl]-2-hydroxybutanamide) + DMF						
0.01	1.011406	453	1.4429	4.41991	8.609	-42.159
0.005	1.01127	432	1.3786	5.35349		
0.0025	1.01221	420	1.3416	6.83175		
0.00125	1.01192	392	1.2520	7.39556		
0.00625	1.01175	371	1.1849	7.12695		
Oxymetazoline(6-tert-butyl-3-(4,5-dihydro-1H-imidazol-2-ylmethyl)-2,4-dimethylphenol) + THF						
0.01	0.88775	125	1.2644	2.64402	5.6488	-30.150
0.005	0.88714	123	1.2432	3.44101		
0.0025	0.88683	123	1.2124	4.25146		
0.00125	0.55668	116	1.1719	4.86352		
0.00625	0.88660	112	1.1312	5.25768		
Amikacin ((2S)-4-amino-N-[(1R,2S,3S,4R,5S)-5-amino-2-[(2S,3R,4S,5S,6R)-4-amino-3,5-dihydroxy-6-(hydroxymethyl)oxan-2-yl]oxy-4-[(2R,3R,4S,5S,6R)-6-(aminomethyl)-3,4,5-trihydroxyoxan-2-yl]oxy-3-hydroxycyclohexyl]-2-hydroxybutanamide) + THF						
0.01	0.88830	126	1.2753	2.75294	4.8386	-21.471
0.005	0.88728	121	1.2335	3.30061		
0.0025	0.88690	117	1.1825	3.64697		
0.00125	0.88671	112	1.1416	4.00782		
0.00625	0.88660	109	1.1113	4.45029		

Table 3: η_r, $\eta_{sp}/\sqrt{c}$, Falkenhagen coefficient (A), Jones-Dole Coefficient (B) of heterocyclic compounds in a different solvent above.

Result and Discussion:

The molar refraction (Rm) and molar polarizability constant (a) values are higher in polar solvents such as ethanol, methanol, and acetone than in non-polar solvents like DMF. This is because polar solvents, which contain hydrogen bonding, can form complexes with the solute, whereas non-polar solvents lack hydrogen bonding and do not form such complexes.

This behaviour may be attributed to the fact that the dipole in the compound is oriented perpendicular to the longer axis of the molecule, leading to intermolecular attraction. As a result, molar refraction and molar polarizability constants increase with higher concentrations of the solution due to the mutual alignment of dipoles.

Tables 1-2 show that molar refractivity and molar polarizability constants decrease with decreasing solution concentration.

Table 3, that the 'A' (Falkenhagen coefficient) values are positive for all systems studied. The positive 'A' values indicate strong solute-solute interactions among the molecules. Conversely, the 'B' (Jones-Dole coefficient) values are negative for all drugs studied. A negative 'B' coefficient characterizes the solute as a "surface breaker," indicating weak solute-solvent interactions.

References

[1]. R. Shukla, A. Kumar, N. Awasthi, U. Srivastava, V. Gangwar, Experimental thermal and fluid science 37, 1-11, (2012) Elsevier.

[2]. R. Shukla, A. Kumar, U. Srivastava, K. Srivastava, V. Gangwar, Arabian Journal of Chemistry 9, S1357-S1367, (2016).

[3]. A. Hagahni, M. Hoffmann, H. Iloukhani, Journal of Chemical & Engineering Data 66 (5), 1956-1969, (2021).

[4]. Y. Liu., Journal of Aerosol Science 39(11):974-986, (2008). Elsevier

[5]. M. Teodorescu, C. Secuianu, Journal of Solution Chemistry 42, 1912-1934, (2013). Springer

[6]. Y. K. Meshram, S.B. Rewatkar, G. R. Nimbarte, R. R. Dharamkar, Indian journal of applied research, 6/7, 2249-555x. (2016).

[7]. S. Pradhan, S. Mishra, Journal of Molecular Liquids 279, 317-326, (2019).

[8]. Hema, T. Bhatt, SN Applied Sciences 2 (1), 43, (2020). Springer

[9]. J. George, N. V. Sastry, S. R. Patel, M. K. Valand, Journal of Chemical & Engineering Data 47 (2), 262-269, (2002).

[10]. A. N. Sonar, N. S. Pawar, Asian journal of physical chemistry, 3(2) 250-254, April. (2010).

[11]. G. R. Nibrate, Journal of Advanced Scientific Research 2021 (ICITNAS), 201-208, (2021).

[12]. M. Patel, N. Malek, Journal of Chemical & Engineering Data 67 (3), 594-606, (2022).

[13]. R Rives, A. Mialdun, V. Yasnou, V. Shevtsova, A. Coronas, The Journal of Chemical Thermodynamics 160, 106484, (2021). Elsevier.

[14]. N. Chaudhary, S. Patel, N. Acharya, M. Prajapati, A. Prajapati, Journal of Electronic Materials, 1-9, (2024). Springer

[15]. A. Sharma, R. Sharma, R. Thakur, L. Singh, Journal of Energy Chemistry 82, 592-626, (2023). Elsevier.

[16]. R. Padmanaban, A. Gayathri, A. Gopalan, D. Lee, K. Venkatramanan, Applied Sciences 13 (13), 7475, (2023).

[17]. P. Devi, P. Rani, J. Kataria, Journal of the Taiwan Institute of Chemical Engineers 159, 105468, (2024).

[18]. Y. Zheng, J. Luo, L. Li, Q. Wang, H. Lv, K. Wang, C. Lai, Journal of Chemical & Engineering Data, (2024).

[19]. Ganesh D Tambatkar, AIP Conference Proceedings 2974 (1), (2024).

[20]. F. Lari, S. Ahmadi, Journal of Molecular Structure 1257, 132651, (2022).

International Journal of Scientific Research in Science and Technology
Available online at : www.ijsrst.com
OPEN ACCESS
Print ISSN: 2395-6011 | Online ISSN: 2395-602X
doi : https://doi.org/10.32628/IJSRST

The Production of Benzothiazoles in an Organic Solvent DMF Catalyzed By Baker's Yeast

Rajani R. Dharamkar[1], Prashant D. Netankar[1], Rohini R. Dharamkar[2], Roshani R. Dharamkar[2]

[1]Department of Chemistry, Maulana Azad College, Aurangabad, Maharashtra, India

[2]Department of Chemistry, G S Science Arts and Commerce College Khamgaon, Dist Buldana, Maharashtra, India

ARTICLEINFO

Article History :

Published : 07 Dec 2024

Publication Issue :
Volume 11, Issue 23
Nov-Dec-2024
Page Number :
259-264

ABSTRACT

Benzothiazoles are an important class of privileged organic compounds of medicinal significance due to their recognized biological and therapeutic activities. As such, these heterocycles constitute key structural motifs that exhibit a wide range of biological properties. Benzothiazoles are bicyclic ring systems. In the 1950s, a number of benzothiazoles were intensively studied as central muscle relaxants. Since then medicinal chemists have not taken active interest in this chemical family. Biologist's attention was drawn to this series when the pharmacological profile of Riluzole was discovered. Riluzole is a drug used to treat amyotrophic lateral sclerosis. After that, benzothiazole derivatives have been studied extensively and found to have diverse chemical reactivity and broad spectrum of biological activities.1 A large number of therapeutic agents are synthesized with the help of benzothiazole nucleus. During recent years there have been some interesting developments in the biological activities of benzothiazole derivatives. These compounds have special significance in the field of medicinal chemistry due to their remarkable pharmacological potentialities.2 The 2-Substitued benzothiazole has emerged in its usage as a core structure in the diversified therapeutic applications. The studies of structure–activity relationship interestingly reveal that change of the structure of substituent group at C-2 position commonly results the change in its bioactivity. It shows different properties like Anti-cancer3-4, Anti-bacterial5,6,7, Anti-tuberculosis8, Anti-diabetic, Anti-inflammatory9-12, Anti-viral,Anti-oxidant13-15. In the present work an efficient and cost effective synthetic protocol have been developed for 2-arylbenzothiazoles using milder reaction conditions, carrying the condensation of 2-aminothiophenols and aryl aldehydes in organic solvent medium like DMF

inpresence of active dry baker's yeast.

Keywords: Benzothiazole, Anti-inflammatory, Anti-bacterial, Baker's yeast, DMF etc

Introduction

Benzothiazole is a fascinating organic compound belonging to the family of bicyclic heterocycles.Its core structure consists of a benzene ring fused to a five-membered thiazole ring, containing both nitrogen and sulfur atoms. This unique arrangement gives benzothiazole a diverse range of properties and applications. It is found naturally in some foods and even in certain marine organisms. It's used as a food additive due to its distinctive sulfurous odor and meaty flavor. Benzothiazole derivatives play a crucial role in the rubber industry as vulcanization accelerators, improving the properties of rubber products. They are also employed as antioxidants to prevent oxidative degradation. Some benzothiazole derivatives act as plant growth regulators, influencing plant development. Benzothiazole and its derivatives exhibit a wide spectrum of biological activities, making them valuable in medicinal chemistry. Some benzothiazole compounds show promising anti-cancer properties, targeting various cancer cell lines.They possess antibacterial activity, inhibiting the growth of bacteria. Certain benzothiazole derivatives are effective against Mycobacterium tuberculosis, the bacteria responsible for tuberculosis.These compounds have shown potential in managing diabetes by regulating blood sugar levels. Benzothiazole derivatives can reduce inflammation, making them useful in treating inflammatory diseases. Some derivatives exhibit antiviral activity, inhibiting the replication of viruses. They possess antioxidant properties, protecting cells from oxidative damage.

These structural frameworks have potent utility as imaging agents for β-amyloids, antituberculotics, chemiluminescents, calcium channel antagonists, antiparasitics and photosensitizers.[16] The benzothiazole moiety with some substitution shows promising antitumor activity. Aminomethylphenyl, carbonitrile and bis amidino substituted 2-styryl benzothiazoles show selective growth inhibitory properties against human cancer cell lines[17] proliferation of cells[18] and cytostatisis[19] respectively. Several chlorinated and fluorinated derivatives of this moiety exhibit excellent *in vitro* as well as *in vivo* antitumor activity.

Literature Review:

These wide biological and synthetic applications have prompted organic chemists to develop convenient synthetic methodologies for obtaining variety of the benzothiazoles. There are numerous methods reported to construct this value added heterocyclic system.Following is a brief review on the methods, practiced for obtaining 2-aryl benzothiazoles.

1. Jacobson cyclization

Simple and effective method to synthesize benzothiazole derivatives includes thecyclization (Jacobson cyclization, **Scheme 1**) of substituted thiobenzanilidine (in the presence of aqueous sodium hydroxide and potassium ferricyanide). But this route requires a multistep reaction sequence.[20]

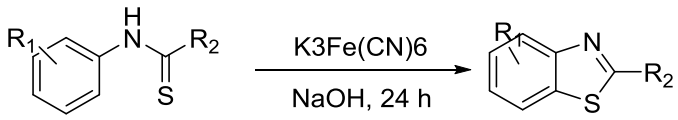

Scheme 1

2. Condensation of 2-aminothiophenols

The most widely used method involves the condensation of 2-aminothiophenol with substituted nitriles, carboxylic acids, aldehydes, acyl chlorides or esters (**Scheme2)**. A number of catalysts, namely, (pmIm)Br, I_2, $ZrOCl_2$:8H_2O, TMSCl, H_2O, PCC,CAN, PTSA, SDS, cyclodextrin, CTAB, P_2O_5/MW, H_2O_2/HCl, phosphoric acid, , have been used in the cyclo condensation of 2- aminothiophenol and aldehydes.[21-26]

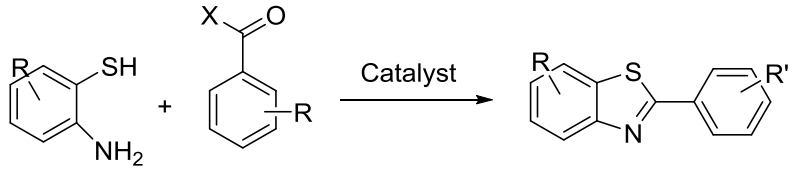

X = H, Cl, OH, OEt Scheme 2

3. **Direct arylation at 2-position of benzothiazoles** (**Scheme 3**) by employing various metal catalyst viz. $Pd(OAc)_2$, $NiBr_2$, PXPd/Cu(Xantphos)I(dichlorobis(chloro-di-tert-butylphosphine)palladium CuI /PPh3 and copper oxide has also been reported.[27-29]

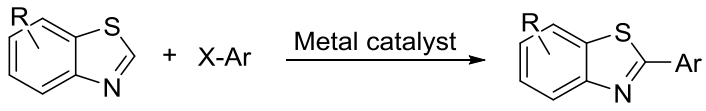

Scheme 3

Recently the cross-coupling condensation of nitro-substituted aryl halides with benzylthiols using KOH and polyethylene glycol has been demonstrated to afford benzothiazole derivatives via a novel synthetic pathway.This condensation has been found to be completed within 2 h at room temperature.[30] (Scheme 4)

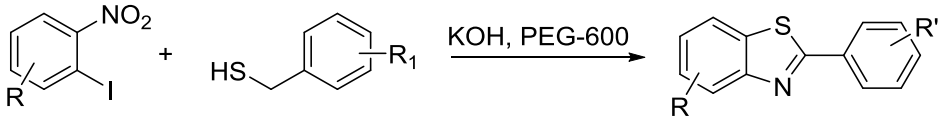

Scheme 4

Methodology:

In the present work an efficient and cost effective synthetic protocol have been developed for 2-arylbenzothiazoles using milder reaction conditions, carrying the condensation of 2-aminothiophenols and aryl aldehydes in organic medium in presence of active dry baker's yeast. It was observed that the yields of benzothiazoles were found to be better.

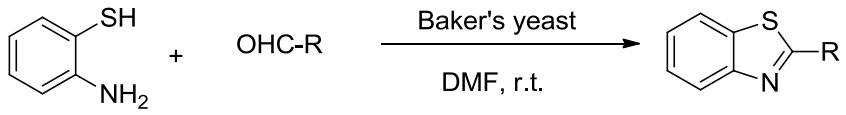

1 2a-2h 3a-3h

Scheme: I

Experimental Section:

General procedure for the synthesis 2-substituted benzothiazoles (3a-3h):

A mixture of aldehydes (8 mmol), 2-aminothiophenol (8 mmol), baker's yeast (2 g), was stirred at room temperature in DMF (25 mL). The progress of the reaction was monitored by thin layer chromatography, using petroleum ether/ethyl acetate (7:3) as a solvent system. After 24 h of stirring reaction mass was filtered through a bed of celite to remove the baker's yeast as a residue and the filtrate was concentrated under reduced pressure. On cooling, the solid product obtained was separated and
crystallized from ethanol to afford the pure benzothiazoles (**Table 2**).

Result and Discussion:

In order to find the best experimental conditions, the cyclocondensation of *p*anisaldehyde and 2-aminothiophenol, carried in the presence of baker's yeast was considered as standard model reaction. To evaluate the effect of the solvents, the model reaction was run in different solvents namely water (H2O), ethanol/water, ethanol (EtOH), methanol (MeOH), 1, 4-dioxane, acetonitrile (ACN) and N, Ndimethylformamide (DMF). The use of water orwater/ethanol as solvent gave poor yields. Solvents like ethanol, methanol, 1,4-dioxane, acetonitrile gave moderate yields. When the reaction was run in N, Ndimethylformamide (DMF),the yield of benzothiazole was found relatively better. Therefore, N, Ndimethylformamide (DMF) was selected as a solvent for this reaction.To examine the catalytic efficiency of baker's yeast, the model reaction was then run in the absence of yeast in dichloromethane. There was no conversion even after 40h. To generalize our methodology with respect to aldehydes, we have synthesized several 2-arylbenzothiazoles by the reactions of various aldehydes and 2-aminothiophenol using baker's yeast in N, Ndimethylformamide (DMF). A variety of aldehydes containing electron donating and electron withdrawing groups were successfully employed to prepare corresponding benzothiazoles. Here for the first time bakers' yeast has been successfully employed to catalyze the condensation of 2-aminothiophenol and aldehydes in N, Ndimethylformamide (DMF) to yield 2-substituted benzothiazoles in moderate to good yields under mild reaction condition. This protocol is user-friendly and could be an attractive tool for the synthesis of highly functionalized bioactive benzothiazoles.

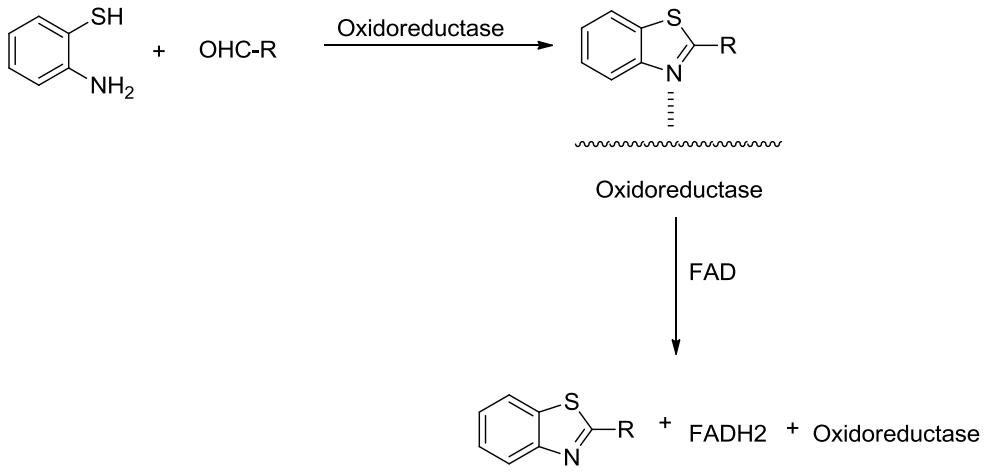

Mechanism for the formation of benzothiazole.

Table 1 Effect of solvents on the synthesis of 2-(4-methoxy phenyl)-benzothiazole, catalyzed by baker's yeast.

Entry	Solvent	Percentage yield (%)
1	H_2O	20
2	EtOH:H_2O	28
3	EtOH	59
4	MeOH	60
5	1,4-dioxane	58
6	ACN	64
7	DMF	75

Spectral data of representative compound of the series, 2-(4-methoxyphenyl) benzothiazole (3a):

1H NMR (DMSO-*d6*, 400 MHz): δ= 3.85 (s, 3H, OCH3), 7.09 (d, *J* = 8.8 Hz, 2H),7.38 (t, *J* = 7.6 Hz, 1H), 7.51 (t, *J* = 8 Hz, 1H), 8.03 (d, 1H), 8.07 (d, *J* = 8.2, 2H) and 8.09 (d, *J* = 7.6 Hz,1H).

13C NMR (75 MHz, CDCl3): δ= 55.6, 114.5, 121.7, 122.9, 124.9, 126.4, 126.5, 129.3,135.0, 159.3, 162.09 and 168.0.

MS (ESI+ mode): m/z = 242.1 (M+).

Table 2 Synthesis of 2-aryl benzothiazole derivatives catalyzed by baker's yeast (**Scheme I**).

Entry	R	Products	Percentage Yield(%)	M.P (°C)
1	4-$OCH_3C_6H_4$	**3a**	85	120-122
2	C_6H_5	**3b**	78	112-115
3	4-$N(CH_3)_2$ C_6H_4	**3c**	80	175-178
4	4-$CH_3C_6H_4$	**3d**	70	87-89
5	2-OH C_6H_4	**3e**	72	130-133
6	2-ClC_6H_4	**3f**	74	72-75
7	4-ClC_6H_4	**3g**	86	114-117
8	4-BrC_6H_4	**3h**	84	130-135

References

[1]. Priyanka, Sharma, N. K.; Jha, K. K. International J. Curr. Pharm. Res. 2010,2, 1.

[2]. Murti, Y. Importance of benzothiazole nucleus in medicinal, Article base,2008.

[3]. a) Mathis, C. A.; Wang, Y.; Holt, D. P.; Huang, G.-F.; Debnath, M. L.; Klunk,W. E. J. Med. Chem. 2003, 46, 2740. b) Hutchinson, I.; Jennings, S. A.;Vishnuvajjala, B. R.; Westwell, A. D.; Stevens, M. F. G. J. Med. Chem. 2002,45, 744. c) Alagille, D.; Baldwin, R. M.; Tamagnan, G. D. Tetrahedron Lett. 2005, 46, 1349.

[4]. Stevens, M. F. G.; Wells, G.; Westwell, A. D.; Poole, T. D. WO 03,004,479,2003; Chem. Abstr. 2003, 138, 106698.

[5]. Caujolle, R.; Loiseau, P.; Payard, M.; Gayral, P.; Kerhir, M. N. Ann. Pharm.Fr. 1989, 47, 68.

[6]. Yamamoto, K.; Fujita, M.; Tabashi, K.; Kawashima, Y.; Kato, E.; Oya, M.;Iso, T.; Iwao, J. J. Med. Chem. 1988, 31, 919.

[7]. Yoshida, H.; Nakao, R.; Nohta, H.; Yamaguchi, M. Dyes Pigments 2000, 47,239.

[8]. Petkov, I.; Deligeorgiev, T.; Markov, P.; Evstatiev, M.; Fakirov, S. Polym.Degrad. Stab. 1991, 33, 1988.

[9]. Kashiyama, E.; Hutchinson, I.; Chua, M. S.; Sherman, F.; Stinson, L. R. J.Med. Chem. 1999; 42, 4172.

[10]. Besson, T.; Benetau, V.; Guillard, J.; Leonce, S.; Pfeiffer, B. J. Med. Chem.1999, 34, 1053.

[11]. Caleta, I.; Gridisa, M.; Mrovs, S. D.; Cetina, M.; Tralic, K. V.; Pavelic, K. IL,Farmaco 2004, 59, 297.

[12]. Hutchinson, I.; Chua, M. S.; Browne, H. L.; Trapani. V.; Bradshaw,T. D.;Westwell, A.D.; J. Med. Chem. 2001, 44, 1446.

[13]. Walczynski, K.; Guryn, R.; Zuiderveld, O. P.; Timmerman, H. IL Farmaco,1999, 54, 684.

[14]. Jayachandran, E.; Bhatia, K.; Naragud, L.V.G.; Roy, A. Indian Drugs. 2003,40, 408.

[15]. Javed, S. A.; Siddiqui, N.; Drabu, S. Ind. J. Heter. Chem. 2004, 13, 287.

[16]. Doroshenko, N. Z.; Maĭskiĭ, V. A.; Pigarev, I. N. Arkh Anat Gistol Embriol.1988, 94, 90.

[17]. Bergman, J. M.; Coleman, P. J.; Cox, C.; Hartman Lindsley, G. D. C.; Mercer,S. P.; Roecker, A. J.; Whitman, D. B. PCT Int. Appl. 2006, WO 2006127550.

[18]. Ali, A.; Taylor, G. E.; Graham, D. W. PCT Int. Appl. 2001, WO 2001028561.

[19]. Koltun, D. O.; Maequart, T. A.; Shenk, K. D.; Elzein, E.; Li, Y.; Nguyen, M.;Kerwar, S.; Zeng, D.; Chu, N.; Soohoo, D.; Hao, J.; Maydanik, V. Y.; Lustig, D. A.; Ng, K. J.; Fraser, H.; Zablocki, J. A. Bioorg. Med. Chem. Letts. 2004,14, 549.

[20]. Mylari, B. L.; Larson, E. R.; Beyer, T. A.; Zembrowski, W. J.; Aldinger, C. E.;Dee, M. F.; Siegel, T. W.; Singleton, D. H. J. Med. Chem. 1991, 34, 108.

[21]. Song, K.; Kim, J. S.; Park, S. M.; Chung, K. C.; Ahn, S.; Chang, S. K. Org.Lett., 2006, 8, 3413.

[22]. Bose, S. D.; Idrees, M.; Srikanth, B. Synthesis 2007, 819.

[23]. Blacker, A. J.; Farah, M. M.; Hall, M. I.; Marsden, S. P.; Saidi, O.; Williams,J. M. J. Org. Lett. 2009, 11, 9.

[24]. Ranu, B. C.; Jana, R.; Dey, S. Chem. Lett. 2004, 33, 274.

[25]. Li, Y.; Wang, Y. L.; Wang, J. Y. Chem. Lett. 2006, 35, 460.

[26]. Moghadhan, F. M.; Ismaili, H.; Bardajee, G. R. Heteroatom Chem. 2006, 17,136.

[27]. Saha, D.; Adak, L.; Ranu, B. C. Tetrahedron Lett. 2010, 51, 5624.

[28]. Ranjit, S.; Liu, X. Chem. Eur. J. 2011, 17,1105.

[29]. Hachiya, H.; Hirano, K.; Satoh, T.; Miura, M. Org. Lett., 2009, 11, 1737.

[30]. Huang, J.; Chan, J.; Chen, Y.; Borths, C. J.; Baucom, K. D.; Larsen, R. D.;Faul, M. M.; J. Am. Chem. Soc. 2010, 132, 3674.

International Journal of Scientific Research in Science and Technology
Available online at : www.ijsrst.com
OPEN ACCESS
Print ISSN: 2395-6011 | Online ISSN: 2395-602X
doi : https://doi.org/10.32628/IJSRST

Environmentally Benign Synthesis of Copper Oxide Nanoparticles from Copper Sulphate Using Ixora Coccinea Leaves Extract

Rajani R. Dharamkar, Prashant D.Netankar, Rohini R. Dharamkar, Roshani R. Dharamkar
Maulana Azad College of Arts, Science and Commerce, Chatrapati Sambhaji Nagar-431003, Maharashtra, India
G S Science Arts and Commerce College Khamgaon 444312, Maharashtra, India

ARTICLEINFO

Article History :

Published : 07 Dec 2024

Publication Issue :
Volume 11, Issue 23
Nov-Dec-2024
Page Number :
265-270

ABSTRACT

Nanoparticles play a crucial role in organic transformations, particularly in the field of catalysis. Nanoparticles provide a high surface area-to-volume ratio, which enhances their catalytic activity. This increased surface area allows for more active sites where chemical reactions can occur, leading to improved efficiency in organic transformations. Nanoparticles catalysts often require lower reaction temperatures and reduced amounts of hazardous reagents, leading to greener and more sustainable organic transformations. They can facilitate reactions under milder conditions, reducing energy consumption and waste generation. Some nanoparticles, such as metal nanoparticles, exhibit unique catalytic properties, used in drug delivery, including size-dependent catalysis and surface plasmon resonance effects. The green approach to synthesizing nanoparticles has many advantages, like environment friendly synthesis, nontoxic, zero contaminants, simple, and do not involve hazardous chemicals, cost effective, large scale production. One of the most important nanometals is copper oxide nanoparticles because of their extensive applications in biotechnology and biomedical fields. copper oxide nanoparticles were usually synthesised by using chemical and physical methods. In the chemical methods, various toxic chemicals are used, which are harmful to the health of living organisms. Therefore, the CuO-NPs were synthesized by using biological methods based on green chemistry for reducing the toxic chemicals. There are various resources for green synthesis of CuO-NPs such as bacteria, fungi, enzyme and plant extracts. Though the CuO-NPs are synthesised by chemical methods but that are suffering from many drawbacks hence here we report the “Environmentally Benign Synthesis of Copper oxide nanoparticles from Copper sulphate Using Ixora Coccinea

Leaves Extract". In conclusion, the research findings suggest that an aqueous extract of Ixora Coccinea Linn Leaves can serve as a viable and environmentally friendly method for producing stable copper oxide nanoparticles with beneficial antioxidant and antibacterial characteristics. The morphology and magnitude of the CuO-NPs were thoroughly examined through the application of (SEM) Scanning electron microscopy.
Keywords: Copper oxide, nanoparicles, Ixora Coccinea , green synthesis, SEM etc

Introduction

Nanoparticles can be immobilized on solid supports, enabling heterogeneous catalysis. This facilitates catalyst separation and recycling, reducing the environmental impact and cost of organic transformations. Nanoparticles can create novel reaction pathways and promote reactions that are not easily achievable with conventional catalysts. This opens up new possibilities for the synthesis of complex organic molecules. In the pharmaceutical industry, specialized in treating cancerous diseases, anti-bacterial and anti-oxidant agents, nanoparticles are used for drug delivery and as catalyst in the synthesis of pharmaceutical compounds, enabling the development of more effective and targeted drugs. In addition to its use in other fields, such as nourishment, farming, fabric industries handling, make-ups, lotion, and anti-larvae agents[1-6]. Chemical methods consume money and time, also causing toxicity at the cellular and genetic levels. At this time, Scientists have attracted methods safer than chemical methods by synthesis nanoparticles using bacteria, fungi, and Yeasts[7-10]. The use of microorganisms in nanoparticle synthesis is a major challenge, especially at the industrial level, Plants have been used as bio-production sources for nanoparticles, providing clean and contaminated-free products to CuO-NPs. Biologic approaches to nanoparticle synthesis have been expanded in recent years[11-14].

Green synthesis of metal oxide-based Nano-particles: In the recent years, CuO-NPs, ZnO-NPs and nanocomposites are exciting inorganic materials can be used in various filed because have generated a great deal of interest such as energy conservation, textiles, electronics, healthcare, catalysis, cosmetics, semiconductor, chemical sensing as a catalyst in organic reactions, environmental technology. Nano particles can be synthesized by various methods (Chemicals, physical and biosynthesis) with multiple properties and large application.[15-16]

Today, the development of an efficient "green method" for synthesis of nanoparticles has become a major focus of researchers. The metal oxide nanoparticles synthesized using green approaches have more advantages than physical and chemical methods. The synthesis of nanoparticles using plants extract is drawing attention because of several advantages like, eco-friendly, non-toxic, and non-pathogenic. In green synthesis of nanoparticles, more secure, sustainable and credible reducing and capping agents are used instead of hazardous chemicals. Nanoparticles synthesized via green synthesis find applications in biomedicine, biology, materials science, electronics, biosensors, pharmaceutical, food, and cosmetic industries[17]. Green synthesis of nanoparticles is less time consuming as compared to physicochemical methods [18]. One of the significant advantage of plant-mediated nano-particles is the higher kinetics for this method than other methods [19]. Here we report CuO-NPs by using Ixora Coccinea Leaves Extract , we first time developed this green methodology.

Ethnomedicinal plant *: Ixora coccinea,* (Rubiaceae) commonly known as the flame of the woods, flame of the forest, jungle flame, burning love, scarlet ixora, jungle of Geranium, and red ixora, is one such evergreen shrub [20,21] The plant is supposed to be originally native to India and Sri Lankahowever, today it can be found growing in the tropical and subtropical climates of the world. The plants have also naturalized to Puerto Rico, Florida, and parts of Nigeria.[22] Ixora coccinea are found growing profusely in dry lands where the soil is slightly acidic.

METHODOLOGY:

Material and Methods

Collection of plants material : The leaves of the plant *Ixora coccinea* were collected from region of Buldana District (MS).

Preparation of Sample extracts: Fresh leaf of *Ixora coccinea* plant was collected and shades dried. After dry were grinded to fine powder. 10g of leaves powder of *Ixora coccinea* was transfer into beaker add 100ml of deionized water once homogenized and the sample was subjected to boiling at 80^{o}C for 3 hours in water bath. After cooling, filtered with vacuum suctions pump then filterate was collected , stored in refrigerator to avoid bacterial growth before its used for bio synthesis.

Green synthesis of CuO NPs

The metal salt 0.1 M of $CuSO_4$ solution(10ml) was prepared in round bottom flask; 90 ml of leaves extract was added to the copper sulphate solution with 30:10(V/V) using separating funnel at 80^{0}C for 3 hrs with continuous stirrer using magnetic stirrer for accelerative bio reduction of CuO-NPs. The reddish-brown colour indicated the formation of CuO-NPs. The fully reduced CuO-NPs solution was centrifuge at 5000 rpm for 5-15 min. The supernant liquid solution was discarded. The residue was purified with distilled water filter it and dry it. Then dry residue was collected in crucible, provides heat treatment/calcinations process at 500^{0}C to dry completely. It is a temperature dependent process and calcinations remove the impurities and give pure nanoparticles. The copper oxide nanoparticles are then separated and packed for further characterization.

Characteristics of Nanoparticles :

The aim of characterization of nanoparticles is to study the main parameters like size, shape, degree of aggregation, surface area and charge. The size, shape and organic ligands present on the surface of nanoparticles change their properties and applications[23]. Different techniques are used in characterization of nanoparticles commonly X-ray diffraction (XRD), scanning electron microscopy (SEM), transmission electron microscopy (TEM) etc. Here we discussed Scanning electron microscope(SEM) scans a focused electron beam over a surface to create an image. SEM is fundamentally diferent than TEM as instead of transmission of electrons, the beam falls on the sample surface and after interaction with sample gives an image pixel by pixel. SEM retains 3D topography of the sample due to large and wide depth than TEM[24].

RESULT AND DISCUSSION:

This method of green synthesis CuO-NPs beings by mixing the plant leaves extracts (natural) with $CuSO_4$ solution with biochemical reduction of cupric sulphate salt color change is observed in the solution indicating synthesis of CuO-NPs. In the present work, we develop an eco-friendly, clean, non-toxic, facile chemically preparative method, for the synthesis of CuO-NPs using the extract of *Ixora coccinea.* Research investigation indicates that the extract of *Ixora coccinea* is one of the new approaches in the field of nanosynthesis. To date, there is no report on the green synthesis of CuO-NPs by utilizing the leaves extract of *Ixora coccinea.* While

performing our research we took (**2.49gm** of $CuSO_4$) and obtain yield of nanoparticles is **0.05gm**. Result shows that the obtain nanoparticles are crystalline in nature having a black color. Nanoparticles have low particle momentum and very high mobility. Due to the small size of nanoparticles, they allow for free movement and therefore heat treatment is necessary in furnace which transfers heat. Synthesized CuO-NPs shows magnetic properties.

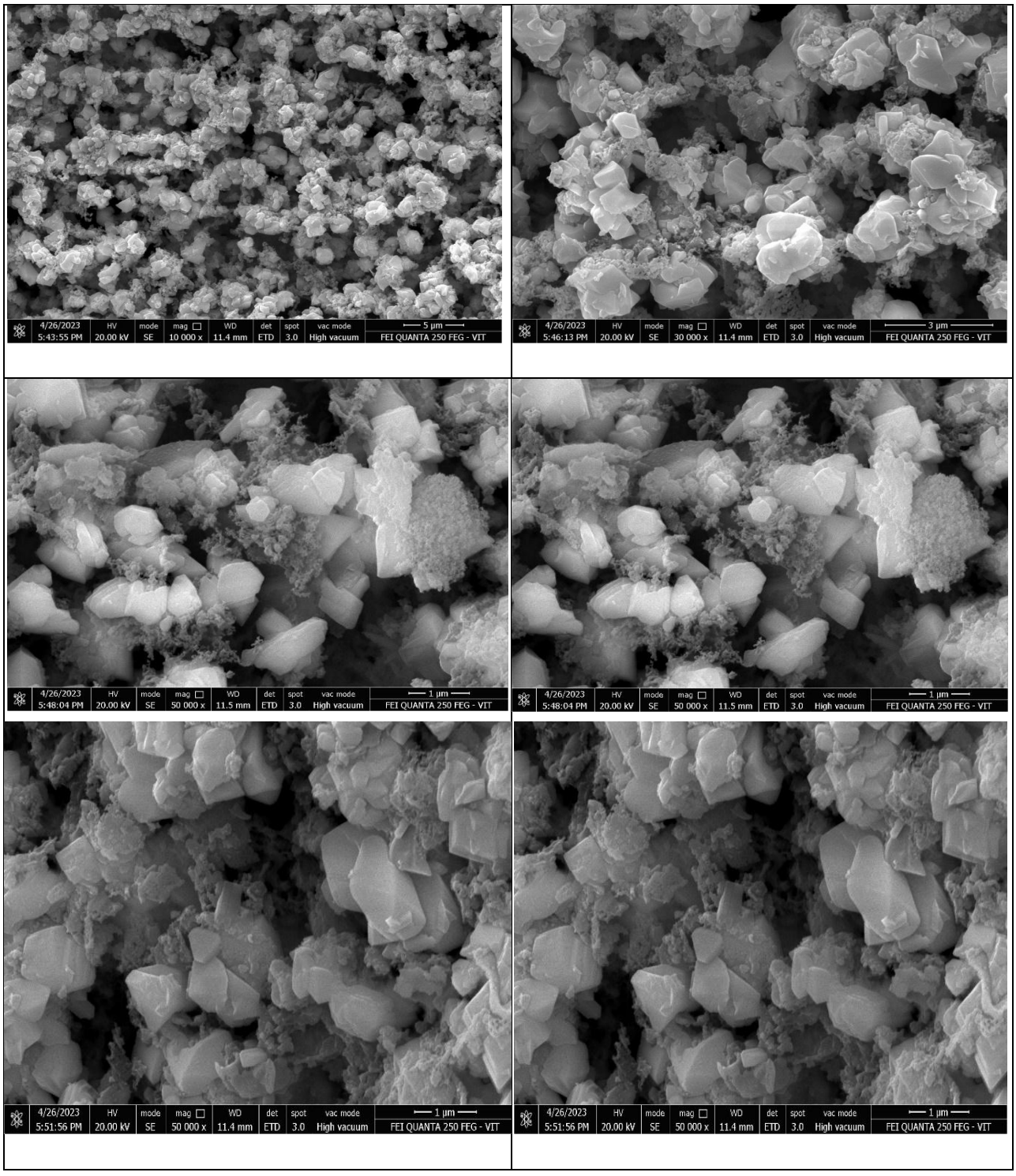

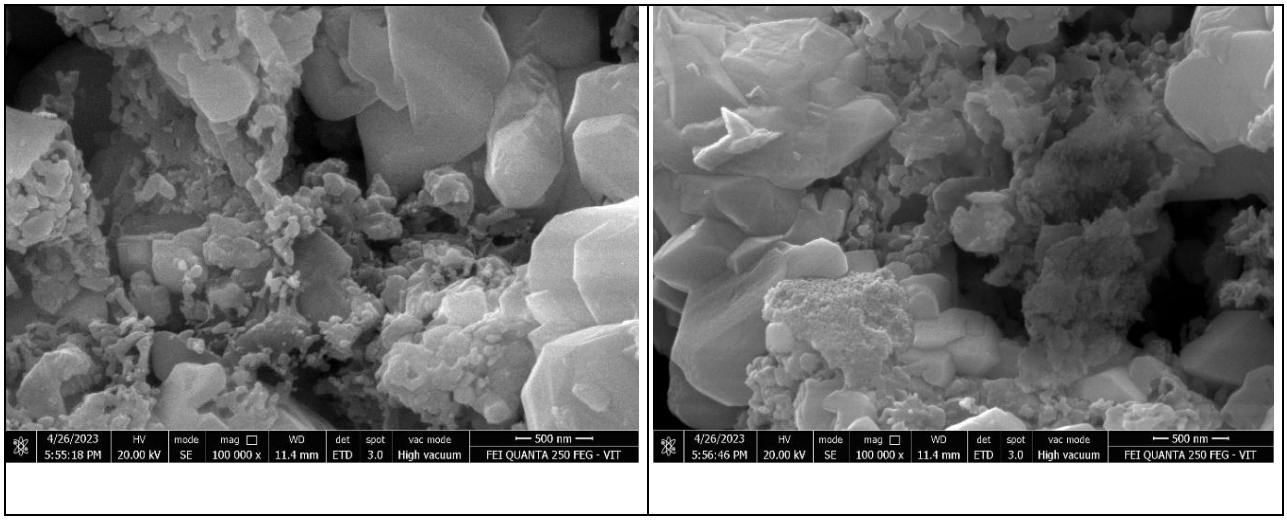

Fig: Scanning Electron Microscopy (SEM) of CuO-NPs

CONCLUSION:

The green synthesis of CuO-NPs by using leaves extract of this plant *Ixora coccinea.* is successfully synthesized. The present research work shows that the leaves extract of this plant *Ixora coccinea.* can are efficiently used for CuO-NPs. Physical, chemical and green synthesis methods are available for synthesis of CuO-NPs, but the physical and chemical methods may be toxic and highly reactive and hence it is risk for environment and human health. Therefore, to search an inexpensive, reliable, safe and "Green" method for synthesis of CuO-NPs with controlled size, shape and stability is highly warranted that is no physical or chemical change when it stored. Ixora coccinea extracts have potential to be developed as antimicrobial agents, in particular against S. aureus and S. flexneri. Further studies on isolation and identification of the active principles and evaluation of possible synergism among these constituents for their antimicrobial activity are currently ongoing.

References

[1]. Ahmed I, Feroz A. Mir, Javid A. Banday :Synthesis of Metal and metal oxide nanoparticles using plant extracts-characterization and applications, Bionanosciences, Springer, 2023 https//doi.org/10.1007/s12668-023-01194-y.

[2]. Jeevanandam, J.; Barhoum, A.; Chan, Y. S.; Dufresne, A.; Danquah, M. K. Review on Nanoparticles and Nanostructured Materials: History, Sources, Toxicity and Regulations. Beilstein J. Nanotechnol.2018, 9 (1), 1050–1074. https://doi.org/10.3762/bjnano.9.98.

[3]. Heiligtag, F. J.; Niederberger, M. The Fascinating World of Nanoparticle Research. Mater. Today2013, 16 (7–8), 262–271. https://doi.org/10.1016/j.mattod.2013.07.004.

[4]. Walter, P.; Welcomme, E.; Hallégot, P.; Zaluzec, N. J.; Deeb, C.; Castaing, J.; Veyssière, P.; Bréniaux, R.; Lévêque, J. L.; Tsoucaris, G. Early Use of PbS Nanotechnology for an Ancient Hair Dyeing Formula. Nano Lett.2006, 6 (10), 2215– 2219. https://doi.org/10.1021/nl061493u.

[5]. Johnson-Mcdaniel, D.; Barrett, C. A.; Sharafi, A.; Salguero, T. T. Nanoscience of an Ancient Pigment. J. Am. Chem. Soc.2013, 135 (5), 1677–1679. https://doi.org/10.1021/ja310587c.

[6]. Hulla, J. E.; Sahu, S. C.; Hayes, A. W. Nanotechnology: History and Future. Hum. Exp. Toxicol.2015, 34 (12), 1318–1321. https://doi.org/10.1177/0960327115603588.

[7]. NNI. National Nanotechnology Initiative Strategic Plan: National Science and Technology Council Committee on Technology Subcommittee on Nanoscale Science , Engineering , and Technology. Natl. Nanotechnol. Initiat.2014.
[8]. Faisal, S.; Jan, H.; Shah, S. A.; Shah, S.; Khan, A.; Akbar, M. T.; Rizwan, M.; Jan, F.; Wajidullah; Akhtar, N.; Khattak, A.; Syed, S. Green Synthesis of Zinc Oxide (ZnO) Nanoparticles Using Aqueous Fruit Extracts of Myristica Fragrans: Their Characterizations and Biological and Environmental Applications. ACS Omega2021, 6 (14), 9709–9722. https://doi.org/10.1021/acsomega.1c00310.
[9]. Gawande, M. B.; Goswami, A.; Felpin, F. X.; Asefa, T.; Huang, X.; Silva, R.; Zou, X.; Zboril, R.; Varma, R. S. Cu and Cu-Based Nanoparticles: Synthesis and Applications in Catalysis. Chem. Rev.2016, 116 (6), 3722–3811.
[10]. Yip S.K., SaulsJ.A., Phys. Rev. Lett., 69 (1992) 2264.
[11]. Kim Y.S., Hwang I.S., Kim S.J., C.Y., Lee J.H., Sens. Actuators B, 135 (2008) 298.
[12]. Yang S., Wang C., Chen L., Chen S., Mater. Chem. Phys.120 (2010) 296.
[13]. Yu T., Cheong. F.C., Sow C.H., Nanotechnology. 15 (2004) 1732.
[14]. Faisal, S.; Jan, H.; Shah, S. A.; Shah, S.; Khan, A.; Akbar, M. T.; Rizwan, M.; Jan, F.; Wajidullah; Akhtar, N.; Khattak, A.; Syed, S. Green Synthesis of Zinc Oxide (ZnO) Nanoparticles Using Aqueous Fruit Extracts of Myristica Fragrans: Their Characterizations and Biological and Environmental Applications. ACS Omega2021, 6 (14), 9709–9722. https://doi.org/10.1021/acsomega.1c00310.
[15]. Gawande, M. B.; Goswami, A.; Felpin, F. X.; Asefa, T.; Huang, X.; Silva, R.; Zou, X.; Zboril, R.; Varma, R. S. Cu and Cu-Based Nanoparticles: Synthesis and Applications in Catalysis. Chem. Rev.2016, 116 (6), 3722–3811 https://doi.org/10.1021/acs.chemrev.5b00482.
[16]. Wang H., Xu J.Z., Zhu J.J., Chen H.Y., J. Cryst. Growth 244 (2002) 88.
[17]. Xu J.F., Ji W., Shen Z.X., Tang S.H., Ye X.R., Jia D.Z., Xin X.Q., J. Solid State Chem.147 (2000) 516.
[18]. Xu C.K., Liu Y.K., Xu G.D., Wang G.H., Mater. Res. Bull. 37 (2002) 2365.
[19]. National Institute of Science Communication and Information Resources. Glossary of Indian medicinal plants with active principles. New Delhi 1992:374.
[20]. National Institute of Science Communication and Information Resources. The wealth of India, dictionary of Indian raw materials and industrial products—raw materials. New Delhi 2002: 351no_name12 (2022-02-15). "40 Florida Shrubs (Flowering, Evergreen, Vines): Pictures and Identification". Leafy Place. Retrieved 2022-08-01a
[21]. Griffiths M. Index of garden plants. Portland: Timber Press; 1994:1234.
[22]. Ramesh C., Hari Prasad M, Ragunathan V., Curr. Nanosci. 7 (2011) 770.
[23]. Sankar R., Manikandan P., Malarvizhi V., Fathima T., Shivashangari K. S., Ravikumar V., Spectrochim. Acta Mol. Biomol. Spectrosc. 121 (2014) 746.

International Journal of Scientific Research in Science and Technology
Available online at : www.ijsrst.com
Print ISSN: 2395-6011 | Online ISSN: 2395-602X
doi : https://doi.org/10.32628/IJSRST

Kinetic and Adsorption Studies Of Acid Red 2G Dye on Pergularia Daemia Leaves

Sanket Sawant[1], Pramila Ghumare[2], Dattatraya Jirekar[2]*

[1]Department of Chemistry, Research Centre, Maulana Azad College, Chh.Sambhajinagar, Maharashtra, India
[2]Department of Chemistry, Anandrao Dhonde Alias Babaji Mahavidyalaya, Kada, Maharashtra, India

ARTICLEINFO

Article History :

Published : 07 Dec 2024

Publication Issue :
Volume 11, Issue 23
Nov-Dec-2024
Page Number :
271-280

ABSTRACT

This article presents an adsorption and kinetic study of Acid red 2G dye on Pergularia daemia (PDL) leaves. This work used a low-cost bio-adsorbent; Pergularia daemia leaves (PDL) powder, to remove Acid red 2G dye from a water based solution. We also conducted an adsorption study using this powder. We found that effect of temperature, adsorbent dose and contact time, all had positive effects on the adsorption of Acid red 2G dye on PDL leaves. Conversely, the initial concentration, the addition of salt, the pH, and the particle size of the adsorbent all had an adverse impact on the adsorption % of Acid red 2G dye. The adsorption data is analyzed through the application of pseudo first and second order kinetic models, revealing that the pseudo second order kinetic model predominantly governs the adsorption process.

In summary, our results indicate that the PDL serves as an efficient and cost-effective adsorbent for the elimination of Acid Red 2G dye molecules.

Keywords: PDL, Adsorbate, Adsorbent, Acid red 2G, Adsorption, Kinetics.

Introduction

The textile industry is among the most water-intensive sectors globally, highlighting the scarcity of water as a critical resource. Textiles are often treated with chemicals and dyes in water baths (Senthil Kumar & Grace Pavithra, 2019). Because of this the textile industry significantly contributes to global environmental degradation by discharging harmful dye effluents(Yaseen & Scholz, 2019). All effluent generated from dye manufacturing and processing of textiles is discharged into water bodies, containing a range of unsafe organic pollutants that pose significant risks to the biodiversity within the aquatic ecosystem. (Homagai, Poudel, Poudel, & Bhattarai, 2022). The decontamination of hazardous dyes from wastewater is an essential global endeavour. as even a small amount of these dyes can be unpleasant and visible(Kumar et al., 2019).So dye removal is necessary before wastewater discharge to address these issues. The best option for treating wastewater is to use an adsorption technique to remove colors, which might be a beneficial choice if the adsorbent is both inexpensive

and easily accessible. Researchers use several non-traditional, low-cost adsorbents to eliminate dyes(Mane & Bhusari, 2012).For example cashew nut shells (Thang, Khang, Hai, Nga, & Tuan, 2021), Ground Nut Waste (Etim, 2019),Pecan nut shells (Aguayo-Villarreal et al., 2013), Poplar Wood(Shokoohi, Vatanpoor, Zarrabi, & Vatani, 2010),Pine cone (Mahmoodi, Hayati, Arami, & Lan, 2011), morus alba L. Leaves (Khan, Zafar, Badar, Hussain, & Shafiq, 2015), Papaya Seeds (Foletto, Weber, Bertuol, & Mazutti, 2013),Rice husk (Safa, Bhatti, Bhatti, & Asgher, 2011),bael shell carbon (Ahmad & Kumar, 2010), activated charcoal (Mohan & Karthikeyan, 1997),Black tea leaves (Ahmed, Rafia, & Hossain, 2021), metal hydroxides sludge (Attallah, Ahmed, & Hamed, 2013),

Specifically, this study shows that PDL carbon can adsorb certain dye molecules and figures out the factors that impact how well Acid red 2G dyes adsorb onto the PDL solid leaf powder.

Materials and Methods:

1.1 Preperation of adsorbate :

In this study used Acid red 2G dye as an adsorbate. We purchased this dye, from SD Fine chem Limited corporation. The molecular formula of this dye is C30H15feN3Na3O15S3 and used a 500 ppm stock solution to determine the λ max we use a Bioera (BE/CI/SP/SB-S-03) single beam spectrophotometer to determine the dye's λ max. The λmax of dye is 715 nm (Bezak-Mazur & Adamczyk, 2012).

1.2 Preperation of adsorbent:

We first dry the leaves in the shade, grind them, and then pass them through three separate sieves to make the fine PDL leaf powder. The leaf particle sizes employed were 425, 600, and 800 microns.We used finely powdered leaves of Pergularia daemia to create a low-cost bioadsorbent for this study.

1.3 Batch adsorption studies:

We conducted this process experiment in batch mode to investigate the impact of various process parameters such as contact time, adsorbent dose, initial dye concentration,(Safa et al., 2011) salt effect, pH, zero point pH, adsorbent particle size, temperature on the adsorption study of Acid red 2G dye. The initial dye concentration is 25 ppm, and the solution volume is 100 ml. The contact time varies from 0 to 60 minutes. Other parameters include adsorbent doses ranging from 0.25 grams to 1.25 grams, initial concentrations from 10 ppm to 50 ppm, salt additions between 0.2 grams and 1.0 gram, temperatures from 301.5Kto 341.5K. degrees, pH levels from 2 to 10, and particle sizes of 425, 600, and 800 microns. C_0 shows the initial concentration of the dye, c_t defines the concentration of the dye at time t, and C_e (Cooper & Bidwell, 2006) indicates the concentration of the dye at equilibrium time. The variables 'qt' and 'qe' define the quantity of dye adsorbed at time t and the equilibrium time. The below equation illustrates percentage adsorption.

$$Qt = (C_0-C_t)/W \quad (1)$$

$$Qe = ((C_0-C_e)/W \quad (2)$$

$$\% \text{ Adsorption} = (C_0-C_t)/C_0 \times 100 \quad (3)$$

Result and Discussion:

Effect of contact time:

We examined the effect of contact time using a 25 ppm Acid re 2G dye solution. Fig.1. demonstrates contact time effect on dye removal efficiency. Figure 1 illustrates how increasing contact time enhanced dye removal. Furthermore, we discovered that dye removal was quick during the first contact time, but as contact time

increased, dye adsorption slowed (Shokoohi et al., 2010). and achieved equilibrium after 60 minutes. This may initially provide more readily available sites for adsorption, but over time, the number of active adsorption sites may decrease.

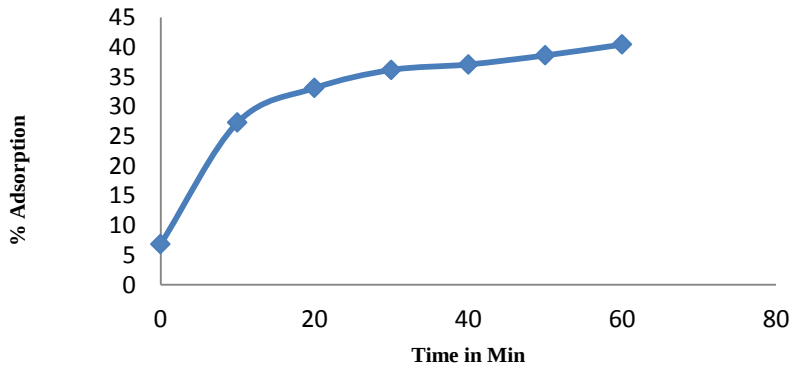

Figure 1. Contact time effect on adsorption of Acid red 2G dye on PDL

Effect of adsorbent dose:

The rate of adsorption can be enhanced by increasing the dosage of the adsorbent (Shokoohi et al., 2010). The same finding indicates that the adsorption percentage rises with an increase in adsorption dosage. The increased dosage could potentially improve the availability of surface active sites (Khenifi, Bouberka, Sekrane, Kameche, & Derriche, 2007). The adsorption percentage increases from 24.27 % to 75.26 % as the adsorption dosage increases from 0.25 grams to 1.25 grams. This is shown by fig.2.

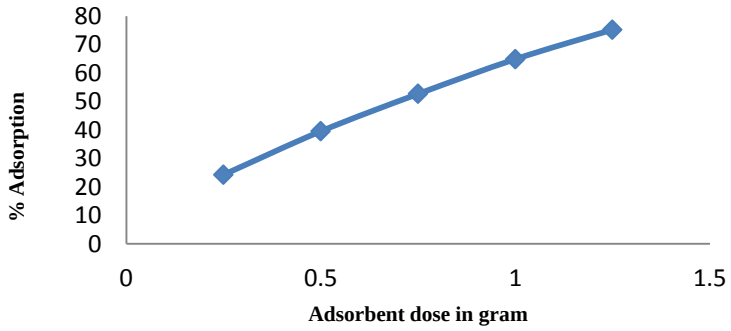

Figure 2. Adsorbent dose effect on adsorption of Acid red 2G dye on PDL

Effect of initial concentration:

Because there were more adsorption sites and fewer dye molecules at low starting concentrations, dye adsorbed up to 67.93%; however, as initial concentration increased, dye molecule adsorption decreased upto 2.7 % shown by fig.3.This is because of the adsorbents' vacant binding sites improved the dye removal efficiency at low initial concentrations. The percentage of dye removal decreased as dye concentration raised as the binding sites became nearly fully occupied at elevated dye concentrations. (Sun, Zhang, Wu, & Liu, 2010).

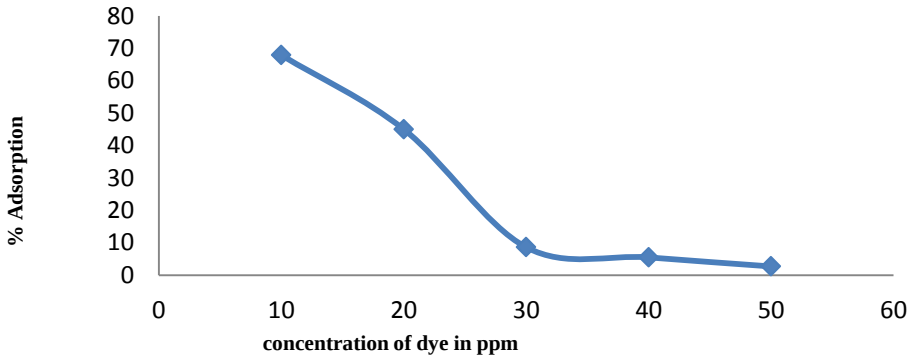

Figure 3. Initial concentration effect on adsorption of Acid red 2G dye on PDL

Effect of temperature:

The adsorption capability of Acid red 2G dye was examined from 301.5K to 341.5 K. Heat enhances Acid green 1dye adsorption, peaking at 341.5 K. The adsorption percentage increased from 43.20% to 65.19% in Figure 4.Adsorption increases with temperature owing to an increase in active adsorption sites, pore size, and pore volume.(Aksu, Tatlı, & Tunç, 2008).

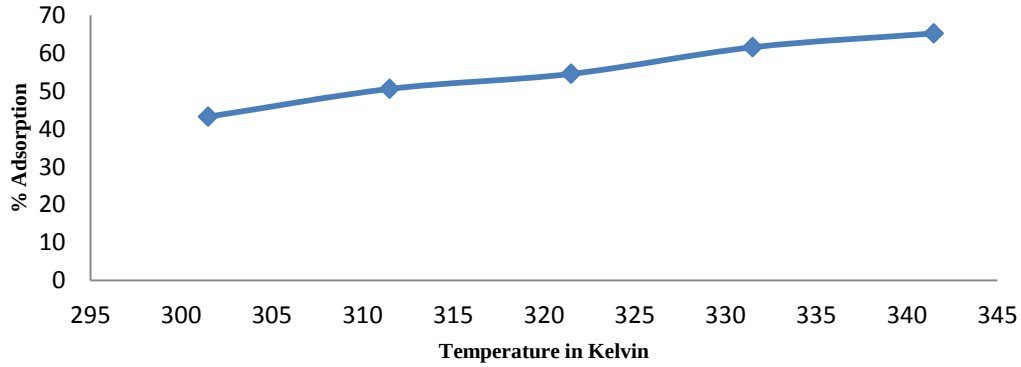

Figure 4. Temperature effect on adsorption of Acid red 2G dye on PDL

Effect of addition of salt:

The elimination of Acid red 2G dye lowers with increasing salt content, as seen in Fig.5. As the salt concentration increased from 0.2 gram to 1.0 gram the dye adsorption percentage decreased from 27.93% to 5.03%. This may be a competition between Cl^- ions and dye molecules for active adsorption sites. Cl^- ions can occupy these active adsorption sites, resulting in a decrease (Aksu & Isoglu, 2006) in the adsorption percentage (FEB_05A_2018_Pp_3226_3872-Libre.Pdf, n.d.).

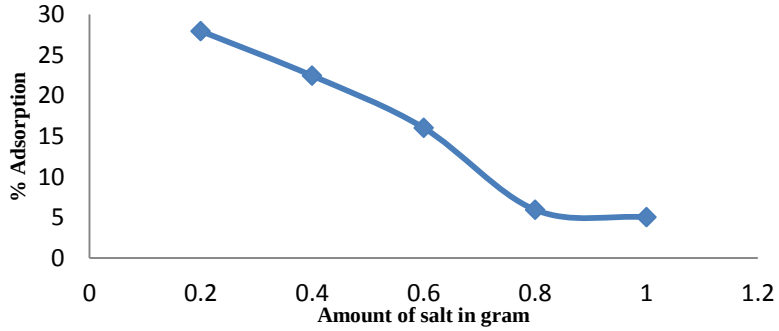

Figure 5. Addition of salt effect on adsorption of Acid red 2G dye on PDL

Effect of pH:

The dye molecule and positively charged adsorbent surface interact strongly electrostatically at acidic pH. The dye adsorption percentage rises. As pH rises, dye molecules reject one another, decreasing dye adsorption. Therefore, % adsorption drops from 97.25% to 25.19% (fig.6).(Shokoohi et al., 2010).

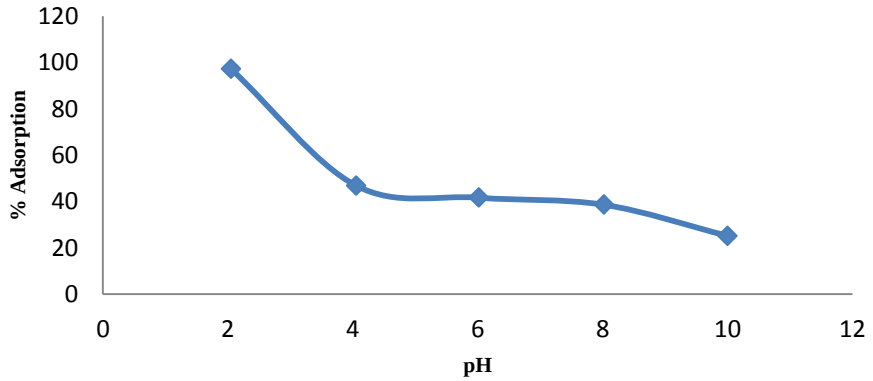

Figure 6. pH effect on adsorption of Acid red 2G dye on PDL

Effect of zero point charge:

We use the powder addition technique to facilitate Acid red 2G dye adsorption, adjusting the pH of the solutions with 0.1 N HCl and 0.1 N NaOH. At an acidic pH, dye molecules adhere strongly to the adsorbent due to the interaction between the negatively charged dye molecules and the positively charged adsorbent surface. The Fig.7 shows a zero point charge of pH=5.3. As pH decreases, dye molecules adhere to the adsorbent much less(Al-Degs, El-Barghouthi, El-Sheikh, & Walker, 2008).

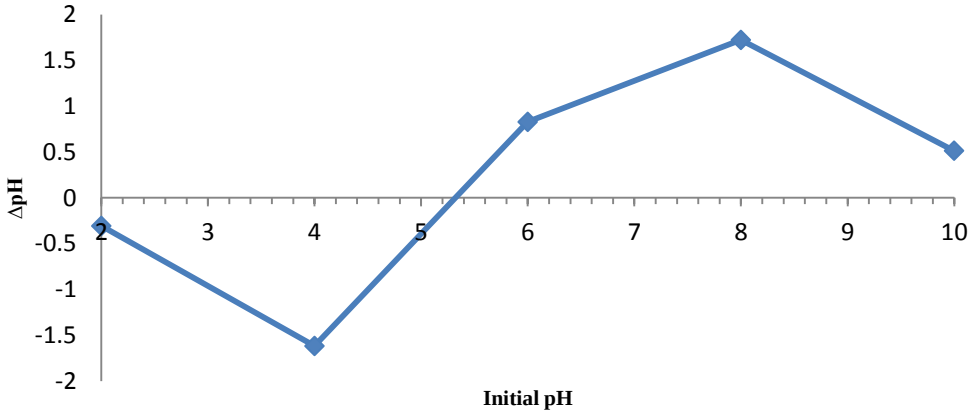

Figure 7. Zero point charge effect on adsorption of Acid red 2G dye on PDL

Effect of particle size of adsorbent:

Adsorbent particle size considerably alters dye adsorption. The amount of dye adsorbed increased with decreasing particle size (Wong, Szeto, Cheung, & McKay, 2008). because big dye molecules had trouble entering the internal pore structure of larger particles.(Wong et al., 2008). Figure 8 demonstrates how increasing the adsorbent's particle size reduces the percentage of adsorption.

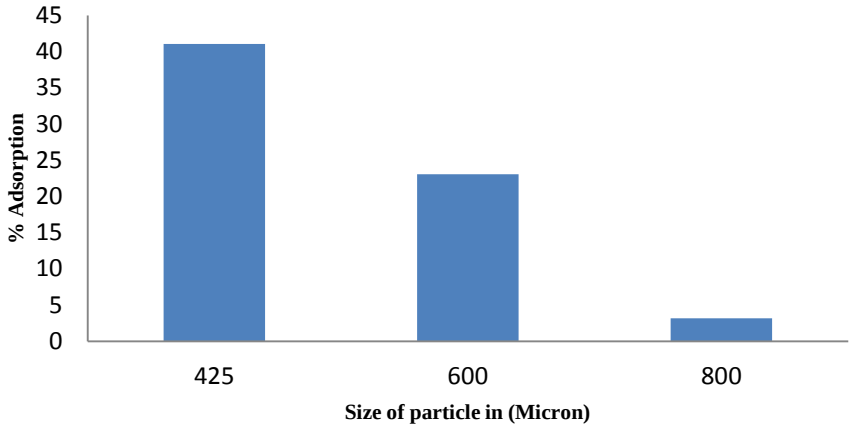

Figure 8. Particle size effect on adsorption of Acid red 2G dye on PDL

Adsorption studies:

Pseudo 1st order

An analysis of the kinetic values was conducted utilizing a pseudo 1st order rate equation. The equation can be expressed in linear form as follows:

$$\log(qe - qt) = \log qe - \frac{k_1}{2.303t} \quad (4)$$

In this context, qe_1 and qt express the quantity of adsorption at an equilibrium time and at any given time 't' respectively. The variable k_1 is the rate constant. The plot of log(qe/qt) versus 't'(Hameed, Ahmad, & Aziz, 2007) demonstrates a linear correlation (Malik, 2003). Table 1.0 displays the values of k_1, qe (Cal.), qe (Exp.), and R^2.

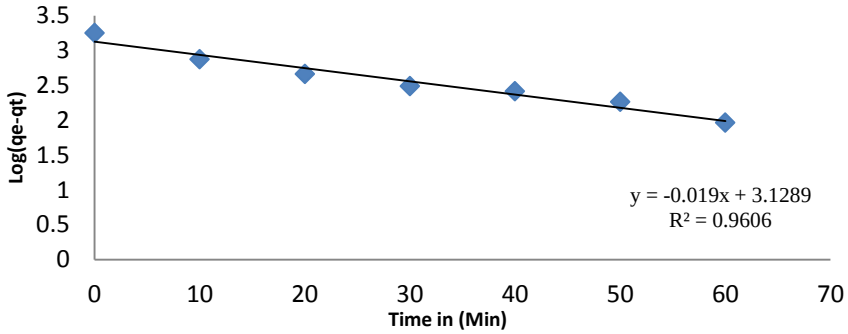

Figure 9. Pseudo first order kinetics of Acid red 2G dye on PDL

Pseudo 2nd order:

We further analyzed the kinetic values using the pseudo-second-order kinetic model. As a result, we express the second-order equation in its linear form is

$$\left(\frac{t}{qt}\right) = (1/k_{2qe^2}) + 1/qe(t) \quad (5)$$

If we apply pseudo-2nd order kinetics, we should see a linear correlation in the graph of t/qt versus t. Table 1.0 shows the k_2, the adsorption capacity at an equilibrium time (qe_2), the calculated and experimental values, and the R^2 values.

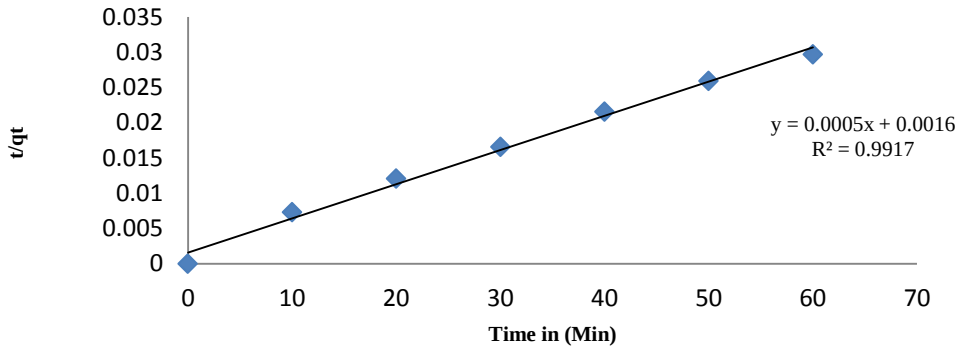

Figure 10. Pseudo second order kinetics of Acid red 2G dye on PDL

Table 1.0:

Sr.No.	Kinetics	Rate constant		Qe (mg/g)		R^2
1	Pseudo 1st order (Min-1)	Exp.	Cal.	Exp.	Cal.	0.9606
		0.066	0.043	2115	1632.63	
2	Pseudo 2nd order (g/mg.min)	$0.01*10^{-3}$	$0.15*10^{-3}$	2115	2000	0.9917

Conclusions:

The previously presented research led to the following conclusions:
Contact time positively affects acid red 2G dye adsorption on PDL; hence, an increase in contact time causes an initial spike in the dye's adsorption percentage, which then declines until it reaches 42.29% at equilibrium. When the adsorbent dosage of PDL leaves powder increases from 0.25 gram to 1.25 gram, the adsorption percentage increases from 24.27% to 75.26%, demonstrating a favorable and substantial effect. Initial concentration negatively affects acid red 2G dye adsorption because higher initial dye concentrations result in a lower adsorption percentage. As the initial dye concentration rises, the adsorption percentage drops. The total volume of adsorption pores grows, leading to an increase in adsorption as the temperature rises. Therefore, increasing the temperature from 301.5K to 341.5K increases the percentage of dye adsorption from 43.20% to 65.19%, indicating a significant and positive influence of temperature on dye adsorption. Salt addition at concentrations ranging from 0.2 to 1.0 grams negatively affects the supplied dye's adsorption process, causing the adsorption percentage to drop from 27.93% to 5.03%. At lower pH levels, dye molecules strongly interact electrostatically with the positively charged surface of an adsorbent. This causes a high percentage of adsorption to happen. Nevertheless, adsorption decreases at higher pH levels because the deposited dye molecule repels the non-adsorbed dye molecule. A pH of 5.3 is the zero point charge for this adsorption process. The ability of dye molecules to stick to adsorbent particles goes down as their size goes up because there is less surface area available for adsorption. Acid-red 2G dye adsorption on PDL leaves follows pseudo-second-order kinetics, according to the kinetic analysis.

References

[1]. Aguayo-Villarreal, I. A., Ramírez-Montoya, L. A., Hernández-Montoya, V., Bonilla-Petriciolet, A., Montes-Morán, M. A., & Ramírez-López, E. M. (2013). Sorption mechanism of anionic dyes on pecan nut

shells (Carya illinoinensis) using batch and continuous systems. Industrial Crops and Products, 48, 89–97. https://doi.org/10.1016/j.indcrop.2013.04.009

[2]. Ahmad, R., & Kumar, R. (2010). Adsorptive removal of congo red dye from aqueous solution using bael shell carbon. Applied Surface Science, 257(5), 1628–1633. Retrieved from https://www.sciencedirect.com/science/article/pii/S016943321001202X

[3]. Ahmed, R., Rafia, R. R., & Hossain, M. A. (2021). Kinetics and thermodynamics of acid red 1 adsorption on used black tea leaves from aqueous solution. International Journal of Sciences, 10(6), 7–15. Retrieved from https://www.researchgate.net/profile/Rasel-Ahmed-5/publication/352040586_Kinetics_and_Thermodynamics_of_Acid_Red_1_Adsorption_on_Used_Black_Tea_Leaves_from_Aqueous_Solution/links/60c7948992851c8e6395b14d/Kinetics-and-Thermodynamics-of-Acid-Red-1-Adsorption-on-Used-Black-Tea-Leaves-from-Aqueous-Solution.pdf

[4]. Aksu, Z., & Isoglu, I. A. (2006). Use of agricultural waste sugar beet pulp for the removal of Gemazol turquoise blue-G reactive dye from aqueous solution. Journal of Hazardous Materials, 137(1), 418–430. Retrieved from https://www.sciencedirect.com/science/article/pii/S0304389406001737

[5]. Aksu, Z., Tatlı, A. İ., & Tunç, Ö. (2008). A comparative adsorption/biosorption study of Acid Blue 161: Effect of temperature on equilibrium and kinetic parameters. Chemical Engineering Journal, 142(1), 23–39. https://doi.org/10.1016/j.cej.2007.11.005

[6]. Al-Degs, Y. S., El-Barghouthi, M. I., El-Sheikh, A. H., & Walker, G. M. (2008). Effect of solution pH, ionic strength, and temperature on adsorption behavior of reactive dyes on activated carbon. Dyes and Pigments, 77(1), 16–23. Retrieved from https://www.sciencedirect.com/science/article/pii/S0143720807000538

[7]. Attallah, M. F., Ahmed, I. M., & Hamed, M. M. (2013). Treatment of industrial wastewater containing Congo Red and Naphthol Green B using low-cost adsorbent. Environmental Science and Pollution Research, 20(2), 1106–1116. https://doi.org/10.1007/s11356-012-0947-4

[8]. Cooper, N. L., & Bidwell, J. R. (2006). Cholinesterase inhibition and impacts on behavior of the Asian clam, Cor-bicula fluminea, after exposure to an organophosphate insecticide. Aquatic Toxicology, 76(3–4), 258–267. Retrieved from https://www.sciencedirect.com/science/article/pii/S0166445X05003498

[9]. Etim, E. U. (2019). Removal of methyl blue dye from aqueous solution by adsorption unto ground nut waste. Bio-medical Journal of Scientific & Technical Research, 15(3), 11365–11371. Retrieved from https://www.academia.edu/download/84727199/BJSTR.MS.ID.002701.pdf

[10]. FEB_05A_2018_Pp_3226_3872-libre.pdf. (n.d.). Retrieved from https://d1wqtxts1xzle7.cloudfront.net/95105316/FEB_05A_2018_Pp_3226_3872-libre.pdf?1669882401=&response-content-disposition=inline%3B+filename%3DComparison_of_real_time_PCR_RT_PCR_and_m.pdf&Expires=1732796974&Signature=faOq2bxVonrFK~-UiaoA6iC1soMHkI1wVSzDduSY6m5VGZR9pWwjDcrSJE0HlP68WpKPsFwqvpoPfWf9NSyLpXnEAxKZ66LSFpd676SrM~C6Dh-SoZayilxPEMMqDTDkX94yQftUld13bmWZlBYgqm6pcTLX7a7b4kxXUApKvGhWm2r9eo-3W7-nG5W1YbeakvTfrbSQMOoTAM6bDe78Kdndt1SCk5u9hcELdRpqN5hmvlpbmWpgnFE2G6fG9AeaJhUU7NJFoa4Lp8SRcJJ8tRkLgIpiaiCrlIP1BAii6C91x3kjzK~8kIKVXq31AGWI~RKDrknIN0B4YSEs4qGyXA__&Key-Pair-Id=APKAJLOHF5GGSLRBV4ZA#page=120

[11]. Foletto, E. L., Weber, C. T., Bertuol, D. A., & Mazutti, M. A. (2013). Application of Papaya Seeds as a Macro-/Mesoporous Biosorbent for the Removal of Large Pollutant Molecule from Aqueous Solution:

Equilib-rium, Kinetic, and Mechanism Studies. Separation Science and Technology, 48(18), 2817–2824. https://doi.org/10.1080/01496395.2013.808213

[12]. Hameed, B. H., Ahmad, A. A., & Aziz, N. (2007). Isotherms, kinetics and thermodynamics of acid dye adsorption on activated palm ash. Chemical Engineering Journal, 133(1–3), 195–203. Retrieved from https://www.sciencedirect.com/science/article/pii/S1385894707000678

[13]. Homagai, P. L., Poudel, R., Poudel, S., & Bhattarai, A. (2022). Adsorption and removal of crystal violet dye from aqueous solution by modified rice husk. Heliyon, 8(4). Retrieved from https://www.cell.com/heliyon/fulltext/S2405-8440(22)00549-7

[14]. Khan, M., Zafar, S., Badar, H., Hussain, M., & Shafiq, Z. (2015). Use of morus alba L. Leaves as biosorbent for the removal of Congo red dye. Fresenius Environmental Bulletin, 24, 2251–2258.

[15]. Khenifi, A., Bouberka, Z., Sekrane, F., Kameche, M., & Derriche, Z. (2007). Adsorption study of an industrial dye by an organic clay. Adsorption, 13(2), 149–158. https://doi.org/10.1007/s10450-007-9016-6

[16]. Kumar, P. S., Joshiba, G. J., Femina, C. C., Varshini, P., Priyadharshini, S., Karthick, M. S. A., & Jothirani, R. (2019). A critical review on recent developments in the low-cost adsorption of dyes from wastewater. Desalination and Water Treatment, 172, 395–416. https://doi.org/10.5004/dwt.2019.24613

[17]. Mahmoodi, N. M., Hayati, B., Arami, M., & Lan, C. (2011). Adsorption of textile dyes on pine cone from colored wastewater: Kinetic, equilibrium and thermodynamic studies. Desalination, 268(1–3), 117–125. Retrieved from https://www.sciencedirect.com/science/article/pii/S0011916410007228

[18]. Malik, P. K. (2003). Use of activated carbons prepared from sawdust and rice-husk for adsorption of acid dyes: A case study of Acid Yellow 36. Dyes and Pigments, 56(3), 239–249. https://doi.org/10.1016/S0143-7208(02)00159-6

[19]. Mane, R. S., & Bhusari, V. N. (2012). Removal of colour (dyes) from textile effluent by adsorption using orange and banana peel. International Journal of Engineering Research and Applications, 2(3), 1997–2004. Re-trieved from https://www.academia.edu/download/43300997/banana_fibre.pdf

[20]. Mohan, S. V., & Karthikeyan, J. (1997). Removal of lignin and tannin colour from aqueous solution by adsorption onto activated charcoal. Environmental Pollution, 97(1–2), 183–187. Retrieved from https://www.sciencedirect.com/science/article/pii/S0269749197000250

[21]. Safa, Y., Bhatti, H. N., Bhatti, I. A., & Asgher, M. (2011). Removal of direct Red‐31 and direct Orange‐26 by low cost rice husk: Influence of immobilisation and pretreatments. The Canadian Journal of Chemical Engineering, 89(6), 1554‐1565. https://doi.org/10.1002/cjce.20473

[22]. Senthil Kumar, P., & Grace Pavithra, K. (2019). Water and Textiles. In Water in Textiles and Fashion (pp. 21–40). Elsevier. https://doi.org/10.1016/B978-0-08-102633-5.00002-6

[23]. Shokoohi, R., Vatanpoor, V., Zarrabi, M., & Vatani, A. (2010). Adsorption of Acid Red 18 (AR18) by Activated Carbon from Poplar Wood‐A Kinetic and Equilibrium Study. Journal of Chemistry, 7(1), 65‐72. https://doi.org/10.1155/2010/958073

[24]. Sun, D., Zhang, X., Wu, Y., & Liu, X. (2010). Adsorption of anionic dyes from aqueous solution on fly ash. Jour-nal of Hazardous Materials, 181(1–3), 335–342. https://doi.org/10.1016/j.jhazmat.2010.05.015

[25]. Thang, N. H., Khang, D. S., Hai, T. D., Nga, D. T., & Tuan, P. D. (2021). Methylene blue adsorption mechanism of activated carbon synthesised from cashew nut shells. RSC Advances, 11(43), 26563–26570. Retrieved from https://pubs.rsc.org/en/content/articlehtml/2021/ra/d1ra04672a

[26]. Wong, Y. C., Szeto, Y. S., Cheung, W. H., & McKay, G. (2008). Effect of temperature, particle size and percentage deacetylation on the adsorption of acid dyes on chitosan. Adsorption, 14(1), 11–20. https://doi.org/10.1007/s10450-007-9041-5

[27]. Yaseen, D. A., & Scholz, M. (2019). Textile dye wastewater characteristics and constituents of synthetic effluents: A critical review. International Journal of Environmental Science and Technology, 16(2), 1193–1226. https://doi.org/10.1007/s13762-018-2130-z

International Journal of Scientific Research in Science and Technology
Available online at : www.ijsrst.com
Print ISSN: 2395-6011 | Online ISSN: 2395-602X
doi : https://doi.org/10.32628/IJSRST

Characterization of Soil Samples from the Lonar Lake, Maharashtra, India

Suryakant B. Borul, Shivshankar P. More
Department of Chemistry, Late Ku Durga K. Banmeru Science College, Lonar, Pin 443302, Dist Buldhana, Maharashtra, India

ARTICLEINFO

Article History :

Published : 07 Dec 2024

Publication Issue :
Volume 11, Issue 23
Nov-Dec-2024
Page Number :
281-285

ABSTRACT

Lonar Lake is an inland saline crater lake of only one of its kind in Asia. The lake is a closed system without any outlet and the lake is unique due to its salinity, alkalinity and biodiversity. It is the natural water body and unique ecosystem with its own feature in Buldhana district of Maharashtra state in India. It is the crater formed by hyper velocity two million-ton meteorite the impacted on the earth. It was formed by hyper velocity meteorite impact and situated in the basaltic terrine. The crater possesses the smallest forest sanctuary with great biological diversity. Soil is the most vital abiotic component of the lake ecosystem and while studying the biodiversity of any lake ecosystem, the Knowledge of the quality of lake soil becomes important. In this regard, a detailed physical and chemical analysis of some soil samples was carried out in different sites of Lonar Lake.

Keywords- Lonar Lake, Lake Soil, Physiochemical analysis.

Introduction

Lonar Lake is an inland saline crater lake of only one of its kind in Asia. The lake is a closed system without any outlet and the lake is unique due to its salinity, alkalinity and biodiversity. The Lonar Lake is originated as a meteorite impact crater around 50-60 thousand years ago having surface area 1.8 km and average depth 150 meters. It is the only crater take created in Basaltic rocks by the hyper-velocity impact. Lonar Lake is the third largest crater in the world and situated to southwest of Lonar village Buldhana district of Maharashtra state in India. It is situated about a kilometer to south west of Lonar town (North Latitude 19°55'; East longitude 75°34') in Buldhana district in Maharashtra state of India. The crater was first brought to be notice in 1823 by British officer CJE Alexander in 1896, and American Geologist G.K. Gilbert conducted studies to prove that the Lonar crater was created due to meteor strikes. Lonar Lake has the attention of world geologists and researcher for investigation of its origin, the source of salinity and quality of Lake Soil and Water. The Lake water is highly alkaline due to the high concentration of sodium carbonates exploited.

Soil is the most vital abiotic component of the lake ecosystem and while studying the biodiversity of any lake ecosystem. The outer region of lake has water with pH value range 7-8.5 while inner region has highly alkaline water with pH value around 8.5-10. Some sudden changes take place in the water and soil of Lonar Lake, such as increase water level of lake, in july 2020 Lonar crater turned pink suddenly. Investigation of the scientists revealed that the pink colour was due to the appearance of salt loving Haloarchaea microbes in large scale. Soil is consists of a solid phase as well as porous phase that holds gases and water. Soil is the system which supplies nutrients to the root of plant. Soil is the mixture of minerals, organic matter, gases and countless organisms that together support plant life. Physical and Chemical analysis of the soil are carried out to indicate the efficiency of soil for supplying plants with nutrients in available forms as well as identification of the factors affecting this efficiency in the soil and reason behind the changes take place in Lonar lake area. Therefore besides perfect sampling in the field, soil samples must be properly prepared and analyzed in order to reach the correct evaluation of the soil. Due to the uniqueness, the crater has evoked much scientific value among researchers and continues to site of attraction for much scientific view. Therefore it was thought to undertake studies on physicochemical quality of soil of Lonar Lake.

Experimental Section

Soil samples was collected from sampling site of Lonar Lake (Fig. 1) in sample bag and carried to the laboratory. The parameter selected for analysis were soil in general test, temperature, pH, Colour, Odour, Electrical Conductivity, Calcium Carbonate, and Organic carbon. Major nutrients Nitrogen, Phosphorous, Potassium, Macronutrients Calcium, Magnesium, Sulphur, Sodium. Micronutrients Copper, Zinc, Ferrous, Manganese, Boron and exchangeable sodium percent.

The pH and temperature recorded by soil water suspension on pH meter and thermometer and rest of the parameters were analyzed in the laboratory by standard methods. In case of detection of major and macro nutrients, AAS method is follow for elemental analysis in soil sample, AAS is an analytical technique used to determine how much of certain elements are in a sample. In case of detection of micronutrients in soil sample DTPA Extraction and AAS method is used. This method is based on the principle that atoms (and ions) can absorb light at a specific, unique wavelength. When this specific wavelength of light is provided, the energy (light) is absorbed by the atom.

Results and Discussion

In this study soil sample was analyzed for the in physicochemical quality of Lonar Lake. The numbers of physicochemical parameters as general test, temperature, pH, Colour, Odour, Electrical Conductivity, Calcium Carbonate, and Organic carbon. Major nutrients Nitrogen, Phosphorous, Potassium and Macronutrients as Calcium, Magnesium, Sulphur, Sodium. Micronutrients Copper, Zinc, Ferrous, Manganese, Boron and exchangeable sodium percent were performed.

In the present study it is observed that, the colour of the crater soil is also dark green because of the dense algal population with predominating spirullina. The odour of lake soil is somewhat an offensive. The pH of Lonar lake soil was found 8.92 it is higher from limit range 6.5-8.5 and temperature 22^0C. The normal value range of Electrical conductivity in between 0.1 to 1.0 dSm^{-1} and actually it was found to be 1.158 dSm^{-1} and it is moderately high value. The normal range of water holding capacity 25-50%, in Lonar lake soil it is found to be 52% that is high value as compare to the normal value. The normal range of Calcium Carbonate is 1.00-5.00%,

in Lonar lake soil it is found to be 5.00%. The normal range of 0.41-0.8% in Lonar lake soil it is found to be 0.507%. Now in case of major nutrients Nitrogen normal range between 281-560 Kg/ha, in Lonar Lake soil it is found 202.8 Kg/ha, that is amount of nitrogen is low. The amount of phosphorous 44.66 Kg/ha, it is very high as compare to normal value range 14-28 Kg/ha. The normal range of Potassium in between 151-250 Kg/ha and it was found to be 177.72Kg/ha value. In Macronutrient, The normal range Magnesium between 251-500 mg/L and it is found 351.17mg/L. The normal range of Calcium in between 500-1000 mg/L and it was found to be 5982.36 mg/L that is very high value. The normal range of Sulphur in between 10-50 mg/L and it was found to be 84.19 mg/L that is very high value. The normal range of Sodium in between up to 400 mg/L and it was found to be 2295.56 mg/L that is high value.

In case of Micronutrient the normal range of Copper in between 0.2 to 5.00 mg/L and it was found to be 1.24 mg/L value. The normal range of Zinc in between 0.6 to 1.2 mg/L and it was found to be 0.18 mg/L it is low very value. The normal range of Ferrous in between 4.5-7.5mg/L and it was found to be 8.12mg/L that is very low value. Manganese normal value 2.0-4.0 mg/L and it is found to be 2.15 mg/L that is normal value. The normal range of Boron in between 0.5-1.0 mg/L and it was found to be 1.26 mg/L that is high value.

Table-1 Physical parameters of Soil samples from selected sites of Lonar Lake

Sr. No.	Parameters	Normal	Results	Remark
GENERAL TEST				
1	Colour	Colourless	Dark green	--
2	Odour	Odour less	Strong Murky	--
3	Temp in ^{o}C	--	$22^{o}C$	--
4	pH	6.5-8.5	8.92	Basic
5	Electrical Conductivity (dSm^{-1})	<1.00	1.158	Moderately High
6	Water Holding Capacity	25-50	52%	High
7	Calcium Carbonate	1.00-5.00	5.00%	Normal
8	Organic Carbon	0.41-0.8	0.507%	Normal
MAJOR NUTRIENTS				
1	Nitrogen (in Kg/ha)	281-560	202.8	Low
2	Phosphorous (in Kg/ha)	14-28	44.66	Very high
3	Potassium (in Kg/ha)	151-250	170.72	Normal
MACRONUTRIENTS				
1	Calcium (in ppm)	500-1000	5982.36	Very high
2	Magnesium (in ppm)	251-500	351.17	Normal
3	Sulphur (in ppm)	10.00-50.00	84.19	Very high
4	Sodium (in ppm)	Upto 400	2295.56	Very high
MICRONUTRIENTS				
1	Copper (in ppm)	0.2-5	1.24	Normal
2	Zinc (in ppm)	0.6-1.2	0.18	Low
3	Ferrous (in ppm)	4.5-7.5	8.12	High
4	Manganese (in ppm)	2.0-4.0	2.15	Normal
5	Boron (in ppm)	0.5-1.0	1.26	High
6	Exchangeable Sodium Present (%)	10-20	23.22	High

Conclusion

In the present study the data revealed that there were considerable variations in the quality with respect to their physicochemical characteristics of soil sample in different season. It is also observed that, the colour of the Lonar Lake soil is also dark green because of the dense algal population with predominating spirullina in Lonar Lake water. In the general test the odour of crater soil is somewhat an offensive and pH, electrical conductivity, water holding capacity are high values. In case of major and macronutrients Phosphorous, Calcium, Sulphur, Sodium is very high values. This study focuses on the highly enriched hydrogen-bounded surface OH groups reveal the high pH in the crater and lake regions while the higher Na and chloride content are responsible for the high salinity of the lake and surroundings.

The higher percentages of S, Fe, P, Na and Ca along with the presence of certain minerals including zeolites get formed by post-impact hydrothermal reactions, which might have been due to an impact with any extra-terrestrial object (the meteor) at the Lonar region. The higher remanent magnetization of the soil samples is indicative of soil-meteorite interaction during impact and also due to post-impact with the passage of time. From this analysis it is clear that the physicochemical characteristics of soil of Lonar Lake are varied and Lonar Lake site is the main source, this is a great treasure for researchers.

ACKNOWLEDGMENT

Authors are grateful to the SAI Pvt. Ltd., Nashik for extending help and support for analysis of samples. We are thankful to Dr. P. K. Banmeru, Principal Late Ku. Durga K. Banmeru Science College, Lonar (MS) for encouraging research and providing laboratory facilities.

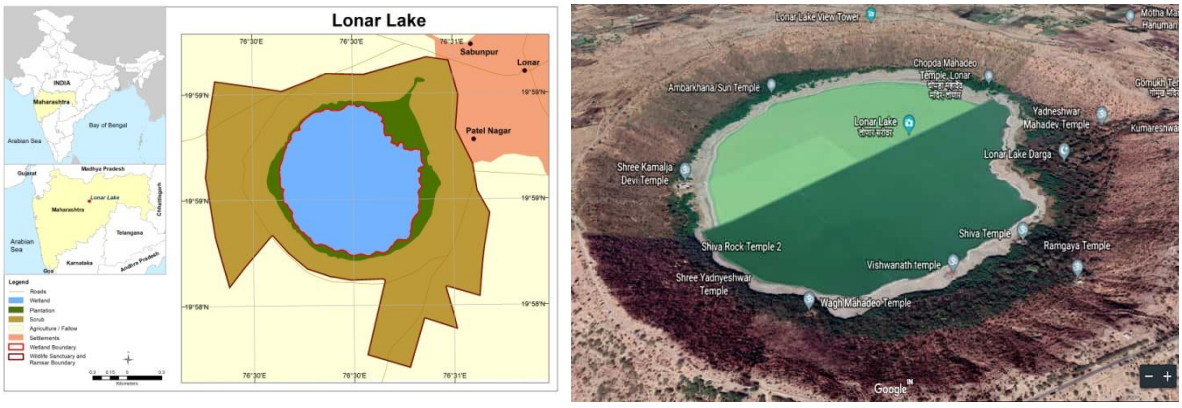

Google Earth satellite imagery of Lonar lake

References

[1]. Majan and Billore, (2014) Assesment of Physicochemical parameters of soil of Nagchoon pond Khanwa, MP. India research journal of chemical science 4(1) 26-30.

[2]. Standard APHA Methods for the examination of soil 22nd Edition, (2012) The data is tabulated and statistically analyzed.

[3]. Mehrothra S C and Bhalerao A S, (2005) Biodiversity of Lonar Crater. Anamaya Publishers, New Delhi, India, pp17-30.

[4]. Joshi A A, Kanekar P, Kelkar A S, Shouche Y S, Wani A A, Borgave S B and Sarnaik S S, (2007) Microb Ecol DOI, 10 1007/s0024.007.9264-8.
[5]. APHA, (1998) Standard Methods for the Examination of Water and Wastewater(20thEd.), Washington DC.
[6]. Ku Smita, Tale, Dr Sangita Ingole. (2015) A Review on Role of Physico Chemical Properties in Soil Quality, Chem Sci Rev Lett.; 4(13):57-66.
[7]. Laboratory manual in Chemistry by Mishra, Bhushan and Sharma, Arya book Depot Delhi.
[8]. Mahrer, Y., Shilo, E., (2012) Physical Principles of Solar Heating of Soils, Soil Solarization, theory and practice, American Phyto pathological Society, St. Paul. pp147-152
[9]. Dr. Sheetal Patel, M. Mahajan, (2024), Study of Physico-Chemical Parameter of Soil Analysis in Burhanpur District, International Journal of Research in Engineering and Science, 2320-9356 Volume 12 Issue 8,pp62-65.
[10]. Acevedo, R. D., Ponce, J. F., Rocca, M., Rabassa, J., and Corbella, H. (2009) "Bajada del Diablo impact crater-strewn field: The largest crater field in the Southern Hemisphere". Geomorphology, 110, pp58-67.
[11]. Das, S. K., Avasthe, R.K.and Reza, S. K. (2014). Importance of Soil Testing in Organic Agriculture. Pb. Sikkim Organic Mission, Gov. of Sikkim, Gangtok, India. pp:311-316.
[12]. Anthony, J. W., Bideaux, R. A., Bladh, K. W., and Nichols, M. C. (2001) "Handbook of Mineralogy", Mineral Data Publishing.
[13]. Wagh P.B.,Deshpande A.D.,Ingle S.R.(2021) "Study of Physico-Chemical Parameter of Soil Analysis in Buldana District".International Journal of Advanced Research in Science,Communication and Technology(IJARSCT)Vol.12.pp256-260.
[14]. P. B. Singare, N.A.Meshram, A. S. Jondhale and V. S. Kadam. (2020)."Need of Soil Testing for Improvement of Soil Heaith and Crop Productivity". Agriculture Observer 1(2), Pp:48-51
[15]. ASTM D 422-63 (2007) Standard test method for particle size analysis of soils. ASTM International, West Conshohocken, PA, USA.
[16]. ASTM D 720-91 (2010) Standard Test Method for Free-Swelling Index of Coal. ASTM International, West Conshohocken, PA, USA.
[17]. ASTM D 2487-11 (2011) Standard classification of soils for engineering purposes (Unified Soil Classification System). ASTM International, West Conshohocken, PA, USA.
[18]. ASTM D 4318-10 (2010) Standard Test Methods for Liquid Limit, Plastic Limit, and Plasticity Index of Soils. ASTM International, West Conshohocken, PA, USA.
[19]. ASTM D4972-13 (2013) Standard Test Method for pH of Soils. ASTM International, West Conshohocken, PA, USA
[20]. Solanke M. R., D. S. Dabhade (2016): Physico-Chemical Analysis of Upper Morna Reservoir, Medsi, District Washim, Maharashtra. Multidisciplinary Research Journal: Indian Stream Research Journal, Vol. 5(12), Jan, 89-99.

International Journal of Scientific Research in Science and Technology
Available online at : www.ijsrst.com
Print ISSN: 2395-6011 | Online ISSN: 2395-602X
doi : https://doi.org/10.32628/IJSRST

Adsorption of Heavy Metals from Waste Water Using Low Cost-Adsorbent: A Review

Shaikh Naushaba Gulrez, Samreen Fatema, Mazahar Farooqui
Post Graduate and Research Canter, Maulana Azad College of Arts, Science and Commerce, Rauza Bagh, Aurangabad (431001), Maharashtra, India

ARTICLEINFO

Article History :

Published : 07 Dec 2024

Publication Issue :
Volume 11, Issue 23
Nov-Dec-2024
Page Number :
286-299

ABSTRACT

Heavy metal pollution is a major problem in the environment. The impact of toxic metal ions can be minimized by different technologies but out of all, adsorption was found to be very effective due to ease of operation and economically feasible properties. The number of low-cost adsorbents has been investigated as a replacement for current costly methods of removing heavy metals from solution. In this review, several low cost adsorbents in the recent literature have been studied. The maximum adsorption capacity and percentage removal were revised and summarized in this review for further reference. Some of the natural adsorbents appeared as good heavy metal removal, while some were not. The objective of this study is to contribute in the search for less expensive adsorbents and their utilization possibilities for various agricultural waste by-products such as seaweed, algae, chitosan, egg shell and saw dust etc. for the elimination of heavy metals from wastewater.

Keywords: Heavy Metals, Wastewater, Adsorption, lowcost Adsorbent

Introduction

Water pollution raises a great concern nowadays. The fast-paced development of industries such as metal mining operations, fertilizers and paper industries metallurgical, chemical, tannery, battery and nuclear, agriculture, shipping and others have discharging various types of pollutants into the environment especially in developing countries[1-2]. Among other issues, water contaminations by heavy metals are more pronounced than other pollutants which may affect the quality of water supply [3]. Some of the hazardous heavy metal ions which pose potential danger threat to human health are nickel, zinc arsenic, mercury, chromium, cadmium, and lead. Heavy metal ions noted are not recyclable and accumulate in living organisms [4-5].

Heavy metals are unique part of the nature and most of them are biogenic means most of them are necessary for nature and human bodies but in small concentrations. Due to continuous exposure of these metals in water could be a reason for high dose in human body may lead toxicity [6]. The present world faces the risk of heavy

metal ions most since they are very toxic and carcinogenic in nature [7]. Heavy metals are non biodegradable pollutants and are very difficult to eliminate naturally from the environment [8] Moreover, since they are toxic, they cause illnesses and diseases such as lung cancer and cancers of other respiratory organs, the kidney and bladder, damage to the brain and reproductive organs, and heart and immune system disorders [9-10].

Hence there is burning need for the removal of heavy metals from the wastewater, to regulate the uncontrollable discharge of these hazardous pollutants in wastewater. Therefore treatment technologies are proposing globally and various technologies that are currently used for the removal of heavy metals are evaporation, Ion exchange, precipitation, membrane filtration, and adsorption [11-12] however these methods have several disadvantages such as high reagent requirement, unpredictable metal ion removal, generation of toxic sludge, etc. Among the mentioned methods, adsorption is considered to be one of the most appropriate techniques, Adsorption process being very simple, economical, effective and versatile has become the most preferred methods for removal of toxic contaminants from wastewater [13-17]

Comparatively, the adsorption process seems to be a significant technique [18] due to its wide applications, such as ease of operation, economic feasibility, wide availability and simplicity of design [19], but there are disadvantages to this method, including small capacity and difficulty for large-scale application, etc [20].Various types of natural materials or wastes have been utilized as adsorbents for the adsorption process due to their potential adsorption capacities. In the category of low-cost adsorbents, both natural adsorbents and bio-adsorbents [21] are used. In natural materials, zeolites, clay, chitosan and red mud are utilized as adsorbents. The main sources of bio-adsorbents are agricultural and animal waste materials. [22]

There are several kinds of adsorbents for removal of heavy metals, such as activated carbon [23] , carbon nanotubes [24] , graphene oxide[25], mesoporous silica, and mesoporous carbon[26], clays, zeolites[27], metal organic frameworks [28], and adsorbents from industrial/agricultural by-product residues[29] . Recently attention has been diverted towards the biomaterials which are byproducts or the wastes from large scale industrial operations and agricultural waste materials. . The use of such materials as low-cost adsorbents has double benefits to the environment. First, these materials are converted into high added value adsorbents, and second, these adsorbents are suitable for water and wastewater purification [30]

These agricultural by-products have been used in their raw form or after some physical or chemical modification [31]. Hydrothermal treatment and conventional pyrolysis are two of the most commonly used methods to increase the adsorption capacity of the agricultural residues[32] Agricultural residues, also called “lingo” cellulosic biomass resource, are defined as a biomass byproduct from the agricultural system and include stalks, leaves, seeds, shell, peels, husks, and straws. [33] Agricultural waste materials being economic and ecofriendly due to their unique chemical composition, availability in abundance, renewable, low in cost and more efficient are seem to be viable option for heavy metal remediation [34].

This review provides detailed information about the use of low-cost materials as adsorbents for the removal of heavy metal ions. A crucial analysis of low-cost adsorbent materials has been made and their features and advantages have been described.

1. Comparison of current treatment methods of various metal ions:

	Methods	advantages	disadvantages	references
1	Ion-Exchange	High quality of metal removal, easy to use, high transformation of components	Expensive, can’t be used on large scale, highly sensitive to pH, removes only limited metals.	[35]

	Methods	advantages	disadvantages	references
2	Chemical Precipitation	Easy to use ,inexpensive,	Excess chemical required, disposal problem, generation and disposal of sludge	[36]
3	Coagulation	Suitable to large scale waste water treatment, cost effective, dewatering qualities	Expensive, large sludge production	[37]
4	Membrane Separation	Large amount of chemical used, less sludge production, lower space require, easy to operate,	High maintenance, operational cost, very expensive, membrane fouling, complex process	[38]
5	Reverse Osmosis	Effective removal	Required chemical cost is high, consumption of high power	[39]
6	Adsorption	Easy operation, less sludge production, utilization of low cost adsorbent	desorption	[40]

Sources and toxicity of heavy metals:

1. Nickel:

Nickel (Ni) is the 24th most abundant element in the Earth's crust, comprising about 3% of the composition of the earth. This metal is used in electroplating, battery production, stainless steel manufacturing. It causes variety of pathologic effects. [41] Its alloys are widely used in the metallurgical, chemical and food processing industries, especially as catalysts and pigments. The nickel salts of greatest commercial importance are nickel chloride, sulphate, nitrate, carbonate, hydroxide, acetate and oxide [42].The high concentration of this metal causes several effects on humans such as headache, dizziness, nausea, vomiting, several lung diseases, dermatitis, chronic asthma and also it is carcinogenic and even in severe condition death may take place. It is also genetoxic and mutagenic. [43-44] According to the US environmental protection agency(EPA) requires Ni not to exceed to 0.015 mg/l in drinking water, and WHO permissible limit is 2.0 mg/l. [45].

Table: 02) Low cost adsorbent used for the adsorption of Nickel:

Sr.No	Adsorbent material	Adsorption capacity(Mg/g)	Percentage removal	references
1	*Lancium domesticum* peel	10.1	90%	[46]
2	Mango peel	39.75	79.42%	[47]
3	Orange peel	162.6	…..	[48]
4	Lemon peel	…..	78%	[49]
5	Banana peel	…..	77.8%	[50]
6	Pomegranate peel	52	…..	[51]
7	Jack fruit peel	12.03	…..	[52]
8	Grape fruit	46.13	97%	[53]
9	Rice straw	35.08	…..	[54]
10	Tea waste	15.26	……	[55]
11	Chestnut shell	2.4	…..	[56]
12	Walnut shell	……	90.0%	[57]
13	Neem bark	…..	84.75%	[58]

Sr.No	Adsorbent material	Adsorption capacity(Mg/g)	Percentage removal	references
14	Corn cob	12	.....	[59]
15	Coconut husk	404.5	……	[60]

2. Lead:

Lead is considered as one of the most hazards and cumulative environmental pollutants that affect all biological systems through exposure to air, water, and food sources but it's also a disease of lifestyle. These are harmful to the nervous system, causes brain and heart disorder, damage fetal brain, diseases of kidney toxicity of the liver, hematopoietic system, and nervous system. Having a carcinogenic risk as well [61] .Lead is used in electroplating, burning of coal, battery manufacturing, paint and pigment production, mining and smelting [62]. Even small quantity of this metal ion can destroy the life of aquatic animal. According to WHO the max permissible concentration of lead is 0.05mg/l [63]

Table: 03) Low cost adsorbent used for the adsorption of Lead:

Sr.No	Peels	Adsorption capacity(Mg/g)	Percentage removal	references
1	Yellow passion fruit	151.6	98%	[64]
2	African wild mango	40	-	[65]
3	Water melon peel	130.23	99.9%	[66]
4	Plntain	85.9	-	[67]
5	Lemon peel	90.91	-	[68]
6	Pomegranate peel	-	95%	[69]
7	Mango peel	75.55	76.45%	[70]
8	Passion fruit	93.9	-	[71]
9	Coconut	6.2	-	[72]
10	Apricot	-	87%	[73]

3. Cadmium:

Cadmium has been included in the red list of priority pollutants by the Department of Environment, UK[74] Sources of cadmium human exposures are fossil fuels, iron and steel production, cement nonferrous metals production, waste incineration, smoking, fertilizers, etc. Refining, mining, welding, electrochemistry, and coating industries, battery production, fertilizers production, [75]. It is cancer causing agent mean carcinogenic. It causes renal disorder, nausea, salivation, diarrhea, muscular cramps, lung insufficiency, bone lesions, hypertension. According to WHO guidelines the permissible concentration of cadmium in drinking water is 0.003mg/l. [76-77]

Table: 04) Low cost adsorbent used for the adsorption of Cadmium:

Sr.No	Peels	Adsorption capacity(Mg/g)	Percentage removal	references
1	Pomegranate peel	23.5	-	[78]
2	Grape peel	42.04	-	[79]
3	Cucumber peel	58.14	-	[80]
4	Banana peel	35.52	95%	[81]
5	Mango eel	68.92	-	[82]

Sr.No	Peels	Adsorption capacity(Mg/g)	Percentage removal	references
6	Wheat straw	14.56	-	[83]
7	Sunflower stalk	42.18	-	[84]
8	Almond shell	8.08		[85]
9	Cassava peel	5.80	73%	[86]

4. Zinc:

Zinc is one of the most important trace elements in the organism, with three major biological roles, as catalyst, structural, and regulatory ion. [87]. Galvanization, paints, and rubber manufacturing fertilizer production. It is carcinogenic agent, causing nausea, vomiting, stomach diseases, anemia, damage pancreases, skin irritation, In many chronic diseases, including atherosclerosis, several malignancies, neurological disorders, autoimmune diseases, aging, age-related degenerative diseases, and Wilson's disease, the concurrent zinc deficiency may complicate the clinical features, affect adversely immunological status, increase oxidative stress, and lead to the generation of inflammatory cytokines[88]. According to WHO and Indian Standard the recommended level of zinc in drinking water is 5mg/l. [89].

Table: 05) Low cost adsorbent used for the adsorption of Zinc:

Sr.No	Peels	Adsorption capacity(Mg/g)	Percentage removal	references
1	Mango peel	28.21	78.30%	[90]
2	Black gram husk	33.81	-	[91]
3	Rice husk ash	14.30	-	[92]
4	Neem bark	13.29	-	[93]
5	Castor seed hull	6.72	-	[94]
6	Coir fibers	2.51	-	[95]
7	Sugarcane bagasse	31.11	-	[96]
8	Banana peel	5.80	-	[97]

5. Chromium:

Chromium (Cr) is a crucial trace element. The total body content of chromium decreases with age[98]. electroplating, leather lanning , Stainless steel production Alloy production Metal and alloy manufacturing Metal and alloy manufacturing Brick lining Chrome plating Leather tanning Textiles Dye and pigment manufacturing, plumping[99]., Inhalation of chromium increases the chances of hypersensitivity reactions like asthma, nasal irritability, nasal ulcers, skin lesions or rashes, lung cancer and contact dermatitis mutagenic, carcinogenic, asthma, failure of kidney and liver , skin allegies, lung carcinoma, [100] According to the Indian standard the permissible limit of Cr(VI) from industrial waste to be discharge to surface water IS 0.1 mg/l. WHO permissible limit 0.05mg/l. , [101]

Table: 06) Low cost adsorbent used for the adsorption of Chromium:

Sr.No	Peels	Adsorption capacity(Mg/g)	Percentage removal	references
1	Orange peel	40.56	82	[102]
2	Banana peel	131.56	80-99%	[103]
3	Peat and coconut fiber	1.25	-	[104]

Sr.No	Peels	Adsorption capacity(Mg/g)	Percentage removal	references
4	Rice husk	102.96	-	[105]
5	Almond	10.62	-	[106]
6	Sugar cane bagasse	13.4	-	[107]
7	eucalyptus bark	45.5		[108]
8	Groundnut hull	40		[109]

6. Copper:

Copper is a hazardous heavy metal that is used in various industries such as Equipment production,mining and smelting, electrical wiring, pestisides and fertilizers[110] ,its excessive uptake causes gasterointestinal ,bleeding, headache, dizziness, anemia, vomiting, insomniya, Wilson disease ,Convulsions,. [111] According to the united states environmental perotection agency the maximum contamination level goal is 1.3mg/l.. [112]

Table: 07) Low cost adsorbent used for the adsorption of Copper:

Sr.No	Peels	Adsorption capacity(Mg/g)	Percentage removal	references
1	Musk melon		90.2%	[113]
2	Orange peel	56.18	86.6%	[114]
3	Pomegranate peel	55	-	[115]
4	Mango peel	46.09	89.02%	[116]
5	Banana peel	4.75	-	[117]
6	Cassava peel	5.80	-	[118]
7	Rice husk	7.1	-	[119]
8	Wood apple shell	151.51	-	[120]
9	Neem leaves	62.97	-	[121]
10	Alfa grass	75.8	-	[122]

References

[1]. Summers, J. K., Shiomi, N., Zambare, V., & Din, M. F. M. (2023). Bioremediation for Global Environmental Conservation. BoD–Books on Demand.

[2]. Anjum, M., Miandad, R., Waqas, M., Gehany, F., & Barakat, M. A. (2019). Remediation of wastewater using various nano-materials. Arabian journal of chemistry, 12(8), 4897-4919.

[3]. Sonone, S. S., Jadhav, S., Sankhla, M. S., & Kumar, R. (2020). Water contamination by heavy metals and their toxic effect on aquaculture and human health through food Chain. Lett. Appl. NanoBioScience, 10(2), 2148-2166.

[4]. Mohammed, A. S., Kapri, A., & Goel, R. (2011). Heavy metal pollution: source, impact, and remedies. Biomanagement of metal-contaminated soils, 1-28.

[5]. Vardhan, K. H., Kumar, P. S., & Panda, R. C. (2019). A review on heavy metal pollution, toxicity and remedial measures: Current trends and future perspectives. Journal of Molecular Liquids, 290, 111197.

[6]. Bradl, H. (Ed.). (2005). Heavy metals in the environment: origin, interaction and remediation. Elsevier.

[7]. Munir, N., Jahangeer, M., Bouyahya, A., El Omari, N., Ghchime, R., Balahbib, A., ... & Shariati, M. A. (2021). Heavy metal contamination of natural foods is a serious health issue: A review. Sustainability, 14(1), 161.

[8]. Khalef, R. N., Hassan, A. I., & Saleh, H. M. (2022). Heavy metal's environmental impact. In Environmental Impact and Remediation of Heavy Metals. IntechOpen.
[9]. Velarde, L., Nabavi, M. S., Escalera, E., Antti, M. L., & Akhtar, F. (2023). Adsorption of heavy metals on natural zeolites: A review. Chemosphere, 328, 138508.
[10]. Fu, Z., & Xi, S. (2020). The effects of heavy metals on human metabolism. Toxicology mechanisms and methods, 30(3), 167-176.
[11]. Mahurpawar, M. (2015). Effects of heavy metals on human health. Int J Res Granthaalayah, 530(516), 1-7.
[12]. Gunatilake, S. K. (2015). Methods of removing heavy metals from industrial wastewater. Methods, 1(1), 14.
[13]. Gupta, V. K., Kumar, R., Nayak, A., Saleh, T. A., & Barakat, M. A. (2013). Adsorptive removal of dyes from aqueous solution onto carbon nanotubes: a review. Advances in colloid and interface science, 193, 24-34.
[14]. Weber, W. J., & Smith, E. H. (1987). Simulation and design models for adsorption processes. Environmental science & technology, 21(11), 1040-1050.
[15]. Meena, A. K., Kadirvelu, K., Mishra, G. K., Rajagopal, C., & Nagar, P. N. (2008). Adsorptive removal of heavy metals from aqueous solution by treated sawdust (Acacia arabica). Journal of hazardous materials, 150(3), 604-611.
[16]. Yu, B., Zhang, Y., Shukla, A., Shukla, S. S., & Dorris, K. L. (2000). The removal of heavy metal from aqueous solutions by sawdust adsorption—removal of copper. Journal of hazardous materials, 80(1-3), 33-42.
[17]. Ismail, U. M., Vohra, M. S., & Onaizi, S. A. (2024). Adsorptive removal of heavy metals from aqueous solutions: Progress of adsorbents development and their effectiveness. Environmental Research, 118562.
[18]. Rashid, R., Shafiq, I., Akhter, P., Iqbal, M. J., & Hussain, M. (2021). A state-of-the-art review on wastewater treatment techniques: the effectiveness of adsorption method. Environmental Science and Pollution Research, 28, 9050-9066.
[19]. Rajendran, S., Priya, A. K., Kumar, P. S., Hoang, T. K., Sekar, K., Chong, K. Y., ... & Show, P. L. (2022). A critical and recent developments on adsorption technique for removal of heavy metals from wastewater-A review. Chemosphere, 303, 135146.
[20]. Chai, W. S., Cheun, J. Y., Kumar, P. S., Mubashir, M., Majeed, Z., Banat, F., ... & Show, P. L. (2021). A review on conventional and novel materials towards heavy metal adsorption in wastewater treatment application. Journal of Cleaner Production, 296, 126589.
[21]. Foroutan, R., Oujifard, A., Papari, F., & Esmaeili, H. (2019). Calcined Umbonium vestiarium snail shell as an efficient adsorbent for treatment of wastewater containing Co (II). 3 Biotech, 9(3), 78.
[22]. Afroze, S., & Sen, T. K. (2018). A review on heavy metal ions and dye adsorption from water by agricultural solid waste adsorbents. Water, Air, & Soil Pollution, 229, 1-50.
[23]. Mariana, M., HPS, A. K., Mistar, E. M., Yahya, E. B., Alfatah, T., Danish, M., & Amayreh, M. (2021). Recent advances in activated carbon modification techniques for enhanced heavy metal adsorption. Journal of Water Process Engineering, 43, 102221.
[24]. Stafiej, A., & Pyrzynska, K. (2007). Adsorption of heavy metal ions with carbon nanotubes. Separation and purification technology, 58(1), 49-52.
[25]. Wang, J., & Chen, B. (2015). Adsorption and coadsorption of organic pollutants and a heavy metal by graphene oxide and reduced graphene materials. Chemical Engineering Journal, 281, 379-388.

[26]. Showkat, A. M., Zhang, Y. P., Kim, M. S., Gopalan, A. I., Reddy, K. R., & Lee, K. P. (2007). Analysis of heavy metal toxic ions by adsorption onto amino-functionalized ordered mesoporous silica. Bulletin of the Korean Chemical Society, 28(11), 1985-1992.

[27]. Jiménez-Castañeda, M. E., & Medina, D. I. (2017). Use of surfactant-modified zeolites and clays for the removal of heavy metals from water. Water, 9(4), 235.

[28]. Efome, J. E., Rana, D., Matsuura, T., & Lan, C. Q. (2018). Metal–organic frameworks supported on nanofibers to remove heavy metals. Journal of Materials Chemistry A, 6(10), 4550-4555.

[29]. Alalwan, H. A., Kadhom, M. A., & Alminshid, A. H. (2020). Removal of heavy metals from wastewater using agricultural byproducts. Journal of Water Supply: Research and Technology—AQUA, 69(2), 99-112.

[30]. Demirbas, A. (2008). Heavy metal adsorption onto agro-based waste materials: a review. Journal of hazardous materials, 157(2-3), 220-229.

[31]. Chen, B., & Chen, Z. (2009). Sorption of naphthalene and 1-naphthol by biochars of orange peels with different pyrolytic temperatures. Chemosphere, 76(1), 127-133.

[32]. He, W., Li, G., Kong, L., Wang, H., Huang, J., & Xu, J. (2008). Application of hydrothermal reaction in resource recovery of organic wastes. Resources, Conservation and Recycling, 52(5), 691-699.

[33]. Maia, L. C., Soares, L. C., & Gurgel, L. V. A. (2021). A review on the use of lignocellulosic materials for arsenic adsorption. Journal of Environmental Management, 288, 112397.

[34]. Renu, Agarwal, M., & Singh, K. (2017). Heavy metal removal from wastewater using various adsorbents: a review. Journal of Water Reuse and Desalination, 7(4), 387-419.

[35]. Vaaramaa, K., & Lehto, J. (2003). Removal of metals and anions from drinking water by ion exchange. Desalination, 155(2), 157-170.

[36]. BrbootI, M. M., Abid, B. A., & Al-ShuwaikI, N. M. (2011). Removal of heavy metals using chemicals precipitation. Eng. Technol. J, 29(3), 595-612.

[37]. Tang, X., Zheng, H., Teng, H., Sun, Y., Guo, J., Xie, W., ... & Chen, W. (2016). Chemical coagulation process for the removal of heavy metals from water: a review. Desalination and water treatment, 57(4), 1733-1748.

[38]. Huang, Y. C., & Koseoglu, S. S. (1993). Separation of heavy metals from industrial waste streams by membrane separation technology. Waste management, 13(5-7), 481-501.

[39]. Bakalár, T., Búgel, M., & Gajdošová, L. (2009). Heavy metal removal using reverse osmosis. Acta Montanistica Slovaca, 14(3), 250.

[40]. Rajendran, S., Priya, A. K., Kumar, P. S., Hoang, T. K., Sekar, K., Chong, K. Y., ... & Show, P. L. (2022). A critical and recent developments on adsorption technique for removal of heavy metals from wastewater-A review. Chemosphere, 303, 135146.

[41]. Cempel, M., & Nikel, G. J. P. J. S. (2006). Nickel: a review of its sources and environmental toxicology. Polish journal of environmental studies, 15(3).

[42]. Friberg, L., & Elinder, C. G. (1993). Biological monitoring of toxic metals. Scandinavian journal of work, environment & health, 7-13.

[43]. Begum, W., Rai, S., Banerjee, S., Bhattacharjee, S., Mondal, M. H., Bhattarai, A., & Saha, B. (2022). A comprehensive review on the sources, essentiality and toxicological profile of nickel. RSC advances, 12(15), 9139-9153.

[44]. Coogan, T. P., Latta, D. M., Snow, E. T., Costa, M., & Lawrence, A. (1989). Toxicity and carcinogenicity of nickel compounds. CRC Critical reviews in toxicology, 19(4), 341-384.

[45]. Meshram, P., & Pandey, B. D. (2019). Advanced review on extraction of nickel from primary and secondary sources. Mineral Processing and Extractive Metallurgy Review.
[46]. Lam, Y. F., Lee, L. Y., Chua, S. J., Lim, S. S., & Gan, S. (2016). Insights into the equilibrium, kinetic and thermodynamics of nickel removal by environmental friendly Lansium domesticum peel biosorbent. Ecotoxicology and environmental safety, 127, 61-70.
[47]. Iqbal, M., Saeed, A., & Kalim, I. (2009). Characterization of adsorptive capacity and investigation of mechanism of Cu2+, Ni2+ and Zn2+ adsorption on mango peel waste from constituted metal solution and genuine electroplating effluent. Separation Science and Technology, 44(15), 3770-3791.
[48]. Feng, N., Guo, X., Liang, S., Zhu, Y., & Liu, J. (2011). Biosorption of heavy metals from aqueous solutions by chemically modified orange peel. Journal of hazardous materials, 185(1), 49-54
[49]. Herrera-Barros, A., Bitar-Castro, N., Villabona-Ortíz, Á., Tejada-Tovar, C., & González-Delgado, Á. D. (2020). Nickel adsorption from aqueous solution using lemon peel biomass chemically modified with TiO2 nanoparticles. Sustainable Chemistry and Pharmacy, 17, 100299
[50]. Olufemi, B., & Eniodunmo, O. (2018). Adsorption of nickel (II) ions from aqueous solution using banana peel and coconut shell. International Journal of Technology, 9(3)
[51]. Bhatnagar, A., & Minocha, A. K. (2010). Biosorption optimization of nickel removal from water using Punica granatum peel waste. Colloids and Surfaces B: Biointerfaces, 76(2), 544-548.
[52]. Ranasinghe, S. H., Navaratne, A. N., & Priyantha, N. (2018). Enhancement of adsorption characteristics of Cr (III) and Ni (II) by surface modification of jackfruit peel biosorbent. Journal of Environmental Chemical Engineering, 6(5), 5670-5682.
[53]. Torab-Mostaedi, M., Asadollahzadeh, M., Hemmati, A., & Khosravi, A. (2013). Equilibrium, kinetic, and thermodynamic studies for biosorption of cadmium and nickel on grapefruit peel. Journal of the Taiwan Institute of Chemical Engineers, 44(2), 295-302.
[54]. El-Sayed, G. O., Dessouki, H. A., & Ibrahim, S. S. (2010). Biosorption of Ni (II) and Cd (II) ions from aqueous solutions onto rice straw. Chemical Sciences Journal, 9, 1-11.
[55]. Malkoc, E., & Nuhoglu, Y. (2005). Investigations of nickel (II) removal from aqueous solutions using tea factory waste. Journal of hazardous materials, 127(1-3), 120-128.
[56]. Vázquez, G., Calvo, M., Freire, M. S., González-Alvarez, J., & Antorrena, G. (2009). Chestnut shell as heavy metal adsorbent: optimization study of lead, copper and zinc cations removal. Journal of Hazardous Materials, 172(2-3), 1402-1414.
[57]. Jalilic, M. C. B. V. I. (2012). A comparative experimental study of the removal of heavy metals using low cost natural adsorbents and commerical activated carbon. International Journal, 3(1).
[58]. Naiya, T. K., Bhattacharya, A. K., & Das, S. K. (2008). Adsorption of Pb (II) by sawdust and neem bark from aqueous solutions. Environmental Progress, 27(3), 313-328.
[59]. Abdelfattah, I., Ismail, A. A., Al Sayed, F., Almedolab, A., & Aboelghait, K. M. (2016). Biosorption of heavy metals ions in real industrial wastewater using peanut husk as efficient and cost effective adsorbent. Environmental Nanotechnology, Monitoring & Management, 6, 176-183.
[60]. Malik, R., & Dahiya, S. (2017). An experimental and quantum chemical study of removal of utmostly quantified heavy metals in wastewater using coconut husk: A novel approach to mechanism. International journal of biological macromolecules, 98, 139-149.
[61]. Ara, A., & Usmani, J. A. (2015). Lead toxicity: a review. Interdisciplinary toxicology, 8(2), 55-64.
[62]. Papanikolaou, N. C., Hatzidaki, E. G., Belivanis, S., Tzanakakis, G. N., & Tsatsakis, A. M. (2005). Lead toxicity update. A brief review. Medical science monitor, 11(10), RA329-RA336.]

[63]. Naja, G. M., & Volesky, B. (2017). Toxicity and sources of Pb, Cd, Hg, Cr, As, and radionuclides in the environment. In Handbook of advanced industrial and hazardous wastes management (pp. 855-903). Crc Press.

[64]. Jacques, R. A., Lima, E. C., Dias, S. L., Mazzocato, A. C., & Pavan, F. A. (2007). Yellow passion-fruit shell as biosorbent to remove Cr (III) and Pb (II) from aqueous solution. Separation and Purification Technology, 57(1), 193-198.

[65]. Adekola, F. A., Adegoke, H. I., & Ajikanle, R. A. (2016). Kinetic and equilibrium studies of Pb (II) and Cd (II) adsorption on African wild mango (Irvingia gabonensis) shell. Bulletin of the Chemical Society of Ethiopia, 30(2), 185-198.

[66]. Moreno-Barbosa, J. J., López-Velandia, C., Maldonado, A. D. P., Giraldo, L., & Moreno-Piraján, J. C. (2013). Removal of lead (II) and zinc (II) ions from aqueous solutions by adsorption onto activated carbon synthesized from watermelon shell and walnut shell. Adsorption, 19, 675-685.

[67]. Sudha, R., & Premkumar, P. (2016). Lead removal by waste organic plant source materials review. International Journal of ChemTech Research, 9(01), 47-57.

[68]. Wanja, N. E., Murungi, J., Ali, A. H., & Wanjau, R. (2016). Efficacy of adsorption of Cu (II), Pb (II) and Cd (II) Ions onto acid activated watermelon peels biomass from water. International Journal of Science and Research, 5(8), 671-679.

[69]. El-Ashtoukhy, E. S., Amin, N. K., & Abdelwahab, O. (2008). Removal of lead (II) and copper (II) from aqueous solution using pomegranate peel as a new adsorbent. Desalination, 223(1-3), 162-173.

[70]. Iqbal, M., Saeed, A., & Zafar, S. I. (2009). FTIR spectrophotometry, kinetics and adsorption isotherms modeling, ion exchange, and EDX analysis for understanding the mechanism of Cd2+ and Pb2+ removal by mango peel waste. Journal of hazardous materials, 164(1), 161-171.

[71]. Chao, H. P., Chang, C. C., & Nieva, A. (2014). Biosorption of heavy metals on Citrus maxima peel, passion fruit shell, and sugarcane bagasse in a fixed-bed column. Journal of Industrial and Engineering Chemistry, 20(5), 3408-3414.

[72]. Okafor, P. C., Okon, P. U., Daniel, E. F., & Ebenso, E. E. (2012). Adsorption capacity of coconut (Cocos nucifera L.) shell for lead, copper, cadmium and arsenic from aqueous solutions. International Journal of Electrochemical Science, 7(12), 12354-12369.

[73]. Šoštarić, T. D., Petrović, M. S., Pastor, F. T., Lončarević, D. R., Petrović, J. T., Milojković, J. V., & Stojanović, M. D. (2018). Study of heavy metals biosorption on native and alkali-treated apricot shells and its application in wastewater treatment. Journal of Molecular Liquids, 259, 340-349.

[74]. Wang, F. Y., Wang, H., & Ma, J. W. (2010). Adsorption of cadmium (II) ions from aqueous solution by a new low-cost adsorbent—Bamboo charcoal. Journal of hazardous materials, 177(1-3), 300-306.

[75]. Dubey, A. M. S. S. A., Mishra, A., & Singhal, S. (2014). Application of dried plant biomass as novel low-cost adsorbent for removal of cadmium from aqueous solution. International journal of environmental science and technology, 11, 1043-1050.

[76]. Tripathi, A., & Ranjan, M. R. (2015). Heavy metal removal from wastewater using low cost adsorbents. J Bioremed Biodeg, 6(6), 315.

[77]. Lim, A. P., & Aris, A. Z. (2014). A review on economically adsorbents on heavy metals removal in water and wastewater. Reviews in Environmental Science and Bio/Technology, 13, 163-181.

[78]. Chen, Y., Wang, H., Zhao, W., & Huang, S. (2018). Four different kinds of peels as adsorbents for the removal of Cd (II) from aqueous solution: Kinetics, isotherm and mechanism. Journal of the Taiwan Institute of Chemical Engineers, 88, 146-151.

[79]. Efficacy and field applicability of Burmese grape leaf extract (BGLE) for cadmium removal: An implication of metal removal from natural water. Ecotoxicol.

[80]. Pandey, R., Ansari, N. G., Prasad, R. L., & Murthy, R. C. (2014). Removal of Cd (II) ions from simulated wastewater by HCl modified Cucumis sativus peel: Equilibrium and kinetic study. Air, Soil and Water Research, 7, ASWR-S16488.

[81]. Memon, J. R., Memon, S. Q., Bhanger, M. I., Memon, G. Z., El-Turki, A., & Allen, G. C. (2008). Characterization of banana peel by scanning electron microscopy and FT-IR spectroscopy and its use for cadmium removal. Colloids and Surfaces B: Biointerfaces, 66(2), 260-265.

[82]. Iqbal, M., Saeed, A., & Zafar, S. I. (2009). FTIR spectrophotometry, kinetics and adsorption isotherms modeling, ion exchange, and EDX analysis for understanding the mechanism of Cd2+ and Pb2+ removal by mango peel waste. Journal of hazardous materials, 164(1), 161-171.

[83]. Dang, V. B. H., Doan, H. D., Dang-Vu, T., & Lohi, A. (2009). Equilibrium and kinetics of biosorption of cadmium (II) and copper (II) ions by wheat straw. Bioresource technology, 100(1), 211-219.p

[84]. Sun, G., & Shi, W. (1998). Sunflower stalks as adsorbents for the removal of metal ions from wastewater. Industrial & engineering chemistry research, 37(4), 1324-1328.

[85]. Pehlivan, E., Altun, T., Cetin, S., & Bhanger, M. I. (2009). Lead sorption by waste biomass of hazelnut and almond shell. Journal of hazardous materials, 167(1-3), 1203-1208.

[86]. Owamah, H. I. (2014). Biosorptive removal of Pb (II) and Cu (II) from wastewater using activated carbon from cassava peels. Journal of Material Cycles and Waste Management, 16, 347-358.

[87]. Prasad, A. S. (2008). Zinc in human health: effect of zinc on immune cells. Molecular medicine, 14, 353-357.

[88]. Frassinetti, S., Bronzetti, G. L., Caltavuturo, L., Cini, M., & Della Croce, C. (2006). The role of zinc in life: a review. Journal of environmental pathology, toxicology and oncology, 25(3).

[89]. Fosmire, G. J. (1990). Zinc toxicity. The American journal of clinical nutrition, 51(2), 225-227.

[90]. Iqbal, M., Saeed, A., & Kalim, I. (2009). Characterization of adsorptive capacity and investigation of mechanism of Cu2+, Ni2+ and Zn2+ adsorption on mango peel waste from constituted metal solution and genuine electroplating effluent. Separation Science and Technology, 44(15), 3770-3791.

[91]. Saeed, A., Iqbal, M., & Akhtar, M. W. (2005). Removal and recovery of lead (II) from single and multimetal (Cd, Cu, Ni, Zn) solutions by crop milling waste (black gram husk). Journal of hazardous materials, 117(1), 65-73.

[92]. Bhattacharya, A. K., Mandal, S. N., & Das, S. K. (2006). Adsorption of Zn (II) from aqueous solution by using different adsorbents. Chemical Engineering Journal, 123(1-2), 43-51.

[93]. Bhattacharya, A. K., Mandal, S. N., & Das, S. K. (2006). Adsorption of Zn (II) from aqueous solution by using different adsorbents. Chemical Engineering Journal, 123(1-2), 43-51.

[94]. Mohammod, M., Sen, T. K., Maitra, S., & Dutta, B. K. (2011). Removal of Zn 2+ from aqueous solution using castor seed hull. Water, Air, & Soil Pollution, 215, 609-620.

[95]. Shukla, S. R., Pai, R. S., & Shendarkar, A. D. (2006). Adsorption of Ni (II), Zn (II) and Fe (II) on modified coir fibres. Separation and purification technology, 47(3), 141-147.

[96]. Mondal, M. K., Singh, R. S., Kumar, A., & Prasad, B. M. (2011). Removal of acid red-94 from aqueous solution using sugar cane dust: An agro-industry waste. Korean Journal of Chemical Engineering, 28, 1386-1392.

[97]. Annadurai, G., Juang, R. S., & Lee, D. J. (2003). Adsorption of heavy metals from water using banana and orange peels. Water science and technology, 47(1), 185-190.

[98]. Adamu, N., & Kumar, J. (2022). Review on chromium: therapeutic uses and toxicological effects on human health. The Journal of Multidisciplinary Research, 23-30.

[99]. Pereira, S. C., Oliveira, P. F., Oliveira, S. R., Pereira, M. D. L., & Alves, M. G. (2021). Impact of environmental and lifestyle use of chromium on male fertility: focus on antioxidant activity and oxidative stress. Antioxidants, 10(9), 1365.

[100]. Ukhurebor, K. E., Aigbe, U. O., Onyancha, R. B., Nwankwo, W., Osibote, O. A., Paumo, H. K., ... & Siloko, I. U. (2021). Effect of hexavalent chromium on the environment and removal techniques: a review. Journal of Environmental Management, 280, 111809.

[101]. DesMarias, T. L., & Costa, M. (2019). Mechanisms of chromium-induced toxicity. Current opinion in toxicology, 14, 1-7.

[102]. Marín, A. P., Ortuno, J. F., Aguilar, M. I., Meseguer, V. F., Sáez, J., & Lloréns, M. (2010). Use of chemical modification to determine the binding of Cd (II), Zn (II) and Cr (III) ions by orange waste. Biochemical Engineering Journal, 53(1), 2-6.

[103]. Memon, J. R., Memon, S. Q., Bhanger, M. I., El-Turki, A., Hallam, K. R., & Allen, G. C. (2009). Banana peel: a green and economical sorbent for the selective removal of Cr (VI) from industrial wastewater. Colloids and surfaces B: Biointerfaces, 70(2), 232-237

[104]. Henryk, K., Jarosław, C., & Witold, Ż. (2016). Peat and coconut fiber as biofilters for chromium adsorption from contaminated wastewaters. Environmental Science and Pollution Research, 23, 527-534.

[105]. Vieira, M. G. A., de Almeida Neto, A. F., Silva, M. G., Nóbrega, C. C., & Melo Filho, A. A. (2012). Characterization and use of in natura and calcined rice husks for biosorption of heavy metals ions from aqueous effluents. Brazilian Journal of Chemical Engineering, 29, 619-634.

[106]. Dakiky, M., Khamis, M., Manassra, A., & Mer'Eb, M. (2002). Selective adsorption of chromium (VI) in industrial wastewater using low-cost abundantly available adsorbents. Advances in environmental research, 6(4), 533-540.

[107]. Sharma, D. C., & Forster, C. F. (1994). A preliminary examination into the adsorption of hexavalent chromium using low-cost adsorbents. Bioresource Technology, 47(3), 257-264.

[108]. Sarin, V., & Pant, K. (2006). Removal of chromium from industrial waste by using eucalyptus bark. Bioresource technology, 97(1), 15-20.

[109]. Qaiser, S., Saleemi, A. R., & Umar, M. (2009). Biosorption of lead (II) and chromium (VI) on groundnut hull: Equilibrium, kinetics and thermodynamics study. Electronic journal of Biotechnology, 12(4), 3-4.

[110]. Aydın, H., Bulut, Y., & Yerlikaya, Ç. (2008). Removal of copper (II) from aqueous solution by adsorption onto low-cost adsorbents. Journal of environmental management, 87(1), 37-45.

[111]. Gupta, M., Gupta, H., & Kharat, D. S. (2018). Adsorption of Cu (II) by low cost adsorbents and the cost analysis. Environmental technology & innovation, 10, 91-101.

[112]. Milicevic, S., Boljanac, T., Martinovic, S., Vlahovic, M., Milosevic, V., & Babic, B. (2012). Removal of copper from aqueous solutions by low cost adsorbent-Kolubara lignite. Fuel Processing Technology, 95, 1-7.

[113]. Khan, T. A., Mukhlif, A. A., & Khan, E. A. (2017). Uptake of Cu2+ and Zn2+ from simulated wastewater using muskmelon peel biochar: Isotherm and kinetic studies. Egyptian journal of basic and applied sciences, 4(3), 236-248.

[114]. FENG, N. C., & GUO, X. Y. (2012). Characterization of adsorptive capacity and mechanisms on adsorption of copper, lead and zinc by modified orange peel. Transactions of Nonferrous Metals Society of China, 22(5), 1224-1231.

[115]. El-Ashtoukhy, E. S., Amin, N. K., & Abdelwahab, O. (2008). Removal of lead (II) and copper (II) from aqueous solution using pomegranate peel as a new adsorbent. Desalination, 223(1-3), 162-173.

[116]. Iqbal, M., Saeed, A., & Kalim, I. (2009). Characterization of adsorptive capacity and investigation of mechanism of Cu2+, Ni2+ and Zn2+ adsorption on mango peel waste from constituted metal solution and genuine electroplating effluent. Separation Science and Technology, 44(15), 3770-3791.

[117]. Annadurai, G., Juang, R. S., & Lee, D. J. (2003). Adsorption of heavy metals from water using banana and orange peels. Water science and technology, 47(1), 185-190.

[118]. Owamah, H. I. (2014). Biosorptive removal of Pb (II) and Cu (II) from wastewater using activated carbon from cassava peels. Journal of Material Cycles and Waste Management, 16, 347-358.

[119]. Nakbanpote, W., Thiravetyan, P., & Kalambaheti, C. (2000). Preconcentration of gold by rice husk ash. Minerals engineering, 13(4), 391-400.

[120]. Doke, K. M., Yusufi, M., Joseph, R. D., & Khan, E. M. (2012). Biosorption of hexavalent chromium onto wood apple shell: equilibrium, kinetic and thermodynamic studies. Desalination and Water Treatment, 50(1-3), 170-179.

[121]. Babu, B. V., & Gupta, S. (2008). Adsorption of Cr (VI) using activated neem leaves: kinetic studies. Adsorption, 14, 85-92.

[122]. Tazrouti, N., & Amrani, M. (2009). CHROMIUM (VI) ADSORPTION ONTO ACTIVATED KRAFT LIGNIN PRODUCED FROM ALFA GRASS (STIPA TENACISSIMA). BioResources, 4(2).

[123]. Chakraborty, R., Asthana, A., Singh, A. K., Jain, B., & Susan, A. B. H. (2022). Adsorption of heavy metal ions by various low-cost adsorbents: a review. International Journal of Environmental Analytical Chemistry, 102(2), 342-379.

[124]. Babel, S., & Kurniawan, T. A. (2003). Low-cost adsorbents for heavy metals uptake from contaminated water: a review. Journal of hazardous materials, 97(1-3), 219-243.

[125]. Habuda-Stanić, M., & Nujić, M. (2015). Arsenic removal by nanoparticles: a review. Environmental Science and Pollution Research, 22, 8094-8123.

[126]. Hao, L., Liu, M., Wang, N., & Li, G. (2018). A critical review on arsenic removal from water using iron-based adsorbents. RSC advances, 8(69), 39545-39560.

[127]. Khan, F. A., Mushtaq, M. A. B., Arif, P. M. A., & Mazahar, M. F. (2023). A Comparative Study of Adsorption of Methylene Blue Dye onto Untreated Platanus orientalis (chinar tree) Leaves Powder and its Biochar-Equilibrium, Kinetic and Thermodynamic Study. Orbital: The Electronic Journal of Chemistry, 163-170.

[128]. Ahmad Khan, F., & Farooqui, M. (2024). Removal of methylene blue dye from aqueous solutions onto Morus nigra L.(mulberry tree) leaves powder and its biochar—equilibrium, kinetic and thermodynamic study. International Journal of Environmental Analytical Chemistry, 104(16), 4364-4383.

[129]. Ahmad Khan, F., Dar, B. A., & Farooqui, M. (2023). Characterization and adsorption of malachite green dye from aqueous solution onto Salix alba L.(Willow tree) leaves powder and its respective biochar. International Journal of Phytoremediation, 25(5), 646-657.

[130]. Khan, F. A., & Farooqui, M. REMOVAL OF CRYSTAL VIOLET DYE FROM AQUEOUS SOLUTION USING MORUS NIGRA L.(MULBERRY TREE) LEAVES BIOCHAR.

[131]. KHAN, F. A., AHAD, A., FATEMA, S., & FAROOQUI, M. (2022). ADSORPTION STUDY OF CRYSTAL VIOLET DYE ONTO Morus nigra L.(MULBERRY TREE) LEAVES POWDER: EQUILIBRIUM, KINETICS AND THERMODYNAMICS STUDY. Indian J. Sci. Res, 12(2), 23-33.

[132]. Jirekar, D. B., Ubale, M., & Farooqui, M. (2016). Evaluation of Adsorption Capacity of Low Cost Adsorbent for the Removal of Congo Red Dye from Aqueous Solution. Orbital: The Electronic Journal of Chemistry, 282-287.

[133]. Jirekar, D. B., Ubale, M., & Farooqui, M. (2016). Evaluation of Adsorption Capacity of Low Cost Adsorbent for the Removal of Congo Red Dye from Aqueous Solution. Orbital: The Electronic Journal of Chemistry, 282-287.

[134]. Jirekar, D. B., Ubale, M., & Farooqui, M. (2016). Evaluation of Adsorption Capacity of Low Cost Adsorbent for the Removal of Congo Red Dye from Aqueous Solution. Orbital: The Electronic Journal of Chemistry, 282-287.

[135]. Jirekar, D. B., Pathan, A. A., & Farooqui, M. (2014). Adsorption studies of methylene blue dye from aqueous solution onto Phaseolus aureus biomaterials. Orient J Chem, 30(3), 1263-1269. Gurgel, L. V. A., de Melo, J. C. P., de Lena, J. C., & Gil, L. F. (2009). Adsorption of chromium (VI) ion from aqueous solution by succinylated mercerized cellulose functionalized with quaternary ammonium groups. Bioresource technology, 100(13), 3214-3220

[136]. Jirekar, D. B., & Farooqui, M. (2013). Adsorption Studies of hexavalent Chromium Ion from Aqueous Solution Using Lenus Esculent (Masoor). International Journal of Recent Trends in Science And Technology, 15-20

International Journal of Scientific Research in Science and Technology
Available online at : www.ijsrst.com
OPEN ACCESS
Print ISSN: 2395-6011 | Online ISSN: 2395-602X
doi : https://doi.org/10.32628/IJSRST

Studies of Complexation of Cerium Metal Ion with Medicinal Drugs in Aqueous Media: Thermodynamic Aspect

Shailendrasingh Thakur[1], Ramesh Ware[1], Hansaraj Joshi[2], Milind Gaikwad[3], Pandit Khakre[4]

[1]Department of Chemistry, Milliya College, Beed, Maharashtra, India

[2]Department of Chemistry, Swa Sawarkar Mahavidyalaya, Beed, Maharashtra, India

[3]Department of Chemistry, Rajmata Jijau Mahavidyalaya, Kille Dharur, Maharashtra, India

[4]Department of Chemistry, Mrs.K.S.K. Mahavidyalaya, Beed, Maharashtra, India

ARTICLEINFO

Article History :

Published : 07 Dec 2024

Publication Issue :
Volume 11, Issue 23
Nov-Dec-2024
Page Number :
300-306

ABSTRACT

We have used a pH metric titration technique in a 20% (v/v) ethanol-water mixture at three different temperatures at an ionic strength of 0.1M NaClO4 to measure the proton-ligand and metal-ligand stability constants of medicinal drugs containing Cerium metal ion. The logK values of the metal-ligand stability constant have been determined using the modified Irving-Rossotti and Calvin-Bjerrum method. The thermodynamic parameters Gibb's free energy change, entropy change and enthalpy change related to the complexation reactions were quantitatively determined.

Keywords: Cerium metal ion, medicinal drugs, Stability constants, Thermodynamic parameters, pH metry etc.

Introduction

For the present investigation, we selected seven medicinal drugs as Metformin hydrochloride(L1), Oxytetracycline hydrochloride(L2), Cefotaxime Sodium(L3), Ceftriaxone Sodium(L4), Imipramine(L5), Isoniazid(L6) and Adenosine (L7). In continuation of our earlier work with complexation of medicinal drugs01-16 and after literature survey, it was thought to be fascinating to look at how temperature may affect thermodynamic parameters such as Gibb's free energy change (ΔG), enthalpy change (ΔH) and entropy change (ΔS) of complexes of seven medicinal drugs with rare earth metal ion Ce3+ pH metrically in 20% (v/v) ethanol-water mixture at constant ionic strength of 0.1M NaClO4.

Methods and Material

All chemicals used were of AR grade. All medicinal drugs are soluble in 20% (v/v) ethanol-water mixture. The solutions used in the pH metric titration were prepared in double distilled water. Water thermostat is used to

maintain the temperature constant. pH measurement was made using Elico L1-120 pH meter. The instrument was calibrated at pH 7.00 and 4.00 using standard buffer solutions. For evaluating the protonation constant of the ligand and the formation constant of the complexes in 20 %(v/v) ethanol-water mixture with Cerium metal ion we prepare the following sets of solutions.

(A) HClO4 (A)

(B) HClO4 + medicinal drug (A + L)

(C) HClO4 + medicinal drug + Cerium metal (A + L+ M)

Above mentioned sets prepared by keeping M : L ratio, concentration of perchloric acid and sodium perchlorate were kept constant for all sets. The volume of every mixture was made up to 50ml with double distilled water and the reaction solution were titrated pH metrically against standard NaOH solution at three different temperatures 298K, 308K and 318K.

Determination of the thermodynamic parameters: The change in Gibb's free energy (ΔG) of the ligands was calculated by using the equation. $\Delta G = -2.303RT \log K$

Where R (ideal gas constant) = 8.314 JK-1mol-1,

K is the dissociation constant for the ligand or the stability constant of the complex and T is absolute temperature in Kelvin.

The change in enthalpy (ΔH) is calculated by plotting logK vs 1/T

The equation utilized for the calculation of changes in enthalpy is as Slope = - ΔH/2.303R

The evaluation of changes in entropy (ΔS) is given by the equation: $\Delta S = ((\Delta H - \Delta G))/T$

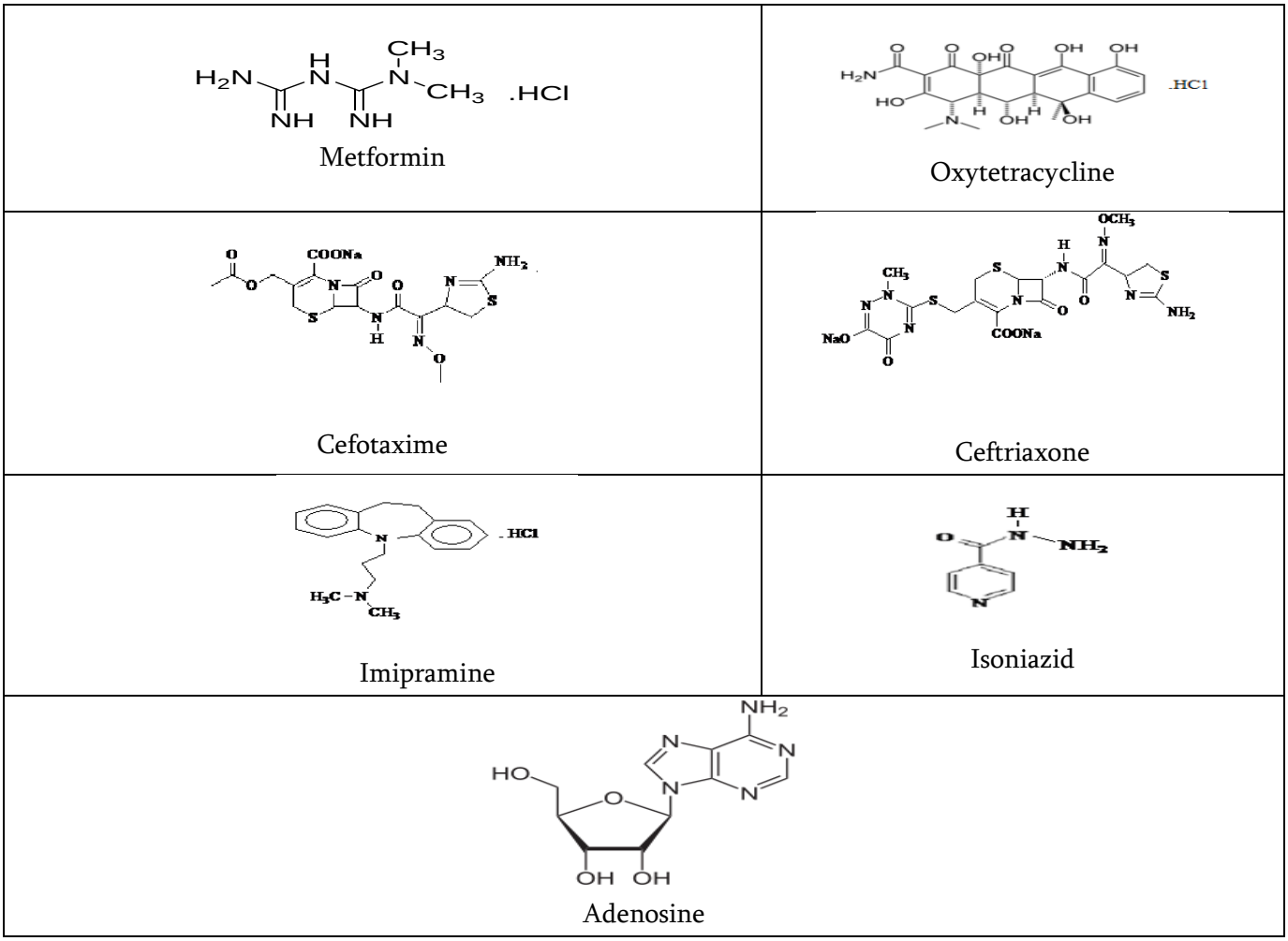

Figure 1. The structure of drugs

Table 1: Proton-ligand stability constant of medicinal drugs

Temperature	Proton-ligand stability constant	Medicinal drugs						
		L_1	L_2	L_3	L_4	L_5	L_6	L_7
298K	pK_1	2.905	-	3.156	4.093	-	3.192	3.292
	pK_2	11.101	4.316	10.764	10.741	9.062	10.657	11.659
308K	pK_1	2.618	-	3.103	3.939	-	3.110	3.082
	pK_2	10.958	4.010	10.611	10.622	8.967	10.391	11.470
318K	pK_1	2.346	-	3.051	3.780	-	2.805	2.988
	pK_2	10.856	3.732	10.340	10.372	8.854	10.214	11.280

Table 2: Ce (III)-ligand stability constant of medicinal drugs

Temperature	298K			308K			318K		
Ce(III)-ligand stability constant → Medicinal drugs ↓	$\log K_1$	$\log K_2$	$\log\beta$	$\log K_1$	$\log K_2$	$\log\beta$	$\log K_1$	$\log K_2$	$\log\beta$
L_1	7.627	6.292	13.918	7.487	6.095	13.582	7.375	5.920	13.295
L_2	4.431	3.426	7.857	4.102	3.267	7.369	3.791	3.092	6.883
L_3	7.470	6.236	13.706	7.283	6.084	13.367	7.047	5.812	12.859
L_4	4.811	4.041	8.852	4.694	3.930	8.624	4.446	3.704	8.150
L_5	5.427	3.557	8.984	5.332	3.485	8.817	5.191	3.390	8.581
L_6	6.477	5.250	11.727	6.206	4.985	11.191	6.029	4.809	10.838
L_7	7.094	5.148	12.242	6.933	4.986	11.919	6.740	4.811	11.551

Table 3: Thermodynamic parameters of medicinal drugs complex formation with Ce(III) at 298K

Medicinal drugs	$-\Delta G_1$	$-\Delta G_2$	$-\Delta H_1$	$-\Delta H_2$	ΔS_1	ΔS_2
	($KJmol^{-1}$)		($KJmol^{-1}$)		($KJK^{-1}mol^{-1}$)	
L_1	43.516	35.898	24.618	33.730	0.0634	0.0073
L_2	25.281	19.547	58.029	30.264	-0.1099	-0.0360
L_3	42.624	35.579	38.395	38.377	0.0142	-0.0094
L_4	27.451	23.057	33.0598	30.5255	-0.0188	-0.0251
L_5	30.963	20.293	21.396	15.100	0.0321	0.0174
L_6	36.957	29.953	40.823	40.093	-0.0130	-0.0340
L_7	40.478	29.374	32.062	30.548	0.0282	-0.0039

Table 4: Thermodynamic parameters of medicinal drugs complex formation with Ce(III) at 308K

Medicinal drugs	$-\Delta G_1$	$-\Delta G_2$	$-\Delta H_1$	$-\Delta H_2$	ΔS_1	ΔS_2
	($KJmol^{-1}$)		($KJmol^{-1}$)		($KJK^{-1}mol^{-1}$)	
L_1	44.153	35.943	24.618	33.730	0.0634	0.0072
L_2	24.189	19.265	58.029	30.264	-0.1099	-0.0357
L_3	42.951	35.879	38.395	38.377	0.0148	-0.0081
L_4	27.680	23.178	33.0598	30.5255	-0.0175	-0.0239
L_5	31.445	20.552	21.396	15.100	0.0326	0.0177

Medicinal drugs	$-\Delta G_1$	$-\Delta G_2$	$-\Delta H_1$	$-\Delta H_2$	ΔS_1	ΔS_2
	($KJmol^{-1}$)		($KJmol^{-1}$)		($KJK^{-1}mol^{-1}$)	
L_6	36.599	29.396	40.823	40.093	-0.0137	-0.0347
L_7	40.886	29.404	32.062	30.548	0.0287	-0.0037

Table 5: Thermodynamic parameters of medicinal drugs complex formation with Ce (III) at 318K

Medicinal drugs	$-\Delta G_1$	$-\Delta G_2$	$-\Delta H_1$	$-\Delta H_2$	ΔS_1	ΔS_2
	($KJmol^{-1}$)		($KJmol^{-1}$)		($KJK^{-1}mol^{-1}$)	
L_1	44.907	36.045	24.618	33.730	0.0638	0.0073
L_2	23.084	18.827	58.029	30.264	-0.1099	-0.0360
L_3	42.908	35.390	38.395	38.377	0.0142	-0.0094
L_4	27.073	22.553	33.0598	30.5255	-0.0188	-0.0251
L_5	31.605	20.642	21.396	15.100	0.0321	0.0174
L_6	36.707	29.278	40.823	40.093	-0.0129	-0.0340
L_7	41.038	29.296	32.062	30.548	0.0282	-0.0039

Results And Discussion

The proton ligand stability constant pKa of all seven medicinal drugs were determined in aqueous medium at three different temperatures at 0.1M NaClO4 ionic strength. (Table 1). The medicinal drugs L2 and L5 has only one pK value where as L1, L3, L4, L6 and L7 have two pK values. The $\bar{n}_A$value ranges between 0.2 to 1.8 indicates the presence of two pK values whereas therange of $\bar{n}_A$ is in between 0.2 to 0.8 shows only one pK value. In the present investigation drugs selected contains amino group(s), carboxyl or hydroxyl groups as bonding sites.

The order of pKa values of seven drugs is as: L7 > L4 > L1 > L3 > L6 > L5 > L2

The above order indicates that Adenosine drug (L7) has lowest basicity, whereas Oxytetracycline drug (L2) has highest basicity. The present drugs are diverse in nature hence it is difficult to correlate pKa values of one drug with other.

i. **Metformin hydrochloride** contains one primary, three secondary and one tertiary –N atom. Out of three secondary amino groups, two are having C=N bond. Hence the electrons present on these N atoms may experiences the force of repulsion due to delocalized π- electrons. One secondary amino group is attached to two carbon atom by single bond. Hence, it might be expected that protonation may be taking place at primary NH2 group as well as at =NH group easily, rather than NH-group. This results in two pKa values 2.905 and 11.101.

ii. **Oxytetracycline hydrochloride** contains four hexacyclic rings. There are six hydroxyl groups attached to different rings, out of six one is phenolic –OH, remaining are cyclic alcoholic –OH groups. The rings also possess two exocyclic carbonyl groups, one tertiary amino group and one amide -CONH2 group. The Oxytetracycline under experimental condition shows only one protonation constant that too in acidic range. Instead of the hydroxyl groups and carbonyl groups, nitrogen of amide or tertiary amino group might be involved in the protonation. The pKa value 4.316 is close to amide group.

iii. **Cefotaxime sodium** consists of ester group, N and S containing hetrocyclic rings, NH-CO group, N-OCH3 groups along with –COO and NH2. As it has been a established fact that carboxylate and amino groups

are most promising co-ordinating groups. Hence, in the present investigation two pKa values, 3.156 corresponding to –COO- and 10.764 corresponding to amino group are obtained.

iv. **Ceftriaxone Sodium** drug shows two pKa values. Since carboxylate and amino groups are most promising co-ordinating groups, the pK1 value 4.093 corresponding to –COO- and pK2 value 10.741 corresponding to amino group.

v. **Imipramine hydrochloride** shows one pKa value. The protonation constant for Imipramine obtained under the experimental condition is 9.062. This is due to presence of two ternary amine nitrogen.

vi. **Isoniazid** shows two pKa values due to two dissociable protons. The pK1 value 3.192 can be assigned to the substituted amide -CONHR group which is near to the pKa value of nicotinamide. The low value of pK1 may be attributed to the weak basic nature of amide group. The pK2 value 10.657 is assigned to the R-NH-NH2 group which is attributed to the deprotonation of primary amino group.

vii. **Adenosine** has N-atom as binding site. The functional group NH2 is mostly responsible for complexation, although there is nitrogen atoms present in the co-ordinate bond formation. Adenosine contains three OH groups, out of these two are attached to cyclic ring and one is to the side chain. The deprotonation of side chain –OH is easier compaired to –OH directly attached to ring. Hence only one deprotonation in the acidic range (3.292) and the other pKa in the basic region correspond to –NH2 group only (11.659).

Metal ligand stability constant logK of Ce(III) metal ion with medicinal drugs are calculated by point wise and half integral method, indicates simultaneous formation of 1:1 complex. We got values of proton-ligand formation number ($\bar{n}_A$) between 0.2 to 0.8 and 1.2 to 1.8 indicating 1:1 and 1:2 complex formations. The proton-ligand stability constant pKa values decrease with increase in temperature i.e. the acidity of the ligands increases, it suggests that the liberation of proton becomes easier at higher temperature.

Order of stability constants log β for Ce(III) metal complexes with medicinal drugs (Table 2) found to be as: L1 > L3 > L7 > L6 > L5 > L4 > L2

The metal-ligand stability of Metformin (L1) found higher while for Oxytetracycline (L2) found lower.

The negative ΔG value indicates that both dissociation of the ligand and the complexation process are spontaneous. A decrease in metal-ligand stability constant logK with an increase in temperature and the negative values of enthalpy change ΔH for the complexation suggests that all the complexation reactions are exothermic, favorable at lower temperature and the metal-ligand binding process is enthalpy driven and metal-ligand bonds are fairly strong.

The positive entropy changes ΔS accompanying a given reaction are due to the release of bound water molecules from the metal chelates. The positive value of ΔS is considered to the principal driving force for the formation of respective complex species. According to Martell -Calvin positive entropy effects was predicted towards an increase in the number of particles after the reaction and positive ΔS is responsible to give more negative ΔG. The positive values of ΔS in some cases indicate that the entropy effect is predominant over enthalpy effect and the formation of these complexes was entropy favored, while negative ΔS values for metal complexes suggesting a highly solvated metal complexes (Table 3-5)

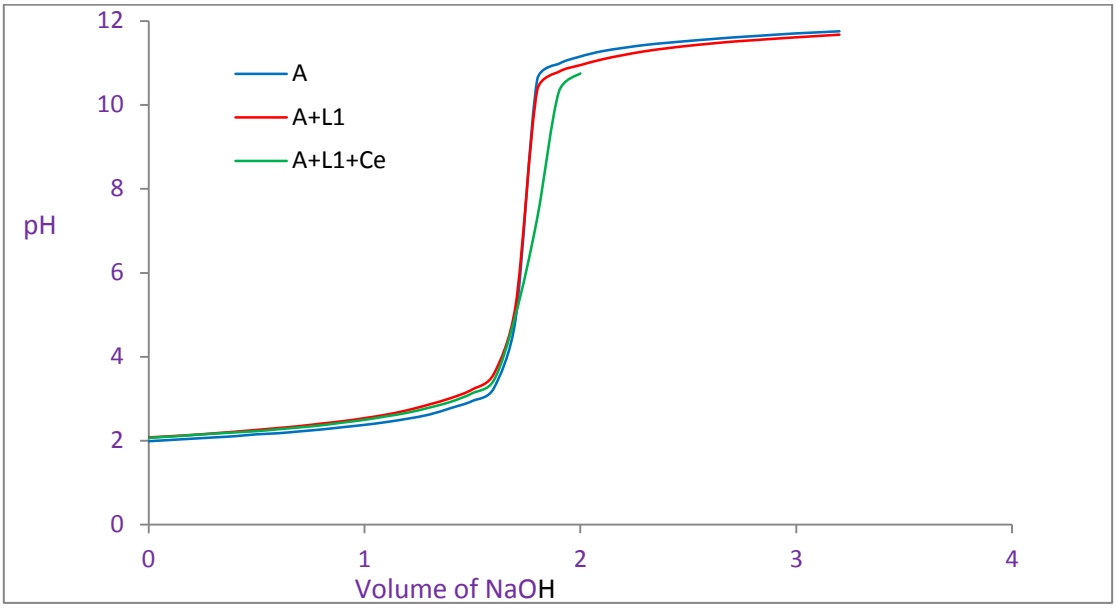

Figure 2: The pH metric titration curve for Ce(III)-L1

Conclusion

Cerium metal ion forms 1:1 and 1:2 complexes with all medicinal drugs. The metal-ligand stability constant logK decreases with an increase in temperature. The negative values of change in enthalpy ΔH for the complexation suggest that all the complexation reactions are exothermic, favourable at lower temperature. The negative change in free energy ΔG values indicates that both dissociation of the ligand and the complexation process are spontaneous. The positive ΔS values for some metal complexes indicated that the formation of these complexes was entropy favoured, while negative ΔS values indicated a highly solvated metal complex.

Acknowledgments

Authors thankful to research guide Principal Dr. Sahebrao Naikwade, Chhatrapati Shahu College, Lasur Station, Chhatrapati Sambhajinagar, Principal Dr. Mazahar Farooqui, Maulana Azad College, Chhatrapati Sambhajinagar and Principal Dr. Mohd. Iliyas Fazil, Milliya College, Beed for providing all research facilities.

References

[1]. Shailendrasingh Thakur, R.L.Ware, MazaharFarooqui, S.D.Naikwade (2012) "Equilibrium studies on Imipramine Hydrochloride-metal ion in 20% ethanol-water mixture."Asian Journal of Research in Chemistry, 5(12), 1464-1465.

[2]. S.V. Thakur, Mazahar Farooqui, S.D.Naikwade (2012) "Stability study of complexation of trivalent rare earth metals with isoniazid: Thermodynamic aspect." International Journal of Research in Inorganic Chemistry, 1(4), 05-07.

[3]. ShailendrasinghThakur, MazaharFarooqui, S.D.Naikwade (2012) "Thermodynamic studies of transition metal complexes with Metformin Hydrochloride drug in 20% (v/v) ethanol-water mixture." Pelagia Research Library, Der Chemica Sinica, , 3(6), 1406-1409.

[4]. Shailendrasingh Thakur, Mazahar Farooqui, S.D.Naikwade (2012) "Potentiometric study of transition metal and rare earth metal complexes with Isoniazid drug in 20% (v/v) ethanol-water mixture."Journal of Chemical and Pharmaceutical Research, 4(9), 4412-4416.

[5]. Shailendrasingh Thakur, Mazahar Farooqui, S.D.Naikwade (2013) "Mixed ligand complexes of cobalt(II) metal ion with medicinal drugs Metformin, Imipramine & Adenosine in mixed solvent system." International Journal of Pharma Tech Research. 5(4), 1508-1515.

[6]. Shailendrasingh Thakur, Mazahar Farooqui, S.D.Naikwade (2013) "Equilibrium Studies on Mixed Ligand Complexes of Zinc (II) Metal Ion with Some Medicinal Drugs and Amino Acids."Asian Journal of Biochemical and Pharmaceutical Research, 3(3), 34-43.

[7]. Shailendrasingh Thakur, Sahebrao Naikwade, Mazahar Farooqui (2013) "Thermodynamics of the formation trivalent Lanthanide complexes carrying Adenosine drug in mixed solvent media." International Journal of Chemical Studies. 1(3), 88-92.

[8]. Shailendrasingh Thakur, Mazahar Farooqui, MA Sakhare, SD Naikwade (2013) "Thermodynamic studies of Oxytetracycline with some transition and rare earth metal ions in mixed solvent media."American Int. J. Research in Formal, Applied & Natural Sciences. 3(1),123-127.

[9]. Shailendrasingh Thakur, Mazahar Farooqui, Sahebrao Naikwade (2013) "Thermodynamics of the formation of transition metal complexes carrying Adenosine drug in mixed solvent system."International Journal of Emerging Technologies in Computational & Applied Sciences. 4(4),389-393.

[10]. Shailendrasingh Thakur, Mazahar Farooqui, Sahebrao Naikwade (2013) "Thermodynamics of the complexation of Imipramine Hydrochloride drug with Lanthanide."International Journal of Emerging Technologies in Computational and Applied Sciences. 4(4), 342-346.

[11]. Shailendrasingh Thakur, Mazahar Farooqui, S.D. Naikwade (2013) "Study of Binary Complexes of transition metal ions and Lanthanide metal ions with Adenosine drug in mixed Solvent System."Acta Chimica & Pharmaceutica Indica, 3(1), 35-39.

[12]. ShailendrasinghThakur, MazaharFarooqui, S.G.Shankarwar, S.D.Naikwade.(2013) "Comparative study of stability constant of antibacterial drugs with rare earth metal ions."International Journal of Chemical Sciences, 11(1), 464- 468.

[13]. S.V. Thakur, Mazahar Farooqui, S.D.Naikwade.(2013) "Thermodynamic studies of rare earth metal complexes with Metformin Hydrochloride drug in mixed solvent system." Journal of Advanced Scientific Research, 4(1), 31-33.

[14]. Shailendrasingh Virendrasingh Thakur, Mazahar Farooqui, Sahebrao Naikwade. (2014) "Formation of transition metal complexes carrying medicinal drugs: Thermodynamic study."Journal of Chemical Biological & Physical Sciences. 4(1), 1-7.

[15]. Shailendrasingh Thakur, Mazahar Farooqui, S.D. Naikwade.(2015) "Complexation behavior of the antibacterial drugs Oxytetracycline, Cefotaxime & Ceftriaxone along with amino acids towards cobalt (II) in aqueous solution." Journal of Medicinal Chemistry & Drug discovery (Special issue ACTRA) 123-127.

[16]. Shailendrasingh Thakur, Mazahar Farooqui, Ramesh Ware. (2019) "Mixed ligand complexes of Zinc metal ion with drug Cefotaxime and amino acids in aqueous media." International Journal of Advance and Innovative Research, 6(1{XVI}), 228-232.

International Journal of Scientific Research in Science and Technology
Available online at : www.ijsrst.com
OPEN ACCESS
Print ISSN: 2395-6011 | Online ISSN: 2395-602X
doi : https://doi.org/10.32628/IJSRST

Nanostructured Catalysts for Environmental Remediation

Siddiqui Alima Fatema

ARTICLEINFO

Article History :

Published : 07 Dec 2024

Publication Issue :
Volume 11, Issue 23
Nov-Dec-2024
Page Number :
307-313

ABSTRACT

Nanotechnology has shown immense potential in environmental remediation, particularly through the use of nanostructured catalysts. These catalysts have proven effective in breaking down pollutants in water, air, and soil, offering an advanced approach to environmental clean-up. This paper explores the role of Nano catalysts in addressing pollution by examining their applications in wastewater treatment, air purification, and soil decontamination. The paper also reviews the potential of Nano catalysts in reducing carbon emissions and combating climate change. Finally, the challenges and future directions in Nano catalyst research for environmental remediation are discussed.

Introduction

Environmental pollution has become one of the most pressing challenges of the 21st century, affecting ecosystems, human health, and biodiversity. Traditional methods of pollution control, such as physical filtration and chemical treatments, often fail to address pollutants efficiently and sustainably. As the need for more effective and eco-friendly solutions grows, nanotechnology has emerged as a promising field for environmental remediation. Specifically, nanostructured catalysts are being investigated for their ability to decompose toxic substances, reduce harmful emissions, and clean up polluted environments.

Nano catalysts are materials with nanoscale dimensions, typically ranging from 1 to 100 nanometres, and possess unique properties such as high surface area, reactivity, and selectivity. These characteristics make them ideal for use in catalytic reactions that break down environmental pollutants. The growing interest in Nano catalysts for environmental remediation is driven by their ability to enhance the efficiency of catalytic processes, lower energy consumption, and provide sustainable solutions to mitigate the effects of pollution.

Mechanisms of Nano catalysts in Environmental Remediation

Nano catalysts are materials that exhibit catalytic properties at the nanoscale (typically 1–100 nanometres). Their unique physical and chemical properties, such as high surface area-to-volume ratio, reactivity, and the ability to be easily functionalized, make them ideal candidates for a variety of applications, particularly in the field of environmental remediation. Environmental remediation aims to remove or neutralize contaminants

from polluted water, soil, and air. Nano catalysts play a pivotal role in accelerating the breakdown of toxic substances, thereby offering a sustainable and efficient approach to tackling environmental pollution. The mechanisms by which Nano catalysts facilitate environmental remediation include:

1. **Photocatalysis**
2. **Fenton-like Reactions**
3. **Electrocatalysis**
4. **Adsorption and Desorption**
5. **Oxidation-Reduction Reactions**

Below, we explore each of these mechanisms in greater detail:

1. Photocatalysis

Photocatalysis involves the acceleration of a chemical reaction under the influence of light, typically ultraviolet (UV) light, although visible light can also be used depending on the catalyst material. Nano catalysts like titanium dioxide (TiO_2) and zinc oxide (ZnO) are among the most widely used photocatalysts due to their strong UV absorption and excellent stability.

Mechanism:

When TiO_2 or similar photocatalysts are exposed to UV light, they absorb the energy and undergo excitation. This results in the creation of electron-hole pairs. The energy from UV light is enough to excite an electron from the valence band to the conduction band, leaving behind a positively charged hole (h^+). These electrons and holes can then interact with water molecules or oxygen in the surrounding environment, generating reactive oxygen species (ROS), such as hydroxyl radicals (•OH) and superoxide anions ($O_2^{\bullet -}$).

- **Hydroxyl radicals (•OH)** are highly reactive and can degrade a wide range of organic pollutants, breaking them down into smaller, less toxic molecules such as carbon dioxide (CO_2) and water (H_2O).
- **Superoxide anions ($O_2^{\bullet -}$)** can also degrade organic pollutants by initiating further chemical reactions.

This mechanism is especially useful in the treatment of organic pollutants like dyes, pesticides, and pharmaceutical residues in wastewater or air (Fujishima, Rao, & Tryk, 2000).

Advantages:

- **Energy efficiency**: Photocatalysis uses sunlight as a natural energy source, making it energy-efficient for large-scale applications.
- **Environmentally friendly**: Photocatalysis generates harmless byproducts (CO_2 and H_2O) and does not require harsh chemicals or solvents.

Applications:

- Degradation of hazardous organic pollutants in water.
- Air purification and the breakdown of volatile organic compounds (VOCs).
- Water disinfection by destroying microbial pathogens.

2. Fenton-like Reactions

Fenton-like reactions are based on the reaction of hydrogen peroxide (H_2O_2) with iron-based nanomaterials to produce hydroxyl radicals (•OH). The traditional Fenton reaction involves iron ions (Fe^{2+}) reacting with hydrogen peroxide to produce hydroxyl radicals, which can then degrade organic contaminants. However, Fenton-like reactions use iron-based nanoparticles, such as nano-zero-valent iron (nZVI) or iron oxide (Fe_2O_3), in a similar process to enhance pollutant degradation.

Mechanism:

In Fenton-like systems, iron nanoparticles (nZVI) or iron oxide catalysts interact with hydrogen peroxide (H_2O_2) in the following manner:

$Fe^{2+}+H_2O_2 \rightarrow Fe^{3+}+\cdot OH+OH^-$

The hydroxyl radicals (·OH) produced are highly reactive and are capable of breaking down a wide range of pollutants, including organic contaminants and toxic metals such as chromium (Cr), arsenic (As), and lead (Pb). These radicals initiate oxidation reactions, converting pollutants into less harmful substances like CO_2, water, or simpler organic compounds.

Advantages:

- **Effective for a wide range of pollutants**: This method is particularly effective in treating both organic and inorganic contaminants, such as chlorinated solvents, pesticides, and heavy metals.
- **Faster reaction rates**: The use of nanomaterials accelerates the reaction rates, making the process more efficient compared to traditional Fenton reactions.

Applications:

- Remediation of contaminated groundwater and soil (e.g., chlorinated solvents).
- Removal of heavy metals like arsenic, lead, and cadmium from contaminated water.
- Degradation of persistent organic pollutants (POPs) in wastewater.

3. Electrocatalysis

Electrocatalysis refers to the use of Nano catalysts to promote electrochemical reactions, which involve the transfer of electrons between the catalyst and the pollutant. Nano catalysts, particularly those composed of metals such as platinum (Pt), palladium (Pd), or gold (Au), can significantly improve the efficiency of electrochemical processes that degrade pollutants in the environment.

Mechanism:

In electrocatalysis, Nano catalysts enhance the efficiency of redox reactions by facilitating electron transfer between the pollutant and the electrode. For example:

- **In wastewater treatment**: Electrochemical cells equipped with Nano catalysts can facilitate the reduction of harmful pollutants (e.g., heavy metals, nitrates, and VOCs), converting them into less harmful or inert substances.
- **In air purification**: Nano catalysts can aid in the electrochemical oxidation of gases, such as nitrogen oxides (NO_x), sulfur dioxide (SO_2), and VOCs, transforming them into non-toxic products.

Nano catalysts are particularly useful in removing metal contaminants, as they can promote reactions that convert soluble metals into insoluble forms, allowing for easy removal.

Advantages:

- **Low energy consumption**: Electrocatalytic reactions can be conducted at low temperatures, making them energy-efficient.
- **Highly selective**: Electrocatalysis allows for targeted pollutant degradation without the production of harmful byproducts.

Applications:

- Removal of heavy metals (e.g., lead, chromium) from water.
- Reduction of nitrogen oxides (NO_x) in industrial exhaust gases.
- Detoxification of industrial wastewater through electrochemical oxidation.

4. Adsorption and Desorption

Nano catalysts also facilitate the adsorption and desorption of pollutants, which is an important mechanism in environmental remediation. Adsorption is the process by which pollutants adhere to the surface of Nano catalysts, while desorption refers to the release of adsorbed pollutants under certain conditions.

Mechanism:

Nano catalysts, such as activated carbon, graphene, and carbon nanotubes (CNTs), have a large surface area that can adsorb a wide range of contaminants, including heavy metals, organic chemicals, and dyes. The pollutants are attracted to the surface of the nanomaterials through physical or chemical interactions, including van der Waals forces, hydrogen bonding, or electrostatic interactions.

Once pollutants are adsorbed, they can be either removed through filtration or chemically treated on the catalyst surface. In some cases, desorption can be triggered by changes in temperature, pressure, or pH, which allows the Nano catalyst to be reused.

Advantages:

- **High capacity for pollutant removal**: The large surface area of nanomaterials enables them to adsorb significant amounts of pollutants.
- **Reusability**: Nano catalysts can be regenerated and reused multiple times, making the process cost-effective and sustainable.

Applications:

- Removal of heavy metals, such as arsenic and mercury, from water.
- Adsorption of organic pollutants, such as pesticides and industrial dyes, from wastewater.
- Capture of CO_2 from industrial exhaust gases.

5. Oxidation-Reduction Reactions

Oxidation-reduction (redox) reactions are central to many catalytic processes involving nanomaterials. Nano catalysts can facilitate both oxidation (loss of electrons) and reduction (gain of electrons) reactions to break down pollutants.

Mechanism:

Nano catalysts like palladium (Pd), platinum (Pt), and copper (Cu) can catalyse redox reactions where pollutants are either oxidized (e.g., organic compounds) or reduced (e.g., toxic metal ions). For instance, in the reduction of chromium (VI) to chromium (III), the following reaction occurs:

$Cr^{6+} + 3e^- \rightarrow Cr^{3+}$

Similarly, in oxidation reactions, Nano catalysts can generate reactive species like hydroxyl radicals (•OH) or superoxide anions ($O_2^{\bullet -}$), which oxidize contaminants, breaking them down into non-toxic compounds.

Advantages:

- **Versatility**: Nano catalysts can be engineered to perform a wide variety of oxidation and reduction reactions, making them applicable for treating different types of contaminants.
- **High reaction rate**: The enhanced reactivity of nanomaterials increases the speed of redox reactions, improving the efficiency of the remediation process.

Applications:

- Reducing toxic metal ions like chromium and arsenic in water.
- Oxidizing organic pollutants in wastewater treatment.
- Breaking down hazardous chemicals like pesticides and herbicides.

Applications of Nano catalysts in Environmental Remediation

3.1. Nano catalysts in Water Treatment

Nano catalysts have shown great promise in removing contaminants from wastewater, including heavy metals, organic pollutants, and pathogens. One of the most widely studied Nano catalysts for water treatment is TiO_2, which can degrade organic pollutants through photocatalysis. This process has been used to remove pharmaceuticals, pesticides, and industrial chemicals from wastewater (Tung et al., 2020). Moreover, Nano catalysts can facilitate the removal of heavy metals, such as arsenic, lead, and mercury, through adsorption and reduction reactions.

For instance, iron-based nanoparticles can be employed to remove arsenic from contaminated water. These nanoparticles undergo reduction reactions that convert toxic arsenic species into less harmful forms, which can then be easily separated (Wang & Chen, 2015).

3.2. Nano catalysts in Air Pollution Control

Air pollution, primarily caused by industrial emissions, vehicle exhaust, and chemical processes, is a major environmental issue. Nano catalysts, especially metal oxide nanoparticles like TiO_2, zinc oxide (ZnO), and cerium oxide (CeO_2), have been investigated for their ability to degrade air pollutants such as nitrogen oxides (NO_x), sulfur dioxide (SO_2), and volatile organic compounds (VOCs). Photocatalytic reactions using these nanomaterials can help break down harmful gases in the atmosphere, converting them into less toxic byproducts (Molina et al., 2017).

For example, TiO_2-based catalysts have been used to remove VOCs from industrial effluents. When exposed to UV light, TiO_2 nanoparticles generate ROS that oxidize VOCs, turning them into harmless compounds like carbon dioxide and water (Zhao et al., 2020).

3.3. Nano catalysts in Soil Remediation

Soil contamination by toxic metals, organic compounds, and pesticides poses significant risks to human health and the environment. Nano catalysts offer a novel approach to decontaminating soils. For instance, nano-iron and nano-zero-valent iron (nZVI) particles have been extensively used for the remediation of chlorinated solvents and heavy metals in soil. These nanoparticles can degrade pollutants through reduction reactions, converting toxic chemicals into safer forms.

Nano catalysts can also be used to remove persistent organic pollutants (POPs) from soils, including pesticides and herbicides. The high surface area and reactivity of these nanomaterials make them effective in breaking down complex organic compounds that are resistant to conventional degradation processes (Jiang et al., 2019).

Potential of Nano catalysts in Reducing Carbon Emissions

One of the most significant applications of Nano catalysts in environmental remediation is their role in reducing carbon emissions. Catalytic processes, such as carbon capture and conversion, are essential for mitigating the effects of climate change. Nano catalysts can enhance the efficiency of CO_2 capture, turning it into useful products like fuels or chemicals.

For example, carbon dioxide can be reduced to methane or other hydrocarbons using Nano catalysts in a process called catalytic CO_2 hydrogenation. Platinum (Pt) and palladium (Pd) nanoparticles are often used as catalysts in this process, as they effectively promote the reaction between CO_2 and hydrogen. By converting CO_2 into valuable chemicals, this process not only helps reduce atmospheric carbon levels but also provides a potential source of renewable energy (Hansen et al., 2020).

Furthermore, Nano catalysts can improve the efficiency of fuel cells, which are used to generate electricity with minimal carbon emissions. The use of nanostructured catalysts in fuel cell reactions increases their performance and reduces the energy required for hydrogen production, further contributing to the reduction of greenhouse gas emissions (Xie et al., 2019).

Challenges and Future Directions

While Nano catalysts show great promise in environmental remediation, several challenges must be addressed before their widespread implementation. One key issue is the stability and reusability of Nano catalysts. Over time, nanomaterials may undergo aggregation or deactivation, reducing their efficiency. Research is ongoing to develop more stable and reusable nano catalysts through surface modification and functionalization.

Another challenge is the potential environmental impact of nanoparticles themselves. The toxicity and mobility of nanomaterials in the environment are still not fully understood, and there is a need for comprehensive studies to evaluate the long-term effects of Nano catalysts on ecosystems and human health.

In the future, research efforts will likely focus on developing more efficient and sustainable nano catalysts, improving their scalability, and integrating them into existing pollution control technologies. Additionally, advances in computational modelling and nanofabrication techniques will enable the design of nano catalysts with tailored properties for specific environmental applications.

Conclusion

Nanostructured catalysts have emerged as powerful tools for environmental remediation, offering innovative solutions for water, air, and soil pollution. Their high reactivity, large surface area, and versatility make them highly effective in degrading a wide range of pollutants. Moreover, Nano catalysts have significant potential in reducing carbon emissions and addressing climate change. While there are still challenges to overcome, the future of Nano catalysts in environmental remediation looks promising, with ongoing research focused on improving their efficiency, stability, and environmental safety.

References

[1]. Fujishima, A., Rao, T. N., & Tryk, D. A. (2000). Titanium dioxide photocatalysis. Journal of Photochemistry and Photobiology C: Photochemistry Reviews, 1(1), 1-21. https://doi.org/10.1016/S1389-5567(00)00002-6

[2]. Hansen, T. W., et al. (2020). Nano catalysts for CO2 hydrogenation: Opportunities and challenges.

[3]. Nature Communications, 11(1), 1-11. https://doi.org/10.1038/s41467-020-15396-9

[4]. Jiang, Z., et al. (2019). Nano-zero-valent iron (nZVI) for soil and groundwater remediation: A review of applications and future directions. Environmental Science & Technology, 53(6), 2935-2949. https://doi.org/10.1021/acs.est.8b05830

[5]. Molina, M. J., et al. (2017). Nanocatalysts for air pollution control: Advances and challenges. Environmental Science & Technology, 51(5), 2630-2640. https://doi.org/10.1021/acs.est.6b06189

[6]. Tung, P. H., et al. (2020). Recent advances in TiO2 photocatalysis for wastewater treatment. Environmental Technology Reviews, 9(1), 91-109. https://doi.org/10.1080/21622515.2020.1735974

[7]. Wang, C., & Chen, G. (2015). Removal of arsenic from drinking water by iron nanoparticles. Environmental Science & Technology, 49(2), 921-928. https://doi.org/10.1021/es505071t

[8]. Xie, J., et al. (2019). Nanocatalysts in fuel cells: Opportunities and challenges. Journal of Power Sources, 430, 52-64. https://doi.org/10.1016/j.jpowsour.2019.05.064

[9]. Zhao, B., et al. (2020). Photocatalytic removal of volatile organic compounds: Recent developments and future prospects. Environmental Science & Technology, 54(13), 7896-7915. https://doi.org/10.1021/acs.est.0c01706

[10]. Zhao, Y., et al. (2021). Electrocatalysis for environmental remediation: Strategies and progress. Environmental Science & Technology, 55(6), 3445-3459. https://doi.org/10.1021/acs.est.0c07683

International Journal of Scientific Research in Science and Technology
Available online at : www.ijsrst.com
OPEN ACCESS
Print ISSN: 2395-6011 | Online ISSN: 2395-602X
doi : https://doi.org/10.32628/IJSRST

Recent Development Nanotechnology in Solar Cell

Sunil B. Aute, Sherkhan Pathan
Kohinoor Arts Commerce and Science College Khultabad Tq. Khultabad, Dist Chhatrapati Sambhajinagar-431101, Maharashtra, India

ARTICLEINFO

Article History :

Published : 07 Dec 2024

Publication Issue :
Volume 11, Issue 23
Nov-Dec-2024
Page Number :
314-324

ABSTRACT

Nanotechnology is fast emerging field in the recent era, in this field nonstop advances and breakthroughs. Numerous nanoscale materials and coatings are already found in consumer goods such Energy, paints, dyes, fibers and textiles, sunscreens, and cosmetics. The smallest components of a computer chip are on a nanoscale. Nanotechnology has demonstrated great potential for energy uses through the manipulation of materials at the molecular level. Distinct optical, electrical, and mechanical characteristics of materials such as perovskite solar cells, Quantum Dot Solar, and dye-sensitized solar cells enable their application in renewable energy generation and pollutant elimination. perovskite solar cells has the maximum power conversion efficiency is 24% that, QuantumDot Solar has the reported PCE about 12.7%,and Dye sensitized solar cell has the maximum PCE reported as a 13%. The swift rise of the worldwide population has markedly heightened energy usage and strain on the environment.

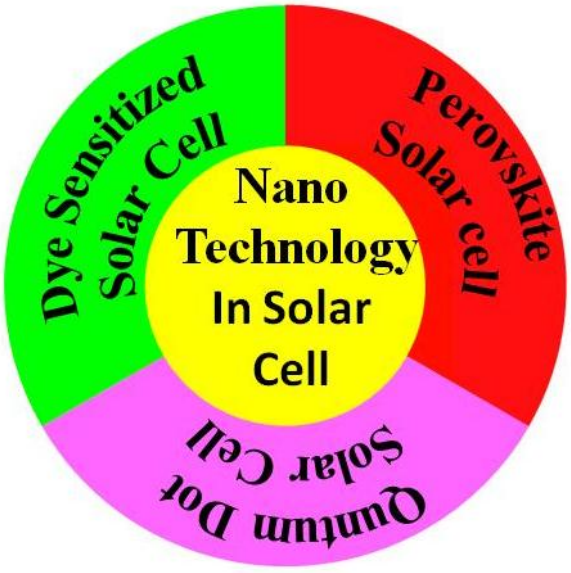

Introduction

In today's evolving landscape and contemporary technological era, energy holds significant importance. It has turned into an essential requirement vital for existence, evident from the rising energy demand due to a growing global population. Energy consumption could potentially double in the next two decades or beyond due to a heightened dependence on non-renewable fossil fuels, resulting in a notable rise in the search for alternative energy sources.Nuclear power produces a significant quantity of energy; however, there are issues regarding safety, waste disposal, and societal implications. Therefore, moving forward, it is essential to shift to alternative energy sources that are both sustainable and renewable.[1] An eventually, solar energy and other renewable sources like geothermal heat, hydropower[2], wind[3], and various natural energy resources are abundant and environmentally friendly on our planet. At present, scientists are investigating solar energy as a potential energy source to fulfil societal demands.Approximately 3 x 10^{24} joules of energy annually reach the Earth's surface as sunlight, which is roughly 108 times greater than global energy consumption. While the Sun gives us a significant amount of energy, it is essential to effectively manage its distribution and storage for efficient use in the future. The conventional inorganic semiconductor silicon photovoltaic (PV) solar cell has certain limitations, including silica purity and elevated manufacturing expenses.[5]Recentdecades, the PCE recorded in the solar system in perovskite solar cells has recorded as 25.%, showing themind blowing outcomes for the commonincorporates in the organometallic trihalide perovskite solar cells. Advances in $CsPbI_3$ (perovskite) solar cells have enabled high efficiency over 15% to be achieved, showing great potential for photovoltaic.[6,7]Cross hybrid halide class perovskites have improve as a capable group of resources with huge potential for effective optoelectronic properties. The especially flexible applications of these system, lie in its unable band gap and carrier dynamics, gettingduring compositional engineering. In mixed hybrid halide perovskites (MHHPs).[8] The quantum dots (QD) have obviouslydissimilar properties with the bulk materials. Their much more inherent dipole moments allowvery good separation of charge.[9] Generally, in the quantum dots their size will in some way enable the bring into play the hot electrons or high-energy to generate multiple charge carriers by single photon inside these nanomaterial. Generally, the QD are made up of inorganic components, alsothese materials are physically and chemically stable in the solar cell system, these material playing the productive life of the QD solar cells.[10]

In year 1991, Gratzel and his group establish the dye-sensitized solar cell (DSSC), and produces a sequence of N_3 dyes in succeeding years. First upon N_3 dye obtaining the highest efficiency (10%) in DSSC Cell as TiO_2 as nanoparticle.[5]As a result in 2014, porphyrin dye compound have recorded PCE that are as good as to or still higher than those of well-established highly efficient DSSCs composed on ruthenium complexes. So far the PCE has improved up to 13% by help of a push–pull porphyrin mechanism with redox shuttle of cobalt base. In this viewpoint, we review the recent developments in the synthetic design of porphyrins and TiO_2 nanoparticle for highly efficient DSSCs.[11]

Perovskite solar cells

In the solar cell rapid progress power conversion efficiency (PCE) to reaches up to 25%, of metal halide perovskite kind solar cells turn out to be a prompt in anefficient photovoltaic device.[6,7] Intense follow up research on structure design, materials chemistry, process engineering, and device physics has been prompted by the development of the solid state perovskite solar cell in 2012. This has led to the revolutionary evolution

of the solid state perovskite solar cell, making it a promising contender for a next generation solar energy harvester.[12]

The advantages of this cell over commercial silicon or other organic and inorganic solar cells are its high efficiency and the low cost of materials and processes. Perovskite materials' unique properties may allow the PCE to develop beyond the Shockley–Queisser limit and beyond what silicon solar cells can provide. The principles underlying the optoelectronic characteristics of perovskite materials and the key strategies for creating high-efficiency perovskite solar cells are outlined in this paper. Additionally, potential next-generation approaches to improving the PCE beyond the Shockley-Queisser limit are examined.[13]

Perovskite structure

The term "perovskites" was first used to refer to a group of minerals bearing the formula $CaTiO_3$.[14]The compositional formula represents the optimal perovskite structure $A^{2+}B^{4+}O_3$, although $A^{1+}B^{5+}O_3$ and $A^{3+}B^{3+}O_3$ are also feasible. Typically, perovskites are represented by the formula ABO3, with the crystal structure illustrated in Fig. 1. In this crystal lattice, A and B are cation positions filled by alkali earth or rare earth elements from the La-series and transition metals, respectively.

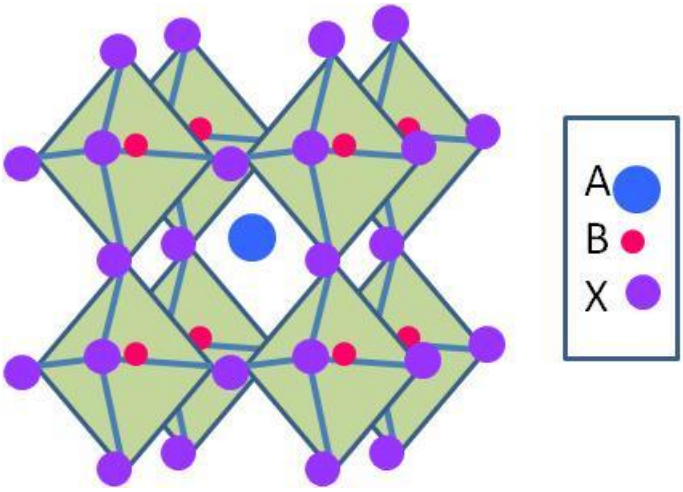

Figure 1 crystal Structural formula of ABO_3 perovskite

The unit cell takes the form of a face-centred cubic crystal, featuring the larger Acations at the corners, the smaller B cation situated in the body-centred position, and the O^{2-} anions positioned at the face-centred locations.

It is important to note that, unlike the unfavorablebehavior of Ln doping seen in semiconductor quantum dots (CdSe, InP, etc.), doping in halide-based perovskites like CsPbX3 (X = Cl, Br, I) is relatively straightforward, as this structure offers a suitable octahedral coordination environment for the Ln ion. As a result, Ln-doped metal halide perovskites have quickly come to the forefront as a novel category of phosphors.[14,15]Metal halide perovskites, particularly the hybrid using organic-inorganic compound $CH_3NH_3PbI_3$, characterize a novel class of optoelectronic materials that have create significant concern for

their application as solution-deposited absorbing layers in solar cells, achieving PCE of up to 20%. In that investigation, Perez-Prietoand co-worker explore a new direction for halide perovskites by developing highly luminescent perovskite-based colloidal quantum dot materials. Perez-Prieto and co-worke successfully synthesized monodisperse colloidal nanocubes with edge lengths ranging from 4 to 15 nm, composed of fully

inorganic cesium lead halide perovskites (CsPbX3, where X can be Cl, Br, or I, including mixed halide systems of Cl/Br and Br/I) utilizing cost-effective commercial precursors.[16,17]

Throughout Structural modulations and quantum size-effects, the energies gap of HOMO and LUMO level and luminescence spectra are effectively tunable over the whole visible spectral region of 410–700 nm. The Photo emission of $CsPbX_3$ nano material is indentified by narrow luminescenceband-widths of 12–42 nm, grandcolour gamut under up to 140% of the NTSC colour benchmark, highest quantum yields nearby 90%, along with radiative lifetimes in the region of 1–29 ns.

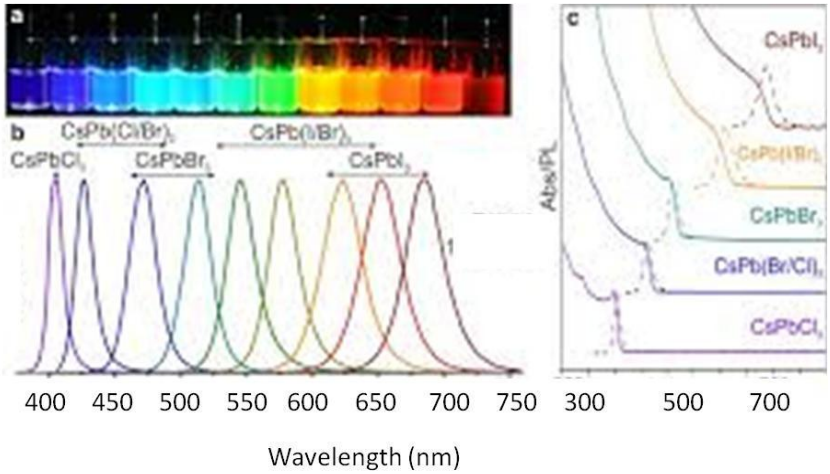

Figure 2 Illustrating the $CsPbX_3$ Perovskite Changing the composition of halide effect to tune the Wavelength of Material

$CsPbX_3$ nonomaterial are attractive for optoelectronic applications due to their strong optical characteristics and chemical stability, especially in the blue and green spectral ranges (410–530 nm), where photodegradation is a problem for conventional metal chalcogenide-based Perovskite.

Mechanism perovoskite solar cell

In a photovoltaic mechanism light absorption process is just the first step; then it create splitting of the holes and electrons quasi Fermi levels E_{Fn} and E_{Fp}, consequently. The greatest free energy available is the difference between these two levels, but it can only be utilized to generate work following the charge separation, the second photovoltaic phase. Charge-selective connections must be used to separately contact each pseudo Fermi level. Because selectivity may be achieved through a variety of methods, the photovoltaic limit is therefore dependent on the selective contacts and the method used to achieve it (see Figure 3).

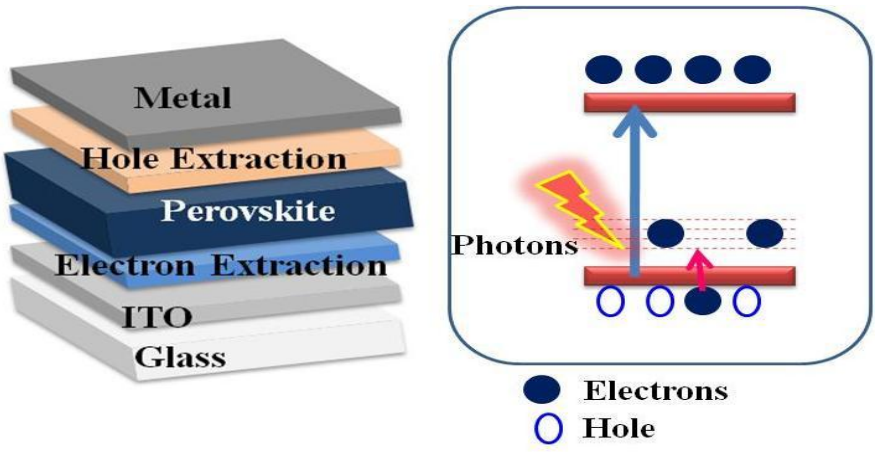

Figure 3. Layer of perovskite solar cell and mechanism of electron excitation

A p-i-n solar cell's band diagram is seen in Figure 3. In this concept, two doped layers, n and p, respectively, come into contact with an inherent light-absorbing semiconductor. The Fermi level, EF0, equilibrates along the whole device in dark circumstances without any bias applied (see Figure 3). The equilibration results in an inherent potential, Vbi, since the n-doped and p-doped layers exhibit low and high work functions, respectively. Their bands are slanted along the whole thickness of the light-absorbing layer due to its intrinsic nature, with an electrical field operating in the intrinsic area. Accordingly, the electrical field that drives electrons and holes to n-doped and p-doped contacts, respectively, is essentially responsible for the contact selectivity in this model. In this case, charge separation and collection are significantly influenced by the drift current. Both the applied bias and the creation of light photocarriers influence the band's inclination. Indeed, when exposed to open circuit illumination, the splitting of Fermi levels results in flat band conditions (refer to Figure 3), where the photocurrent is annulled due to the removal of the electrical field and the resulting cancellation of the collection driving force. In this instance, the contacts' work duties place restrictions on the Voc. The Voc in organic solar cells and amorphous Si solar cells has been explained by this approach.[18]

Quantum dot nanotechnology:

The initial studies on the decreased dimensionality of semiconductors, which gave rise to the idea of "artificial atoms," or quantum dots (QDs), were conducted many years ago. The optical and electrical characteristics of these semiconductor nanocrystals, which have dimensions of nanometers, show quantum size effects.[19,20] Specifically, several QD material systems now routinely accomplish core-shell architectures, narrow emission, photochemical stability, and adjustable and efficient photoluminescence (PL). Consequently, QDs have been integrated as active components in several gadgets and uses. Many of these applications like QD-based displays are already commercially accessible and used in many aspects of our everyday lives. QD synthesis, characterization, and applications remain a very active area of research even though they are already a part of established technologies. Although group IV and III–V compounds were the main focus of early QD research, advancements in synthesis over time have broadened the elemental composition. Nowadays, transition-metal dichalcogenides, perovskites, carbon, and II–VI and I–III–VI compounds are also the basis for QDs. The primary basis for QD applications is their involvement in light emission, conversion, and detection as well as their excellent optical characteristics.As a result, QDs have many different applications. The recent developments in QD research have been covered by ACS Applied Nano Materials, an interdisciplinary magazine that covers topics related to nanomaterial applications. These papers have now been collected in this virtual issue. We have categorized these nanomaterials according to their intended use in order to showcase these papers.[21,22]

Structure of QD

In order to prevent toxicity, the structure of quantum dots consists of an exterior shell composed of zinc sulfide (ZnS) and cadmium sulfide (CdS) and a semiconductor core composed of heavy metals such as cadmium selenide (CdSe), lead selenide (PbSe), or indium arsenide (InAs). At the moment, the most widely accessible commercial items are CdSe/ZnS quantum dots.[23]

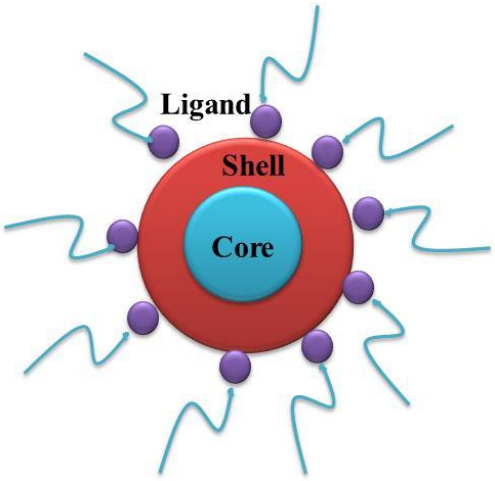

Figure 4. Basic Structure of Quantum Dots

Quantum dots have been created using a variety of techniques, including viral assembly, electrochemical assembly, and plasma synthesis. The most often used method is still colloidal synthesis.[24]

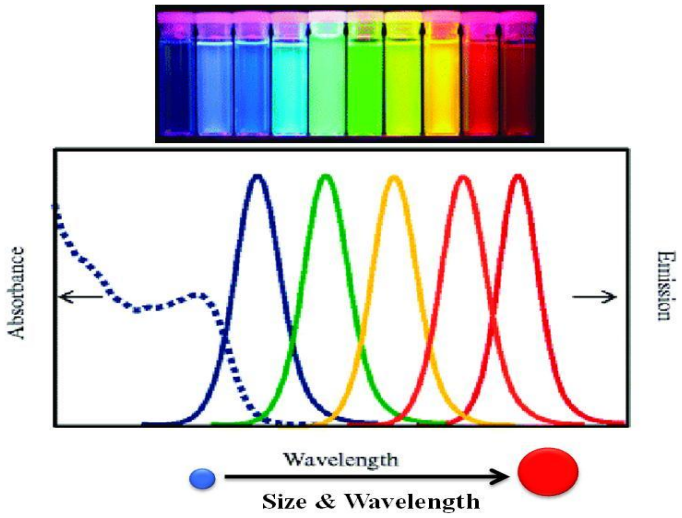

Figure 5. Increasing size of the Nanoparticle emission wavelength shifted to red Region

Due to its characteristics, which include narrow and symmetric emission with customizable colors, high quantum yield, high stability, and programmable shape, semiconductor quantum dots have garnered a lot of interest in the biosensing field. A variety of ligands, antibodies, peptides, or nucleic acids may be conjugated for a wider range of more intelligent applications by adding different reactive functional groups to the surface of semiconductor quantum dots. Aptamers stand out among these ligands because to their small size, excellent chemical stability, ease of synthesis, high batch-to-batch uniformity, and ease of modification.More significantly, aptamer-based sensing devices may easily be made more sensitive by adding nanomaterials and/or nucleic acid amplification techniques. Thus, aptamers and semiconductor quantum dots together open up new bioanalysis possibilities. Here, we provide an overview of current developments in biosensing applications using aptamer-functionalized semiconductor quantum dots. First, we go over the characteristics and composition of semiconductor aptamers and quantum dots.[23] The use of biosensors based on semiconductor quantum dots modified by aptamers via various signal transducing mechanisms, such as optical, electrochemical, and electrogeneratedchemiluminescence techniques, is then covered.

Mechanism of QD solar cell

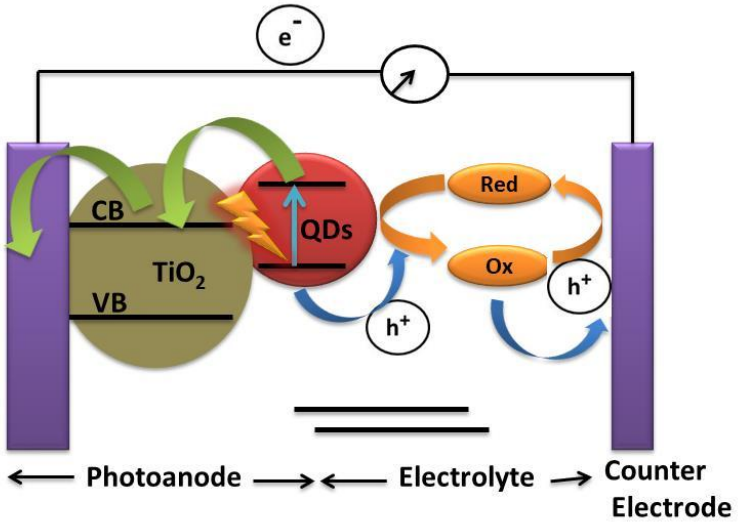

Figure 6. Mechanism of the DQ solar Cell electron and hole transfer

DSSC operates in a manner akin to DSSC. The fundamental architecture and the pathway of electron movement in a QDSSC are depicted in Figure 6. The primary distinctions between QDSSC and DSSC lie in the materials used for light absorption and the electrolyte system. Generally, QDSSC functions when illuminated by light, wherein the light-absorbing material reacts to a particular wavelength range within the visible light spectrum, facilitating the transition of electrons from the valence band to the conduction band.[22] In this process, the electrons within the light-absorbing material are described as having been "excited." These excited electrons subsequently migrate through the network of wide band gap oxide materials. Typically, the light-absorbing materials are connected to this network of wide band gap oxides. Ultimately, the excited electrons arrive at the conducting substrate and proceed to the external circuit, where they are utilized by the load to generate electricity. Concurrently, as the electrons become "excited," the light-absorbing material undergoes oxidation, resulting in an electron deficiency. Consequently, it necessitates additional electrons to stabilize its condition. Therefore, the electrolyte system provides its electrons to the light-absorbing material to meet this electron demand. When the electrons traveling through the external circuit reach the counter electrode, they are promptly returned to the electrolyte system, allowing it to attain a stable state as well. This entire cycle will persist as long as there is light exposure.[23]

Dye sensitise Solar Cell

Since energy is crucial to the expansion, development, and enhancement of the agricultural, mechanical, and defense industries, it is widely acknowledged that a state's financial progress is largely reliant on this sector. It is anticipated that a reliable energy supply will raise society's standards for daily comforts. Electricity is necessary for modern industrial development, which is essential for any country. The primary cause of the energy crisis is the sharp rise in the consumption of hydrocarbon resources. Therefore, using renewable resources is crucial to solving this problem. Our environment is negatively impacted by the use of hydrocarbon fuels and their emissions. The newest and most promising alternative in solar cells are third-generation photovoltaic (solar) cells. Nowadays, inorganic (ruthenium) sensitizers and organic (natural and manufactured) dyes are used in dye-sensitized solar cells (DSSC). Due to the nature of this dye and other factors, its application has changed.Because of their low cast, ease of use, plentiful resource availability, and lack of environmental harm,

natural dyes are a viable substitute for costly and scarce ruthenium dye. The dyes often used in DSSC are covered in this review. The development of natural and inorganic dyes is tracked, and the DSSC criteria and components are described. This analysis will be helpful to scientists working on this new technology. The estimated global power requirement in 2050 is 28 terawatts (TW), assuming reasonable population growth and electricity output.[25] In the near future, solar energy has the most potential to meet the world's need for sustainable power sources. The 1.7×10^5 TW solar energy that reaches our planet's surface is used to estimate the useful Earth-bound global solar power potential estimate at around 600 TW. Therefore, over 60 TW of energy might potentially be generated by using 10% of productive farms that are reliant on sunshine. In contrast, during the past 15 years, the development of solar power cells has advanced at a rate of around 30% annually. Before discussing the research and development efforts done for the different DSSC components, a brief overview of worldwide research on various DSSC components has been provided below. This includes some noteworthy works on the international state of DSSC research progress. shows the photoconversion efficiency of several solar cell types, including DSSC, based on a year-by-year analysis from 1980 to the present with data from NREL (USA). It is important to note that, despite PSCs becoming viable photovoltaic technologies in a relatively short ten years, no material has been discovered to improve the efficiency of DSSCs over the previous 20 years.We will talk about some of the major research and innovation projects that have been conducted on the many DSSC components over the last ten to fifteen years all over the world. The data indicates that the majority of research efforts have focused on developing DSSCs that are economical, environmentally benign, stable, and efficient.[26] The most nanomaterial investigatedphotoanode materials for DSSCs are still TiO_2 and ZnO. A some TiO_2improvedphotoanodes, such as $SiO_2/Ag/TiO_2$,[27] g-C_3N_4 and ZnO/TiO_2,[28] multilayer TiO_2,Ag/TiO_2,[27] have demonstrated promising photovoltaic capabilities. also capable ZnO-based photoanodes, indicating promising electron transport in the photoanode and enlarged cell efficiency. On exposure to light, dye substrate generates photoexcited electron, and are thus regarded as the most crucial part of DSSCs.

Mechanism of solar cell

A schematic representation of DSSCs is shown in Fig. 4, where the structure is made from four fundamental parts.

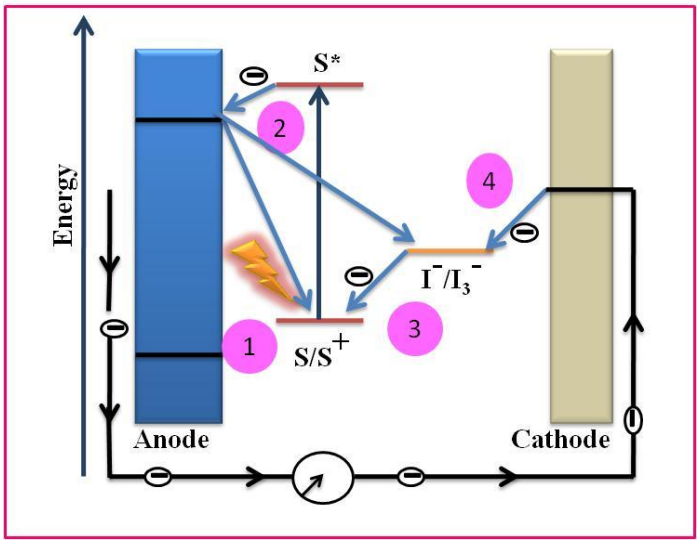

Figure 7. Schematic Illustration of Dye Sensitised Solar Cell

STEP 1: At first, the dye molecule is in its ground state (S). At this energy level (close to the valence band), the anode's semiconductor material is nonconductive.

Equation 1 shows that dye molecules are stimulated from their ground state to a higher energy state (S*) when light strikes the cell.

$S + hv \rightarrow S^*$…….. (1)

The excited dye molecule surpasses the semiconductor's band gap and has a larger energy content.

STEP 2: An electron is introduced into the semiconductor's conduction band when the excited dye molecule (S*) is oxidized (refer to equation 2). At this energy level, the semiconductor becomes conductive, allowing electrons to flow freely.

$S^* \rightarrow S^+ + e^-$…….. (2)

Diffusion mechanisms are then used to move the electrons to the anode's current collector. If connected, an electrical load can be powered.

STEP 3: The oxidized dye substrate (S^+) is again recharged by electron donation from the iodide in the electrolyte (see equation 3).

$S^+ + \frac{3}{2}I^- \rightarrow S + \frac{1}{2}I_3^-$…….. (3)

STEP 4: In finally the iodide is recharged by reduction of triiodide on the cathode (see equation 4).

$\frac{1}{2}I_3^- + e^- \rightarrow 3/2I^-$…….. (4)

Conclusion

Nanotechnology is emerging field nowadays in that several Nanomaterials playing their role in several filed like solar, medical, material etc. In that energy in is very important factor in our day to day life. Solar energy is available in our planet. There are different type of solar cell in that we are seen here first one is Perovskite Solar cell, these solar cell is nanomaterial based solar cell having PCE up to the 25%. The Second solar cell is the Quantum Dot Solar cell this also a nanomaterial based solar cell. QDSC having PCE up to the 12-13% and third one we are seen here the Dye sensitised Solar Cell these solar cell also used TiO_2 nanomaterial. In DSSC with help of TiO_2 Nanomaterial the PCE is up to the 13%. Here in these three system the Perovskite solar cell has getting maximum PCE because of the that the Perovskite solar cell is prominent nanomaterial in Current Scenario of Solar Cell.

References

[1]. Jeff Johnson, special to C&EN, 2016, 94 (34), p 16.

[2]. Anon.Mr. Brush's Windmill Dynamo, Scientific American, Vol. 63 No. 25, 20 December 1890, p. 54.

[3]. Kreis, Steven (2001). Retrieved19 June 2010.

[4]. IEA Renewable Energy Working Party (2002). Renewable Energy. into the mainstream, p. 9

[5]. M. Gratzel, Nature 2001, 414, 338.

[6]. Dong In Kim, Ji Won Lee, Rak Hyun Jeong, Jin-Hyo Boo, Scientific Reports volume 12, Article number: 697 (2022)

[7]. Anthony Kipkorir, Bo-An Chen, Prashant V. Kamat. Anion-Driven Bandgap Tuning of AgIn(SxSe1–x) 2 Quantum Dots. ACS Nano 2024, 18 (41) , 28170-28177.

[8]. GourabSarkar, PriyankaDeswal, Dibyajyoti Ghosh. Ion Diffusion Dynamics and Halogen Mixing at the Heterojunction of Halide Perovskites: Atomistic Insights. The Journal of Physical Chemistry C 2024, 128 (4) , 1762-1772

[9]. R. Vogel, K. Pohl, H. WellerSensitization of highly porous, polycrystalline TiO2 electrodes by quantum sized CdSChem. Phys. Lett., 174 (3) (1990), pp. 241-246,

[10]. R.D. Schaller, V.I. Klimov High efficiency carrier multiplication in PbSenanocrystals: implications for solar energy conversion Phys. Rev. Lett., 92 (18) (2004), Article 186601,

[11]. Mathew, S., Yella, A., Gao, P. et al. Dye-sensitized solar cells with 13% efficiency achieved through the molecular engineering of porphyrin sensitizers. Nature Chem 6, 242–247 (2014).

[12]. AsirElietMagdalin, Peter Daniel Nixon, ElangovanJayaseelan, MurugesanSivakumar, Suresh Kumar Narmadha Devi, M.S.P. Subathra, Nallapaneni Manoj Kumar, NallamuthuAnanthi, Development of lead-free perovskite solar cells: Opportunities, challenges, and future technologies, Results in Engineering, Volume 20, 2023,101438,

[13]. Kim JY, Lee JW, Jung HS, Shin H, Park NG. High-Efficiency Perovskite Solar Cells. Chem Rev. 2020 Aug 12;120(15):7867-7918.

[14]. Wenk, H.-R.; Bulakh, A. Minerals: Their Constitution and Origin; Cambridge University Press, 2016.

[15]. AirtonGermanoBispo-Jr, Amanda Justino de Morais, Claudia Manuela Santos Calado, ItaloOdoneMazali, Fernando AparecidoSigoli, Lanthanide-doped luminescent perovskites: A review of synthesis, properties, and applications,Journal of Luminescence,Volume 252,2022,119406,

[16]. L. C. Schmidt, A. Pertega´s, S. Gonza´lez-Carrero,O. Malinkiewicz, S. Agouram, G. Mı´nguezEspallargas,H. J. Bolink, R. E. Galian and J. Perez-Prieto, J. Am. Chem.Soc., 2014, 136, 850–853.

[17]. LoredanaProtesescu,SergiiYakunin,Maryna I. Bodnarchuk,Franziska Krieg, Riccarda Caputo, Christopher H. Hendon,Ruo Xi Yang, Aron Walsh, Maksym V. KovalenkoNanocrystals of Cesium Lead Halide Perovskites (CsPbX3, X = Cl, Br, and I): Novel Optoelectronic Materials Showing Bright Emission with Wide Color GamutNano Lett. 2015, 15, 6, 3692–3696

[18]. Wehrenfennig, C.; Eperon, G.E.; Johnston, M.B.; Snaith, H.J.; Herz, L.M. High Charge Carrier Mobilities and Lifetimes in Organolead Trihalide Perovskites. Adv. Mat. Res. 2013, 26, 1584–1589

[19]. Alferov, Zh.I. The history and future of semiconductorheterostructures. Semiconductors 1998, 32, 1–14.

[20]. Ashoori, R. C. Electrons in artificial atoms. Nature 1996, 379,413–419.

[21]. Kubendhiran, S.; Bao, Z.; Dave, K.; Liu, R.-S. MicrofluidicSynthesis of Semiconducting Colloidal Quantum Dots and TheirApplications. ACS Appl. Nano Mater. 2019, 2, 1773–1790.

[22]. Shirasaki, Y.; Supran, G. J.; Bawendi, M. G.; Bulovic, V.Emergence of colloidal quantum-dot light-emitting technologies. Nat.Photonics 2013, 7, 13–23.

[23]. Han, M.; Gao, X.; Su, J.Z.; Nie, S. Quantum-dot-tagged microbeads for multiplexed optical coding of biomolecules. Nat. Biotechnol. 2001, 19, 631–635

[24]. Guyot-Sionnest, P. Charging colloidal quantum dots by electrochemistry. Microchim. Acta 2008, 160, 309–314.

[25]. Jeff Johnson, special to C&EN, 2016, 94 (34), p 16.

[26]. Anon.Mr. Brush's Windmill Dynamo, Scientific American, Vol. 63 No. 25, 20 December 1890, p. 54

[27]. Luís Pinho, María Rojas, Maria J. Mosquera, Ag–SiO2–TiO2 nanocomposite coatings with enhanced photoactivity for self-cleaning application on building materials, Applied Catalysis B: Environmental, Volume 178, 2015, Pages 144-154

[28]. Nguyen T. B.; Hwang M. J.; Ryu K. S. Synthesis and high photocatalytic activity of Zn-doped TiO2 nanoparticles by sol-gel and ammonia-evaporation method. Bull. Korean Chem. Soc. 2012, 33, 243–247. 10.5012

International Journal of Scientific Research in Science and Technology
Available online at : www.ijsrst.com
OPEN ACCESS
Print ISSN: 2395-6011 | Online ISSN: 2395-602X
doi : https://doi.org/10.32628/IJSRST

Recent Advances in Green Chemistry: Innovations towards a Sustainable Future

Nilesh P. Tale *

Department of Chemistry, Late B.S. Arts, Prof. N.G. Science and A.G. Commerce College Sakharkherda Tq. Sindkhed Raja, Dist. Buldhana, Maharashtra, India

ARTICLEINFO

Article History :

Published : 07 Dec 2024

Publication Issue :
Volume 11, Issue 23
Nov-Dec-2024
Page Number :
325-328

ABSTRACT

Green chemistry, often referred to as the chemistry of sustainability, focuses on designing chemical products and processes that minimize environmental impact, reduce waste, and enhance energy efficiency. Recent advances in green chemistry have led to significant innovations across various domains, including renewable energy, waste reduction, and the development of environmentally benign materials and processes. This review article explores the latest breakthroughs in green chemistry, emphasizing key innovations such as the use of renewable feedstock's, energy-efficient catalytic processes, sustainable solvent systems, and biocatalysis.

Keywords:- Green Chemistry, Sustainable Chemistry, Renewable Feedstock's, Environmental Impact, Catalysis, Biocatalysis, Energy Efficiency, Sustainable Solvents, Waste Reduction.

Introduction

The field of green chemistry has emerged as a critical discipline in the quest for sustainable solutions to global environmental challenges. Green chemistry, by definition, seeks to minimize the environmental footprint of chemical processes by promoting the use of renewable resources, reducing waste, and enhancing energy efficiency. As the world faces increasing concerns related to climate change, resource depletion, and pollution, the importance of developing environmentally responsible chemical technologies has never been greater.[1] In recent years, there has been a surge of innovations in green chemistry, driven by advances in catalytic processes, sustainable materials, renewable energy technologies, and biocatalysis. These innovations are reshaping industrial practices, offering new avenues for reducing the reliance on hazardous chemicals, conserving resources, and mitigating environmental degradation. From the development of green solvents and waste-minimizing reaction pathways to the integration of renewable feedstock's and energy-efficient processes, green chemistry is fostering a paradigm shift towards more sustainable chemical production.[2] This review explores the most recent breakthroughs in green chemistry, highlighting key advancements in areas such as catalysis,

sustainable manufacturing, and bio-based chemistry. The integration of green chemistry principles into industrial settings not only enhances the environmental sustainability of chemical processes but also offers economic benefits, such as cost reduction and improved efficiency. Furthermore, we discuss the potential of these innovations to support the transition to a circular economy, where waste is minimized, and materials are continuously recycled and reused.[3] Despite the progress made, challenges remain in scaling up green technologies for widespread industrial adoption. The ongoing need for innovation in green chemical processes, coupled with a supportive policy framework, will be crucial in realizing a truly sustainable future. In this context, this article aims to provide a comprehensive overview of the latest advancements in green chemistry, offering insights into their current impact and future potential for fostering sustainability in both scientific and industrial sectors.[4]

Key Advances in Green Chemistry

1. **Renewable Feedstock's:-** The shift from fossil-derived raw materials to renewable feedstock's has been one of the most significant advancements in green chemistry. Biorefineries, which convert plant-based materials into chemicals, fuels, and other useful products, are a prime example. These advancements have led to the development of bio-based plastics, biofuels, and biopolymers. For example, the conversion of lignocelluloses biomass (such as agricultural waste) into biofuels, including ethanol and butanol, has seen remarkable improvements in efficiency.[5]
2. **Solvent-Free and Green Solvents :-**Solvents are crucial in many chemical processes, but their environmental impact has been a major concern due to toxicity, waste generation, and energy consumption. Researchers have made significant strides in reducing or eliminating solvent use altogether. Solvent-free synthesis methods, such as mechanochemical and microwave-assisted synthesis, are being adopted for their efficiency and minimal environmental impact. Additionally, the development of "green solvents" such as ionic liquids, supercritical fluids, and deep eutectic solvents has enabled safer and more sustainable reactions.[6]
3. **Catalysis and Biocatalysis:-** Catalysis plays a crucial role in enhancing the efficiency of chemical reactions, and recent advancements have focused on developing more efficient, selective, and environmentally benign catalysts. The use of enzymes (biocatalysts) in chemical processes has gained traction due to their specificity, mild reaction conditions, and renewable nature. Advances in enzyme engineering and immobilization techniques have broadened the scope of biocatalysis for industrial applications.

In addition, there has been significant progress in the development of heterogeneous catalysts that can be easily recovered and reused, reducing waste and costs. One example is the development of metal-organic frameworks (MOFs) as highly efficient and recyclable catalysts for various reactions.[7]

4. **Waste Minimization and Atom Economy:-** Reducing waste generation is a core tenet of green chemistry. Advances in reaction design, such as those that promote atom economy, aim to ensure that the maximum possible amount of reactants is converted into useful products, thus minimizing waste. One notable example is the development of reaction pathways that use fewer reagents, produce fewer by-products, and require less energy. Green chemistry advocates for using techniques like flow chemistry, which allows for continuous reactions with better control over reaction conditions, minimizing waste and optimizing yield.[8]
5. **Energy Efficiency and Sustainable Processes:-**The green chemistry field is also focused on reducing energy consumption in chemical processes. Innovations such as the development of energy-efficient reaction pathways, better thermal management, and the use of renewable energy sources (e.g., solar, wind, or

bioenergy) are gaining momentum. For instance, the integration of solar energy in industrial chemical processes can reduce the need for high-temperature operations, which are traditionally energy-intensive.

Another notable advancement is the development of electrochemical processes. Electrochemistry offers cleaner, more energy-efficient alternatives to traditional thermal processes in fields like synthetic organic chemistry and materials production. Advances in battery technologies, like those for storing energy from renewable sources, are also contributing to greener industrial practices.[9]

6. **Green Chemistry in Pharmaceuticals and Agrochemicals:-**The pharmaceutical industry has been a significant adopter of green chemistry practices due to increasing pressure for sustainable practices. Many pharmaceutical companies now focus on reducing the environmental impact of drug synthesis, including minimizing hazardous reagents and solvents, increasing the selectivity of reactions, and optimizing process efficiency.

Green chemistry principles have also been applied to the agrochemical industry, which traditionally relies on harmful chemicals for pest control and crop management. Biopesticides, which are derived from natural sources such as bacteria, fungi, or plants, have been developed as a safer alternative to conventional synthetic pesticides. Furthermore, the application of nanotechnology to fertilizers is helping to optimize nutrient delivery and reduce environmental impact.[10]

7. **Circular Economy and Green Chemistry:-** The circular economy model, which emphasizes the reuse, recycling, and repurposing of materials, has found strong synergy with green chemistry principles. Chemists are developing new methods for recycling plastics and other materials using less energy and fewer chemicals. Notable efforts include the development of enzymatic methods for breaking down synthetic polymers, such as PET, and processes that enable the regeneration of valuable metals used in industrial processes.[11]
8. **Green Chemistry in Education and Policy:-** As the need for sustainable practices grows, so too does the importance of incorporating green chemistry into educational curricula and policy-making. Increased training in green chemistry is preparing the next generation of scientists and engineers to design safer and more sustainable chemicals and processes. On the policy front, governments around the world are beginning to establish stricter regulations and incentives for businesses to adopt green chemistry practices, creating a more favorable environment for innovation.[12]

Challenges and Future Directions:-

Despite the progress, several challenges remain in the widespread adoption of green chemistry. Economic and regulatory barriers, such as the cost of developing new technologies and the lack of standardized regulations, continue to limit its broader implementation. Additionally, while many green chemistry methods are more sustainable, they can still require significant research and development before they can be scaled up for industrial applications.

Looking forward, the future of green chemistry lies in further integration with other fields, such as biotechnology, materials science, and renewable energy. Innovations in artificial intelligence and machine learning also hold the potential to accelerate the design of new green processes and materials by predicting the outcomes of chemical reactions and optimizing reaction conditions.[13]

Conclusion:-

Green chemistry represents a paradigm shift in the chemical sciences, focusing not only on the development of safer chemicals but also on creating more sustainable industrial practices. Through innovations in renewable feedstock's, green solvents, catalysis, and waste reduction, the field has made great strides in minimizing the environmental impact of chemical processes. While challenges remain, ongoing research and collaboration across industries will continue to drive progress toward a greener and more sustainable future.

References

[1]. Sala, O. E., et al. (2000). Global biodiversity scenarios for the year 2100. Science, 287(5459), 1770–1774.

[2]. Cavallo, L. R. (2003). Green Chemistry and Sustainable Development: Future Directions. Science, 302(5644), 212–214.

[3]. Beller, M., & Tundo, P. (2005). Green Catalysis in the Chemical Industry. Angewandte Chemie International Edition, 44(32), 5192–5194.

[4]. Georgakopoulos, D., et al. (2020). Sustainable Industry 4.0: A Comprehensive Review of Key Challenges and Future Prospects. Sustainable Production and Consumption, 24, 58–80

[5]. Xu, F., et al. (2023). Renewable Biomass Feedstocks for Biofuels: Advancements and Challenges in Conversion Technologies. Biotechnology Advances, 60, 107971.

[6]. Shaterian, H. R., &Mirkhani, V. (2023). Solvent-Free Organic Synthesis: Principles and Applications. Green Chemistry Letters and Reviews, 17(1), 45-60.

[7]. Zhang, H., et al. (2023). Biocatalysis in Green Chemistry: Recent Developments and Challenges. Green Chemistry, 25(2), 318-331.

[8]. Sheldon, R. A. (2023). Atom Economy: A New Approach to Green Chemistry. Nature Sustainability, 6(1), 3-10.

[9]. Leiva, D., et al. (2023). Energy Efficiency in Chemical Manufacturing: Challenges and Opportunities. Journal of Cleaner Production, 394, 136487.

[10]. Ghosh, M., &Pathak, S. (2023). Green Chemistry in Pharmaceutical Industry: Innovations and Applications. Green Chemistry, 25(6), 1689-1705.

[11]. Anastas, P. T., & Zimmerman, J. B. (2023). The Role of Green Chemistry in Supporting a Circular Economy. Nature Sustainability, 6(2), 131-141.

[12]. Allen, D. T., & Armstrong, P. (2023). Green Chemistry in Education: A Review of Current Approaches and Future Directions. Journal of Chemical Education, 100(3), 933-944.

[13]. Patel, R., & Singh, A. (2023). Challenges and Future Directions in Green Chemistry. Green Chemistry, 25(9), 3201-3220.

International Journal of Scientific Research in Science and Technology
Available online at : www.ijsrst.com
OPEN ACCESS
Print ISSN: 2395-6011 | Online ISSN: 2395-602X
doi : https://doi.org/10.32628/IJSRST

Synthesis, Characterisation and Antimicrobial Studies of Transition Metal Complexes of Bidentate Ligand

V. A. Shelke[1], S. M. Jadhav[2], C. G. Devkate[1], S. G. Shankarwar[3]

[1]Department of Chemistry, Indraraj Arts, Science and Commerce College Sillod, Dist. Chh. Sambhajinagar–431112, Maharashtra, India

[2]Department of Chemistry, Siddharth Arts, Science and Commerce College Jafrabad Dist. Jalna -431206, Maharashtra, India

[3]Department of Chemistry, Dr. Babasaheb Ambedkar Marathwada University Aurangabad Dist-Chh. Sambhajinagar 431001, Maharashtra, India

ARTICLEINFO

Article History :

Published : 07 Dec 2024

Publication Issue :
Volume 11, Issue 23
Nov-Dec-2024
Page Number :
329-339

ABSTRACT

The solid complexes of Mn(II), Fe(III), Ni(II) and Cu(II) have been synthesized Schiff base derived from 2-hyhdroxybenzohydrazide and 2-Methyl benzaldehyde. And characterized by spectral and other physicochemical techniques such as 1H-NMR, UV-vis molar conductivity, magnetic susceptibility, thermal analysis, X-ray diffraction, FTIR, and mass spectroscopy. The analytical data of these metal complexes showed metal: ligand ratio (1:2). The physico–chemical study supports the presence of square planar geometry around Cu(II) and Ni(II) and octahedral geometry around Mn(II), and Fe(III). The IR spectral data reveal that the ligand behaves as bidentate with ON donor atom sequence towards central metal ion. The molar conductance values of metal complexes suggest their non electrolyte nature. The X-ray diffraction data suggest orthorombic crystal system for these complexes. Thermal behavior (TG/DTA) and kinetic parameters calculated by Coats-Redfern method are suggestive of more ordered activated state in complex formation. The ligand and their metal complexes were screened for antibacterial activity against Staphylococcus aureus, Escherichia coli and fungicidal activity against Aspergillus Niger and Trichoderma.

Keywords: Bidentate Schiff base, Metal complexes, Thermal analysis, XRD, Antimicrobial study.

Introduction

Many organic compounds, heterocyclic aromatic compounds in particular like benzimidazoles, benzothiazoles are reported to posses a variety of physiological activities such as fungicidal, insecticidal, antimicrobial and anesthetic properties. Schiff bases derived from aromatic amines and aromatic aldehydes have a wide variety of applications in many fields like biological, inorganic and analytical chemistry[1-2]. The development of the field of bioinorganic chemistry has increased the interest in Schiff base complexes since it has been recoganised that many of these complexes may serve as models for biologically important species [3-5].The study of ligands involving such hydrazones is interesting as they demonstrate versatility in coordination, a tendency to yield stereochemistry of higher coordination number[6] an ability to behave as neutral or deprotonated ligands and flexibility in assuming different conformations. Recently, several metal complexes of Schiff bases containing N, S and N, O donors have been synthesized and studied [7–9].

In the present article Mn(II), Fe(III), Ni(II), and Cu(II), complexes with Schiff base derived from 2-hyhdroxybenzohydrazide and 2-Methyl benzaldehyde. These have been characterized on the basis of physicochemical and spectral analysis. The antibacterial and antifungal activities of the ligand and its metal complexes were also tested. Unfortunately most schiff bases are chemically unstable and show a tendency to be involved in varius equalibrium, like tautomaric interconversion hydrolysis or formation of ionsised species [1, 2]

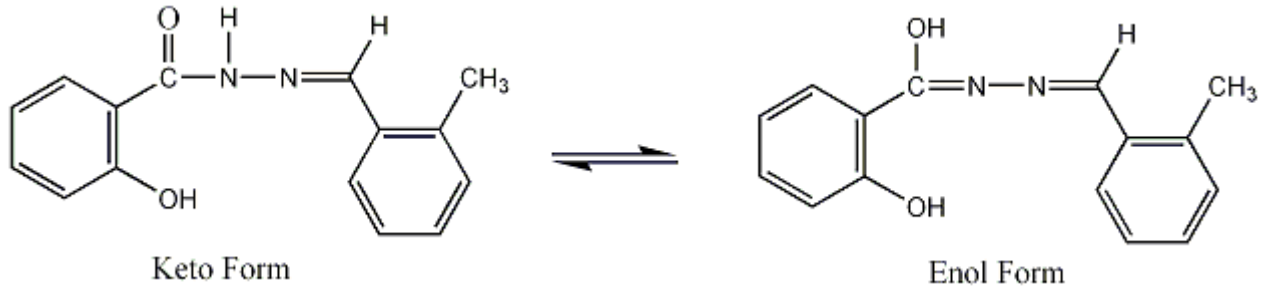

Figure 1. Keto and enol form of ligand.

EXPERIMENTAL

Materials

All chemicals used were of the analytical grade (AR) and of highest purity. Methyl 2-hydroxybezoate, hydrazine and benzaldehyde were purchased from E-Merk (AR grade) and were used for synthesis of ligand. AR grade metal chlorides of S. D. Fine chemicals were used for complex preparation. Spectral grade solvents were used for spectral measurements. The carbon, hydrogen and nitrogen contents were determined on Perkin Elmer (2400) CHNS analyzer. IR spectra for ligand and metal complexes were recorded on Jasco FT-IR-4100 spectrometer using KBr pellets in the range of 4000-400 cm^{-1}. ^{1}H-NMR spectra of the ligand was measured in $CDCl_3$ using TMS as an internal standard. The TG/DTA analysis was recorded on Perkin Elmer TA/SDT-2960 with heating rate 10°c/min. XRD was recorded on Philips 3701 employing CuK_α radiation (λ=1.541Å) in the range 20° to 90°. The UV-vis spectra of the complexes were recorded on Jasco UV-530 Spectrophotometer. Magnetic susceptibility measurements were carried out on Guoy balance at room temperature using $Hg[Co(SCN)_4]$ as a calibrant. Conductance was measured on Elico CM-180 conductometer using 1 mM solution in dimethyl sulphoxide.

Synthesis of Ligand

Step-I

50 mL ethanolic solution of 0.001 mol (0.168g.) of methyl salicylate was taken in round bottomed flask and to this 0.001 mol (0.108g.) of hydrazine in ethanol was added slowly under stirring. The resulting mixture was refluxed for about 4-5 h. It was naturally cooled to room temperature. After cooling, the solid residue was washed with hot ethanol and used for further study. (Yield 75%)

Step-II

Above synthesised intermediate 0.001 mol was refluxed with 0.001 mol of 2-methyl benzaldehyde in super dry ethanol for 5 h. The precipitate thus formed was filtered, dried in vacuum in presence of $CaCl_2$ and recrystallised in ethanol (yield: 79%).

Fig. 2

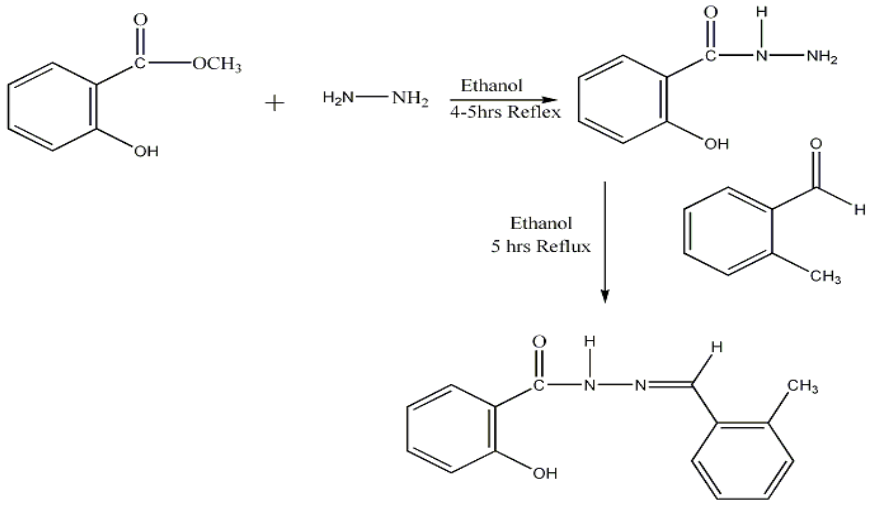

Figure 2.Synthesis of ligand.

Preparation of Complexes

To a hot solution of ligand (0.02 mol) in chloroform (25mL), methanolic solution of metal chloride (0.01 mol) was added under constant stirring. The pH of the reaction mixture was adjusted to 7.5-8.5 by adding 10 % ethanolic ammonia solution and refluxed for about 5 h. The precipitated solid metal complex was filtered and washed with hot methanol, followed by petroleum ether, ethyl acetate and dried over $CaCl_2$ in vacuum desiccator (yield 61%).

Fig.III. The proposed structure of the complexes

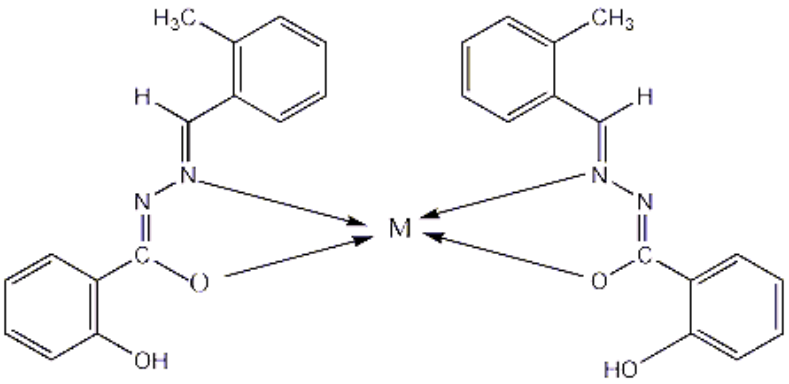

III-a

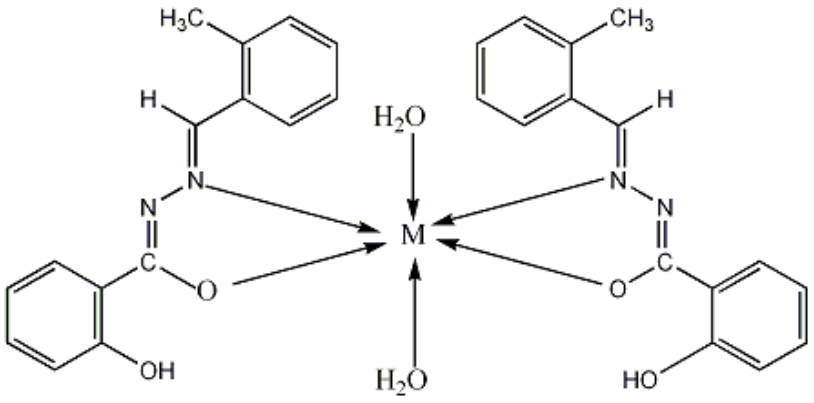

Fig.III b

Fig.III. The proposed structure of the complexes a. when M = Cu(II) and Fe(III) b. when M = Mn(II)and Ni(II)

Table I. Physical characterization, analytical and molar conductance data of compounds.

Compound	F.W.	M.P./ Decom. Temp °C	Colour	Molar conductance Mho $cm^2 mol^{-1}$	%C (calcd.)	%H (calcd.)	%N (calcd.)	%M (calcd.)
H_2L	266	258	White		70.10 (70.85)	5.45 (5.54)	11.25 (11.01)	
[MnL]	544.93	>300	Yellow	4.74	63.59 (63.94)	4.95 (5.00)	9.60 (9.94)	10.01 (9.74)
[FeL]	545.84	230	Black	5.2	63.95 (63.84)	4.58 (4.99)	9.72 (9.92)	9.59 (9.89)
[NiL]	548.69	270	Brown	4.86	63.22 (63.52)	4.88 (4.97)	9.42 (9.87)	10.30 (10.36)
[CuL]	553.54	280	Pale green	17.66	62.22 (62.98)	4.88 (4.93)	9.42 (9.79)	10.38 (10.34)

RESULT AND DISCUSSION

All the complexes are coloured solids, air stable and are having line solubility in polar solvents DMF and DMSO. The elemental analysis show 1:2 (metal: ligand) stoichiometry for all the complexes. Micro analytical data and molar conductance values are given in Table I. The metal contents in complexes were estimated by gravimetric analysis [10]. All the complexes show low conductance which indicates their non-electrolytic nature. The magnetic measurement studies suggest paramagnetic behavior of all these complexes

^{1}H-NMR spectra

^{1}H-NMR spectra of synthesiysed ligand was recorded in $CDCl_3$. It shows signals at 7.59 δ (s,1H, -C-N-H), 7.08 δ (dd, 2H, Ar-H), 7.22 δ (dd, 2H, Ar-H), 7.01-7.75 δ (dd, 4H, Ar-H), 7.85 δ (s, 1H, N=C-H), 2.50 δ (s, 3H, Ar-H) and 6.10 δ (s,1H, Ar-OH).

Mass spectra of the ligand

Mass spectra of the ligand H_2L has been recorded which show the molecular ion peak (M^+) at m/z = 255.28 corresponding to its molecular mass.

IR spectra

The FT-IR spectrum of the free ligand shows four characteristic bands at 3240-3210, 3260, 1651 and 1615 cm^{-1} assignable to (υ -N-H), free (-O-H) stretching phenolic moiety, amide carbonyl (-C=O) and azomethine (-C=N), stretching modes respectively. The absence of a weak broad band in 3270-3300 cm^{-1} region, noted in the spectra of the metal complexes indicates deprotonation of bonded (-NH) group during the complexation and subsequent coordination of the oxygen of amide carbonyl to metal ion enolization[11]. The υ(C=N) band is shifted to lower frequency with respect to free ligand, indicating that the nitrogen of the azomethine group is coordinated to the metal ion, which was further confirmed by observation of the red shift in the υ(N-N) stretching frequency from 923 cm^{-1} to 953 cm^{-1} regions[12-14]. New bands observed in the complexes at 1621 and 1624 cm^{-1} are attributed to the >C=N-N=C< group[13]. The spectra of metal chelates showed new bands in the 460-540 and 407-478 cm^{-1} regions which can be assigned to υ (M-O) and (M-N) vibrations respectively[15]. The spectra of Mn(II) and Fe(III). showed a strong band at 3020-3500 cm^{-1} region, suggesting the presence of coordinated water in these metal complexes[10]. The presence of coordinated water is further confirmed by the appearance of non-ligand band in 827-846 cm^{-1} region[16]. The presence of coordinated water is also established and supported by TG/DTA analysis of these complexes. Hence co-ordination takes place via oxygen of amide and nitrogen of azomethine group of ligand molecule [17].

Electronic absorption spectra and magnetic measurements

The electronic spectra of Mn(II) complex in DMSO show bands at 12225, 16009, 27823 cm^{-1} assignable to a $^4T_{1g} \rightarrow T_{2g}$, $^4T_{1g} \rightarrow A_{2g}$ transition and charge transfer respectively. The electronic spectral data coupled with observed magnetic moment 5.8 B.M. suggest octahedral geometry for Mn(II) complex [18,19]. Fe(III) complex exhibits three bands at 16501, 24280 and 27871 cm^{-1} assignable to $^6A_{1g} \rightarrow {}^4T_{1g}$, $^6A_{1g} \rightarrow {}^4T_{2g}$ (F) transitions and charge transfer respectively. These transitions and observed magnetic moment 5.7 B.M indicate square planer geometry of the complex[20]. Ni(II) complex exhibits three bands at 12280, 16118 and 27270 cm^{-1} assignable to $^4T_{1g} \rightarrow T_{2g}$, $^4T_{1g} \rightarrow {}^4A_{2g}$ transitions and charge transfer respectively. These transitions and observed magnetic moment 2.6 B.M indicate octahedral geometry of the complex[17,21]. The electronic spectra of Cu(II) complex .show bands at 12600, 17980, 23475 cm^{-1} assignable to a $^6A_{1g} \rightarrow {}^1T_{2g}$ transition and charge transfer respectively. The electronic spectral data coupled with observed magnetic moment 1.8 B.M. suggest square planar geometry for Cu(II) complex.[17].

Table I. Physical characterization, analytical and molar conductance data of compounds.

Compound	F.W.	M.P./ Decom. Temp °C	Colour	Molar conductance Mho $cm^2 mol^{-1}$	%C (calcd.)	%H (calcd.)	%N (calcd.)	%M (calcd.)
H_2L	266	258	White		70.10 (70.85)	5.45 (5.54)	11.25 (11.01)	

Compound	F.W.	M.P./ Decom. Temp °C	Colour	Molar conduc tance Mho $cm^2 mol^{-1}$	%C (calcd.)	%H (calcd.)	%N (calcd.)	%M (calcd.)
[MnL]	544.93	>300	Yellow	4.74	63.59 (63.94)	4.95 (5.00)	9.60 (9.94)	10.01 (9.74)
[FeL]	545.84	230	Black	5.2	63.95 (63.84)	4.58 (4.99)	9.72 (9.92)	9.59 (9.89)
[NiL]	548.69	270	Brown	4.86	63.22 (63.52)	4.88 (4.97)	9.42 (9.87)	10.30 (10.36)
[CuL]	553.54	280	Pale green	17.66	62.22 (62.98)	4.88 (4.93)	9.42 (9.79)	10.38 (10.34)

X-ray diffraction study

The X-ray diffractogram of a representative metal complex Mn(II) was scanned in the range 10-80° at wavelength 1.54 A° (Fig. 3). The diffractogram and associated data depict 2θ values for each peak, relative intensity and inter planar spacing (d-values). The diffractogram of Mn(II) complex showed fourteen reflections with maxima at 2θ (68.61°) corresponding to d value 1.35 Å. The X-ray diffraction pattern of the complex with respect to major peaks having relative intensity greater than 10 % have been indexed by using computer programme [22]. The above indexing method also yields Miller indices (hkl), unit cell parameters and volume. The unit cell of Mn(II) complex yielded values of lattice constants, a =7.55 Å, b =7.63 Å, c =8.11 Å and unit cell volume, V = 471.24 $(Å)^3$. In concurrence with these cell parameters of Mn(II) complex, the condition a≠ b≠c and α =β =γ = 90° required for the compound to be orthorhombic lattice type. The diffractogram of Fe(III) complex shows eight reflections with maxima at 2θ =61.81 corresponding to d value 1.50A. The observed values of lattice constants, a= 4.71A˚, b = 4.91A˚, c = 5.40A˚ and α =β = 90° γ =120°. Fe(III) complex satisfies the condition a≠ b≠c and α =β = 90° γ =120° required for the compound to be monoclinic lattice type. The diffractogram of Ni(II) complex shows eight reflections with maxima at 2θ =62.38 corresponding to d value 1.43A. The observed values of lattice constants, a= 9.70A˚, b = 9.70A˚, c = 6.63A˚ and α =β = γ =.90° Ni(II) complex satisfies the condition a=b≠c and α =β =γ = 90° required for the compound to be tetragonal lattice type. The diffractogram of Cu(II) complex shows thirteen reflections with maxima at 2θ =31.00 corresponding to d value 2.88A. The observed values of lattice constants, a= 7.23A˚, b=7.48A˚, c = 6.31A˚ and α =β = 90° γ= 120° Cu(II) complex satisfies the condition a≠ b≠c and α =β = 90° γ= 120 ° required for the compound to be monoclinic lattice type. The above values indicate that the metal complex has orthorhombic crystal system. Experimental density value of the complex was determined by using specific gravity method [23].

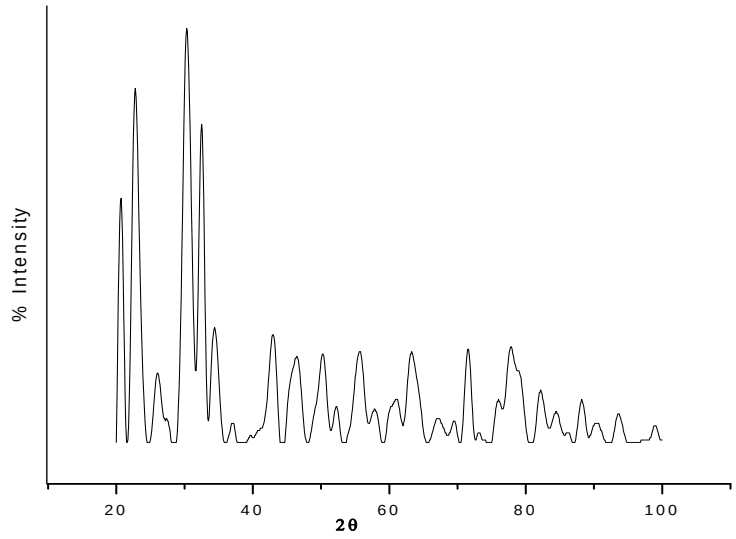

Fig. 3. X-ray diffractogram of Co(II) complex.

Thermal analysis.

The simultaneous TG/DT analysis of metal complexes was studied from ambient temperature to 1000 ºC in nitrogen atmosphere using α-Al_2O_3 as reference. The thermogram curve of Cu(II) metal complex shows mass loss 5.7 % (calcd.5.85 %) representative in the range 160-230ºC. An endothermic peak in this region ΔT_{max} = 120ºC indicating presence of two coordinated water molecules [10]. The TG curve of Cu(II) complex, then show slow decomposition from 270ºC to 480ºC with mass loss 52.10% (calcd.51.20%). An exothermic peak ΔT_{max} = 310ºC in DTA may be attributed to the decomposition of non coordinated part of ligand. The second slow step from 510 to 790ºC with mass loss of 21.20% (calcd.21.50%) corresponds to decomposition of coordinated part of ligand. A broad endotherm ΔT_{max} = 740ºC in DTA is observed for this. The mass of final residue 15.90 % (calcd.16.10 %) corresponds to stable CuO. All other metal complexes show similar behavior.

Kinetic calculations

The kinetic and thermodynamic parameters viz order of reaction (n), energy of activation (E_a), pre-exponential factor (z), entropy of activation (ΔS) and free energy change (ΔG) together with correlation coefficient (r) for non-isothermal decomposition of metal complexes have been determined by Horowitz-Metzer (HM) approximation method and Coats-Redfern integral method[24] [34]. The data is given in Table III. The results show that the value obtained by two methods is comparable. The calculated value of energy of activation of the Co(II) and Ni(II) complexes is relatively low indicating the autocatalytic effect of metal ion on thermal decomposition of the metal complex[25,26]. The negative value of entropy of activation indicates that the activated complex is more ordered than the reactant and that the reaction is slow. The more ordered nature may be due to the polarization of bonds in activated state which might happen through charge transfer electronic transition.

Table III. The kinetic parameter of metal complexes calculated by the methods Horowitz-Metzger (HM) and Coats-Redfern (CR).

Complex	Step	n	Method	E_a (kJmol$^{1)}$	Z S^{-1}	ΔS# $JK^{-1}mol^{-1}$	ΔG# (kJmol^{-1})	Corelation coefficient (r)
Ni(II)	I	1.3	HM	12.25	3.7×10^5	-175	50.23	0.9989
			CR	16.45	4.2×10^4	-195	47.25	0.9990
	II	1.1	HM	21.45	3.7×10^3	-161	61.47	0.9989
			CR	16.15	5.2×10^4	-198	52.40	0.9989
Cu(II)	I	1.3	HM	24.47	6.6×10^6	-214	41.35	0.9988
			CR	22.40	8.2×10^4	-242	38.11	0.9995
	II	1.1	HM	11.35	8.6×10^5	-236	40.41	0.9992
			CR	14.40	6.2×10^4	-283	39.33	0.9995

Antimicrobial activity

The antimicrobial activity of ligand and its metal complexes were tested in vitro against bacteria such as Staphylococcus aureus and Escherichia coli by paper disc plate method [27]. The compounds were tested at the concentration 500 and 1000 μg cm^{-3} in DMF and compared with known antibiotics viz ciproflaxin (Table IV). For fungicidal activity, compounds were screened in vitro against Aspergillus Niger and Trichoderma by mycelia dry weight method [28] with glucose nitrate media. The compounds were tested at the concentration 250and 500 μg cm^{-3} in DMF and compared with control (Table V). From Table 4 and 5, it is clear that the inhibition by metal chelates is higher than that of a ligand and metal salts. The results are in good agreement with previous findings with respect to comparative activity of free ligand and its complexes[17,20]. The metal chelates have higher antibacterial activity than the corresponding free ligand and control against the same microorganism under identical experimental conditions. Such enhanced activity of metal chelates is due to increased lipophilic nature of the metal ions in complexes[29]. The increase in activity with concentration is due to the effect of metal ions on the normal process.

The microbial results are presented in Tables IV and V. In case of antibacterial studies it was observed that, the ligand is moderately active towards Stapylococcus and less active towards E.Coli. Comparison of activities of the ligand and its metal chelates showed that the copper complex is approximately found to be more active than the ligand Cu(II) complex show higher activity than other metal complexes. The cobalt and manganese complexes show the activity comparable to copper complex. However Fe(III) and Ni(II) complexes show less activity against E.Coli and Stapylococcus. The activity of these complexes follow the order Cu>Co>Mn>Ni>Fe.

Investigation of antifungal activity of the ligand and its metal complexes revealed that all metal chelates are more fungi toxic than their parent ligand Table V. The antifungal activity of the ligand is found to enhance several times on being coordinated with metal ions. The activity of these complexes follow the order of Aspergillus Niger Cu> Ni >Mn>Fe and that of Trichoderma Cu > Ni > Mn >Fe.

As a result, metal complexes of Cu(II) and Mn(II) show good antibacterial and Cu > Ni show good antifungal activity, where as Fe(III) complexe shows comparatively less activity.

Table IV. Antibacterial activity of ligand and its metal complexes.

Test Compound	inhibition zone (mm)			
	E. Coli		**Staphylococus**	
	500ppm	1000ppm	500ppm	1000ppm
Ciproflaxin	29	32	31	35
$[C_{30}H_{28}N_4O_4]$ (H_2L)	12	15	13	17
$[C_{30}H_{28}N_4O_4Mn]$	17	20	16	19
$[C_{30}H_{28}N_4O_4Fe]$	12	16	13	17
$[C_{30}H_{28}N_4O_4Ni]$	14	16	12	18
$[C_{30}H_{28}N_4O_4Cu]$	17	24	16	20

Table V. Antifungal activity of compounds yield of mycelial dry weight in mg (% inhibition)

Test Compound	**A.niger**		**Trichoderma**	
	250ppm	500ppm	250ppm	500ppm
Control	79	79	70	70
$[C_{30}H_{28}N_4O_4]$ H_2L	61 (22)	27 (65)	40 (42)	20 (72)
$[C_{30}H_{28}N_4O_4Mn]$	53 (32)	15 (81)	32 (54)	08 (87)
$[C_{30}H_{28}N_4O_4Fe]$	50 (36)	20 (74)	32 (54)	07 (90)
$[C_{30}H_{28}N_4O_4Ni]$	45 (43)	14 (82)	21 (70)	05 (93)
$[C_{30}H_{28}N_4O_4Cu]$	41 (48)	12 (84)	23 (68)	05 (93)

CONCLUSIONS

In the light of above discussion we have proposed square-planar geometry for Cu(II) and Ni(II) complex and octahedral geometry for Mn(II) and Fe(III) complexes. On the basis of the physico-chemical and spectral data discussed above, one can assume that the ligand behave as monobasic, ON bidentate, coordinating via amide oxygen and azomethine nitrogen as illustrated in Fig.4. The complexes are biologically active and are having enhanced antimicrobial activities compared to free ligand. Thermal study reveals thermal stability of metal complexes. The XRD study suggests monoclinic crystal system for Cu (II) and Fe(III) complex, Mn(II) complex show orthorhombic crystal structure, and Ni(III) shows tetragonal crystal structure.

References

[1]. Naik, V.M.; Sambrani, M.I.; Mallur, M.B. 2008, Synthesis, Characterization and Biological Activities of Manganese(II) Complex: Molecular Modeling of DNA Interactions, Ind.J. of Chemistry, 47, 1793.

[2]. Narang, K.K.; Singh, V.P., 1997, Hydrazone as complexing agent: Synthesis, structural characterization and biological studies of some complexes, Synth. React. Inorg. Met.-Org. Chem., 27, 721.

[3]. Chowdhury, D.A.; Uddin, M.N.; Sarker, M.A.H. 2008, Metal Complexes of Schiff Bases Derived from 2-Thiophenecarboxaldehyde and Mono/Diamine as the Antibacterial Agents, Chiang Mai J. Sci., 35, 483.

[4]. Clear, M.J. Coord. 1974, Transition metal complexes in cancer chemotherapy, Chem. Rev.x, 12, 349.

[5]. M.T.H.Tarafder, M.A.Jalil MiahR.N.Bose, M.Akbar Ali 1981, Metal complexes of some schiff bases derived from s-benzyldithiocarbazate, J. Inorg. Nucl. Chem. Volume 43, Issue 12, , Pages 3151-3157.

[6]. Maurya, R.C.; Verma, R.; Singh, T. 2003, Synthesis, Magnetic, and Spectral Studies of Some Mono - and Binuclear Dioxomolybdenum(VI) Complexes with Chelating Hydrazones Derived from Acid Hydrazides and Furfural or Thiophene - 2 - aldehyde, Synth. React. Inorg. Met.-Org.Chem.,.33, 309

[7]. Ali, M.A.; Livingstone, S. E. 1974, Metal complexes of sulphur-nitrogen chelating agents, Coord. Chem. Rev., 13, 101.

[8]. Williams, D.R. 1972, Metals, ligands, and cancer, Chem. Rev., 72, 203.

[9]. Loncle, C.; Brunel, J.M.; Vidal, N.; Dherbomez, M.; Letourneux, Y. 2004, Synthesis and antifungal activity of cholesterol-hydrazone derivatives, Eur. J.Med.Chem., 39, 1067.

[10]. Ku¨ c¸u¨ kgu¨ zel S.G.; Mazi A.; Sahin F.; O¨ ztu¨ rk S.; Stables, J. 2003, Synthesis and biological activities of diflunisal hydrazide–hydrazones, Eur. J. Med. Chem., 38, 1005.

[11]. Todeschini, R.; de Miranda, A.L.P.; da Silva, K.C.M.; Parrini, S.C., Barreiro, E.J. 1998, Synthesis and evaluation of analgesic, antiinflammatory and antiplatelet properties of new 2-pyridylarylhydrazone derivatives, Eur. J. Med. Chem., ,33,189.

[12]. Melnyk, P.; Leroux, V.; Sergheraert, C.; Grellier, P.; Sergheraert, C. 2006, Design, synthesis and in vitro antimalarial activity of an acylhydrazone library, Bioorg. Med. Chem. Lett., 16, 31.

[13]. Lima, P.C.; Lima, L.M.; da Silva, K.C.M.; O. Le´da, P.H.; de Miranda, A.L.P.; Fraga, C.A.M.; Barreiro, E.J. 2000, Synthesis and analgesic activity of novel N-acylarylhydrazones and isosters, derived from natural safrole, Eur. J. Med. Chem., 35, 187.

[14]. V.A.ShelkeaS.M.JadhavaV.R.PatharkaraS.G.ShankarwaraA.S.MundebT.K.Chondhekar, 2012, Synthesis, spectroscopic characterization and thermal studies of some rare earth metal complexes of unsymmetrical tetradentate Schiff base ligand, Arabian Journal of Chemistry, Volume 5, Issue 4, October, Pages 501-507

[15]. Bedia, K.K.; U. Seda, O. Elc.; Fatma, K.; Nathaly, S.; Sevim, R.; Dimoglo, A. 2006, Synthesis and characterization of novel hydrazide–hydrazones and the study of their structure–antituberculosis activity, Eur. J. Med. Chem., 41, 1253.

[16]. Terzioglu, N.; Gu¨ rsoy, A. 2003, Synthesis and anticancer evaluation of some new hydrazone derivatives of 2,6-dimethylimidazo[2,1-b][1,3,4]thiadiazole-5-carbohydrazide, Eur. J. Med. Chem., 38, 781.

[17]. K. Ramana Kumar , A. Raghavendra Guru Prasad, V. Srilalitha, G. Narayana Swami and L.K. Ravindranath, 2012, Synthesis and Characterization of Iron Complexes of Resacetophenone Salicyloyl Hydrazone, Chem. Bull. "POLITEHNICA" Univ. Volume 57(71), 1.

[18]. Sreeja, P.B.; Sreekanth, A.; Nayar, C.R.; PrathapachandraKurup, M.R.; Usman, A.; Razak, I.A.; Chantrapromma, S.; Fun, H.K. 2003, Synthesis, spectral studies and structure of 2-hydroxyacetophenone nicotinic acid hydrazone, J. of Molecular Structure, .645, 221.

[19]. Salam, M.A.; Chowdhury, D. A. Bull. Pure & Appl. Sci. 2001, 20, 89.

[20]. Vogel, A.I.; 1975 , "A Text Book of Quantitative Inorganic Analysis," 3rd.ed., Longmans, London,. PP 540.

[21]. Baliger, R.S.; Revankar, V.K. 2006, Coordination diversity of new mononucleating hydrazone in 3d metal complexes: synthesis, characterization and structural studies, J.Serb.Chem.Soc., 71, 1301.

[22]. Hueso-Urena, F.; Illan-Cabeza, N.A.; Moreno-Carretero, M.N.; Penans Chamorro, A.L., 2000, Ni(Ii), Cu(Ii), Zn(Ii) And Cd(Ii) Complexes With Dinegative N,N,Otridentate Uracil-Derived Hydrazones, Acta Chem. Solv., 47, 481.

[23]. Narang, K.K.; Aggarwal, A. 1974, Salicylaldehyde salicylhydrazone complexes of some transition metal ions, Inorg. Chim. Acta , 9, 137.

[24]. Synthesis, characterization, antibacterial and antifungal studies of some transition and rare earth metal complexes of N-benzylidene-2-hydroxybenzohydrazide

[25]. Blout, E.R.; Fields, M.; Karplus, R. J. 1948, Absorption Spectra. VI. The Infrared Spectra of Certain Compounds Containing Conjugated Double Bonds, Am. Chem. Soc., 70, 194.
[26]. Natrajan, R.; Antonysamy, K.; Thangaraja, C. 2003, Redox and antimicrobial studies of transition metal(II) tetradentate Schiff base complexes, Transition Met. Chem. 28, 29-36.
[27]. Munde, A.S.; Jagdale, A.N.; Jadhav, S.M.; Chondhekar, T.K. 2009, Synthesis and characterization of some transition metal complexes of unsymmetrical tetradentate Schiff base ligand, J. of the Korean Chemical Society., 53, 415.
[28]. Natrajan, R.; Antonysamy, K.; Thangaraja, C. 2003, Redox and antimicrobial studies of transition metal(II) tetradentate Schiff base complexes, Transition Met. Chem. 28, 29.
[29]. Raman, N.; Pitchaikaniraja, Y.; Kulandaisamy, A. 2001, Synthesis and characterisation of Cu(II), Ni(II), Mn(II), Zn(II) and VO(II) Schiff base complexes derived fromo-phenylenediamine and acetoacetanilide, Proc. Indian Acad. Sci (Chem.Sci.), 113, 183.

International Journal of Scientific Research in Science and Technology
Available online at : www.ijsrst.com
Print ISSN: 2395-6011 | Online ISSN: 2395-602X
doi : https://doi.org/10.32628/IJSRST

Pyruvic Acid Catalysed One Pot-Multicomponent Synthesis, Characterization and Biological Activities of 3-Methyl-4-Arylmethylene-Isoxazole-5(4H)-Ones.

Vishal Naiknaware[1], Hansaraj Joshi[1], Prashant Dixit[2], Ramesh Ware[3], Mazhar Farooqui[4], Syed Abed[5]

[1]Department of Chemistry, Swa Sawarkar College, Beed, Maharashtra, India
[2]Dr. B.A.M. University Sub Center, Dharashiv, Maharashtra, India
[3]Milliya College, Beed, Maharashtra, India
[4]Moulana Azad College, Aurangabad, Maharashtra, India
[5]Govt.college of Arts & Science, Aurangabad, Maharashtra, India

ARTICLEINFO

Article History :

Published : 07 Dec 2024

Publication Issue :
Volume 11, Issue 23
Nov-Dec-2024
Page Number :
340-346

ABSTRACT

A swift, environmental-friendly and efficient protocol for the synthesis of 3-Methyl-4-Arylmethylene-isoxazole-5(4H)-one derivatives through multicomponent reaction of substituted aldehydes, ethyl acetoacetate and hydroxylamine are synthesised by pyruvic acid catalyst easily available and less harmful. The noticeable features of this protocol are simple handling, environmental-benign catalyst, avoid of harmful effect on environment, short reaction time, energy conserving, no toxic by-products and excellent yields (78–93%).

Keywords: Isoxazole, One-pot synthesis, Multicomponent reaction, pyruvic acid Catalyst, Biological activities.

Introduction

Multicomponent reactions (MCRs) have developed progressively prevalent through the last two decades. MCRs are three or more reactants pooled in a one-pot process to afford a single molecule without any intermediate isolation [1–6]. MCRs have progressed from unsystematic academic quirks to plan methods in medicinal, combinatorial, pharmaceutical and agro chemistry [1]. Further, MCRs offer a potent tool to one-pot synthesis of various and complex molecules besides minor and drug-like heterocyclic compounds. They are environmentally and economically valuable because multi-step preparations produce huge amounts of waste mostly due to complex isolation processes normally containing expensive and harmful solvents after to each step [6-9].

This non-classical heating approach has ripened from a research laboratory interest to proven method that is greatly applied in both academic and industrial fields [10]. One of the several benefits of consuming quick

'microwave flash heating' for green synthesis is the theatrical decrease in reaction times (hours to seconds) [11]. Further, it was also exhibited that the reaction rate was enhanced by several times under microwave irradiation condition compared with traditional reaction conditions [12]. The influence of a MWI field on dielectric constituents is to prompt fast rotation of the polarized dipoles in the reactants. It creates more heat owing to rubbing, concurrently growing the possibility of interaction between the reactants, therefore improving the decreasing the activation energy and reaction rate [12-14]. MWI offers several benefits such as mild reaction conditions, rapid reaction optimization, minimized chemical wastes, excellent yield and solvent consumption. Although there are many methods were reported for the synthesis or modification of the isoxazole ring [15-20]. In the literature, it was found that α,β-unsaturated isoxazol-5(4H)-one derivatives have been prepared via one-pot three component condensation reaction of β-oxoesters, hydroxylamine hydrochloride and substituted aldehydes by use of catalytic amounts of sodium benzoate, sodium sulphide, sodium silicate, tartaric acid, pyridine, sodium ascorbate, sodium tetraborate and boric acid[21].

Isoxazole and its derivatives are a significant class of heterocyclic chemistry, which are major in nature and also exhibit interesting pharmaceutical, medicinal and agrochemical properties [22,23]. They are considered a key framework compound in the drug discovery and combinatorial synthesis [18]. Further, these isoxazole derivatives display several biological activities like antimicrobial, antioxidant, antibacterial, antiviral, anti-inflammatory, anti-tubercular, antifungal, antiprotozoal, and antagonist activities etc. [22-26]. But these methods have some limitations such as harsh reaction conditions, expensive procedure, tedious work-up process, less product yield, less atom economy and completion of reaction time was also more. Based on these fundings and our on-going efforts towards synthesis of isoxazole derivatives, in this paper we reported one-pot three components clean and facile synthesis of isoxazole derivatives in presence of pyruvic acid as a catalyst. Moderate to excellent product yield, less reaction time, reduce use of strong acids and bases, high atom economy are some merits of present methodology.

Experimental

All chemicals were used for AR grade purchased from reputed chemical Company such as spectrochem and solvents commercially available were purchased from local provider and used as without further purification. The melting point apparatus, Stuart model SMP3, was used for measuring melting points. FT-IR spectra were recorded on a PerkinElmer series II spectrum. 1HNMR spectra were recorded in DMSO-d6 using Bruker Avance Neo 500 MHz NMR Spectrometer and proton chemical shifts were recorded in δ relative to TMS as an internal standard using DMSO as solvent and the LC-MS spectra of synthesised compounds have been carried out with Water Micro mass Q-Tof Micro instrument.

General Procedure for the synthesis of 3-Methyl-4-arylmetheylene-isoxazol-5(4H)-ones.

Ethyl acetoacetate (20 mmol), hydroxylamine hydrochloride (20 mmol) and pyruvic acid solution (20% mmol) in ethanol: water (10 ml) Mixed in Round bottom flask and they were stirred for 05 min, after then substituted aromatic aldehyde (20 mmol) was added in the same slowly with shaking and the mixture was further stirred on magnetic stirrer till the completion of the reaction (monitored by TLC). The prepared compound was filtered off and washed with cold 5% aqueous ethanol (2 × 30 ml), and recrystallized from ethanol (95%) to afford the pure product. The Products were obtained likes 3-Methyl-4-arylmethylene-isoxazol-5(4H)-ones. These synthesized compounds were identified by spectral studies.

Characterization of 3-Methyl-4-arylmetheylene-isoxazol-5(4H)-ones.

1) 4-(4-Methoxybenzylidene)-3-methylisoxazol-5(4H)-one (4a)

M.p. 173–174°C; Yield: 88%; ^{1}HNMR (DMSO-d_6, 400MHz) (ppm) d: 8.49 (d, J=8.3Hz, 2H), 7.83(s,1H),7.12(d, J=8.3Hz,2H),3.86(s,3H),2.23(s,3H); MS(LCMS)m/z: observed. 217.

2) 4-(2-Hydroxybenzylidene)-3-methylisoxazol-5(4H)-one (4b)

M.p. 199–201C; Yield: 89%; ^{1}H NMR (DMSO-d_6, 400MHz) (ppm) d: 10.96 (s, 1H), 8.70 (d, J =8.0Hz, 1H), 8.05 (s, 1H), 7.47–7.41 (m, 1H), 6.98–6.88 (m, 2H), 2.22(s, 3H); MS (LCMS) m/ z: observed. 203.

3) 4-(4-Chlorobenzylidene)-3-methylisoxazol-5(4H)-one (4c)

M.p. 118–120°C; Yield: 89%; ^{1}H NMR (DMSO-d_6, 400MHz) (ppm) d: 8.44 (d, J=10.4Hz, 4H), 7.77 (s, 1H), 6.94 (d, J=11.0Hz, 2H), 2.22 (s, 3H); MS (LCMS) m/z: observed. 221.

4) 4-(2-Naphthylmethylidene)-3-methylisoxazol-5(4H)-one (4d)

M.p. 169–171°C; Yield: 90%; ^{1}H NMR (DMSO-d_6, 400MHz) (ppm) d: 8.63 (d, J=8.9Hz, 1H), 8.42 (d, J=7.1Hz, 1H), 8.28 (d, J=8.0Hz, 1H), 8.17 (d, J=7.5Hz, 1H), 8.03 (d, J=7.6Hz, 1H),7.67 (m, 3H), 2.40 (s, 3H); MS (LCMS) m/z: observed. 237.

Bioassay

Protocol for antibacterial activity

The antibacterial activity of the compounds was performed by enumerating feasible number of cells upon in the nutrient broth containing various concentrations of compounds. The feasible number is represented by colony control method. The test organisms on which the antibacterial activity was performed were *Pseudomous aeruginosa*, *Bacillus subtilis, Salmonella typhi, Escherichia coli* and *Staphylococcus areas*. In this method, the cells of test organisms were grown in nutrient broth till mid log phase and used as an inoculum for performing antimicrobial test. An approximately, 1*106 cells/ml test organisms were each incubated with 0 to 500 ug/ml concentrations of different compounds, separately, and each incubated for 13 to 15 at 37 °C. During this incubation cells tend to grow and multiply in number. However, if the compounds interfere with growth of the cells, the number of cells of decrease. After, 13 to 15 hrs. available number of cells were recorded by spreading an aliquot, from the broth, inoculated with test organisms and compounds as colony forming units per millilitre.

Protocol for antifungal activity

The Antifungal activity was evaluated against different functional strains such as *Aspergillus niger* and *Saccharomyces cerevisiae*. The medium yeast nitrogen base was dissolved in phosphate buffer pH 7 and it was autoclaved in 110 °C for 10 min. The suitable concentration of standard was incorporated in medium. With each set of growth control of without the antifungal agents and solvent control DMSO were included. The fungal strains were freshly sub cultured on to Sabouraud dextrose agar (SDA) and incubated at 25°C for 72 hrs. The fugal cells were deferred in sterile distilled water and dilute to get 105 cells/ml. 10 microlitre of uniform suspension was inoculated on to the control plates and the media were combined with the antifungal agents. The inoculated plates were incubated at 25°C for 48 hrs. The readings were taken at the end of 48 hrs and 72 hrs. Minimum inhibitory concentration (MIC) values were determined using standard agar method as per CLSI guidelines.

Results and Discussion

One-pot-multicomponent reaction, 4-substitued benzylidine3-Methyl-isoxazol-5(4H)ones compounds synthesized from ethyl acetoacetate (20mmol), Hydroxylamine hydrochloride (20mmol) and sub. Aromatic aldehydes (20mmol) added in R B flask in presence of pyruvic acid as a catalyst(20%) with 5 ml ethanol

solvent stirring in room temperature. These synthesised isoxazole-5(4H)ones were agree with their spectral analysed data as per reaction in Figer 1.

Figure 1. synthesis of substituted 3-Methyl-4-arylmethylene-isoxazol-5(4H)-ones by pyruvic acid as a catalyst in alcoholic medium

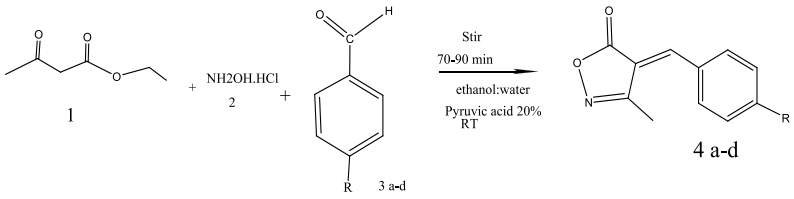

Spectral Characterization

IR Spectra

In the Spectroscopic technique IR spectra of Isoxazole compounds the band at 1668 cm-1 shows presence of conjugated carbonyl group and its frequency were disappeared in the compounds. The 1548 cm-1 region is assigned C=N band, this band of isoxazole undergoes lower frequencies. IR spectra 1162 cm-1 show C-N band and 838 cm-1 for N-O bonding spectra. They also show 764 cm-1 for C-Cl band and 1085 shows for C-O band with the literature data. **^{1}HNMR Spectra**

In the ^{1}HNMR Spectra of the synthesized compounds appears δ 2.12 s, with 3H indicates presence of methyl group bonding with conjugated or aromatic compounds. δ 3.02 s, 1H bonded on C=C group & δ 6.85-8.19 s or m indicates presence of Ar-H means presence of phenyl ring in this structure as per the literature.

LC-MS Spectra

In the present investigation, the mass spectrum of 4-Arylidine-3-Methyl-5(4H)ones shows molecular ion peaks at m/z=[188] corresponding to [$C_{11}H_{10}NO_3$] ion. The spectrum also exhibits peaks for the mass spectra of 4 position sub. Synthesised isoxazole-5(4H)one compounds exhibits molecular ion peaks at m/z [217M+], [203M+], [221] and [237M+] ion respectively that are equivalent to their molecular weight studied with the literature.

Biological activity

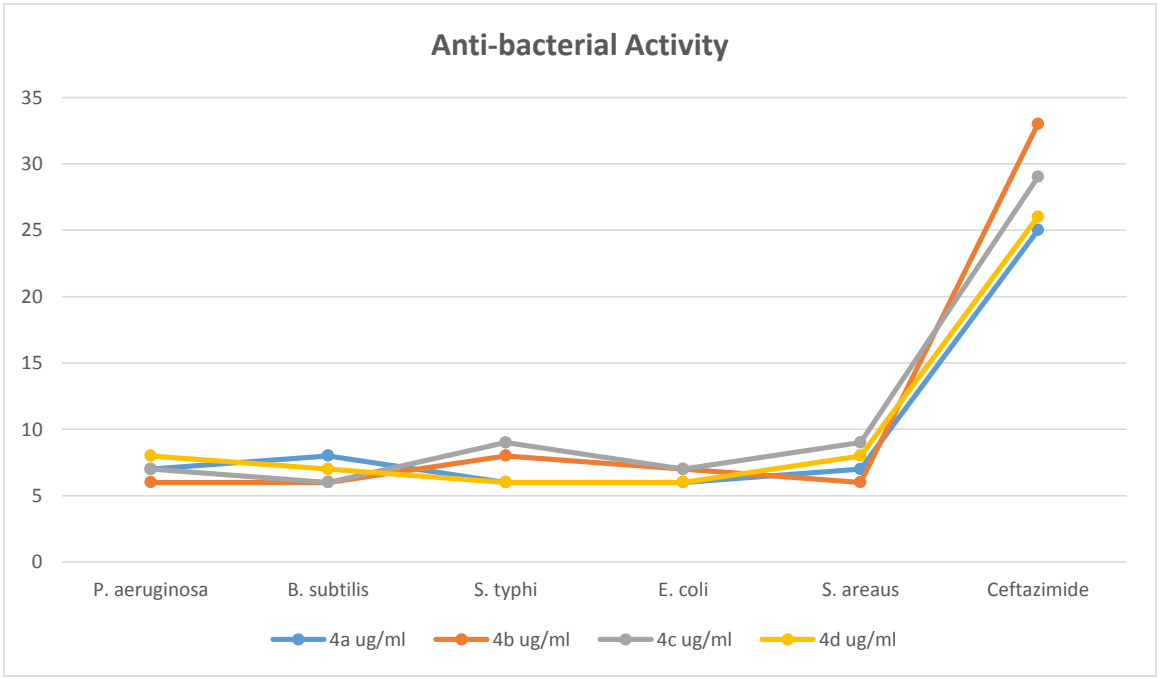

The graphically representation of antibacterial activity

The 4-(4-Methoxybenzylidene)-3-methylisoxazol-5(4H)-one exhibits Minimum inhibitory concentration (MIC) against various bacteria were compare with the MIC values of standard drug Ceftazimide. The MIC values of the synthesised 4-(4-Methoxybenzylidene)-3-methylisoxazol-5(4H)-one (4a) was observed to be 07 ug/ml, 08 ug/ml, 06 ug/ml, 06 ug/ml and 07 ug/ml against *Pseudomonas aeruginosa*, *Bacillus subtilis*, *Salmonella typhi*, *Escherichia coli* & *Staphylococcus aureus* respectively the values exhibit similar activities as compared with standard drug Ceftazimide, they show moderate activity. The MIC values of 4-(2-Hydroxybenzylidene)-3-methylisoxazol-5(4H)-one [4b] exhibits 06 ug/ml, 06 ug/ml, 08ug/ml, 07 ug/ml & 06 ug/ml against *Pseudomonas aeruginosa*, *Bacillus subtilis*, *Salmonella typhi*, *Escherichia coli* & *Staphylococcus aureus* respectively the values exhibit good activities as equated with the standard drug Ceftazimide. The MIC values of 4-(4-Chlorobenzylidene)-3-methylisoxazol-5(4H)-one [4c] exhibits 07 ug/ml, 06 ug/ml, 09 ug/ml, 07 ug/ml and 09 ug/ml against *Pseudomonas aeruginosa*, *Bacillus subtilis*, *Salmonella typhi*, *Escherichia coli* & *Staphylococcus aureus* respectively the MIC value compared with standard drug Ceftazimide moderate activities. The MIC values of synthesised compound 4-(2-Naphthylmethylidene)-3-methylisoxazol-5(4H)-one [4d] exhibits 08 ug/ml, 07 ug/ml, 06 ug/ml, 06 ug/ml and 8 ug/ml against *Pseudomonas aeruginosa*, *Bacillus subtilis*, *Salmonella typhi*, *Escherichia coli* & *Staphylococcus aureus* respectively the MIC value compared with standard drugs to show moderate activity.

Anti-Fungal activity

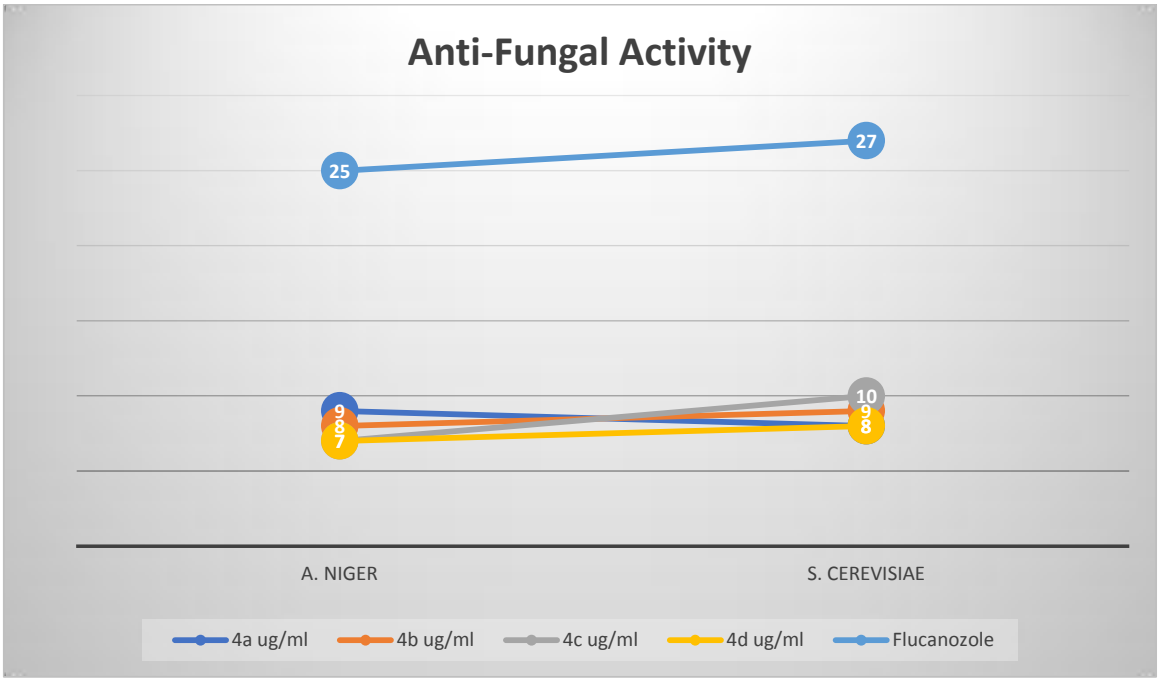

The graphically representative of antifungal activity. In the antifungal activity, the MIC values of the 3-Methyl-4-(arylidene Isoxazol)-5(4H)ones compounds of 4a, 4b, 4c and 4d synthesised compounds exhibits moderate activity as compared to standard drug. The results observed by the analysis for *Aspergillus niger* 9ug/ml, 8 ug/ml, 7ug/ml and 7ug/ml and for *Saccharomyces cerevisiae* shows 8 ug/ml, 9ug/ml, 10 ug/ml and 8 ug/ml equated with standard drug Flucanozole against shows MIC value of 25 ug/ml and 27 ug/ml, they indicate better activities.

Conclusion

Multicomponent-One-Potsynthesised 3-methyl-4(4-sub.Arylidene-Isoxazol-)-5(4H)-ones by using new catalyst Pyruvic acid and characterised through various spectral analysis, from this spectroscopic data, structure of the prepared multicomponent 3-Methyl-4(sub. arylmethylene-Isoxazol)-5(4H) ones compounds have been confirmed. These compounds were characterised by various biological activities such as antibacterial and antifungal activities. The *P. aeruginosa, B. subtilus, S. typhi, E. coli* and *S. aureus* for performing antibacterial activity, the result indicated that the activity exhibited above isoxazole compounds comparable to Ceftazimide standard drugs. Concurrently, the fungal strains such as *A. niger* and *S. cerevisiae* for carrying the antifungal activity as compared to Fluconazole standard drugs and all the compound also exhibited moderate activity compared to standard drugs.

References

[1]. N. Kerru, L. Gummidi, S. Maddila, S.B. Jonnalagadda, Curr. Org. Chem. 25 (2021) 1.

[2]. N. Kerru, L. Gummidi, S.N. Maddila, S.V.H.S. Bhaskaruni, S. Maddila, S.B. Jonnalagadda, RSC Adv. 10 (2020) 19803.

[3]. N. Kerru, L. Gummidi, S. Maddila, K.K. Gangu, S.B. Jonnalagadda, ChemistrySelect 5 (2020) 4104.

[4]. S. Harikrishna, A.R. Robert, H. Ganja, S. Maddila, S.B. Jonnalagadda, Sustain. Chem. Pharm. 16 (2020) 100265.

[5]. N. Kerru, L. Gummidi, S. Maddila, S.B. Jonnalagadda, Sustain. Chem. Pharm. 18 (2020) 100316.

[6]. K.K. Gangu, V. Pothala, T.V.S.P.V.S. Guru, S. Maddila, S.B. Jonnalagadda, Inorg. Chem. Commun. 119 (2020) 108084.

[7]. S.V.H.S. Bhaskaruni, S. Maddila, K.K. Gangu, S.B. Jonnalagadda, Arab. J. Chem. 13 (2020) 1142.

[8]. H. Ganja, A.R. Robert, P. Lavanya, S. Chinnam, S. Maddila, S.B. Jonnalagadda, Inorg. Chem. Commun. 114 (2020) 107807.

[9]. L.S. Venigalla, S. Maddila, S.B. Jonnalagadda, J. Iran. Chem. Soc. 17 (2020) 1539.

[10]. M.R. Khumalo, S.N. Maddila, S. Maddila, S.B. Jonnalagadda, ChemistrySelect. 4 (2019) 12503.

[11]. S. Maddila, K. Nagaraju, S. Chinnam, S.B. Jonnalagadda, ChemistrySelect 4 (2019) 9451. [12] M.R. Khumalo, S.N. Maddila, S. Maddila, S.B. Jonnalagadda, BMC Chem. 13 (2019) 132. [13] M.R. Khumalo, S.N. Maddila, S. Maddila, S.B. Jonnalagadda, RSC Advan. 9 (2019) 30768. [14] S. Moloi, S. Maddila, S.B. Jonnalagadda, Res. Chem. Intermed. 43 (2017) 6233.

[12]. Zhu J, Mo J, Lin HZ, Chen Y, Sun HP. The recent progress of isoxazole in medicinal chemistry. Bioorganic and Medicinal Chemistry 2018; 26 (12): 3065–3075. doi: 10.1016/j.bmc.2018.05.013.

[13]. Sysak A, Obminska-Mrukowicz B. Isoxazole ring as a useful scaffold in a search for new therapeutic agents. European Journal of Medicinal Chemistry 2017;137:292-309. doi: 10.1016/j.ejmech.2017.06.002.

[14]. Beam CF, Dyer MCD, Schwarz RA, Hauser CR. A new synthesis of isoxazoles from 1,4-dianions of oximes having an alpha hydrogen - mass spectrometry. Journal of Organic Chemistry 1970; 35 (6): 1806-1810. doi: 10.1021/jo00831a020.

[15]. Parul S, Ruchi B, Renu S. Various synthetic pathways for the synthesis of 3,4-disubstituted isoxazole by one pot multicomponent reaction. Orbital: The Electronic Journal of Chemistry 2020; 12 (4): 267-275. doi: 10.17807/orbital.v12i4.1549.

[16]. Rizvana KK, Hareeshbabu E. Synthesis and antimicrobial screening of modified isoxazoles: a short review. International Journal of Pharmacy and Pharmaceutical Research 2019; 15 (3): 136-148.

[17]. Chikkula KV, Raja S. Isoxazole -a potent pharmacophore. International Journal of Pharmacy and Pharmaceutical Sciences 2017; 9 (7): 13-24. doi: 10.22159/ijpps.2017.v9i7.1-9097.
[18]. Vekariya, R. H., Patel, K. D. & Patel, H. D. Fruit juice of Citrus limon as a biodegradable and reusable catalyst for facile, eco-friendly and green synthesis of 3, 4-disubstituted isoxazol-5 (4 H)-ones and dihydropyrano [2, 3-c]-pyrazole derivatives. Res. Chem. Intermed. 42, 7559–7579 (2016).
[19]. A.A. Abu-Hashem, M. El-Shazly, Med. Chem. 14 (2018) 356.
[20]. K.M. Naidu, S. Srinivasarao, N. Agnieszka, A.K. Ewa, M.M. Kumar, K.V. Chandra Sekhar, Bioorg. Med. Chem. Lett. 26 (2016) 2245.
[21]. D.A. Patrick, S.A. Bakunov, S.M. Bakunova, T. Wenzler, R. Brun, R.R. Tidwell, Bioorg. Med. Chem. 22 (2014) 559.
[22]. G.H. Cho, T. Kim, W.S. Son, S.H. Seo, S.J. Min, Y.S. Cho, G. Keum, K.S. Jeong, H.Y. Koh, J. Lee, A.N. Pae, Bioorg. Med. Chem. Lett. 25 (2015) 1324.
[23]. N. Agrawal, P. Mishra, Comput. Biol. Chem. 79 (2019) 63.

International Journal of Scientific Research in Science and Technology
Available online at : www.ijsrst.com
OPEN ACCESS
Print ISSN: 2395-6011 | Online ISSN: 2395-602X
doi : https://doi.org/10.32628/IJSRST

Complexation of Cobalt with Medicinal Drugs in Ethanol-Water Media

Ramesh Ware[1], Vishal Naiknaware[2], Shailendrasingh Thakur[1], Hansaraj Joshi[2]*

[1]Department of Chemistry, Milliya Art's, Science & Management Science College, Beed, Maharashtra, India

[2]Department of Chemistry, Swa Sawarkar College, Beed, Maharashtra, India

ARTICLEINFO

Article History :

Published : 07 Dec 2024

Publication Issue :
Volume 11, Issue 23
Nov-Dec-2024
Page Number :
347-352

ABSTRACT

Stability constant of medicinal drugs Diphenhydramine, Lisinopril, Labetalol, Benazepril, Topiramate, Efavirenz and Ibuprofen with Co(II) metal ion were investigate using pH metric titration technique in 20%(v/v) ethanol-water mixture at 300 K temperature and at an ionic strength of 0.1M NaClO4. {metal to ligand ratio = 1:5 and 1:1} The method of Calvin and Bjerrum as adopted by Irving and Rossotti has been employed to determine proton- ligand pKa and metal-ligand stability constant logK values. It is observed that cobalt metal ion forms 1:1 and 1:2 complexes.

Keywords: Stability Constant, Cobalt metal, medicinal drugs, pH metry

Introduction

The metal complexes like cisplatin and auranofin are used as drugs on the treatment of genitourinary, head and neck tumours and rheumatoid arthritis respectively. Jannik Bjerrum developed the general method for determination and calculation of stability constants of metal amine complexes. Further studies were carried by Neil Bjerrum on kinetics and equilibrium study to explain stepwise formation constants. Martell et.al carried work on stability constant of metal complexes of inorganic, organic, biological ligands and significantly contributed towards coordination chemistry.

Most of the d-block elements form complexes. For the present investigation, we selected medicinal drugs as Diphenhydramine (L_1), Lisinopril (L_2), Labetalol (L_3), Benazepril (L_4), Topiramate (L_5), Efavirenz (L_6) and Ibuprofen(L_7)

In continuation of our earlier work with complexation of medicinal drugs[01-18] and after literature survey we have carried out a solution study on the complexation of seven medicinal drugs with transition metal ion Co^{2+} pH metrically in 20% (v/v) ethanol-water mixture at constant ionic strength of 0.1M $NaClO_4$.

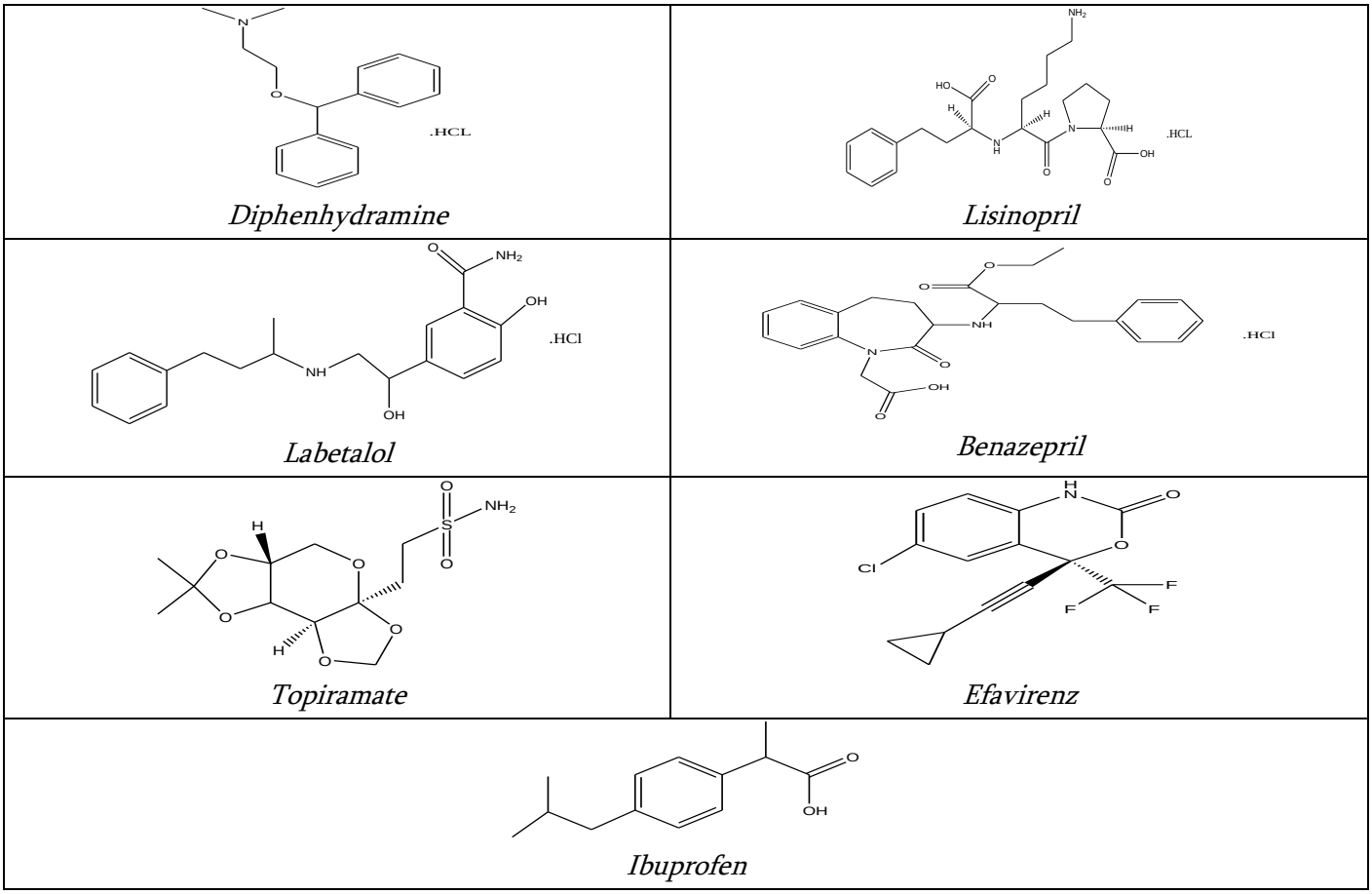

Figure 1. The structure of drugs

Methods And Material

NaOH, $NaClO_4$, $HClO_4$, Cobalt metal salt were of AR grade. All medicinal drugs are soluble in 20% (v/v) ethanol-water mixture. The solutions used in the pH metric titration were prepared in double distilled water. NaOH solution was standardized against oxalic acid solution and standard alkali solution was again used for standardization of $HClO_4$. The measurements were made at temperature 300K in 20% (v/v) ethanol-water mixture at ionic strength 0.1M $NaClO_4$. Water thermostat is used to maintain the temperature constant. pH measurement was made using Elico L_1-120 pH meter in conjunction with glass and reference calomel electrode. The instrument was calibrated at pH 7.00 and 4.00 using standard buffer solutions.

For evaluating the protonation constant of the ligand and the formation constant of the complexes in 20 %(v/v) ethanol-water mixture with Cobalt metal ion we prepare the following sets of solutions.

(A) $HClO_4$ (A)

(B) $HClO_4$+ medicinal drug (A+ L)

(C) $HClO_4$+ medicinal drug + Cobalt metal (A+ L+ M)

Above mentioned sets prepared by keeping M : L ratio, concentration of perchloric acid and sodium perchlorate were kept constant for all sets. The volume of every mixture was made up to 50ml with double distilled water and the reaction solution were pH meterically titrated against the standard alkali at temperature 300K.

Table 1: Proton-ligand stability constant of medicinal drugs in 20% (v/v) ethanol-water medium

Sr. No.	Ligands (Drug)	Proton-ligand stability constant	
		pK_1	pK_2

1	Diphenhydramine Hydrochloride (L_1)	…….	9.3814
2	Lisinopril Hydrochloride (L_2)	3.3231	7.5482
3	Labetalol Hydrochloride (L_3)	---	7.7424
4	Benazepril Hydrochloride (L_4)	---	3.6486
5	Topiramate (L_5)	---	8.9864
6	Efavirenz (L_6)	---	10.7206
7	Ibuprofen (L_7)	---	5.2366

TABLE 2: Metal-ligand stability constant of medicinal drugs in 20% (v/v) ethanol-water medium {Metal to ligand ratio =1:5}

Sr. No.	Ligands (Drug)	Metal-ligand stability constant		
		$\log K_1$	$\log K_2$	$\log\beta$
1	Diphenhydramine Hydrochloride(L_1)	3.8609	3.5360	7.3969
2	Lisinopril Hydrochloride(L_2)	4.4357	3.1107	7.5464
3	Labetalol Hydrochloride(L_3)	2.8805	2.7794	5.6599
4	Benazepril Hydrochloride(L_4)	2.9307	2.8569	5.7876
5	Topiramate (L_5)	3.0797	3.0439	6.1236
6	Efavirenz (L_6)	4.9052	4.4247	9.3299
7	Ibuprofen (L_7)	3.3615	3.0264	6.3879

TABLE 3: Metal -ligand stability constant of medicinal drugs in 20% (v/v) ethanol-water medium {Metal to ligand ratio =1:1}

Sr. No.	Ligands (Drug)	Metal-ligand stability constant		
		$\log K_1$	$\log K_2$	$\log\beta$
1	Diphenhydramine Hydrochloride (L_1)	--	--	--
2	Lisinopril Hydrochloride (L_2)	3.8393	--	3.8393
3	Labetalol Hydrochloride (L_3)	3.8464	--	3.8464
4	Benazepril Hydrochloride (L_4)	3.8413	--	3.8413
5	Topiramate (L_5)	3.6810	--	3.6810
6	Efavirenz (L_6)	5.9379	--	5.9379
7	Ibuprofen (L_7)	4.0322	--	4.0322

Result And Discussion

The proton ligand stability constants of all seven drugs were determined in 20% (v/v) ethanol-water medium at 300K temperature and at 0.1M ionic strength ($NaClO_4$). The proton-ligand stability constants of all the drugs are presented in Table 1.The drug L_2 have two pK values where as L_1, L_3, L_4, L_5, L_6 and L_7 has only one pK value. The $\bar{n}_A$ value ranges between 0.2 to 1.8 indicates the presence of two pK values whereas the range of $\bar{n}_A$ is in

between 0.2 to 0.8 shows one pK value. In the present investigation drugs selected contains amino group(s), carboxyl or hydroxyl groups as bonding sites.

The order of pKa values of seven drugs is as follows.

$L_2 > L_6 > L_1 > L_5 > L_3 > L_7 > L_4$

The above order indicates that L_2 (Lisinopril) has highest basicity whereas L_4 (Benazepril) has lowest basicity. The present drugs are diverse in nature hence it is difficult to correlate pKa values of one drug with other.

The experimentally calculated values of $logK_1$, $logK_2$ and $log\beta$ of the complexes of drugs with Co(II) metal ion are presented in **Table 2**. An examination of titration curve indicates that complex formation takes place in solution on following grounds. The metal titration curve of solution shows displacement with respect to ligand titration curve of solution along volume axis. This indicates affinity of ligand to metal ions which release proton and produce volume difference. In another words on addition of metal ion to free ligand solution shifted the buffer region of ligand to lower pH value. A large decrease in pH for metal titration curves relative to ligand titration curve might be attributed to strong metal-ligand interactions. In all the systems studied, the deviation of metal titration curve from ligand titration curve lies in the region where hydrolysis is not expected and so chelation has taken place. The hydrolysis of metal ion was suppressed due to the complex formation and precipitate did not appear during titration. The metal solution in the present study used is (0.0004M), therefore polynuclear complexes are not expected. The metal Cobalt is used in perchlorate form. Order of stability constant (log β) for Co(II) complexes with medicinal drugs found to be as follows:

$L_6 > L_2 > L_1 > L_7 > L_5 > L_4 > L_3$ {Metal to ligand ratio =1:5}

And **$L_6 > L_7 > L_3 > L_2 > L_4 > L_5 > L_1$** {Metal to ligand ratio =1:1}

The metal-ligand stability of medicinal drug Efavirenz found higher for both ratios. The metal-ligand stability of medicinal drug Labetalol found lower for metal to ligand ratio1:5 while the metal-ligand stability of drug Topiramate found lower and for drug Diphenhydramine found nil for metal to ligand ratio 1:1

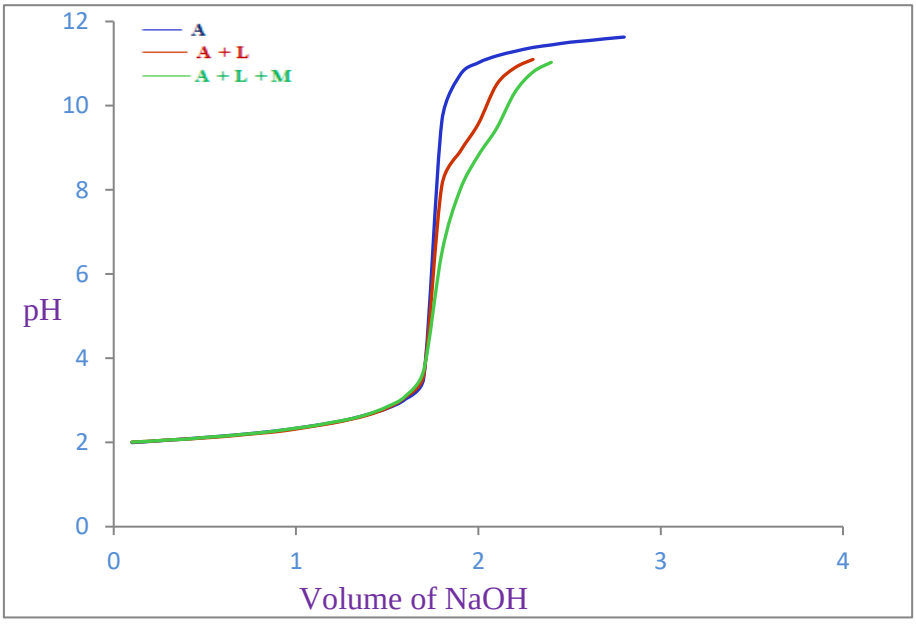

Figure: The Potentiometric titration curve for Co (II)-L_6

Conclusion

In the present investigation, stability constants of Cobalt metal with medicinal drugs at 1:5 and 1:1 metal-ligand ratio were studied at 300K. It is found that stability constant of Co (II) transition metal complexes when metal-ligand ratio 1:5 is greater than those of Cobalt metal complexes when metal-ligand ratio is 1:1. **This indicates that at higher concentration of ligand more stable complexes are formed.** The Cobalt metal ion forms 1:1 and 1:2 complexes with medicinal drug.

Acknowledgments

Authors thankful to research guide Principal Dr. Sahebrao Naikwade, Chhatrapati Shahu College, Lasur Station, Chhatrapati Sambhajinager and Principal Dr. Mazahar Farooqui, Maulana Azad College, Chhatrapati Sambhajinager for providing all research facilities.

References

[1]. Shailendrasingh Thakur,S.A. Peerzade, A.J.Khan, R.L.Ware. (2017) "Mixed ligand complexes of zinc metal ion with antibacterial drug Isoniazid and some amino acids in aqueous solution."International Multilingual Research Journal Printing Area, (Special Issue),47-51.

[2]. Ramesh L. Ware, Kishore N. Koinkar, Shailendrasingh V. Thakur.(2018) "Mixed ligand complex formation of Copper metal ion with some amino acids and drug Efavirenz in ethanol-water medium."International Journal of Universal Science and Technology, 3(6), 284-288.

[3]. Ramesh Ware, Shoeb Peerzade and Shailendrasingh Thakur. (2018) "Potentiometric investigation of complexation of Benazepril hydrochloride drug with transition metal ions." International Journal of Universal Science and Technology, 3 (5), 238-241.

[4]. Ramesh Ware and Shailendrasingh Thakur.(2018) "Mixed ligand complexes of Copper metal ion with drug Diphenhydramine hydrochloride drug and amino acids in aqueous media." International Journal of Universal print,4(4),254-260.

[5]. Ramesh Ware, Shoeb Peerzade and Shailendrasingh Thakur.(2018) "pH metric investigation of complexation of Ibuprofen drug with transition metals in mixed solvent media."International Journal of Universal print, 4(5), 274-278.

[6]. Shailendrasingh Thakur, Mazahar Farooqui, Ramesh Ware. (2019) "Mixed ligand complexes of Zinc metal ion with drug Cefotaxime and amino acids in aqueous media." International Journal of Advance and Innovative Research, 6(1{XVI}), 228-232.

[7]. Shailendrasingh Thakur and Ramesh Ware. (2019) "Mixed Ligand Complexes of Copper Metal Ion withIbuprofen Drug and Amino Acids in Aqueous Medium."Journal of Global Resources, 5(2), 224-229.

[8]. Ramesh Ware and Shailendrasingh Thakur. (2019) "pH Metric Study of Mixed Ligand Complexes of Cadmium Metal ion With Benazepril Drug and Amino Acids in 20% (v/v) Ethanol-water Medium."Journal of Global Resources, 5(2),265-269,

[9]. Ramesh Ware, P.P.Ghumare, D.B.Jirekar, Shailendrasingh Thakur. (2019) "Mixed Ligand Complexes of Cadmium Metal Ion With Ibuprofen Drug and Amino Acids in Aqueous Medium."RESEARCH JOURNEY International Multidisciplinary E-Research Journal, Special Issue 199, 64-70.

[10]. Shailendrasingh Thakur, H.U.Joshi, M.A. Sakhare, Ramesh Ware. (2019) "Mixed Ligand Complexes of Cadmium Metal IonWith Diphenhydramine and Amino Acids in Aqueous Medium." RESEARCH JOURNEY International Multidisciplinary E-Research Journal, Special Issue 199,71-77.

[11]. Rajpal Jadhav,Ramesh Ware, Shailendrasingh Thakur. (2020) "Potentiometric investigation of complexation of Benazepril drug with alkaline earth metal ions in aqueous media."Journal of Research and Development, 10(02), 40-42.

[12]. Ramesh Ware, MA Sakhare, Shukat Patel, Shailendrasingh Thakur. (2020), "Complexation of lisinopril drug with alkaline earth and transition metal ions in mixed solvent media." Innovare Journal of sciences, 8(1),132-133.

[13]. Ramesh Ware,D. B. Jirekar, P. P. Ghumare, Shailendrasingh Thakur.(2020), "Formation of Alkaline Earth and Transition Metal Complexes with Efavirenz Drug in Ethanol-Water Media."To Chemistry Journal, 6(1), 69-72.

[14]. Shailendrasingh Thakur, M. A. Sakhare, D. B. Jirekar, P. P. Ghumare, Ramesh Ware. (2020), "Studies of Complexation of Transition Metal Ions With Benazepril Drug in Aqueous Media: Thermodynamic Aspect."To Chemistry Journal,6(1),73-78.

[15]. Ramesh Ware, Hansaraj Joshi, Rafeeque Shaikh,Shailendrasingh Thakur. (2022), "Thermodynamic Study of the formation of transition metal ion Complexes Carrying medicinal drug in mixed solvent media" Journal of Science and Technology, 7(3),103-108.

[16]. Ramesh Ware, Kishore Koinkar, Ashish Katariya, Shailendrasingh Thakur (2024),"Formation of alkaline earth and transition metal complexes with labetalol drug in ethanol water medium,"Int Journal of Scientific Research in Chemistry, 9(7), 243-246.

[17]. Ramesh Ware, Kishore Koinker, Ashish Katariya, Hansaraj Joshi, Shailendrasingh Thakur.(2024), "Formation of Copper Metal Complexes with Medicinal Drugs in Ethanol Water Media, Int Journal of Scientific Research in Chemical Sciences, 11(5), 19-22.

[18]. Ramesh Ware, Rajpal Jadhav, Hansaraj Joshi, Shailendrasingh Thakur.(2024),"Complexation of zinc Metal with Medicinal Drugs in Mixed Solvent Media, Int Journal of Scientific Research in Science and Technology, 11(21), 58-63. doi: https://doi.org/10.32628/IJSRST

International Journal of Scientific Research in Science and Technology
Available online at : www.ijsrst.com
Print ISSN: 2395-6011 | Online ISSN: 2395-602X
doi : https://doi.org/10.32628/IJSRST

Photocatalytic Degradation of Methylene Blue Dye by Zinc Chromite Spinel (Zncr2o4) Nanoparticles under UV-Vis Irradiation

Yogesh Kadlag, Samreen Fatema, Pathan Mohd Arif, Sayyad Sultan
Department of Chemistry, Maulana Azad College of Arts Science and Commerce, Aurangabad 431 001, Maharashtra, India

ARTICLEINFO

Article History :

Published : 07 Dec 2024

Publication Issue :
Volume 11, Issue 23
Nov-Dec-2024
Page Number :
353-362

ABSTRACT

Pure Zinc Chromite (ZnCr2O4) nanostructures were produced by the simple sol-gel method. The current work examines the production of zinc chromite spinel (ZnCr2O4) using the aqueous sol-gel method and effective use for the photocatalytic breakdown of methylene blue (MB) dye under UV-Vis irradiation. The phase purity of the synthesized zinc chromite (ZnCr2O4) nanostructures was characterized by powder X-ray diffraction analysis (XRD) indicated an average crystalline size of 51 nm. and The structural, morphological, and optical characteristics of the produced NPs were examined using characterization methods such UV-Vis, FTIR, SEM-EDX, and TEM-SEAD. The maximum absorbance of methylene blue (MB) dye was observed at 660 nm. At two different pH levels (pH 8 and pH 10), the photocatalytic activity of ZnCr2O4NPs toward the degradation of methylene blue (MB) dye was examined under UV-Vis irradiation. The produced ZnCr2O4 NPs showed excellent photocatalytic activity, as evidenced by their 42.30% and 57.57 % degradation rates at pH 8 and pH 10, respectively. The findings of this investigation demonstrate that ZrCr2O4 NPs have the potential to be an efficient photocatalyst for the breakdown of organic contaminants like methylene blue (MB) dye.

Keywords: Zinc chromite, sol-gel, FTIR, XRD, SEM. methylene blue

Graphical Abstract:

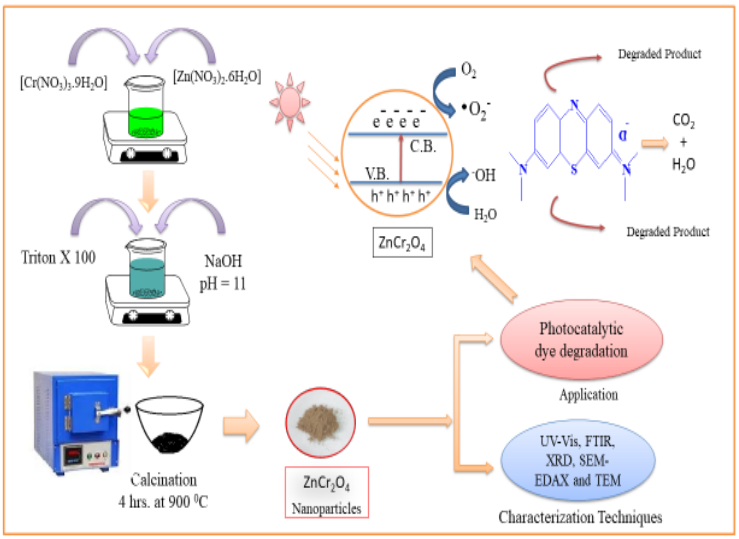

Figure 1. Graphical Abstract

Introduction

Spinel-structured oxide has gained significant attention in recent years due to its unique physical and chemical properties, making it an ideal compound for various applications, including catalysis, energy storage, electronic [1] magnetic materials [2] super hard materials [3], high-temperature ceramics [4], solid electrolytes or semiconductors as the active elements [5] [6]. catalytic combustion of hydrocarbons [7], reduction of several organic molecules [8], and sensing properties [9] Spinel compounds have the general formula AB_2O_4, with divalent cations occupying the tetrahedral A-site and trivalent cations occupying the octahedral B-site ($A^{2+}B_2^{3+}O_4^{2-}$). Zn^{2+} occupied the tetrahedral (A) sites and Cr^{3+} occupied the octahedral (B) sites. Metal oxides with special qualities like high surface area, thermal stability, and electrical conductivity, like TiO_2, Fe_2O_3, and CuO, have been extensively researched [10]. These characteristics make them the perfect choice for a number of uses, such as energy storage, electronic devices, and catalysis. Several techniques have been reported in the literature for the preparation of $ZnCr_2O_4$ materials such as mechanical activation [11] [12], spray pyrolysis [13], high-temperature solid-state reactions [14] [15] [16], and micro-emulsion method [17]

Textile industry waste waters pose a significant risk to aquatic life and human health due to their detrimental effects on the environment. They are loaded with pollutants, like organic dyes, which are widely used in industrial processes but are hazardous and non-biodegradable. Organic pollution is continuously produced by different industries and released into the environment, which is a major global concern [18]. Worldwide natural ecosystems have shown the dangers of various pollutants, including heavy metals, phenolic compounds, dyes, and pharmaceutical contaminants [19] [20]. Pollutants are removed from contaminated water using various treatment techniques and processes. Adsorption is a widely used and cost-effective method for purifying water [21].

In the present investigation, we used the sol-gel method to synthesize $ZnCr_2O_4$ nanoparticles and examined its optical and photocatalytic properties for the first time.

Experimental section:

2.1. Materials

The $ZnCr_2O_4$ nanoparticle was produced chemically, without the need for further purification. Laboratory-grade Zinc nitrate $Zn(NO_3)_2.6H_2O$, chromium nitrate $Cr(NO_3)_3.9H_2O$, 2N Sodium hydroxide and Triton X-100 are among the compound.

2.2. Synthesis of Zinc (II) Chromite nanoparticles

The nanoparticle $ZnCr_2O_4$ was prepared by the using sol-gel method of Zinc nitrate [$Zn(NO_3)_2.6H_2O$] and chromium nitrate [$Cr(NO_3)_3.9H_2O$] as precursors and Triton X 100 as a surfactant. Precursor stoichiometry was maintained in the final particles the initial composition is determined to be Zn:Cr = 1:2 cations ratio. Sodium hydroxide (2M) solution was added gradually drop by drop. While vigorously starring to obtain a precipitate solution with a pH of 11. The precipitate was filtered and dried at 110 ºC for four hours. The dry product was grind with mortar pestle into a fine powder and it was then calcinated for 4 hours at 900 ºC to eliminate contaminations.

2.3. Characterization

The analytical techniques were used to characterize zinc chromite. Crystal phase of prepared product was identifying by the X-ray power diffraction pattern. Bruker D8 advanced instrument at 40 kV and 35 mA with Cu Ka radiation at 0.154 nm wavelength (λ) = 0.154 nm. Bragg's scanning angle changing from 10^0- 80^0 was used to establish the phase purity of the product. The Fourier transform infrared (FTIR) spectra observed in the range of 4000 cm^{-1} to 100 cm^{-1} were recorded on a Thermo Nicolet iS50 spectrometer. UV Visible absorption spectra were recorded using a Perkin Elmer Lambda 365 UV VIS spectrophotometer in the range 200 nm to 1000 nm. The morphology of zinc chromite was observed by SEM. The crystal structure, particle size and distribution information are provided by the TEM.

2.4. Photocatalytic activity Measurement

The photocatalytic activity of the $ZnCr_2O_4$ was investigated for the breakdown of methylene blue dye molecules under UV light irradiation. Before irradiation, the combine solution was stirred using magnetic stirrer in dark for 30 minutes to achieve adsorption equilibrium between the methylene blue molecule and the synthesized catalyst. After the period of time the methylene blue molecules are adsorbed on the surface of the catalyst. The sample of the reaction mixture where taken from the reactor under UV-Vis (400-800 nm) light irradiation at appropriate time intervals, in order to monitor the dye degradation was identifying by the taking absorbance of the solution.

Result and Discussion

3.1. X-ray diffraction studies

Fig. 2 shows the CuKα radiation was used to create X-ray diffraction pattern of spinel -type $ZnCr_2O_4$ after calcining the gel at 900 ºC for 4 hours. The diffraction peaks at 2Θ angle occurred. Scattering from the spinel crystal lattice's (111), (220), (311), (222), (400), (331), (422), (511), (440), and (620) planes can be assigned to the following coordinates: 18.44°, 30.34°, 32.19°, 34.19°, 35.74°, 37.38°, 43.44°, 51.48°, 53.90º, 57.46º and 63.10º. The cubic phase has an a = 8.2800(0)A°, volume = 567.66A° [22], Z = 8, and space group Fd3*m* (No.227). The phases definitely match the phase provided in the powder diffraction database (JCPDS card no. 01-072-0775) and are certainly $ZnCr_2O_4$ phases, as confirm by the XRD peaks. Particle size can be calculated by Scherrer's formula $D = k\lambda/\beta\cos\theta$, where D is the mean crystallite size, k is Scherrer constant (k = 0.9), λ is the X-ray wavelength (λ=

0.154 nm). β is full width at half maximum (FWHM) of the diffraction peak, θ is the angle of diffraction. The average nanoparticles size determines as 51.93 nm.

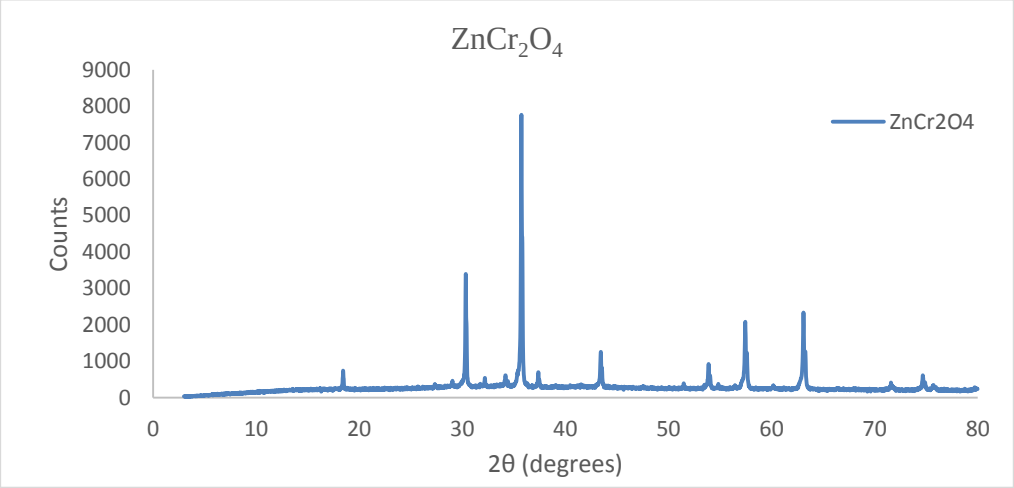

Figure 1. XRD peaks of $ZnCr_2O_4$

3.2. Optical investigation

The optical absorption spectra of $ZnCr_2O_4$ nanoparticles are shows in Fig.3. Two distinct absorption properties are localized. $ZnCr_2O_4$ has a band gap of 395 nm (3.1 eV). By using UV-vis spectroscopy, the band gap of $ZnCr_2O_4$ produced in this study was calculated to be around 3.1 eV. As demonstrated by the product's predicted band gap using these techniques (1240/λ max in PL spectroscopy and Tauc equation in UV-vis)

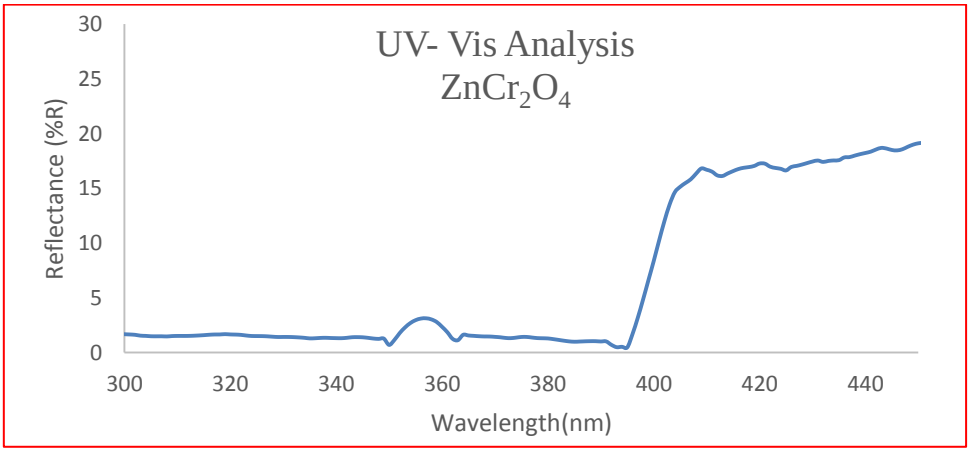

Figure 2 UV–Vis absorbance spectrum of $ZnCr_2O_4$

3.3. FT-IR Spectra of Nanoparticles

Spectroscopic analysis is a useful tool for analyzing the structural and chemical changes that occur throughout the calcination process. The $ZnCr_2O_4$ nanoparticles' infrared spectra are displayed in Fig. 4 The calcine nanoparticls shows the characteristic bands at about 607, 458, 357 and 181cm^{-1}. The absorption peaks at 607cm^{-1} and 375 cm^{-1} correspond to the stretching vibration and bending vibration, respectively, of the Cr-O bond in the chromate ion ($CrO4^{2-}$). The absorption peak at 458 cm-1 attributed to the bending vibration of the Zn-O-Cr bond. The crystal structure of $ZnCr_2O_4$ is corresponds to the lattice vibration mode absorption peak at 181 cm-1.

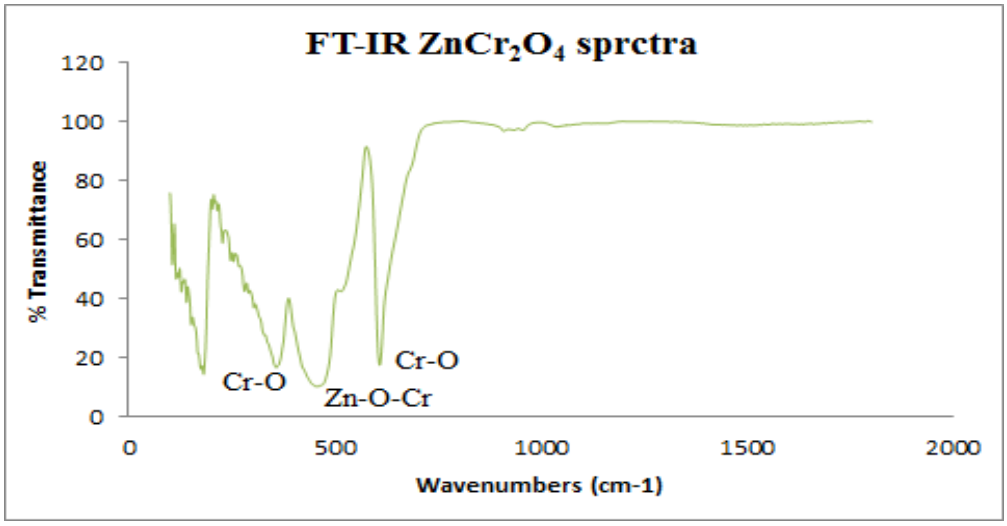

Figure 3 FT-IR spectrum of $ZnCr_2O_4$.

3.4. Morphological studies

SEM images of the sample generated using the sol-gel technique shown in Fig. 5 the particles in these samples had an average size of 51.93 nm. The particles were agglomerated and impacted. The SEM image shows a mesoporous $ZnCr_2O_4$ material with a large surface area, composed of agglomerated nanoparticles. The particles have a rough, uneven surface and sponge-like structure, indicating great porosity. The crystal facets are plainly visible, indicating great crystallinity. It had a consistent particle size and an octahedron-shaped morphology that was well characterized. The following surfaces (111), (220), (311), (222), (400), (331), (422), (511), (440), and (620) are appropriate for the cubic spinel lattice. [23] $ZnCr_2O_4$ has a normal spinel structure, which is a cubic crystal system with a face-centred cubic lattice so belongs to the space group Fm-3m (No. 225)

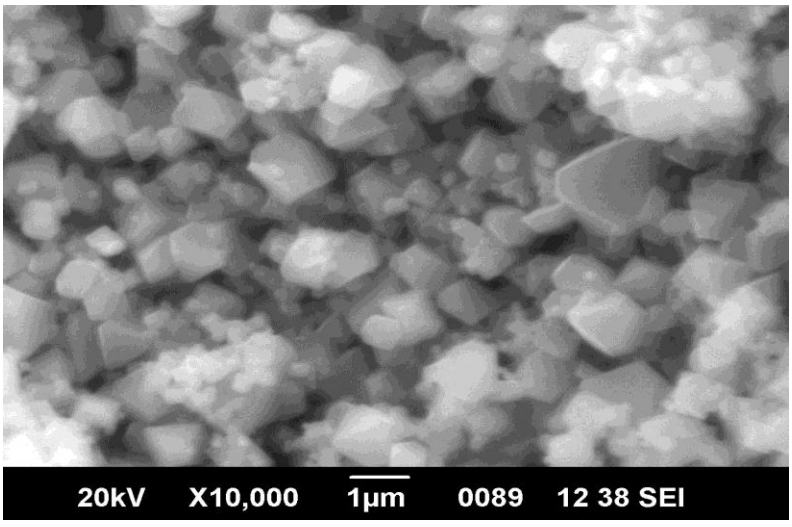

Figure 4 SEM micrograph of $ZnCr_2O_4$

Significant amounts of oxygen (49.52%), chromium (32.31%), iron (1.8%), and zinc (16.98%) were found in the compound according to the EDAX analysis fig.6 The presence of chromium, iron, and zinc suggests that the compound may be a metal oxide or a spinel compound, whereas the high percentage of oxygen suggests that the compound may be an oxide. The molecular formula of the compound can be ascertained using the exact ratios of these constituents. From the given molecular percentage $ZnCr_2O_4$ molecular formula is revealed out.

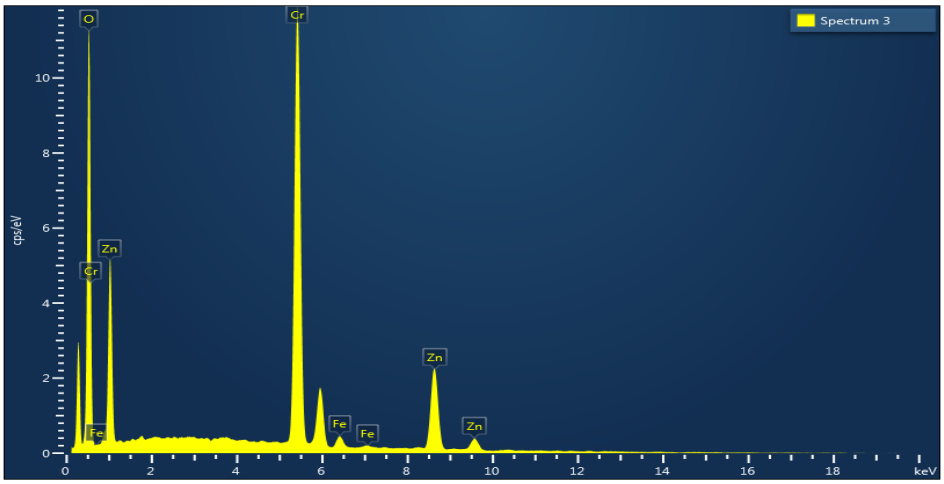

Figure 5 Energy dispersive X-ray (EDX) spectra of $ZnCr_2O_4$ Nanoparticles

3.5. TEM analysis Studies

High-resolution TEM (HRTEM) fig.7 a) images reveal a $ZnCr_2O_4$ nanoparticles exhibit a spherical morphology, uniform size distribution and crystalline structure with an average dimeter of 51 nm. The SED pattern fig.7 b) confirm the polycrystalline nature of the nanoparticles. The crystalline structure with a lattice spacing of 0.24 nm corresponding to the (311) plane of $ZnCr_2O_4$

a)

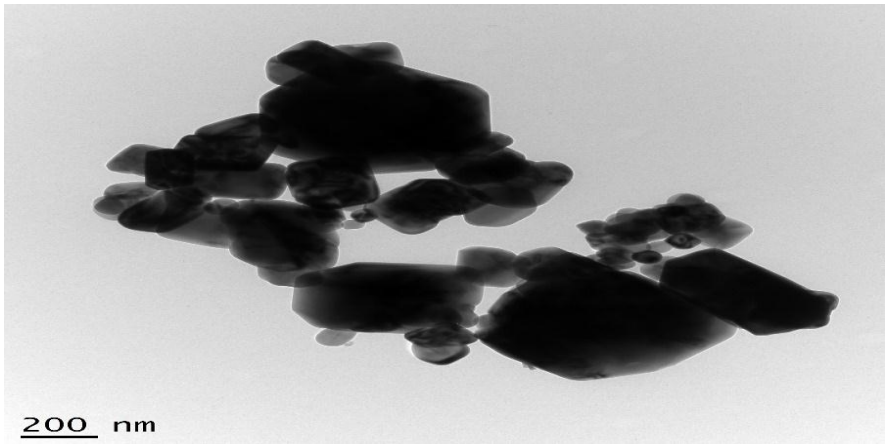

b)

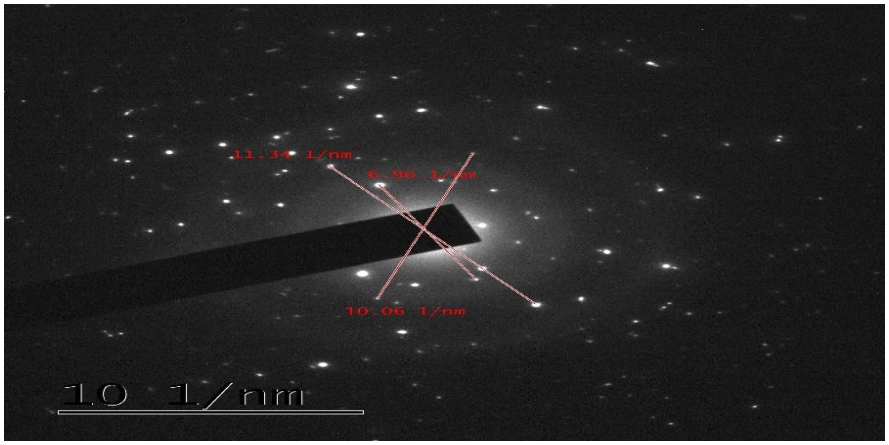

Figure 6 a) HRTEM b) SED pattern of $ZnCr_2O_4$

3.6. Photocatalytic study

According to the Lambert-Beer law, sometimes referred to as Beer's law, absorption is proportional to concentration. The degradation percentage of the process may be calculated using the relationship.

$$\%D = \frac{C_0 - C_t}{C_0} \times 100\% = \frac{A_0 - A_t}{A_0} \times 100\%$$

Where %D is degradation percentage, C_0 is initial concentration before irradiation; C_t is concentration after time t of irradiation, A_0 is absorbance before irradiation, A_t is absorbance after time t of irradiation.

3.6.1 The effect of pH

The initial pH of the solution has been adjusted to be between 8 and 10, as the pH of the solution is a crucial parameter on removing dye molecules [24]. The findings demonstrated that pH has a significant impact on methylene blue elimination. Removal rate calculated by

$$Removal\ rate\ \% = \frac{C_0 - C_t}{C_0} \times 100$$

where Co and Ct are the initial concentration and concentration of methylene blue at time t, respectively. Above 42.30 % and 57.57 % of the methylene blue (MB) was eliminated at pH = 8 and pH =10 respectively. Therefore, $ZnCr_2O_4$ nanoparticles should be used to remove methylene blue (MB) at a pH of 10. This pH has been chosen for future experimentation and investigation.

3.6.2 The effect of contact time

Fig.8 demonstrates how $ZnCr_2O_4$ nanoparticles remove methylene blue (MB) based on contact time. The figure indicates a rapid rate of removal methylene blue (MB) concentration decreases over time due to its adsorption by $ZnCr_2O_4$ nanoparticles.

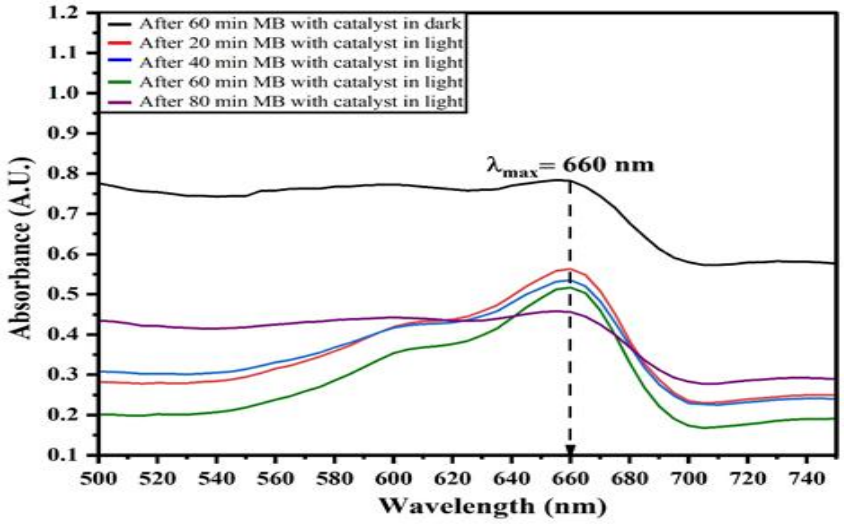

Figure 8 Degradation of MB dye = 10^{-5} M and pH = 8 at visible light

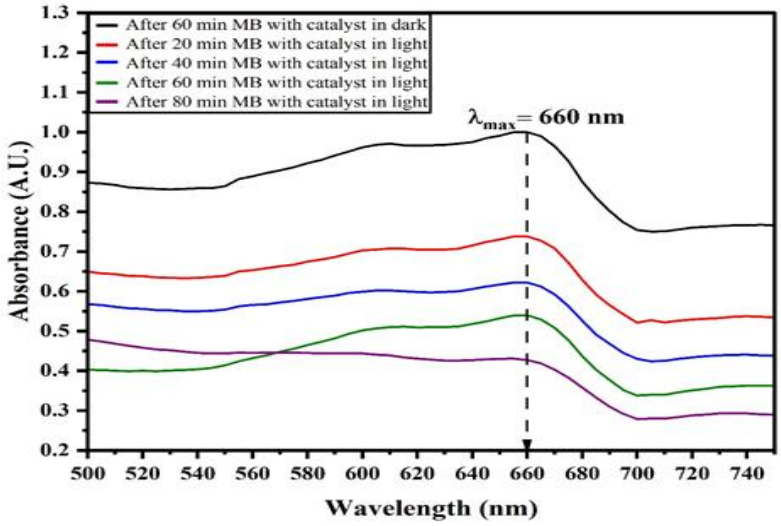

Figure 7 Degradation of MB dye = 10-5 M and pH = 10 at visible light

3.6.3 The effect of adsorbent concentration

The effect of adsorbent dosage of methylene blue (MB) adsorption onto $ZnCr_2O_4$ nanoparticles was examined. The investigation observed that increasing the adsorbent dose led to a higher percentage of dye removal. This is due to an increase in binding sites in the adsorbent.

Conclusion

In summary, $ZnCr_2O_4$ nanoparticles have been successfully synthesized from $Zn(NO_3)_2$. $6H_2O$, $CrCl_3$. $6H_2O$ by a simple sol gel method, with average crystallite size 51 nm after heat treatment at 900°C. The particle size of nanoparticles is small in comparison with those prepared by conventional methods. [25] XRD and SEM-EDAX analysis show that $ZnCr_2O_4$ nanoparticles manufactured. $ZnCr_2O_4$ nanoparticles exhibit a spherical morphology, uniform size distribution and crystalline structure with an average dimeter of 51 nm. The crystalline structure with a lattice spacing of 0.24 nm corresponding to the (311) plane of $ZnCr_2O_4$. The IR spectra confirmed the structure of generated nanoparticles. The adsorption studies have been carried out for contact time, different pH values, and adsorbent doses separately. $ZnCr_2O_4$ nanoparticles have been also proven to removal methylene blue (MB) dye at pH= 10 effectively. Increasing the adsorbent dose led to a higher percentage of dye removal.

Acknowledgment

This research was financially supported by the Chhatrapati Shahu Maharaj Research, Training and Human Development Institute (SARTHI), Pune, as well as Sophisticated Test and Instrumentation Centre (STIC) Cochin University of Science & Technology Campus, Kochi to provide the analysis report. We also acknowledge Department of Chemistry Maulana Azad College, Chatrapati Sambhajinagar, for his continued help, encouragement, and support.

References

[1]. Y. W. H. L. X. L. Z. W. X. a. Z. J. Li, "ZnCr2O4: A promising material for energy storage and conversion," Journal of Materials Chemistry A, vol. 7, no. 10, pp. 5311-5322, 2019.

[2]. H. M. N. O. S. J. A. R. C. G.-A. J. Martinho, “Magnetic properties of the frustrated anti-ferromagnetic,” Phys.Rev. B., vol. 64, p. 1–6, 2001.

[3]. A. M. G. S. G. S. M. K. E. R. R. e. a. Zerr, “Synthesis of cubic silicon nitride,” Nature, vol. 400, p. 340–342., 1999.

[4]. B. N. H. K. M. K. a. S. Y. Kim, “A high-strain-rate superplastic ceramic,” Nature, vol. 413, p. 288–291, 2001.

[5]. F. J.G. and A. V.R.W, “Reliability and reproducibility of ceramic sensors: Part. III. Humidity sensors.,” Am. Ceram. Soc. Bull, no. 72, pp. 119-129, 1993.

[6]. Y. Y., U. S., H. M. and H. H., “Microstructure and humidity- sensitive properties of ZnCr2O4-LiZnVO4 ceramics sensors.,” Sens. Actuators, no. 4, pp. 599-606, 1983.

[7]. M. P. N. Guilhaume, “Catalytic combustion of methane: copper oxide supported on high-specific-area spinels synthesized by a sol–gel process,” J. Chem. Soc. Faraday Trans., vol. 90, p. 1541–1545, 1994.

[8]. D. C. W. T. X. Wei, “Preparation and characterization of the spinel oxide ZnCo2O4 obtained by sol–gel method,” Mater. Chem. Phys., vol. 103, p. 54–58, 2007.

[9]. B. J. K. N. S. Pokhrel, “Humidity-sensing properties of ZnCr2O4–ZnO composites,” Mater. Lett, vol. 57, p. 3543–3548, 2003.

[10]. Y. L. X. W. H. Z. J. L. Q. Z. Y. W. X. Chen, “Metal oxides: A review of their properties and applications.,” Materials Science and Engineering: R: Reports, no. 140, p. 100534, 2020.

[11]. Z. V. M. L. V. P. a. M. O. Marinkovic, “Microstructural characterization of mechanically activated ZnO–Cr2O3 system,” J. Eur. Ceram. Soc, vol. 25, p. 2081–2084, 2005.

[12]. Z. V. L. V. P. a. M. O. Marinkovic, “The influence of mechanical activation on the stoichiometry and defect structure of a sintered ZnO–Cr2O3 system,” Mater. Sci. Forum, vol. 453/454, p. 423–428, 2004.

[13]. Z. V. M. L. M. R. a. M. O. Marinkovic, “Preparation of nanostructured Zn-Cr-O spinel powders by ultrasonic spray pyrolysis.,” J. Eur. Ceram. Soc., vol. 21, p. 2051–2055., 2001.

[14]. D. D. V. P. A. D. M. a. S. A. Levy, “P–V equation of state, thermal expansion, and P–T stability of synthetic (ZnCr2O4 spinel),” Am. Mineral, vol. 90, p. 1157–1162, 2005.

[15]. Z. V. R. N. a. S. B. Marinkovic, “Spectroscopic study of spinel ZnCr2O4 obtained from mechanically activated ZnO–Cr2O3 mixtures,” J. Eur. Ceram. Soc., vol. 27, p. 903–907, 2006.

[16]. Z. L. P. S. S. K. a. A. G. Wang, “High-pressure Raman spectroscopic study of spinel (ZnCr2O4),” J. Solid State Chem., vol. 165, p. 165–170, 2002.

[17]. X. D. W. a. D. W. Niu, “Preparation and gas sensing properties of ZnM2O4 (M = Fe, Co, Cr).,” Sens. Actuators B, vol. 99, p. 405–409, 2004.

[18]. C. F. K. W. Y. Z. Y. X. Q. Z. C. L. M. L. Z. Z. W. W. M. Zhao, “Photocatalytic degradation of antibacterials using BixOyXz with optimized morphologies and adjusted structures - a review,” J. Alloys. Compd., vol. 852, p. 156698., 2021.

[19]. M. H. D. K. A. M. Shabani, “Haghighi, Mesoporous-mixed-phase of hierarchical bismuth oxychlorides nanophotocatalyst with enhanced photocatalytic application in treatment of antibiotic effluents,” J. Clean. Prod, vol. 207, p. 444–457, 2019.

[20]. A. H.-Y. S. P. M. Mousavi, “Review on magnetically separable graphitic carbon nitride-based nanocomposites as promising visible-light-driven photocatalysts,” J. Mater. Sci. Mater. Electron, vol. 29, p. 1719–1747, 2018.

[21]. Q. Jiuhu, “Research progress of novel adsorption processes in water purification: a review,” J. Environ. Sci., vol. 20, p. 1–32, 2008.

[22]. B. N. H. K. M. K. a. S. Y. A. Kim, "high-strain-rate superplastic," Nature, pp. 288-291, 2001.

[23]. D. J. G. R. W. R. A. L. a. G. D. H. Binks, "Morphology and structure of ZnCr2O4 spinel crystallites," J. Mater. Sci., p. 1151–1156., 1996.

[24]. G. C. M. A. G. Bayramoglu, "Biosorption of reactive blue 4 dye by native," J. Hazard. Mater. B., vol. 137, p. 1689–1697, 2006.

[25]. S. N. F. H. H. K. H. S. Y. K. Y. Xue, "Low temperature X-ray diffraction study of ZnCr2O4 and Ni0.5Zn0.5Cr2O4," J. Low Temp. Phys., p. 1193–1204., 2008.

International Journal of Scientific Research in Science and Technology
Available online at : www.ijsrst.com
OPEN ACCESS
Print ISSN: 2395-6011 | Online ISSN: 2395-602X
doi : https://doi.org/10.32628/IJSRST

Synthesis of Formazan Derivatives Physicochemical Properties Study and Effect of Electronic Factor on Their Antimicrobial Activity

Y S Thakare
P.G. Department of Chemistry, Shri Shivaji Science College, Amravati, Maharashtra, India

ARTICLEINFO

Article History :

Published : 07 Dec 2024

Publication Issue :
Volume 11, Issue 23
Nov-Dec-2024
Page Number :
363-370

ABSTRACT

In present work formazan derivatives were prepared through the reaction of benzaldehyde-phenylhydrazon with substituted aniline. The structure of the formazan derivatives were fully established by physical and spectral methods. The study was extended to antimicrobial activity and physicochemical measurements at different concentration in binary solvent system. In viscometric study it was observed that viscosity of solution increases with increase in concentration. Positive value of B-coefficient may attribute to strong solute-solvent interaction on other hand value of A-coefficient is almost negative which indicates weak solute-solute interaction. Study was extended to find conductivity of synthesized derivative in different solvents. Formazan derivatives 4–phenyl –(4 nitrophenyl)-5-phenyl and 4-phenyl –(4 chlorophenyl)-5-phenyl showed best activity against Staphylococcus aureus and poor activity against Escherichia coli bacterial strains.

Keywords: Formazan derivative, Viscosity, Conductivity, Antimicrobial activity.

Introduction

Reaction between benzaldehyde phenylhydrazone with substituted aromatic and hetero aromatic amines form different derivatives of formazan [1-2]. Formazan derivatives possess beautiful colors and used as dyes, ligands, reagents as indicators for redox reactions shows antibacterial activity and was studied against breast cancer cell [3-5]. Wide scope of Formazan compounds in pharmaceutical, biological, medical, industrial and chemical applications in various fields as well as their usefulness in analytical chemistry have attracted the interest of many researchers [6].

Literature survey demonstrates that a lot of formazans have been described to possess broad spectrum of biological activities and pharmacological applications such as antimicrobial, antiviral, anti-inflammatory, anti-

fertility, anticancer, anti tubercular activity and anti corrosion properties [7-8]. Substituted formazan derivatives has been synthesized from corresponding aryl diazonium chloride and Schiff base in pyridine [9-11]. Cyclic formazan was studied as medical nanomaterials [12-13]. Scope to synthesize Formazan using effective functional these compounds exhibits high resistance to the spread of cancerous tumors, bacteria and fungi [14]. Electronic factor and presence of electronegative nitrogen atoms responsible for its stability and different activity towards various pathogens. Formazan possess high molar mass, solid colour compound and relatively low melting point. It is soluble in various polar and non-polar solvents [15-16]. Here efforts were taken to prepare different formazan derivatives using substituted aldehyde and amine. These compounds exposed to study physicochemical properties and its conductivity measurement in 70% ethanol – water and dioxane-water system. Considering importance of formazan derivative towards its biological activity antimicrobial studies were carried out which shows exciting results.

Experimental

Synthesis of 4–phenyl –(4 nitrophenyl)-5-phenyl formazan

Step 1- Preparation of 4- chlorobenzaldehyde phenylhydrazone derivatives – phenyl hydrazine (0.01 mol) drop wise added to a well stirred mixture of 3- chlorobenzaldehyde (0.01 mol) diluted in acetic acid (2%) in a 100 ml conical flask at room temperature. The reaction mixture was further stirred for 1 hours and kept at room temperature for 30 minutes. Precipitated yellow crystalline mass was filtered and dried in a oven at 60°C. The crude product was recrystallized with ethanol. Finally, fine colourless needles like product of 3-chlorobenzaldehyde phenylhydrazone was obtained.

Step 2 - Preparation of 4–phenyl –(4 nitro phenyl)-5-phenyl formazan derivative - 0.01 mol of 4 nitroaniline was dissolved in a 1:1 mixture (10 ml) of concentrated HCl and water taken in a 100 ml conical flask, with constant stirring. The reaction mixture was placed in ice bath with maintaining the temperature below 5°C. In Another beaker sodium nitrite (1.6 g) was taken and was dissolved in 7.5 ml of water. It was cooled in ice bath maintaining the temperature below 5°C in an ice bath. Subject to the temperature condition not more than 10°C sodium nitrite solution was added drop wise to aniline mixture with vigorous shaking. The diazonium salts solution of aryl and hetero aryl amine was filtered then added drop wise with continue stirring to a solution of 3- chlorobenzaldehyde phenylhydrazone (0.01M) in pyridine (20ml), temperature was maintained below 10°C. The reaction mixture was allowed to stand for 4 hours then it was poured into 250 ml of ice-cold water with continue stirring. The dark coloured solid which separated out was filtered, washed successively with cold water followed by hot water and finally with methanol and dried in air. Melting point of compound – 200^{o}C and colour was deep red

^{1}H-NMR :δ 7.94 (d) 1H, 6.72 (d) 1H, 7.50 (s) 1H, 6.40 (d) 1H, 7.3 (d) 1H

IR (KBr) :ν_{max}1683,1338,750,1516 – 1396, 3068

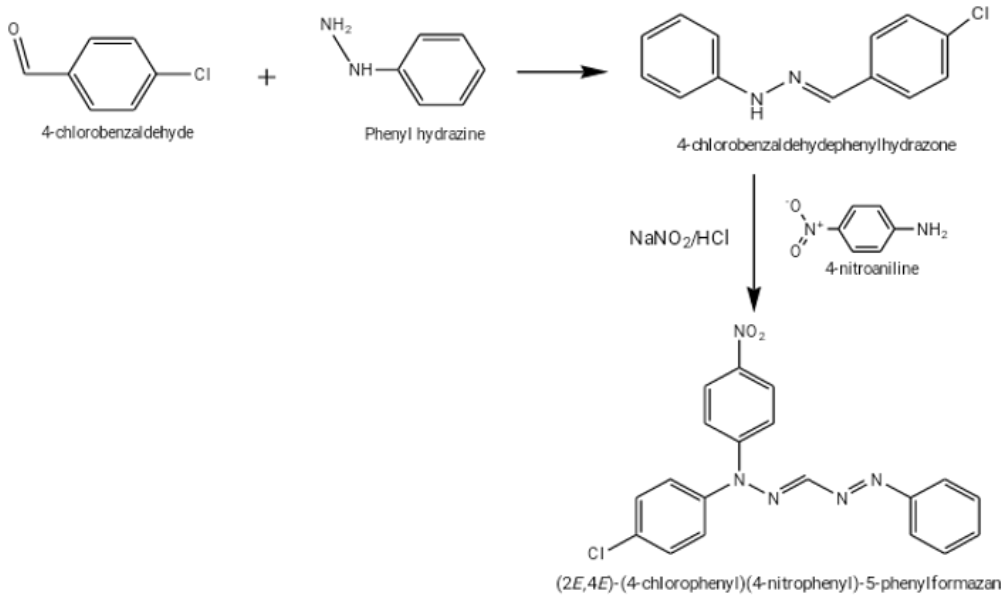

Synthesis of 4-phenyl –(4 chlorophenyl)-5-phenyl formazan :

Step 1 - Preparation of 4- chlorobenzaldehyde phenylhydrazone derivatives –

0.01 mol of phenyl hydrazine was added drop wise to a well stirred mixture of 0.01 mol of 3-chlorobenzaldehyde dilute in acetic acid (2%) in a 100 ml conical flask at room temperature. The reaction mixture was further stirred for 1 hours and kept at room temperature for 30 minutes. The precipitated yellow crystalline mass was filtered and dried in a oven at 60°C. The crude product was crystallized with ethanol. 3-chlorobenzaldehyde phenylhydrazone was obtained as a fine colourless needles.

Step 2 - Synthesis of 4-phenyl –(4 chlorophenyl)-5-phenyl formazan derivative :- 0.01 mol of 4 – chloroaniline was dissolved in a mixture of 5 ml concentrated hydrochloric acid (HCl) and 5 ml water taken in a 100 ml conical flask, with constant stirring. The reaction mixture was cooled in ice bath until the temperature fall below 5°C. Separately, 1.6 g of sodium nitrite ($NaNO_2$) solution was dissolved in 7.5 ml of water and chilled in an ice bath below 5°C. The sodium nitrite solution was filtered then added drop wise to aniline mixture with vigorous shaking, temperature was not allowed to rise above 10°C. The diazonium salts solution of aryl and hetroaryl amine was filtered then added drop wise with continue stirring to a solution of 3-chlorobenzaldehyde phenylhydrazone (0.01M) in pyridine (20ml), temperature was maintained below 10°C. The reaction mixture was allowed to stand for 4 hours then it was poured into 250 ml of ice-cold water with continue stirring, the dark coloured solid which separated out was filtered, washed successively with cold water followed by hot water and finally with methanol and dried in air. Melting point of compound – 65°C and colour of compound – deep red

^{1}H-NMR :δ 7.02 (d) 1H, 6.40 (d) 1H, 7.3 (d) 1H, 7.50 (s) 1H

IR (KBr) :ν_{max}1348, 3061, 754-827.

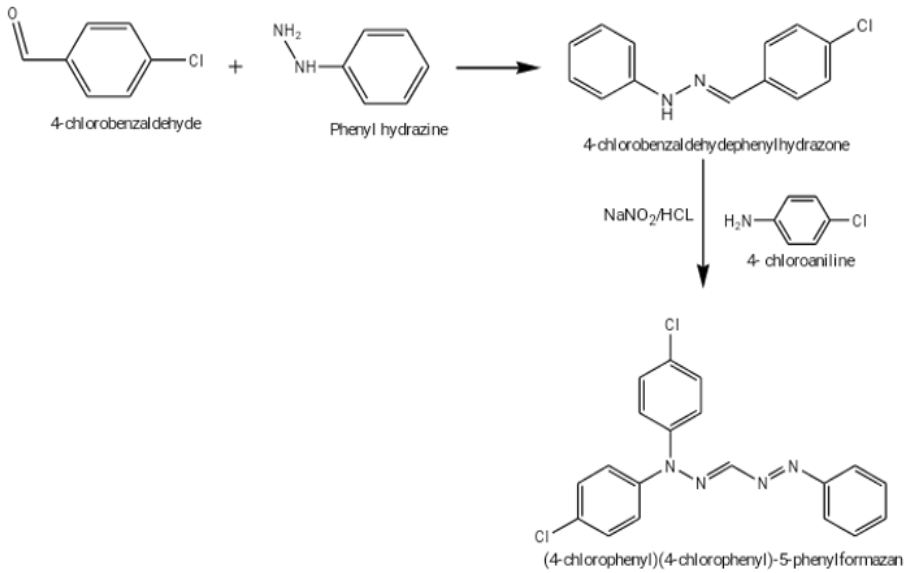

Result And Discussion

Viscometric Measurements -In present study ,viscometric study of formazan derivative at different concentration by using binary solvent system was carried out. To measure the viscosity The most common instrument known as Ostwald's viscometer was used. Relative viscosity was determined by the formula,(η_r)=(η_{liq} – η_{water}) whereas relative viscosity has been analysed by Jones- Dole equation; η_r–1/√c =A + B × √c. Where, 'C' is molar concentration of compound solution. 'A' is the co efficient which is the measure of solute–solute interaction and 'B' is the Jones-Dole co efficient which is the measure of solute-solvent interaction. The graphs are plotted between (ηr - 1)/√c verses √c for binary solvent system 70% ethanol-water and 70% dioxane-water system for formazan derivatives which gives straight line showing validity of Jones-Dole equation From the graph (nr-1)/√cgives the straight line and Jones-Dole co efficient A and B has been calculated. The intercept of the graph gives value of 'A' which is the measures of solute-solute interactions and slope of the graph gives value of 'B' which is the measure of solute-solvent interaction.

Table 1-Viscometric study with variation in concentration

System	Medium	Conc. (M)	√c	Time flow (sec)	Relative viscosity (η_r)	Specific viscosity (η_{sp})	A coefficient	B coefficient
4-Chlorophenyl-(4-nitrophenyl)-5-phenyl formazan	70% Ethanol water system	0.01 0.005 0.0025	0.1 0.070 0.05	80 57 45	0.6283 0.4442 0.3643	-0.371 -0.555 -0.635	-0.8739	4.4983
4-Chlorophenyl-(4-nitrophenyl)-5-phenyl formazan	70% Dioxane water system	0.01 0.005 0.0025	0.1 0.070 0.05	56 50 47	0.6609 0.5041 0.4028	-0.3390 -0.4958 -0.5971	-1.0804	4.2763
4-Chlorophenyl-(4chlorophenyl)-5-	70% Ethanol	0.01 0.005	0.1 0.070	82 67	0.6701 0.507	-0.3298 -0.493	-0.5515	3.8236

phenyl formazan	water system	0.0025	0.05	59	0.4527	-0.5472		
4-Chlorophenyl-(4chlorophenyl)-5-phenyl formazan	70% Dioxane water system	0.01 0.005 0.0025	0.1 0.070 0.05	70 57 51	0.8077 0.6688 0.6026	-0.1922 -0.3311 -0.3973	-1.1577	3.0122

It was observed from above table that the values of co-efficient A are almost negative in all the binary solvent systems which shows weak solute-solute interaction and is also supported by decrease in relative viscosity. Again the values A are more negative in non-polar solvent as compare to polar solvent. It show strong solute-solute interaction in non-polar solvent as compare to polar solvent Besides that the coefficient B is positive, shows strong solute-solvent interaction. The value of B coefficient is more positive in polar solvent as compare to non-polar solvent. These different result for all the tested ligand may be due to different polarity index of polar solvent and non-polar solvent

Graphical Representation :- Plot between Specific viscosity (nr-1)√C V/S √c

Ligand -1: (4-chlorophenyl)-(4-nitrophenyl)-5-phenyl formazan :-

70% Ethanol-Water System **70% Dioxane-Water System**

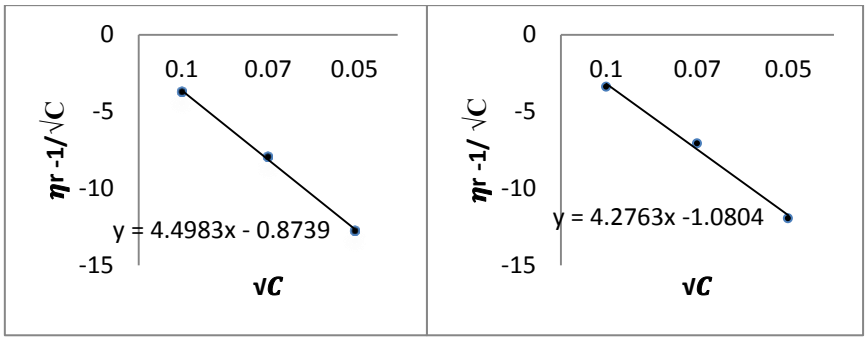

Ligand -2: (4-chlorophenyl)-(4-chlorophenyl)-5-phenyl formazan

70% Ethanol-Water System **70% Dioxane-Water System**

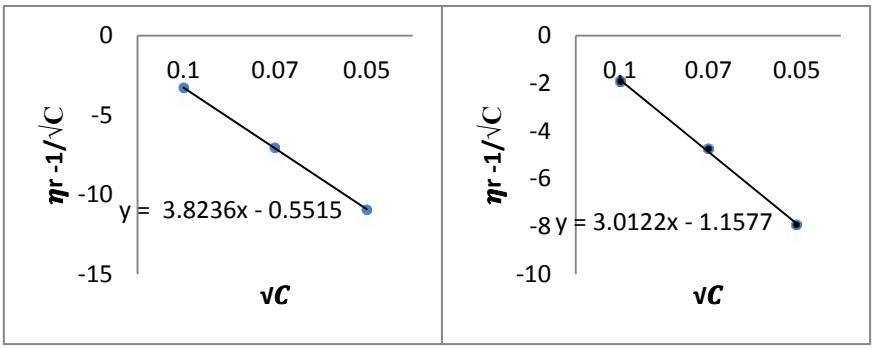

From the graph (nr-1)/√c gives the straight line and Jones-Dole co efficient A and B has been calculated. The intercept of the graph gives value of 'A' which is the measures of solute-solute interactions and slope of the graph gives value of 'B' which is the measure of solute-solvent interaction.

Conductometric Measurement

Conductivity depends on number of ions of an electrolyte present in the system. It also depends on behaviour of solute towards different solvent system.

Table 2- Observe Conductance of formazan derivative

System	Concentration	Medium 70% Ethanol-water Specific Conductance	Medium 70% Dioxane-water Observed Conductance
4-phenyl-(4-nitrophenyl)-5-phenyl formazan	0.01 0.005 0.0025	0.073 0.023 0.003	0.025 0.018 0.013
4-phenyl-(4-chlorophenyl)-5-phenyl formazan	0.01 0.005 0.0025	0.067 0.045 0.006	0.038 0.020 0.011

It was observed that both the ligand shows different conductivity in both the solvent system. Observed conductance decreases with decrease in concentration. In ethanol-water system the value of observed conductivity is high as compare to dioxane-water system for both ligand.

Antimicrobial Activity of formazan derivative

The antibacterial activities of synthesized compounds were tested on against gram positive and gram negative microorganisms using disc diffusion method. The bacteria used in the present investigations included - *Escherichia coli, Staphylococcus aureus.* Tetracycline was used as standard antibiotics. The diameter of zone of inhibition and the MIC results for the compounds are presented in Tables 3. Antibacterial activity of compounds (conc. 10 mg/disc) tested by disc-diffusion method

Table 3- Antimicrobial activity of formazan derivative

Sr. No.	**Compound Code**	**Zone of Inhibition in mm**	
		E. Coli	**S. Aur**
1	Formazan Ligand-1	08 ±0.9	21 ±0.4
2	Formazan Ligand-2	11.00	19 ±0.8
Tetracycline		**28**	**30**

The Minimum inhibitory concentration (MIC) was evaluated for compounds which showed higher antibacterial activity. Zone of inhibition and MIC of all compounds is illustrated in images of Antibacterial screening discs.

Antibacterial Screening

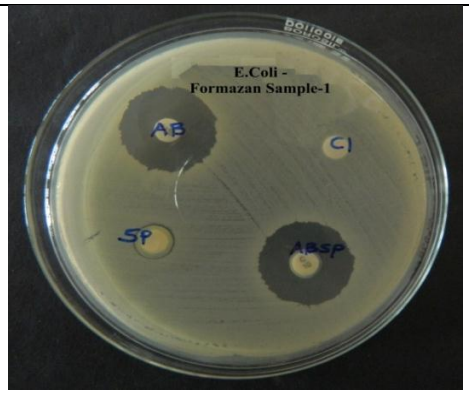	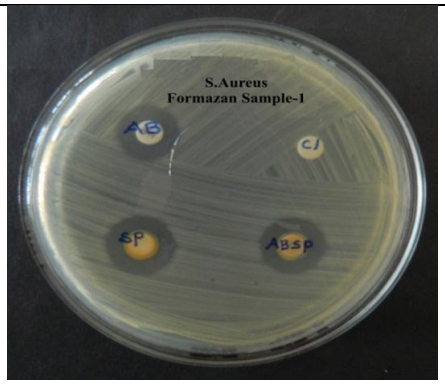
E. Coli – Formazan Ligand – 1	**S. Aureus – Formazan Ligand – 1**
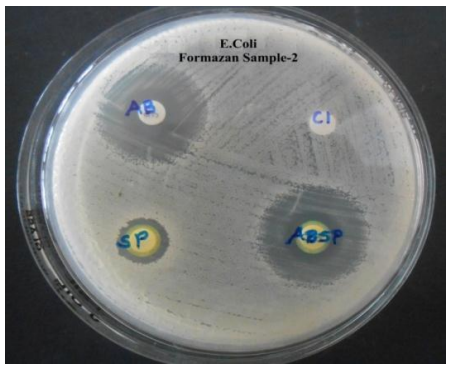	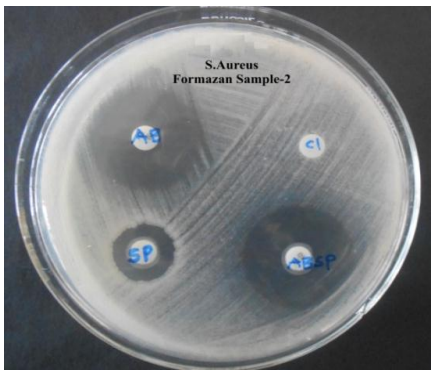
E. Coli – Formazan Ligand – 2	**S. Aureus – Formazan Ligand – 2**

The compound Fomazan Ligand-2 show good activity against *Staphylococcus aureus* whereas it showed moderate activity against *Escherichia coli* bacteria; Compound Formazan Ligand-1 showed best activity against *Staphylococcus aureus* and poor activity against *Escherichia coli* bacterial strains.

Conclusion

Versatile biological activity of formazan derivatives makes it more interesting in medicinal chemistry. In present work Spectroscopic methods were used to characterize structures of all synthesized compounds. The viscometric measurement have been carried out in different percentage solvent system. Viscosity increases with increases in concentration for all the tested derivatives may be attributed to the increases in solute – solvent interactions. Study was extended to find conductivity of synthesized derivative in different solvents. The data obtained was used to evaluate nature, magnitude of ion-solvent and ion-ion interactions. The primary purpose of this study to evaluate antibacterial activity against Gram-positive and Gram-negative pathogens. It was observed that the compounds show poor or good activity. which depend upon electronic factor of the phenyl ring of formazan.

References

[1]. G. Marippan, R Korim, N. M. Joshi, F. A. R. Hazarika, D. Kumar, and T. Uriah, "Synthesis and biological evaluation of formazan derivatives", J. Adv. Pharm. Technol. Res., Vol. 1, no.4, (2010), pp. 396-400.

[2]. G. Turkoglu and S. Akkoc, “Synthesis, optical, electrochemical and antiproliferative activity studies of novel farmazan derivatives”, J. Mole. Str., Vol. 1211, no. 128028, (2020).

[3]. H. M. Azeez, N. M. Aljamali, “Synthesis and Characterization of New trimethoprim-Farmazan Derivatives with Studying Them against Breast Cancer”, Inter. J. Biochem. Biomolecul., Vol. 7, no. 1, (2021), pp. 25-61.

[4]. Y. H. Al-Araji, J. K. Shneine, and A. A. Ahmed, “Chemistry of Farmazan” Inter. J. Res. Pharm Chem., Vol. 5, no.1, (2015), pp. 41-76

[5]. A. Shakir, S. Adnan, “Synthesis and Characterization of some new Formazan Derivatives from 2-Amino-4-Hydroxy-6-Methyl Pyrimidine and Study the Biological Activity” Inter J. Pharm Qual. Assurance., Vol. 11 no. 1, (2020), pp-53-59

[6]. O. A. Mohammed and O. S. Dahham., “Synthesis, Characterization, and Study of Antibacterial Activity of Some New Formazan Dyes Derivatives, Derived from 2-Mercapto Benzoxazole” Mater. Sci. Eng., Vol. 454 no. 1, (2015), pp. 1-11

[7]. J. P. Raval, P. R. Patel, N. H. Patel, P. S. Patel, V. D. Bhatt and K. N. Patel, “Synthesis, Characeterization and in vitro antibacterial activity of novel 3-(4-methoxyphenyl)-1-isonicotinoyl-5- (substituted phenyl)-formazans”., Inter. J. Chem. Tech. Res., Vol. 1, no. 3(2009), pp. 610-615.

[8]. H. K. Mahmoud. B. H. Asghar, M. F. Harras, T. A. Farghaly, “Nano-sized formazan analogues: Synthesis, structure elucidation, antimicrobial activity and docking study for COVID-19”., Bioorg. Chem., Vol. 105, no. 104354, (2020), pp. 1-14.

[9]. S. I. Marjadi, J. H. Solanki,1 and A. L. Patel, “Synthesis and antimicrobial activity of some new farmazan derivative” e- J. Chem., Vol. 6, no. 3, (2009), pp. 844-848.

[10]. H. G. J. Alqaraguli, Z. Y. Kadhim, A. N. Seewan, “Synthesis, Characterization , Theoretical study, Antioxidant activity and in Vitro Cytotoxicity Study of Novel Farmazan Derivatives Towards MCF -7 Cells”., Egypt. J. Chem., Vol. 65, no. 6, (2022), pp.181-188.

[11]. S. R. Chavan, P.P. Bhosale, A. P. Khadake, “Formazans in Pharmaceutical Chemistry”., Res. J. Pharm. Technol., Vol. 4, no. 4, (2011), pp. 510-514.

[12]. N. M. Aljamali, “Inventing of Macrocyclic Formazan Compounds with Their Evaluation in Nano-Behavior in the Scanning Microscope and Chromatography” Biomed. J. Scientific Tech. Res., Vol. 41, no. 3, (2022), pp. 32783-32792

[13]. M. E. Khalifa, E. A. Elkhawass, A. Pardede., M. Ninomiya, K. Tanaka and M. Koketsu., “A facile synthesis of formazon dyes conjugated with plasmonic nanoparticled as photosensitizers in photodynamic theapy against leukemia cell line”. Monatshefte Fur. Chemi., Vol. 149, no, 12, (2018), pp. 2195-2206.

[14]. H. A. Ahmed and N. M. Aljamali., “Preparation, Characteriztion, Antibacterial study, Toxicity study of new phenylene diamine-Formazan Derivatives”., Ind. J. Fore. Med. Toxico., Vol. 15, no. 2, (2021), pp. 3102-3112.

[15]. S. E. M. Reda, L. Moradi, N. M. Aljamali, “Preparation and Characterization of Novel types of formazon derivatives”, J. Pharm. Neg. Results., Vol. 13, no. 7, (2022), pp. 7167-7191

[16]. L. A. Khaleel, S. Adnan, J. H. Mohmmed, “Synthesis, Charecterization of new formazon derivatives and study of biological and anticancer activity”., AIP Conf. Proc. 2845, 020018 (2023)

International Journal of Scientific Research in Science and Technology
Available online at : www.ijsrst.com
Print ISSN: 2395-6011 | Online ISSN: 2395-602X
doi : https://doi.org/10.32628/IJSRST

Emerging Trends in Farming - A Review

Rohini Bhagyawant[1], Ashvini Sonone[2]
[1]Department of Botany, Siddharth Art's, Commerce and Science College, Jafrabad, Maharashtra, India
[2]Department of Chemistry, Siddharth Art's, Commerce and Science College, Jafrabad, Maharashtra, India

ARTICLEINFO

Article History :

Published : 07 Dec 2024

Publication Issue :
Volume 11, Issue 23
Nov-Dec-2024
Page Number :
371-379

ABSTRACT

In recent year, agriculture field undergoes to various transformative changes, which navigates the technological advancements, environmental challenges. This literature review focuses on different techniques of forming such as Electro culture, Hydroponic farming, Organic farming and Vertical farming. These trends increase yield of crops and strengthen the agricultural sector to overcome emerging challenges. The fourth revolution is thought to be a potential way to boost agricultureal growth and fairly, resiliently and sustainably meet the needs of the world's population in the future. In agriculture, farming technologies to be successfully implemented low-cost, easy-to-use techniques requiring fewer workers and lower overall setup and operating costs are essential.

Keywords: Agriculture, Electro culture, Hydroponic farming, Organic farming and Vertical farming, Emerging challenges.

Introduction

The process of farming was begun when man chosen certain plants species for cultivation and domestication, they started cultivation of wild species under the management of humans. Egyptians and Babylonians around 10,000 BC and 4000 BC started farming on large scale. Agriculture developed independently in many regions of world and wild varieties of plants were domesticated at different times and different places. In India the farming began, around 9000 BC (Stain, Burton 1998) Wheat, barley and jujuba were firstly cultivated in India and its subcontinents.

The food grain production in world was increased with the development of civilization. New techniques and methods were developed to increase the yield of crop plants. For increasing the production of crop different types of pesticides and fertilizers are used in the farming with the help of this production and yield of crop plants was increased. In the world, area under cultivation was 4.8 billion hector and this area increases day by day. In India, around 159.7 million hector areas are under cultivation. Food grain production in India was increased from 54.92 million tonnes to 127.06 million tones, it about 224% during 1949 to 1986 period of 36 years. India become self sufficient in foodgrain production but the population of growing India is at alarming

rate 2.5% per year, so that, it is necessary to increase the production of foodgrain to fulfill the need of foodgrain production increase the area of crop cultivation. Use of fertilizers, pesticides, irrigation of water, improve cultivation practices, improve crop verities, and improve the management practices help to increase the yield of foodgrain, but still there is need of quality food for increasing population hence, different farming techniques were evolved these are

1. **Electro culture**
2. **Hydroponic farming**
3. **Organic farming**
4. **Vertical farming**

1. Electroculture

The word electro culture comes from Latin word electro means electric or electrically. Culture means way of life. Electrical way of life is known as Electro culture. It is a way to grow plants in agriculture with using electricity to stimulate plant growth by inserting electricity into plant nutrient by using different techniques. The idea of increasing the yield of agriculture by the use of electricity this technique is not new many successful experiments conducted by scientist. Electro culture is a group of technique, in that electricity and magnetism were use to assess the plant growth. Electricity plays an important role in plant life with the help of electro culture technique, can increase the yield of crop plants many researchers study the different techniques of electric culture such as Muller (L E 1966, Radzevicius 1885, Shabrangi 1906).

In the year 1749, Antonie Nollet studied effect of electricity on vegetation. Actual experimental study of electro culture begins in 18th century. Elfving in 1882 studied galvanotropic response of roots toward the current and electric discharge. After Elfving, many researchers work on the electricity and its work in plant development with the help of experiments. Nowadays researchers from different countries are starting to use electroculture in farming and are sharing their interest in it. These countries are trying to replace electricity with traditional fertilizers. China is one of the leading country to use electricity in the agriculture field and discovered techniques to increase food production using electricity and found that electricity boosted the yield of vegetables.

The different methods used in electroculture

It includes Antenna, Static electricity, Direct and Alternating current techniques can be applied to seed, soil, plant, water, and nutrients.

1) **Antenna system**
2) **Electrostatic system**
3) **Direct current**
4) **Alternating current**
5) **Electromagnetic seed treatment**

1) Advantages of electroculture

Electricity can help improve soil in several ways, like through processes called electro migration, electrophoresis, and electro osmosis. It helps separate plant nutrients from soil particles, making it easier for plant to absorb them. Normally, these nutrients are tied up in the soil, but when electricity is applied, they can break free. With these nutrients available, plants can grow better and develop faster.

The application of Electrostatic field was simple and powerful method to increase seed germination, shoot length and seed vigor, in tomato Gandhare Z W (2014).

Electricity not only increases the seed germination, also increase the effects on water uptake capacity of the seed, it leads to an increase in seed germination, germination percentage, and speed of germination in thyme (Mohammed S T 2021).

Application of electroculture, significantly effect on yield of crop plant to increases the height of plant, growth, height of stem and length of roots, in rice, Brassica plant.

Electroculture not only effect on germination and yield parameter of crop plant but it significantly increases the phenolic content of plant Electric field with different electric intensities significantly increases phenolic content in carrot plants (P Barman, R Bhattacharya, 2016).

Application of electro culture, increase the protein, carbohydrates and fats in wheat and groundnut.

2) Hydroponic farming-

Farming using water instead of soil is not new; ancient Babylonians used it around 600 BC. The Aztecs also used similar methods with floating gardens between 900 and 1000 AD. This type of farming is called hydroponics, where plants grow in nutrient-rich water. Hydroponic farming uses less water, land, and resources, which helps protect the environment.

In traditional farming, plants grow in soil. However, in hydroponic farming, soil is not needed. Instead, a special nutrient solution is used. Soil contains important nutrients that help plants grow, and in regular framing, plants get these nutrients through their roots, which takes a lot of energy and time. In hydroponic farming, these nutrients are given directly to the plants, making it easier and quicker for them to absorb what they need. The word "hydroponic" comes from Greek, where "hydro" means water and "ponics" means labor. In hydroponic framing, plants receive the right nutrients at the right time, which helps them grow better and produce more. There are six different types of hydroponic systems used in this method.

1. Wick system
2. Water culture
3. EBB and flow
4. Drip
5. NFT [nutrient field technology]
6. Aeroponic system

Advantages of hydroponic farming

Hydroponic farming is an alternative to traditional farming method. It reduced the requirement of water and useful in the areas where soil degradation and availability less water. This method of farming is eco-friendly because no use of fertilizers and pesticides (M. Kammae et al, 2022).

This method of farming is knows as future of farming. NASA with the help of this, astronauts can grow crop in space. Number of plants can grow in small area, but in traditional farming, it requires large area for cultivation. In hydroponic farming, it provides controlled environment for growing plants due to this there is no effect of climatic changes like floods, droughts etc.

As environment and climatic conditions artificially controlled in hydroponic farming, seasonal vegetable and fruit can cultivated thought out the year.

In traditional farming, large amount of water is utilized in farming but in hydroponic farming, only 10% water is used and can avoid water wastage which helps in water conservation.

Use of hydroponic farming reduces the time for yield and offering number of benefits. Hydroponic farming having ability to reuse of nutrients and water, it prevents soil born diseases (Lommen et al, 200, Molitor 1990).

3) Organic farming

Organic farming is a method of farming that focuses on cultivation of crops and raising livestock without the use of synthetic chemicals, pesticides, or genetically modified organisms (GMOs). The primary principles of organic farming include sustainability, conservation of biodiversity, and maintaining soil health through natural practices. The goal is to produce food that is both healthy for consumers and environmentally friendly, promoting long-term ecological balance (D. Rigby, D. Caceres, 2001).

Organic farming include:

- **Crop rotation**: Growing different crops in a specific sequence to improve soil health and reduce pest buildup.
- **Composting**: Using organic waste materials to improve soil fertility.
- **Biological pest control**: Using natural predators or organic-approved substances to manage pests and diseases.
- **Minimal or no use of synthetic chemicals**: Avoiding synthetic fertilizers, pesticides, and herbicides.

History of Organic Farming

The origins of organic farming can be traced back to the early 20th century, when concerns about the environmental impact of industrial agriculture began to surface. However, it was not until the mid-1900s that organic farming became a formal movement.

1. **Early Foundations (Pre-1900s)**:
    - Many early agricultural practices around the world, especially in traditional farming systems, were in line with organic principles, relying on natural methods and local resources.
    - Figures such as Sir Albert Howard, a British agricultural scientist, were influential in promoting the idea of returning to more traditional, nature-based methods of farming. His work with composting and soil health laid the foundation for the modern organic movement.
2. **Early 20th Century (1920s-1940s)**:
    - The development of organic farming can be linked to the work of pioneers like **Rudolf Steiner** (founder of biodynamic farming), and **E.F. Schumacher**, who promoted sustainable, small-scale farming techniques.
    - Steiner introduced the idea of **biodynamics**, a holistic form of organic farming that integrates spiritual, ecological, and agricultural practices.
3. **Post-WWII and Industrialization (1950s-1970s)**:
    - After World War II, the widespread use of synthetic fertilizers and pesticides became common, revolutionizing modern agriculture.
    - However, by the 1950s and 1960s, concerns about the environmental and health effects of industrial farming practices began to rise. Pioneers like **Rachel Carson** (author of *Silent Spring*) drew attention to the dangers of chemical pesticides.
    - Organic farming began to gain more traction as an alternative, particularly in Europe and North America. Key organizations like the **Soil Association** (UK, founded in 1946) and **Rodale Institute** (USA, founded in 1947) began to advocate for organic practices.
4. **1980s-1990s**:
    - The establishment of organic certification programs, particularly in the United States and Europe, helped standardize organic farming practices and distinguish organic products from conventional ones.
    - In 1990, the **Organic Foods Production Act** was passed in the U.S., which led to the creation of the USDA Organic certification system.

- In 1991, the **International Federation of Organic Agriculture Movements** (IFOAM) was founded to coordinate the global organic farming movement.

Recent Trends in Organic Farming

In recent years, organic farming has experienced significant growth and transformation, influenced by changing consumer preferences, advances in sustainable agricultural technology, and global efforts to address climate change and food security.

1. **Growth of Organic Market**:
   - The global market for organic food has expanded dramatically. Organic food sales reached **$120 billion globally** in 2020, with significant growth in regions like North America, Europe, and Asia. Consumers are increasingly willing to pay a premium for food that is perceived to be healthier and more environmentally friendly.
   - In the U.S., organic food sales were valued at over **$60 billion** in 2022, and the organic sector now represents a significant portion of agricultural sales.
2. **Advancements in Organic Technology**:
   - While organic farming has always focused on low-tech, natural approaches, there have been technological advancements that have supported its growth. These include:
     - **Precision farming** techniques adapted for organic methods, using GPS and sensors to optimize irrigation, monitor soil health, and reduce resource waste.
     - The development of **biological pest control** methods, such as introducing beneficial insects or using bio-based pesticides.
     - Innovations in organic **weed control** strategies, such as mechanical weeders and organic herbicides.
3. **Integration of Agroecology and Regenerative Agriculture**:
   - There is a growing movement towards **regenerative agriculture**, which seeks to go beyond sustainability by improving soil health and sequestering carbon. This includes practices like cover cropping, agroforestry, and holistic livestock management.
   - **Agroecology**, a framework that integrates ecological principles with agricultural practices, is being widely adopted within the organic movement. Agroecological practices support biodiversity, conserve water, and improve soil fertility.
4. **Environmental and Climate Change Focus**:
   - Organic farming has been increasingly seen as part of the solution to climate change. It is viewed as a more resilient approach to farming that is less reliant on external inputs (e.g., fossil fuels for synthetic fertilizers and pesticides) and can sequester carbon in soil.
   - Additionally, organic farming's emphasis on crop diversity and ecological balance can help improve biodiversity, reduce pollution, and mitigate the effects of extreme weather events.
5. **Expansion in Developing Countries**:
   - Organic farming is gaining momentum in developing countries, especially in Africa and Asia, where it is often used as a strategy for smallholder farmers to increase yields and access premium markets. However, challenges such as limited access to organic inputs and market infrastructure remain.
6. **Regulatory and Certification Challenges**:
   - As demand for organic products grows, the regulatory frameworks governing organic certification are becoming stricter. While this has led to increased consumer confidence, there are concerns over the complexity and cost of certification for small farmers.

- Additionally, issues such as **organic fraud** (the mislabelling of products as organic) and debates over the definition of "organic" are ongoing.

7. **Rise of Plant-Based and Vegan Trends**:
   - The increasing popularity of plant-based and vegan diets is aligning well with the growth of organic farming, as many consumers who prioritize sustainability and animal welfare are also drawn to organic food choices.
8. **Local and Regional Organic Farming**:
   - Local food movements are gaining momentum, with consumers increasingly looking for locally grown organic produce. This trend is driven by concerns over food miles, environmental impact, and the desire to support local economies.

Urban agriculture, including rooftop gardens and community-supported agriculture (CSA), is becoming more popular in cities, providing consumers with direct access to organic, locally grown food.

Organic farming evolved from a niche movement to a significant part of global agriculture. The history of organic farming is intertwined with concerns over environmental degradation, health issues related to synthetic chemicals, and the search for more sustainable food systems. Today, organic farming continues to grow in popularity and sophistication, influenced by technological advances, shifting consumer preferences, and a focus on environmental sustainability. As the world faces challenges like climate change, soil degradation, and biodiversity loss, organic farming offers a promising pathway toward a more resilient and sustainable food system.

4) Vertical Farming-

Vertical farming is a method of growing crops in vertically stacked layers, usually within controlled indoor environments. These systems can be used to grow a variety of plants, such as leafy greens, herbs, fruits, and even some types of grains. It typically relies on technologies like hydroponics, aeroponics, and aquaponics, which enable plants to grow without soil by using nutrient-rich water or mist. Vertical farming takes place in urban areas or within structures like warehouses, skyscrapers, or shipping containers, making it a viable option for growing food in cities where traditional farming may not be feasible due to space or resource constraints (Purabi Barui, 2022).

History of Vertical Farming

Vertical farming, as a modern agricultural concept, emerged in the 1990s. Dickson Despommier, a professor of environmental health at Columbia University, who envisioned transforming urban spaces into farming hubs to address food shortages and environmental degradation, first popularized the idea.

1. **Early Concepts (Vertical Gardening):**
   - The idea of growing plants in multi-story structures dates back centuries, as seen in the hanging gardens of Babylon (circa 600 BC). However, the modern concept of vertical farming involves more sophisticated methods and technologies.
2. **1999 - The Birth of the Modern Vertical Farming Concept:**
   - Dickson Despommier introduced an idea about "Vertical Farms" as a sustainable solution for urban food production. His work focused on utilizing vertical space in cities to provide fresh produce while reducing the environmental footprint of traditional farming.
3. **2000s - The First Pilot Projects:**
   - As the concept gained traction, several pilot projects and experiments began to emerge, especially in places like Japan, Singapore, and the United States. In 2010, the first commercial vertical farm, "The Plant," was established in Chicago, which helped to demonstrate the viability of such systems.

4. **Present Day:**
    - Vertical farming has expanded globally, with significant investment in the technology, research, and infrastructure of vertical farms. Major companies like **Plenty**, **Bowery Farming**, and **Aerofarms** are leading the way in scaling up vertical farming operations, particularly in urban environments.

Benefits of Vertical Farming

1. **Space Efficiency:**
    - One of the most significant benefits of vertical farming is its ability to grow crops in stacked layers, utilizing the vertical space in buildings, warehouses, or unused urban areas. This can significantly increase food production in cities with limited space.
2. **Water Efficiency:**
    - Traditional farming uses vast amounts of water, much of which is lost through evaporation, runoff, or irrigation. Vertical farms typically use hydroponics (growing plants in nutrient-rich water) or aeroponics (growing plants in mist) which are more water-efficient methods. These systems recycle water, often reducing consumption by up to 90% compared to traditional farming.
3. **Reduced Environmental Impact:**
    - Vertical farming reduces the need for large-scale agricultural land, reducing deforestation and the degradation of ecosystems. Furthermore, since these farms are often powered by renewable energy sources like solar or wind, they can have a lower carbon footprint compared to traditional agriculture, which heavily relies on fossil fuels.
4. **Year-Round Crop Production:**
    - Because vertical farms are housed in controlled environments (often indoors), they are not affected by external weather conditions. This means crops can be grown year-round, leading to consistent yields and fresh produce even in regions with harsh climates or off-seasons.
5. **Reduction in Food Miles:**
    - Vertical farming allows food to be grown closer to urban centers, reducing the need for long-distance transportation, which contributes to carbon emissions and food spoilage. This is particularly important in cities where fresh produce may be imported from faraway regions.
6. **Increased Crop Yield:**
    - The controlled environment of vertical farming allows for precise regulation of variables like light, temperature, humidity, and nutrients. This can lead to faster growth cycles and higher crop yields compared to traditional farming methods, which are subject to weather patterns and soil health.

Features of Vertical Farming Systems

1. **Hydroponics:**
    - Hydroponics is the most common method used in vertical farming. It involves growing plants in a nutrient-rich water solution, bypassing the need for soil. The roots of the plants are submerged in the solution, which provides all the necessary nutrients for growth.
2. **Aeroponics:**
    - Aeroponics is another advanced method used in vertical farming. In this system, plants grow with their roots suspended in air and misted with nutrient-rich water. Aeroponics is known for its water efficiency and promotes faster plant growth due to the high oxygen levels around the roots.

3. **Aquaponics:**
    - Aquaponics is a combination of hydroponics and aquaculture (fish farming). In this system, fish are raised in tanks, and their waste provides nutrients for the plants. In turn, the plants help filter and clean the water, creating a sustainable, symbiotic relationship between the plants and fish.
4. **LED Lighting:**
    - Vertical farms often use LED (light-emitting diode) lights to provide the necessary light for photosynthesis, particularly in indoor environments where natural sunlight may not be sufficient. LEDs are energy-efficient and can be tailored to emit specific wavelengths of light that optimize plant growth.
5. **Automation and Data Analytics:**
    - Many vertical farms use sensors, robotics, and automated systems to monitor and optimize the growing conditions. Data analytics and machine learning can predict crop yield, water usage, and environmental conditions, ensuring optimal performance and resource usage.
6. **Climate Control:**
    - Vertical farming systems often incorporate advanced climate control technology to maintain optimal growing conditions, such as temperature, humidity, and CO2 levels. This enables crops to grow faster and more consistently.

Challenges of Vertical Farming

While vertical farming holds many promises, it also faces challenges:

1. **High Initial Capital Investment:**
    - Setting up vertical farms requires significant upfront investment in infrastructure, technology, and systems. While operational costs may be lower over time, the high initial cost can be a barrier to entry.
2. **Energy Consumption:**
    - Although vertical farming reduces water and land use, it often relies on artificial lighting (LEDs) and climate control systems, which can result in high energy consumption. However, using renewable energy sources can mitigate this impact.
3. **Technical Expertise:**
    - Vertical farming requires specialized knowledge and expertise in areas like horticulture, engineering, and technology. This can make it difficult to scale rapidly and requires skilled labor.
4. **Limited Crop Variety:**
    - Vertical farming is most effective for certain types of crops, especially leafy greens and herbs. Growing larger crops, such as grains, fruits, or root vegetables, can be more challenging due to space and resource constraints.

Vertical farming offers a promising solution to many of the challenges faced by conventional agriculture, particularly in urban settings. It can help reduce land use, water consumption, and the carbon footprint associated with traditional farming. However, it requires substantial investment, technical expertise, and innovation to reach its full potential. As technology advances, vertical farming may become an increasingly important tool in feeding the world's growing population sustainably.

References

[1]. Stein, Burton (1998), A History of India, Blackwell Publishing, ISBN 0-631-205462.

[2]. Murr LE (1966). Plant physiology in simulated geoelectric and geomagnetic fields. Advancing Frontiers of Plant Science 15, 97-120.

[3]. Radzevicius Audrius , Sandra Sakalauskienė, Mindaunas Danys Rimantas Simniskis Rasa Zemdirbyste (1885). The effect of strong microwave electric field radiation on:(1) vegetable seed germination and seedling growth rate. Agriculture 100(2);179-184.
[4]. Shabrangi Azita, Majd Ahmad, Sheidai Masoud, Mohammad Nabyouni, Davoud Dorranian (1906). Comparing effects of extremely low frequency electromagnetic fields on the biomass weight of C3 and C4 plants in early vegetative growth. Progress in Electromagnetics Research 593.
[5]. Nollette Jean-Antoine (1749). Recherches sur les causes particulières des phénomènes électriques, et sur les effets nuisibles ou avantageux qu'on peut en attendre. Par M. l'Abbé Nollet.chez les freres Guerin, rue S. Jacques, à S. Thomas d'Aquin.444.
[6]. Patwardhan MS, Gandhare WZ, , (2014). A New Approach of Electric Field Adoption for Germination Improvement. Journal of Power and Energy Engineering 2(4):13-18.
[7]. Barman, P., & Bhattacharya, R. (2016). Impact of electric and magnetic field exposure on young plants-A review. International journal of current research and academic review, 4(2), 182-192.
[8]. Reddy, B. Suresh (2010). Organic Farming: Status, Issues and Prospects – A Review. Agricultural Economics Research Review. Vol. 23 July-December 2010 pp 343-358.
[9]. Alam, Anwar and Wani Shafiq, A. (2003) Status of organic agriculture worldwide–An overview, In: Proceedings of National Seminar on Organic Products and their Future Prospects, Sher-e-Kashmir, University of Agricultural Sciences and Technology, Srinagar, pp. 95-103.
[10]. Barui, P., Ghosh, P., & Debangshi, U. (2022). Vertical farming-an overview. Plant Archives (09725210), 22(2).
[11]. Dickson Despommier (2010). The Vertical Farm: Feeding the World in the 21st Century. Thomas Dunne Books.
[12]. Despommier, D. (2013). "The Vertical Farm: A Review of the Literature." Sustainability.
[13]. David J. (2019). The Future of Agriculture: How Technology Will Change the Way We Farm. Wiley.
[14]. "Vertical Farming: The Future of Food?" (2018). BBC News. Aerofarms (2020). Annual Report on Vertical Farming

International Journal of Scientific Research in Science and Technology
Available online at : www.ijsrst.com
Print ISSN: 2395-6011 | Online ISSN: 2395-602X
doi : https://doi.org/10.32628/IJSRST

Adsorption of Heavy Metals from Waste Water Using Low Cost-Adsorbent: A Review

Shaikh Naushaba Gulrez, Samreen Fatema, Mazahar Farooqui
Post Graduate and Research Canter, Maulana Azad College of Arts, Science and Commerce, Rauza Bagh, Aurangabad (431001), Maharashtra, India

ARTICLEINFO

Article History :

Published : 07 Dec 2024

Publication Issue :
Volume 11, Issue 23
Nov-Dec-2024
Page Number :
380-393

ABSTRACT

Heavy metal pollution is a major problem in the environment. The impact of toxic metal ions can be minimized by different technologies but out of all, adsorption was found to be very effective due to ease of operation and economically feasible properties. The number of low-cost adsorbents has been investigated as a replacement for current costly methods of removing heavy metals from solution. In this review, several low cost adsorbents in the recent literature have been studied. The maximum adsorption capacity and percentage removal were revised and summarized in this review for further reference. Some of the natural adsorbents appeared as good heavy metal removal, while some were not. The objective of this study is to contribute in the search for less expensive adsorbents and their utilization possibilities for various agricultural waste by-products such as seaweed, algae, chitosan, egg shell and saw dust etc. for the elimination of heavy metals from wastewater.

Keywords: Heavy Metals, Wastewater, Adsorption, lowcost Adsorbent

Introduction

Water pollution raises a great concern nowadays. The fast-paced development of industries such as metal mining operations, fertilizers and paper industries metallurgical, chemical, tannery, battery and nuclear, agriculture, shipping and others have discharging various types of pollutants into the environment especially in developing countries[1-2]. Among other issues, water contaminations by heavy metals are more pronounced than other pollutants which may affect the quality of water supply [3]. Some of the hazardous heavy metal ions which pose potential danger threat to human health are nickel, zinc arsenic, mercury, chromium, cadmium, and lead. Heavy metal ions noted are not recyclable and accumulate in living organisms [4-5].

Heavy metals are unique part of the nature and most of them are biogenic means most of them are necessary for nature and human bodies but in small concentrations. Due to continuous exposure of these metals in water could be a reason for high dose in human body may lead toxicity [6]. The present world faces the risk of heavy

metal ions most since they are very toxic and carcinogenic in nature [7]. Heavy metals are non biodegradable pollutants and are very difficult to eliminate naturally from the environment [8] Moreover, since they are toxic, they cause illnesses and diseases such as lung cancer and cancers of other respiratory organs, the kidney and bladder, damage to the brain and reproductive organs, and heart and immune system disorders [9-10].

Hence there is burning need for the removal of heavy metals from the wastewater, to regulate the uncontrollable discharge of these hazardous pollutants in wastewater. Therefore treatment technologies are proposing globally and various technologies that are currently used for the removal of heavy metals are evaporation, Ion exchange, precipitation, membrane filtration, and adsorption [11-12] however these methods have several disadvantages such as high reagent requirement, unpredictable metal ion removal, generation of toxic sludge, etc. Among the mentioned methods, adsorption is considered to be one of the most appropriate techniques, Adsorption process being very simple, economical, effective and versatile has become the most preferred methods for removal of toxic contaminants from wastewater [13-17]

Comparatively, the adsorption process seems to be a significant technique [18] due to its wide applications, such as ease of operation, economic feasibility, wide availability and simplicity of design [19], but there are disadvantages to this method, including small capacity and difficulty for large-scale application, etc [20].Various types of natural materials or wastes have been utilized as adsorbents for the adsorption process due to their potential adsorption capacities. In the category of low-cost adsorbents, both natural adsorbents and bio-adsorbents [21] are used. In natural materials, zeolites, clay, chitosan and red mud are utilized as adsorbents. The main sources of bio-adsorbents are agricultural and animal waste materials. [22]

There are several kinds of adsorbents for removal of heavy metals, such as activated carbon [23] , carbon nanotubes [24] , graphene oxide[25], mesoporous silica, and mesoporous carbon[26], clays, zeolites[27], metal organic frameworks [28], and adsorbents from industrial/agricultural by-product residues[29] . Recently attention has been diverted towards the biomaterials which are byproducts or the wastes from large scale industrial operations and agricultural waste materials. . The use of such materials as low-cost adsorbents has double benefits to the environment. First, these materials are converted into high added value adsorbents, and second, these adsorbents are suitable for water and wastewater purification [30]

These agricultural by-products have been used in their raw form or after some physical or chemical modification [31]. Hydrothermal treatment and conventional pyrolysis are two of the most commonly used methods to increase the adsorption capacity of the agricultural residues[32] Agricultural residues, also called “lingo” cellulosic biomass resource, are defined as a biomass byproduct from the agricultural system and include stalks, leaves, seeds, shell, peels, husks, and straws. [33] Agricultural waste materials being economic and ecofriendly due to their unique chemical composition, availability in abundance, renewable, low in cost and more efficient are seem to be viable option for heavy metal remediation [34].

This review provides detailed information about the use of low-cost materials as adsorbents for the removal of heavy metal ions. A crucial analysis of low-cost adsorbent materials has been made and their features and advantages have been described.

1. Comparison of current treatment methods of various metal ions:

	Methods	advantages	disadvantages	references
1	Ion-Exchange	High quality of metal removal, easy to use, high transformation of components	Expensive, can’t be used on large scale, highly sensitive to pH, removes only limited metals.	[35]

	Methods	advantages	disadvantages	references
2	Chemical Precipitation	Easy to use ,inexpensive,	Excess chemical required, disposal problem, generation and disposal of sludge	[36]
3	Coagulation	Suitable to large scale waste water treatment, cost effective, dewatering qualities	Expensive, large sludge production	[37]
4	Membrane Separation	Large amount of chemical used, less sludge production, lower space require, easy to operate,	High maintenance, operational cost, very expensive, membrane fouling, complex process	[38]
5	Reverse Osmosis	Effective removal	Required chemical cost is high, consumption of high power	[39]
6	Adsorption	Easy operation, less sludge production, utilization of low cost adsorbent	desorption	[40]

Sources and toxicity of heavy metals:

1. Nickel:

Nickel (Ni) is the 24th most abundant element in the Earth's crust, comprising about 3% of the composition of the earth. This metal is used in electroplating, battery production, stainless steel manufacturing. It causes variety of pathologic effects. [41] Its alloys are widely used in the metallurgical, chemical and food processing industries, especially as catalysts and pigments. The nickel salts of greatest commercial importance are nickel chloride, sulphate, nitrate, carbonate, hydroxide, acetate and oxide [42].The high concentration of this metal causes several effects on humans such as headache, dizziness, nausea, vomiting, several lung diseases, dermatitis, chronic asthma and also it is carcinogenic and even in severe condition death may take place. It is also genetoxic and mutagenic. [43-44] According to the US environmental protection agency(EPA) requires Ni not to exceed to 0.015 mg/l in drinking water, and WHO permissible limit is 2.0 mg/l. [45].

Table: 02) Low cost adsorbent used for the adsorption of Nickel:

Sr.No	Adsorbent material	Adsorption capacity(Mg/g)	Percentage removal	references
1	*Lancium domesticum* peel	10.1	90%	[46]
2	Mango peel	39.75	79.42%	[47]
3	Orange peel	162.6	…..	[48]
4	Lemon peel	…..	78%	[49]
5	Banana peel	…..	77.8%	[50]
6	Pomegranate peel	52	…..	[51]
7	Jack fruit peel	12.03	…..	[52]
8	Grape fruit	46.13	97%	[53]
9	Rice straw	35.08	…..	[54]
10	Tea waste	15.26	……	[55]
11	Chestnut shell	2.4	…..	[56]
12	Walnut shell	……	90.0%	[57]

Sr.No	Adsorbent material	Adsorption capacity(Mg/g)	Percentage removal	references
13	Neem bark	…..	84.75%	[58]
14	Corn cob	12	.....	[59]
15	Coconut husk	404.5	……	[60]

2. Lead:

Lead is considered as one of the most hazards and cumulative environmental pollutants that affect all biological systems through exposure to air, water, and food sources but it's also a disease of lifestyle. These are harmful to the nervous system, causes brain and heart disorder, damage fetal brain, diseases of kidney toxicity of the liver, hematopoietic system, and nervous system. Having a carcinogenic risk as well [61] .Lead is used in electroplating, burning of coal, battery manufacturing, paint and pigment production, mining and smelting [62]. Even small quantity of this metal ion can destroy the life of aquatic animal. According to WHO the max permissible concentration of lead is 0.05mg/l [63]

Table: 03) Low cost adsorbent used for the adsorption of Lead:

Sr.No	Peels	Adsorption capacity(Mg/g)	Percentage removal	references
1	Yellow passion fruit	151.6	98%	[64]
2	African wild mango	40	-	[65]
3	Water melon peel	130.23	99.9%	[66]
4	Plntain	85.9	-	[67]
5	Lemon peel	90.91	-	[68]
6	Pomegranate peel	-	95%	[69]
7	Mango peel	75.55	76.45%	[70]
8	Passion fruit	93.9	-	[71]
9	Coconut	6.2	-	[72]
10	Apricot	-	87%	[73]

3. Cadmium:

Cadmium has been included in the red list of priority pollutants by the Department of Environment, UK[74] Sources of cadmium human exposures are fossil fuels, iron and steel production, cement nonferrous metals production, waste incineration, smoking, fertilizers, etc. Refining, mining, welding, electrochemistry, and coating industries, battery production, fertilizers production, [75]. It is cancer causing agent mean carcinogenic. It causes renal disorder, nausea, salivation, diarrhea, muscular cramps, lung insufficiency, bone lesions, hypertension. According to WHO guidelines the permissible concentration of cadmium in drinking water is 0.003mg/l. [76-77]

Table: 04) Low cost adsorbent used for the adsorption of Cadmium:

Sr.No	Peels	Adsorption capacity(Mg/g)	Percentage removal	references
1	Pomegranate peel	23.5	-	[78]
2	Grape peel	42.04	-	[79]
3	Cucumber peel	58.14	-	[80]
4	Banana peel	35.52	95%	[81]

Sr.No	Peels	Adsorption capacity(Mg/g)	Percentage removal	references
5	Mango eel	68.92	-	[82]
6	Wheat straw	14.56	-	[83]
7	Sunflower stalk	42.18	-	[84]
8	Almond shell	8.08		[85]
9	Cassava peel	5.80	73%	[86]

4. Zinc:

Zinc is one of the most important trace elements in the organism, with three major biological roles, as catalyst, structural, and regulatory ion. [87]. Galvanization, paints, and rubber manufacturing fertilizer production. It is carcinogenic agent, causing nausea, vomiting, stomach diseases, anemia, damage pancreases, skin irritation, In many chronic diseases, including atherosclerosis, several malignancies, neurological disorders, autoimmune diseases, aging, age-related degenerative diseases, and Wilson's disease, the concurrent zinc deficiency may complicate the clinical features, affect adversely immunological status, increase oxidative stress, and lead to the generation of inflammatory cytokines[88]. According to WHO and Indian Standard the recommended level of zinc in drinking water is 5mg/l. [89].

Table: 05) Low cost adsorbent used for the adsorption of Zinc:

Sr.No	Peels	Adsorption capacity(Mg/g)	Percentage removal	references
1	Mango peel	28.21	78.30%	[90]
2	Black gram husk	33.81	-	[91]
3	Rice husk ash	14.30	-	[92]
4	Neem bark	13.29	-	[93]
5	Castor seed hull	6.72	-	[94]
6	Coir fibers	2.51	-	[95]
7	Sugarcane bagasse	31.11	-	[96]
8	Banana peel	5.80	-	[97]

5. Chromium:

Chromium (Cr) is a crucial trace element. The total body content of chromium decreases with age[98]. electroplating, leather lanning , Stainless steel production Alloy production Metal and alloy manufacturing Metal and alloy manufacturing Brick lining Chrome plating Leather tanning Textiles Dye and pigment manufacturing, plumping[99]., Inhalation of chromium increases the chances of hypersensitivity reactions like asthma, nasal irritability, nasal ulcers, skin lesions or rashes, lung cancer and contact dermatitis mutagenic, carcinogenic, asthma, failure of kidney and liver , skin allegies, lung carcinoma, [100] According to the Indian standard the permissible limit of Cr(VI) from industrial waste to be discharge to surface water IS 0.1 mg/l. WHO permissible limit 0.05mg/l. , [101]

Table: 06) Low cost adsorbent used for the adsorption of Chromium:

Sr.No	Peels	Adsorption capacity(Mg/g)	Percentage removal	references
1	Orange peel	40.56	82	[102]
2	Banana peel	131.56	80-99%	[103]

Sr.No	Peels	Adsorption capacity(Mg/g)	Percentage removal	references
3	Peat and coconut fiber	1.25	-	[104]
4	Rice husk	102.96	-	[105]
5	Almond	10.62	-	[106]
6	Sugar cane bagasse	13.4	-	[107]
7	eucalyptus bark	45.5		[108]
8	Groundnut hull	40		[109]

6. Copper:

Copper is a hazardous heavy metal that is used in various industries such as Equipment production,mining and smelting, electrical wiring, pestisides and fertilizers[110] ,its excessive uptake causes gasterointestinal ,bleeding, headache, dizziness, anemia, vomiting, insomniya, Wilson disease ,Convulsions,. [111] According to the united states environmental perotection agency the maximum contamination level goal is 1.3mg/l.. [112]

Table: 07) Low cost adsorbent used for the adsorption of Copper:

Sr.No	Peels	Adsorption capacity(Mg/g)	Percentage removal	references
1	Musk melon		90.2%	[113]
2	Orange peel	56.18	86.6%	[114]
3	Pomegranate peel	55	-	[115]
4	Mango peel	46.09	89.02%	[116]
5	Banana peel	4.75	-	[117]
6	Cassava peel	5.80	-	[118]
7	Rice husk	7.1	-	[119]
8	Wood apple shell	151.51	-	[120]
9	Neem leaves	62.97	-	[121]
10	Alfa grass	75.8	-	[122]

References

[1]. Summers, J. K., Shiomi, N., Zambare, V., & Din, M. F. M. (2023). Bioremediation for Global Environmental Conservation. BoD–Books on Demand.

[2]. Anjum, M., Miandad, R., Waqas, M., Gehany, F., & Barakat, M. A. (2019). Remediation of wastewater using various nano-materials. Arabian journal of chemistry, 12(8), 4897-4919.

[3]. Sonone, S. S., Jadhav, S., Sankhla, M. S., & Kumar, R. (2020). Water contamination by heavy metals and their toxic effect on aquaculture and human health through food Chain. Lett. Appl. NanoBioScience, 10(2), 2148-2166.

[4]. Mohammed, A. S., Kapri, A., & Goel, R. (2011). Heavy metal pollution: source, impact, and remedies. Biomanagement of metal-contaminated soils, 1-28.

[5]. Vardhan, K. H., Kumar, P. S., & Panda, R. C. (2019). A review on heavy metal pollution, toxicity and remedial measures: Current trends and future perspectives. Journal of Molecular Liquids, 290, 111197.

[6]. Bradl, H. (Ed.). (2005). Heavy metals in the environment: origin, interaction and remediation. Elsevier.

[7]. Munir, N., Jahangeer, M., Bouyahya, A., El Omari, N., Ghchime, R., Balahbib, A., ... & Shariati, M. A. (2021). Heavy metal contamination of natural foods is a serious health issue: A review. Sustainability, 14(1), 161.

[8]. Khalef, R. N., Hassan, A. I., & Saleh, H. M. (2022). Heavy metal's environmental impact. In Environmental Impact and Remediation of Heavy Metals. IntechOpen.

[9]. Velarde, L., Nabavi, M. S., Escalera, E., Antti, M. L., & Akhtar, F. (2023). Adsorption of heavy metals on natural zeolites: A review. Chemosphere, 328, 138508.

[10]. Fu, Z., & Xi, S. (2020). The effects of heavy metals on human metabolism. Toxicology mechanisms and methods, 30(3), 167-176.

[11]. Mahurpawar, M. (2015). Effects of heavy metals on human health. Int J Res Granthaalayah, 530(516), 1-7.

[12]. Gunatilake, S. K. (2015). Methods of removing heavy metals from industrial wastewater. Methods, 1(1), 14.

[13]. Gupta, V. K., Kumar, R., Nayak, A., Saleh, T. A., & Barakat, M. A. (2013). Adsorptive removal of dyes from aqueous solution onto carbon nanotubes: a review. Advances in colloid and interface science, 193, 24-34.

[14]. Weber, W. J., & Smith, E. H. (1987). Simulation and design models for adsorption processes. Environmental science & technology, 21(11), 1040-1050.

[15]. Meena, A. K., Kadirvelu, K., Mishra, G. K., Rajagopal, C., & Nagar, P. N. (2008). Adsorptive removal of heavy metals from aqueous solution by treated sawdust (Acacia arabica). Journal of hazardous materials, 150(3), 604-611.

[16]. Yu, B., Zhang, Y., Shukla, A., Shukla, S. S., & Dorris, K. L. (2000). The removal of heavy metal from aqueous solutions by sawdust adsorption—removal of copper. Journal of hazardous materials, 80(1-3), 33-42.

[17]. Ismail, U. M., Vohra, M. S., & Onaizi, S. A. (2024). Adsorptive removal of heavy metals from aqueous solutions: Progress of adsorbents development and their effectiveness. Environmental Research, 118562.

[18]. Rashid, R., Shafiq, I., Akhter, P., Iqbal, M. J., & Hussain, M. (2021). A state-of-the-art review on wastewater treatment techniques: the effectiveness of adsorption method. Environmental Science and Pollution Research, 28, 9050-9066.

[19]. Rajendran, S., Priya, A. K., Kumar, P. S., Hoang, T. K., Sekar, K., Chong, K. Y., ... & Show, P. L. (2022). A critical and recent developments on adsorption technique for removal of heavy metals from wastewater-A review. Chemosphere, 303, 135146.

[20]. Chai, W. S., Cheun, J. Y., Kumar, P. S., Mubashir, M., Majeed, Z., Banat, F., ... & Show, P. L. (2021). A review on conventional and novel materials towards heavy metal adsorption in wastewater treatment application. Journal of Cleaner Production, 296, 126589.

[21]. Foroutan, R., Oujifard, A., Papari, F., & Esmaeili, H. (2019). Calcined Umbonium vestiarium snail shell as an efficient adsorbent for treatment of wastewater containing Co (II). 3 Biotech, 9(3), 78.

[22]. Afroze, S., & Sen, T. K. (2018). A review on heavy metal ions and dye adsorption from water by agricultural solid waste adsorbents. Water, Air, & Soil Pollution, 229, 1-50.

[23]. Mariana, M., HPS, A. K., Mistar, E. M., Yahya, E. B., Alfatah, T., Danish, M., & Amayreh, M. (2021). Recent advances in activated carbon modification techniques for enhanced heavy metal adsorption. Journal of Water Process Engineering, 43, 102221.

[24]. Stafiej, A., & Pyrzynska, K. (2007). Adsorption of heavy metal ions with carbon nanotubes. Separation and purification technology, 58(1), 49-52.

[25]. Wang, J., & Chen, B. (2015). Adsorption and coadsorption of organic pollutants and a heavy metal by graphene oxide and reduced graphene materials. Chemical Engineering Journal, 281, 379-388.
[26]. Showkat, A. M., Zhang, Y. P., Kim, M. S., Gopalan, A. I., Reddy, K. R., & Lee, K. P. (2007). Analysis of heavy metal toxic ions by adsorption onto amino-functionalized ordered mesoporous silica. Bulletin of the Korean Chemical Society, 28(11), 1985-1992.
[27]. Jiménez-Castañeda, M. E., & Medina, D. I. (2017). Use of surfactant-modified zeolites and clays for the removal of heavy metals from water. Water, 9(4), 235.
[28]. Efome, J. E., Rana, D., Matsuura, T., & Lan, C. Q. (2018). Metal–organic frameworks supported on nanofibers to remove heavy metals. Journal of Materials Chemistry A, 6(10), 4550-4555.
[29]. Alalwan, H. A., Kadhom, M. A., & Alminshid, A. H. (2020). Removal of heavy metals from wastewater using agricultural byproducts. Journal of Water Supply: Research and Technology—AQUA, 69(2), 99-112.
[30]. Demirbas, A. (2008). Heavy metal adsorption onto agro-based waste materials: a review. Journal of hazardous materials, 157(2-3), 220-229.
[31]. Chen, B., & Chen, Z. (2009). Sorption of naphthalene and 1-naphthol by biochars of orange peels with different pyrolytic temperatures. Chemosphere, 76(1), 127-133.
[32]. He, W., Li, G., Kong, L., Wang, H., Huang, J., & Xu, J. (2008). Application of hydrothermal reaction in resource recovery of organic wastes. Resources, Conservation and Recycling, 52(5), 691-699.
[33]. Maia, L. C., Soares, L. C., & Gurgel, L. V. A. (2021). A review on the use of lignocellulosic materials for arsenic adsorption. Journal of Environmental Management, 288, 112397.
[34]. Renu, Agarwal, M., & Singh, K. (2017). Heavy metal removal from wastewater using various adsorbents: a review. Journal of Water Reuse and Desalination, 7(4), 387-419.
[35]. Vaaramaa, K., & Lehto, J. (2003). Removal of metals and anions from drinking water by ion exchange. Desalination, 155(2), 157-170.
[36]. BrbootI, M. M., Abid, B. A., & Al-ShuwaikI, N. M. (2011). Removal of heavy metals using chemicals precipitation. Eng. Technol. J, 29(3), 595-612.
[37]. Tang, X., Zheng, H., Teng, H., Sun, Y., Guo, J., Xie, W., ... & Chen, W. (2016). Chemical coagulation process for the removal of heavy metals from water: a review. Desalination and water treatment, 57(4), 1733-1748.
[38]. Huang, Y. C., & Koseoglu, S. S. (1993). Separation of heavy metals from industrial waste streams by membrane separation technology. Waste management, 13(5-7), 481-501.
[39]. Bakalár, T., Búgel, M., & Gajdošová, L. (2009). Heavy metal removal using reverse osmosis. Acta Montanistica Slovaca, 14(3), 250.
[40]. Rajendran, S., Priya, A. K., Kumar, P. S., Hoang, T. K., Sekar, K., Chong, K. Y., ... & Show, P. L. (2022). A critical and recent developments on adsorption technique for removal of heavy metals from wastewater-A review. Chemosphere, 303, 135146.
[41]. Cempel, M., & Nikel, G. J. P. J. S. (2006). Nickel: a review of its sources and environmental toxicology. Polish journal of environmental studies, 15(3).
[42]. Friberg, L., & Elinder, C. G. (1993). Biological monitoring of toxic metals. Scandinavian journal of work, environment & health, 7-13.
[43]. Begum, W., Rai, S., Banerjee, S., Bhattacharjee, S., Mondal, M. H., Bhattarai, A., & Saha, B. (2022). A comprehensive review on the sources, essentiality and toxicological profile of nickel. RSC advances, 12(15), 9139-9153.

[44]. Coogan, T. P., Latta, D. M., Snow, E. T., Costa, M., & Lawrence, A. (1989). Toxicity and carcinogenicity of nickel compounds. CRC Critical reviews in toxicology, 19(4), 341-384.
[45]. Meshram, P., & Pandey, B. D. (2019). Advanced review on extraction of nickel from primary and secondary sources. Mineral Processing and Extractive Metallurgy Review.
[46]. Lam, Y. F., Lee, L. Y., Chua, S. J., Lim, S. S., & Gan, S. (2016). Insights into the equilibrium, kinetic and thermodynamics of nickel removal by environmental friendly Lansium domesticum peel biosorbent. Ecotoxicology and environmental safety, 127, 61-70.
[47]. Iqbal, M., Saeed, A., & Kalim, I. (2009). Characterization of adsorptive capacity and investigation of mechanism of Cu2+, Ni2+ and Zn2+ adsorption on mango peel waste from constituted metal solution and genuine electroplating effluent. Separation Science and Technology, 44(15), 3770-3791.
[48]. Feng, N., Guo, X., Liang, S., Zhu, Y., & Liu, J. (2011). Biosorption of heavy metals from aqueous solutions by chemically modified orange peel. Journal of hazardous materials, 185(1), 49-54
[49]. Herrera-Barros, A., Bitar-Castro, N., Villabona-Ortíz, Á., Tejada-Tovar, C., & González-Delgado, Á. D. (2020). Nickel adsorption from aqueous solution using lemon peel biomass chemically modified with TiO2 nanoparticles. Sustainable Chemistry and Pharmacy, 17, 100299
[50]. Olufemi, B., & Eniodunmo, O. (2018). Adsorption of nickel (II) ions from aqueous solution using banana peel and coconut shell. International Journal of Technology, 9(3)
[51]. Bhatnagar, A., & Minocha, A. K. (2010). Biosorption optimization of nickel removal from water using Punica granatum peel waste. Colloids and Surfaces B: Biointerfaces, 76(2), 544-548.
[52]. Ranasinghe, S. H., Navaratne, A. N., & Priyantha, N. (2018). Enhancement of adsorption characteristics of Cr (III) and Ni (II) by surface modification of jackfruit peel biosorbent. Journal of Environmental Chemical Engineering, 6(5), 5670-5682.
[53]. Torab-Mostaedi, M., Asadollahzadeh, M., Hemmati, A., & Khosravi, A. (2013). Equilibrium, kinetic, and thermodynamic studies for biosorption of cadmium and nickel on grapefruit peel. Journal of the Taiwan Institute of Chemical Engineers, 44(2), 295-302.
[54]. El-Sayed, G. O., Dessouki, H. A., & Ibrahim, S. S. (2010). Biosorption of Ni (II) and Cd (II) ions from aqueous solutions onto rice straw. Chemical Sciences Journal, 9, 1-11.
[55]. Malkoc, E., & Nuhoglu, Y. (2005). Investigations of nickel (II) removal from aqueous solutions using tea factory waste. Journal of hazardous materials, 127(1-3), 120-128.
[56]. Vázquez, G., Calvo, M., Freire, M. S., González-Alvarez, J., & Antorrena, G. (2009). Chestnut shell as heavy metal adsorbent: optimization study of lead, copper and zinc cations removal. Journal of Hazardous Materials, 172(2-3), 1402-1414.
[57]. Jalilic, M. C. B. V. I. (2012). A comparative experimental study of the removal of heavy metals using low cost natural adsorbents and commerical activated carbon. International Journal, 3(1).
[58]. Naiya, T. K., Bhattacharya, A. K., & Das, S. K. (2008). Adsorption of Pb (II) by sawdust and neem bark from aqueous solutions. Environmental Progress, 27(3), 313-328.
[59]. Abdelfattah, I., Ismail, A. A., Al Sayed, F., Almedolab, A., & Aboelghait, K. M. (2016). Biosorption of heavy metals ions in real industrial wastewater using peanut husk as efficient and cost effective adsorbent. Environmental Nanotechnology, Monitoring & Management, 6, 176-183.
[60]. Malik, R., & Dahiya, S. (2017). An experimental and quantum chemical study of removal of utmostly quantified heavy metals in wastewater using coconut husk: A novel approach to mechanism. International journal of biological macromolecules, 98, 139-149.
[61]. Ara, A., & Usmani, J. A. (2015). Lead toxicity: a review. Interdisciplinary toxicology, 8(2), 55-64.

[62]. Papanikolaou, N. C., Hatzidaki, E. G., Belivanis, S., Tzanakakis, G. N., & Tsatsakis, A. M. (2005). Lead toxicity update. A brief review. Medical science monitor, 11(10), RA329-RA336.]

[63]. Naja, G. M., & Volesky, B. (2017). Toxicity and sources of Pb, Cd, Hg, Cr, As, and radionuclides in the environment. In Handbook of advanced industrial and hazardous wastes management (pp. 855-903). Crc Press.

[64]. Jacques, R. A., Lima, E. C., Dias, S. L., Mazzocato, A. C., & Pavan, F. A. (2007). Yellow passion-fruit shell as biosorbent to remove Cr (III) and Pb (II) from aqueous solution. Separation and Purification Technology, 57(1), 193-198.

[65]. Adekola, F. A., Adegoke, H. I., & Ajikanle, R. A. (2016). Kinetic and equilibrium studies of Pb (II) and Cd (II) adsorption on African wild mango (Irvingia gabonensis) shell. Bulletin of the Chemical Society of Ethiopia, 30(2), 185-198.

[66]. Moreno-Barbosa, J. J., López-Velandia, C., Maldonado, A. D. P., Giraldo, L., & Moreno-Piraján, J. C. (2013). Removal of lead (II) and zinc (II) ions from aqueous solutions by adsorption onto activated carbon synthesized from watermelon shell and walnut shell. Adsorption, 19, 675-685.

[67]. Sudha, R., & Premkumar, P. (2016). Lead removal by waste organic plant source materials review. International Journal of ChemTech Research, 9(01), 47-57.

[68]. Wanja, N. E., Murungi, J., Ali, A. H., & Wanjau, R. (2016). Efficacy of adsorption of Cu (II), Pb (II) and Cd (II) Ions onto acid activated watermelon peels biomass from water. International Journal of Science and Research, 5(8), 671-679.

[69]. El-Ashtoukhy, E. S., Amin, N. K., & Abdelwahab, O. (2008). Removal of lead (II) and copper (II) from aqueous solution using pomegranate peel as a new adsorbent. Desalination, 223(1-3), 162-173.

[70]. Iqbal, M., Saeed, A., & Zafar, S. I. (2009). FTIR spectrophotometry, kinetics and adsorption isotherms modeling, ion exchange, and EDX analysis for understanding the mechanism of Cd2+ and Pb2+ removal by mango peel waste. Journal of hazardous materials, 164(1), 161-171.

[71]. Chao, H. P., Chang, C. C., & Nieva, A. (2014). Biosorption of heavy metals on Citrus maxima peel, passion fruit shell, and sugarcane bagasse in a fixed-bed column. Journal of Industrial and Engineering Chemistry, 20(5), 3408-3414.

[72]. Okafor, P. C., Okon, P. U., Daniel, E. F., & Ebenso, E. E. (2012). Adsorption capacity of coconut (Cocos nucifera L.) shell for lead, copper, cadmium and arsenic from aqueous solutions. International Journal of Electrochemical Science, 7(12), 12354-12369.

[73]. Šoštarić, T. D., Petrović, M. S., Pastor, F. T., Lončarević, D. R., Petrović, J. T., Milojković, J. V., & Stojanović, M. D. (2018). Study of heavy metals biosorption on native and alkali-treated apricot shells and its application in wastewater treatment. Journal of Molecular Liquids, 259, 340-349.

[74]. Wang, F. Y., Wang, H., & Ma, J. W. (2010). Adsorption of cadmium (II) ions from aqueous solution by a new low-cost adsorbent—Bamboo charcoal. Journal of hazardous materials, 177(1-3), 300-306.

[75]. Dubey, A. M. S. S. A., Mishra, A., & Singhal, S. (2014). Application of dried plant biomass as novel low-cost adsorbent for removal of cadmium from aqueous solution. International journal of environmental science and technology, 11, 1043-1050.

[76]. Tripathi, A., & Ranjan, M. R. (2015). Heavy metal removal from wastewater using low cost adsorbents. J Bioremed Biodeg, 6(6), 315.

[77]. Lim, A. P., & Aris, A. Z. (2014). A review on economically adsorbents on heavy metals removal in water and wastewater. Reviews in Environmental Science and Bio/Technology, 13, 163-181.

[78]. Chen, Y., Wang, H., Zhao, W., & Huang, S. (2018). Four different kinds of peels as adsorbents for the removal of Cd (II) from aqueous solution: Kinetics, isotherm and mechanism. Journal of the Taiwan Institute of Chemical Engineers, 88, 146-151.

[79]. Efficacy and field applicability of Burmese grape leaf extract (BGLE) for cadmium removal: An implication of metal removal from natural water. Ecotoxicol.

[80]. Pandey, R., Ansari, N. G., Prasad, R. L., & Murthy, R. C. (2014). Removal of Cd (II) ions from simulated wastewater by HCl modified Cucumis sativus peel: Equilibrium and kinetic study. Air, Soil and Water Research, 7, ASWR-S16488.

[81]. Memon, J. R., Memon, S. Q., Bhanger, M. I., Memon, G. Z., El-Turki, A., & Allen, G. C. (2008). Characterization of banana peel by scanning electron microscopy and FT-IR spectroscopy and its use for cadmium removal. Colloids and Surfaces B: Biointerfaces, 66(2), 260-265.

[82]. Iqbal, M., Saeed, A., & Zafar, S. I. (2009). FTIR spectrophotometry, kinetics and adsorption isotherms modeling, ion exchange, and EDX analysis for understanding the mechanism of Cd2+ and Pb2+ removal by mango peel waste. Journal of hazardous materials, 164(1), 161-171.

[83]. Dang, V. B. H., Doan, H. D., Dang-Vu, T., & Lohi, A. (2009). Equilibrium and kinetics of biosorption of cadmium (II) and copper (II) ions by wheat straw. Bioresource technology, 100(1), 211-219.p

[84]. Sun, G., & Shi, W. (1998). Sunflower stalks as adsorbents for the removal of metal ions from wastewater. Industrial & engineering chemistry research, 37(4), 1324-1328.

[85]. Pehlivan, E., Altun, T., Cetin, S., & Bhanger, M. I. (2009). Lead sorption by waste biomass of hazelnut and almond shell. Journal of hazardous materials, 167(1-3), 1203-1208.

[86]. Owamah, H. I. (2014). Biosorptive removal of Pb (II) and Cu (II) from wastewater using activated carbon from cassava peels. Journal of Material Cycles and Waste Management, 16, 347-358.

[87]. Prasad, A. S. (2008). Zinc in human health: effect of zinc on immune cells. Molecular medicine, 14, 353-357.

[88]. Frassinetti, S., Bronzetti, G. L., Caltavuturo, L., Cini, M., & Della Croce, C. (2006). The role of zinc in life: a review. Journal of environmental pathology, toxicology and oncology, 25(3).

[89]. Fosmire, G. J. (1990). Zinc toxicity. The American journal of clinical nutrition, 51(2), 225-227.

[90]. Iqbal, M., Saeed, A., & Kalim, I. (2009). Characterization of adsorptive capacity and investigation of mechanism of Cu2+, Ni2+ and Zn2+ adsorption on mango peel waste from constituted metal solution and genuine electroplating effluent. Separation Science and Technology, 44(15), 3770-3791.

[91]. Saeed, A., Iqbal, M., & Akhtar, M. W. (2005). Removal and recovery of lead (II) from single and multimetal (Cd, Cu, Ni, Zn) solutions by crop milling waste (black gram husk). Journal of hazardous materials, 117(1), 65-73.

[92]. Bhattacharya, A. K., Mandal, S. N., & Das, S. K. (2006). Adsorption of Zn (II) from aqueous solution by using different adsorbents. Chemical Engineering Journal, 123(1-2), 43-51.

[93]. Bhattacharya, A. K., Mandal, S. N., & Das, S. K. (2006). Adsorption of Zn (II) from aqueous solution by using different adsorbents. Chemical Engineering Journal, 123(1-2), 43-51.

[94]. Mohammod, M., Sen, T. K., Maitra, S., & Dutta, B. K. (2011). Removal of Zn 2+ from aqueous solution using castor seed hull. Water, Air, & Soil Pollution, 215, 609-620.

[95]. Shukla, S. R., Pai, R. S., & Shendarkar, A. D. (2006). Adsorption of Ni (II), Zn (II) and Fe (II) on modified coir fibres. Separation and purification technology, 47(3), 141-147.

[96]. Mondal, M. K., Singh, R. S., Kumar, A., & Prasad, B. M. (2011). Removal of acid red-94 from aqueous solution using sugar cane dust: An agro-industry waste. Korean Journal of Chemical Engineering, 28, 1386-1392.

[97]. Annadurai, G., Juang, R. S., & Lee, D. J. (2003). Adsorption of heavy metals from water using banana and orange peels. Water science and technology, 47(1), 185-190.

[98]. Adamu, N., & Kumar, J. (2022). Review on chromium: therapeutic uses and toxicological effects on human health. The Journal of Multidisciplinary Research, 23-30.

[99]. Pereira, S. C., Oliveira, P. F., Oliveira, S. R., Pereira, M. D. L., & Alves, M. G. (2021). Impact of environmental and lifestyle use of chromium on male fertility: focus on antioxidant activity and oxidative stress. Antioxidants, 10(9), 1365.

[100]. Ukhurebor, K. E., Aigbe, U. O., Onyancha, R. B., Nwankwo, W., Osibote, O. A., Paumo, H. K., ... & Siloko, I. U. (2021). Effect of hexavalent chromium on the environment and removal techniques: a review. Journal of Environmental Management, 280, 111809.

[101]. DesMarias, T. L., & Costa, M. (2019). Mechanisms of chromium-induced toxicity. Current opinion in toxicology, 14, 1-7.

[102]. Marín, A. P., Ortuno, J. F., Aguilar, M. I., Meseguer, V. F., Sáez, J., & Lloréns, M. (2010). Use of chemical modification to determine the binding of Cd (II), Zn (II) and Cr (III) ions by orange waste. Biochemical Engineering Journal, 53(1), 2-6.

[103]. Memon, J. R., Memon, S. Q., Bhanger, M. I., El-Turki, A., Hallam, K. R., & Allen, G. C. (2009). Banana peel: a green and economical sorbent for the selective removal of Cr (VI) from industrial wastewater. Colloids and surfaces B: Biointerfaces, 70(2), 232-237

[104]. Henryk, K., Jarosław, C., & Witold, Ż. (2016). Peat and coconut fiber as biofilters for chromium adsorption from contaminated wastewaters. Environmental Science and Pollution Research, 23, 527-534.

[105]. Vieira, M. G. A., de Almeida Neto, A. F., Silva, M. G., Nóbrega, C. C., & Melo Filho, A. A. (2012). Characterization and use of in natura and calcined rice husks for biosorption of heavy metals ions from aqueous effluents. Brazilian Journal of Chemical Engineering, 29, 619-634.

[106]. Dakiky, M., Khamis, M., Manassra, A., & Mer'Eb, M. (2002). Selective adsorption of chromium (VI) in industrial wastewater using low-cost abundantly available adsorbents. Advances in environmental research, 6(4), 533-540.

[107]. Sharma, D. C., & Forster, C. F. (1994). A preliminary examination into the adsorption of hexavalent chromium using low-cost adsorbents. Bioresource Technology, 47(3), 257-264.

[108]. Sarin, V., & Pant, K. (2006). Removal of chromium from industrial waste by using eucalyptus bark. Bioresource technology, 97(1), 15-20.

[109]. Qaiser, S., Saleemi, A. R., & Umar, M. (2009). Biosorption of lead (II) and chromium (VI) on groundnut hull: Equilibrium, kinetics and thermodynamics study. Electronic journal of Biotechnology, 12(4), 3-4.

[110]. Aydın, H., Bulut, Y., & Yerlikaya, Ç. (2008). Removal of copper (II) from aqueous solution by adsorption onto low-cost adsorbents. Journal of environmental management, 87(1), 37-45.

[111]. Gupta, M., Gupta, H., & Kharat, D. S. (2018). Adsorption of Cu (II) by low cost adsorbents and the cost analysis. Environmental technology & innovation, 10, 91-101.

[112]. Milicevic, S., Boljanac, T., Martinovic, S., Vlahovic, M., Milosevic, V., & Babic, B. (2012). Removal of copper from aqueous solutions by low cost adsorbent-Kolubara lignite. Fuel Processing Technology, 95, 1-7.

[113]. Khan, T. A., Mukhlif, A. A., & Khan, E. A. (2017). Uptake of Cu2+ and Zn2+ from simulated wastewater using muskmelon peel biochar: Isotherm and kinetic studies. Egyptian journal of basic and applied sciences, 4(3), 236-248.

[114]. FENG, N. C., & GUO, X. Y. (2012). Characterization of adsorptive capacity and mechanisms on adsorption of copper, lead and zinc by modified orange peel. Transactions of Nonferrous Metals Society of China, 22(5), 1224-1231.

[115]. El-Ashtoukhy, E. S., Amin, N. K., & Abdelwahab, O. (2008). Removal of lead (II) and copper (II) from aqueous solution using pomegranate peel as a new adsorbent. Desalination, 223(1-3), 162-173.

[116]. Iqbal, M., Saeed, A., & Kalim, I. (2009). Characterization of adsorptive capacity and investigation of mechanism of Cu2+, Ni2+ and Zn2+ adsorption on mango peel waste from constituted metal solution and genuine electroplating effluent. Separation Science and Technology, 44(15), 3770-3791.

[117]. Annadurai, G., Juang, R. S., & Lee, D. J. (2003). Adsorption of heavy metals from water using banana and orange peels. Water science and technology, 47(1), 185-190.

[118]. Owamah, H. I. (2014). Biosorptive removal of Pb (II) and Cu (II) from wastewater using activated carbon from cassava peels. Journal of Material Cycles and Waste Management, 16, 347-358.

[119]. Nakbanpote, W., Thiravetyan, P., & Kalambaheti, C. (2000). Preconcentration of gold by rice husk ash. Minerals engineering, 13(4), 391-400.

[120]. Doke, K. M., Yusufi, M., Joseph, R. D., & Khan, E. M. (2012). Biosorption of hexavalent chromium onto wood apple shell: equilibrium, kinetic and thermodynamic studies. Desalination and Water Treatment, 50(1-3), 170-179.

[121]. Babu, B. V., & Gupta, S. (2008). Adsorption of Cr (VI) using activated neem leaves: kinetic studies. Adsorption, 14, 85-92.

[122]. Tazrouti, N., & Amrani, M. (2009). CHROMIUM (VI) ADSORPTION ONTO ACTIVATED KRAFT LIGNIN PRODUCED FROM ALFA GRASS (STIPA TENACISSIMA). BioResources, 4(2).

[123]. Chakraborty, R., Asthana, A., Singh, A. K., Jain, B., & Susan, A. B. H. (2022). Adsorption of heavy metal ions by various low-cost adsorbents: a review. International Journal of Environmental Analytical Chemistry, 102(2), 342-379.

[124]. Babel, S., & Kurniawan, T. A. (2003). Low-cost adsorbents for heavy metals uptake from contaminated water: a review. Journal of hazardous materials, 97(1-3), 219-243.

[125]. Habuda-Stanić, M., & Nujić, M. (2015). Arsenic removal by nanoparticles: a review. Environmental Science and Pollution Research, 22, 8094-8123.

[126]. Hao, L., Liu, M., Wang, N., & Li, G. (2018). A critical review on arsenic removal from water using iron-based adsorbents. RSC advances, 8(69), 39545-39560.

[127]. Khan, F. A., Mushtaq, M. A. B., Arif, P. M. A., & Mazahar, M. F. (2023). A Comparative Study of Adsorption of Methylene Blue Dye onto Untreated Platanus orientalis (chinar tree) Leaves Powder and its Biochar-Equilibrium, Kinetic and Thermodynamic Study. Orbital: The Electronic Journal of Chemistry, 163-170.

[128]. Ahmad Khan, F., & Farooqui, M. (2024). Removal of methylene blue dye from aqueous solutions onto Morus nigra L.(mulberry tree) leaves powder and its biochar—equilibrium, kinetic and thermodynamic study. International Journal of Environmental Analytical Chemistry, 104(16), 4364-4383.

[129]. Ahmad Khan, F., Dar, B. A., & Farooqui, M. (2023). Characterization and adsorption of malachite green dye from aqueous solution onto Salix alba L.(Willow tree) leaves powder and its respective biochar. International Journal of Phytoremediation, 25(5), 646-657.

[130]. Khan, F. A., & Farooqui, M. REMOVAL OF CRYSTAL VIOLET DYE FROM AQUEOUS SOLUTION USING MORUS NIGRA L.(MULBERRY TREE) LEAVES BIOCHAR.

[131]. KHAN, F. A., AHAD, A., FATEMA, S., & FAROOQUI, M. (2022). ADSORPTION STUDY OF CRYSTAL VIOLET DYE ONTO Morus nigra L.(MULBERRY TREE) LEAVES POWDER: EQUILIBRIUM, KINETICS AND THERMODYNAMICS STUDY. Indian J. Sci. Res, 12(2), 23-33.

[132]. Jirekar, D. B., Ubale, M., & Farooqui, M. (2016). Evaluation of Adsorption Capacity of Low Cost Adsorbent for the Removal of Congo Red Dye from Aqueous Solution. Orbital: The Electronic Journal of Chemistry, 282-287.

[133]. Jirekar, D. B., Ubale, M., & Farooqui, M. (2016). Evaluation of Adsorption Capacity of Low Cost Adsorbent for the Removal of Congo Red Dye from Aqueous Solution. Orbital: The Electronic Journal of Chemistry, 282-287.

[134]. Jirekar, D. B., Ubale, M., & Farooqui, M. (2016). Evaluation of Adsorption Capacity of Low Cost Adsorbent for the Removal of Congo Red Dye from Aqueous Solution. Orbital: The Electronic Journal of Chemistry, 282-287.

[135]. Jirekar, D. B., Pathan, A. A., & Farooqui, M. (2014). Adsorption studies of methylene blue dye from aqueous solution onto Phaseolus aureus biomaterials. Orient J Chem, 30(3), 1263-1269. Gurgel, L. V. A., de Melo, J. C. P., de Lena, J. C., & Gil, L. F. (2009). Adsorption of chromium (VI) ion from aqueous solution by succinylated mercerized cellulose functionalized with quaternary ammonium groups. Bioresource technology, 100(13), 3214-3220

[136]. Jirekar, D. B., & Farooqui, M. (2013). Adsorption Studies of hexavalent Chromium Ion from Aqueous Solution Using Lenus Esculent (Masoor). International Journal of Recent Trends in Science And Technology, 15-20

International Journal of Scientific Research in Science and Technology
Available online at : www.ijsrst.com
OPEN ACCESS
Print ISSN: 2395-6011 | Online ISSN: 2395-602X
doi : https://doi.org/10.32628/IJSRST

Soil Geochemical Treatment to Enhance the Fertility of Acidic Soil with Effluent Industrial Waste.- A Case Study of Lanzi and Hirapur of Waluj Area , Aurangabad District, Maharashtra India

Mr. Muneeb ur Rahman[1], Mr. M. A. Malik[1], Ms. Mahejabeen N.A.Sayyad[2]

[1]Assistant Professor, Department of Geology, Maulana Azad College of Arts, Science and Commerce, Ch. Sambhajinagar, Maharashtra, India

[2]Assistant Professor, Department of Microbiology, Maulana Azad College of Arts, Science and Commerce, Ch. Sambhajinagar, Maharashtra, India

ARTICLEINFO

Article History :

Published : 07 Dec 2024

Publication Issue :
Volume 11, Issue 23
Nov-Dec-2024
Page Number :
394-400

ABSTRACT

An industrial effluent is a regime in the soil pollution but the characteristics of the waste water are to be utilized for development fertility with neutralizing acidic soil. Acidic soils in agricultural regions are hinder crop productivity by reducing nutrient availability and increasing infertility in the soil. This study explores the potential of using industrial wastewater to ameliorate acidic soils in Lanzi and Hirapur villages, Waluj area Aurangabad district, Maharashtra. Treatment with industrial wastewater was applied to the soil of the study area, and its impact on pH, nutrient availability, and crop productivity was assessed. This study highlights the dual benefits of wastewater reuse: sustainable soil management and environmental conservation. This study explores the use of treated industrial waste effluents for the treatment of acidic soils, with a focus on the geological and geomorphological characteristics of the study area. The underlain rocks are highly rich in iron sulphides the traces in weathering shows iron sulfide grain in soil. In another study highly fertilizers are highly used for agricultural purposes are residue in the soil. The acidic nature of the soil is increased to diminished the acidic pH will be neutralize by alkaline industrial waste water. The yield of the agriculture land using the ground water from the dug wells or bore wells (pH- 5.4 to 6.2) gives less yield, while the cultivation by the industrial waste water from the effluent of Waluj industrial area the stream known as (ganda naala). The water from ganda naala having pH value varied in between (9.2 to 10.8). The farmers use the effluent water for their crop cultivation instead of their bore or dug well waters. The results

demonstrate that treated effluents not only neutralize soil acidity but also improve nutrient availability, leading to enhanced crop productivity. This research offers a sustainable solution to mitigate soil degradation in industrially affected areas. The results revealed significant improvements in soil pH and fertility, along with a reduction in toxic metal concentrations. which will be useful for international and national level natural hazards healing.
Keywords:-Acidic Soil, treated waste water, Basic water.

Introduction

1.1 Background

Soil pH is a critical issue that hampers agricultural productivity by reducing nutrient availability and increasing infertility. Lanzi and Hirapur villages, located near Aurangabad district, are facing severe soil acidification due to its mineral composition in rocks. Soil acidity, characterized by a low pH (5.5 to 6.0), is a critical issue in the agricultural lands of Lanzi and Hirapur villages in Aurangabad district. This condition is exacerbated by natural soil composition and poor land management practices. Acidic soils restrict nutrient availability, inhibit microbial activity, and increase the solubility of some elements such as Iron Sulphides like (Pyrite) which is severely affecting crop yields. However, these effluents, when treated with industrial waste, contain alkaline pH valuable nutrients that can be used for soil reclamation. Industrial wastewater is having a high (9 to 11 pH), with essential elements nutrients, making it a potential alternative for soil amelioration. This study investigates the feasibility of using treated industrial wastewater to neutralize soil acidity and improve agricultural productivity in the study area. Understanding the geochemical and geomorphological context of these areas is vital to comprehending the soil's response to industrial effluent application and its overall impact on agricultural sustainability.

1.2 Objectives

This study aims to:

1. To analyze the geochemical constituents with geology and geomorphology of Lanzi and Hirapur villages.
2. Investigate the effects of industrial waste effluents on acidic soil.
3. Evaluate the impact of effluent-treated soil on crop productivity.

Study Area

The research was conducted in Lanzi and Hirapur villages, located in Aurangabad district, Maharashtra. These villages are situated near industrial zones Waluj (budruk), with acidic soils (pH 5.5 to 6.0) identified as a significant agricultural constraint.

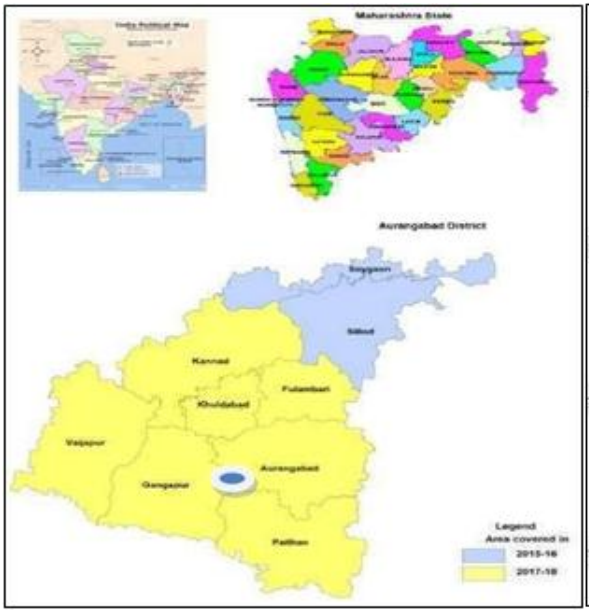

Fig: 2.1. Index Map

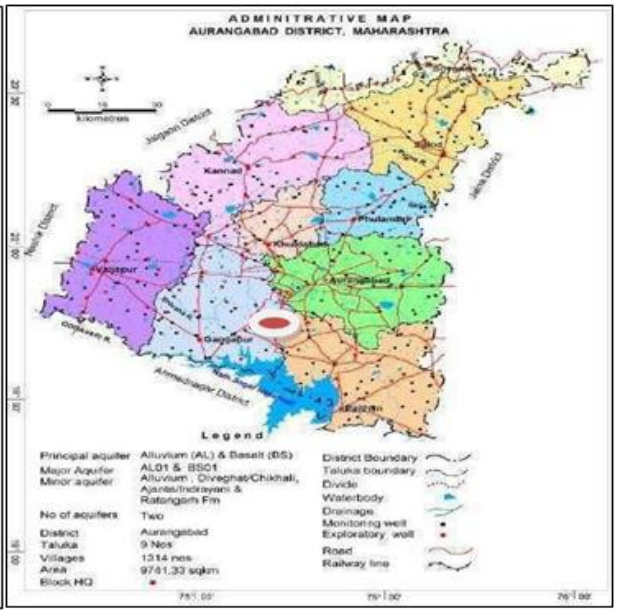

Fig: 2.2. Administrative map

Geological and Geomorphological Studies of the Study Area

3.1. Geological Context

The study area, located in the Aurangabad district, lies in the Deccan Traps, a large igneous province formed during the late Cretaceous to early Paleocene period. Geologically, Basalt formation (Deccan traps) is the major rock formation in the district. The major part of the district is underlain by a sequence of basaltic lava flows while alluvium occupies a small portion. The Deccan Trap has succession of flows in the elevation range and are normally horizontally disposed over a wide stretch plain topography also known as plateau. These flows occur in layered sequence ranging in thickness from meters to tens of meters. Each individual Basaltic rocks flow is massive at the bottom and vesicular/amygdaloidal towards the top. The generalized geological sequence is characterized by:

Basaltic Lava Flows: The dominant rock type in the area is tholeiitic basalt, which weathers to form clayey soils.

Fractures and Joints: The basaltic flows contain fractures and joints, influencing groundwater movement and soil development.

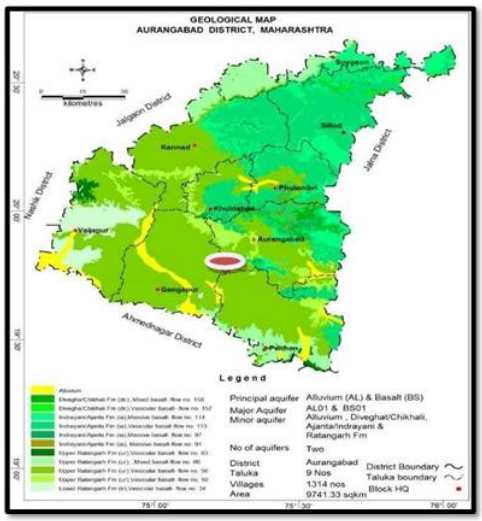

Fig: 3.1. Geology of the study area

3.2. Geomorphological Context

Geomorphologic-ally, the district comprises of varied topographic features and landscape consisting of high hills and plains and low lying hills. The average elevation of the district is in the order of 550 m msl. Within it are flat topped hill ranges extending over wide area and also hills separated by broad valleys.

The geomorphological features of Lanzi and Hirapur villages include: Flat to Undulating Plains: Predominantly flat terrain with slight undulations, suitable for agriculture.Alluvial Deposits: Areas near streams and rivers contain alluvial soils, which are moderately fertile.

Drainage Patterns: The villages are drained by ephemeral streams, dendritic pattern of streams is usually seen that flow during the monsoon, contributing to localized erosion and deposition.

3.3. Soil Characteristics:-

The soils in the study area are classified as vertisols and alfisols, characterized by:

1. Low pH (5.5 to 6.0) before treatment due to acidification.
2. Moderate organic carbon content but poor micronutrient availability (N, P, K).

Understanding the geology and geomorphology provides a foundation for evaluating the impact of industrial effluent treatments on soil properties.

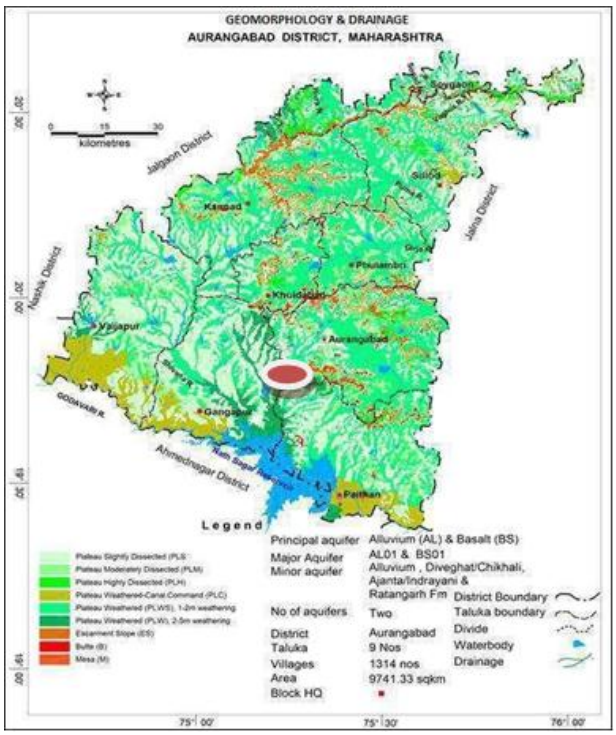

Fig: 3.2 Geomorphology and drainage of study area.

Materials and Methods

4.1. Effluent Collection and Treatment

Industrial effluents water was collected from nearby drainage system of the study area. Treatment involved:

1. Neutralization: Effluent waste water was used to neutralize the pH of the effluent to 7.6 to 8.4.

4.2. Soil Sampling:

Soil samples were collected from ten locations in each village two samples were collected at depths of 15 cm. The samples were sieved, and analyzed for initial properties, including pH (pH 5.5 to 6.0), and heavy metal concentrations like Iron Sulphides (Pyrite).

4.3. Experimental Design

Field trials were conducted on plots (10 mÂ² each) with three treatments:

1. Control (C): Untreated acidic soil.
2. Effluent Treatment (ET): Treated effluent applied at 10% v/v.

Results and Discussion

5.1. Impact of Treated Effluents on Soil Properties

1. Soil pH after the treatment with Effluent-the treated soils showed significant pH improvement 5 to 7.7

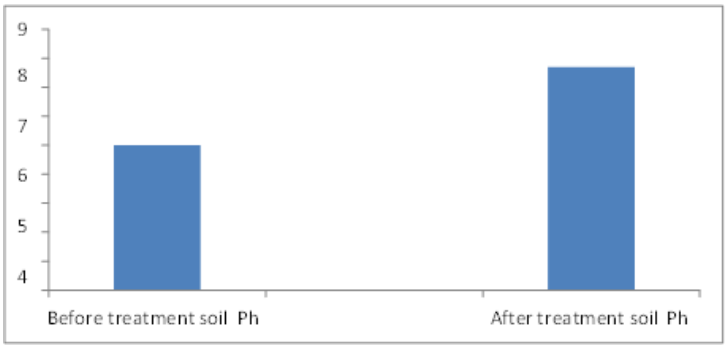

Fig: 5.1 Ph Bar graph representation of soil treatment

Sr. No	Treatment	Ph of soil
01	Before treatment	05
02	After treatment	7.7

2. **Nutrient Enrichment:** After the treatment the study area shows enrichments in the nutrients value like nitrogen content increased by 35% in soils compared to control. Phosphorus content increased by 37% in soils and potassium levels content increased by 11 % in soils also improved significantly.

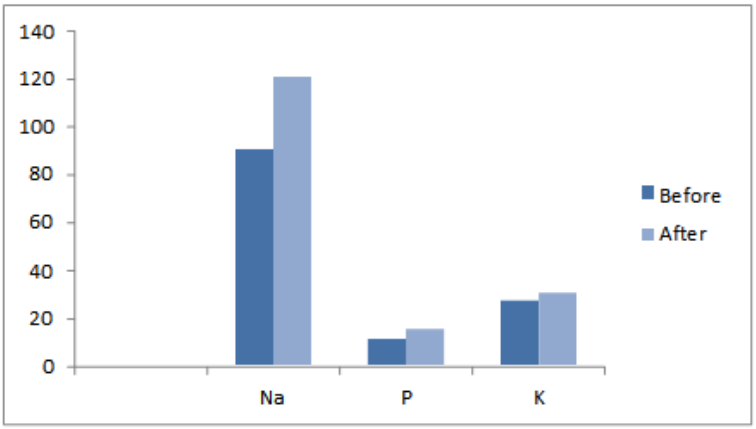

Fig:- 5.1.2 . Comparison table of Nutrients before and after Treatment

Nutrients	Before	After
Na	90	120
P	11	15
K	27	30

5.2. Crop Productivity: The crops which are cultivated in the study area majorly are wheat, cotton, jowar and bajra, maize etc,. One example is of maize yields increased significantly in effluent-treated plots (2.4 tons/ha) or by 35 % in the treated area as compared to lime-treated (2.1 tons/ha) the lime concentration is increased by 20%.

Sr. No	Cropping Pattern Treated with effluent water	Values in Tons	Cropping Pattern Treated with Lime	Values in Tons
01	Maize yields in tons before treatment	40	Maize yields in tons before treatment	40
02	Maize yields in tons after treatment	52	Maize yields in tons after treatment	48

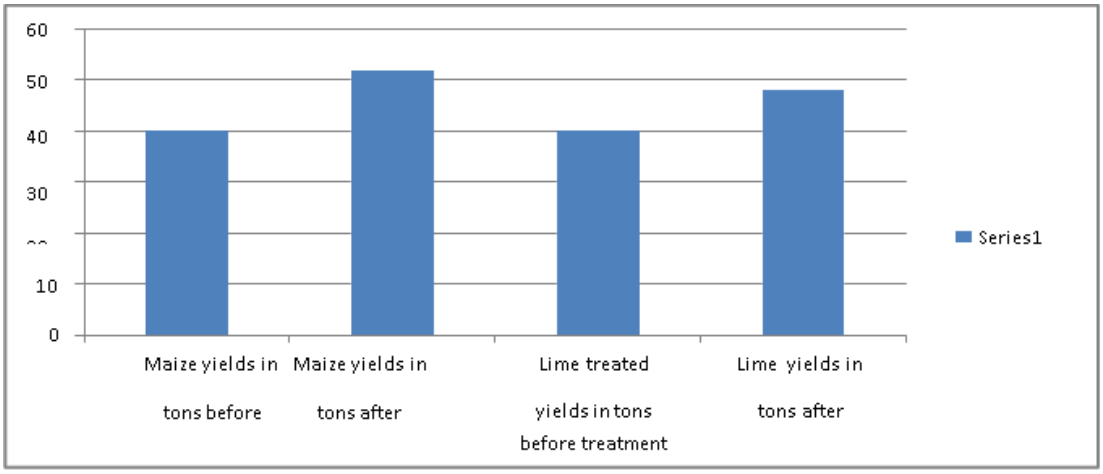

Fig:- 5.1.3 . Comparison table of crop yielding before and after Treatment

Impact on Soil Properties

6.1. Changes in Soil pH: 5.5-6.0 from acidic soil to neutral pH, and increase in the Nutrient availability of the soil.

6.2. Treated wastewater significantly increased available N, P, and K compared.

6.3. Crop Productivity

In the region significantly increased in the crop of maize yields which has been increased by 35% in wastewater-treated farmlands, compared to the control and by 20% compared to lime- treated plots.

Conclusion

A seasonal flowing stream geographically present in industrial area becomes perennial stream (ganda naala) because in which industrial effluent wastewater is added. The geological and geomorphological characteristics of Lanzi and Hirapur villages of Aurangabad city play a significant role in the agriculture farming because they are closer to the urban population.

This study demonstrates that industrial effluents can effectively neutralize acidic soils, improve nutrient availability, and enhance crop productivity. Analytical study shows soil and water in different localities of this study area soil is acidic in nature because of rich in iron sulphide content while the stream water of Gandanala

9 pH (alkaline).This study can be apply alkaline water to the acidic soil to enhance the fertility instead of using dug well water 5.8 pH practices shows good results. Farmers practice start with small farmers acquiring a small piece of land they try to cultivate this industrial waste water by lifting of water by pipeline finding good results and this technique was adopted by various farmers to their agriculture land in the region. These practices play a significant role in the response of soils to industrial effluent treatments. These findings provide a sustainable solution for soil reclamation treatment and waste water management in industrially affected regions.

Recommendations

1. Establish effluent treatment near industrial zones.
2. Educate farmers on the safe application of effluents where it is necessory.
3. Conduct long-term studies to monitor heavy metal accumulation in soils and crops.
4. This Practice should be applied in different regions, wherever the industrial waste suites to enhance fertility of soil.

References

[1]. Subbarao, G. V., & Johansen, C. (1998). Strategies for improving acidic soils. Agricultural Systems, 56(1), 75-91.

[2]. Roy, S., & Sharma, A. (2019). Soil acidification and reclamation in basaltic terrains. Journal of Geology, 45(3), 123-134.

[3]. Shah, R. M., & Jadhav, M. S. (2020). Industrial waste management and soil health. Environmental Pollution Research, 27(6), 445-462.

[4]. Brady, N. C., & Weil, R. R. (2017). The Nature and Properties of Soils. Pearson Education.

[5]. Singh, A., & Agrawal, M. (2010). Effects of treated industrial wastewater on soil and crops. Environmental Pollution, 158(6), 2344 to 2353.

[6]. Fageria, N. K., & Baligar, V. C. (2008). Amelioration of acidic soils for sustainable crop production. Advances in Agronomy, 99, 345 to 399.

[7]. Jackson, M. L. (1973). Soil Chemical Analysis. Prentice Hall of India Pvt. Ltd.

[8]. Sharma, R. K., & Agrawal, M. (2005). Potential use of wastewater in agriculture. Environmental Science and Technology, 39(6), 4321 to 4327.

[9]. Central Ground Water Board (2019) Aquifer Mapping and Management of Ground Water Resources Aurangabad district, Maharashtra Central Region Nagpur, Department of water resources river development and Ganga rejuvenation, Ministry of Jal Shakti Government of India. P.203.

[10]. Balpande U.S (. 2013) Central region Nagpur, Govt. of India ministry of water resources central ground water board, Ground water information Aurangabad district Maharashtra. P.167.

Figures and Graphical Data Representation

1. Figure 1: Study map of the area
2. Figure 2: Geological and Geomorphology map of the study area.
3. Figure 3: Line graph showing changes in soil pH and Effluent treatments.
4. Figure 4: Bar graph comparing nutrient content (N, P, K) in soils for different treatments.
5. Figure 5:Crop productivity (tons/ha) under different treatments.

International Journal of Scientific Research in Science and Technology
Available online at : www.ijsrst.com
OPEN ACCESS
Print ISSN: 2395-6011 | Online ISSN: 2395-602X
doi : https://doi.org/10.32628/IJSRST

Solvent-Based Extraction of Ficus racemosa Leaves: Phytochemical and Antimicrobial Investigation

Dr. Santosh G. Badne, Prof .Mahesh A. Pawar,Dr. Gajanan W. Belsare
Department of Chemistry, Shri Shivaji College of Arts Commerce and Science, Akola, Maharashtra, India

ARTICLEINFO

Article History :

Published : 07 Dec 2024

Publication Issue :
Volume 11, Issue 23
Nov-Dec-2024
Page Number :
401-405

ABSTRACT

The present study deals with physicochemical, phytochemical and microbial study of leaves extract of medical Ficus racemosa, commonly known as the cluster fig tree, it is a medicinal plant with notable therapeutic application. This study investigates the extraction of bioactive compounds from its leaves in various solvents of varying polarities, such as hot water, ethanol, chloroform, and 1:1 ethanol and water, to optimize phytochemical yield. Phytochemical screening confirmed the presence of alkaloids, tannins, saponins, tannins steroids and carbohydrates. Methanolic and Ethanolic extracts demonstrated superior phytochemical yields and significant antimicrobial activity compared to chloroform and aqueous extracts, highlighting the importance of solvent selection. Antimicrobial activity was evaluated. These findings validate the medicinal potential of Ficus racemosa leaves and provide a foundation for further studies to isolate and develop bioactive compounds for medicinal applications.

Keywords: Ficus racemosa, solvent extraction, phytochemicals, antimicrobial screening,

Introduction

Medicinal plants have been a cornerstone of traditional medicine systems and continue to be a significant source of bioactive compounds for modern therapeutic applications. Among these, Ficus racemosa (commonly known as the cluster fig or Indian fig tree) holds a prominent place due to its extensive ethnopharmacological uses. Belonging to the family Moraceae, this plant is widely distributed across tropical and subtropical regions and has been traditionally employed to treat various ailments such as diabetes, inflammation, diarrhea, and skin disorders[1,2]. The therapeutic properties of Ficus racemosa are attributed to its rich phytochemical profile, which includes alkaloids, flavonoids, tannins, saponins, and phenolics. These bioactive compounds exhibit diverse biological activities, including antimicrobial, antioxidant, anti- inflammatory, and antidiabetic effects. The extraction of these phytochemicals using solvents of different polarities is critical to maximizing the yield of

specific compounds and evaluating their bioactivities 5.In recent years, the increasing prevalence of microbial resistance has highlighted the need for novel antimicrobial agents. Plants like Ficus racemosa offer a promising avenue for the discovery of new bioactive compounds with potential antimicrobial properties. However, a systematic study on the solvent-dependent extraction of its phytochemicals and the evaluation of their antimicrobial efficacy remains limited 3.This research aims to extract and analyze the phytochemical constituents of Ficus racemosa leaves using solvents of varying polarities, including methanol, ethanol, chloroform, and water. Furthermore, the study evaluates the antimicrobial potential of these extracts against gram- positive and gram-negative bacteria and fungal strains. By identifying the most effective solvent for extraction and its corresponding bioactivity, this study seeks to contribute to the growing body of knowledge on the medicinal potential of Ficus racemosa and its application in combating microbial infections 4.

Material and Method

Plant materials of Ficus racemosa were collected from area of katepurna dam Akola district as per the standard method 6.The plant was identified and authenticated by Dr. Nikhil Chaukhande, Department of Botany, Shri Shivaji College of Arts Commerce and Science Akola . Fresh leaves were collected then bring to the laboratory and thoroughly washed with distilled water and shade dried at 28 º C. The completely dried leaves were ground well into a fine powder in a mixer grinder. The powder was stored in a polythene bags at room temperatures.

Preparation of leaves extract

Extraction of leaves done both manually and by soxhlet. The powdered plant material underwent extraction using the hot continuous extraction technique in a Soxhlet apparatus. The process involved sequentially extracting the material with solvents of increasing polarity, specifically methanol, acetone, ethyl acetate, and hot water. This systematic approach ensured the efficient recovery of a diverse range of phyto constituents by taking advantage of the varying solubility of plant compounds in these solvents. Following each extraction cycle, the resulting liquid extracts were carefully collected into pre-weighed (tarred) conical flasks. To concentrate the extracts, the solvents were removed through distillation, leaving behind the residues containing the extracted phytochemicals. The concentrated extracts were subsequently analyzed through a series of qualitative chemical tests designed to detect and confirm the presence of specific phytoconstituents, including alkaloids, flavonoids, tannins, saponins, and other biologically active compounds. This meticulous extraction and analysis workflow provided valuable insights into the phytochemical composition of the plant material, laying the groundwork for further investigations into its biological properties or pharmacological potential.

Fig: 1 Leave Extract of Ficus racemosa

Preliminary Phytochemical Screening

Phytochemical screening of the Leave Extract of Ficus racemosa was done by the standard procedures prescribed by Kokate and Harborne [7, 8].

Result and Discussion:

Table 1: phytochemical test of Soxhlet Extract

S.N.	Tests	Hot Water extract	Ethanol extract	1:1 Water-Ethanol extract	Chloroform extract
1	**Alkaloids** Wagner's Test	P os itive	N egative	Pos itive	N egative
2	**Terpenoids** Salkowski's Test	N egative	P os itive	Negative	N egative
3	**Steroids** Salkowski's Test	P os itive	N egative	Negative	N egative
4	**Tanins** FeCl3 Test	P os itive	P os itive	Pos itive	N egative
5	**Saponins** Foam Test	N egative	N egative	Negative	N egative
6	**Flavonoids** Lead Acetate Test	N egative	N egative	Negative	N egative
7	**Carbohydrates**	P os itive	P os itive	Pos itive	P os itive

S.N.	Tests	Hot Water extract	Ethanol extract	1:1 Water-Ethanol extract	Chloroform extract
	Fehling Test				
8	**Cardiac Glycosides** Keller-Killiani Test	N egative	P os itive	Ngative	N egative
9	**Quinines** Naoh Test	P os itive	P os itive	Ngative	N egative
10	**Protein** Biuret Test	N egative	N egative	os itive	N egative

Phytochemical profiling was carried out on different solvent extracts of Ficus racemosa, prepared using hot water, ethanol, chloroform, and a 1:1 water-ethanol mixture. Each extract underwent systematic evaluation to determine the presence of various bioactive compounds, offering a detailed understanding of the plant's chemical composition.

- **Hot Water Extract:** The phytochemical analysis identified alkaloids, steroids, tannins, carbohydrates, and quinones. The use of hot water as the solvent enabled the extraction of a wide spectrum of polar and semi-polar compounds, demonstrating its efficiency in isolating multiple active constituents.
- **Ethanolic Extract:** This extract contained terpenoids, tannins, carbohydrates, and glycosides. Ethanol, with its intermediate polarity, effectively extracted both polar and non-polar compounds, including terpenoids and glycosides, reflecting its versatility as a solvent.
- **1:1 Water-Ethanol Extract:** The combination of water and ethanol extracted alkaloids, tannins, carbohydrates, and proteins. The mixed solvent system facilitated the recovery of compounds that are soluble in both highly polar and moderately polar environments, offering a balanced extraction profile.
- **Chloroform Extract:** The analysis of the chloroform extract revealed the presence of carbohydrate glycosides. As a non-polar solvent, chloroform selectively extracted less polar compounds, aligning with its chemical properties.

in Ficus racemosa and underscore the importance of solvent selection in phytochemical extraction. This research holds significance for the evaluation of the crude drug's quality and purity, laying a foundation for standardization and validation. Moreover, understanding the plant's chemical profile is essential for assessing its potential therapeutic efficacy and guiding further studies into its pharmacological applications.

Anti-Microbial Activity Study

The zone of inhibition in mm for the tested organism with the ethanolic extract leaf extract of Ficus racemosa and by agar well diffusion method is shown below.

Results for Anti-Microbial Activity Study

In this study, the ethanolic leaf extract of Ficus racemosa, obtained through Soxhlet extraction, was evaluated for its phytochemical properties to determine the presence or absence of various bioactive compounds. These compounds are known for their potential in treating a wide range of diseases and ailments. The antimicrobial

activity of the leaf extract was tested against two pathogenic microorganisms, Staphylococcus aureus and Escherichia coli, using the agar well diffusion method. The results demonstrated significant antimicrobial efficacy, with a zone of inhibition measuring 19.2 mm against S. aureus and 16.8 mm against E. coli.These findings highlight the antimicrobial potential of the ethanolic leaf extract of Ficus racemosa. The extract exhibited notable inhibitory effects on both gram-positive and gram- negative bacteria, indicating its efficiency in controlling microbial growth and its potential as a natural antimicrobial agent.

Fig.2 Antimicrobial study of leaf extract of Ficus racemosa.

The phytochemical analysis of Ficus racemosa leaf extract revealed the presence of several bioactive compounds, including alkaloids, steroids, tannins, carbohydrates, and proteins. These constituents support the therapeutic potential of the plant, particularly in traditional medical treatments. In India, there is a growing trend toward the use of medicinal plants and phytochemicals for healthcare purposes. Traditional systems of medicine, such as Ayurveda, Unani, and Siddha, have long utilized a wide variety of medicinal plants for healing.The findings from this study, including the results of phytochemical screening, contribute valuable knowledge for the identification and authentication of Ficus racemosa as a medicinal plant. These standardization parameters are essential for ensuring the quality, efficacy, and safety of herbal medicines, further emphasizing the importance of Ficus racemosa in traditional and modern healthcare practices.

References

[1]. Mendoza N, Silva EME. Introduction to Phytochemicals: Secondary Metabolites from Plants with Active Principles for Pharmacological Importance. Phytochemicals - Source of Antioxidants and Role in Disease Prevention. 2018..

[2]. Fabricant DS, Farnsworth NR. The Value of Plants Used in Traditional Medicine for Drug Discovery. Environmental Health Perspectives. 2001.

[3]. Shiksharthi AR, Mittal S. Ficus racemosa: Phytochemistry, traditional uses, and pharmacological properties: A review. Int J Adv Pharm Res. 2011.

[4]. Dubey S, Maity S, Singh M, Saraf SA, Saha S. Phytochemistry, pharmacology and toxicology of Spilanthes acmella: A review. Adv Pharmacol Sci 2013.

[5]. Council of Scientific and Industrial Research. 4. New Delhi, India: The wealth of India- A Dictionary of Indian Raw Material. Publications and Information Directorate; 1956.

[6]. Jain, S.K. and R.R. Rao (1977).A Handbook ofField andHerbarium Methods. Today and Tomorrow'sPrinters and Publishers, New Delhi

[7]. Kokate, C. K. (1994). Practical Pharmacognosy, 4thedn.VallabhPrakan, New Delhi, 179-181.

[8]. Harbone, J.B and B. L. Turner (1984).Plant chemosystematics.Academic press, London.pp:61-62.

International Journal of Scientific Research in Science and Technology
Available online at : www.ijsrst.com
Print ISSN: 2395-6011 | Online ISSN: 2395-602X
doi : https://doi.org/10.32628/IJSRST

Neat Reaction Strategies for Organic Transformation: A Mini Review

Sabreena Yameen Pathan, Atufa A. Shaikh, Pathan Mohd Arif, Prashant D. Netankar
Department of Chemistry, Maulana Azad College of Arts, Science and Commerce, Rauza Bagh, Chh. Sambhajinagar, Maharashtra, India

ARTICLEINFO

Article History :

Published : 07 Dec 2024

Publication Issue :
Volume 11, Issue 23
Nov-Dec-2024
Page Number :
406-416

ABSTRACT

The solvents and reagents used in conventional methods in organic synthesis cause many side effects on human health as well as on the environment. To prevent the side effects, researchers are adopting different ways following the 12 principles of green chemistry. Neat method for organic transformation is the method where reagents and substrates are used without solvents. These reactions typically involve the direct mixing of reactants, often under heat or irradiation, to facilitate chemical transformations. The absence of solvents eliminates waste and reduces the need for solvent disposal, aligning with green chemistry principles. This review outlines the synthesis of different heterocyclic compounds using a neat reaction strategy.

Keywords- ball milling, green chemistry, neat reaction, microwave-assisted and ultrasound-assisted

Introduction

Conventional methods in organic synthesis refer to the methods used to synthesize organic compounds through chemical reactions that include the use of solvents, reagents, catalysts, and heating methods and they require harsh conditions, produce waste, and rely on toxic solvents and reagents. Most commonly used solvents and reagents in synthesis are dichloromethane (DCM), chloroform, acetonitrile, dimethylformamide (DMF), dimethylsulfoxide (DMSO), xylene, benzene and toluene etc.

These conventional methods have adverse side effects on human health as well as on the environment. To prevent these hazards, researchers are adopting different ways in accordance with the 12 principles of green chemistry[1]. Some of them include the grinding or ball milling methods[2], microwave and ultrasound-assisted[3,4], use of green solvents[5,6] and heterogeneous or nanocatalysts[7] and neat(solvent-free) reactions[8,9].

Neat methods for organic transformations are the methods where reagents and substrates are used without solvents. These reactions typically involve the direct mixing of reactants, often under heat or irradiation, to

facilitate chemical transformations. The absence of solvents eliminates waste and reduces the need for solvent disposal, aligning with green chemistry principles. Neat conditions can enhance reaction rates, improve yields, and promote selectivity due to the concentrated nature of the reactants.[10]

Heterocyclic compounds play a very important role as they are frequently found in enzymes, vitamins, and natural products. Most of the drugs contain the heterocyclic nucleus which possesses many biological activities such as anti-inflammatory, antibacterial, antifungal, antioxidant, antiallergic, enzyme inhibitors, anticonvulsant, anti-HIV, antidiabetic, anticancer activity, insecticidal agents, etc.[11]

A. NEAT SYNTHESIS OF PYRROLES

Mukherjee et al.[12] demonstrated an environmentally benign one-pot method for the synthesis of chromeno[4,3-b]pyrrol-4(1H)-one derivatives. Three-component domino reaction of 4-aminocoumarins, arylglyoxal monohydrates, and nucleophilic substrates yields functionalized chromeno[4,3-b]pyrrol-4(1H)-ones, catalyzed by $Fe_3O_4@SiO_2$-SO_3H magnetic nanoparticles under solvent-free conditions. The procedure has numerous advantages like atom-economy fashion, short reaction time, good yield of the products, use of a recyclable nanocatalyst, and avoiding the use of hazardous solvents as well as expensive catalysts/reagents. (Scheme-1)

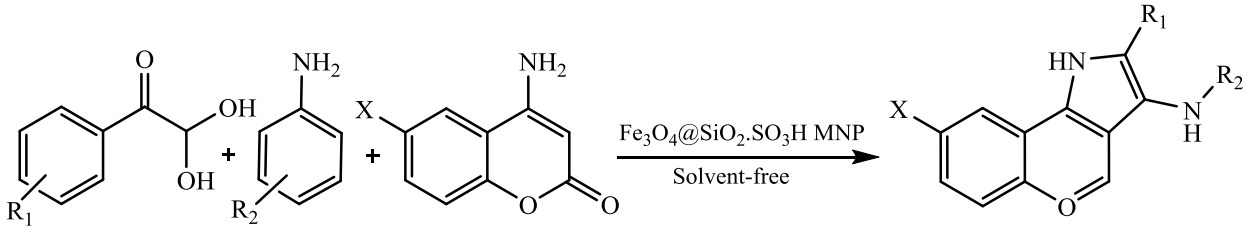

Scheme-1

Surya De[13] reported N-substituted pyrrole derivatives were synthesized by the reaction of hexane-2,5-dione, aniline and $Pr(OTf)_3$ as a catalyst under solvent-free conditions. The reaction was also tested in different solvents such as DCM, MeOH and THF and the best results were obtained in solvent-free neat conditions. (Scheme-2)

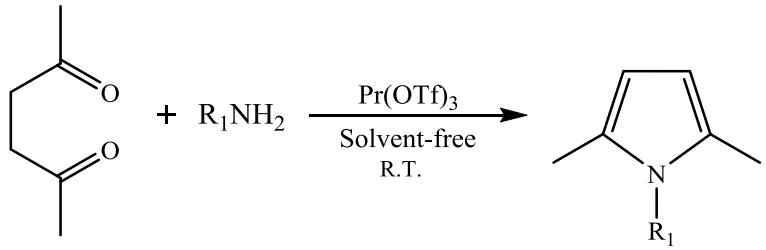

Scheme-2

Attanasi and coworkers[14] synthesized the polysubstituted pyrroles one-pot three component reaction between primary aliphatic amines,1,2-diaza-1,3-diene and active methylene compounds. The reaction was performed without using any catalyst and solvent. The mechanism involved the 3+2 cycloaddition of simple secondary enamines with 1,2-diaza-1,3-diene. (Scheme-3)

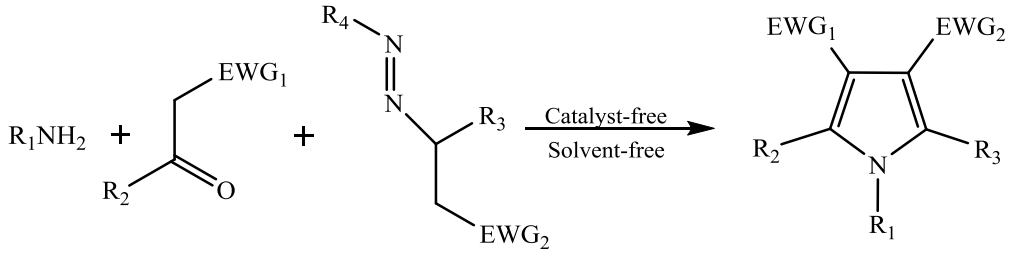

Scheme-3

Wani et al.[15] reported the synthesis of N-substituted pyrroles using alkaline earth metal-based catalyst. Reaction was carried out between 2,5-dimethoxytetrahydrofuran with aliphatic/aromatic amines and catalytic amount of $Ca(NO_3)_2.4H_2O$. It was observed that good to excellent yield of product was obtained solvent-free condition with the presence of electron donating groups on amines. (Scheme-4)

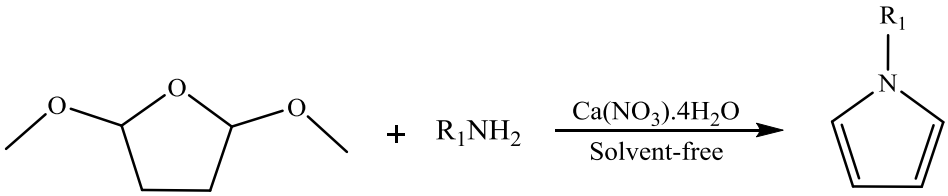

Scheme-4

Borghs and researchers[16] successfully prepared the 2,5-disubstituted pyrroles using biomass-derived primary diols and amines catalyzed by manganese/potassium carbonate under neat method which produces water and hydrogen gas as the byproducts. (Scheme-5)

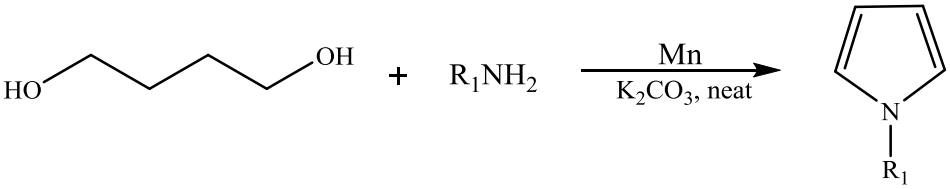

Scheme-5

Rostami and Shiri [17] developed an efficient one-pot multicomponent protocol for the synthesis of N-substituted pyrroles by using aniline derivatives, β-ketoesters/β-diketones and β-nitrostyrene catalyzed by Fe_3O_4@SiO_2–CPTMS–Guanidine–SO_3H under solvent-free conditions. The reactions were investigated at different temperatures and with the use of various polar solvents and the best results were obtained under solvent-free conditions at 50°C. (Scheme-6)

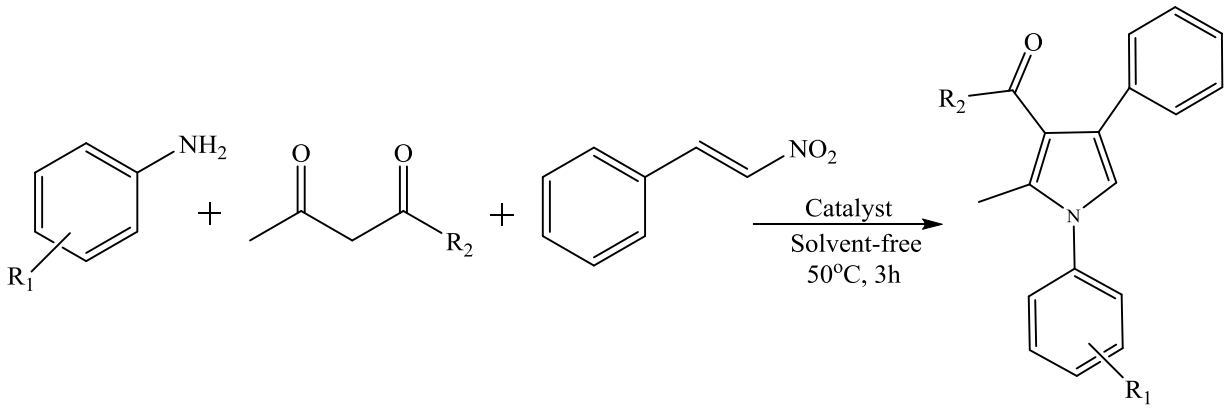

Scheme-6

For the preparation of pyrrole derivatives, an environment-friendly neat procedure was reported by Marvi and Nahzomi[18] using Paal-Knorr condensation reaction between 2,5-hexandione and different aromatic amines catalyzed by smectite clays as heterogeneous Lewis acid catalysts. (Scheme-7)

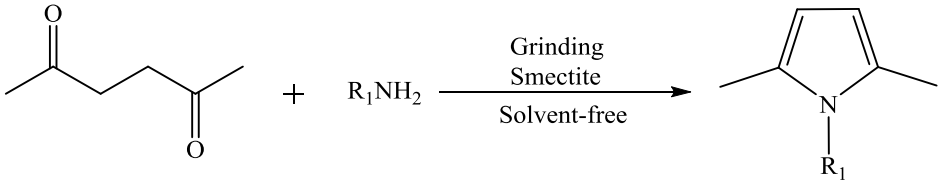

Scheme-7

B. NEAT SYNTHESIS OF PYRAZOLES

Shaterian and Kangani [19] synthesized 1,4-dihydropyrano[2,3-c]pyrazoles using hydrazine monohydrate, ethyl acetoacetate, aryl aldehydes and malononitrile in the presence of P_2O_5/SiO_2, H_3PO_4/ Al_2O_3, cellulose sulfuric acid or starch sulfuric acid as a green catalyst under solvent free conditions. (Scheme-8)

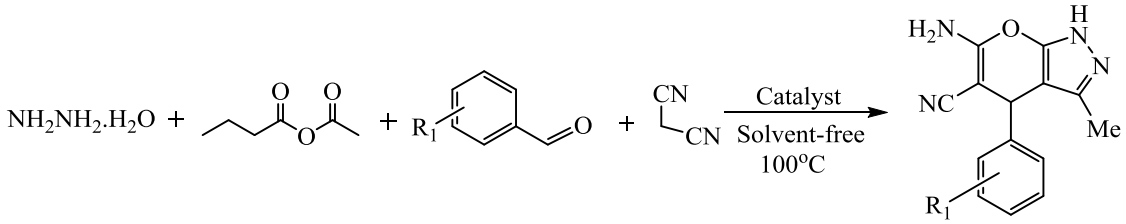

Scheme-8

Soltanzadeh et al.[20] described the synthesis of pyrazole derivatives under solvent free conditions. They used 4-phenylurazole or 1,2-dibenzoylhydrazines, dialkyl acetylene dicarboxylates, isocyanides and tetrabutylammonium bromide (TBAB) and obtained the product in good yield. (Scheme-9)

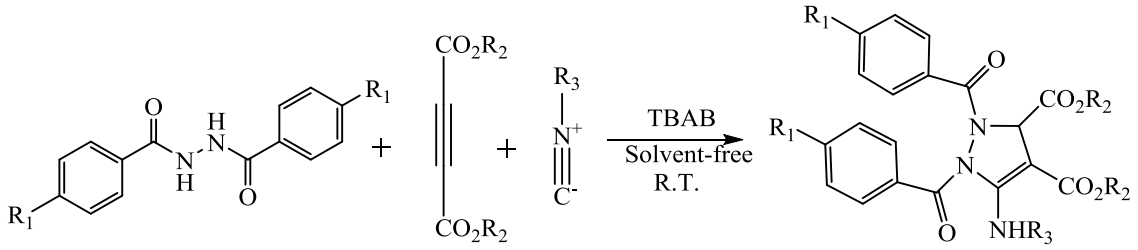

Scheme-9

Mallah and Mirjalili[21] reported the effective and green ball milling method for the synthesis of dihydropyrano[2,3-c]pyrazole using nano-silica/aminoethylpiperazine as a metal-free catalyst. They carried the reaction at room temperature and without using any solvent by obtaining the product in good to excellent yield. (Scheme-10)

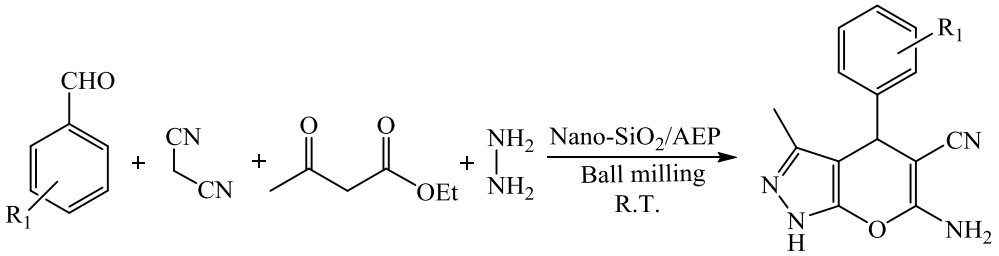

Scheme-10

Vuluga and coworkers[22] synthesized pyrazoles by 1,3-dipolar cycloaddition of diazo compounds and alkynes at 80°C under solvent-free conditions. They reported the method is simple and clean and the reaction affords pyrazoles in excellent yields. (Scheme-11)

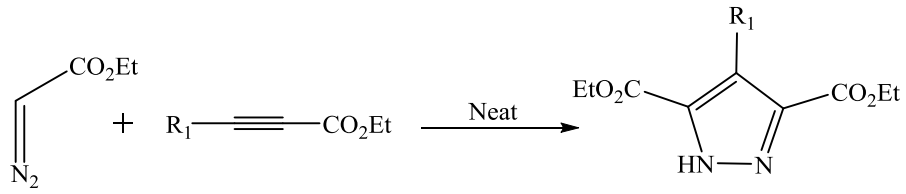

Scheme-11

Shaabani and co-researchers[23] reported the synthesis of Pyrazolo[1,2-a]Pyrazoles and Pyrano[2,3-c]Pyrazoles by using four component reaction between dialkyl acetylenedicarboxylates, isocyanides and ethyl acetoacetate with hydrazine hydrate or phenylhydrazine. They used different reaction conditions and concluded that they obtained the product in excellent yield under solvent-free conditions at 70°C. (Scheme-12)

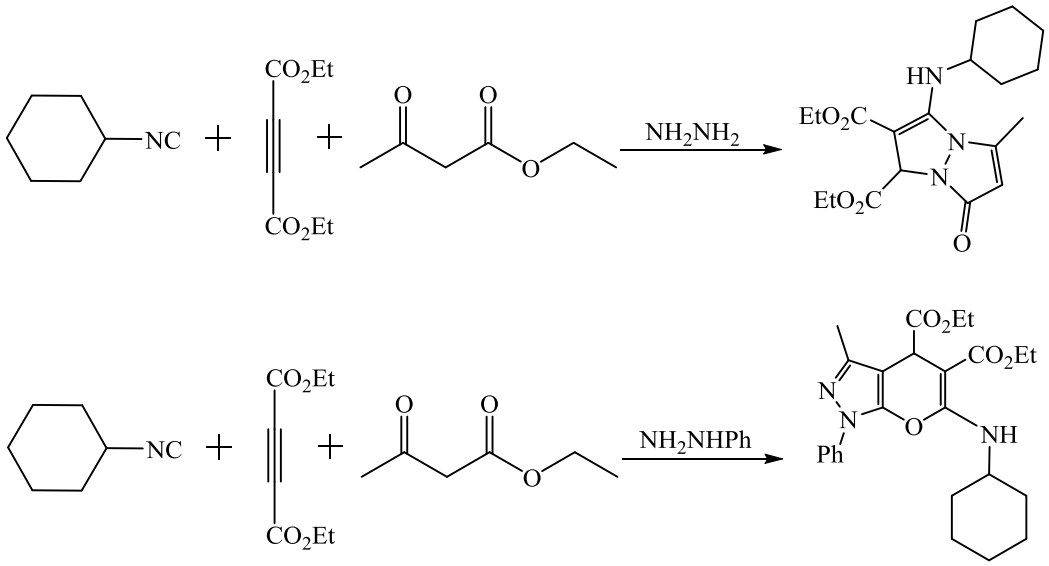

Scheme-12

Siddiqui and Farooq[24] reported the synthesis of substituted pyrazoles catalyzed by silica supported sodium hydrogen sulfate ($NaHSO_4.SiO_2$) under solvent-free conditions by the reaction of β-enaminones and hydrazine hydrate. (Scheme-13)

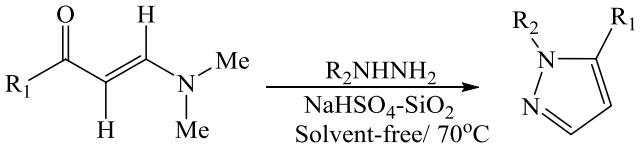

Scheme-13

Sapkal and researchers[25] reported an efficient and facile one pot multicomponent synthesis of Pyrano [2,3-c] pyrazoles in good to excellent yield using different substituted benzaldehyde, malononitrile, ethyl acetoacetate, hydrazine hydrate under solvent free condition using ionic liquid N-methyl pyridinium toluene sulfonate (NMPyTs) as a catalyst by grinding method. (Scheme-14)

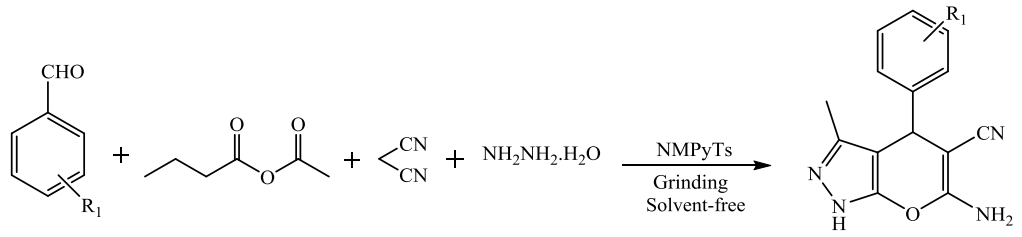

Scheme-14

Longhi and team [26] synthesized the series of NH-pyrazoles using β-dimethylamino-vinyl ketones and hydrazine sulfate in solid state on grinding under solvent-free conditions. They used four different catalysts viz SiO_2, PTSA, $KHSO_4$, and $NaHSO_4$ and found PTSA (p-toluenesulfonic acid) as an efficient catalyst. (Scheme-15)

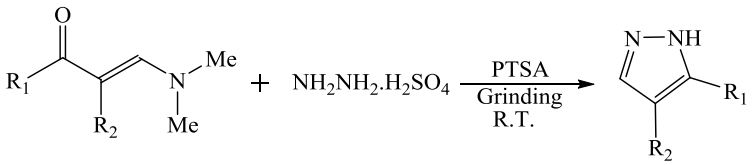

Scheme-15

C. NEAT SYNTHESIS OF IMIDAZOLES

Zhang et al.[27] reported one-pot synthesis of imidazole derivatives using different substituted benzaldehyde, benzil or aromatic o-phenylenediamines and ammonium acetate under solvent-free conditions at 70°C and obtained the product in high yields. (Scheme-16)

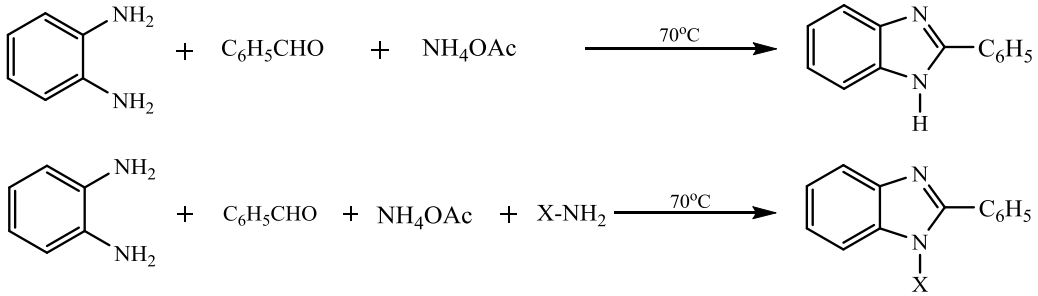

Scheme-16

The derivatives of 2,4,5-trisubstituted-1H-imidazole and 1,2,4,5-tetrasubstituted-imidazole were synthesized by Pandit and researchers[28] by benzyl, aryl aldehydes, ammonium acetate and aromatic amines in presence of Amberlyst A-15 as a reusable catalyst under microwave irradiations. (Scheme-17)

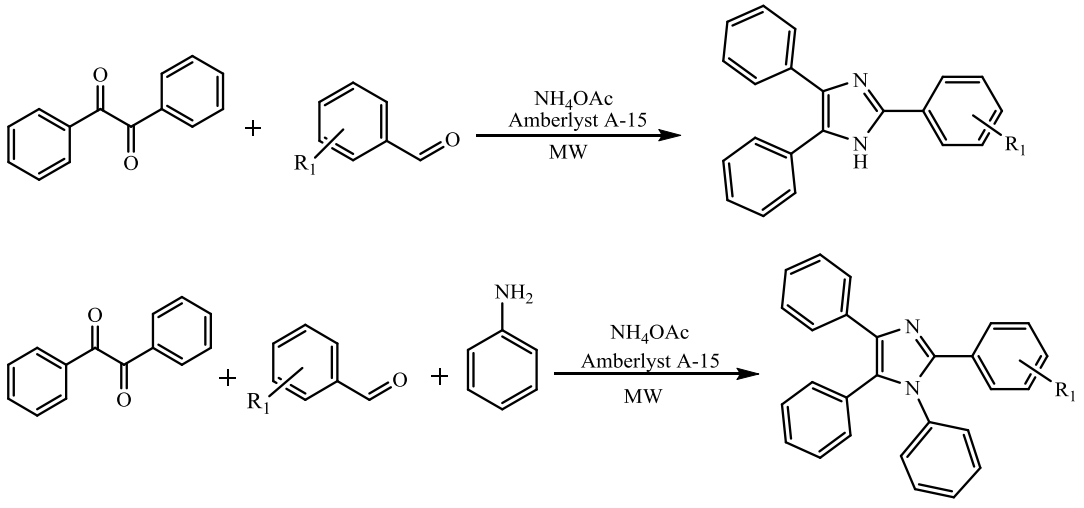

Scheme-17

Sangwan et al.[29] synthesized substituted imidazoles by reacting aromatic aldehydes, benzil, and ammonium acetate in presence of solid acid catalyst viz. Rice Husk Ash.SO_3H (RHA.SO_3H) at room temperature. They reported the synthesized products showed herbicidal activity against Raphanus sativus L. seeds and also screened for their antifungal activity against Rhizoctonia solani and Aspergillus niger. (Scheme-18)

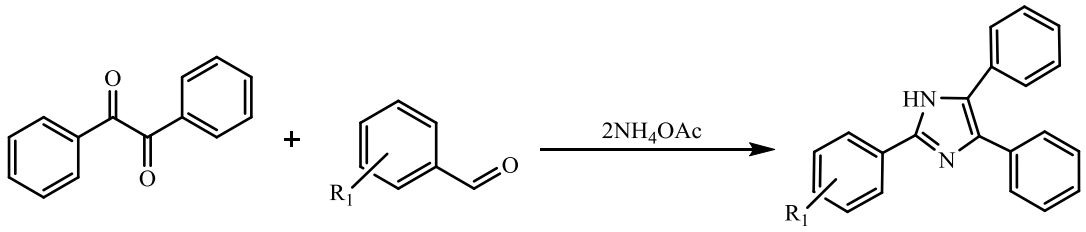

Scheme-18

Cyclocondensation of 1,2-diketone, aldehyde, ammonium acetate, primary amine and Antimony trichloride absorbed on silica gel ($SbCl_3/SiO_2$) as a catalyst under solvent-free conditions gives 1,2,3,5-tetrasubstituted imidazole derivatives as reported by Safari and team[30]. (Scheme-19)

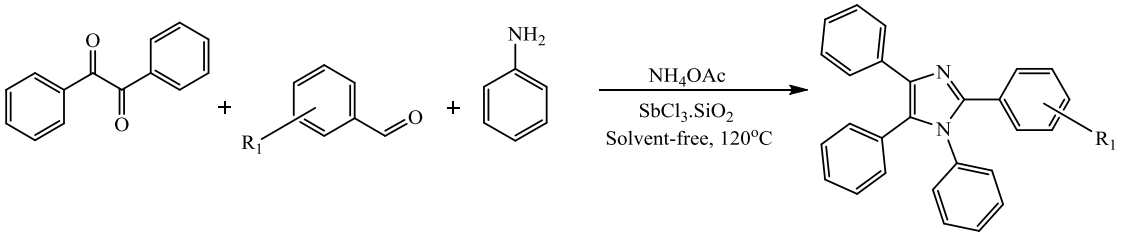

Scheme-19

Mahmoudiani et al.[31] prepared a new nano-Fe_3O_4@$Ca_3(PO_4)_2$ catalyst from an egg-shell as a solid waste with Fe_3O_4 nanoparticles. The synthesized nano-Fe_3O_4@$Ca_3(PO_4)_2$ catalyst was used as a promoter for the synthesis of 1,2,4,5-tetra-substituted imidazole derivatives by using various benzaldehydes, anilines, benzoin, and ammonium acetate at 95°C under solvent-free conditions. (Scheme-20)

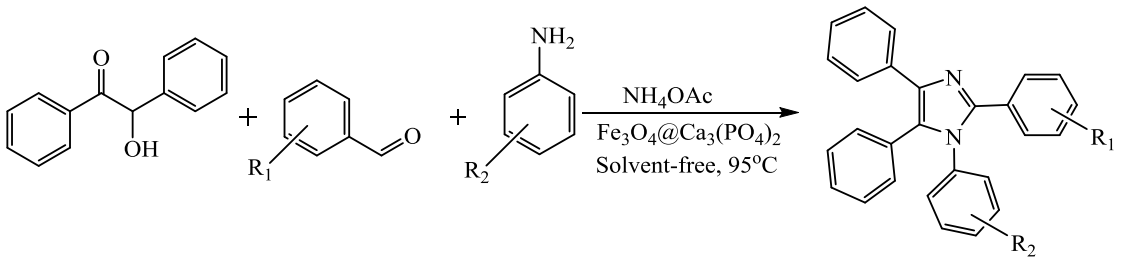

Scheme-20

Thwin and researchers[32] reported the synthesis of 1,2,4,5-tetrasubstituted imidazole derivatives using benzil, benzaldehydes, benzalamines, and ammonium acetate in the presence of Cu@imine/Fe_3O_4 MNPs as a catalyst at 80°C under solvent-free conditions. (Scheme-21)

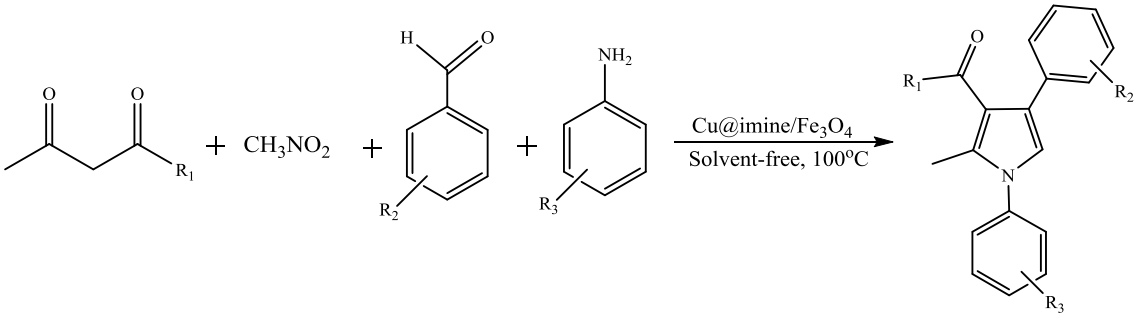

Scheme-21

D. NEAT SYNTHESIS OF PYRIDINES

Rong and researchers[33] discussed a green protocol for the synthesis of polysubstituted pyridines without using any solvent and catalyst. The reaction was carried out between aromatic aldehydes, cyclopentanone and ammonium acetate and obtained the products in excellent yield. (Scheme-22)

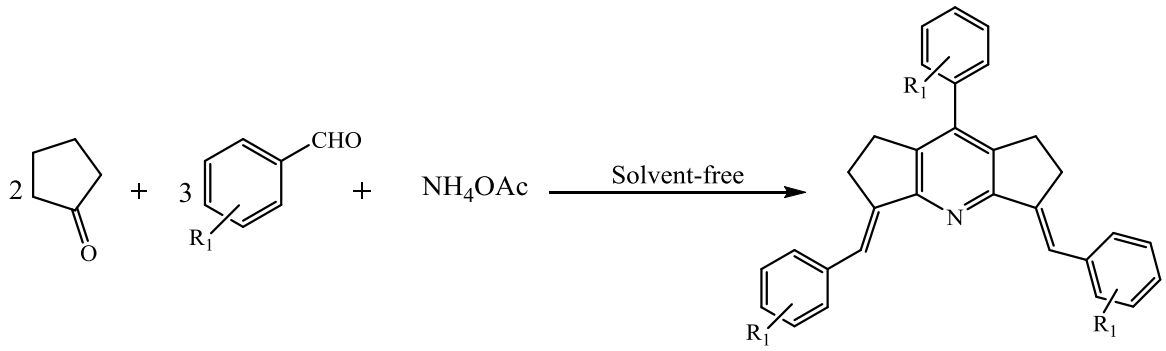

Scheme-22

Mobinikhaledi et al.[34] synthesized highly substituted pyridines by one-pot multicomponent reaction of aldehydes, malononitrile, and ammonium acetate in the presence of triethylamine(NEt_3) as a catalyst under solvent-free conditions. The reaction was investigated using various solvents and obtained the high yield of products under solvent free conditions at 100°C. (Scheme-23)

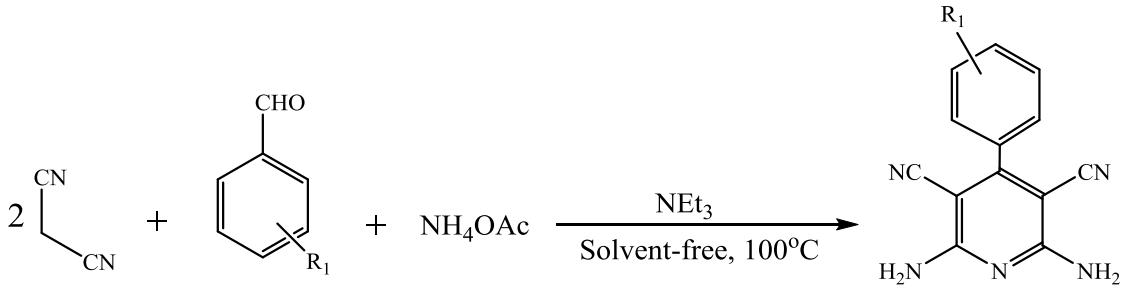

Scheme-23

Adib and coworkers[35] and researchers reported the novel method for synthesizing 2,4,6-triaryl pyridines through the reaction of 1,3-diaryl-2-propen-1-ones with ammonium acetate in the presence of a catalytic amount of acetic acid at 100°C for 4 hours, under solvent-free conditions. This method offers several advantages, including solvent-free conditions, high yields, and a simplified purification process. (Scheme-24)

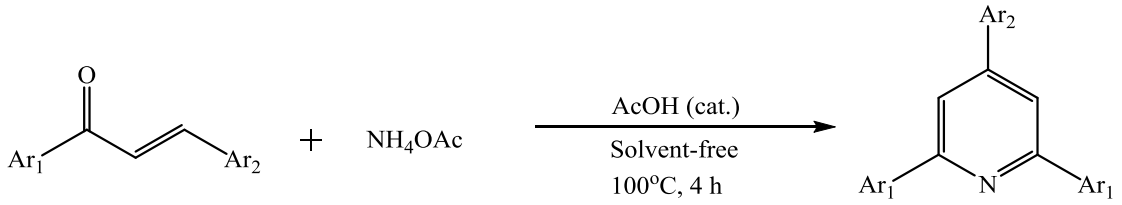

Scheme-24

Jiang and researchers[36] reported a domino reaction of malononitrile, cycloketones and ammonium acetate under microwave-irradiation and solvent-free conditions to yield highly substituted 2,4-diaminopyridine-3,5-dicarbonitriles. The method was tested in different solvents but the product was obtained in excellent yield under solvent-free conditions. (Scheme-25)

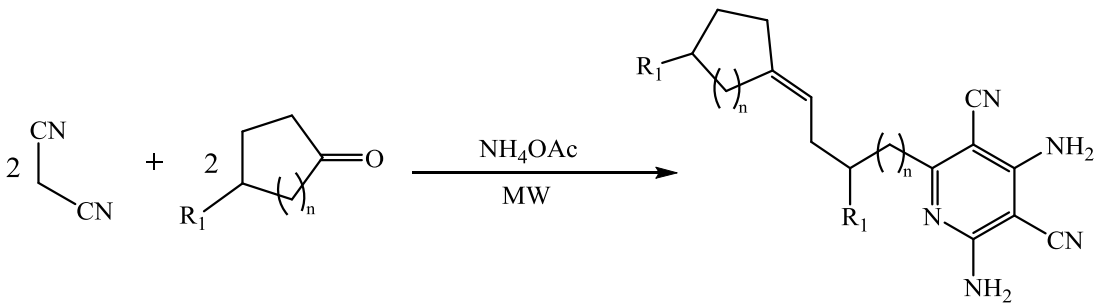

Scheme-25

Conclusion

Neat reaction strategies, which eliminate the need for solvents and catalysts, have emerged as a vital tools in modern organic synthesis. This review has highlighted various neat reaction methods, including room-temperature reactions, microwave irradiation, grinding and ball milling. These approaches not only reduce waste and environmental impact but also offer simplicity, efficiency, and cost-effectiveness. This approach enables the straightforward synthesis of various compounds, including pyrroles, pyrazoles, imidazoles, and pyridines.

As the chemical industry focuses more on sustainability and protecting the environment, neat reaction strategies will become more important. Future research should work on improving these methods, finding new uses for them, and using them in large-scale industrial processes. In the end, using neat reaction strategies will help create chemical processes that are more efficient, sustainable, and better for the environment.

References

[1]. P. Anastas and N. Eghbali, "Green Chemistry: Principles and Practice," Chem. Soc. Rev., vol. 39, no. 1, pp. 301–312, 2010, doi: 10.1039/b918763b.

[2]. C. A. Tao and J. F. Wang, "Synthesis of metal organic frameworks by ball-milling," Crystals, vol. 11, no. 1, pp. 1–20, 2021, doi: 10.3390/cryst11010015.

[3]. F. Frecentese et al., "The Application of Microwaves, Ultrasounds, and Their Combination in the Synthesis of Nitrogen-Containing Bicyclic Heterocycles," Int. J. Mol. Sci., vol. 24, no. 13, 2023, doi: 10.3390/ijms241310722.

[4]. D. S. Wagare, P. D. Netankar, M. Shaikh, M. Farooqui, and A. Durrani, "Highly efficient microwave-assisted one-pot synthesis of 4-aryl-2-aminothiazoles in aqueous medium," Environ. Chem. Lett., vol. 15, no. 3, pp. 475–479, 2017, doi: 10.1007/s10311-017-0619-1.

[5]. D. S. Wagare, S. E. Shirsath, M. Shaikh, and P. Netankar, "Sustainable solvents in chemical synthesis: a review," Environ. Chem. Lett., vol. 19, no. 4, pp. 3263–3282, 2021, doi: 10.1007/s10311-020-01176-6.

[6]. V. B. Jagrut, D. L. Lingampalle, P. D. Netankar, and W. N. Jadhav, "Glycerol mediated safer synthetic route for pyrazolines bearing quinolino and benzene sulfonamido pharmacophores," Der Pharma Chem., vol. 5, no. 1, pp. 8–11, 2013.

[7]. M. Kashezheva et al., "Harnessing Nanocatalysts for Sustainable Chemical Processes: Innovations in Green Chemistry," Asian J. Green Chem., vol. 9, no. 1, pp. 57–82, 2025, doi: 10.48309/AJGC.2025.483172.1564.

[8]. H. M. Marvaniya, K. N. Modi, and D. J. Sen, "International Journal of Drug Development & Research Available online http://www.ijddr.in Covered in Official Product of Elsevier , The Netherlands © 2010 IJDDR GREENER REACTIONS UNDER SOLVENT FREE CONDITIONS," vol. 3, no. 2, pp. 42–51, 2011.

[9]. T. S. Choudhare, D. S. Wagare, V. T. Kadam, A. A. Kharpe, and P. D. Netankar, "Rapid One-Pot Multicomponent Dioxane-HCl Complex Catalyzed Solvent-Free Synthesis of 3,4-Dihydropyrimidine-2-One Derivatives," Polycycl. Aromat. Compd., vol. 42, no. 6, pp. 3865–3873, 2022, doi: 10.1080/10406638.2021.1873808.

[10]. N. R. Candeias, L. C. Branco, P. M. P. Gois, C. A. M. Afonso, and A. F. Trindade, "More sustainable approaches for the synthesis of n-based heterocycles," Chem. Rev., vol. 109, no. 6, pp. 2703–2802, 2009, doi: 10.1021/cr800462w.

[11]. Al-Mulla. A., "A Review: Biological Importance of Heterocyclic Compounds," Der Pharma Chem., vol. 9, no. 13, pp. 141–147, 2017.

[12]. S. Mukherjee, S. Sarkar, and A. Pramanik, "A Sustainable Synthesis of Functionalized Pyrrole Fused Coumarins under Solvent-Free Conditions Using Magnetic Nanocatalyst and a New Route to Polyaromatic Indolocoumarins," ChemistrySelect, vol. 3, no. 5, pp. 1537–1544, 2018, doi: 10.1002/slct.201703146.

[13]. S. K. De, "Simple synthesis of pyrroles under solvent-free conditions," Synth. Commun., vol. 38, no. 16, pp. 2768–2774, 2008, doi: 10.1080/00397910701833791.

[14]. O. A. Attanasi, G. Favi, F. Mantellini, G. Moscatelli, and S. Santeusanio, "Synthesis of functionalized pyrroles via catalyst- and solvent-free sequential three-component enamine-azoene annulation," J. Org. Chem., vol. 76, no. 8, pp. 2860–2866, 2011, doi: 10.1021/jo200287k.

[15]. R. R. Wani, H. K. Chaudhari, and B. S. Takale, "Solvent Free Synthesis of N-Substituted Pyrroles Catalyzed by Calcium Nitrate," J. Heterocycl. Chem., vol. 56, no. 4, pp. 1337–1340, 2019, doi: 10.1002/jhet.3507.

[16]. J. C. Borghs, Y. Lebedev, M. Rueping, and O. El-Sepelgy, "Sustainable Manganese-Catalyzed Solvent-Free Synthesis of Pyrroles from 1,4-Diols and Primary Amines," Org. Lett., vol. 21, no. 1, pp. 70–74, 2019, doi: 10.1021/acs.orglett.8b03506.

[17]. H. Rostami and L. Shiri, "Fe3O4@SiO2—CPTMS—Guanidine—SO3H-catalyzed One-Pot Multicomponent Synthesis of Polysubstituted Pyrrole Derivatives under Solvent-Free Conditions," Russ. J. Org. Chem., vol. 55, no. 8, pp. 1204–1211, 2019, doi: 10.1134/S1070428019080207.

[18]. O. Marvi and H. T. Nahzomi, "Grinding solvent-free paal-knorr pyrrole synthesis on smectites as recyclable and green catalysts," Bull. Chem. Soc. Ethiop., vol. 32, no. 1, pp. 139–147, 2018, doi: 10.4314/bcse.v32i1.13.

[19]. H. R. Shaterian and M. Kangani, "Synthesis of 6-amino-4-aryl-3-methyl-1,4-dihydropyrano[2,3-c]pyrazole-5- carbonitriles by heterogeneous reusable catalysts," Res. Chem. Intermed., vol. 40, no. 5, pp. 1997–2005, 2014, doi: 10.1007/s11164-013-1097-0.

[20]. Z. Soltanzadeh, G. Imanzadeh, N. Noroozi-Pesyan, and E. Şahin, "Green synthesis of pyrazole systems under solvent-free conditions," Green Chem. Lett. Rev., vol. 10, no. 3, pp. 148–153, 2017, doi: 10.1080/17518253.2017.1330428.

[21]. D. Mallah and B. B. F. Mirjalili, "A green protocol ball milling synthesis of dihydropyrano[2,3-c]pyrazole using nano-silica/aminoethylpiperazine as a metal-free catalyst," BMC Chem., vol. 17, no. 1, pp. 1–10, 2023, doi: 10.1186/s13065-023-00934-1.

[22]. D. Vuluga, J. Legros, B. Crousse, and D. Bonnet-Delpon, "Synthesis of pyrazoles through catalyst-free cycloaddition of diazo compounds to alkynes," Green Chem., vol. 11, no. 2, pp. 156–15, 2009, doi: 10.1039/b812242c.

[23]. A. Shaabani, H. Sepahvand, and M. Keramati Nejad, "A re-engineering approach: Synthesis of pyrazolo[1,2-a]pyrazoles and pyrano[2,3-c]pyrazoles via an isocyanide-based four-component reaction

under solvent-free conditions," Tetrahedron Lett., vol. 57, no. 13, pp. 1435–1437, 2016, doi: 10.1016/j.tetlet.2016.02.051.

[24]. Z. N. Siddiqui and F. Farooq, "Journal of Molecular Catalysis A : Chemical Silica supported sodium hydrogen sulfate (NaHSO 4 – SiO 2): A novel , green catalyst for synthesis of pyrazole and pyranyl pyridine derivatives under solvent-free condition via heterocyclic ketene aminals -enaminones," "Journal Mol. Catal. A, Chem., vol. 363–364, pp. 451–459, 2012, doi: 10.1016/j.molcata.2012.07.024.

[25]. A. V Sapkal, D. L. Lingampalle, and B. R. Madje, "Solvent Free Synthesis Of Pyrano [2 , 3-c] pyrazoles Derivatives By Green Protocol Using NMPyTs .," vol. 7, no. 4, pp. 1135–1139, 2020.

[26]. K. Longhi et al., "An efficient solvent-free synthesis of NH-pyrazoles from β-dimethylaminovinylketones and hydrazine on grinding," Tetrahedron Lett., vol. 51, no. 24, pp. 3193–3196, 2010, doi: 10.1016/j.tetlet.2010.04.038.

[27]. Q. G. Zhang et al., "One-pot synthesis of imidazole derivatives under solvent-free condition," Asian J. Chem., vol. 24, no. 10, pp. 4611–4613, 2012.

[28]. S. S. Pandit, S. K. Bhalerao, U. S. Aher, G. L. Adhav, and V. U. Pandit, "Amberlyst A-15: Reusable catalyst for the synthesis of 2,4,5-trisubstituted and 1,2,4,5-Tetrasubstituted-1H-Imidazoles under MW irradiation," J. Chem. Sci., vol. 123, no. 4, pp. 421–426, 2011, doi: 10.1007/s12039-011-0097-0.

[29]. S. Sangwan, R. Singh, S. Gulati, S. Rana, J. Punia, and K. Malik, "Solvent-free rice husk mediated efficient approach for synthesis of novel imidazoles and their In vitro bio evaluation," Curr. Res. Green Sustain. Chem., vol. 5, no. January, p. 100250, 2022, doi: 10.1016/j.crgsc.2021.100250.

[30]. J. Safari, S. Gandomi‐Ravandi, and S. Naseh, "ChemInform Abstract: Efficient, Green and Solvent‐Free Synthesis of Tetrasubstituted Imidazoles Using SbCl 3 /SiO 2 as Heterogeneous Catalyst.," ChemInform, vol. 44, no. 51, pp. 827‐833, 2013, doi: 10.1002/chin.201351147.

[31]. M. Mahmoudiani Gilan, A. Khazaei, and N. Sarmasti, "Utilization of eggshell waste as green catalyst for application in the synthesis of 1,2,4,5-tetra-substituted imidazole derivatives," Res. Chem. Intermed., vol. 47, no. 5, pp. 2173–2188, 2021, doi: 10.1007/s11164-018-03724-w.

[32]. M. Thwin, B. Mahmoudi, O. A. Ivaschuk, and Q. A. Yousif, "An efficient and recyclable nanocatalyst for the green and rapid synthesis of biologically active polysubstituted pyrroles and 1,2,4,5-tetrasubstituted imidazole derivatives," RSC Adv., vol. 9, no. 28, pp. 15966–15975, 2019, doi: 10.1039/c9ra02325a.

[33]. L. Rong, H. Han, S. Wang, and Q. Zhuang, "Efficient synthesis of polysubstituted pyridine under solvent-free conditions without using any catalysts," Synth. Commun., vol. 38, no. 11, pp. 1808–1814, 2008, doi: 10.1080/00397910801991184.

[34]. A. Mobinikhaledi, S. Asadbegi, and M. A. Bodaghifard, "Convenient, multicomponent, one-pot synthesis of highly substituted pyridines under solvent-free conditions," Synth. Commun., vol. 46, no. 19, pp. 1605–1611, 2016, doi: 10.1080/00397911.2016.1218516.

[35]. M. Adib, H. Tahermansouri, S. A. Koloogani, B. Mohammadi, and H. R. Bijanzadeh, "Kröhnke pyridines: an efficient solvent-free synthesis of 2,4,6-triarylpyridines," Tetrahedron Lett., vol. 47, no. 33, pp. 5957–5960, 2006, doi: 10.1016/j.tetlet.2006.01.162.

[36]. B. Jiang, X. Wang, F. Shi, S. J. Tu, and G. Li, "New multicomponent cyclization: Domino synthesis of pentasubstituted pyridines under solvent-free conditions," Org. Biomol. Chem., vol. 9, no. 11, pp. 4025–4028, 2011, doi: 10.1039/c0ob01258k.

International Journal of Scientific Research in Science and Technology
Available online at : www.ijsrst.com
Print ISSN: 2395-6011 | Online ISSN: 2395-602X
doi : https://doi.org/10.32628/IJSRST

A One-Pot Three-Component Synthesis of 4,6-Diarylpyrimidin-2(1H)-One's Derivatives and its Characterization

M.S. More[1], D.L. Maske[2], B.S. Bhise[3], B.G.Kharode[1], S.S.Wagh[4]

[1]Department of Chemistry, R.A. Art's, Shri M.K. Commerce and S.R. Rathi Scienece Mahavidhyalaya Washim, Maharashtra, India

[2]Department of Chemistry, Vasantrao Naik Science College Dharni, Dist Amravati, Maharashtra, India

[3]Department of Chemistry, Shri Shivaji Art's Commerce and Science College Motala, Dist Buldhana, Maharashtra, India

[4]Department of Chemistry Adarsh College Hingoli, Dist. Hingoli, Maharashtra, India

ARTICLEINFO

Article History :

Published : 07 Dec 2024

Publication Issue :
Volume 11, Issue 23
Nov-Dec-2024
Page Number :
417-419

ABSTRACT

In the Present work first simple and an efficient procedure for the synthesis of 4,6-diarylpyrimidin-2(1H)-ones derivatives using different catalyst one-pot three-component Biginelli-like cyclocondensation of an aldehyde, a methyl ketone and urea under ultrasonic condition is developed . The physical measurement and structural elucidation by spectrum like UV-Vis, FT-IR, 1H-NMR, used in this work.

Keywords: Aromatic Aldehyde, aromatic Ketone, diarylpyrimidin, Ethanol,

Introduction

In recent years' synthesis of biological active compounds is in great demand. Pyrimidine nucleus is found in many natural bioactive products possessing multiple biological and medical properties [1]. Some of these compounds serve as antihypertensive, antibacterial, and anti-inflammatory agents [2]. The batzelladine alkaloids containing 3,4-DHPM isolated from marine sources inhibits the binding of HIV envelope protein gp-120 to human CD4 cells [3]. Such properties make these pyrimidones highly important. There are only a few methods reported for the synthesis of DHPMs, wherein a one-pot cyclocondensation of methyl ketones with aldehydes and urea instead of 1,3-diketones is reported [4]. Heravi et al. used TMSCl and sulfamic acid as catalysts for the synthesis of 4,6-diarylpyrimidin-2(1H)-ones (DAPMs) [5], Khosropour et al. used $Bi(TFA)_3$ immobilized on [nbpy]$FeCl_4$ [6], and Cai-hui used con. HCl in ionic liquid [BMIM][BF_4] to promote this reaction [7]. Other reported methods for the synthesis of DAPMs are from urea and 1,3-diphenylpropenone or 1,3-

diphenylpropynone or 1,3-diphenylpropane-1,3-dione in the presence of NaOEt/Et_3N or cyanuric chloride /CF_3SO_3 Zn as catalysts [8–11]. The above reported methods suffer from drawbacks such as use of stoichiometric amounts of catalysts, expensive reagents, prolonged reaction time, and varying yields of the products.

Experimental

Solvents were employed as commercial anhydrous grade. Melting points were determined in open capillary tube and are uncorrected. ^1H and ^{13}C NMR spectra were recorded on Bruker advance II-400 MHz spectrometer.

Material and Methods:

All solvents were labouring as commercial anhydrous mark without further Refining. The column chromatography was carried out over silica gel (100120esh). Melting points determined by open capillary tube. ^1H NMR spectra were recorded on a Bruker 300 MHz spectrometer in DCl3 solvent TMS as internal standard. The crude product was recrystallizing from 80 percentage ethanol.

General procedure for synthesis of 3, 4-dihydro4, 6-diphenylpyrimidine-2(1H)-one and its derivatives:

A mixture of [0.01M] of substituted Aldehyde and ketone with [0.01M] of urea and thiourea were refluxed for in 30 ml ethanol, Then the reacting mixture was cooled and poured into crushed ice, then the solid product was precipitate out, then it was filtered, dried & recrystallized from ethanol gives substituted 3,4-dihydro-4, 6-diphenylpyrimidine-2(1H)-thione. The reaction is monitored by TLC. All the compounds are characterized by physical and spectral data.

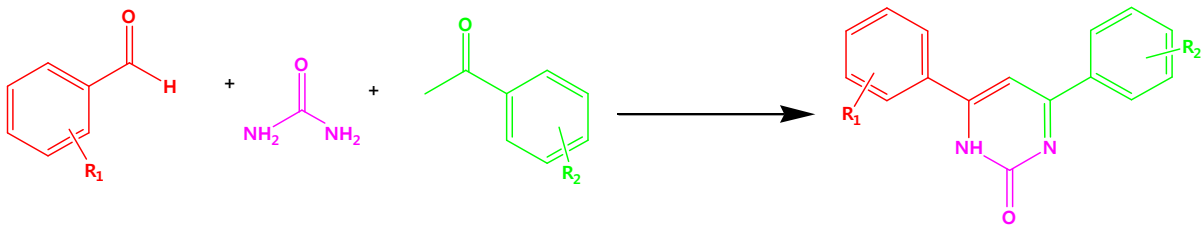

1 2 3

4,6-diphenylpyrimidin-2(1*H*)-one

4

(A25-A32)

Table 1: An effective synthesis Metal Complex of Schiff base & Manganese (A1-A8)

Sr.N.	Aldehyde (R_1)	Ketone (R_2)	Product	M. P. (°C)	Yield[b] (%)
1	$3NO_2$	$4N(CH_3)_2$	**A_{25}**	280	66
2	2Cl	$2CH_3$	**A_{26}**	288	80
3	$2OCH_3$	3Cl	**A_{27}**	235	81
4	$4OCH_3$	2Br	**A_{28}**	292	55
5	2OH	H	**A_{29}**	255	61
6	4OH	H	**A_{30}**	261	78
7	-H	2OH	**A_{31}**	258	68
8	-H	$4NO_2$	**A_{32}**	235	81

1) **A_1**

M.P.280 ^{0}C IR (KBr): 3358, 3159, 2960, 1612, 1502 cm^{-1};

H^1 NMR (DMSO, 300 MHz): d 7.1–7.15, HAr and CH), 7.3–7.6 (m, 7H, HAr), 7.88–7.92 (HAr), 7.99 (s, 1H, NH) ppm;

2) **A_2**

M.P. 288 ^{0}C;

IR (KBr): 3429, 3230, 3083, 1605, 1549, 1509 cm^{-1}

H NMR (DMSO, 500 MHz): d 7.59 (d, 2H, J = 7.33 Hz, HAr), 7.60–7.69 (m, 4H, HAr and H-5), 8.16 (d, 2H, J = 7.45 Hz, HAr), 8.22 (d, 2H, J = 8.32 Hz, HAr) ppm;

3) **A_3**

m.p. 235 ^{0}C; IR (KBr): m 3389, 2922, 1613, 1515, 1450 cm^1 ;

1 H NMR (DMSO, 500 MHz): d 6.96–7.04 (m, 3H, NH and H-4), 7.52–7.71 (m, 5H, HAr and H-5), 8.05–8.16 (m, 5H, HAr), 11 (s, 1H, OH) ppm

Result and Discussion

We have developed an efficient synthesis of 4,6-diarylpyrimidin-2(1H)-ones by a one-pot three-component cyclo-condensation reaction between an aldehyde, a Aryl ketone and urea using atomized sodium in THF under sonic condition. This new protocol has advantages such as:

References

[1]. C.O. Kappe,, Tetrahedron 49 (1993) 6937–6963.

[2]. (a) K.S. Atwal, G.C. Rovnyak, S.D. Kimball, D.M. Floyd, S. Moreland, B.N. Swanson, J.Z. Gougoutas, J. Schwartz, K.M. Smillie, M.F. Malley, J. Med. Chem. 33 (1990) 2629–2635;

[3]. A.D. Patil, N.V. Kumar, W.C. Kokke, M.F. Bean, A.J. Freyer, C. DeBrosse, S. Mai, A. Truneh, D.J. Faulkner, B. Carte, A.L. Breen, R.P. Hertzberg, R.K. Johnson, J.R. Westley, B.C.M. Pott J. Org. Chem. 60 (1995) 1182–1188.

[4]. P. Biginelli Gazz. Chim. Ital. 23 (1893) 360–413.

[5]. M.M. Heravi, L. Ranjbar, F. Derikvand, B. Alimadadi, Mol. Diversity 12 (2008) 191–196.

[6]. A.R. Khosropour, B.I. Mohammad-poor, H. Ghorbankhani, Bi(TFA)3 immobilized in [nbpy]FeCl4: Catal. Commun. 7 (2006) 713–716.

[7]. W. Hui, C. Xiu-mei, W. Yu, Y. Ling, X. Hai-qiang, X. Hua-hong, P. Li-ling, M. Rui, Y. Cai-hui J. Chem. Res., Synop. 12 (2008) 711–714.

[8]. S. Goswami, S. Jana, S. Dey, A.K. Adak, , Aust. J.Chem. 60 (2) (2007) 120–123.

[9]. E.K. Dora, B. Dash, C.S. Panda, J. Heterocycl. Chem. 20 (3) (1983) 691–696.

[10]. J. Nasielski, A. Standaert, R. Nasielski-Hinkens, Efficient Coupling of 2-alopyrimidines to 2,20 - Bipyrimidines, Synth. Commun. 21 (7) (1991) 901–906.

[11]. F.C. Baddar, F.H. Al-Hajjar, N.R. El-Rayyes, J. Heterocycl. Chem. 13 (2) (1976) 257–268.

International Journal of Scientific Research in Science and Technology
Available online at : www.ijsrst.com
OPEN ACCESS
Print ISSN: 2395-6011 | Online ISSN: 2395-602X
doi : https://doi.org/10.32628/IJSRST

Biological Sensors to Detect Mutagenicity of Synthetic Food Colors

Aditi Bhattacharya*, Madhuri Sahasrabudhe[1]
*Professor and Head, Department of Microbiology,Maulana Azad College of Arts, Science and Commerce, Aurangabad
1- Professor, Department of Microbiology,Maulana Azad College of Arts, Science and Commerce, Aurangabad

ARTICLEINFO

Article History :

Published : 07 Dec 2024

Publication Issue :
Volume 11, Issue 23
Nov-Dec-2024
Page Number :
420-422

ABSTRACT

Consumption of artificial food dye has increased manifold in the last 50 years. Food dyes such as erythrosine, Carnosine, Tartrazine, have been implicated in liver cancers. Azo dyes. Triphenylmethanes are adulterants added illegally as food dyes. The metabolic effects result in formation of amines that attack DNA. Apart from this, the flavoring agents, food additives pesticide residues, packing material can all pose for potential risk hazards. A strong mutagenic agent can trigger genetic and thus resultant metabolic changes in organisms. Such changes can be detected and can be used to report mutagenicity and thus possibility of carcinogenicity of the material being tested.

Keywords : Food colors, mutagenicity, carcinogenicity, test organism

Introduction

Food for comfort, food for satiating hunger, food for mindfulness, luxury food, fatty food, processed food are terms that have been heard a number of times. We have consciously moved away from natural colors to non-natural colors and modern food processing techniques. Food additives such as colorants, preservatives, artificial sweeteners, anticaking agents, taste enhancers are often being added without addressing safety concerns of cytotoxicity, genotoxicity, known mutagenicity or ability to induce changes in DNA.

Increase in shelf life and visual appeal of the food with the help of preservation methods, chemical preservatives along with synthetic coloring materials have over looked the possible hazards to health. Permissible food colors being costly are often being replaced by colors whose toxicity testing has not been done.

Review of literature:

Many synthetic colors have been widely used as food additives for economic reasons, and for their bright color and stability. Safety data for all synthetic food colors have been repeatedly determined and evaluated by the Food and Agricultural Organisation (FAO) and World Health Organization (WHO). Furthermore, they are generally used after evaluation of their safety by regulatory agents in the country of use. (Ozaki et al., 1996)

There are further reports mentioned by Ozaki et al (1996) of food additives being decomposed by light (Ishizaki et al., 1978, Ishizaki et al., 1979; Price and Buescher, 1996; Uezawa et al., 1990), by oxygen (Tonogai et al., 1978a), heat (Taru and Takaoka, 1982), and by reaction with chemicals such as other food additives or ingredients (Hisada et al., 1996; Nonaka et al., 1990). As the decomposition may render some of the food additives toxic, it is necessary to examine the toxicity of both virgin food additives and the decomposition products.

Some of the food colors are permitted in some countries and not permitted elsewhere. Ozaki et al (1976) has reported that Food Red Nos 3 (Erythrosine B) and No. 40 (Allura Red AC), Food Blue Nos 1 (Brilliant Blue FCF) and No 2 (Indigo carmine) are widely used and permitted by the regulatory agencies of many countries, including the USA and Japan. Food Red No 102 (new coccine) is permitted in Japan but not in the USA.

Food colors can be oxidized, reduced to toxic products as has been observed in animal studies. One of the reasons for mutagenicity of Azo dyes is through their reduction to toxic amines.

Brown et al (1978) tested 37 azo , Xanthine and Triphenyl methane dyes including those approved for use in USA and tested the same through Ames test . Approved dyes were not found to be mutagenic. They have reported that several azo dyes were directly mutagenic such as Acid Alizarin yellow R and G. Some required microsomal activation or required chemical reduction and microsomal activation, such as Acid Alizarin Red B, Methyl Red and Acid Alizarin violet N, Sudan IV respectively. Two xanthine dyes out of those tested were also found to be mutagenic.

As such the exposures to UV irradiation can occur from natural and artificial sources, mainly from sun. On the other hand, different doses of artificial UV irradiation are widely administered to increase the shelf life of the food products on account if its germicidal property. Herein the interactions between UV radiations and the additives are not being separately assessed for safety.

Ozaki et al (1998) tested the genotoxicity of five of the synthetic food colors. Food Red Nos 3, 40 and 102 and food blues Nos 1 and 2 along with their irradiated products for mutagenic activity by Ames test using *Salmonella typhimurium* strains TA 98 and TA 100 as well as rec assay using *B.subtilis* H 17 and M45 strains that showed DNA damaging effects. Irradiated products of food blue no – 2 were found to be mutagenic that increased with increasing irradiation period.

Food colours Brown FK and its constituents were assayed by Venitt and Bushell (1976) for mutagenicity in *Salmonella typhimurium* TA 1535, 1537 and 1538 strains. Three of the Brown FK samples were found to be mutagenic in TA 1538 when metabolically activated by native supernatant fraction. Mutagenicity was found to be dose dependent. A 16 fold increase in rate of mutation was detected at dye concentration of 4 mg/plate. They inferred that the conversion of products to reactive triamines by the gut microflora was thought to be the main metabolic pathway by which Brown PK produced its myotoxic and proposed mutagenic effects.
Drake (1975) reviewed the UK safety aspects of additives, food colors and preservatives.

Thomas and Adegoke (2015) reported that consumer goods have to be presented with good aesthetics, so as to mask uninviting colors, offensive odors and increase the taste. These are being added and thus consumed

frequently or occasionally as per individual preferences. They observed that chronic exposure to such substances must be emphasized to prevent occurrence of subtle yet terrible side effects from consuming sub toxic doses of the additives over a period of time.

Prival et al (1988) observed the mutagenicity of four azo dyes (FD and C Yellow no – 5 , 6 , Red no. – 40 and amaranth) using four different variation of the Ames plate incorporation assay . In such assays only, the ether extracted portion showed mutagenicity. This was further attributed to an impurity that got reduced and further extracted in ether i.e. an ether extractable mutagen.

Santos et al (2022) reported that among the food additives used in the food industry, food dyes are considered the most toxic. He noted a tartarazine induced concentration dependent toxic effect on the test system. Cytotoxicity was noted in fibroblast and human gastric cells. It also showed mutagenic effect on *Allium cepa* test system. Tartrazine therefore excreted a toxic effect on test systems and a prolonged use may also trigger carcinogenesis.

Conclusion:

It may be thus concluded that biological sensors and tests such as the Ames test, the in vitro comet assay, in vitro micronucleus assay, and the mouse lymphoma assay can be used to identify chemicals that can cause genetic mutations. The several interactions between food additives, packaging material, product processing can render it to be potentially hazardous, gentoxic, mutagenic and thus possibly carcinogenic entities and is of concern on account of its increasing use in food products.

References

1) A Ozaki a, M Kitano b, N Itoh a, K Kuroda c, N Furusawa a, T Masuda d, H Yamaguchi b. 1998. Mutagenicity and DNA-damaging Activity of Decomposed Products of Food Colours under UV irradiation. Food and Chemical Toxicology, Vol 36 (9-10),pp 811-817.

2) P. Brown, Gerald W. Roehm, Ronald J. Brown. 1978. Mutagenicity testing of certified food colors and related azo, xanthene and triphenylmethane dyes with the Salmonella/microsome system, Mutation Research/Fundamental and Molecular Mechanisms of Mutagenesis, Volume 56 (3) , pp 249-271

3) S. Venitt, C.T. Bushell. 1976. Mutagenicity of the food colour brown FK and constituents in Salmonella typhimurium.
Mutation Research/Genetic Toxicology, Vol40(4) ,pp- 309-315. https://doi.org/10.1016/0165-1218(76)90029-X

4) J.J.-P. Drake.1975. Food colours — harmless aesthetics or epicurean luxuries? Toxicology, Vol 5(1) pp- 3-42

5) Michael J. Prival , Valerie M. Davis , Martha D. Peiperl, Sandra J. Bell.1988. Evaluation of azo food dyes for mutagenicity and inhibition of mutagenicity by methods using *Salmonella typhimurium,* Vol 206 (2) pp 247-259.

6) Jailson Rodrigues dos Santos, Larissa de Sousa Soares, João Marcelo de Castro e Sousa.2022. Cytotoxic and mutagenic effects of the food additive tartrazine on eukaryotic cells. *BMC Pharmacology and Toxicology* vol 23, Article number: 95

International Journal of Scientific Research in Science and Technology
Available online at : www.ijsrst.com
Print ISSN: 2395-6011 | Online ISSN: 2395-602X
doi : https://doi.org/10.32628/IJSRST

Comparative Studies of Bacterial Degradation of Azo Dye Reactive Orange 16

Sahasrabudhe Madhuri, Aditi Bhattacharya
Professor, Dept of Microbiology, Maulana Azad College of Arts, Science and Commerce, Aurangabad, Maharashtra, India

ARTICLEINFO

Article History :

Published : 07 Dec 2024

Publication Issue :
Volume 11, Issue 23
Nov-Dec-2024
Page Number :
423-429

ABSTRACT

Azo dyes are one of the oldest xenobiotic compounds extensively used in textile and printing. Approximately 10%-15% of the dyes are released into the environment during manufacturing and usage. Textile and dye industries generate large volumes of waste water. The generation and disposal of insufficiently treated coloured wastewaters is environmentally hazardous. Discharge of azo dyes into the water bodies is unsafe not only for aesthetic reasons but also because many azo dyes and their breakdown products are toxic toward aquatic life and mutagenic for humans. Biological treatment methods are cheap and offer best alternative as compared to physico-chemical methods.

Microbial decolourization and degradation is environmentally friendly and cost competitive alternative to physico-chemical decomposition processes for the industrial effluents. In the present study, Reactive Orange 16 was used a model azo dye. Bacteria selected for the study include Enterococcus faecalis, Georgeniasp, Micrococcus glutamicusNCIM 2168, Bacillus cereus and Pseudomonas sp. Effect of various physico chemical factors was studied to detect optima for pH, temperature and dye concentration. Degradation was confirmed by Uv-Vis absorption, TLC, HPLC studies. Enzymes involved in degradation studies were found to be oxidoreductases. Toxicity studies revealed nontoxic nature of the degradation products.

Hence the isolates having ability to degrade and detoxify the dye can be successfully used for treatment of coloured wastewater.

Introduction

Biodegradation of synthetic dyes using different bacteria is becoming an accepted approach for treating azo dye wastewater to mitigate many environmental problems. Azo dyes are used on a large scale due to their cost-effectiveness, ease of production, and versatility for various applications. Synthetic dyes are diverse and they are

broadly categorized into acid, basic, direct, disperse, reactive, sulphur, and vat. Acid dyes are commonly applied to cosmetics, acrylic, nylon, silk, and wool as acidic dye solutions. They are typically used for textiles, leather goods, and food. (Tang et.al. 2022).

Biodegradation of synthetic dyes not only results in the decolorization of the dyes but also in the disintegration of the dye molecules into smaller and simpler parts. Various microorganisms including fungi, bacteria, yeasts, and algae, have been used to decolorize and degrade synthetic dyes. The wastewater from industries such as plastics, textiles, paper and leather printing contains large amounts of one or more synthetic azo bonds. These chemicals pose significant ecological hazards, including carcinogenic and mutagenic effects. (Awady E. et. Al, 2024). The azoreductases are considered to be the most potent group of enzymes active in the biodegradation of synthetic azo dyes. They accomplish the reductive cleavage of synthetic azo dyes bonds. (A. Hassan et.al, 2023) Hence, it was found essential to study the bacteria degrading dyes and its possible role in degradation of waste water.

2. MATERIAL AND METHODS:

2.1 Culture used:

The cultures used were isolated and identified by 16 S r-RNA sequencing and were in the present study. The isolates identified were *Enterococcus faecalis* YZ 66, *Georgenia* CC-NMPT-T3, *Bacillus cereus* PCS 8 and *Pseudomonas aeruginosa* strain MZA 85. The culture of *Micrococcus glutamicus* NCIM 2168 was obtained from National Collection of Industrial Microorganisms (NCIM), National Chemical Laboratory, Pune, India. The culture was selected for its known property of dye degradation.

2.2 Chemicals and reagents:

All chemicals and reagents used were of high purity. Reactive orange 16 was supplied by Spectrum dyes and chemicals Pvt Ltd., Surat, India

2.3 Optimization of process parameters:

2.3.1 Decolourization experiment:

Decolourization experiment was carried out with the initial concentration of 50 mg/L of the dye Reactive orange 16 under static condition at pH 7and at 28°C. Aliquot of inoculated broth was taken after every two hours, subjected to centrifugation at 10000g for 10 min. and supernatant was used for absorption studies by spectrophotometer at the λ_{max} of 495 nm of the dye. The experiment was carried out in triplicate. Control tubes without inoculated culture were kept throughout the experiments. Percentage decolourization was calculated from initial (A_0) and final(A_t) absorbance by using the formula as stated in Sartale et al. 2009.

% Decolorization = A0 – At/ A0 X 100.

2.3.2 Effect of pH:

The ability of the selected culture to decolourize the dye was studied by using basal nutrient medium Nutrient broth (M 002)Hi Media of pH ranging from 3 to 8. The mean of the three readings was taken.

2.3.3 Effect of temperature:

The temperature plays a key role in decolourization and degradation of the dye. Hence, the decolourization was carried out at temperature ranging from 28 to 50°C under static condition.

2.3.4 Effect of dye concentration:

Ability of the selected culture to decolourize the increasing concentration of the dye was studied by using the dye concentration from 5.-500 mg/L.

2.4 Analysis of the degradation products:

The decolourized broth was subjected to centrifugation for separation of the bacterial cells. Metabolites formed during the degradation were extracted in twice the amount of dicholorometahne . Then it was evaporated and the residue was dissolved in small quantity of HPLC grade methanol. The same is used for analyses.

2.4.1 UV absorbance study

The extracted metabolites were scanned from 200-1000 nm using SL 244 Elico double beam spectrophotometer at room temperature.

2.4.2 TLC

In order to confirm degradation of the dye Thin layer chromatographic separation of the degraded products was carried out. The separation was done on precoated silica gel 60 F_{254} plates 'Merck' 20 X 20 cm aluminum plates. TLC plate were developed using iodine. The mobile phase used for TLC of the dye and metabolites was composed of methanol: ethyl acetate: n-propanol: water: acetic acid in proportion of 1:2:3:1:0.2 (v/v) (Kalyani et al., 2008).

2.4.3 HPLC

HPLC analysis was performed in an isocratic system(Shimadzu SCL 10 AVP) and equipped with dual absorbance detector using C 18 column with HPLC grade methanol as mobile phase at the flow rate of 1.0 mL/min for 10 min at λ_{max} of the respective dye (Sartale et al., 2009).

2.4.4 Enzymes involved in degradation

Cell free extract was obtained by centrifugation followed by sonication. The homogenate was subjected to centrifugation , supernatant was used as a source of enzymes for carrying out assay of oxidoreductase enzymes as per Kalyani et al., 2008.

2.4.5 Toxicity studies

For confirmation of nontoxic nature of the metabolites, toxicity assay was carried out using *Sorghum vulgare Phaseolus mungo* . Ten seeds were irrigated by water as a control, the dye and the metabolites of degradation respectively. Three sets of the same experiment were kept

2.4.6 Statistical analysis was done by ANOVA

3 RESULTS AND DISCUSSION:

3.1 Optimization of process parameters:

3.1.1 Decolourization experiment:

Sulphonated azo dye RO 16 was completely decolourized by *E.faecalis* within 4 h. *Georgenia sp.* and *M.glutamicus* decolourized 94.2% and 99.62 % of the dye within 8 h, respectively while Bacillus cereus, *P.aeruginosa* and the consortium took 10 h to decolourize 83.63, 86.96 and 76.51%, respectively.

Decolourization efficiency is higher under static condition. This is because oxygen is essential for the growth of the organism but adversely affects the activity of azoreductase enzyme (Ogugbue et al., 2012). This enzymes plays a key role in degradation of the azo bond. Decolourization was associated with increase in wet weight indicating growth of the culture in presence of the selected dye. The selected cultures were found to decolourize mixture of five azo dyes as well as dye industry effluent.

3.1.2 Effect of pH on dye decolourization:

The optimum pH for colour removal is often at a neutral pH values (Junnarkar *et. al*, 2006) or slightly alkaline and the rate of colour removal tends to decrease rapidly at strongly acidic or strongly alkaline pH values (Pearce *et al.*, 2003).

Reactive orange 16 was decolourized by *E. faecalis* YZ 66 by 96.56 % at pH 6.0 within 2 h while at pH 7 and 8 it showed 94 % decolourization within 2 h. *Georgenia* decolourized RO16 96 -97 % at pH range 6 – 8 within 12-13 h. RO16 was 84.48 % decolourized at pH 7.0 within 13 h by *Bacillus cereus*. No decolourization was observed at pH 3 and 4 .Highest decolourization of 94.5 % was shown by *Micrococcus glutamicus* within 16 h at pH 8 while there was no decolourization at pH 3 and 4. .*Pseudomonas aeruginosa* decolourized 90.50 % of RO16 at pH 6.0 within 13 h. The consortium showed 81.63% decolourization within 14 h at pH 7.0

3.1.3 Effect of temperature:

Pearce *et al.* (2003) reported that the rate of colour removal increases with increasing temperature within a defined range that depends up on the system. The temperature required to produce the maximum rate of colour removal tends to correspond with the optimum cell culture growth temperature of 35-45ºC.It was reported by Mathew *et al.* (2004) that various microorganisms showed their survival at various temperature ranging from 25 – 50 ºC. The decline in colour removal activity at higher temperature can be attributed to the loss of cell viability or to the denaturation/ inhibition of the azoreductase enzyme.

Overall results showed that 28-37°C temperature range is significant for decolourization of selected dyes / mixture of dyes using our isolates/ consortium

3.1.4 Effect of dye concentration :

As dye concentration increased , the rate of decolourization was increased upto 350mg/L , above which the efficiency decolourization at increased dye concentration was decreased remarkably. It was observed that the culture could decolourize 88.11% of the dye at 500mg/L in 72 h. This may be due to the toxicity exerted by the increased dye concentration on the organism. Bheemaraddi et al ,2014 reported that decolourization decreased slowly with increase in dye concentration. Same is also reported by Parshetti et al 2009.

Decolourization of different concentrations of the dye ranging from 50-500 mg/L was studied under static anoxic condition. Among promising isolates *E.faecalis* YZ 66 was able to decolourize 96.65% of RR 195 up to 500 mg/L in 13 h. The rate of decolourization was increased up to dye concentration of 300 mg/L, above which the time required for decolourization was increased. This was observed in decolourization of the dye by all the isolates. *Georgenia* sp. decolourized 92.08% of the dye in 48 h at dye concentration 250mg/L but it took 96 h for 68.54% at 500mg/L. *B.cereus* was found to decolourize the dyes 97% in 24 h at 50mg/L. The rate of decolourization increased up to 250 mg/L but onwards it decreased. It took 72 h for about 55.42% decolourization of 500mg/L of the dyes by *B.cereus*. *M.glutamicus* showed about 90.85% decolourization in 45 h up to 300mg/L but at 500 mg/L dye concentration it required 70 h to decolourize 66.08% of the dye. *P.aeruginosa* required 76 h for 77.92% of the dye decolourization at 500 mg/L.

3.2 Analysis of the degradation products:

3.2.1 UV absorbance study:

In order to confirm biodegradation of the dye, the degradation product was subjected to Ultra violet spectrophotometric analysis. The dye RO 16 gave maximum absorption at 495 nm. The degradation product showed sharp peak at 240nm. Absence of the peak at λ_{max} of the dye confirm degradation of the dye. Reactive orange 16 with λ_{max} of 495 nm which changes to 302,294.5, 294.5,292,319 and 294 nm by *E.faecalis*, *Georgenia*, *B.cereus*, *M.glutamicus*, *P.aeruginosa* and the consortium, respectively.

3.2.2 TLC : TLC analysis revealed a sharp spot at R_f value 0.92 of RO 16 . Degradation products showed spots at R_f 0.85, 0.81.0.87,0.76 and 0.80 *E.faecalis*, *Georgenia*, *B.cereus*, *M.glutamicus*, and *P.aeruginosa*, respectively.

Sr. No.	Dye	Name of the isolate	Rf value
19	RO 16	-	0.92
20		*E.faecalis*	0.85
21		*Georgenia sp.*	0.81
22		*B.cereus*	0.87
23		*M.glutamicus*	0.76
24		*P.aeruginosa*	0.80

3.2.3 HPLC

RO16 showed peaks 1.65, 1.94, 2.93and 3.39 while degradation products of *E. faecalis* YZ 66 showed peaks at 2.709, 2.795, 2.923, 3.008 and 3.13min. Degradation products by *Georgenia sp.* show 2.668, 2.741, 2.912, 3.008, 3.467 and 3.851 min. *B.cereus* showed peaks at 2.720, 2.880, 2.976, 3.413 and 3.787 min. *M.glutamicus* showed peaks at 2.912, 3.019, and 3.083, 3.36, 3.445 and 3.616 min. *P.aeruginosa* degradation product showed peaks at 2.816, 3.029, 3.381, 3.605 and 3.829 min.

3.2.4 Enzymes involved in degradation

Decolourization performance was based on the structure of dye as well as the status of different biotransformation enzymes produced during decolourization. The dye molecule or its metabolite was responsible for an induction or inhibition of different biotransformation enzymes that bring decolourization and subsequent detoxification process. Degradation not only depends on the type of the enzymes but appropriate concentration also (Gomare *et al.*, 2009).

Culture	Dye	Lignin peroxidase	Laccase	NADH-DCIP reductase	Azoreductase
E.faecalis	RO 16	0.6573±0.0090	0.8833±0.0267	1.511±0.0516	0.325±0.021
Georgenia sp		1.4083±0.0927	1.4958±0.0556	0.3897±0.0099	0.306±0.012
B.cereus		0.7358±0.0453	0.8813±0.0172	0.43±0.02685	0.212±0.014
M.glutamicus		1.132±0.0095	0.8886±0.0205	0.653±0.032	0.21±0.016
P.aeruginosa		0.3483±0.0073	0.2243±0.0061	0.4344±0.0002	0.138±0.001

Significant induction in all four enzymes tested was observed in induced cells of *E.faecalis* and *Georgenia* sp. during decolourization of RO 16. Lip, laccase and azoreductase levels were enhanced in *B.cereus*. *M.glutamicus* showed significant induction in Lip, NADH-DCIP reductase and azoreductase. In *P. aeruginosa*, induction of NADH-DCIP reductase and azoreductase was noted

3.2.5 Phytotoxicity study of dyes and their degradation products by the isolates

Culture	Dye	*Sorghum vulgare*			*Phaseolus mungo*		
		RL	SL	% G	RL	SL	%G
	RO 16	6.04±0.51	8.77±1.17	90	4.40±0.86	8.06±1.5	80

E.faecalis	RO 16	8.38±1.21	9.68±1.31	100	6.36±1.48	10.09±1.45	100
Georgenia sp.		8.61±0.61	10.89±0.64	100	6.87±1.32	10.91±1.21	100
B.cereus		8.44±0.85	10.68±0.48	100	7.09±0.97	10.88±1.24	100
M.glutamicus		9.22±0.67	11.39±0.44	100	7.68±0.90	11.44±0.97	100
P.aeruginosa		9.26±0.95	11.31±0.57	100	8.04±0.69	11.36±0.72	100

The water from water bodies in which dye waste water is disposed is many times used for agricultural purposes hence it was essential to study phytotoxicity.

The results of the phytotoxicity revealed that there is no significant difference in the root and shoot length in case of wheat and mung irrigated with the dye but in case of metabolite irrigated wheat and mung the root and shoot length was significantly increased ($p \leq 0.001$) as compared to control.

Hence the isolates having ability to degrade and detoxify the dye can be successfully used for treatment of coloured wastewater.

REFERENCES

1. Alzain H, Kalimugogo V, Hussein K, Karkadan M. (2023). A Review of Bacterial Degradation of Azo Dyes. *International Journal of Research and Review* , 10 , 443-462.
2. AwadyM. , El-Shall F., Mohamed G., Abd-Elaziz A., Mohamed O. Abdel-Monem M. El Awady M. and Hassan M. (2024). Exploring the decolorization efficiencyand biodegradation mechanisms of different functional textile azo dyes by Streptomycesalbidoflavus 3MGH. BMC Microbiology, 24, 210.
3. Bheemaraddi, M.C., Patil, S., Shivannavar, C.T., Gaddad, S.M. (2014) Isolation and Characterization of Paracoccus sp. GSM2 Capable of Degrading Textile Azo Dye Reactive Violet 5. Hindawi Publishing Corporation e Scientific World Journal
DOI: https://doi.org/10.1155/2014/410704
4. Gomare S. and Govindwar S.P. (2009) Brevibacillus laterosporus MTCC 2298: a potential azo dye degrader. *J Appl Microbiol* ,106,993– 1004.
5. Junnarkar N. D., Murty S., Bhatt N. and Madamwar D.(2006) Decolourization of diazo dye Direct Red 81 by a novel bacterial consortium, *World Jr. of Micro& Biotech*., 22, 163-168.
6. Kalyani, D.C., Patil, P.S., Jadhav, J.P., Govindwar, S.P. (2008) Biodegradation of reactive textile dye Red BLI by an isolated bacterium *Pseudomonas* sp.SUK1. *Bioresour Technol* 994635-4641.
7. Mathew S, and Madamwar D (2004) Decolourization of Ranocid Fast Blue dye by bacterial consortium SV5. *Appl Biochem Biotechnol* ,118,371–381.

8. Ogugbue, C.J., Sawidis., T., Oranusi, N.A. (2012) Bioremoval of chemically different synthetic dyes by Aeromonas hydrophila in simulated wastewater containing dyeing auxiliaries, Ann. Microbiol, 62,1141–1153 https://doi.org/10.1007/s13213-011-0354-y.
9. Parshetti, G., Saratale G., Telke, A., Govindwar S. (2009) Biodegradation of hazardous triphenylmethane dye methyl violet by *Rhizobium radiobacter* (MTCC 8161) *Journal of Basic Microbiology,* 49, S36–S42.
10. Pearce CI, Lloyed JR, Guthrie JT (2003) The removal of colour from textile wastewater using whole bacterial cells: a review. *Dyes Pigm* 58,179–196.
11. Saratale, R.G., Saratale, G.D., Chang, J.S., Govindwar, S.P. (2009) Ecofriendly degradation of sulphonated diazo dye C.I. Reactive Green 19A using *Micrococcus glutamicus* NCIM-2168. *Bioresour Technol* 100, 3897-3907.
12. Tang K, Darwish N., Alkahtani A., AbdelGawwad M., Karácsony P. (2022). Biological Removal of Dyes from Wastewater: A Review of Its Efficiency and Advances. *Tropical Aquatic and Soil Pollution* 2, 59-75.

International Journal of Scientific Research in Science and Technology
Available online at : www.ijsrst.com
Print ISSN: 2395-6011 | Online ISSN: 2395-602X
doi : https://doi.org/10.32628/IJSRST

Study of Elemental Analysis Fertilizers to improvement of soil fertility using parameters : Methods and Importance

Kele K.V.
Dept. of Chemistry, Vaishnavi Mahavidyalaya Wadwani, Wadwani Dist. Beed, India

ARTICLEINFO

Article History :

Published : 07 Dec 2024

Publication Issue :
Volume 11, Issue 23
Nov-Dec-2024
Page Number :
430-439

ABSTRACT

In India agriculture is most important to economy. More than 50% population of India depends on agriculture. The analysis of fertilizer containing NPK essential elements which is important to development of soil fertility with the help of its methods and importance's such as supply of plant nutrients, liming materials, soil amendments and percentage of fertilizers, this is increases the plant growth and productivity of crops yield. The increment of soil fertility depending on the natural fertilizer or artificial fertilizer also organic fertilizer and inorganic fertilizer among these which is good fertilizers, advantages of disadvantages of fertilizers. Without fertilizers, nature struggles to replenish the nutrients in the soil. When crops are harvested, important nutrients are removed from the soil, because they follow the crop and end up at the dinner table. Although organic fertiliser increases the soil's physical and biological activity, a greater amount is needed for plant development because of its relatively low nutritional concentration. On the other hand, inorganic fertiliser typically contains all of the nutrients that plants need and is readily available. However, persistent use of inorganic fertilisers alone results in environmental contamination, soil acidity, and deterioration of soil organic matter.

Keywords : NPK Fertilizer, Importance of Fertilizer's, Organic or Inorganic Fertilizers

Introduction

The fertilizer is a American English or fertiliser is a British English spelling names. Fertilizers are the organic or inorganic any material of natural or synthetic origin that is applied to soil or to plant tissues to supply **plant nutrients**. Plant nutrient is the chemical elements and compounds essential for plant growth and reproduction, plant metabolism and their external supply. The total essential plant nutrients include seventeen different elements: carbon, oxygen and hydrogen which are absorbed from the air, whereas other nutrients including nitrogen are typically obtained from the soil (exceptions include some parasitic or carnivorous plants). Plants

must obtain the following mineral nutrients from their growing medium:[2] the macronutrients: nitrogen (N), phosphorus (P), potassium (K), calcium (Ca), Sulfur (S), magnesium (Mg), carbon (C), hydrogen (H), oxygen (O) the micronutrients (or trace minerals): iron (Fe), boron (B), chlorine (Cl), manganese (Mn), zinc (Zn), copper (Cu), molybdenum (Mo), nickel (Ni) These elements stay beneath soil as salts, so plants absorb these elements as ions. Fertilizers may be distinct from **liming materials.** Liming materials is an application of calcium and magnesium-luminous materials in various forms including chalk, limestone, marl burnt or hydrated lime to soil these material neutralise to soil this is improves plant growth and enhance the activity of soil bacteria or other non-nutrient **soil amendments.** To improve the soil's physical quantity, usually fertility that is the ability to provide nutrition for plant which is product soil conditioner added to soil. The most soil conditions across the world can provide plants adapted to that climate and soil with sufficient nutrition for a complete life cycle, without the addition of nutrients as fertilizer. However, if the soil is cropped it is necessary to artificially modify soil fertility through the addition of fertilizer to promote vigorous growth and increase or sustain yield. This is done because, even with adequate water and light, nutrient deficiency can limit growth and crop yield. The term "soil conditioner" is often thought of as a subset of the category soil amendments (or soil improvement, soil condition), which more often is understood to include a wide range of fertilizers and non-organic materials. Soil conditioners can be used to improve poor soils, or to rebuild soils which have been damaged by improper soil management. They can make poor soils more usable, and can be used to maintain soils in peak condition.

The many sources of fertilizer exist, it is produced natural and industrially. For most modern agricultural practices, fertilization focuses on three main macro nutrients: nitrogen (N), phosphorus (P), and potassium (K) with occasional addition of supplements like rock flour for micronutrients. Farmers apply these fertilizers in a variety of ways: through dry or pelletized or liquid application processes, using large agricultural equipment or hand-tool methods. The NPK fertilizer, if overused, harms the soil. These are often harmful to the soil food web.

Fertilizer analysis

The guaranteed analysis or fertilizer grade, 16-4-8, indicates the percentage by weight of nitrogen (N), phosphate (P_2O5) and potash (K_2O). They're often simply expressed as N-P-K (nitrogen (N), phosphorus (P) and potassium (K)). In this manner, the first number is always the amount of nitrogen (N), the second number is the amount of phosphate (P_2O5), and the third number is the amount of potash (K_2O). Together, they represent the primary nutrients your plant needs: nitrogen (N) – phosphorus (P) – potassium (K). The method of analysis will help to assess the main components, the primary nutrient, and also the harmful components in fertilizers. These tests are very important and pivotal to identifying the type of nutrients in the fertilizers and also the quality and composition of the final product. Major two-component fertilizers provide both nitrogen and phosphorus to the plants. These are called NP fertilizers. The main NP fertilizers are monoammonium phosphate (MAP) and diammonium phosphate (DAP).

Elemental of Fertilizers

The macronutrients, phosphorus, nitrogen, and potassium in fertilizer determine its quality. At the same time, certain secondary elements such as magnesium, calcium, Sulfur, and trace amounts of boron, copper, cobalt, iron, molybdenum, manganese, and zinc are present in small amounts but are essential for plant growth. The fertilizer solution can be tested using two different methods: sending a sample off to a laboratory or in-house testing with an electrical conductivity (E.C.) meter. Laboratory testing determines the amount of each fertilizer element in the fertilizer solution and the application rate. However, starting in the 19th century, after

innovations in plant nutrition, an agricultural industry developed around synthetically created fertilizers. This transition was important in transforming the global food system, allowing for larger-scale industrial agriculture with large crop yields. Nitrogen-fixing chemical processes, such as the Haber process invented at the beginning of the 20th century, and amplified by production capacity created during World War II, led to a boom in using nitrogen fertilizers. In the latter half of the 20th century, increased use of nitrogen fertilizers (800% increase between 1961 and 2019) has been a crucial component of the increased productivity of conventional food systems (more than 30% per capita) as part of the so-called "Green Revolution".

These changes in agriculture began in developed countries in the early 20th century and spread globally till the late 1980s. In the late 1960s, farmers began incorporating new technologies such as high-yielding varieties of cereals, particularly dwarf wheat and rice, and the widespread use of chemical fertilizers (to produce their high yields, the new seeds require far more fertilizer than traditional varieties, **pesticides, and controlled irrigation.)**

The Green Revolution was a period that began in the 1960s during which agriculture in India was converted into a modern industrial system by the adoption of technology, such as the use of high yielding variety (HYV) seeds, mechanised farm tools, irrigation facilities, pesticides, and fertilizers. Mainly led by agricultural scientist M. S. Swami Nathan in India, this period was part of the larger Green Revolution endeavour initiated by Norman Borlaug, which leveraged agricultural research and technology to increase agricultural productivity in the developing world. Varieties or strains of crops can be selected by breeding for various useful characteristics such as disease resistance, response to fertilizers, product quality and high yields.

Significance of fertilizers

The use of artificial and industrially-applied fertilizers has caused environmental consequences such as water pollution and eutrophication due to nutritional runoff; carbon and other emissions from fertilizer production and mining; and contamination and pollution of soil. Various sustainable-agriculture practices can be implemented to reduce the adverse environmental effects of fertilizer and pesticide use as well as other environmental damage caused by industrial agriculture. The Green Revolution, or the Third Agricultural Revolution, was a period of technology transfer initiatives that saw greatly increased crop yields.

- Provide nutrients that are not found in the soil.
- Replace nutrients that were removed during harvest.
- To improve the quality of your food and increase your yield, balance the nutrients.
- It increases the water-holding capacity of the soil.
- It makes the soil porous and facilitates the exchange of gases.
- The texture of the soil improves.
- The number of microbes increases in the soil.
- They are quick in providing plant nutrients and restoring soil fertility.
- They are portable and easy to transport.
- Plants easily absorb fertilizers.
- Fertilizers improve and increase the productivity of many crops such as wheat, maize, and rice.

Even though chemical fertilizers boost agricultural productivity, their excessive usage has harmed both human health and the environment by hardening the soil, reducing fertility, enhancing insecticides, polluting air and water, and releasing greenhouse gases. Because of this in our country enhance crop production to use of field

crop fertilizers. It is counted from the year 2017 is 91.37% to 2021 is 93.1 % this value indicate the effect of fertilizers uses also horticulture crop fertilizer market value increases. With the increase horticulture cultivation areas (under horticulture cultivation in 2017 was 8.6 million hectares and 8.9 million hectares in 2021) as well as consumption of fertilizers also increase to get high yield. Recently government has been focused on self-sufficient, developing various strategies such as greenhouse ornamental flower production, which is anticipated to boost the fertilizers market in the region during the forecast period.

Necessity and Requirements of Good Fertilizer

Necessity:

Farmers become option to select which fertilizer use for good fertility of soil. It may be natural or synthetic fertilizers. To grow healthy crops full of nutrients, farmers need to ensure they have healthy soil. Without fertilizers, nature struggles to replenish the nutrients in the soil. When crops are harvested, important nutrients are removed from the soil, because they follow the crop and end up at the dinner table.

Fertilizers can be easily absorbed by the plants, as they are water-soluble and help by providing essential nutrients for the plants and improve the production of crops. Fertilizers are predictable and reliable, which increase the crop yield and provide enough food to feed a large population.

Requirements:

Fertiliser requirements are affected by soil type and nutrient content, previous cropping, the expected length of the growing season and variety grown.

a. Free-flowing (easily applied).
b. Consistent in particle size with smooth and hard granules.
c. Easily spread – ensuring even distribution patterns.
d. Quickly dissolve when in contact with moist soil or water (avoid run-off)
e. Free from contaminants and additives.

There are 17 essential nutrients that all plants need, including carbon, hydrogen, and oxygen, which plants get from air and water. Nitrogen, phosphorus, and potassium are needed in larger amounts than other nutrients; they are considered primary macronutrients.

Acidity and basicity of fertilizers: The amount of $CaCO_3$

Importance of NPK fertilizers

1) Nitrogen Fertilizers

- Nitrogen fertilizers have the nitrogen that crops need to grow.
- It is a component of protein and an amino acid in plants.
- Fertilizers containing nitrogen increase the quantity and caliber of agricultural output.
- The Haber-Bosch process produces ammonia (NH_3), which is used to make nitrogen fertilizers.
- The hydrogen (CH_4) is commonly supplied by natural gas (CH_4), and the nitrogen (N_2) is obtained from the air in this energy-intensive process. All other nitrogen fertilizers, such as anhydrous ammonium nitrate (NH_4NO_3) and urea ($CO(NH_2)_2$), need this ammonia as a feedstock.
- The Atacama Desert in Chile also has deposits of sodium nitrate ($NaNO_3$) (Chilean saltpetre), which was one of the first nitrogen-rich fertilisers employed around 1830. Fertilizer is still mined from it.
- The Ostwald technique also produces nitrates from ammonia.

2) Phosphorus Fertilizer

- Phosphorus is the principal nutrient in phosphorus fertilizers.

- The effective phosphorus concentration, fertilization techniques, soil characteristics, and crop strains all affect how successful a fertilizer is.
- The protoplasm of the cell contains phosphorus, which is crucial for cell growth and proliferation.
- Phosphate fertilizers are made from phosphate rock, which comprises the minerals fluorapatite $Ca_5(PO_4)3F$ (CFA) and hydroxyapatite $Ca_5(PO_4)3F$, which contain phosphorus. Treatment with sulfuric (H_2SO_4) or phosphoric acids converts these minerals into water-soluble phosphate salts (H_3PO_4). This application is the driving force behind the large-scale manufacture of sulfuric acid.
- The nitro phosphate process, also known as the Odda process, involves dissolving phosphate rock containing up to 20% phosphorus (P) in nitric acid (HNO_3) to produce a combination of phosphoric acid (H_3PO_4) and calcium nitrate ($Ca(NO_3)_2$). This mixture can be used with potassium fertilizer to provide a compound fertilizer that contains the three macronutrients N, P, and K in easily soluble form.

3) Fertilizer Potassium

- One of the 17 basic minerals that plants need for development and reproduction is potassium (K).
- Potassium is associated with the movement of water, nutrients and carbohydrates in plant tissue. It's involved with enzyme activation within the plant, which affects protein, starch and adenosine triphosphate (ATP) production. The production of ATP can regulate the rate of photosynthesis.
- Potassium also helps regulate the opening and closing of the stomata, which regulates the exchange of water vapour, oxygen and carbon dioxide. If K is deficient or not supplied in adequate amounts, it stunts plant growth and reduces yield.
- Potassium is categorized as a macronutrient (nutrient required in large quantity) along with nitrogen (N) and phosphorus (P).
- A set of minerals and salts that contain potassium are referred to as "potash. "Numerous potassium fertilizer sources, such as muriate of potash (KCl), sulphate of potash (K_2SO_4), double sulphate of potash and magnesium (K_2SO_4 $2MgSO_4$), and nitrate of potash (KNO_3), are used.
- Potash is a mixture of potassium minerals that are used to generate potassium fertilizers (chemical symbol: K). Because potash is water-soluble, the primary effort in extracting this nutrient from the ore entails several purification stages, such as removing sodium chloride (NaCl) (common salt). Potash is sometimes referred to as K2O for the sake of simplicity when discussing potassium content.
- Potassium chloride, potassium sulphate, potassium carbonate, and potassium nitrate are the most common potash fertilizers.
- Increases root growth and improve drought resistance.
- Maintains turgor; reduces water loss and wilting.
- Aids in photosynthesis and food formation.
- Reduces respiration, preventing energy losses.
- Enhances translocation of sugars and starch.
- Produces grain rich in starch.
- Increases plants' protein content.
- Builds cellulose and reduces lodging.
- Helps retard crop diseases.

Natural Fertilizers/Organic fertilizer

- Fertilizers derived from plants and animals are known as organic fertilizers.
- By adding carbonic molecules necessary for plant growth, it enriches the soil.
- Organic fertilizers boost the amount of organic matter in the soil, encourage microbial reproduction, and alter the physical and chemical composition of the soil.
- It is regarded as one of the essential elements for foods that are green.
- The following items can be used to make organic fertilizers:
  Livestock, Agricultural Waste, Sludge from municipal and Industrial waste

Methods:

1) **Analysis of Nitrogen by Kjeldahl's Method:**

This method was developed by Johan Kjeldahl in 1883. Johan Gustav Christoffer Thorsager Kjeldahl. The Kjeldahl method or Kjeldahl digestion (Danish pronunciation: [ˈkʰelˌtɛˀl]) was a Danish chemist who developed a method for determining the amount of nitrogen in certain organic compounds using a laboratory technique which was named the Kjeldahl method after him. In analytical chemistry is a method for the quantitative determination of a sample's organic nitrogen plus ammonia/ammonium. (NH_3/NH_4+). Without modification, other forms of inorganic nitrogen, for instance nitrate, are not included in this measurement. Using an empirical relation between Kjeldahl nitrogen and protein, it is an important method for indirectly quantifying protein content of a sample.

Kjeldahl's Method:

The end of the condenser is dipped into a known volume of standard acid (i.e. acid of known concentration). A weak acid like boric acid (H_3BO_3) in excess of ammonia is often used. Standardized HCl, H_2SO_4 or some other strong acid can be used instead, but this is less commonplace.

- The sample solution is then distilled with a small amount of sodium hydroxide (NaOH).
- NaOH can also be added with a dropping funnel.
- NaOH react the ammonium (NH_4+) to ammonia (NH_3), which boils off the sample solution. Ammonia bubbles through the standard acid solution and reacts back to ammonium salts with the weak or strong acid.
- Ammonium ion concentration in the acid solution and thus the amount of nitrogen in the sample is measured via titration. If boric acid (or some other weak acid) was used, direct acid–base titration is done with a strong acid of known concentration. HCl or H_2SO_4 can be used.
- Indirect back titration is used instead if strong acids were used to make the standard acid solution: strong base of known concentration (like NaOH) is used to neutralize the solution. In this case, the amount of ammonia is calculated as the difference between the amount of HCl and NaOH.
- In the case of direct titration, it is not necessary to know the exact amount of weak acid (e.g. boric acid) because it does not interfere with the titration (it does have to be in excess of ammonia to efficiently trap it). Thus, one standard solution is needed (e.g. HCl) in the direct titration, while two are needed (e.g. HCl and NaOH) in the back-action.
- One of the suitable indicators for these titration reactions is Tashiro's indicator. It is a mixed indicator composed of a solution of methylene blue (0.1%) and methyl red (0.03%) in ethanol or in methanol.
- Writhen the methyl red is above pH 4.3, the yellow of the methyl red plus the blue of methylene blue gives aa green solution. The change from green to purple on addition of acid in titrating bck to the

original pH of boric acid is very sharp. When methyl red is used, there is a sharp change from yellowish brown to pink.

2) Analysis of Phosphorus by Phosphomolybdate Method:

This method is for the determination of phosphorus in the extracts from fertilisers.

The method is applicable to all extracts of fertilisers, for the determination of the different forms of phosphorus. After hydrolysis, phosphorus is precipitated in an acid solution in the form of quinoline phosphomolybdate. The precipitate is collected, washed, dried at 250°C and weighed.

In the above conditions, compounds likely to be found in the solution (mineral and organic acids, ammonium ions, soluble silicates, etc….) will not interfere provided that a reagent based on sodium molybdate or ammonium molybdate is used in the precipitation. Concentrated nitric acid (d = 1.40 g/ml).

Phosphomolybdate Method:

1. Phosphomolybdate assay. This assay is based on the reduction of phosphomolybdate ion in the presence of an antioxidant resulting in the formation of a green phosphate/MoV complex which is measured spectrophotometrically.
2. Reagent for preparation: 1) 0.6 M (0.6 mole/L) sulfuric acid (H_2SO_4), 2)28 mM (28 mmole/L) sodium phosphate (Na_3PO_4) $_3$) 4 mM (4 mmole/L) ammonium molybdate. Method: 1) Transfer 0.05 g ground tissue to a cooled epp endorf and add 1 ml methanol. C or. at -20.4) C. 3) Centrifuge samples for 10 min at 4. 5. O.
3. The determination of total phosphorus (TP) in an aqueous sample is based on digestion of the sample to convert phosphorus compounds into orthophosphate, which can then be determined based on spectrophotometry.
4. The total phosphorus test measures all the forms of phosphorus in the sample (orthophosphate, condensed phosphate, and organic phosphate). This is accomplished by first "digesting" (heating and acidifying) the sample to convert all the other forms to orthophosphate.

The two common colorimetric methods of measuring orthophosphate are: Ascorbic Acid/"Blue" Method and Molybdovanadate/"Yellow" Method. Both methods combine orthophosphate with molybdate in an acidic environment but differ in how they form the final compound, which creates the blue or yellow colour.

Solubility of Phosphorus:

- Phosphorus soluble in mineral acids, water soluble phosphorus, phosphorus soluble in solutions of ammonium citrate, phosphorus soluble in 2% citric acid and phosphorus soluble in 2% formic acid.
- 21 ml when the solution to be precipitated contains more than 15 ml of citrate solution (neutral citrate, Petermann or Joulie alkaline citrate).

Analysis of Potassium by Sodium Tetraphenylborate Method

Potassium in the sample reacts with sodium tetraphenylborate to form potassium tetraphenylborate, an insoluble white solid. The amount of turbidity produced is proportional to the potassium concentration. The measurement wavelength is 650 nm for spectrophotometers or 610 nm for colorimeters.

Potassium is extracted from the soil by shaking a 1-gram scoop of air-dried soil for 5 minutes with 10 millilitres of (pH7) 1 N ammonium acetate (NH4OAc). Plant-available potassium is measured by analyzing the filtered extract on an atomic absorption spectrometer set on emission mode at 766.5 nm.

The soil test for K is the best management tool for predicting the amount of potash needed in a fertilizer program. Available K in soils is estimated by measuring the total of solution K (water = soluble K) and exchangeable K.

Potassium (K) is an essential nutrient for plant growth. It's classified as a macronutrient because plants take up large quantities of K during their life cycle.

Minnesota soils can supply some K for crop production, but when the supply from the soil isn't adequate, a fertilizer program must supply the K.

Here, we'll give you a basic understanding of K, including plants' K nutrition, how it reacts in soils and its function in plants and its role in efficient crop production. In addition, you'll find information about soil tests, K sources, predicting potash needs and effectively applying K to your fields.

- Potassium in soils

The total K content of soils frequently exceeds 20,000 ppm (parts per million). While the supply of total K in soils is quite large, relatively small amounts are available for plant growth at any one time. That's because nearly all of this K is in the structural component of soil minerals and isn't available for plant growth. The amount of K supplied by soils varies due to large differences in soil parent materials and the effect weathering has on these materials. Therefore, the need for K in a fertilizer program varies across the United States.

Three forms of K are unavailable, slowly available or fixed and readily available or exchangeable are exist in equilibrium in the soil system. Below, we describe these forms and their relationship to one another.

- Soil moisture: Higher soil moisture usually means greater K availability. Increasing soil moisture increases K's movement to plant roots and enhances availability. Research has generally shown more responses to K fertilization in dry years.
- Soil aeration and oxygen level: Air is necessary for root respiration and K uptake. Root activity and subsequent K uptake decrease as soil moisture content increases to saturation. Oxygen levels are very low in saturated soils.
- Soil temperature: Root activity, plant functions and physiological processes all increase as soil temperature increases. And increased physiological activity leads to increased K uptake.
- Tillage system: Availability of soil K reduces in no-till and ridge-till planting systems. The exact cause of this reduction isn't known, although research results point to restricted root growth combined with a restricted distribution of roots in the soil.

Soil testing labs commonly air dry soil samples prior to analysis. Drying soils high in clay can affect the amount of K extracted. If K is fixed by clay, the soil test will extract less K and underestimate the available K, leading to the over application of potash fertilizer. Similarly, with clays that release K, availability tends to be overestimated and fertilizer needs underestimated. Influencing factors

Factors that determine whether K is fixed or released:

a) The type of clay that dominates the soil clay fraction.

b) The soil test K level.

c) The native level of K available from parent material.

d) Recent K fertilizer applications.

- Soil in Minnesota

Soils in Minnesota contain a mixture of clays, with smectite (the name of a pure clay mineral phase) and illite (any of a group of clay minerals having essentially the crystal structure of muscovite.) being the most abundant clay types. Iron is a structural component of clay minerals, and reducing Fe^{3+} to Fe^{2+} can affect fixation and release of K. As Fe^{3+} is reduced, K can be trapped (fixed) between clay layers for smectite and K will be released from illite. As soils get wet and dry off, the two types of clays will affect the availability of K to the crop.

We can apply potassium fertilizer either in the fall or spring for most soils in Minnesota. Sandy soils with a low cation exchange capacity have a low ability to hold K. Consider potassium to be partially mobile on sandy soils and apply it closer to the time of planting. There's a higher probability of successful establishment of perennial crops such as alfalfa and grasses if the soil test for K is in the medium range or higher.

- Liquid forms of potassium

Liquid forms of potassium are available for in-furrow application as a starter fertilizer. These forms of fertilizer are manufactured with either potassium chloride (KCl) or potassium hydroxide (KOH). Fertilizer sources containing KCl pose a greater risk for stand damage due to salts in solution.

If a fertilizer source contains KCl, apply no more than 10 pounds of N + K_2O in loamy soils and 4 pounds of N + K_2O in sandy soils. Fertilizers containing KOH are safer for seed placement as they form potassium-phosphate compounds that don't contribute to the fertilizer's salt content. Low-salt fertilizer sources manufactured with KOH cost more and may contain a very low concentration of K. Applying fertilizer on the corn seed as an in-furrow application cannot supply all the needed K in a K-responsive soil.

Potassium thiosulfate is a liquid fertilizer containing K and S. Applying fertilizer containing thiosulfate can negatively impact seedling emergence and isn't suggested for in-furrow application.

Conclusion and Result

Potassium is present in all crops grown for food and helps plants resist lodging. This is due to its impact on cell will stability, osmosis and turgor pressure. It promotes a high concentration of sugars in cells making fruits sweeter. It is very crucial for high crop yielding. It helps balance crop growth with nitrogen, ensuring healthier crops. This is acts as an antifreeze agent and result in improved frost tolerance is a crop's ability to survive a frost or below freezing temperatures. This is particularly helpful for winter crop. Phosphorous is present in every living cell thus is essential the same way's water or oxygen in all crops grown for food. It helps to capture and transform the sun's energy into chemical energy (photosynthesis) and this energy required for extract all nutrients from the soils. Phosphorous is also ensures optimal growth and maturities of crops. Phosphorus is an essential mineral for human tissue bone formation and is required by every cell in the body for normal function. Nitrogen is key component Chlorophyll to photosynthesis. It is essential for DNA in the form of nucleic acids and also Protein and amino acids. Storage N in leaves is mainly in the forms of nitrate, amino acid, and Protein Nitrate in leaves is mostly stored in vacuoles, accounting for 58–99% of total leaf nitrate. In the soil nitrogen are form by the nitrogeneas enzymes reduces the dinitrogen to ammonia and this biological proses are important in agriculture.

Potash is a mixture of potassium minerals that are used to generate potassium fertilizers (chemical symbol: K). Because potash is water-soluble, the primary effort in extracting this nutrient from the ore entails several purification stages, such as removing sodium chloride (NaCl) (common salt). Potash is sometimes referred to as K2O for the sake of simplicity when discussing potassium content. Potassium is associated with the movement of water, nutrients and carbohydrates in plant tissue. It's involved with enzyme activation within the plant, which affects protein, starch and adenosine triphosphate (ATP) production. The production of ATP

can regulate the rate of photosynthesis. Potassium also helps regulate the opening and closing of the stomata, which regulates the exchange of water vapour, oxygen and carbon dioxide. If K is deficient or not supplied in adequate amounts, it stunts plant growth and reduces yield.

Reference:

1. Lay La Burgess, © 2022 HGIC, Clemson Extension.
2. Daniel E. Kaiser, Extension nutrient management specialist and Carl J. Rosen, Extension nutrient management specialist.
3. https://www.mordorintelligence.com/industry-reports/india-fertilizers-market.
4. Millard, 1988; Nordin and Näsholm, 1997; Tegeder et al., 2018.
5. Martinoia et al., 1981; Granstedt and Huffaker, 1982.
6. Rasaynik khate Book by Dr. Jayvant H Dongle, 2003.
7. Adunikn Sendriy Khate Adunikn Sendriy Sheti Book Dr. S. D. More, 2005.
8. Sendriy Khate Nirmiti – Udoyg by Mr. Ashok Kothare, 1998.
9. Brar, B.S., Singh, J., Singh, G. and Kaur, G. (2015) Effects of Long Term Application of Inorganic and Organic Fertilizers on Soil Organic Carbon and Physical Properties in Maize-Wheat Rotation. Agronomy, 5, 220-238.
10. Han, S.H., Young, J., Hwang, J., Kima, S.B. and Parka, B. (2016) the Effects of Organic Manure and Chemical Fertilizer on the Growth and Nutrient Concentrations of Yellow Poplar (Liriodendron tulipifera Lin.) in a Nursery System. Forest Science and Technology, 12, 137-143. https://doi.org/10.1080/21580103.2015.1135827.

International Journal of Scientific Research in Science and Technology
Available online at : www.ijsrst.com
Print ISSN: 2395-6011 | Online ISSN: 2395-602X
doi : https://doi.org/10.32628/IJSRST

Nanomaterials: Exploring Classification and Innovative Synthesis Techniques

Aarti Jathar*[1], Samreen Fatema[1], Mazahar Farooqui[1], Dattaraya Jirekar[2], Pramila Ghumare[2]
[1]Post Graduate and Research Center, Maulana Azad College of Arts, Science and Commerce, Aurangabad, Maharashtra, India
[2]Anandrao Dhonde Alias Babaji Mahavidyalaya Kada, Beed, Maharashtra, India

ARTICLEINFO

Article History :

Published : 07 Dec 2024

Publication Issue :
Volume 11, Issue 23
Nov-Dec-2024

Page Number :
440-454

ABSTRACT

Recent technological developments and advanced research have undeniably demonstrated the pivotal role of nanotechnology and nanoscience in driving progress across various scientific domains. This comprehensive review article aims to explore the details of nanomaterials, focusing on their classification and synthesis techniques. Nanotechnology, as a collaborative field encompassing physics, chemistry, materials science, and engineering science, has revolutionized the scientific landscape. This review provides a detailed understanding of the types and classifications of nanomaterials, and highlighted their intricate structures, properties and synthesis methods. Various experimental techniques, including physical, chemical and biological processes, are thoroughly discussed, shedding light on the synthesis of nanomaterials. By offering an extensive overview of recent advances and synthesis techniques, this review article served as a valuable resource for researchers, scientists and engineers. This study not only provided essential insights into the potential of nanomaterials but also eased further exploration and development in this exciting field, contributing to the advancement of science and technology.

Keywords : Nanomaterials, Green synthesis, Surface functionalization, Self-assembly, Bottom-up synthesis, Top-down synthesis

1. Introduction:

Nanotechnology, which involves the application, synthesis and processing of nanometer-sized materials, has revolutionized various industries by enabling the development of new materials, devices and systems (Chaudhry et al. 2008; Farhang et al. 2007). Nanotechnology encompasses disciplines such as physics, chemistry, materials science, and engineering science, and its impact on society continues to grow (Roco 2003; Sanguansri and Augustin 2006). NanoparticlesNPs, with their unique physical, chemical, magnetic, and optical properties, have gained increasing amounts of attention and are being increasingly studied in the field of Earth Science (Banfield and Zhang 2001). With their regulated microstructural features, nanostructured materials (NsMs) offer novel properties and functionalities, making them a focus of nanotechnology research and development

(Gleiter 2000). Compared with bulk materials, nanomaterials (NMs) have gained significance due to their enhanced physical, chemical, and biological properties (Jeevanandam et al. 2018; Tiwari et al. 2012). Although there is no universally accepted definition of NMs, they generally refer to materials with a length of 1-100 nm in at least one dimension (Boverhof et al. 2015). Different organizations have provided varying definitions, emphasizing the unique features and dimension-dependent behaviors of NMs (United Nations 2012; USFDA 2011; ISO/TS 2010; Potocnik 2014).

Recently, the British Standards Institution provided definitions for commonly used scientific terms related to nanotechnology. The nanoscale is defined as a size range spanning from 1 to 1000 nm. Nanoscience involves the study of matter at the nanoscale, focusing on understanding the size- and structure-dependent features and comparing them to the behavior of individual atoms, molecules, or bulk materials. Nanotechnology refers to the modification and control of matter at the nanoscale, employing scientific knowledge for a wide range of industrial and biomedical applications. A nanomaterial is characterized by its interior or exterior nanoscale dimensional structures. A nano-object possesses one or more extrinsic nanoscale dimensions. NPs are nano substances with three outer dimensions, and if the longest and shortest axis lengths of a nano-object differ, they are referred to as nanorods or nanoplates instead of nanoparticles. Nanofibers, on the other hand, are nanomaterials with two comparable external nanoscale dimensions and a third larger dimension. A nanocomposite is a multiphase structure that has at least one nanoscale dimension, while a nanostructure refers to a nanoscale structure composed of interconnected constituent parts. Nanostructured materials include materials with internal or external nanostructures (Pas, 2011). The use of different definitions for nanomaterials across countries poses a significant barrier to establishing regulatory frameworks, as it leads to uncertainty in applying legislative guidelines to similar nanomaterials. Reconciling these disparate considerations becomes crucial in defining a unified international definition for nanomaterials (Jeevanandam et al., 2018). Controlling the characteristics of nanoparticles produces distinct effects due to the interplay of their size, atomic structure, and chemical composition. These effects include size impacts, changes in system dimensionality, changes in atomic structure, and the alloying of components that are immiscible in the solid and/or molten state (Gleiter, 2000).

2. Types and Classification:

Over the past few decades, a multitude of new nanomaterials (NMs) have emerged, necessitating the development of classification systems. It is important to differentiate between nanostructures (NSs) and nanoscale materials (NSMs). NSs are characterized by their shape and structure, while NSMs are defined by their composition. Therefore, NSs must be accurately identified based on their dimensionality, which encompasses size, shape, and form. While bulk 3D materials can have a wide range of shapes, the atomic differences between certain NSs shapes of the same dimensions become negligible as they transition into the nanoscale domain. As a result, the number of distinct NS classes has become limited, posing challenges in the current categorization of NSs (Pokropivny and Skorokhod, 2007). Most existing nanoparticles (NPs) and NSMs can be classified into four material-based groups.

(i) Organic-based nanomaterials:

This category primarily includes organic NMs and excludes carbon-based or inorganic NMs. Weak noncovalent interactions facilitate self-assembly and molecular design, resulting in desirable structures such as dendrimers,

ferritin, micelles, liposomes, and polymeric NPs. These structures exhibit sensitivity to electromagnetic radiation and thermal impacts and are predominantly used for targeted drug delivery due to their effective drug delivery potential and low toxicity (Behari et al., 2008).

(ii) Inorganic-based nanomaterials:

Inorganic NPs are composed of substances without carbon and can be further classified into two main categories: metals and metal oxide NPs. Metals such as platinum (Pt), gold (Au), silver (Ag), copper (Cu), cadmium (Cd), iron (Fe), zinc (Zn), and cobalt (Co) are utilized in NP synthesis. Metal oxides NPs are synthesized to enhance their efficiency, reactivity, and modification properties. Commonly used metal oxide NPs include zinc oxide (ZnO), iron oxide (Fe2O3), aluminum oxide (Al2O3), titanium oxide (TiO2), cerium oxide (CeO2), and silicon dioxide (SiO2). These nanoparticles exhibit distinct sizes, shapes, surface areas, and densities.

(iii) Carbon-based nanomaterials:

Carbon-based NPs are derived from carbon and widely applied in biomedical fields. They have various morphologies, such as hollow tubes, ellipsoids, or spheres. Carbon-based NMs include fullerenes (C60), carbon nanotubes (CNTs), carbon nanofibers, soot, and graphene (Gr). Key production processes for these carbon-based materials (excluding carbon black) include laser ablation, arc discharge, and chemical vapor deposition (CVD) (Kumar and Kumbhat, 2016; Jeyarajet et al., 2019).

(iv) Composite-based nanomaterials:

Composite NMs consist of multiphase NPs and NSMs, where one phase has nanoscale dimensions. These composites can combine NPs with other NPs, larger materials, or more complex structures, such as metal-organic frameworks. Composites can be formed by combining carbon-based, metal-based, or organic-based NMs with various forms of metal, ceramic, or polymer bulk materials. NMs synthesized in various forms, such as nanosheets, nanowires, nanoporous materials, and nanofibers, among others, are tailored to exhibit specific properties required for their intended applications (Jeevanandam et al., 2018).

2.1 Classification of nanomaterials based on their dimensions:

The production of conventional nanoscale products has played a crucial role in the economic advancement of many countries and is expected to continue doing so. As a result, the identification and classification of various types of nanoparticles (NPs) and nanoscale materials (NSMs) have become imperative. Initially, the classification of NMs proposed by Gleiter in 2000 was based on their crystalline morphologies and chemical content. However, this approach does not consider the dimensionality of NPs and NSMs, rendering it incomplete. In 2007, Pokropivny and Skorokhod introduced a new classification scheme for NMs, incorporating emerging composites known as 0D, 1D, 2D, and 3D NMs, as depicted in Figure 1. This classification heavily relies on the movement of electrons along the dimensions of the NMs. For instance, in 0D NMs, electrons are confined to a dimensionless space, while NMs with 1D allow electron movement along the x-axis within a range of less than 100 nm. Similarly, 2D and 3D NMs exhibit electron movement along the x-y-axis and the x-, y-, and z-axes, respectively (Pokropivny and Skorokhod, 2007).

Additionally, the classification of NPs often considers morphology, size, shape, content, homogeneity, and aggregation. Recently, three primary morphologies of NPs have been identified: spherical, crystalline, and planar. NPs are further classified into four types based on the dimension of electron movement, as illustrated in Figure- 1: 0D NPs, 1D NPs (including thin films widely used in electronic devices and sensors), 2D NPs (such as carbon nanotubes known for their high absorption and stability), and 3D NPs (including dendrimers and quantum dots) (Behari et al., 2008). Moreover, these NPs are categorized as inorganic, organic, or carbon-based (fullerenes) depending on their chemical structure (Jeyarajet et al., 2019).

2.2 Classification of nanomaterials based on their origin:

The categorization of nanoparticles (NPs) and nanoscale materials (NSMs) extends beyond dimensions and material-based classifications to consider their origin, distinguishing between natural and synthetic nanomaterials.

(i) Natural nanomaterials are generated through either biological species or natural transpiration due to anthropogenic activities. Natural sources provide surfaces with unique micro- and nanoscale templates and properties that can be utilized for technological applications. These naturally occurring nanomaterials exist in various spheres of the Earth, including the hydrosphere, atmosphere, lithosphere, and biosphere, and remain unaffected by human intervention. Earth is abundant, with naturally formed nanomaterials found in different spheres, such as the atmosphere encompassing the troposphere,; the hydrosphere containing oceans, lakes, rivers, groundwater, and hydrothermal vents,; the lithosphere comprising rocks, soils, magma, or lava at various stages of evolution,; and the biosphere encompassing microorganisms, higher organisms, and humans (Hochella et al.; Sharma V. et al., 2015).

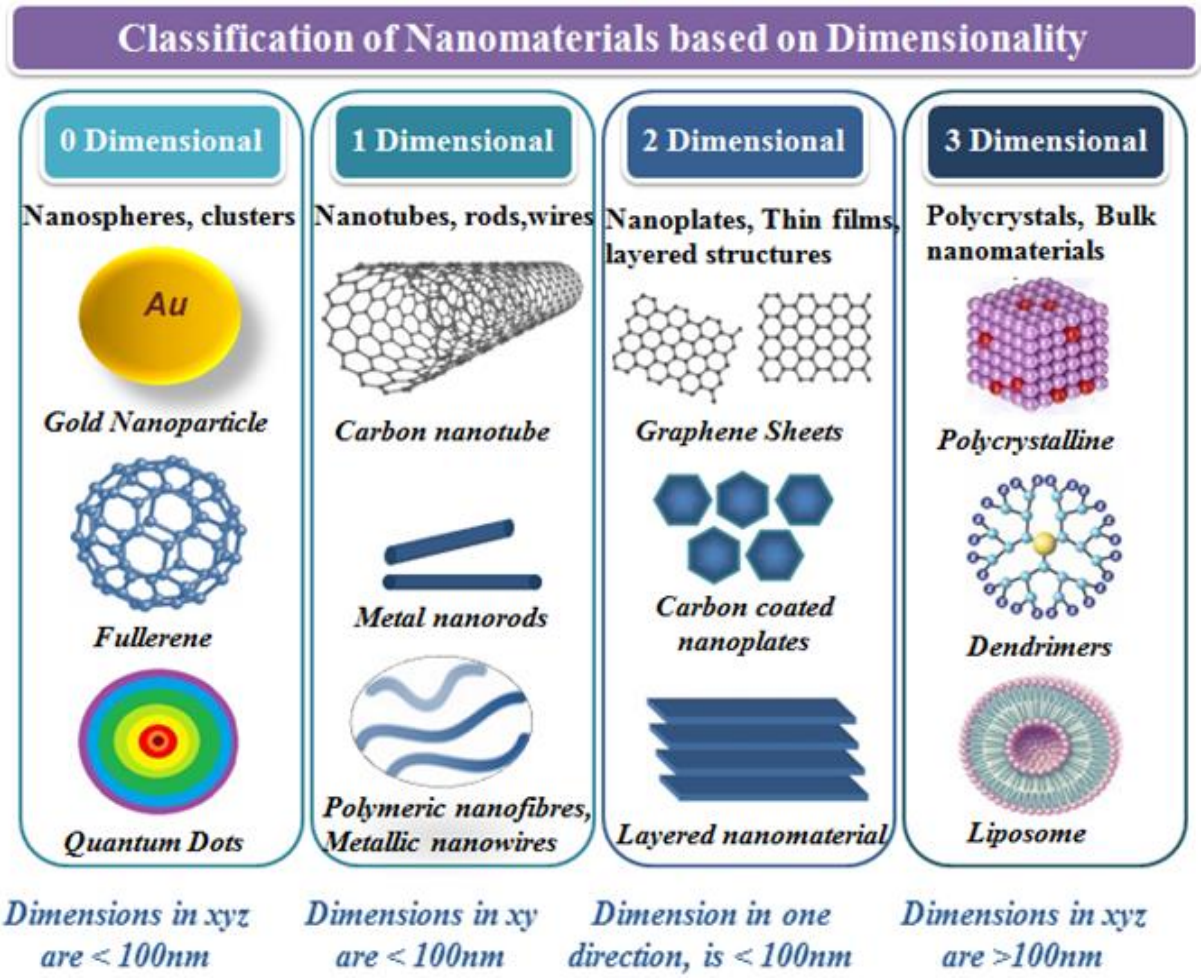

Figure-1: Classification of Nanomaterials based on their dimensions

(ii) Synthetic (engineered) nanomaterials are manufactured through processes such as mechanical grinding, engine exhaust, smoke, or synthesis via physical, chemical, biological, or hybrid methods. With the increasing production and utilization of engineered nanomaterials in consumer and industrial applications, the issue of risk assessment strategies has emerged. These strategies play a crucial role in predicting the behavior and fate of engineered nanomaterials in different environmental media. The main challenge with manufactured nanomaterials lies in determining whether existing knowledge is sufficient to predict their behavior or whether they exhibit distinct environmental behavior compared to that of natural nanomaterials. Currently, various sources relevant to their intended applications are employed for the synthesis of manufactured nanomaterials (Wagner et al., 2014).

3. Synthesis of nanomaterials: Nanomaterials can be synthesized using a diverse range of materials, such as proteins, polysaccharides, and synthetic polymers. Several factors influence the choice of matrix materials, including the following:

The synthesis of nanoparticles can be achieved through three different approaches, as depicted in Figure-2:
1. Physical synthesis.

2. Chemical synthesis.
3. Biological synthesis.

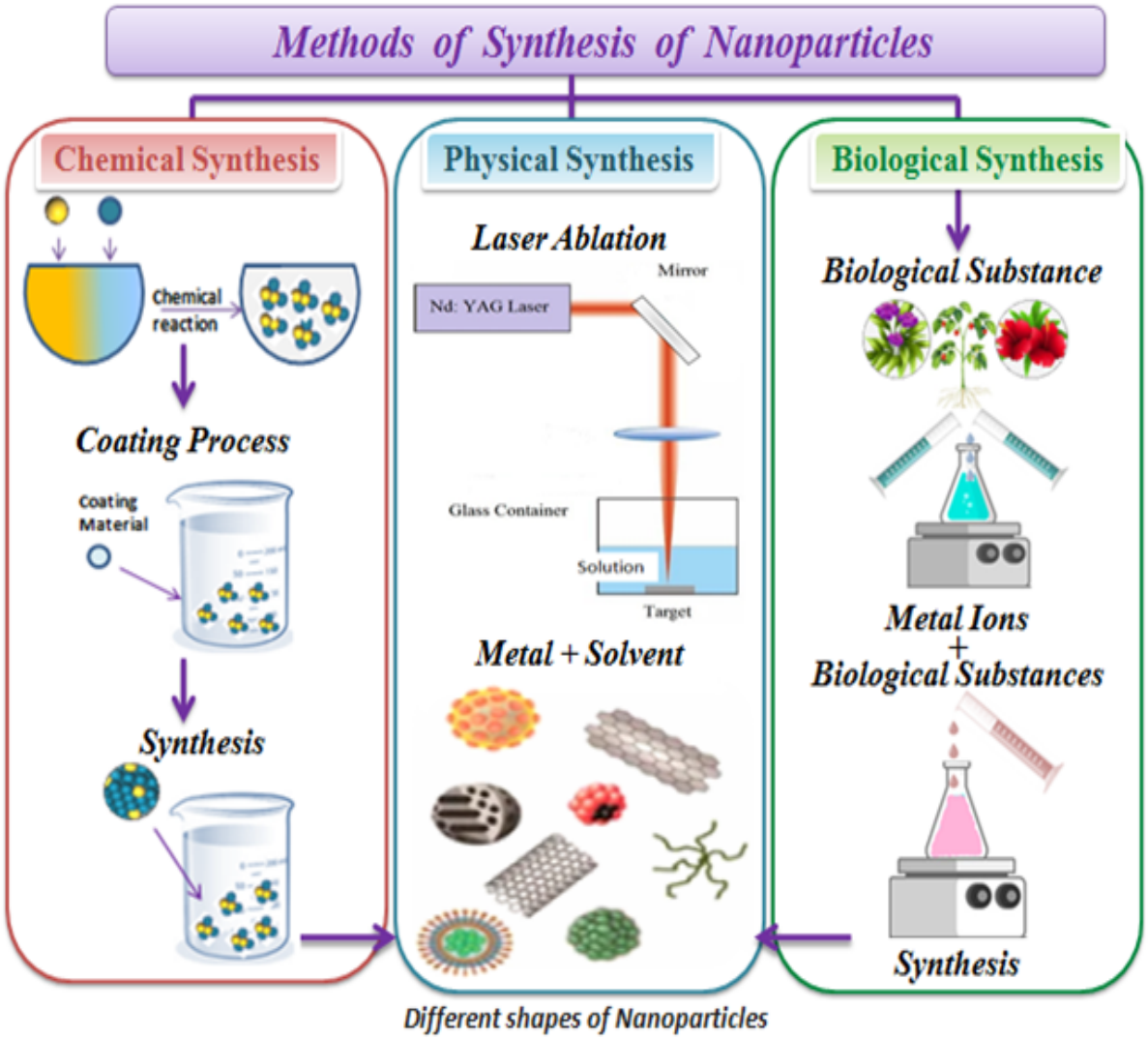

Figure-2: Conventional methods for the synthesis of nanoparticles.

1. Physical synthesis of nanoparticles (NPs):

NPs are synthesized using various physical methods, which can be classified as either top-down or bottom-up approaches. A simplified representation of this process is depicted in Figure- 3.

3.1 Top-down methods:

Top-down methods involve reducing a bulk material to particles at the nanoscale level. Some widely used techniques for nanoparticle synthesis include mechanical milling, nanolithography, laser ablation, sputtering, and thermal decomposition, as illustrated in Figure- 4.

3.1.1 Thermal decomposition:

Thermal decomposition refers to the chemical degradation caused by heat, leading to the breaking of chemical bonds within a substance (Salavati-Niasari et al., 2008). At specific temperatures, the metal undergoes chemical degradation, resulting in the formation of nanoparticles.

3.1.2 Mechanical milling:

Mechanical milling is a commonly employed top-down approach for producing various types of nanoparticles. Among the different methods, mechanical milling is extensively used to synthesize nanoparticles through milling and post-annealing of different elements in an inert atmosphere (Yadav et al., 2012). Plastic deformation, fracture, and cold- welding are influencing factors in mechanical milling, affecting the particle shape, size reduction, and size increase, respectively.

3.1.3 Laser ablation:

Laser ablation synthesis in solution (LASiS) is a typical method for producing nanoparticles from different solvents. By irradiating a metal immersed in a liquid solution with a laser beam, a plasma plume is condensed, leading to nanoparticle formation (Amendola and Meneghetti, 2009). This top-down method offers an alternative to the conventional chemical reduction of metals for synthesizing metal-based nanoparticles. LASiS is considered a "green" process because it allows sustainable nanoparticle production in organic solvents and water without the need for stabilizing agents or chemicals.

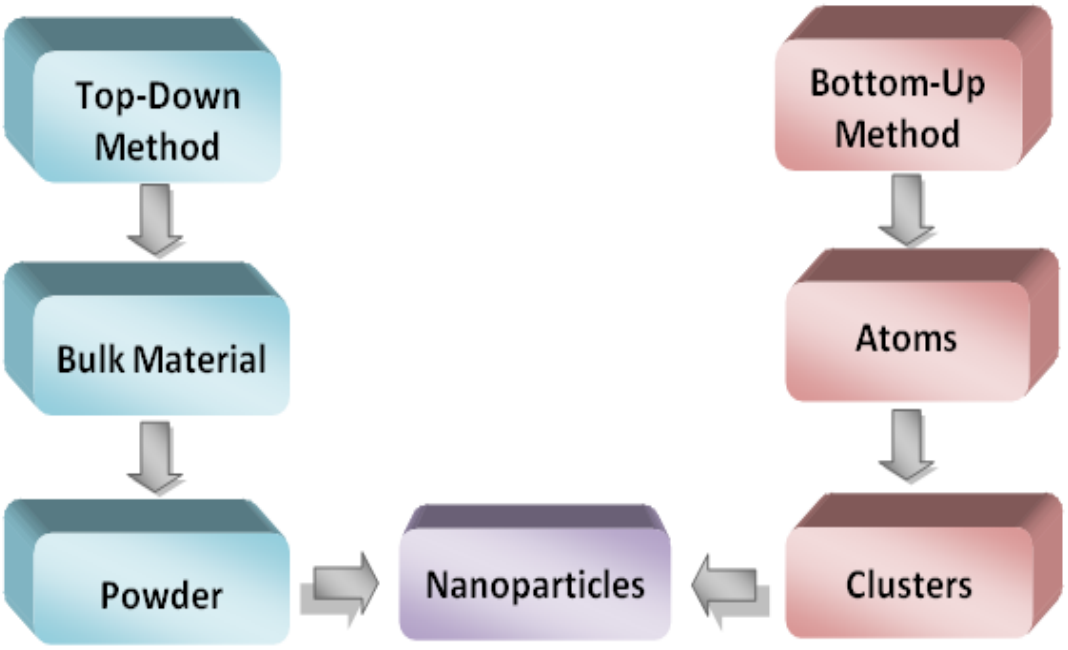

Figure-3: Process of Synthesis of nanoparticles.

3.1.4 Nanolithography:

Nanolithography involves the production of structures at the nanoscale, typically with at least one dimension ranging from 1 to 100 nm. Various nanolithographic processes exist, including optical, electron-beam, multiphoton, nanoimprint, and scanning probe lithography (Pimpin and Srituravanich, 2012). In general, nanolithography entails printing the desired shape or structure onto a photosensitive material, selectively

removing a portion of the material to create the desired shape, and structure. One advantage of nanolithography is the ability to create clusters with the desired shape and size from a single nanoparticle. However, the complexity of the equipment and associated costs are notable disadvantages.

3.1.5 Sputtering:

Sputtering involves depositing nanoparticles onto a surface by ejecting particles through ion collision (Shah and Gavrin, 2006). Typically, sputtering entails depositing a thin layer of nanoparticles followed by annealing. Factors such as layer thickness, annealing temperature and duration, and the type of substrate determine the structure and size of the nanoparticles (Lugscheider et al., 1998).

3.1.6 Chemical Etching:

Chemical etching, also known as chemical milling or photo etching, is a subtractive sheet metal machining process that utilizes chemical etchants to create precise components from various metals. This technique is employed in microfabrication to selectively remove layers from the surface of a wafer during manufacturing. Etching plays a crucial role in the fabrication process, with each wafer undergoing multiple etching steps before completion. A masking material, such as a photoresist patterned using photolithography or silicon nitride, is used to protect certain areas of the wafer from the etchant. In some cases, chemical etching of Ag/C nanowires can be utilized to fabricate high-quality carbonaceous nanotubes (Liu et al., 2010).

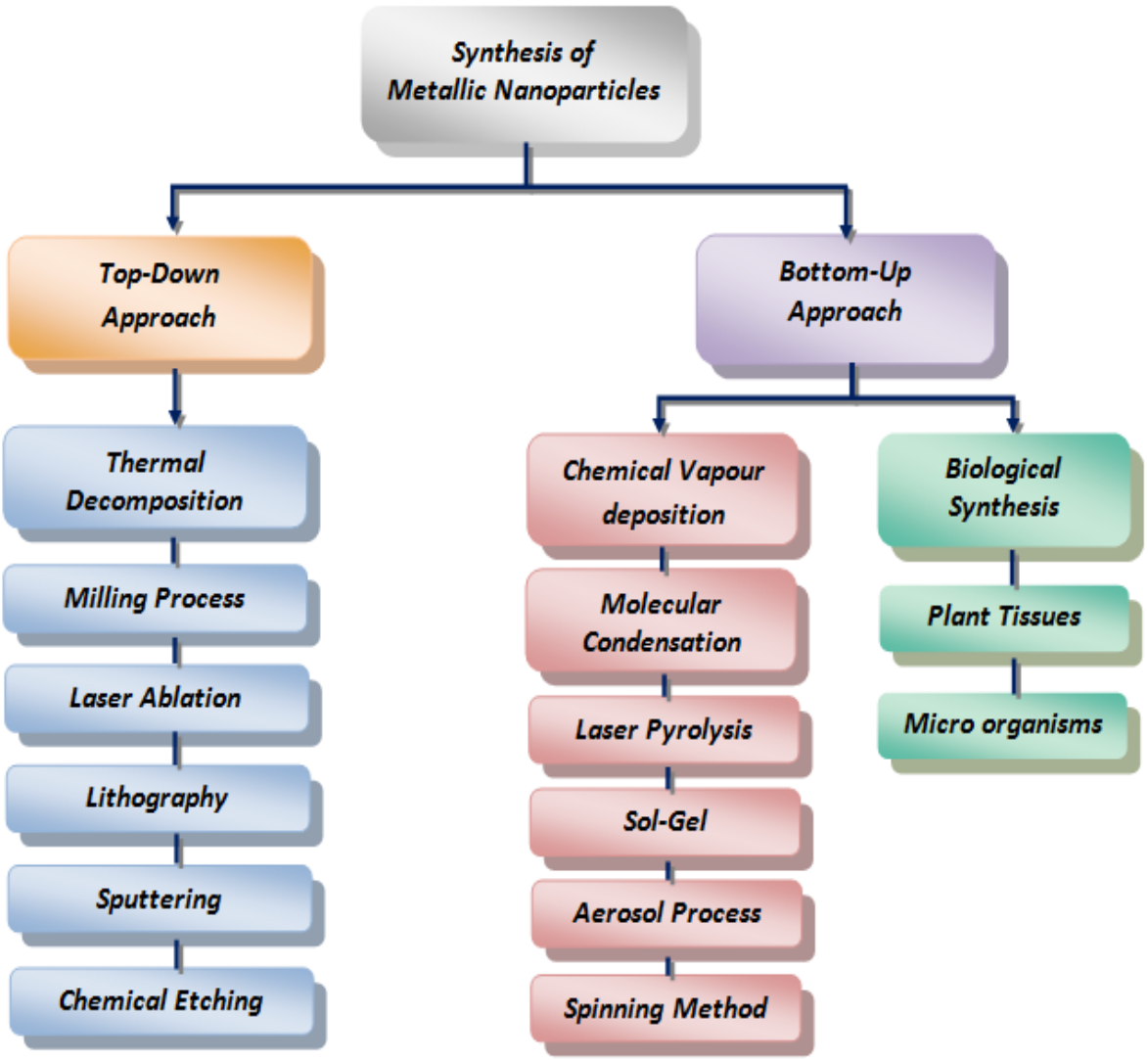

Figure-4: Different methods for the Synthesis of nanoparticles.

3.2. Bottom-up methods:

The bottom-up or constructive process involves the assembly of materials from atoms to clusters and eventually to nanoparticles. Widely used bottom-up methods for nanoparticle production include sol-gel, spinning, chemical vapor deposition (CVD), pyrolysis and biosynthesis, as shown in Figure- 4.

3.2.1. Chemical Vapor Deposition (CVD):

Chemical vapor deposition entails depositing a thin layer of gaseous reactants onto a substrate. In a reaction chamber at room temperature, gas molecules are combined, and a chemical reaction occurs when a heated substrate comes into contact with the gas mixture (Bhaviripudi et al., 2007). This reaction results in the formation of a thin film of the desired product on the surface of the substrate. The substrate temperature plays a crucial role in CVD. The advantages of CVD include high purity, uniformity, and the production of strong and hard nanoparticles. However, special equipment is required for CVD and gaseous byproducts can be highly toxic.

3.2.2. Pyrolysis:

Pyrolysis is a commonly employed industrial process for large-scale nanoparticle production. This process involves the combustion of a precursor using a flame. The precursor, either in liquid or vapor form, is introduced under high pressure through a small hole into a furnace, where it burns (Kammler et al., 2001). The combustion or derived gases are then collected and classified in the air to recover the nanoparticles. Some furnaces use lasers and plasma to achieve high temperatures for efficient evaporation (Amato et al., 2013). The advantages of pyrolysis include its simplicity, efficiency, low cost, and continuous process with high yield.

3.2.3. Sol-gel:

Sol-gel is a preferred bottom-up method for nanoparticle synthesis, involving a colloidal solution of suspended particles in a liquid phase (sol) and a solid macromolecule submerged in a solvent (gel). This method is widely used due to its simplicity, and most nanoparticles can be synthesized using this approach. The sol-gel process is a wet-chemical process that utilizes a chemical solution that acts as a precursor to form discrete particles. Metal oxides and chlorides are commonly used precursors in the sol-gel process (Ramesh, 2013). The precursor is dispersed in a host liquid through agitation, stirring, or sonication, resulting in a system containing both a liquid and a solid phase. NPs are recovered through phase separation via methods such as sedimentation, filtration, or centrifugation, followed by drying to remove moisture (Mann et al., 1997).

3.2.4. Spinning:

Nanoparticle synthesis through spinning involves the use of a spinning disc reactor (SDR). The SDR consists of a rotating disc within a chamber or reactor, where physical parameters such as temperature can be controlled. A reactor is typically filled with nitrogen or other inert gases to remove oxygen and prevent unwanted chemical reactions (Tai et al., 2007). The disc rotates at varying speeds, while the precursor liquid and water are pumped in. Spinning causes the fusion and precipitation of atoms or molecules, which are then collected and dried (Mohammadi et al., 2014). Various operating parameters, including the liquid flow rate, disc rotation speed, liquid-to-precursor ratio, feed location, and disc surface, determine the characteristics of the synthesized nanoparticles using SDR.

3.3. Biological synthesis of nanoparticles:

Biological synthesis offers an environmentally friendly, easy, and simple approach to nanoparticle synthesis that result in nontoxic and biodegradable nanoparticles (Kuppusamy et al., 2016). Microorganisms, bacteria, plant extracts, fungi, and algae are utilized in biosynthesis, replacing traditional chemicals for bio-reduction and capping purposes. Biosynthesized nanoparticles possess unique and enhanced properties, making them suitable for various biomedical applications.

3.3.1. Bacterial synthesis:

Bacteria-based bio-mineralization processes are often employed in nanoparticle synthesis, utilizing proteins. For instance, under anaerobic conditions, magneto-tactic microorganisms on the sea floor, utilize protein-coated magnetosomes to synthesize magnetic iron oxide nanocrystals, resembling a compass pointing toward their preferred environment (Krishnan, 2016). Homogeneous particles with core diameters of 20-45 nm can be produced in vitro (Faivre and Schüler, 2008; Timko, 2013). Magneto-somes exhibit excellent magnetic properties and have potential applications in hyperthermia (Molcan et al., 2016). Additionally, photosynthetic

bacteria such as Rhodopseudomonas capsulata have been utilized to extracellularly produce gold nanoparticles with sizes ranging from 10 to 20 nm (Guo et al., 2007). Pseudomonas cells found at the Alpine site have also been reported to be capable of extracellularly producing palladium nanoparticles (Schluter et al., 2014).

3.3.2. Algal synthesis:

Researchers, such as Singaravelu et al., have proposed the use of Sargassum wightii algae to prepare extracellular gold nanoparticles. They achieved a production yield of 95% within 12 hours of incubation. However, further exploration of nanoparticle preparation using algae is necessary. It should be noted that certain bacteria, fungi, and algae can be pathogenic, requiring the development of appropriate safety measures (Singaravelu et al., 2007).

3.3.3. Fungal synthesis:

Fungi are attractive agents for the biogenic synthesis of silver nanoparticles due to their high metal tolerance and ease of manipulation (Balaji et al., 2009). They also secrete significant amounts of extracellular proteins that contribute to the stability of nanoparticles (Du et al., 2015; Netala et al., 2016). Trichoderma reesei, a mesophilic and filamentous fungus, is widely utilized in various industries, including food, animal feed, pharmaceuticals, textiles, and paper production. A. Fumigatus is used for the production of extracellular silver nanoparticles (Silver NPs) (Bhainsa and D'Souza, 2006). Silver nanoparticles have also been synthesized using Fusarium oxysporum, and the reduction of silver ions was attributed to the action of the enzyme nitrate reductase and anthraquinones (Duran et al., 2005). Another study revealed that extracellular NADPH-structured nitrate reductase enzymes and quinones from the same fungus were responsible for nanoparticle formation, as demonstrated using purified nitrate reductase and phyto-chelatins (Anil Kumar et al., 2007).

3.3.4. Biological template synthesis:

Nanomaterials can be synthesized inside organisms using biological processes. Unique nanostructures can be produced using biological templates such as DNA and proteins, enabling the design of biosensors, bioNEMS, and bioelectronic systems (Zhans et al., 2019). For example, Wu et al. synthesized yttrium phosphate radionuclide nanoparticles inside apoferritin and conjugated them with biotin (Wu et al., 2008).

3.3.5. Plant-based synthesis:

Plants and their extracts have been utilized for nanoparticle synthesis. Metallic nanoparticles, such as flavones, organic acids, and quinones, which act as effective reducing agents, are reduced by the phytochemicals present in plants. Gold nanoparticles of different shapes are synthesized from the biomass of plants such as Medicago sativa (Alfalfa) (Gardea-Torresdey et al., 2003) and Pelargonium graveolens (Geranium) leaves (Pandian, 2013). Azadirachta indica (Neem) leaves have been used to synthesize bimetallic gold-silver nanoparticles, with sugars and/or terpenoids in the plant acting as reducing agents (Shankar et al., 2004). Various plants, including Brassica juncea (Indian mustard) and Helianthus annuus (sunflower), have been used to synthesize silver, nickel, cobalt, zinc, and copper nanoparticles (Madhuchanda et al., 2014).

4. Conclusions:

In this article, we have provided a detailed overview of nanoparticles, including their types, classification and synthesis methods. While significant progress has been made in the fields of biomedicine, electronic storage devices, and sensors, there is still room for further research and advancement in these areas. This review article serves as a valuable resource for general information on nanoparticles. However, it is essential to address concerns regarding the health hazards associated with their uncontrolled use and release into the environment, to promote the safe and environmentally friendly utilization of nanoparticles.

References:

[1] Amato, R. D., Falconieri, M., Gagliardi, S. et al. (2013). From research to applications J. Anal. Appl. Pyrolysis. J Anal Appl pyrrol synth Ceram nanoparticles laser pyrrol, 104, 461–469.

[2] Amendola, V., & Meneghetti, M. (2009). Laser ablation synthesis in solution and size manipulation of noble metal nanoparticles 3805–21. Physical Chemistry Chemical Physics, 11(20), 3805–3821. https://doi.org/10.1039/b900654k

[3] Anil Kumar, S., Abyaneh, M. K., Gosavi, S. W., Kulkarni, S. K., Pasricha, R., Ahmad, A., & Khan, M. I. (2007). Nitrate reductase-mediated synthesis of silver nanoparticles from $AgNO_3$. Biotechnology Letters, 29(3), 439–445. https://doi.org/10.1007/s10529-006-9256-7

[4] Balaji, D. S., Basavaraja, S., Deshpande, R., Mahesh, D. B., Prabhakar, B. K., & Venkataraman, A. (2009). Extracellular biosynthesis of functionalized silver nanoparticles by strains of Cladosporium cladosporioides fungus. Colloids and Surfaces. B, Biointerfaces, 68(1), 88–92. https://doi.org/10.1016/j.colsurfb.2008.09.022

[5] Banfield, J. F., & Zhang, H. (2001). Nanoparticles in the environment. Reviews in Mineralogy and Geochemistry, 44(1), 1–58. https://doi.org/10.2138/rmg.2001.44.01

[6] Baudot, C., Tan, C. M., & Kong, J. C. (2010). FTIR spectroscopy as a tool for nano-material characterization. Infrared Physics and Technology, 53(6), 434–438. https://doi.org/10.1016/j.infrared.2010.09.002

[7] Behari, J., Tiwari, D. K., & Sen, P. (2008). Application of nanoparticles in Waste Water treatment. World. Journal of Applied Sciences, 3, 417–433.

[8] Bhainsa, K. C., & D'Souza, S. F. (February 1, 2006). Extracellular biosynthesis of silver nanoparticles using the fungus Aspergillus fumigatus. Colloids and Surfaces. B, Biointerfaces, 47(2), 160–164. https://doi.org/10.1016/j.colsurfb.2005.11.026

[9] Bhaviripudi, S., Mile, E., III, Sas, Z. A. T., & Dresselhaus, M. S. (1516–17). Belcher A M and Kong J 2007 CVD synthesis of single-walled carbon nanotubes from gold nanoparticle catalysts.

[10] Boverhof, D. R., Bramante, C. M., Butala, J. H., Clancy, S. F., Lafranconi, M., West, J., & Gordon, S. C. (2015). Comparative assessment of nanomaterial definitions and safety evaluation considerations. Regulatory Toxicology and Pharmacology, 73(1), 137–150. https://doi.org/10.1016/j.yrtph.2015.06.001

[11] Chaudhry, Q., Scotter, M., Blackburn, J., Ross, B., Boxall, A., Castle, L., Aitken, R., & Watkins, R. (2008). Applications and implications of nanotechnologies for the food sector. Food Additives and Contaminants. Part A, Chemistry, Analysis, Control, Exposure and Risk Assessment, 25(3), 241–258. https://doi.org/10.1080/02652030701744538

[12] Du, L., Xu, Q., Huang, M., Xian, L., & Feng, J.-X. (2015). Synthesis of small silver nanoparticles under light radiation by fungus Penicillium oxalicum and its application for the catalytic reduction of methylene blue. Materials Chemistry and Physics, 160, 40–47. https://doi.org/10.1016/j.matchemphys.2015.04.003

[13] Durán, N., Marcato, P. D., Alves, O. L., De Souza, G. I. H., & Esposito, E. (2005). Mechanistic aspects of biosynthesis of silver nanoparticles by several Fusarium oxysporum strains. Journal of Nanobiotechnology, 3, 8. https://doi.org/10.1186/1477-3155-3-8

[14] Faivre, D., & Schüler, D. (2008). Magnetotactic bacteria and magnetosomes. Chemical Reviews, 108(11), 4875–4898. https://doi.org/10.1021/cr078258w

[15] Farhang, D., Kottegoda, N., & Sigmund, W. (2007). Nanotechnology and the development of new structural materials. Journal of Materials Science, 2024-2029-20312024-2029, 42(6). https://doi.org/10.1007/s10853-006-0687-y

[16] Gardea-Torresdey, J. L., Gomez, E., Peralta-Videa, J. R., Parsons, J. G., Troiani, H., & Jose-Yacaman, M. (2003). Alfalfa sprouts: A natural source for the synthesis of silver nanoparticles. Langmuir, 19(4), 1357–1361. https://doi.org/10.1021/la020835i

[17] Gleiter, H. (2000). Nanostructured materials: Basic concepts and microstructure. Acta Materialia, 48(1), 1–29. https://doi.org/10.1016/S1359-6454(99)00285-2

[18] Guo, Z., Y., Zhans, S., Zhang, W. N., & Gu, M. Lt. (2007). S, H, 61(18), 3984–3987.

[19] Hochella, M. F., Jr., Spencer, M. G., & Jones, K. L. (2015). Nanotechnology: Nature's gift or scientists' brainchild? Environmental Science: Nano, 2(2), 114–119. https://doi.org/10.1039/C4EN00145A

[20] ISO, & T. S. (2010). 80004-1:2010, nanotechnology—Vocabulary – Part 1: Core terms. https://www.iso.org/standard/51240. html. Retrieved July 17, 2017. International Organization for Standardization.

[21] Jeevanandam, J., Barhoum, A., Chan, Y. S., Dufresne, A., & Danquah, M. K. (2018). Review on nanoparticles and nanostructured materials: History, sources, toxicity and regulations. Beilstein Journal of Nanotechnology, 9, 1050–1074. https://doi.org/10.3762/bjnano.9.98

[22] Jeyaraj, M., Gurunathan, S., Qasim, M., Kang, M. H., & Kim, J. H. (2019). A comprehensive review on the synthesis, characterization, and biomedical application of platinum nanoparticles. Nanomaterials, 9(12), 1719. https://doi.org/10.3390/nano9121719

[23] Kammler, B. H. K., Mädler, L., & Pratsinis, S. E. (2001). Flame Synthesis of Nanoparticles, 24, (583–596).

[24] Kreuter, J. (1994). Nanoparticles. In M. Dekker (Ed.), Colloidal drug delivery systems, J, K (pp. 219–342). New York.

[25] Krishnan, K. (2016). Fundamentals and applications of magnetic materials. Oxford University Press.

[26] Kumar, N., Kumbhat, S., & Nanomaterials, C.-B. (2016). Essentials in nanoscience and nanotechnology (pp. 189–236). John Wiley & Sons, Inc.. https://doi.org/10.1002/9781119096122.ch5

[27] Kuppusamy, P., Yusoff, M. M., Maniam, G. P., & Govindan, N. (2016). Biosynthesis of metallic nanoparticles using plant derivatives and their new avenues in pharmacological applications—An updated report. Saudi Pharmaceutical Journal, 24(4), 473–484. https://doi.org/10.1016/j.jsps.2014.11.013

[28] Liu, Z., Zhou, X., & Qian, Y. (2010). Synthetic methodologies for carbon nanomaterials. Advanced Materials, 22(17), 1963–1966. https://doi.org/10.1002/adma.200903813

[29] Lugscheider, E., Bärwulf, S., Barimani, C., Riester, M., & Hilgers, H. (1998). Magnetron-sputtered hard material coatings on thermoplastic polymers for clean room applications. Surface and Coatings Technology, 108–109, 398–402. https://doi.org/10.1016/S0257-8972(98)00627-6

[30] Madhuchanda, B. et al. (2014). Energy, 69, 695–699.

[31] Mann, S., Burkett, S. L., Davis, S. A., Fowler, C. E., Mendelson, N. H., Sims, S. D., Walsh, D., & Whilton, N. T. (1997). Sol–gel synthesis of organized matter. Chemistry of Materials, 9(11), 2300–2310. https://doi.org/10.1021/cm970274u

[32] Mohammadi, S., Harvey, A., & Boodhoo, K. V. K. (2014). Synthesis of TiO_2 nanoparticles in a spinning disc reactor. Chemical Engineering Journal, 258, 171–184. https://doi.org/10.1016/j.cej.2014.07.042

[33] Mohanraj, V. J., & Chen, Y. (June 2006). Nanoparticles—A review, Orchid chemicals and pharmaceuticals limited, Chennai, India 2. Tropical Journal of Pharmaceutical Research, (Benin City, Nigeria). School of Pharmacy, Curtin University of Technology, 5(1), 561–573.

[34] Molcan, M., Gojzewski, H., & Skumiel, A. (2016). Dut Kovac, S., Kubovikwa Kopcansky, M., Vekas, L., & Timko, M. Phys. D. Applied Physics, 49(36). PubMed: 365002

[35] Netala, V. R., Bethu, M. S., Pushpalatha, B., Baki, V. B., Aishwarya, S., Rao, J. V., & Tartte, V. (2016). Biogenesis of silver nanoparticles using endophytic fungus Pestalotiopsis microspora and evaluation of their antioxidant and anticancer activities. International Journal of Nanomedicine, 11, 5683–5696. https://doi.org/10.2147/IJN.S112857

[36] Pandian, M. (2013). Aml. Nanoscience and Nanotechnology, 1(2), 57.

[37] Pas, S. J. (2011). Terms relating to nanomaterials. British Standards Institution. https://committee.iso.org/files/live/sites/isoorg/files/store/en/PUB100397.pdf

[38] Pimpin, A., & Srituravanich, W. (2012). Review on micro- and nanolithography techniques and their applications. Engineering Journal, 16(1), 37–56. https://doi.org/10.4186/ej.2012.16.1.37

[39] Pokropivny, V. V., & Skorokhod, V. V. (2007). Classification of nanostructures by dimensionality and concept of surface forms engineering in nanomaterial science, V. V. Materials Science and Engineering, 27(5–8), 990–993. https://doi.org/10.1016/j.msec.2006.09.023

[40] Potocnik, J. (2011). Official Journal of the European Communities. Legislation, L275, 38–40. https://doi.org/10.3000/19770677.L_2011.275.eng

[41] Ramesh, S. (2013). Sol—Ggel Ssynthesis and characterization of 2013, 2013.

[42] Roco, M. C. (2003). Nanotechnology: Convergence with modern biology and medicine. Current Opinion in Biotechnology, 14(3), 337–346. https://doi.org/10.1016/s0958-1669(03)00068-5

[43] Salavati-Niasari, M., Davar, F., & Mir, N. (2008). Synthesis and Characterization of Metallic Copper Nanoparticles Via Thermal Decomposition Polyhedron, 27, (3514–3518).

[44] Sanguansri, P., & Augustin, M. A. (2006). Nanoscale materials development-A food industry perspective. Trends in Food Science and Technology, 17(10), 547–556. https://doi.org/10.1016/j.tifs.2006.04.010

[45] Schlüter, M., & Hentzel, T. CSuarez, M. Koch, W. Lorenz, L Bohm, R. During. K Kainis, M. Bunge Chemisphen 117 2014) 462-470.

[46] Shah, P., & Gavrin, A. Ã. (2006). Synthesis of nanoparticles using high-pressure sputtering for magnetic domain imaging. Journal of Magnetism and Magnetic Materials, 301(1), 118–123. https://doi.org/10.1016/j.jmmm.2005.06.023

[47] Shankar, S. S., Rai, A., Ahmad, A., & Sastry, M. (2004). Rapid synthesis of Au, Ag, and bimetallic au core-Ag shell nanoparticles using Neem (Azadirachta indica) leaf broth. Journal of Colloid and Interface Science, 275(2), 496–502. https://doi.org/10.1016/j.jcis.2004.03.003

[48] Sharma, V. K., Filip, J., Zboril, R., & Varma, R. S. (2015). Natural inorganic nanoparticles-Formation, fate, and toxicity in the environment. Chemical Society Reviews, 44(23), 8410–8423. https://doi.org/10.1039/C5CS00236B

[49] Singaravelu, G., Arockiamary, J. S., Kumar, V. G., & Govindaraju, K. (2007). A novel extracellular synthesis of monodisperse gold nanoparticles using marine alga, Sargassum wightii Greville. Colloids and Surfaces. B, Biointerfaces, 57(1), 97–101. https://doi.org/10.1016/j.colsurfb.2007.01.010

[50] Tai, C. Y., Tai, C., Chang, M., & Liu, H. (2007). Synthesis of magnesium hydroxide and oxide nanoparticles using à spinning disk reactor 5536–5541.

[51] Timko, M., Molcan, M., Hashim, A., Skumiel, A., Muller, M., Gojzewski, H., Jozefczak, A., Kovac, J., Rajnak, M., Makowski, M., & Kopcansky, P. (2013). Hyperthermic effect in suspension of magnetosomes prepared by various methods. IEEE Transactions on Magnetics, 49(1), 250–254. https://doi.org/10.1109/TMAG.2012.2224098

[52] United Nations. (2012). The world at 7 billion. Population division, department of economic and social affairs. United Nations. https://doi.org/10.18356/920a0e23-en

[53] United States Food and Drug Administration. (2011). Guidance for industry: Considering whether an FDA-regulated product involves the application of nanotechnology, 10. U. S. Food and Drug Administration. https://doi.org/10.1016/S0140-6736(11)60401-8

[54] Wagner, S., Gondikas, A., Neubauer, E., Hofmann, T., & von der Kammer, F. (2014). Spot the difference: Engineered and natural nanoparticles in the environment-Release, behavior, and fate. Angewandte Chemie, 53(46), 12398–12419. https://doi.org/10.1002/anie.201405050

[55] Wu, H., Wang, J., Wang, Z., D., Fisher, Y., & NaniciNanotechnol, L. I. (2008), 8(5), 2316–2322.

[56] Yadav, T. P., Yadav, R. M., & Singh, D. P. (2012). Mechanical milling: A top down approach for the synthesis of nanomaterials and nanocomposites, 2, 22–48.

[57] Zhans, N. Y., Oi, M., Wang, Z., Wans, Z., Chen, M., Shum, K. L. P., & Wei, L. (2019). Sensors and Actuators. Part B. https://doi.org/10.1016/j.snb, 2019.01.166

International Journal of Scientific Research in Science and Technology
Available online at : www.ijsrst.com
Print ISSN: 2395-6011 | Online ISSN: 2395-602X
doi : https://doi.org/10.32628/IJSRST

Synthesis, of Schiff Base Ligand and their Transition Metal Complexes Derived from (E)-N'-((1H-indol-3-yl)methylene) benzohydrazide

Dnyaneshwar T. Nagre [a], Sanjay S. Kotalwar [b], Amol D. Kale[b], Sushil K. Ghumbre[C], Sadasive N. Sinkar[d] and Ram B. Kohire[a*]

[a] Department of Chemistry, RMIG College, Jalna, (M.S.)- , India

[a*] Department of Chemistry Swami Vivakanand Sr. College Mantha ,Dist. Jalna (M.S.)-431504 India

[b] Department of Chemistry, L. B.S.College, Partur, Dist.-Jalna(M.S.)-431501 India

[c] Department of Chemistry I.C.S. College of Art's, Commerce and Science, Khed (M.S.)- 415709 , India

[d] Department of Chemistry; MSS'S Arts Science and Commerce College Ambad, Dist. Jalna, India

ARTICLEINFO

Article History :

Published : 07 Dec 2024

Publication Issue :
Volume 11, Issue 23
Nov-Dec-2024
Page Number :
455-461

ABSTRACT

This synthesis Of Schiff base ligand of (E)-N'-((1H-indol-3-yl)methylene)benzohydrazide and its transition metal complexe of Cu(II), were prepared under microwave irradiation as a green approach compared to the conventional method. The structures of these Schiff base and its metal complexes were confirmed by different spectroscopic techanics. i.e, UV, IR, ^{1}H-NMR, , IR, and Powder XRD and electronic spectra of the synthesized complexes explained their geometrical structures. The thermal stability of metal complexes was studied by thermo-gravimetric analyses (TGA). The elemental analysis revealed metal to ligand stoichiometry was 1:2 molar ratio and screened for biological activities (antimicrobial)

Keywords : Microwave Synthesis, NO,ONO Donor Schiff Base, Thermal Study, Biological Activity.

1. Introduction

The indole Schiff bases have been reported some important biological activities such as antifungal, antibacterial and DNA cleavage, anticorrosive, antimicrobial, anti-inflammatory, ulcerogenic properties.Hydrazones are known to be a significant class of nitrogen oxygen donor ligands because of their variable bonding modes towards transition metal ions and their extremely fascinating chemical, biological and medicinal applications. Among this great family of molecules, chromones are of great interest due to their extensive pharmacological activity1-3]. The characterization and elucidation of the structure of the prepared compounds were performed by elemental analysis, FT-IR, ESI-MS, electronic, ^{1}H NMR and ^{13}C NMR spectral methods.

Coordination complexes are formed by ligands that have various donor sites generally heterocyclic rings, for example: -ONO, - NNO or NNS and NO. Among the ligands hydrazone playing a significant role since coordination complexes of these compounds are at present extensively used for the treatment of numerous diseases, in analytical and synthetic chemistry as heterogeneous catalysts in the oxidation-reduction reaction process and a variety of chemical, photochemical reactions as well as different industrial significance in the field of science and technology [3-5].

2. Experimental

2.1. | Materials

All chemicals and solvents employed in synthesis were of extra-pure grade and used as received without anyfurther purification. Solvents were purified and dried according to literature method [6]. All chemicals were obtained from Sigma–Aldrich chemical used without purification. They 1H-indole-3-carbaldehyde and Benzohydrazide, remaining all chemical solvents were purchased from spectrochem ltd.

2.2. Physical measurements

Elemental analysis (C, H, N,) was performed using Perkin Elmer CHN analyzer. TLC was visualized by VL-6-LC, UVlamp.IR spectra of the ligands and their metal complexes were recorded on Bruker spectrometer within the range of 4000–400 cm^{-1}. The UV spectra of compounds were recorded by UV-Vis. Spectrophotometer (UV-1700, Shimadzu). Thermal studies of the complexes were carried out on a Perkin Elmer diamond TGA instrument. ^{1}H-NMR and ^{13}C-NMR spectra of the ligands were recorded on Bruker spectrometer using DMSO-d6 as a solvent and TMS as internal standard. Mass spectra were recorded on water, Qt of micromass (ESI-MS).

2.3 | Synthesis of the Schiff base ligand

The Schiff base has been synthesized by reacting 1H-indole-3-carbaldehyde (1.00 mmole) and Benzohydrazide (1.00 mmole).The reaction was carried out in a microwave oven for 30 minutes. The irradiated product was washed with dry ether and filtered. The final product was recrystallized from ethanol to give pale yellow crystals. The purity of the product was monitored by the use of TLC, using n-hexane and ethyl acetate (7:3) ratio.

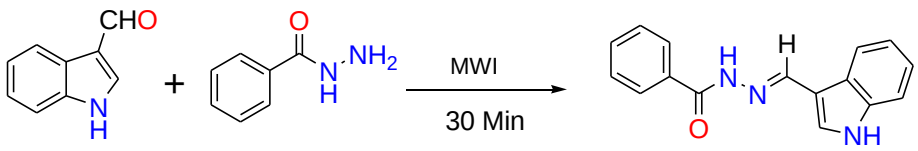

1*H*-indole-3-carbaldehyde Benzohydrazide (*E*)-*N*'-((1*H*-indol-3-yl)methylene)benzohydrazide

Scheme: The schematic route for synthesis of Schiff base (L)

2.4 Spectral data of ligand:

Color: Violet , Yield: 83%, M.P.: 248°C, Selected FT-IR bands (KBr, cm^{-1}) : 3210 ν (NH), 1679 ν(C=O), 1632 ν (ν(C=N); ^{1}H- NMR (DMSO-d6, δ ppm) 12.41 (1H,s, iminolic -OH); 8.11 (S, 1H, HC=N), 6.80-8.24 (m, 4H, Ar-H); 2.90 (S, 3H, $-CH_3$); ^{13}C NMR (DMSO-d6, δ ppm) 160.51 (C=O hydrazone), 154.48 (-HC=N), 15.22

2.5 Synthesis of metal complexes

The Schiff base ligand and metal salts were mixed in a grinder 1:1 (metal: ligand) ratio. The reaction mixture was then irradiated in a microwave oven. The reaction was completed in a short time, between 60-180 sec. The progress of the reaction and purity of the product was monitored by TLC plate. Each product was recrystallized from ethanol and ether, and finally, different colored crystals were obtained. (Yield: 62 %)

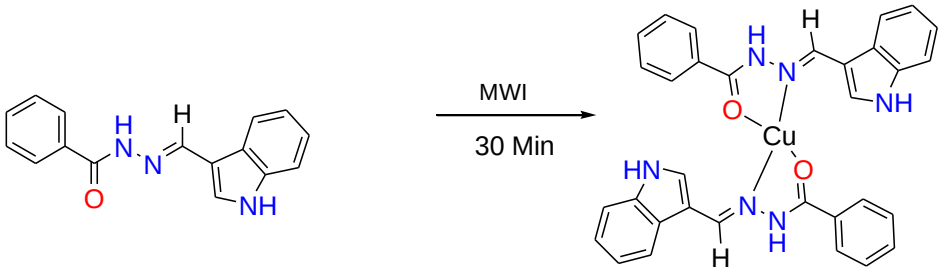

(*E*)-*N*'-((1*H*-indol-3-yl)methylene)benzohydrazide

Scheme: The schematic route for synthesis of Cu metal complexe

3. Results and discussion

In the present study of the microwave-assisted synthesis, it was observed that the reaction time had been drastically reduced with a better yield of the products. The difference was observed probably due to the strong microwave effect and the high enhancement of reaction rate. The conformation of results was also checked by repeating the synthesis process [6-8]. The microwave irradiation technique was completed with 60-180 Sec. and yield 62%. The metal complexe Of Cu colored, solid and stable towards air and moisture at room temperature. They possess a sharp melting point. The complexes are soluble in dimethylformamide and dimethyl sulfoxide but insoluble in common organic solvents 3.1.Elemental analysis.

Table-1: Physical and analytical data of L and its metal complexes.

Compound	Mol. Formulae (F.W.)	M.P.°C	Colour	Elemental analysis found (calculated.)%			
				% C (cal.)	% H (cal.)	% N (cal.)	% M (cal.)
Ligand (L)	$C_{16}H_{13}N_3O$ (263)	248°C	Violet	72.99 (72.33)	4.98 (4.80)	15.96 (15.62)	-
$[Cu(L)_2]$	$C_{33}H_{29}CuN_6O_2$ (605)	>280°C	Violet	65.49 (65.10)	4.83 (4.22)	12.54 (13.44)	10.50 (7.66)

3.1FT-Infrared spectra

The characteristic IR bands of the chromone hydrazones give important information about the various functional groups present in it .The ligands showed a Strong band at 1679cm^{-1} which is due to ν (C=O) group. This Strong band was shifted to lower wave number region 10–35 cm^{-1} in their corresponding metal complexes, indicating the coordination of oxygen atom of carbonyl group. The stretching vibration of the azomethine group (C=N) was observed at 1632 cm^{-1} in the ligand. This band was shifted to lower wave number region 20-40 cm^{-1} in their metal complexes, indicating the participation of nitrogen atom of azomethine group in coordination to the metal ion.. The coordination of nitrogen and oxygen atoms was supported by the appearance of a non-ligand bands in the range 525cm^{-1} and 448cm^{-1} region due to the ν(M–O) and ν(M–N),

respectively. From the above spectral data, it was concluded that schiff base ligand acts as bident ateThe FT-IR spectral data containing relevant vibrational bands of the ligands and their metal complexes are listed in Table 2.

Table-2: The selective Infrared frequencies of ligand (L) and its metal complexes

Compound Name	ν(C=O)	ν(C=N)	ν(M-O)	ν(M-N)
L	1679	1632	-	
$[Cu(L)_2]$	1666	1533	525	448

3.23.2Electronic spectra

In UV-Visible spectra the intra ligand transitions of copper (II) complexes are assigned to bands in the range λ_{max} (DMF) **logε (L mol^{-1} cm^{-1})** 280 -366 nm (35844 -27398 cm^{-1}) and 426-482 nm (23532-15420 cm^{-1}) It is due to the Intra ligand transition, $^2B_1 \rightarrow {}^2E(dx^2\text{-}y^2 \rightarrow dxz, dyz)$, $^2B_1 \rightarrow {}^2B_2$ $(dx^2\text{-}y^2 \rightarrow dxy)$, $^2B_1 \rightarrow {}^2A_1$ $(dx^2\text{-}y^2 \rightarrow dz_2)$ and $n\rightarrow\pi^*$ and $\pi\rightarrow\pi^*$ transitions of hydrazone ligands suffered a marginal shift up on complexation. The shift of the bands may be caused by intra ligand transitions which weakening of the C=N bond and extension of conjugation upon complexation.

In UV-Visible spectra the intra ligand transitions of Ni(II) complexes are assigned to bands in the range λ_{max} (DMF) **logε (L mol^{-1} cm^{-1})** 284 nm (35233 cm^{-1}) 326-308,658 (30759 -19822,15424 cm^{-1}) It is due to the Intra ligand transition, $^3A_{2g}(F)\rightarrow{}^3T_{1g}(F)$, and $^3A_{2g}(F)\rightarrow{}^3T_{1g}(F)$ and $n\rightarrow\pi^*$ and $\pi\rightarrow\pi^*$ transitions of hydrazone ligands suffered a marginal shift up on complexation. The shift of the bands may be caused by intra ligand transitions which weakening of the C=N bond and extension of conjugation upon complexation.

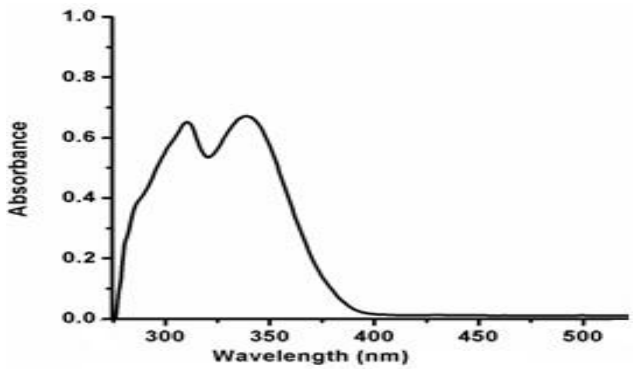

Figure 3.33 UV-visible spectrum of $[Cu(L)_2]$

3.5: Powder XRD studies

The X-ray diffractograms of Cu(II) complexes were recorded in between the range 5-80° at wavelength 1.541551 Å. The unit cell parameters and calculation were performed using powder-X software. Average particle size was calculated using grain software. gives the summary of unit cell parameters and average particle size. Miller's indices and the calculated lattice constants correspond to monoclinic system for Cu(II) complex.

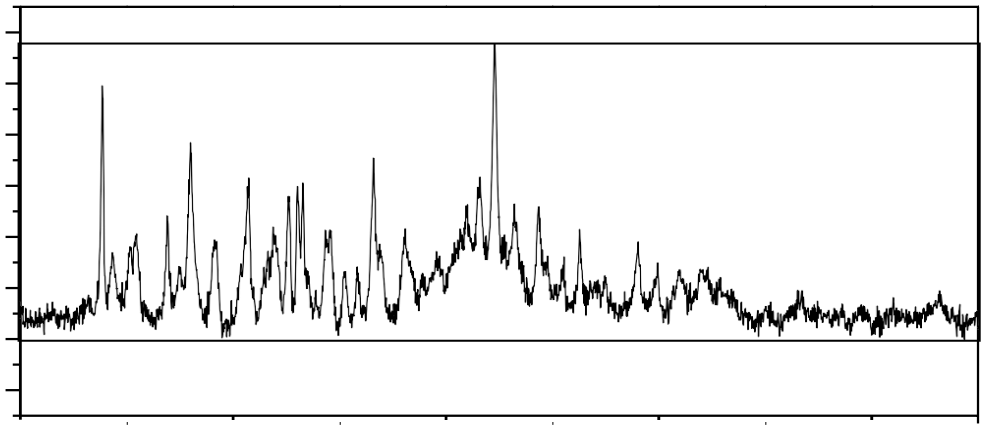

Figure-: Powder X-ray diffractogram pattern of $[Cu(L)_2]$

Table-5 : X-ray diffractogram data of Cu(II)

Parameters	$[Cu(L)_2]$
Temperature	298K
Wavelength (Å)	1.541551
Radiation	CuKα
Crystal system	Monoclinic
Unit Cell Dimension	
α(°)	90
β(°)	106.21
γ (°)	90
Average particle size (nm)	14.923436

3.6 Antimicrobial activity

The in vitro antimicrobial screening of synthesized ligand and metal complexes was tested against four bacteria (*S. Aureus, S. Pyogenes, E. Coli & S. Typhi*) and two fungi (*C. Albicans & T. Rubrum*) by petri-plate containing 30 ml potato dextrose agar and nutrient agar medium, the plates were incubated for 20-24 hr and 24-48 hr for bacteria and fungi stains, respectively. The activities were measured in terms of zone of inhibition in mm. Cefotaxime, Azithromycin and Clotrimazole were used as standard drugs for bacteria and fungi, respectively at 500 ppm concentration of sample as well as drugs. The results of antimicrobial activity of ligand and metal complexes are shown in Table 4.

The metal complexes exhibit higher inhibition against tested microorganism compared to the free ligand. [12-16]. The value in the above table indicates that the activity of the Schiff base ligand became more pronounced when coordinated with the metal ions. The presence of azomethine moiety and chelation effect with central metal enhances the antibacterial activities. This enhancement in antibacterial activity of these metal complexes can be explained based on the chelation theory [17-20].

When a metal ion is chelated with a ligand, its polarity will be reduced to a greater extent due to the overlap of ligand orbital and the partial sharing of the positive charge of the metal ion with donor groups. Furthermore, the chelation process increases the delocalization of the π-electrons over the whole chelate ring, which results

in an increase in the lipophilicity of the metal complexes. Consequently, the metal complexes can easily penetrate into the lipid membranes and block the metal binding sites of enzymes of the microorganisms. These metal complexes also affect the respiration process of the cell and thus block the synthesis of proteins, which restrict further growth of the organism[18-24].

Table 6: Results of antimicrobial activity of synthesized compounds

Compounds	Zone of Inhibition in mm					
	Gm +ve bacteria		Gm -ve bacteria		Antifungal activity	
	S. Aureus	S. Pyogenes	E. Coli	S. Typhi	C. Albicans	T. Rubrum
Ligand (L)	10	09	10	08	-	10
$[Cu(L)_2]$	08	08	08	09	08	09
Cefotaxime	-	-	**24**	**22**	**-**	-
Azithromycin	**22**	**24**		-	**-**	-
Clotrimazole	-	-	-	-	**12**	**14**

Figure-: Selected images of antimicrobial activity of ligands L its metal complexes.

4. Conclusion

The study of the reaction between the transition metal **Cu(II)** and the derived Schiff base indicates its high stability. This encourages the synthesis and careful investigation of the nature of bonding between the Schiff base and the transition metal cation of important biological role, using physicochemical method of analyses. In the present work, **Cu(II)** complexes were prepared from (E)-N'-((1H-indol-3-yl)methylene)benzohydrazide These Schiff base are characterized using various spectral techniques. All hydrazones were characterized by physiochemical methods such as elemental, FT-IR spectra, UV-Vis., spectra and ^{1}HNMR spectra. All these studies give good evidence for the synthesized compounds are crystalline and pure.

IR spectra revealed coordination of Schiff base ligand with metal ion through azomethine nitrogen, carbonyl oxygen of chromone moiety and carbonyl oxygen of hydrazide moiety. The structural elucidation studies by various spectral techniques (IR, TGA and ^{1}H NMR) suggested the nature of ligand is bidentate and geometry of the metal complexes are squar planer. Antimicrobial studies suggest that Schiff base and its complexes play a vital role in developing a new class of antibiotics.

References

[1] C. Selvam, S. M. Jachak, R. Thilagavathi, A. K. Chakraborti, Bioorganic Med. Chem. Lett., 15 (2005) 1793.

[2] B. Kupcewicz, G. B. Czerniak, M. Małecka, P. Paneth, U. Krajewska, M. Rozalski, Bioorganic Med. Chem. Lett., 23 (2013) 4102.

[3] E. Venkateswararao, V. K. Sharma, M. Manickam, J. Yun, S. Jung, Bioorganic Med. Chem. Lett., 24 (2014) 5256.

[4] M. L. Neuhouser, Nutr. Cancer, 50 (2004) 1.

[5] J. P. Cornard, J. C. Merlin, J. Inorg. Biochem., 92 (2002) 19

[6] B. G. Turner, M. F. Summers, J. Mol. Biol., 285 (1999) 1.

[7] M. Shebl, J. Mol. Struct., 1128 (2017) 79.

[8] Y. Sun, G. Liu, H. Huang, P. Yu, Phytochemistry, 75 (2012) 169.

[9] M. S. Masoud, A. A. Soayed, A. F. El-Husseiny, Spectrochim. Acta A, 99 (2012) 365.

[10] K. M. Khan, N. Ambreen, U. R. Mughal, S. Jalil, S. Perveen, M. I. Choudhary, Eur. J. Med. Chem., 45 (2010) 4058.

[11] S. Y. Ebrahimipour, I. Sheikhshoaie, A. Crochet, M. Khaleghi, K. M. Fromm, J. Mol. Struct., 1072 (2014) 267.

[12] T. Sedaghat, M. Yousefi, G. Bruno, H. A. Rudbari, H. Motamedi, V. Nobakht, Polyhedron, 79 (2014) 88.

[13] I. Babahan, E. P. Coban, H. Biyik, Int. J. Sci. Technol., 7 (2013) 26.

[14] A. C. Pinheiro, C. R. Kaiser, T. C. Nogueira, S. A. Carvalho, E. F. da Silva, A. L. Candea, M. C. Lourenco, M. V. de Souza, Med Chem., 7 (2011) 611.

[15] B. C. Raju, R. N. Rao, P. Suman, P. Yogeeswari, D. Sriram, T. B. Shaik, S. V. Kalivendi, Bioorganic Med. Chem. Lett., 21 (2011) 2855.

[16] N. Kavitha, P. V. Ananthalakshmi, J. Saudi Chem. Soc., 7 (2017) S457.

[17] S. M. Saadeh, Arab. J. Chem., 6 (2013) 191.

[18] S. Kumar, A. Hansda, A. Chandra, A. Kumar, M. Kumar, M. Sithambaresan, V. Kumar, R. P. John, Polyhedron, 134 (2017) 11.

[19] M. Sahin, N. Kocak, D. Erdenay, U. Arslan, Spectrochim. Acta A, 103 (2013) 400.

[20] I. A. Tossidis, C. A. Bolos, Inorg. Chimi. Acta., 112 (1986) 93.

[21] A. A. Abu-Hashem, M. M. Youssef, Molecules., 16 (2011) 1956.

[22] (a) J. D. Hepworth, in: A. J. Boulton, A. McKillop (Edn.), Comprehensive Heterocyclic Chemistry 3, Pergamon Press, Oxford, 1984, 835. (b) M.R. Detty, Organometallics., 17 (1988) 2188.

[23] (a) S. V. Jovanovic, S. Steenken, M. Tosic, B. Marjanovic, M.G. Simic. J. A. C. S., 116 (1994) 4846. (b) S. Martens, A. Mithofer, Phytochemistry., 66 (2005) 2399.

[24] M. Kuroda, S. Uchida, K. Watanabe, K. Mimaki, Phytochemistry 70 (2009) 288.

National conference on Chemistry Innovations, Applications and Sustainability

Organized By

Department of Chemistry,
Late Ku. Durga K. Banmeru Science College, Lonar, India

Publisher

Technoscience Academy

Website : www.technoscienceacademy.com

Email : editor@ijsrst.com Website : http://ijsrst.com